Scientific Research Support Fund

The Hashemite Kingdom of Jordan

The University of Jordan

المجلة الأردنية في العلوم الصيدلانية

مجلة علمية عالمية متخصصة تصدر بدعم من صندوق دعم البحث العلمي والابتكار

Jordan Journal of PHARMACEUTICAL Sciences

Specialized International Referreed Journal

Issued by the Scientific Research Support Fund

This title is indexed in Scopus

مجلد (18) العدد (2)، حزيران 2025

Volume 18, No. 2, June 2025

Established 2007

ISSN: 1995-7157

EISSN: 2707-6253

Publisher

The University of Jordan
Deanship of Scientific Research
Amman 11942 Jordan
Fax: +962-6-5300815

National Deposit
(23.3/2008/D)
(Journal's National Deposit Number at the Jordanian National Library)

Jordan Journal of Pharmaceutical Sciences

Volume 18, Number (2), *June* 2025

Jordan Journal of Pharmaceutical Sciences

Aims & Scopes:

***Jordan Journal of Pharmaceutical Sciences* (*JJPS*)** is a bimonthly open-access peer reviewed journal funded by the Scientific Research Fund at Ministry of Higher Education and Research and hosted by the Deanship of Research at the University of Jordan. JJPS is dedicated to various disciplines of pharmaceutical and allied sciences. JJPS publishes manuscripts on original work, either experimental or theoretical in the following areas:

- Pharmaceutics & Biopharmaceutics
- Drug Delivery systems
- Nanotechnology & Nanomedicine
- Organic & Medicinal Chemistry
- Pharmacognosy & Phytochemistry
- Pharmacology, Toxicology, and Experimental Therapeutics
- Pharmaceutical Biotechnology
- Microbiology
- Pharmacy Practice
- Clinical Pharmacy & Hospital Pharmacy
- Pharmacovigilance & Drug Safety
- Health Outcomes and Economics
- Pharmaceutical Health Care Services
- Natural Product Research
- Drug Regulatory Affairs
- Health Policy
- Pharmaceutical Marketing

Instructions to Authors

Preparation and Submission of Manuscripts

Type of Manuscripts

JJPS publishes original research articles, full reviews, research reports, short communications, case studies, commentaries, and short reviews.

Manuscript Preparation

Research paper should be typed on the computer; double spaced, and shouldn't exceed 15 pages (3000 words, font size 12). Spelling, punctuation, sentence structure, spacing, length, and consistency in form and descriptions should be checked before submission. References should also be checked for accuracy. Ensure that all figures and tables are mentioned in the text, and that all references are cited in the text.

Title Page

A separate title page should be submitted separately with the manuscript. The title should be followed by the author(s) name(s) and full affiliations including institution name and address. The title, author(s) name(s), and affiliations should all appear on their own respective line of text. Place an asterisk after the name of the author to whom enquiries regarding the paper should be directed and include that author's telephone and fax numbers and e-mail address. Author(s) affiliation (s) must be mentioned for each one in order.

Abstract

Authors should submit with their research two abstracts, one in English and it should be typed at the beginning of the paper followed by the keywords before the introduction.

The abstract, detailing in one paragraph the problem, experimental approach, major findings, and conclusions, should appear on the second page. It should be double spaced and should not exceed 200 words for **Full Papers and Reviews or l00 words for Case Studies and Short Communications.**

Compounds mentioned in the abstract, given as specific Arabic numbers in the text, should also be accompanied in the abstract by that same numeral. The abstract should appear on a separate page and should be untitled.

Authors are required to submit an Arabic abstract (Required only for Arab native speakers) which should be appended at the end of the submitted manuscript on a separate sheet, including author(s) name(s) and affiliation(s).

Keywords

Should be included at the end of the abstract page, separated by semicolons, not exceeding seven both in Arabic and in English.

Introduction

The manuscript should include an introduction stating the purpose of the research detailed in the manuscript and summaries previous literature leading to the idea and method described in the manuscript.

Results

The results should be presented concisely. Tables and figures should be designed to maximize the presentation and comprehension of the experimental data. Data present in tables and figures should not be redundant in the manuscript's text.

Discussion

The discussion section should interpret the results and relate them to existing knowledge in the field in as clearly and brief as possible. For Full Papers, subheadings may be included within the Results and Discussion sections.

Bolded structural code numbers should only be used for new compounds and for those known compounds for which new biological data or spectroscopic values are being reported. Other known compounds should be referred to in the text by name, wherever necessary.

Experimental Section

The presentation of specific details about instruments used, sources of specialized chemicals and related experimental details should be incorporated into the text of the Experimental Section as a paragraph headed General Experimental.

Acknowledgments

The Acknowledgments section should include credits [initial(s) and last name(s)] for technical assistance, and other appropriate recognition.

Conflict of Interest

Authors should declare any pertaining conflicts in their work, otherwise the authors should clearly indicate that no conflict is present.

Funding

Authors should declare any received funding, indicating the funding institution and grant number. Otherwise, the receipt of no funding should be indicated.

References and Notes

References to the literature and all notes, regardless of their nature, should be numbered in order of appearance in the manuscript, and then cited under the heading References and Notes with superscript numbers. Each reference may have its own citation number, then should be assigned its own number in this section. References and notes should follow the format shown:

Journal

Taha M., Al-Bakri A. and Zalloum W. Discovery of potent inhibitors of pseudomonal quorum sensing via pharmacophore modeling and silico screening. *Bioorg. Med. Chem. Lett.* 2006; 16:5902-5906.

Book

Ancel H. C., Allen L. V. and Popovich N. G. *Pharmaceutical Dosage Forms and Drug Delivery Systems*; Lippicott Williams & Wilkins: New York. 1999, p 45.

Chapter in a Book

Aburjai T., Natsheh F. and Qasem A.: *In: Contemporary Perspective on Clinical Pharmaceutics*. Kohli K. (Ed).; Elsevier New York, 2006; 1st edition, Chapter 57, pp 623-633.

Chemical or Biological Abstract

Al-Hiari Y., Qaisi A., El-Abadelah M. and Wolfgamg V., *Monatshefte fuer Chemei*. 2006; 137(2) 243-248, *Chem. Abstr*. 2007; 145, 397308.

Ph.D. or M. Sc. Thesis

Alkhalil S. The Alkaloids of *Thalictrum isopyroides*. Ph.D. Thesis, Pittsburgh University, PA. 1986, p 115.

Patent

Davis R. U.S. Patent 5,708,591, 1998.

The author is responsible for the accuracy and completeness of all references.

All references must be numbered and written "superscript "without parentheses in the Manuscript (*e.g....according to guidelines pertaining to these techniques*[5,6,7] **);but with parentheses around in the references list (***e.g. (1) Alkhalil S. The Alkaloids of Thalictrum isopyroides. Ph.D. Thesis, Pittsburgh University, PA. 1986, p 115).*

Nomenclature

It is the responsibility of the author(s) to provide correct nomenclature.

Insofar as possible, authors should use systematic names similar to those used by Chemical Abstracts Service.

Abbreviations

Standard abbreviations should be used throughout the manuscript. All nonstandard abbreviations should be kept to a minimum and must be defined in the text following their first use. The preferred forms of some of the more commonly used abbreviations are: mp, bp, °C, K, s, min, h, mL, . ***μ***L, kg, g, mg, ng, ***μ***g, cm, mm, nm, mnl, mmol, , ***μ***mol, ppm, TLC, GC, HPLC, NMR, MS, UV, and IR.

Graphics

The quality of the illustrations printed depends on the quality of the originals provided. Figures cannot be modified or enhanced by the journal production staff. Whenever possible, the graphic files furnished by authors on CD with revised submissions of accepted manuscripts are used in production of the Journal.

A- Layout

In preparing structures for direct photoreproduction, layout is critical. Equations, schemes and blocks of structures are presented in the Journal either in one-column or two-column format.

B- Content

Abbreviations such as Me for CH_3, Et for C_2H_5 and Ph (but not Φ) for C_6H_5 are acceptable.

C- Dimensions

For best results, illustrations should be submitted in the actual size at which they should appear in the Journal. Only original work or high quality photographic prints of originals should be submitted; photocopies do not reproduce well.

Chemical Structures

Structures should be produced with the use of a drawing program such as Chem-Draw. Structure drawing preferences are as follows:

1- Drawing settings:

Chain angle 120^o

Bond spacing 18% of width

Fixed length 14.4 pt (0.508 cm, 0.2 in.), Bold width 2.0 pt (0.071 cm, 0.0278 in.), Line width 0.6 pt (0.021 cm, 0.0084 in.), Margin width 1.6 pt (0.056 cm, 0.0222 in.), Hash spacing 2.5 pt (0.088 cm, 0.0347 in.)

2- Text settings:

Font: Arial/Helvetica

Size: 10 pt

3- Preference:

Units: points

Tolerance: 3 pixels

4- Page setup:

Paper: US Letter

Scale: 100%

Tables

These should be numbered consecutively with Arabic numerals and should be arranged within the manuscript.

Footnotes in tables should be given lowercase letter designations and be cited in the table by italic superscript letter.

Figures

Figures should be constructed in keeping with the column width and line width. All illustrations should be numbered as "Figures", with Arabic numerals.

The Arabic numbers (not the roman ones or the alphabets) are used to number the Tables and Figures which are not abbreviated into Fig. or Tab.

Informed Consent

All manuscripts reporting the results of experimental investigation involving human subjects should include a statement confirming that an informed consent was obtained from each subject or subject's guardian, after the approval of the experimental protocol by a local human ethics committee or IRB.

Copyright Status Form

A properly completed Copyright Status Form with an original signature in ink must be provided for each submitted manuscript.

Manuscript Submission

Manuscripts (in English), together with a cover letter from the corresponding author, should be submitted. A valid e-mail address should be listed when submitting manuscripts.

Manuscript submission via **Website**: **https://jjournals.ju.edu.jo/index.php/jjps/**

Galley Proofs

Page proofs will be sent to the author who submitted the paper. The standard delivery method for galley proofs is by mail.

Correspondence

Correspondence regarding accepted papers and proofs should be directed to Jordan Journal of Pharmaceutical Sciences.

Deanship of Scientific Research
The University of Jordan
Amman 11942, Jordan
Phone: +962 6 5355000 Ext. 25106
Fax: 00962 6 5300815
E-mail: jjps@ju.edu.jo
Website: **https://jjournals.ju.edu.jo/index.php/jjps/**

INTRODUCTION

The Jordan Journal of Pharmaceutical Sciences (**JJPS**) is a peer-reviewed Journal, which publishes original research work that contributes significantly to further the scientific knowledge in pharmaceutical sciences' fields including pharmaceutical/medicinal chemistry, drug design and microbiology, biotechnology and industrial pharmacy, instrumental analysis, phytochemistry, biopharmaceutics and Pharmacokinetics, clinical pharmacy and pharmaceutical care, pharmacogenomics, bioinformatics, and also **JJPS** is welcoming submissions in pharmaceutical business domain such as pharmacoeconomics, pharmaceutical marketing, and management. Intellectual property rights for pharmaceuticals, regulations and legislations are also interesting topics welcomed from our colleagues in Schools of Law.

On a current topic in Pharmaceutical Sciences are also considered for publication by the Journal. **JJPS** is indexed in SCOPUS (Q3). It's a journal that publishes 4 issues per year since 2021 in (**March, June, September, December**). The Editorial Team wishes to thank all colleagues who have submitted their work to JJPS). If you have any comments or constructive criticism, please do not hesitate to contact us at jjps@ju.edu.jo. We hope that your comments will help us to constantly develop **JJPS** as it would be appealing to all our readers.

Prof Ibrahim Alabbadi
Editor-in-Chief
School of Pharmacy- The University of Jordan
Amman 11942- Jordan

Volume 18, 2025

Letter from the Editor-in-Chief

Life is about demand and supply. While this may sound like a business-related phrase, it is embedded in every stage of human life. The foundation of this concept is **value**—no one will buy something they perceive as worthless. However, value is subjective and depends on the buyer's perspective. For example, what is valuable to Hanan may not be valuable to Najah, even though they share the same environment and culture. The key factor here is **perception**—a term that highlights how people assess value based on their personal needs rather than through an objective and accurate evaluation. This subjectivity is also evident in research articles and submissions to the *Jordan Journal of Pharmaceutical Sciences (JJPS)*. Sometimes, two referees provide widely differing opinions on the same paper, making the decision process extremely challenging, even with a third opinion. As a result, some researchers feel discouraged when *JJPS* declines their submission. However, such decisions are never taken lightly. We strive to be as scientific, transparent, and logical as possible in our evaluations.

I am sharing this brief introduction to emphasize that all editorial board members, including myself, always strive to be as objective as possible when making decisions about accepting or rejecting submitted articles. As I write my final introduction for this year's volume of *JJPS*, I encourage all researchers to accept and understand both the outcomes that bring them joy and those that may disappoint them. After six years of continuous dedication and teamwork with my colleagues, this September I am stepping down from my position, hopeful that we will achieve a *SCOPUS Q2* ranking this year.

Over the past five years, we have made significant progress: increasing the number of issues per year from three to four, expanding the number of articles per issue from 5 to 20, and raising the total number of published articles from 15 per year to 80 in 2024, providing researchers with greater flexibility to have their valuable work published sooner. The average waiting time from submission to decision has been drastically reduced, dropping from 28 weeks to just 2.78 weeks in 2024. We have also broadened the journal's scope, ensuring a balanced and logical distribution of research across various pharmaceutical fields, including but not limited to medicinal chemistry and instrumental analysis, pharmacognosy and phytochemistry, pharmaceutics and industrial pharmacy, pharmacokinetics and pharmacodynamics, clinical pharmacy and pharmaceutical care, as well as pharmaceutical business, including pharmacoeconomics and pharmaceutical marketing. I am grateful for this journey and for the opportunity to contribute to the growth and success of *JJPS*, and I extend my sincere thanks to my colleagues and all researchers who have been part of this endeavor.

Submissions have increased dramatically, rising more than fivefold (e.g., 446 submissions in 2024) with an acceptance rate of 28.7% in the same year. Furthermore, we have received a wider diversification of submissions from countries including the USA, Canada, Australia, Europe, Iran, India, Pakistan, Bangladesh, Malaysia, Indonesia, Vietnam, Singapore, Morocco, Algeria, Tunisia, Egypt, Libya, Saudi Arabia and Gulf countries, Yemen, Lebanon, Iraq, Syria, and Jordan, submitted by researchers from both governmental and private universities, as well as scientific research institutes.

As a final note, I would like to express my sincere gratitude to my colleagues—the editorial board members, advisory board members, our dedicated editorial secretary, and the team responsible for English language editing and production. I wish them all the best, along with *JJPS*, for even greater achievements in the years to come.

Best regards

Prof Ibrahim Alabbadi
Editor-in-Chief

CONTENTS

Instructions to Authors		**iv**
Introduction		**ix**
Letter from the Editor		**x**
	ORIGINAL ARTICLES	
Emmy Yuanita *Ima Arum Lestarini* *Ni Komang Tri Dharmayani* *Baiq Nila Sari Ningsih* *Maulida Septiyana* *Maria Ulfa,* *Sudirman* *Taufan Hari Sugara*	Sulfonated Hydroxyxanthone as Anti-Tuberculosis Agent: One-Step Sequence Synthesis, Characterization, And Molecular Docking Preevaluation	**305**
Cheryl Rhea Lewis	Investigating the Mechanistic Target of Rapamycin and Analogous Pathways in Cardiovascular Diseases to Augment Cardiac Functionality	**317**
Nadine N. Abdelhadi *Alaa Dabbous* *Saad M Jaddoua*	Role of Clinical Pharmacy Services in Vitamin Supplementation in Critically Ill Cancer Patients: A 3-Year Retrospective Study at a Comprehensive Cancer Centre	**332**
C. Hima Bindu *T. Farmaan* *K. Aparna* *M. Sadan* *T. Reshma*	Nano-Analytical Techniques in Pharmaceutical Analysis	**341**
Belal Rahhal *Heba Salah* *Leen Abu Abdoh* *Noor Almasri* *Shahd Al-Tarsha* *Shoroq Bsharat* *Jumana Najjar*	Effect of Mannitol on Renal Function during Cardiac Surgery and Immediate Post-Operative in Selected Private Hospitals in Nablus City/ Palestine	**377**
Tahani Alwidyan *Rawan Abudalo* *Mohannad Odeh PhD* *May Tayyem* *Aya Banat*	Community Pharmacists' Attitudes Toward the Implementation of Good Pharmacy Practice Guidelines in Jordan: A Cross-Sectional Survey	**389**

Hamad Haider Khan *Faiz Ullah Khan* *Tawseef Ahmad* *Hui Guo* *Bingyin Shi*	Evaluation of Health-Related Quality of Life in Patients with Type 2 Diabetes Mellitus through EQ-5D-3L: in public sector hospitals of Quetta, Pakistan	**410**
Amaresh Prusty *Chinmaya Keshari Sahoo* *Sanjit Kumar Senapati* *Priyanka Singh* *Gyanranjan Behera*	Formulation and Characterization of Methyldopa Floating Tablets Using Polymeric Excipients: A Study on Gastroretentive Drug Delivery System	**423**
Aaiza Mumtaz *Muhammad Umair* *Hadia Hussain* *Wasla Ali* *Muhammad Sajid*	In-silico innovative mRNA Vaccine development using multi-epitopes of SopD protein for Enteric Fever caused by *Salmonella enterica*	**437**
Sawsan I. Khdair *Seham Zarour* *May Almajawleh* *Feras A. Khudeir*	Single Nucleotide Pleomorphisms of Different Cytokines among Jordanian Patients with Lupus Nephritis: A Pilot Study	**461**
Razan Hasan *Nader Abdalla* *Maram Bilal*	Pre treatment neutrophil to lymphocyte ratio and total cholesterol levels as biomarkers for breast cancer	**472**
Djahra Ali Boutlelis *Benkaddour Mounia* *Benkherara Salah* *Laib Ibtissam* *Benine Chaima* *Chrait Sabrina*	The Remedial Effect of *Ziziphus lotus* Extract against Oxidative Stress Induced by Deltamethrin Pesticide in Rats	**483**
Hebah Ayash *Muhammed Hamitoğlu* *Soodabeh Davaran* *Ahmet Aydin*	Review on the Application of Electrospun Herbal Extract-Loaded Metallized Nanofiber Composites as Wound Healing Promoter: Fabrication, Efficacy, and Safety	**496**
Belal Rahhal *Nidal Jaradat* *Linda Issa* *Fatimah Hussein* *Gidaa Amara* *Leen Gazawi* *Sahar Alheen* *Waed Jbara* *Zan Baransi* *Zena keadan*	Unveiling the Phytochemical Profiling, hypolipidemic, hypoglycemic and antioxidant effects of different extracts from *Lavandula stoechas* L. (French lavender) grown in Palestine	**509**

Ahmed Naji Alfalahi *Sina M. Matalqah* *Reem Issa* *Hala I. AL-Daghistani* *Anas Abed*	Evaluation of Cytotoxicity and Antibacterial Activity of Green Synthesized Silver Nanoparticles using *Hedera helix* extract	**524**
Kajol, Aditi Kaushik *Nikhil Sharma*	Stability Indicating Rp-Hplc for Method Development and Validation for Simultaneous Estimation of Empagliflozin and Nateglinide in Bulk Drug	**538**
Sindhu K.C *Atisammodavardhana Kaundinnyayana* *Prabhat Kumar Jha* *Sandesh Poudel* *Rajib Tiwari* *Ram Kishor Yadav* *Sistu K.C.* *Kushal Subedi*	Phytochemical Constituents and in-vitro antioxidant Activity of *Aleuritopteris bicolor* Leaves, *Crinum amoenum* Bulbs, and *Drynaria coronans* Rhizomes of Nepal	**555**
Boyeekati Mohammad Rizwan *Nawaz Mahammed* *Shaik Farheen Taj* *V. Sivasai Bharath Kumar* *B. Yamuna*	A Review on Puncturing Potential: Microneedles' Present Landscape And Prospective Horizons	**566**
Issa Yusuf *Rama Ibrahim*	The Predictive Value of Neutrophil/Lymphocyte Ratio for CK-MB Elevation in Myocardial Infarction: A Study in Syrian ACS Patients	**586**
Hassan Badaoui *Marwa Alaqarbeh* *Youness Moukhliss* *Hanane Zaki* *Moulay Ahfid El alaouy* *M'barek Choukrad* *Abdelouahid Sbai* *Hamid Maghat* *Tahar Lakhlifi* *Mohammed Bouachrine*	Integrated Computational Exploring of Benzoyl Thienopyrimidine Derivatives as Potential ERα Regulators in Breast Cancer Treatment	**596**

Sulfonated Hydroxyxanthone as Anti-Tuberculosis Agent: One-Step Sequence Synthesis, Characterization, And Molecular Docking Preevaluation

Emmy Yuanita*[1], Ima Arum Lestarini[2], Ni Komang Tri Dharmayani[1], Baiq Nila Sari Ningsih[1], Maulida Septiyana[1], Maria Ulfa1, Sudirman[1], Taufan Hari Sugara[3,4]

[1]Department of Chemistry, Faculty of Mathematic and Natural Science, Universitas Mataram, Mataram, Indonesia.
[2]Department of Medical, Faculty of Medical, Universitas Mataram, Mataram, Indonesia.
[3]University of Muhammadiyah Mataram, West Lombok, Indonesia.
[4]Research Center for Marine and Land Bioindustry, BRIN, Mataram, Indonesia.

ABSTRACT

The synthesis of sulfonated hydroxyxanthones (4a and 4b) was streamlined into a single sequence to reduce steps and enhance efficiency. This study also investigated the molecular docking of these synthesized compounds as potential anti-TB agents. Using AutoDock Vina, the docking results indicated that compounds 4a and 4b exhibit promising anti-TB activity by effectively binding to the DHPS enzyme. This enzyme, crucial for *Mycobacterium tuberculosis* growth, was specifically targeted in the study, underscoring the compounds' potential to inhibit DHPS and their suitability as anti-TB drugs.

Keywords: *Hydroxyxanthone, Sulfonated, Docking, anti-TB.*

INTRODUCTION

The multidrug resistance in pathogenic bacteria, particularly Mycobacterium tuberculosis (Mtb), has become the major problem that causes this disease to be difficult to cure and increases mortality [1]. Commercial anti-TB drugs such as Rifabutin (RBT), Rifapentine (RPT), Rifampicin (RIF), Isoniazid (INH), Pyrazinamide (PZA), Ethambutol (EMB), D-Cycloserine (DCS), Streptomycin (STC) which are in chemical structure containing polyphenol, amine, and amide group in aromatic and aliphatic formed, are indicated resistance in battle toward Mtb [2, 3].

Antimicrobial resistance is created naturally through how the mechanism of the bacteria combat and adapt to an antibacterial agent. Moreover, it is believed that the misuse and overuse of antibiotics are a primary reason for the growing antibiotic crisis [4, 5]. However, several solutions can be proposed to tackle this growing antimicrobial resistance, such as the development of rapid diagnostics, modifying existing drugs, combining existing drugs, and discovering new antimicrobials [6] such as taraxasterol that isolated from *Euphorbia hirta L* [7], as well as in embattle the Mtb, discovery and development of new effective anti-TB drugs is extremely needed. By observing the active functional group attached to the standard anti-TB drugs and previous study on Quantitative Structure-Activity Relationship, Xanthone and its derivatives have potential as anti-TB. The QSAR equation generated was Log MIC = 3.113 + 11.627 qC1 + 15.955 qC4 + 11.702 qC9, which implies that the 3,6 dihydroxy and 1,3,6 trihydroxy xanthone with amide, sulfoxide, and carboxylate groups have good activity as a drug for anti-tuberculosis. In addition, docking studies showed that sulfonamide-substituted xanthone has an inhibitory

Corresponding author: Emmy Yuanita
emmy_yuanita@unram.ac.id
Received: 28/06/2024 Accepted: 18/07/2024.
DOI: https://doi.org/10.35516/jjps.v18i2.2850

mechanism like KasA for anti-TB drug activity [8]. Furthermore, xanthone is designated as anti-TB since xanthone as heterocyclic compound has been regarded as an important chemical compound in the search for bioactivity such as antioxidant [9], antibacterial [10, 11] , cancer chemotherapy [12, 13, 14], antimalarial [15], and as therapeutic agent for covid-19 [16]. These biological activities of xanthone are based on their tricyclic scaffold and the nature and or position of their substituents. Among the substituents that could attach to these compounds are hydroxy, methoxy, phenyl, alkoxy, halogens, sulfonamide, and sulfoxide [11].

Therefore, the aims of the project were to synthesize derivatives of hydroxyxantone with sulfonate substituent, as it has been done before in the modification of Isoniazid (INH), in which the addition of sulfonate and hydrazine group generated Isoniazid a better activity in TB treatment [17]. Secondly, the docking analysis of the synthesized hydroxyxanthone as an anti-TB agent is a strategic approach to reduce the cost associated with the biological evaluation of these compounds. A previous study also showed that the presence of sulfonate and sulfoxide groups inhibited KasA (4C6X.pdb), an enzyme involved in the biosynthesis of mycolic acid, which plays a vital role in the life cycle of *Mycobacterium tuberculosis* (Mtb) [8] Additionally, para-aminobenzoic acid (pABA) plays a prominent role in the outgrowth of Mtb. Therefore, molecular docking studies in this project were carried out to target 7,8-dihydropteroate synthase (DHPS), a transferase enzyme from Mycobacterium tuberculosis H37Rv (1EYE.pdb). DHPS catalyzes the condensation reaction of pABA with 6-hydroxymethyl-7,8-dihydropterin pyrophosphate to produce 7,8-dihydropteroate and pyrophosphate [18].

Experimental Section

General

All reagents were purchased commercially from Merck and Sigma-Aldrich, and the reaction conditions are shown in Figure 1. Compounds 3a and 3b were prepared based on the method of [9, 10, 19, 11, 14] which is a modification of the method of Chan., et al [20]. Furthermore, the obtained compounds were purified by recrystallization.

1,3-dihydroxy-9H-xanthen-9-one (3a), reddish solid (75.5%), m.p: 224°C. FTIR (KBr, ν, cm-^{1}): 3240 (OH), 1612 (C=O), 1458 (C-C aromatic), 1296 (C-O-C). 1H-NMR (CD3OD; 500 MHz) δ (ppm): 6.24 (1H, d, J= 1.20 Hz), 6.40 (1H, and J= 1.2 Hz), 7.78 (1H, dd, J= 1.2 Hz and J= 7.9 Hz), 7.85 (1H, td, J= 7.2 Hz; J = 7.7 Hz and J= 1.3Hz), 7.59 (1H, dd, J= 8.50 Hz and J= 1.50Hz), 8.13 (1H, dd, J= 7.9 Hz and J= 1.2 0Hz; 12.82 (OH, S); MS (EI) m/z: 228 (M+1).

1,3,7-trihydroxy-9H-xanthen-9-one (3b), light yellow solid (75%), 322.5°C. FTIR (KBr, ν, cm-^{1}): 3387 (OH), 1612 (C=O), 1450 (C-C aromatic), 1288 (C-O). 1H-NMR (DMSO-d6; 500 MHz) δ (ppm): 6.16 (1H, d, J= 2.05 Hz), 6.34 (1H, d, J= 2.0 Hz), 6.79 (1H, d, J= 2.16 Hz), 6.389 (1H, dd, J= 2.2Hz and 8,75 Hz), 7.9 (1H, d, J= 8.75 Hz), 13.01 (0H, s); MS (EI) m/z: 244 (M+1).

Synthesis of sulfonate-substituted hydroxyxanthone (4a-b)

All reagents and conditions of synthesis are shown in Scheme 1. Compounds 4a-b were prepared based on the method of [21] and modified from [22]. The synthesis was applied by reacting the result of 1 mmol of each hydroxyxanthones 3a and 3b with 2 to 5 mL chlorosulfonic acid, which used ethanol as a solvent. The addition of chlorosulfonic acid was carried out dropwise at (0±3) °C for 1 hour. The precipitate which is formerd was filtered and then washed with water to give a solid product.

Sulfonate substituted 1,3-dihydroxyxanthone (4a). Yellow (71 %). FTIR (KBr, ν; cm^{-1}): 3433(O-H), 1635(C=O), 1381 (C-C aromatic), 1226 (C-O-C), 1165 (O=S=O), 1018 (S=O), 763 (S-O). ^{1}H-NMR (DMSO-d$_6$; 500 MHz) δ (ppm): 12.81 (OH, *s*), 11.11 (OH, *s*), 6.21 (1H, *s*), 7.46 (1H, *t, J* = 7.5 Hz), 7.58 (1H, *d, J* = 5 Hz), 7.84 (1H, *t, J* = 7.5 Hz), 8.12 (1H, *d, J* = 10 Hz), 1.16 (2H, *t, J* = 5 Hz).

Sulfonate substituted 1,3,7-trihydroxyxanthone (4b). Red Solid (44 %). FTIR (KBr, ν; cm^{-1}): 3435 (O-H), 1638 (C=O), 1482 (C=C aromatic), 1250 (C-O-C), 1196

(O=S=O), 1060 (S=O); ^{1}H-NMR (DMSO-d_6; 500 MHz) δ (ppm): 12.90 (OH, *s*), 11.21 (OH, *s*), 10.00 (OH, *s*), 6.19 (1H, *d*, *J* = 2.1 Hz), 7.13 (1H, *d*, *J* = 8.7 Hz), 7.29 (1H, *dd*, *J* = 9.0; 3.1 Hz), 7.92 (1H, *s*), 1.23 (2H, *s*).

Molecular Docking

Molecular docking studies were conducted on compounds 4a and 4b against the 1EYE protein structure using AutoDock Vina and visualized with Discovery Studio Visualizer software. The candidate compounds were optimized using Gaussian software with semi-empirical calculations. The 1EYE structure represents the crystal structure of the binary complex of 6-hydroxymethyl pterin monophosphate (PtP) with dihydropteroate synthase (DHPS) from *Mycobacterium tuberculosis* (Mtb), a pathogen responsible for the deaths of millions of people each year. The crystal structure used in this study was obtained from the Protein Data Bank. The inhibitory activity of the compounds is attributed to their ability to block the catalytic condensation reaction between para-aminobenzoic acid (pABA) and 6-hydroxymethyl-7,8-dihydropterin pyrophosphate, thereby preventing the formation of 7,8-dihydropteroate and pyrophosphate, which are essential for bacterial growth and survival.

RESULTS AND DISCUSSION

Synthesis and Characterization

Sequential one-pot syntheses are effective for constructing complex targets, such as sulfonate-substituted hydroxyxanthones, and can significantly reduce the number of steps required for the overall reaction. The synthesized compounds 4a and 4b were derived from intermediates 3a and 3b through a condensation reaction between hydroxybenzoic acid derivatives (1a–b) and phloroglucinol (2). This method has been reported in previous studies [9, 10, 19, 11, 14]. All reactions were catalyzed using Eaton's reagent. The formation of hydroxyxanthones via this reaction is illustrated in Scheme 1.

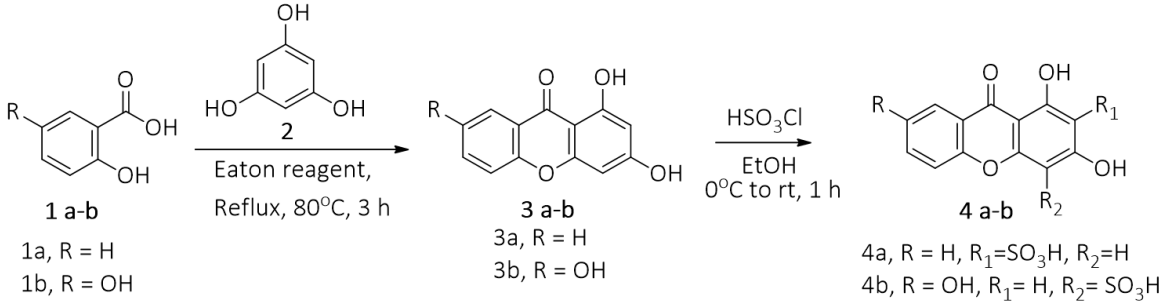

Scheme 1. Synthesis route of sulfonated hydroxyxanthone

A one-sequence reaction refers to a process in which all reactions occur in a single pot and proceed directly to subsequent stages without purification of intermediate products. Sulfonation was carried out by carefully adding chlorosulfonic acid into the reaction mixture. The sulfonation mechanism of hydroxyxanthone proceeds via electrophilic substitution, beginning with the interaction of the π bond from the xanthone ring with an electrophile—specifically, a sulfate species. A proton is then abstracted from an adjacent carbon to restore the aromatic system, either at the original position or via isomerization. Regioselectivity was observed in the synthesis of compounds 4a and 4b, where the products displayed different substitution positions. This regioselectivity is attributed to steric and electronic effects during the electrophilic attack [23, 24]. Scheme 2 illustrates the proposed reaction mechanism for the sulfonation of xanthone. Sulfonation of xanthones 3a and 3b yielded substitution at the ortho position for compound 4a and at the para position for compound 4b, respectively.

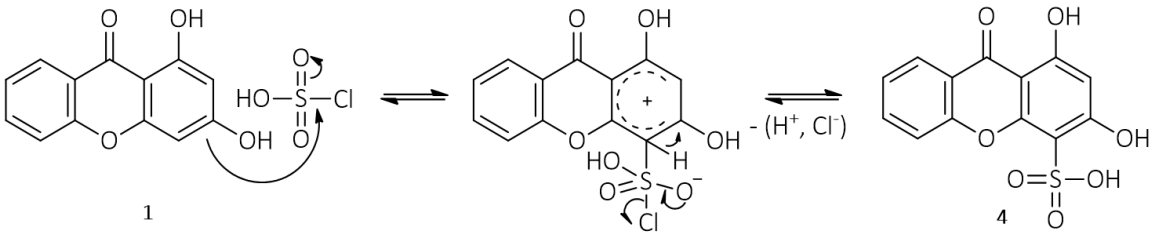

Scheme 2. Mechanism reaction of substitution of sulfonic to xanthone

Changes in the wave number of the IR spectrum and chemical shift of the 1H-NMR spectrum are shown in Figure 1 and Figure 2. The synthesized IR data shows a shift in the wave number of the aromatic alkene group from 1450 cm-^{1} to 1381 cm-^{1}, which indicates a change in the alkene carbon. The occurrence of sulfonation is also confirmed based on IR data from poly (ether-ether ketone) sulfonate compounds at wave numbers 1165, 1018 and 763 cm-^{1}, indicating respectively of the spectrum for O=S=O, S=O and S-O. Meanwhile, the spectrum at wave numbers 1226 cm-^{1}, 1635 cm-^{1} and 3433 cm-^{1} indicates C-O-C, C=O and O-H.

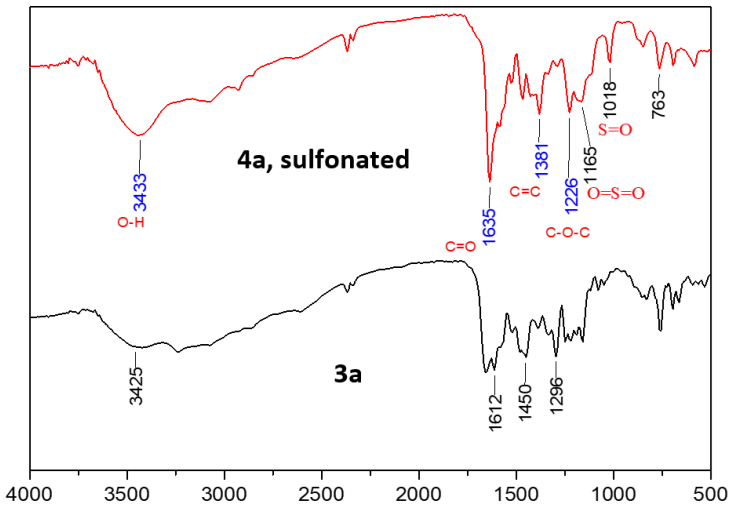

Figure 1. FTIR spectra of compound 3a and 4a

Moreover, based on the 1^11H-NMR spectrum, the presence of the sulfonate group is indicated by the chemical shifts of five aromatic protons in the range of 6.00 to 9.00 ppm. A singlet signal at 6.59 ppm (1H, s) corresponds to the proton at the C-2 position, which is isolated and shows no coupling with neighboring protons. This isolation is due to the presence of the sulfonate substituent at the C-4 position. The remaining four aromatic protons appear at 8.64 ppm (1H, d, J = 7.15 Hz), 7.59 ppm (1H, d, J = 7.15 Hz), 7.25 ppm (1H, t, J = 7.25 Hz), and 7.01 ppm (1H, t, J = 5.70 Hz). The multiplicity and coupling constants of these signals indicate that the protons are adjacent and correspond to positions C-5, C-6, C-7, and C-8, respectively.

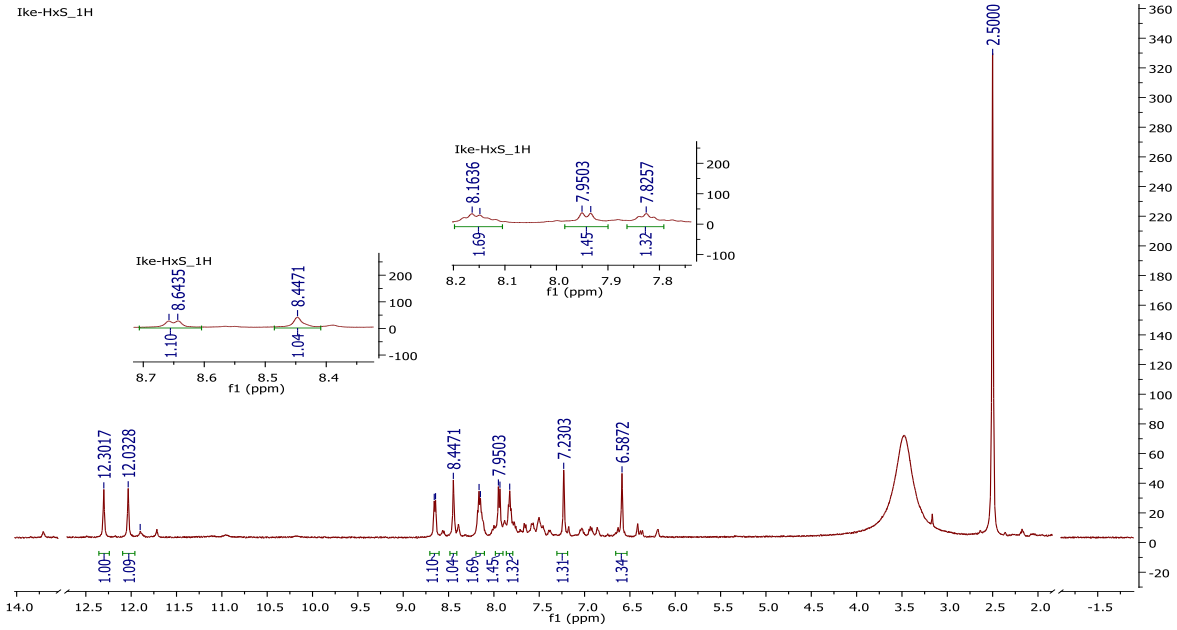

Figure 2. 1H NMR spectra of compound 4a sulfonated 1,3-dihydroxyxanthone

The characterization of compound 4b shows different results, with the estimated position of sulfonation at the C-2 position. The hydroxyl group at C-1 forms a chelate with the carbonyl group, suggesting that substitution or sulfonation is likely to occur at C-2. A previous study by Qin et al. also indicated that substitution at the C-2 position is relatively more stable [25]. Compound 4b was confirmed by FTIR and 1-HNMR spectra. In the FTIR spectrum, characteristic vibrations of the xanthone core appear, 1020, dan 709 cm-[1], along with additional peaks corresponding to O=S=O, S=O, and S–O stretching vibrations. The vibration of the aromatic carbon bonded to sulfur in the sulfonate group is observed at 660 cm-1 [26, 27].

Table 1. FTIR of compound 3b and 4b

Gugus Fungsi	Bilangan Gelombang (cm-1)	
	(3b)	(4b)
O-H	3432	3435
C=O	1637	1638
C=C	1484	1482
C-O-C	1185	1250
O=S=O	-	1196
S=O	-	1060
S-O	-	820

The 1H-NMR spectrum of compound 4b shows four aromatic proton signals in the range of 6–8 ppm, indicating that one aromatic proton present in compound 3b has been substituted. A singlet observed at 8.43 ppm corresponds to the hydroxyl proton of the sulfonate group in compound 4b, further confirming successful sulfonation.

Table 2. 1H-NMR of compounds 3b and 4b

C	Compound 3b	Compound 4b
2	6.14 (1H, d, J=2.1 Hz)	-
4	6.28 (1H, d, J=2.1 Hz)	6.18 (1H, d, J=2.1 Hz)
5	7.58 (1H, d, J=3.0 Hz)	7.38 (1H, d, J=3.0 Hz)
6	7.73 (1H, dd, J=3.0; 9.0 Hz)	7.64 (1H, dd , J=3.0; 9.2 Hz)
8	7.90 (1H, d, J=9.0 Hz)	7.86 (1H, d, J=9.0 Hz)
1-OH	12.83 (OH, s)	12.88 (OH, s)
3-OH	12.48 (OH, s)	11.73 (OH, s)
7-OH	12.58 (OH, s)	10.33 (OH, s)
S-OH	-	8.43 (OH, s)

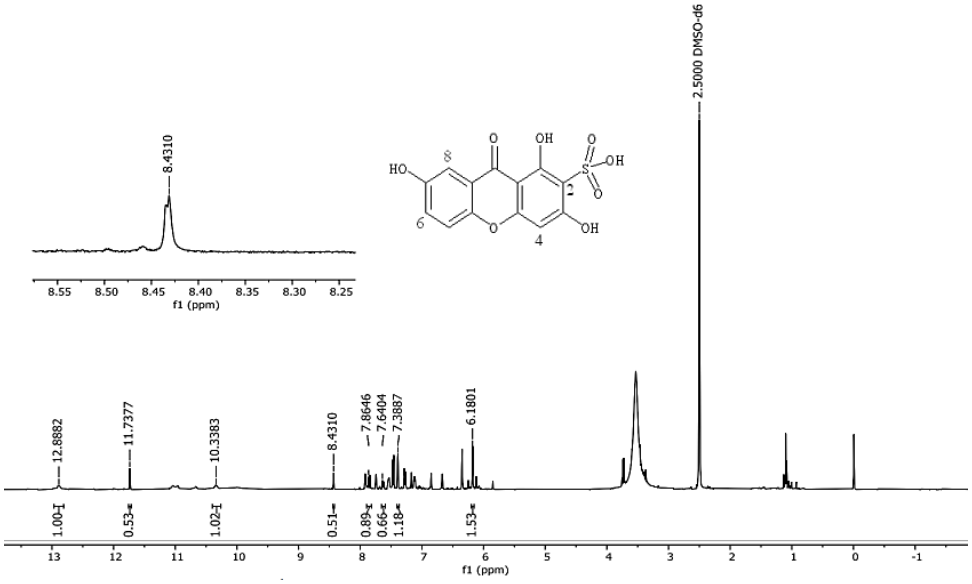

Figure 3. 1H-NMR of compound 4b sulfonated of 1,3,7-trihydroxyxanthone

Molecular Docking

The primary objective of molecular docking is to gain insights into and predict molecular recognition. This involves two key aspects: first, identifying potential binding modes at the structural level, and second, estimating binding strength or affinity [28]. Molecular docking is a valuable tool in the discovery of new compounds with therapeutic potential. It enables the prediction of interactions between ligands and targets at the molecular level, as well as the exploration of structure–activity relationships (SAR), even without prior knowledge of the chemical structures of other target modulators. Although initially developed to elucidate molecular recognition mechanisms between small and large molecules, the applications of molecular docking in drug discovery have expanded significantly in recent years [13]. One prominent application is the repurposing of existing compounds for new therapeutic targets through reverse screening approaches, which identify novel molecular targets for known ligands based on structural complementarity [29]. In this study, the compounds tested were sulfonated hydroxyxanthones (4a and 4b), docked against Mycobacterium tuberculosis DHPS (1EYE.pdb), as shown in Figure 4.

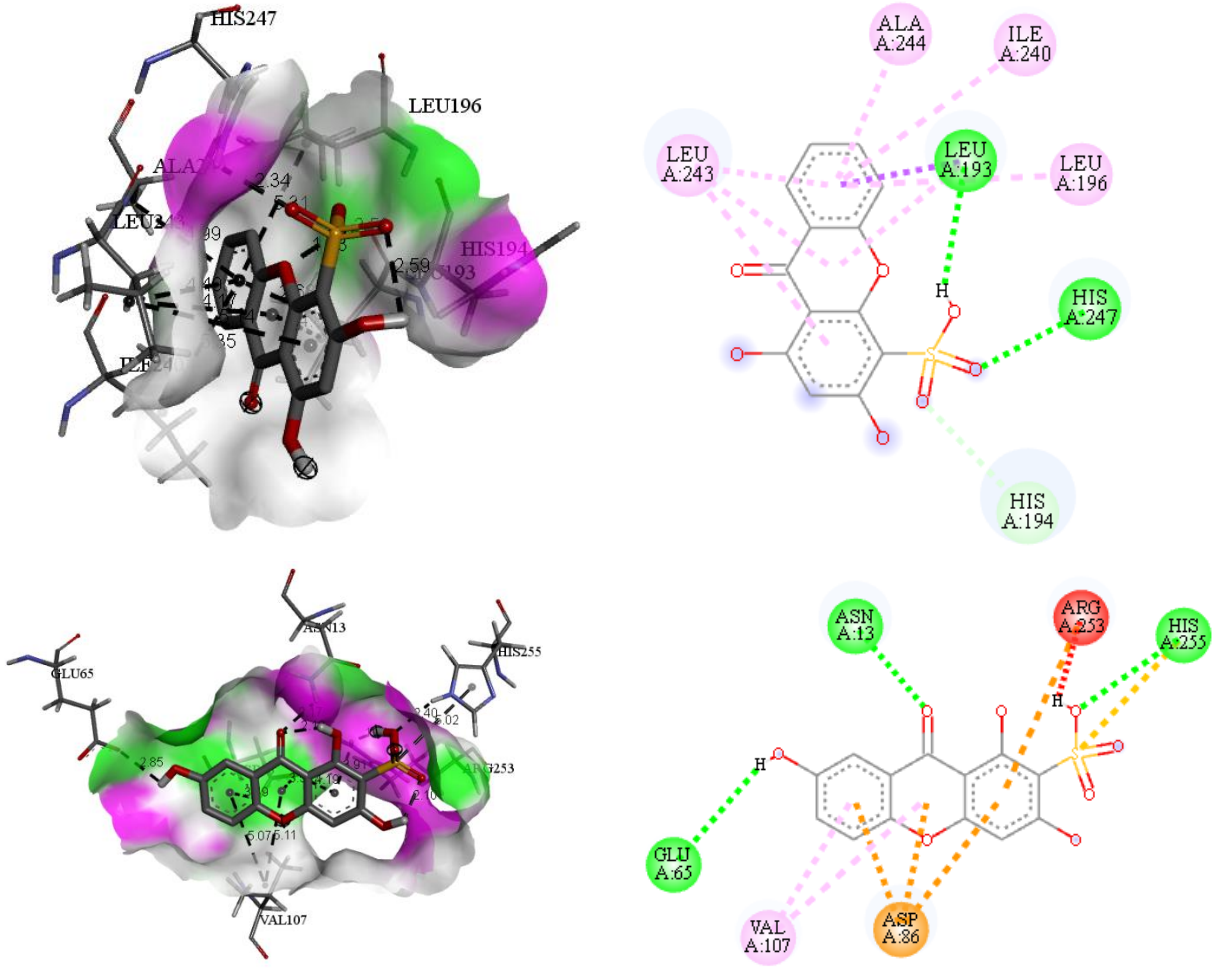

Figure 4. 2D and 3D predicted binding mode from docking simulation of 4a and 4b into the active site of MTB DHPS (1EYE.pdb)

Table 3. Binding Interaction, Distance, energy interaction of hydroxyxanthone substituted sulfonate (4a-b)

Compound	Affinity/Energy (Kcal/mol)	Binding Interaction (Amino acid residue)	Hydrogen Bond Length
Native Ligand	-6.3	Asn105; Lys213, Arg253; Asp86 dan Gly20	3.07; 2.97; 2.73; 3.06; 2.79; 2.78; and 3.13
4a	-7.5	Leu193 and His 194	2.55 and 2.73
4b	-7.6	AsN13, His255 and Glu65	2.17; 2.39, and 2.85

Compound 4b exhibits a lower binding energy compared to compound 4a and the native ligand of DHPS, indicating that the lower the energy, the more stable the ligand–protein complex formed. As a reference, compound 4a forms two hydrogen bonds with Leu193 and His194. In contrast, compound 4b forms three hydrogen

bonds with Asn13, His255, and Glu65. These hydrogen bonds differ somewhat from those in the native DHPS ligand, which involves seven hydrogen bonds distributed among Asn105, Lys213, Arg253, Asp86, and Gly20.

Hydroxyxanthones with sulfonate substituents can inhibit the DHPS enzyme, which catalyzes the condensation of para-aminobenzoic acid (pABA) with 6-hydroxymethyl-7,8-dihydropterin pyrophosphate to produce 7,8-dihydropteroate and pyrophosphate via hydrogen bonding interactions. DHPS plays a crucial role in de novo folate synthesis in prokaryotes, lower eukaryotes, and plants, but is absent in mammals. The binding mechanism of sulfonated xanthones 4a and 4b with DHPS is analogous to that of sulfonamide drugs, which act as DHPS inhibitors [30]. Sulfa-containing drugs, such as sulfamethoxazole (a sulfonamide) combined with trimethoprim (a diaminopyrimidine) as co-trimoxazole, have been used to treat drug-resistant tuberculosis. Similar findings have been reported for sulfamoyl pentanamida groups in leucine derivatives [31]. However, the antibacterial activity of amide, imine, and hydroxamic acid derivatives was found to be low or nonexistent against some Gram-positive and Gram-negative bacteria [32]. Moreover, the structure of hydroxyxanthones 4a and 4b potentially binds with pABA, facilitating the formation of an oxygen bridge, as illustrated in Figure 5. Therefore, the lower binding energy and inhibitory interactions of compounds 4a and 4b with the pABA synthesis pathway in *Mycobacterium tuberculosis* suggest their potential as anti-TB agents.

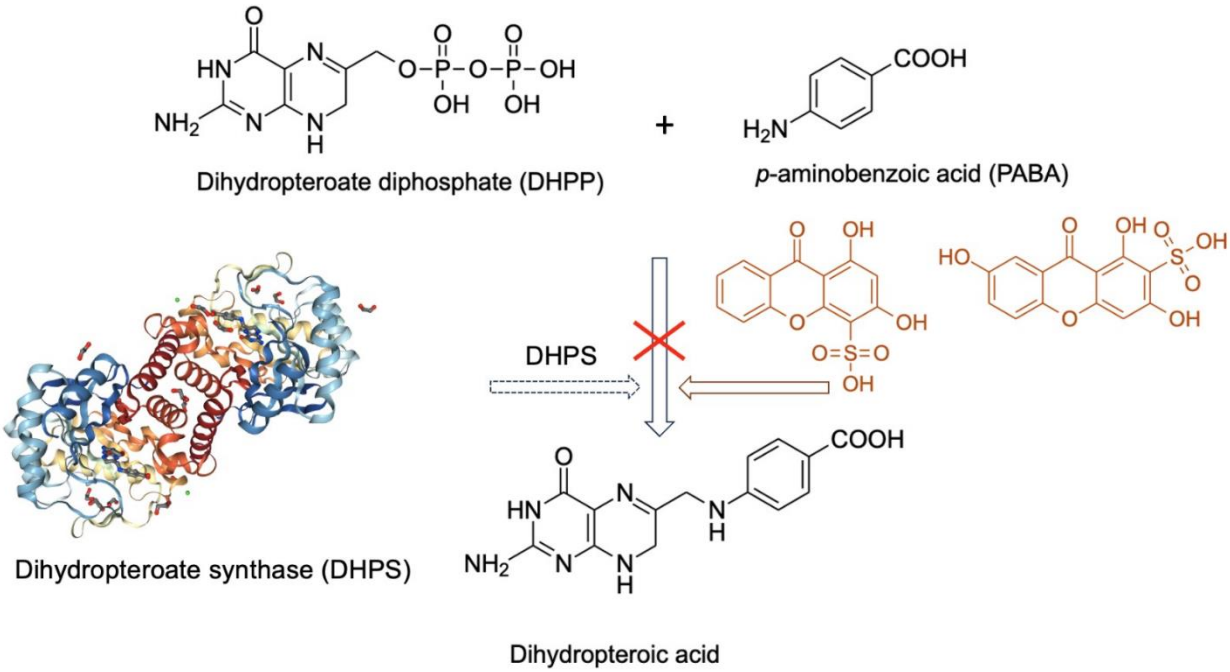

Figure 5. Schematic representation of the anti-tuberculossis activity mechanism of hydroxyxanthone sulfonate (4a-b). Molecular surface representation of DHPS with the co-crystallized DHPP and pABA (1EYE.pdb)

The mechanism of inhibition of hydroxyxanthones on the DHPS (7,8-dihydropteroate synthase) enzyme in *Mycobacterium tuberculosis* (Mtb) involves disrupting the enzyme's normal function, thereby interfering with folate biosynthesis, which is essential for bacterial growth and survival. DHPS is crucial for synthesizing

dihydropteroate, a key precursor in the folate biosynthesis pathway of Mtb. Hydroxyxanthones, such as compounds 4a and 4b, bind to the active site of the DHPS enzyme. This binding occurs through interactions such as hydrogen bonding, hydrophobic interactions, and other specific contacts depending on the chemical structure of the hydroxyxanthones.

Once bound, hydroxyxanthones inhibit the enzymatic activity of DHPS, preventing the conversion of para-aminobenzoic acid (pABA) and 6-hydroxymethyl-7,8-dihydropterin pyrophosphate (DHPPP) into dihydropteroate. Without dihydropteroate, folate synthesis is interrupted. Folate is essential for the synthesis of nucleotides and amino acids, which are crucial for DNA replication and protein synthesis in bacteria, including Mtb. By inhibiting DHPS and thus folate biosynthesis, hydroxyxanthones disrupt these vital processes, leading to inhibition of bacterial growth and potentially bactericidal effects.

The specificity of hydroxyxanthones for DHPS in Mtb makes them promising candidates for anti-TB drugs. This study likely evaluated the binding affinity and efficacy of compounds 4a and 4b using molecular docking methods (such as AutoDock Vina), which simulate how well these compounds bind to the enzyme's active site and inhibit its function.

In summary, hydroxyxanthones inhibit the DHPS enzyme in Mtb by binding to its active site and disrupting folate biosynthesis, thereby impairing essential metabolic processes and inhibiting bacterial growth—highlighting their potential as effective anti-TB agents.

CONCLUSION

The synthesis of sulfonated hydroxyxanthones (4a and 4b) was consolidated into a single sequence to streamline the process and improve efficiency. Additionally, this study investigated the molecular docking of these synthesized compounds as potential anti-TB agents. AutoDock Vina analysis revealed that compounds 4a and 4b exhibit significant anti-TB activity by effectively binding to the DHPS enzyme. In summary, hydroxyxanthones inhibit the DHPS enzyme in *Mycobacterium tuberculosis* by binding to its active site and disrupting folate biosynthesis, thereby impairing essential metabolic processes and inhibiting bacterial growth, highlighting their potential as effective anti-TB agents.

Acknowledgment

Financial support for these works from Penelitian Fundamental Reguler of Kementerian Pendidikan, Kebudayaan, Riset, dan Teknologi-Indonesia is gratefully acknowledged for years 2023 with grand number 3181/UN18.L1/PP/2023.

Authors' Declaration

The authors declare that they have no known competing financial interests or personal relationships that could have appeared to influence the work reported in this paper.

Authors' Contribution Statement

Emmy Yuanita contributed to conceptualization, methodology, and supervision. Baiq Nila Sari Ningsih handled software and validation for docking, while Taufan Hari Sugara was responsible for writing and data curation. Ni Komang Tri Dharmayani collected data for synthesis and spectroscopy evaluation. Ima Arum Lestarini contributed to methodology for activity evaluation. Maria Ulfa and Maulida Septiyana provided review, writing, and editing support. Sudirman contributed to data curation and software.

REFERENCES

1. Jones R. M., Adams K. N., Eldesouky H. E. and Sherman D. R. The evolving biology of Mycobacterium tuberculosis drug resistance. *Front Cell Infect Microbiol*. 2022; 12:1027394.
2. Seung K. J., Keshavjee S. and Rich M. L. Multidrug-Resistant Tuberculosis and Extensively Drug-Resistant Tuberculosis. *Cold Spring Harb Perspect Med*. 2015; 5(9).
3. Tripathi R. P., Tewari N., Dwivedi N. and Tiwari V. K. Fighting tuberculosis: an old disease with new challenges. *Med Res Rev*. 2005; 25(1):93-131.
4. Miethke M., Pieroni M., Weber T., Brönstrup M., Hammann P., Halby L., Arimondo P. B., Glaser P., Aigle B., Bode H. B., Moreira R., Li Y., Luzhetskyy A., Medema M. H., Pernodet J.-L., Stadler M., Tormo J. R., Genilloud O. and et al. Towards the sustainable discovery and development of new antibiotics. *Nat Rev Chem*. 2021; 5(10):726-749.
5. Ventola C. L. The antibiotic resistance crisis: part 1: causes and threats. *P T*. 2015; 40(4):277-283.
6. O'Neill J. Tackling a Global Health Crisis: Initial step. Wellcome Collection, London, 2015.
7. Irianti T., Pratiwi S. U. T. and Yasmin I. F. Antituberculosis Activity of Active Compound of Ethyl Acetate Extract for Patikan Kebo (Euphorbia hirta L.). *Jordan J Pharm Sci*. 2022; 15(4):461-473.
8. Yuanita E., Sudirman, Dharmayani N. K. T., Ulfa M. and Syahri J. Quantitative structure-activity relationship (QSAR) and molecular docking of xanthone derivatives as anti-tuberculosis agents. *J Clin Tuberc Other Mycobact Dis*. 2020; 21:100203.
9. Yuanita E., Pranowo H. D., Siswanta D., Swasono R. T., Mustofa M., Zulkarnain A. K., Syahri J. and Jumina J. One-Pot Synthesis, Antioxidant Activity and Toxicity Evaluation of Some Hydroxyxanthones. *Chem Chem Technol*. 2018; 12(3):290-295.
10. Yuanita E., Jannah B. K., Ulfa M., Sudirman, Ningsih B. N. S. and Dharmayani N. K. T. C-prenylation of 1,3 dihydroxyxanthone: synthesis, characterization and antibacterial activity. *Acta Chim Asiana*. 2023; 6(1):279-286.
11. Yuanita E., Sudarma I. M., Sudewiningsih N. M., Syahri J., Dharmayani N. K. T., Sudirman, Ulfa M. and Sumarlan I. Antibacterial activity and molecular docking studies of series hydroxyxanthone. *AIP Conf Proc*. 2020; 2243(1):020032.
12. Yuanita E., Pranowo H. D., Jumina J. and Mustofa M. Design of Hydroxy Xanthones Derivatives as Anticancer Using Quantitative Structure-Activity Relationship. *Asian J Pharm Clin Res*. 2016; 9(2):180-185.
13. Pinzi L. and Rastelli G. Molecular Docking: Shifting Paradigms in Drug Discovery. *Int J Mol Sci*. 2019; 20(18).
14. Yuanita E., Ulfa M., Sudirman, Sumarlan I., Sudarma I. M., Dharmayani N. K. T., Syahri J. and Jumina J. Synthesis, Cytotoxic Evaluation and Molecular Docking of Bromo-Substituted 1,3,6-Trihydroxyxanthone as Protein Tyrosine Kinase Inhibitor. *Malays J Biochem Mol Biol*. 2021; 23:24-32.
15. Syahri J., Yuanita E., Nurohmah B. A., Wathon M. B., Syafri R., Armunanto R. and Purnowo B. Xanthone as Antimalarial: QSAR Analysis, Synthesis, Molecular Docking and In-vitro Antimalarial Evaluation. *Orient J Chem*. 2017; 33(1):29-40.
16. Yuanita E., Sudirman, Dharmayani N. K. T., Ulfa M., Hadisaputra S. and Syahri J. Molecular docking of xanthone derivatives as therapeutic agent for Covid-19. *Molekul*. 2022; 17(1):1-9.
17. Aslan E. K., Han M. I., Khrisna V. S., Tamhev R., Dengiz C., Dogan S. D., Lhebert C., Mourey L., Tonjum T. and Gunduz M. G. Isoniazid Linked to Sulfonate Esters via Hydrazone Functionality: Design, Synthesis, and Evaluation of Antitubercular Activity. *Pharmaceuticals (Basel)*. 2022; 15(10).

A. Baca M. A., Sirawaraporn R., Turley S., Sirawaraporn W. and Hol W. G. J. Crystal structure of *Mycobacterium tuberculosis* 7,8-dihydropteroate synthase in complex with pterin monophosphate: new insight into the enzymatic mechanism and sulfa-drug action. *J Mol Biol*. 2000; 302(5):1193-1212.

18. Yuanita E., Pranowo H. D., Mustofa M., Swasono R. T., Syahri J. and Jumina J. Synthesis, Characterization and Molecular Docking of Chloro-substituted Hydroxyxanthone Derivatives. *Chem J Moldova*. 2019; 14(1):68-76.
19. Kiang L. C., Thơ L., Kim Y., Shah S. A. and Webber J. ChemInform Abstract: Synthesis of 1,3,6-Trioxygenated Prenylated Xanthone Derivatives as Potential Antitumor Agents. *ChemInform*. 2013; 44.
20. Yuanita E., Hidayah N., Umami M. R., Ningsih B. N. S., Dharmayani N. K. T., Sudirman and Ulfa M. Simple synthesis and characterization of sulfonate ester-substituted hydroxyxanthone. *AIP Conf Proc*. 2024; 3055(1):03000.
21. Sudarma M., Yuanita E. and Suana I. W. Markovnikov addition of chlorosulfuric acid to eugenol isolated from clove oil. *Indones J Chem*. 2013; 13(2):181-184.
22. Mondal M., Puranik V. G. and Argade N. P. Facile Synthesis of 1,3,7-Trihydroxyxanthone and Its Regioselective Coupling Reactions with Prenal: Simple and Efficient Access to Osajaxanthone and Nigrolineaxanthone F. *J Org Chem*. 2006; 71(13):4992-4995.
23. Zhao and Larock R. C. Synthesis of xanthones, thioxanthones, and acridones by the coupling of arynes and substituted benzoates. *J Org Chem*. 2007; 72(2):583-588.
24. Qin W., Lan Z., Liu J., Huang H., Tang H. and Wang H. Synthesis and biological evaluation of 1,3-dihydroxyxanthone mannich base derivatives as anticholinesterase agents. *Chem Cent J*. 2013; 7(1):78.
25. Sanabria E., Esteso M., Pérez-Redondo A., Vargas E. and Maldonado M. Synthesis and characterization of two sulfonated resorcinarenes: a new example of a linear array of sodium centers and macrocycles. *Molecules*. 2015; 20(6):1420-3049.
26. Chuesutham T., Sirivat A., Paradee N., Changkhamchom S., Wattanakul K., Anumart S., Krathumkhet N. and Khampim J. Improvement of sulfonated poly(ether ether ketone)/Y zeolite -SO3H via organo-functionalization method for direct methanol fuel cell. *Renew Energy*. 2019; 138:243-249.
27. Stanzione F., Giangreco I. and Cole J.C. Use of molecular docking computational tools in drug discovery. *Prog Med Chem*. 2021; 60:273-343.
28. Kharkar P.S., Warrier S. and Gaud R.S. Reverse docking: a powerful tool for drug repositioning and drug rescue. *Future Med Chem*. 2014; 6(3):333-342.
29. Palomino J.C. and Martin A. The potential role of trimethoprim-sulfamethoxazole in the treatment of drug-resistant tuberculosis. *Future Microbiol*. 2016; 11(4):539-547.
30. Egbujoe C., Okonkwo V.I., Onyeije U.C., Emeruwa C.N., Nkuzinna O.C., Egwuatu P.I., Amasiatu I.S., Onyemeziri A.C. and Okoro U.C. Design, synthesis, molecular docking and biological evaluation of novel leucine derived sulfamoyl pentanamides as antimicrobial and antioxidant agents. *Jordan J Pharm Sci*. 2024; 17(4):687-705.
31. Hussein B., Bourghli L.M.S., Alzweiri M., Al-Hiari Y., Sini M.A., Alnabulsi S. and Al-Ghwairi B. Synthesis and biological evaluation of carbonic anhydrase III and IX inhibitors using gas chromatography with modified pH-sensitive pellets. *Jordan J Pharm Sci*. 2023; 16(2):426-439.

السولفونات من الهيدروكسيكسانثون كعامل مضاد للسل: التوليف التسلسلي في خطوة واحدة، التحليل، والتقييم المبدئي باستخدام التفاعل الجزيئي

إمي يوانيتا[1*]، إما أروم ليستارييني[2]، ني كومانغ تري دارمايانى[1]، بايق نيلا ساري نينغسيه[1]، موليدا سيبتيانا[1]، ماريا أولفا[1]، سوديرمان[1]، توفان هاري سوغارا[3،4]

[1] قسم الكيمياء، كلية الرياضيات والعلوم الطبيعية، جامعة ماتارام، ماتارام، إندونيسيا

[2] قسم الطب، كلية الطب، جامعة ماتارام، ماتارام، إندونيسيا

[3] جامعة محمدية ماتارام، لومبوك الغربية، إندونيسيا

[4] مركز أبحاث الصناعات البيولوجية البحرية والبرية، BRIN، ماتارام، إندونيسيا

ملخص

تم تبسيط توليف المركبات السولفونية من الهيدروكسيكسانثون (a4 وb4) إلى تسلسل واحد بهدف تقليل عدد الخطوات وزيادة الكفاءة. كما درست هذه الدراسة التفاعل الجزيئي لهذه المركبات المحضرة كعوامل محتملة ضد مرض السل. باستخدام برنامج AutoDock Vina، أظهرت نتائج التفاعل الجزيئي أن المركبات a4 وb4 تظهر نشاطًا واعدًا ضد مرض السل من خلال ارتباطها الفعال بأنزيم .DHPSهذا الإنزيم، الذي يعد أمرًا حيويًا لنمو المتفطرة السلية، كان الهدف المحدد في الدراسة، مما يبرز قدرة المركبات على تثبيط DHPS وملاءمتها كأدوية مضادة للسل.

الكلمات الدالة: هيدروكسيكسانثون، سولفوني، تفاعل جزيئي، مضاد للسل.

[*] ***المؤلف المراسل: إمي يوانيتا***

emmy_yuanita@unram.ac.id

تاريخ استلام البحث 2024/06/28 وتاريخ قبوله للنشر 2024/07/18.

Jordan Journal of Pharmaceutical Sciences, Volume 18, No. 2, 2025

Investigating the Mechanistic Target of Rapamycin and Analogous Pathways in Cardiovascular Diseases to Augment Cardiac Functionality

Cheryl Rhea Lewis*[1]

[1] Department of Pharmacology, Kasturba Medical College, Manipal Academy of Higher Education, Manipal – 576104, Karnataka, India

ABSTRACT

Cardiovascular diseases (CVDs) are the leading cause of global mortality, especially in low- to middle-income countries, with heart failure accounting for 34% of deaths, totaling 62.5 million premature deaths in the past decade. Despite initial improvements in survival rates, mortality due to heart failure remains concerning, indicating a decline in the heart's compensatory capacity as age advances. To understand the molecular complexities of CVDs, this narrative review extensively explored databases such as Scopus, Web of Science, and PubMed using specific inclusion criteria to select articles from experimental studies, clinical trials, animal studies, and observational studies published after the year 2000. Conversely, exclusion criteria were applied to omit articles irrelevant to the topic or published before 2000. The extensive literature search revealed, surprisingly, the largely unexplored potential of targeting the mTOR pathway for the treatment of CVDs. Previous studies suggest that mTOR modulation could reshape cardiac disease pathways, though clinical evidence remains limited. Recent findings underscore mTOR dysregulation in cardiac diseases and show promise in mitigating dysfunction through mTOR inhibition, despite challenges in clinical translation. Understanding mTOR's crosstalk with other pathways illuminates the complexity of cardiac disease. This review emphasizes mTOR's significance in coronary artery disease (CAD) and ischemic heart disease (IHD), suggesting avenues for further research and clinical applications to improve cardiovascular disease management and reduce heart failure-related mortality.

Keywords: coronary artery disease; ischaemic heart disease; mTOR pathway.

INTRODUCTION

The mechanistic Target of Rapamycin (mTOR) is a highly conserved serine/threonine protein kinase that functions as a central regulator of cellular growth, proliferation, metabolism, and survival. It is a key component of two distinct multiprotein complexes: mTOR Complex 1 (mTORC1) and mTOR Complex 2 (mTORC2)[13]. mTORC1 is primarily known for its role in regulating protein synthesis, cell growth, and metabolism in response to nutrient availability, growth factors, and energy status. Activation of mTORC1 promotes anabolic processes such as protein synthesis and lipid biosynthesis while inhibiting catabolic processes such as autophagy[13]. Key upstream regulators of mTORC1 include the PI3K/Akt pathway, which is activated by growth factors such as insulin and insulin-like growth factor 1 (IGF-1), and the AMP-activated protein kinase (AMPK) pathway, which senses cellular energy levels. Upon activation, mTORC1 phosphorylates downstream targets such as ribosomal protein S6 kinase 1 (S6K1) and eukaryotic translation initiation factor 4E-binding protein 1 (4E-BP1), leading to enhanced protein synthesis and cell growth[31].

mTORC2, on the other hand, regulates cell survival, cytoskeletal organization, and metabolism. Akt phosphorylation at Serine 473 by mTORC2 is crucial for

Corresponding author: Cheryl Rhea Lewis
rheadsouza30@rediffmail.com
Received: 31/01/2024 Accepted: 22/08/2024.
DOI: https://doi.org/10.35516/jjps.v18i2.2313

its full activation and plays a central role in promoting cell survival and proliferation. Additionally, mTORC2 has been closely associated with the regulation of cytoskeletal dynamics through its phosphorylation of substrates such as protein kinase C alpha (PKCα) and serum/glucocorticoid-regulated kinase 1 (SGK1)[31].

Dysregulation of mTOR signalling has been implicated in a wide range of diseases, including cancer, metabolic disorders, neurodegenerative, and cardiovascular diseases[33]. In cancer, aberrant activation of mTOR signalling is commonly observed due to mutations or alterations in upstream regulators such as PI3K, Akt, and PTEN, leading to uncontrolled cell growth and proliferation. Abnormal mTOR signalling has also been implicated in metabolic disorders such as obesity, type 2 diabetes, and insulin resistance highlighting the complex interplay between mTOR signalling and metabolic homeostasis[33] making it an attractive target for therapeutic intervention in several pathologies including cardiovascular.

1) Coronary Artery Disease (CAD)

The pathophysiology of coronary artery disease

In the genesis of coronary artery disease (CAD), the initiation of atherosclerotic plaque formation emerges as a pivotal precursor (Figure 1). Atherosclerosis, a multifactorial phenomenon linked to predisposing conditions including diabetes, hypertension, chronic infection, lipid abnormalities, intra-abdominal/visceral obesity, and hypertension, assumes a paramount role in this intricate process.[1] Notably, heightened levels of visceral adipose tissue significantly augment the susceptibility to coronary artery disease. Substantial evidence implicates inflammation as a pivotal player in atherosclerotic plaque development.[2] This inflammatory cascade is orchestrated through the activation of nuclear factor kappa B (NfκB) and transforming growth factor beta (TGFβ) pathways, culminating in the release of cytokines, inflammatory cells, and adhesion factors that contribute to endothelial dysfunction. Additionally, hemodynamic forces induced by blood flow elicit endothelial dysfunction, characterized by the upregulation of factors such as endothelin, vascular endothelial growth factors (VEGF), cytokines, adhesion factors, and other pro-inflammatory mediators.[3]

Furthermore, the increased uptake of oxidized low-density lipoprotein (oxLDL) serves as a potent chemo-attractant for lymphocytes and macrophages into the intima of the blood vessel. Macrophages laden with oxLDL, along with T cells, platelets, and smooth muscle cells, coalesce to form fatty streaks, arresting motility and fostering atherogenic microenvironments. Foam cells within the intimal wall release growth factors, promoting stromal cell proliferation and extracellular remodelling, thereby propelling the progression of fatty streaks into granuloma formation. Neovascularization of the plaque surfaces culminates in the development of an atheroma plaque.[4] The p53 signalling pathway, integral to apoptosis, precipitates the rupture of atherosclerotic plaques, prompting subsequent platelet aggregation at the rupture site and the clinical manifestation of coronary artery disease symptoms.[2]

Research endeavours underscore the pivotal role of nutrients, particularly lipids and carbohydrates, in regulating gene expressions of glycolytic and lipogenic enzymes. These molecular signals exert their influence through key genes such as sterol responsive element-binding protein, 1 and 2 (SREBP) and the mammalian target of rapamycin (mTOR).

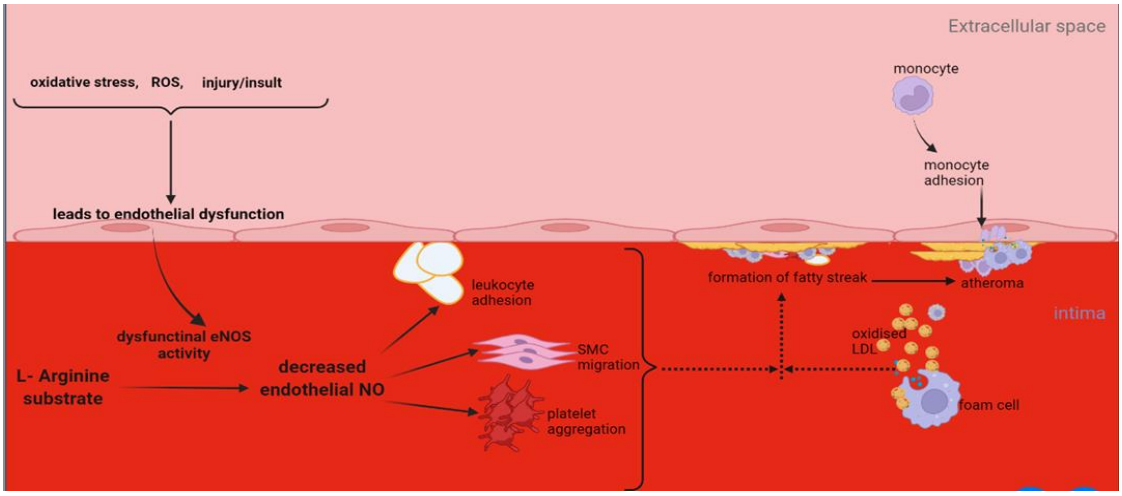

Created using biorender.com

Figure 1. Pathophysiology of coronary artery disease

Figure 1 illustrates the development of an atherosclerotic plaque. The initial trigger for atherogenesis is either oxidative stress or injury/insult to the arterial wall. The resulting injury leads to endothelial dysfunction, characterized by impaired eNOS activity. Consequently, smooth muscle cells migrate, leukocytes adhere, and platelets aggregate, culminating in the formation of a fatty streak within the vessel wall's intima. Simultaneously, LDL oxidation occurs, accompanied by the accumulation of monocytes, macrophages, and oxidized LDL, which give rise to foam cells. These foam cells adhere to the fatty streak, leading to the formation of an atherosclerotic plaque. Clinical manifestations of coronary artery disease occur when the atherosclerotic plaque ruptures.

Role of mTOR in CAD

mTOR assumes a pivotal role in diverse pathophysiological processes within the cardiovascular system.[5] Specifically, mTORC1, a component of the mTOR complex orchestrates the synthesis of membrane lipids in cells by activating SREBP1/2 and transcription factor genes governing fatty acid and cholesterol metabolism.[5] The activation of SREBP1/2 by mTORC1 can occur directly through the phosphorylation of S6K-1 or indirectly via the phosphorylation of Lipin 1, a negative regulator of SREBP1/2.[6] Dysregulation of SREBPs induces dysfunction in lipogenesis and fatty acid metabolism, contributing to cardiovascular diseases, diabetes mellitus, and obesity.[7] In specific cardiovascular conditions such as coronary artery disease, SREBP genes exhibit significant expression in epicardial adipose tissue (EAT), situated between the epicardium and the pericardium.[8] Overexpression of SREBPs is linked to the exacerbation of coronary atheroma, and studies associate the upregulation of SREBP genes with early-stage atherosclerosis, even at normal plasma lipid levels.[9]

Endothelial dysfunction serves as a pivotal element in the progression from a plaque to an atheroma, primarily driven by reduced availability of endothelial nitric oxide (eNO). eNO, synthesized by endothelial nitric oxide synthetase (eNOS), encoded by chromosome 7 in humans, predominantly exists in the vasculature, regulating vessel permeability and promoting angiogenesis.[10,11] Additionally, eNOS plays a vital role in inhibiting leukocyte adhesion to the endothelial wall, preventing the migration of smooth muscle cells (SMC), and averting platelet aggregation in the cardiovascular system.[12] eNOS phosphorylation is regulated through various pathways involving calmodulin and multiple phosphorylation events, with serine 1177 phosphorylation

being the primary regulator.[13] (Figure 2). Among the kinases involved in eNOS phosphorylation, phosphor kinase B and C (PKB and PKC) play a significant role.[14] The phosphorylation of serine 1177 occurs downstream of the phosphoinositide 3 kinase pathway.[15,16] Insulin, HDL, estradiol, and VEGF can enhance serine 1177 phosphorylation through the AKT/PKB pathway, while the phosphorylation of threonine at 459 reduces eNOS activity. VEGF, in particular, phosphorylates Ser1177 and dephosphorylates threonine 459.[17] Conversely, PKC dephosphorylates Ser1177 and phosphorylates threonine 459, decreasing eNOS activity.[18] A defective AKT/eNOS mechanism resulting in increased phosphorylation of eNOS at Ser1177 leads to endothelial dysfunction and accelerated atherogenesis.

The impairment of endothelial function due to injury or insult manifests as alterations in eNO and serves as an early indicator of vascular diseases.[19] Conditions such as oxidative stress and the presence of reactive oxygen species (ROS) render eNOS pro-atherogenic through 'uncoupling of eNOS', causing dysfunctional eNOS activity.[13] Under normal physiologic conditions, the generation of endothelial nitric oxide by eNOS depends on the co-factor tetrahydrobiopterin (BH4).[20] In pathological conditions like atherosclerosis, there is a decrease in endothelial BH4 production, an increase in the formation of the eNOS inhibitor asymmetric dimethyl arginine (ADMA), and an increase in arginase activity, which collectively reduce the substrate of eNOS, L-arginine into urea and ornithine. This leads to superoxide anion (O2-) production and decreased NO release, initiating a cascade of oxidative damage that disrupts endothelial function and overall cardiac health.[21,22] Recent studies on mice reported that an increase in S6 kinase activity, a downstream target of mTORC1, enhances superoxide generation and decreases NO function due to eNOS uncoupling.[23] (Figure 2). Therefore, it can be inferred that S6 kinase activation by mTORC1 phosphorylates eNOS, leading to oxidative stress and endothelial dysfunction- precursors to atherosclerosis and coronary artery disease. Given the crucial role of mTORC1 in cellular metabolism and nitric oxide signalling, a comprehensive understanding of the implications of mTORC1-mediated phosphorylation of eNOS is imperative.

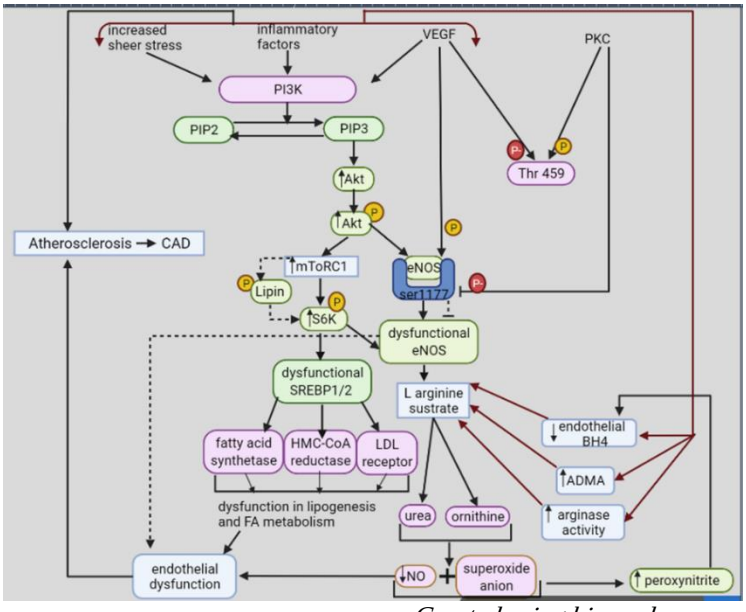

Created using biorender.com

Figure 2. The Role of mTOR in the pathogenesis of CAD

Figure 2 depicts the involvement of mTOR in the development of coronary artery disease (CAD). The activation of mTORC1, facilitated by upstream Akt signaling, initiates the phosphorylation of its downstream substrate, S6 Kinase. This phosphorylation event precedes the disruption of lipogenesis and fatty acid metabolism through the dysregulation of SREBP1/2. Additionally, the activation of upstream Akt also impairs eNOS function and its activity on its substrate, L-arginine, ultimately leading to the generation of free radicals such as superoxide and peroxynitrite. These free radicals contribute to endothelial dysfunction, which serves as a precursor to CAD. Factors such as increased shear stress, inflammatory mediators, and VEGF indirectly promote endothelial dysfunction by reducing the availability of endothelial BH4, a critical co-factor for eNOS, and increasing levels of ADMA.

mTORC1, orchestrates the synthesis of membrane lipids in cells by activating SREBP1/2 and transcription factor genes governing fatty acid and cholesterol metabolism.

↓

The activation of SREBP1/2 by mTORC1 can occur directly through the phosphorylation of S6K-1 or indirectly via the phosphorylation of Lipin 1.

↓

In coronary artery disease, SREBP genes exhibit significant expression in epicardial adipose tissue (EAT). Overexpression of SREBPs is linked to the exacerbation of coronary atheroma.

↓

Endothelial dysfunction serves as a pivotal element in the progression from a plaque to an atheroma, primarily driven by reduced availability of endothelial nitric oxide (eNO), synthesized by endothelial nitric oxide synthetase (eNOS).

↓

Oxidative stress and the presence of reactive oxygen species (ROS) render eNOS pro-atherogenic causing dysfunctional eNOS activity.

↓

A defective AKT/eNOS mechanism resulting in increased phosphorylation of eNOS at Ser1177 leads to endothelial dysfunction and accelerated atherogenesis.

↓

In atherosclerosis, there is a decrease in endothelial BH4 production, an increase in the formation of the eNOS inhibitor asymmetric dimethyl arginine (ADMA), and an increase in arginase activity, which collectively reduce the substrate of eNOS - L-arginine, into urea and ornithine. This leads to superoxide anion (O2-) production and decreased NO release, initiating a cascade of oxidative damage that disrupts endothelial function.

Flowchart representing mTOR involvement in development of atherosclerosis

Inhibition/ knockout of mTOR in CAD

mTOR, a pivotal regulator of cellular energy and nutrient homeostasis, can be effectively hindered by mTOR inhibitors such as rapamycin and everolimus. This intervention leads to the suppression of lymphocyte cell proliferation directed towards the atherosclerotic region and hampers cell cycle progression.[24] Rapamycin specifically targets mTORC1, resulting in the inhibition of p70S6K, which, in turn,

downregulates cyclooxygenase -2 (COX-2) and inducible nitric oxide synthase (iNOS). These proteins are crucial contributors to inflammation and have been implicated in the heightened production of VEGF.[24]

Various animal experimental models have employed rapamycin or rapalogs like everolimus to impede mTOR and scrutinize its impact on atherosclerosis progression. These models have demonstrated that rapalogs effectively inhibit mTORC1, eliciting a potent anti-atherosclerotic effect by:[25]

i) Curtailing smooth muscle cell proliferation,

ii) Suppressing macrophage activity,

iii) Hampering the recruitment and migration of monocytes to the vessel wall, and

iv) Diminishing de novo protein synthesis through the dephosphorylation of downstream mTORC1 targets, specifically p70S6K and 4E-BP1.

Conversely, mTORC1 inhibition prompts the activation of the mTORC2 pathway, instigating cell survival and autophagy. This molecular cascade prevents the transition of early-stage atherosclerotic plaques into fully formed plaques.[26] Investigations on the inflammatory response in arterial atherosclerotic plaques in Apo-E knockout mice have unveiled that mTORC1 inhibition in early plaques results in eNOS phosphorylation within the atherosclerotic regions. This phenomenon leads to reduced migration of smooth muscle cells and diminished adhesion of monocytes to the area, effectively curtailing the size of fatty streaks.[27] Notably, treatment with mTOR inhibitors in LDLR-/- mice has demonstrated substantial delays in the progression of small-sized plaques into fully developed atherosclerotic plaques.[28]

Key findings:

Role of mTORC1 in Lipid Metabolism: The involvement of mTORC1 in regulating lipid synthesis via SREBP1/2 activation elucidates its contribution to cardiovascular diseases such as atherosclerosis. Dysregulation of SREBPs leads to dysfunction in lipogenesis and fatty acid metabolism, exacerbating conditions like coronary artery disease. Understanding these pathways highlights potential therapeutic targets aimed at modulating mTORC1 activity to mitigate lipid-related cardiovascular risks.

Impact of Endothelial Dysfunction on Atherogenesis: The elucidation of endothelial dysfunction mechanisms, particularly involving eNOS phosphorylation, underscores its pivotal role in atherosclerosis development. Dysfunctional eNOS activity, influenced by factors like oxidative stress and ROS, leads to impaired endothelial function and reduced nitric oxide availability, initiating a cascade of events culminating in atherosclerotic plaque formation. Targeting pathways involved in eNOS regulation, such as the AKT/PKB pathway, may offer therapeutic avenues for restoring endothelial function and preventing atherogenesis.

Link between mTORC1 Activation and Endothelial Dysfunction: The identified association between mTORC1 activation, S6 kinase activity, and eNOS phosphorylation provides further insights into the role of mTOR signalling in endothelial dysfunction and atherosclerosis. Enhanced S6 kinase activity, downstream of mTORC1, contributes to eNOS uncoupling and subsequent oxidative stress, further exacerbating endothelial dysfunction and promoting atherogenesis. This highlights the potential of targeting mTORC1 signalling pathways to alleviate endothelial dysfunction and prevent cardiovascular diseases.

Overall, these findings underscore the intricate interplay between mTOR signalling, lipid metabolism, endothelial function, and atherosclerosis, offering potential therapeutic targets for intervention in cardiovascular diseases. A comprehensive understanding of these pathways is crucial for developing targeted therapies aimed at improving cardiac health and preventing the progression of cardiovascular diseases.

2. Ischaemic Heart Disease (IHD)

The pathophysiology of Ischaemic Heart Disease (IHD)

Myocardial infarction (MI), stemming from the

occlusion of coronary arteries, represents a sudden cardiac event with potential fatal outcomes irrespective of age, gender, or ethnicity. Despite heightened awareness and endeavors in resuscitation the mortality rate persists at approximately 10% during the acute phase and around 25% during the chronic phase of MI.[29] The restoration of blood flow to the myocardium following ischemia induces a paradoxical damage known as "ischemia/reperfusion injury," often culminating in heart failure despite successful reperfusion. Consequently, an episode of acute myocardial infarction comprises two primary phases: the ischemic phase, stemming from coronary artery occlusion and the formation of an infarct zone in the myocardium, and the reperfusion phase, wherein blood flow is reinstated.[29] Both ischemia and reperfusion events inflict detrimental effects on cardiac tissue.[29] (Figure 3). Given the substantial impact of ventricular remodeling on the prognosis of MI, it becomes imperative to discern pathways that either facilitate or impede this process to formulate safer therapeutic interventions. Molecules such as phosphoinositide-kinase 3 and Akt exhibit cardioprotective effects through the mTOR pathway, which assumes a pivotal role as the primary regulator of cellular functions and the central coordinator of diverse signaling pathways.[30]

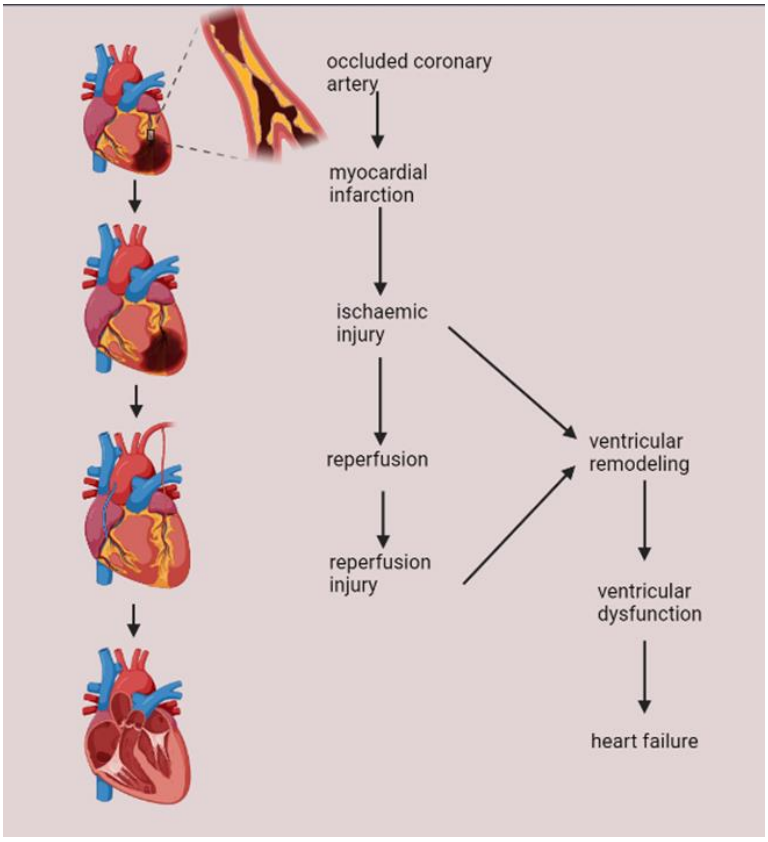

Created using biorender.com

Figure 3. Pathophysiology of Ischaemic Heart Disease (IHD)

Fig. 3 depicts representation of coronary artery occlusion due to long term predisposing factors lead to sudden cardiac events like myocardial infarction. The episode of a MI has two phases, an ischaemic phase where there is reduced or no blood supply beyond the point of occlusion and a reperfusion phase in which blood supply is restored. Each of these phases cause cardiac injury and activates signalling pathways both detrimental and beneficial to cardiac recovery.

Role of mTOR in IHD

Investigations utilizing myocardial infarction (MI) models in mice have delineated the nuanced influence of the mTOR signalling pathway, specifically governed by mTOR phosphorylation and the dynamics of mTORC1 and mTORC2.[31] In the context of MI, both mTORC1 and mTORC2 undergo phosphorylation, and the induction of mTORC2 expression through autophagy manifests a protective effect during the ischemic phase of ischemia-reperfusion, whereas mTORC1 proves beneficial during the reperfusion phase.[32] (Figure 4). Notably, research underscores the cardioprotective role of mTORC2 activation in cardiomyocytes, with its genetic deletion or knockdown of Rictor, a downstream substrate of mTORC2, exacerbating cell survival.[33] The inhibition of Rictor leads to diminished phosphorylation of Akt at Serine 473, inadequate phosphorylation of downstream Akt targets like Forkhead box protein O (FoxO), and heightened cell death.[34] Previous investigations have proposed that mTORC2 governs substrate specificity for downstream Akt targets, including FoxO, glycogen synthase kinase-3 (GSK-3), and tuberous sclerosis 2 (TSC-2).[35]

During the reperfusion phase, the activation of p70S6 kinase, a downstream target of mTORC1, stimulates protein synthesis and eventual myocardial hypertrophy in response to MI. Conversely, phosphorylation of 4E-BP1, another downstream substrate of mTOR, inhibits protein synthesis, with mTOR inactivating 4E-BP1 during hypertrophy.[36] Downstream, inhibition of the ubiquitin-proteasome system attenuates the pro-inflammatory response mediated by NfkB.[37] PRAS40, a proline-rich Akt substrate, acts as both a substrate and a component of mTORC1, inhibiting mTORC1 activity post-infarction.[38] Phosphorylation of PRAS40 by either Akt or mTORC1 prompts its dissociation from mTORC1, relieving its inhibitory effect on mTORC1.[38] Elevated expression of PRAS40 confers protection post-myocardial infarction by mitigating against ischemic injury and steering myocytes towards mTORC2 signaling.[39]

Ras homolog enriched in brain (Rheb), functioning as an upstream regulator of mTOR and an energy sensor, undergoes regulation by various kinases, including Akt, AMPK, and glycogen synthase kinase-3β, through tuberous sclerosis complex proteins 1/2 (TSC).[40] In conditions of low cellular energy, such as ischemia, AMPK activates TSC1/2, culminating in the inhibition of Rheb and subsequent suppression of mTORC1. This suppression mitigates the phosphorylation of p70S6K and 4E-BP1, leading to diminished protein synthesis and energy conservation during the ischemic phase. Glucose deprivation during ischemia redirects cardiomyocytes towards the activation of the mTORC2 pathway and autophagy. Animal models with Rheb overexpression exhibited a reduction in autophagy genes under conditions of energy deprivation, emphasizing the pivotal role of Rheb in autophagy regulation as a protective mechanism for cardiomyocytes in the ischemic state.[41]

However, prolonged ischemia induces dephosphorylation and activation of GSK-3β, while reperfusion inhibits its activity. GSK-3β, expressed via the mTOR pathway, exhibits cardioprotective effects during both ischemia and reperfusion. The upstream regulation of GSK-3β by Akt,[42] which phosphorylates TSC2, resulting in mTORC1 inactivation,[43] plays a pivotal role. The suppression of GSK-3β during reperfusion facilitates cardioprotection by regulating the opening of the mitochondrial permeability transition pore (mPTP) through direct phosphorylation.[44]

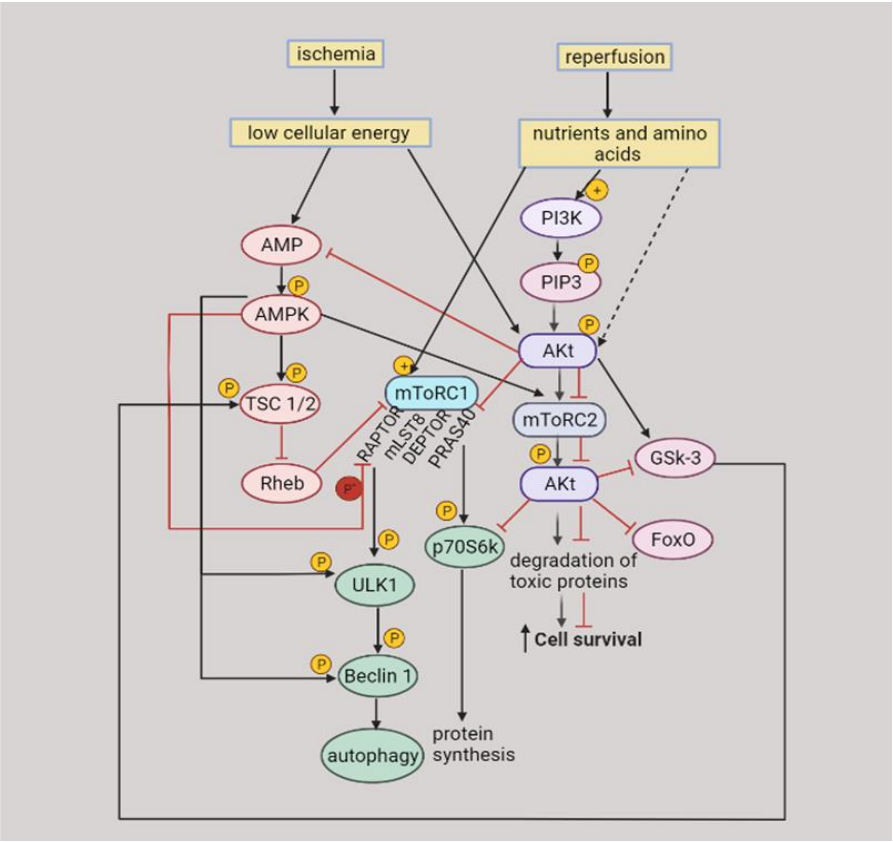

Created using biorender.com

Figure 4. Role of mTOR in pathogenesis of IHD

Fig.6 The two components of mTOR – mTORC1 and mTORC2 have a role to play during the reperfusion and ischemic phases respectively. mTORC1 is activated during the reperfusion phase when blood supply is restored and in the presence of nutrients and amino acids leading to protein synthesis and eventual myocardial hypertrophy, while mTORC2 is activated during the ischemic phase via the AMPK-Akt pathway which inhibits mTORC1 and activates autophagy genes like beclin, FOXO and Atg 7, ulk which bring about cell survival through degradation of toxic proteins which is a protective mechanism for cardiomyocytes in ischemic state

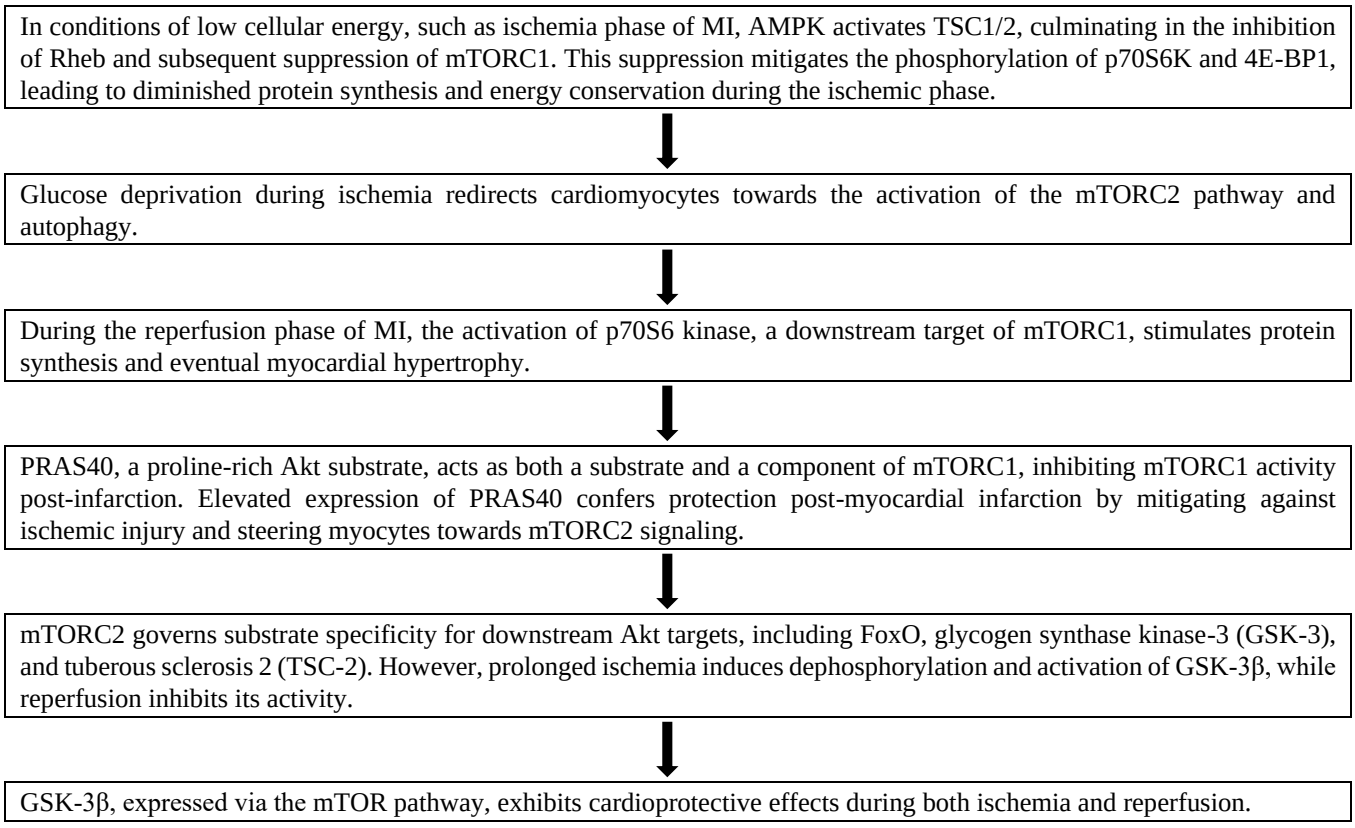

Flowchart representing mTOR involvement in development of ischemic heart disease

Inhibition/ knockout of mTOR in IHD

In vivo experiments utilizing Langendorff-perfused rat and rabbit hearts involved the administration of the mTOR inhibitor rapamycin, either preceding the onset of reperfusion subsequent to ischemia or before the commencement of ischemia itself. Notably, when rapamycin was given before the initiation of reperfusion, the absence of ischemic preconditioning, which typically imparts cardioprotection in ischemia-reperfusion injury, was observed. However, administration of rapamycin prior to the onset of ischemia proved effective in limiting the size of the ensuing infarction.[45] In GSK-3β knock-out C57BL/6J mice, the adverse effects associated with GSK-3β inhibition during prolonged ischemia were ameliorated upon treatment with rapamycin.[42]

Key findings

Understanding Ischemia/Reperfusion Injury: The description of MI's two primary phases, ischemia, and reperfusion, underscores the complex nature of the cardiac damage inflicted during these events. Ischemia/reperfusion injury, characterized by paradoxical damage upon restoration of blood flow, significantly contributes to the development of heart failure post-MI. This recognition emphasizes the importance of developing therapeutic strategies targeting both ischemic and reperfusion phases to mitigate cardiac damage and improve outcomes.

Role of mTOR Pathway in Cardio-protection: The identification of molecules such as phosphoinositide-kinase 3 and Akt, which exhibit cardioprotective effects through the mTOR pathway, offers promising therapeutic targets for MI treatment. The mTOR pathway's central role in regulating cellular functions and coordinating various signalling pathways suggests its potential as a key

mediator in modulating cardiac response to ischemic injury. Targeting this pathway could potentially mitigate ischemia/reperfusion injury and improve cardiac outcomes post-MI.

In essence, these findings enhance our understanding of the pathophysiology of MI, particularly the detrimental effects of ischemia/reperfusion injury, and provide insights into potential therapeutic interventions. Developing targeted therapies that modulate the mTOR pathway to protect against cardiac damage may represent a promising approach for improving outcomes in MI patients.

Current research and emerging perspectives

In cardiovascular biology, mTORC1 activation is pivotal for facilitating adaptive cardiac hypertrophy, while mTORC2 safeguards cardiomyocyte viability during pressure overload[46]. mTORC1 inhibition holds promise in ameliorating cardiac remodelling and failure, thereby extending longevity in murine models and potentially affording cardio-protection in humans. Despite limited clinical evidence, pharmacologically targeting mTOR, emerges as a prospective therapeutic avenue for cardiovascular diseases.

Rapamycin and rapalogs such as everolimus have emerged as effective agents in mitigating cardiac dysfunction and remodelling, in animal models of cardiac hypertrophy and heart failure, induced by transverse aortic constriction. These findings underscore the therapeutic promise of targeting mTOR via rapamycin and rapalogs like everolimus as nanoparticles [51] in addressing hypertrophic disease and its associated heart failure[48]. Compelling evidence also suggests that metformin indirectly modulates mTORC1 activity via both AMPK-dependent and -independent mechanisms, exhibiting efficacy in attenuating atherosclerosis in multiple animal models [49]. Although phytopharmaceuticals have demonstrated potential in laboratory studies, challenges remain in effectively translating their efficacy into clinical applications, especially regarding their delivery [50].

The specificity of mTOR inhibitors and the potential for off-target effects pose significant considerations. The complex involvement of mTOR in cardiovascular pathologies underscores the need for highly selective modulators capable of selectively targeting mTOR complexes. Novel compounds with drug-likeness properties should undergo rigorous evaluation in both preclinical models and clinical trials [52], specifically designed to assess their impact on cardiac development, physiology, and stress response following mTOR modulation. Rigorous preclinical and clinical studies are imperative to ascertain the long-term safety and efficacy of targeting mTOR across diverse scenarios of cardiac diseases. A profound understanding of the intricate crosstalk between mTOR and other signalling pathways will not only provide new insights into the complexity of cardiac disease pathophysiology but also offer a comprehensive perspective on the multifaceted role of mTOR in cardiovascular diseases.

Acknowledgements & Conflict of interest

The author is the sole contributor to this review article and declares that there is no financial, academic, or personal interests that have influenced the work reported in this paper.

REFERENCES

1. Hansson G.K. Inflammation, atherosclerosis, and coronary artery disease. *N. Engl. J. Med.* 2005; 352(16):1685-1695.
2. Pawitan J. Molecular pathogenesis of atherosclerosis and implication for therapy. *Int. Med. J. Malays.* 2010; 9(2):7-14.
3. Walpola P.L., Gotlieb A.I., Cybulsky M.I. and Langille B.L. Expression of ICAM-1 and VCAM-1 and monocyte adherence in arteries exposed to altered shear stress. *Arterioscler. Thromb. Vasc. Biol.* 1995; 15(1):2-10.
4. Samson S., Mundkur L. and Kakkar V.V. Immune response to lipoproteins in atherosclerosis. *Cholesterol* 2012; 2012:571846.
5. Düvel K., Yecies J.L., Menon S., Raman P., Lipovsky A.I., Souza A.L. et al. Activation of a metabolic gene regulatory network downstream of mTOR complex 1. *Mol. Cell* 2010; 39(2):171-183.
6. Peterson T.R., Sengupta S.S., Harris T.E., Carmack A.E., Kang S.A., Balderas E. et al. mTOR complex 1 regulates lipin 1 localization to control the SREBP pathway. *Cell* 2011; 146(3):408-420.
7. Brown M.S. and Goldstein J.L. The SREBP pathway: regulation of cholesterol metabolism by proteolysis of a membrane-bound transcription factor. *Cell* 1997; 89(3):331-340.
8. Pérez-Belmonte L.M., Moreno-Santos I., Cabrera-Bueno F., Sánchez-Espín G., Castellano D., Such M. et al. Expression of sterol regulatory element-binding proteins in epicardial adipose tissue in patients with coronary artery disease and diabetes mellitus: preliminary study. *Int. J. Med. Sci.* 2017; 14(3):268-274.
9. Robinet P., Védie B., Chironi G., Gariépy J., Simon A., Moatti N. et al. Characterization of polymorphic structure of SREBP-2 gene: role in atherosclerosis. *Atherosclerosis* 2003; 168(2):381-387.
10. Halcox J.P., Schenke W.H., Zalos G., Mincemoyer R., Prasad A., Waclawiw M.A. et al. Prognostic value of coronary vascular endothelial dysfunction. *Circulation* 2002; 106(6):653-658.
11. Förstermann U. and Sessa W.C. Nitric oxide synthases: regulation and function. *Eur. Heart J.* 2012; 33(7):829-837.
12. Davies M.G. and Hagen P.O. The vascular endothelium. A new horizon. *Ann. Surg.* 1993; 218(5):593-609.
13. Yang Z. and Ming X.F. mTOR signalling: the molecular interface connecting metabolic stress, aging and cardiovascular diseases. *Obes. Rev.* 2012; 13 Suppl 2:58-68.
14. Sessa W.C. eNOS at a glance. *J. Cell Sci.* 2004; 117(Pt 12):2427-2429.
15. Fulton D., Gratton J.P., McCabe T.J., Fontana J., Fujio Y., Walsh K. et al. Regulation of endothelium-derived nitric oxide production by the protein kinase Akt. *Nature* 1999; 399(6736):597-601.
16. Huang P.L. eNOS, metabolic syndrome and cardiovascular disease. *Trends Endocrinol. Metab.* 2009; 20(6):295-302.
17. Dimmeler S., Dernbach E., Zeiher A.M. Phosphorylation of the endothelial nitric oxide synthase at ser-1177 is required for VEGF-induced endothelial cell migration. *FEBS Lett.* 2000; 477(3):258-262.
18. Michell B.J., Chen Z.P., Tiganis T., Stapleton D., Katsis F., Power D.A. et al. Coordinated control of endothelial nitric-oxide synthase phosphorylation by protein kinase C and the cAMP-dependent protein kinase. *J. Biol. Chem.* 2001; 276(21):17625-17628.
19. Davignon J. and Ganz P. Role of endothelial dysfunction in atherosclerosis. *Circulation* 2004; 109(23 Suppl 1):III27-III32.
20. Tiefenbacher C.P., Bleeke T., Vahl C., Amann K., Vogt A., Kübler W. Endothelial dysfunction of coronary resistance arteries is improved by tetrahydrobiopterin in atherosclerosis. *Circulation* 2000; 102(18):2172-2179.
21. Alp N.J., McAteer M.A., Khoo J., Choudhury R.P.,

Channon K.M. Increased endothelial tetrahydrobiopterin synthesis by targeted transgenic GTP-cyclohydrolase I overexpression reduces endothelial dysfunction and atherosclerosis in ApoE-knockout mice. *Arterioscler. Thromb. Vasc. Biol.* 2004; 24(3):445-450.

22. Peng H., Zhuang Y., Harbeck M.C., He D., Xie L., Chen W. Serine 1179 Phosphorylation of Endothelial Nitric Oxide Synthase Increases Superoxide Generation and Alters Cofactor Regulation. *PLoS One* 2015; 10(11):e0142854.
23. Rajapakse A.G., Yepuri G., Carvas J.M., Stein S., Matter C.M., Scerri I. et al. Hyperactive S6K1 mediates oxidative stress and endothelial dysfunction in aging: inhibition by resveratrol. *PLoS One* 2011; 6(4):e19237.
24. Tarantino G., Capone D. Inhibition of the mTOR pathway: a possible protective role in coronary artery disease. *Ann. Med.* 2013; 45(4):348-356.
25. Marx S.O., Jayaraman T., Go L.O., Marks A.R. Rapamycin-FKBP inhibits cell cycle regulators of proliferation in vascular smooth muscle cells. *Circ. Res.* 1995; 76(3):412-417.
26. Jung C.H., Ro S.H., Cao J., Otto N.M., Kim D.H. mTOR regulation of autophagy. *FEBS Lett.* 2010; 584(7):1287-1295.
27. Naoum J.J., Woodside K.J., Zhang S., Rychahou P.G., Hunter G.C. Effects of rapamycin on the arterial inflammatory response in atherosclerotic plaques in Apo-E knockout mice. *Transplant. Proc.* 2005; 37(4):1880-1884.
28. Mueller M.A., Beutner F., Teupser D., Ceglarek U., Thiery J. Prevention of atherosclerosis by the mTOR inhibitor everolimus in LDLR-/- mice despite severe hypercholesterolemia. *Atherosclerosis* 2008; 198(1):39-48.
29. Nallamothu B.K., Bradley E.H., Krumholz H.M. Time to treatment in primary percutaneous coronary intervention. *N. Engl. J. Med.* 2007; 357(16):1631-1638.
30. Dazert E., Hall M.N. mTOR signaling in disease. *Curr. Opin. Cell Biol.* 2011; 23(6):744-755.
31. Zoncu R., Efeyan A., Sabatini D.M. mTOR: from growth signal integration to cancer, diabetes and ageing. *Nat. Rev. Mol. Cell Biol.* 2011; 12(1):21-35..
32. Aoyagi T., Kusakari Y., Xiao C.Y., Inouye B.T., Takahashi M., Scherrer-Crosbie M. Cardiac mTOR protects the heart against ischemia-reperfusion injury. *Am. J. Physiol. Heart Circ. Physiol.* 2012; 303(1):H75-H85.
33. Hung C.M., Garcia-Haro L., Sparks C.A., Guertin D.A. mTOR-dependent cell survival mechanisms. *Cold Spring Harb. Perspect. Biol.* 2012; 4(12):a008771.
34. Ronnebaum S.M., Patterson C. The FoxO family in cardiac function and dysfunction. *Annu. Rev. Physiol.* 2010; 72:81-94.
35. Guertin D.A., Stevens D.M., Thoreen C.C., Burds A.A., Kalaany N.Y., Moffat J. Ablation in mice of the mTORC components raptor, rictor, or mLST8 reveals that mTORC2 is required for signaling to Akt-FOXO and PKCalpha, but not S6K1. *Dev. Cell* 2006; 11(6):859-871.
36. Pham F.H., Sugden P.H., Clerk A. Regulation of protein kinase B and 4E-BP1 by oxidative stress in cardiac myocytes. *Circ. Res.* 2000; 86(12):1252-1258.
37. Pye J., Ardeshirpour F., McCain A., Bellinger D.A., Merricks E., Adams J. Proteasome inhibition ablates activation of NF-kappa B in myocardial reperfusion and reduces reperfusion injury. *Am. J. Physiol. Heart Circ. Physiol.* 2003; 284(3):H919-H926.
38. Wiza C., Nascimento E.B., Ouwens D.M. Role of PRAS40 in Akt and mTOR signaling in health and disease. *Am. J. Physiol. Endocrinol. Metab.* 2012; 302(12):E1453-E1460. PMID: 22354785.
39. Völkers M., Toko H., Doroudgar S., Din S., Quijada P., Joyo A.Y. Pathological hypertrophy amelioration by PRAS40-mediated inhibition of mTORC1. *Proc. Natl. Acad. Sci. U. S. A.* 2013; 110(31):12661-12666.
40. Inoki K., Li Y., Xu T., Guan K.L. Rheb GTPase is a direct target of TSC2 GAP activity and regulates mTOR signaling. *Genes Dev.* 2003; 17(15):1829-1834.
41. Sciarretta S., Zhai P., Volpe M., Sadoshima J.

Pharmacological modulation of autophagy during cardiac stress. *J. Cardiovasc. Pharmacol.* 2012; 60(3):235-241.

42. Zhai P., Sciarretta S., Galeotti J., Volpe M., Sadoshima J. Differential roles of GSK-3β during myocardial ischemia and ischemia/reperfusion. *Circ. Res.* 2011; 109(5):502-511.
43. Matsui Y., Takagi H., Qu X., Abdellatif M., Sakoda H., Asano T. Distinct roles of autophagy in the heart during ischemia and reperfusion: roles of AMP-activated protein kinase and Beclin 1 in mediating autophagy. *Circ. Res.* 2007; 100(6):914-922.
44. Juhaszova M., Zorov D.B., Kim S.H., Pepe S., Fu Q., Fishbein K.W. Glycogen synthase kinase-3beta mediates convergence of protection signaling to inhibit the mitochondrial permeability transition pore. *J. Clin. Invest.* 2004; 113(11):1535-1549.
45. Fuglesteg B.N., Tiron C., Jonassen A.K., Mjøs O.D., Ytrehus K. Pretreatment with insulin before ischaemia reduces infarct size in Langendorff-perfused rat hearts. *Acta Physiol. (Oxf.)* 2009; 195(2):273-282.
46. Sciarretta S., Forte M., Frati G., Sadoshima J. New insights into the role of mTOR signaling in the cardiovascular system. *Circ. Res.* 2018; 122(3):489-505.
47. Sanches-Silva A., Testai L., Nabavi S.F., Battino M., Pandima Devi K., Tejada S., et al. Therapeutic potential of polyphenols in cardiovascular diseases: Regulation of mTOR signaling pathway. *Pharmacol. Res.* 2020; 152:104626. https://doi.org/10.1016/j.phrs.2019.104626
48. Bishu K., Ogut O., Kushwaha S., Mohammed S.F., Ohtani T., Xu X., et al. Anti-remodeling effects of rapamycin in experimental heart failure: dose response and interaction with angiotensin receptor blockade. *PLoS One.* 2013; 8:e81325.
49. Griffin S.J., Leaver J.K., Irving G.J. Impact of metformin on cardiovascular disease: a meta-analysis of randomised trials among people with type 2 diabetes. *Diabetologia.* 2017; 60:1620-1629.
50. K P., V M. A review of safety, quality, regulation, and delivery approaches for phytopharmaceuticals. *Jordan J. Pharm. Sci.* 2024 Jun. Available from: https://jjournals.ju.edu.jo/index.php/jjps/article/view/1768
51. Kzar H.H., Al-Gazally M.E., Wtwt M.A. Everolimus loaded NPs with FOL targeting: preparation, characterization and study of its cytotoxicity action on MCF-7 breast cancer cell lines. *Jordan J. Pharm. Sci.* 2022 Mar 1. Available from: https://jjournals.ju.edu.jo/index.php/jjps/article/view/286
52. Widyananda M.H., Kurniasari C.A., Alam F.M., Rizky W.C., Dings T.G.A., Ansori A.N.M., Antonius Y. Exploration of potentially bioactive compounds from fingerroot (Boesenbergia rotunda L.) as inhibitor of atherosclerosis-related proteins (CETP, ACAT1, OSC, sPLA2): An in silico study. *Jordan J. Pharm. Sci.* 2023 Sep 23. Available from: https://jjournals.ju.edu.jo/index.php/jjps/article/view/1609

التحقيق في الهدف الميكانيكي للرابامايسين والمسارات المماثلة في أمراض القلب والأوعية الدموية لزيادة وظائف القلب

شيريل ريا لويس[1]*

[1] قسم علم الأدوية، كلية كاستوربا الطبية، أكاديمية مانيبال للتعليم العالي، مانيبال، كارناتاكا، الهند.

ملخص

تعد أمراض القلب والأوعية الدموية السبب الرئيسي للوفيات العالمية، خاصة في البلدان المنخفضة الدخل إلى المتوسطة الدخل، حيث يمثل قصور القلب 34٪ من الوفيات، حيث بلغ مجموعها 62.5 مليون حالة وفاة مبكرة في العقد الماضي. على الرغم من التحسينات الأولية في معدلات البقاء على قيد الحياة، لا تزال الوفاة بسبب قصور القلب مثيرة للقلق، مما يشير إلى انخفاض في القدرة التعويضية للقلب مع تقدم العمر. من أجل فهم التعقيدات الجزيئية للأمراض القلبية الوعائية، استكشفت هذه المراجعة السردية على نطاق واسع قواعد البيانات مثل Scopus وWeb of Science وPubMed مع معايير إدراج محددة لاختيار مقالات من الدراسات التجريبية والتجارب السريرية والدراسات على والدراسات القائمة على الملاحظة المنشورة بعد عام 2000. وعلى العكس من ذلك، استخدمت معايير الاستبعاد لاستبعاد المقالات التي لا صلة لها بالعنوان أو التي نشرت قبل عام 2000. كشف البحث المكثف في الأدبيات، بشكل مدهش، عن الإمكانات غير المستكشفة لاستهداف مسار mTOR لعلاج الأمراض القلبية الوعائية. تشير الدراسات السابقة إلى أن تعديل mTOR يمكن أن يعيد تشكيل مسارات أمراض القلب، على الرغم من أن الأدلة السريرية محدودة. تؤكد الأدلة الحديثة على عدم تنظيم mTOR في أمراض القلب، مما يبشر بالخير في التخفيف من الخلل الوظيفي من خلال تثبيط mTOR، على الرغم من التحديات في الترجمة السريرية. إن فهم الحديث المتبادل ل mTOR مع المسارات الأخرى يسلط الضوء على تعقيد أمراض القلب. تؤكد المراجعة على أهمية mTOR في مرض الشريان التاجي CAD وأمراض القلب الإقفارية IHD، مما يقترح طرقا لمزيد من البحث والتطبيقات السريرية لتحسين إدارة أمراض القلب والأوعية الدموية وتقليل الوفيات المرتبطة بقصور القلب.

الكلمات الدالة: مرض الشريان التاجي. مرض القلب الإقفاري. مسار mTOR.

* ***المؤلف المراسل: شيريل ريا لويس***

rheadsouza30@rediffmail.com

تاريخ استلام البحث 2024/01/31 وتاريخ قبوله للنشر 2024/08/22.

Role of Clinical Pharmacy Services in Vitamin Supplementation in Critically Ill Cancer Patients: A 3-Year Retrospective Study at a Comprehensive Cancer Centre

Nadine N. Abdelhadi[1]*, Alaa Dabbous[2], Saad M Jaddoua[2]

[1] Faculty of Pharmacy, Aqaba University of Technology, Aqaba, Jordan
[2] Department of Pharmacy, King Hussein Cancer Center, Amman, Jordan

ABSTRACT

Background: Clinical pharmacists provide nutrition support pharmacy services, including evaluating micronutrient status and managing vitamin use. However, only a limited number of studies have explored the role of clinical pharmacists in managing vitamin supplementation.

Objective: To explore clinical pharmacists' interventions in managing vitamin supplementation in critically ill cancer patients admitted to intensive care units.

Methods: This retrospective analysis reviewed 9,949 electronically reported clinical pharmacist interventions for patients admitted to the ICU from January 2020 to December 2022. All patient records with clinical pharmacists' interventions related to vitamin supplementation in ICU cancer patients were extracted and analyzed.

Results: The total number of interventions related to vitamin management was 129 (1.30%). Vitamin D was the most commonly used vitamin supplement (n = 39, 30.2%). Initiation of vitamin supplementation (n = 55, 42.6%) was the most frequent intervention by clinical pharmacists. The acceptance rate by physicians was 100%.

Conclusion: Clinical pharmacists play a key role in managing nutrition support therapy and vitamin supplementation in critically ill cancer patients. This study represents the first experience in Jordan and serves as a role model. Further research is needed to investigate barriers to implementing nutrition support pharmacy services and vitamin supplementation in Jordan, as well as to explore the impact of these services on patient outcomes.

Keywords: Clinical pharmacy services, nutrition support pharmacy, vitamins, critical care.

1. INTRODUCTION

Clinical pharmacy aims to optimize the use of medicines [1]. It represents a field of professional practice and research that encompasses pharmaceutical care but is not limited to it [1]. The clinical pharmacy discipline has evolved into many specialties, including nutrition support pharmacy [2]. Clinical pharmacists are essential members of critical care health teams, contributing to the safety and management of medications for this vulnerable population [3–11]. Vitamins are nutrients that the body needs in small amounts to function properly and maintain health. They are classified as either fat-soluble or water-soluble [13]. Clinical pharmacists provide nutrition support pharmacy services, including evaluating micronutrient status and managing vitamin supplementation [11,12]. These activities have been shown to improve patient outcomes and reduce healthcare-related costs [12,17–19]. Timely nutritional therapy should be considered for patients undergoing anticancer treatment who are at risk of malnutrition [14–16].

Oxidative stress and inflammation are physiological responses to injury during critical illness. Under normal conditions, the human antioxidant defense system counteracts inflammation and oxidative stress. However,

***Corresponding author: Nadine N. Abdelhadi**
nadine_abdelhadi@yahoo.com
Received: 16/4/2024 Accepted: 22/8/2024.
DOI: https://doi.org/10.35516/jjps.v18i2.2557

this antioxidant capacity is often significantly compromised, and serum levels of micronutrients, including vitamins, are markedly depleted in critically ill patients [21]. Although the evidence remains inconclusive, treating micronutrient deficiencies is expected to enhance clinical outcomes in critically ill patients [20].

Vitamins and minerals are among the most commonly recommended and dispensed classes of complementary medicines by pharmacists [22]. A lack of scientific evidence and reliable information sources are common barriers to the practice of complementary medicine [22,23].

A limited number of studies have explored the role of clinical pharmacists in managing vitamin use, particularly in critical care settings [26–32].

Based on the above and due to the lack of information about the role of clinical pharmacists in vitamin supplementation in critically ill cancer patients in Jordan, this study aimed to analyze clinical pharmacists' interventions in managing vitamin use in ICU cancer patients at King Hussein Cancer Center (KHCC).

2. METHODS

Ethical approval was granted by the Institutional Review Board (IRB) at King Hussein Cancer Centre (KHCC) on 25 October 2021 (approval number RC/2021/153).

This retrospective analysis included electronically reported clinical pharmacist interventions for 9,949 patients admitted to intensive care units at KHCC in Amman, Jordan, from January 2020 to December 2022. All patient records with clinical pharmacist interventions related to managing vitamin supplementation in ICU cancer patients were extracted and analyzed. The time taken by clinical pharmacists to intervene was routinely recorded in the pharmacy database. Intervention times were collected and analyzed for all cases.

Patients were categorized into two age groups: adults (older than 18 years) and pediatrics (18 years or younger). Descriptive statistics were used to present the results as frequencies and percentages.

The Mann–Whitney U test was applied to compare the time taken by clinical pharmacists to intervene between the pediatric and adult ICU patient groups.

All analyses were performed using the Jamovi statistical package (2022) [24,25]. A p-value of less than 0.05 was considered statistically significant.

3. RESULTS

3.1. Participants characteristics

The study population comprised pediatric patients (n = 29, 22.5%) and adult patients (n = 100, 77.5%). Most participants were male (n = 78, 60.5%). The majority of patients were admitted to the ICU in 2020 (44.2%), followed by 2021 (35.7%). Table 1 summarizes the participants' characteristics.

Table 1: Characteristics of participants

										Percentiles		
Age group			Gender	N	Median	IQR	25th	50th	75th			
Age (years)	Adult	F	40	59.50	15.25	47.75	59.50	63.0				
		M	60	57.00	18.00	50.25	57.00	68.3				
	Pediatric	F	11	11	10.00	6.00	11.00	16.0				
		M	18	9.50	12.25	4.75	9.50	17.0				
Date	Adult	F	40	2021.00	1.00	2020.00	2021.00	2021.0				
		M	60	2020.00	1.00	2020.00	2020.00	2021.0				
	Pediatric	F	11	2021	1.00	2021.00	2021.00	2022.0				
		M	18	2021.00	1.00	2021.00	2021.00	2022.0				

3.2. Vitamin supplement use in critically ill cancer patients admitted to ICU.

Fat-soluble vitamins (n = 68, 52.7%) were the most commonly used vitamin supplements (Figure 1). Vitamin D was the most frequently used individual supplement (n = 39, 30.2%), followed by vitamin C (n = 29, 22.5%), vitamin K (n = 28, 21.7%), and folic acid (n = 14, 10.9%). The forms of vitamin D supplementation included cholecalciferol (n = 29, 74.4%) and alfacalcidiol (n = 10, 25.6%). Table 2 shows the frequencies of these supplements.

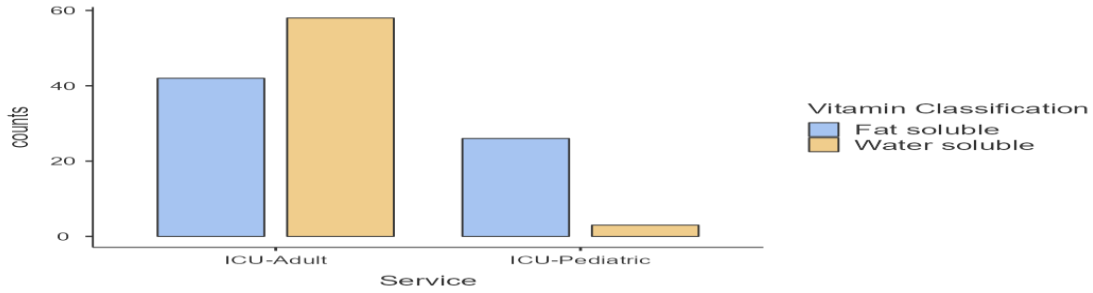

Figure 1: Frequency of use of fat-soluble and water-soluble vitamins in critically ill cancer patients admitted to ICU at KHCC

Table 2: Frequencies of supplements

Supplement	Gender	Age group	Counts	% of Total	Cumulative %
Folic acid	F	Adult	3	2.3 %	2.3 %
		Pediatric	0	0.0 %	2.3 %
	M	Adult	11	8.5 %	10.9 %
		Pediatric	0	0.0 %	10.9 %
Thiamine	F	Adult	3	2.3 %	13.2 %
		Pediatric	1	0.8 %	14.0 %
	M	Adult	7	5.4 %	19.4 %
		Pediatric	1	0.8 %	20.2 %
Vitamin B12	F	Adult	1	0.8 %	20.9 %
		Pediatric	0	0.0 %	20.9 %
	M	Adult	4	3.1 %	24.0 %
		Pediatric	1	0.8 %	24.8 %
Vitamin C	F	Adult	13	10.1 %	34.9 %
		Pediatric	0	0.0 %	34.9 %
	M	Adult	16	12.4 %	47.3 %
		Pediatric	0	0.0 %	47.3 %
Vitamin D	F	Adult	15	11.6 %	58.9 %
		Pediatric	3	2.3 %	61.2 %
	M	Adult	17	13.2 %	74.4 %
		Pediatric	4	3.1 %	77.5 %
Vitamin E	F	Adult	0	0.0 %	77.5 %
		Pediatric	0	0.0 %	77.5 %
	M	Adult	0	0.0 %	77.5 %

Supplement	Gender	Age group	Counts	% of Total	Cumulative %
		Pediatric	1	0.8 %	78.3 %
Vitamin K	F	Adult	5	3.9 %	82.2 %
		Pediatric	7	5.4 %	87.6 %
	M	Adult	5	3.9 %	91.5 %
		Pediatric	11	8.5 %	100.0 %

3.3. Role of clinical pharmacists in the management of vitamin supplementation

The initiation of vitamin supplementation (n = 55, 42.6%) was the most frequent clinical pharmacist intervention in managing vitamins for ICU cancer patients, followed by discontinuation of vitamin supplementation (n = 32, 24.8%). Table 3 provides details on the frequency of interventions. The total number of interventions related to vitamin management was 129 (1.30%). The total time spent on these interventions was 1,845 minutes, with a minimum of 1 minute and a maximum of 40 minutes per intervention (Table 4).

Table 3: Frequencies of interventions for the management of vitamin supplementation.

Intervention	Counts	% of Total	Cumulative %
Clarification of orders	2	1.6 %	1.6 %
Dose clarified/evaluated	17	13.2 %	14.7 %
Drug Information provided	2	1.6 %	16.3 %
Duration of RX Order Clarified	5	3.9 %	20.2 %
Lab Evaluation	1	0.8 %	20.9 %
Medication reconciliation/admission	14	10.9 %	31.8 %
Route of administration clarified.	1	0.8 %	32.6 %
Initiation of vitamin supplementation	55	42.6 %	75.2 %
Discontinuation of the vitamin supplementation	32	24.8 %	100.0 %

Table 4: Times taken by clinical pharmacists to intervene in vitamin supplementation in ICU cancer patients at KHCC

					Percentiles		
	Intervention	N	Median	IQR	25th	50th	75th
Time Taken	Clarification of orders	2	11.50	8.50	7.25	11.50	15.75
	Dose clarified/evaluated.	17	15	5.00	10.00	15.00	15.00
	Drug Information provided	2	3.00	0.00	3.00	3.00	3.00
	Duration of RX Order Clarified	5	10	0.00	10.00	10.00	10.00
	Lab Evaluation	1	25	0.00	25.00	25.00	25.00
	Medication reconciliation/admission	14	15.00	0.00	15.00	15.00	15.00
	Route of administration clarified.	1	40	0.00	40.00	40.00	40.00
	Therapy recommendation / Initiation	55	15	0.00	15.00	15.00	15.00
	Therapy recommendation/Discontinue	32	15.00	0.00	15.00	15.00	15.00

The Mann-Whitney U test was used to compare the time clinical pharmacists took to intervene between the pediatric and adult ICU groups. The test showed no significant difference between the two groups' intervention times (Table 5).

Table 5: Mann-Whitney U test

		Statistic	p
Time Taken	**Mann-Whitney U**	**1393**	**0.630**
Note. H_a $\mu_{\text{ICU-Adult}} \neq \mu_{\text{ICU-Pediatric}}$			

4. Discussion

Clinical pharmacists play a role in managing vitamin supplementation in critically ill cancer patients in Jordan. Vitamin D was the most commonly used vitamin. The most frequent intervention by clinical pharmacists was initiating vitamin supplementation. The number of clinical pharmacists' interventions related to vitamin supplementation was relatively low compared to the total number of clinical pharmacist interventions in the ICU, which is consistent with a prospective study conducted at an academic hospital in China [26].

Although the number of interventions in vitamin supplementation was relatively low compared to overall clinical pharmacist interventions in the ICU, it is considered significant as this represents the first experience of its kind in Jordan. The nutrition support pharmacy services at KHCC are regarded as a role model. Further research is needed to explore barriers to implementing nutrition support pharmacy services, including the assessment of vitamin deficiencies and provision of vitamin supplements. Additional studies are also required to investigate the impact of vitamin supplementation and nutrition support pharmacy services on patient outcomes, healthcare expenditures, and length of hospital stay.

Most available evidence has focused on the role of community pharmacists in recommending complementary and alternative medicines, including vitamins and minerals [22,23]. This is the first study to provide insights into clinical pharmacists' interventions in managing vitamin supplementation in critically ill cancer patients admitted to intensive care units in the Middle East. Only a few studies have investigated the role of clinical pharmacists in intensive care units generally [26-29]. None of the previous studies in the literature have explored the role of clinical pharmacists in vitamin supplementation specifically in critically ill cancer patients, which is one of the strengths of the current study.

This study explored the use of vitamin supplements in critically ill cancer patients, including different supplement forms. To our knowledge, it is the first study to examine the mean time clinical pharmacists took to intervene in vitamin supplementation in intensive care units at a comprehensive cancer center, which represents another strength of the study.

Clinical pharmacists' interventions ranged from 1 to 40 minutes, contrasting with a related study where most pharmacist interventions in a university hospital setting took 15 to 30 minutes to complete [29]. The current study focused exclusively on the role of clinical pharmacists in vitamin supplementation for cancer patients admitted to intensive care units. In contrast, the other study was conducted across various university hospital departments, which may explain the differences in findings between the two studies.

Further research is needed across different hospital departments and patient populations to identify factors affecting micronutrient supplementation and nutrition support pharmacy services. This is critical to improving the efficiency of these services.

A limitation of the current study, which should be acknowledged, is the likely incomplete documentation of interventions due to its retrospective design.

5. Conclusion

Clinical pharmacists play an important role in managing vitamin supplementation in Jordan. The initiation of vitamin supplementation is the most common clinical pharmacist intervention among critically ill cancer patients admitted to intensive care units. Nutrition support pharmacy services for these patients, including vitamin supplementation, remain uncommon in Jordan and have thus far only been reported at King Hussein Cancer Center. Although the number of clinical pharmacist interventions related to vitamin supplementation was relatively low compared to the total number of interventions in the ICU, this finding is significant as it represents the first documented experience of its kind in Jordan. Further studies are needed to identify the barriers hindering the implementation of nutrition support pharmacy services, including vitamin supplementation, for critically ill cancer patients. Additional research is also required to assess the impact of these services on patient outcomes.

Funding

No specific funding was obtained for this work.

Conflict of interest

No potential conflict of interest relevant to this study was reported.

REFERENCES

1. ACCP. Definition of Clinical Pharmacy. *ACCP Compass* [Internet]. 2024 [cited 2024 Mar 1]. Available from: https://www.accp.com/stunet/compass/definition.aspx
2. Dreischulte T., van den Bemt B., Steurbaut S.; European Society of Clinical Pharmacy. European Society of Clinical Pharmacy definition of the term clinical pharmacy and its relationship to pharmaceutical care: a position paper. *Int. J. Clin. Pharm.* 2022; 44(4):837–842.
3. Board of Pharmacy Specialties. BPS specialties. *Board of Pharmacy Specialties* [Internet]. 2024 [cited 2024 Mar 1]. Available from: https://bpsweb.org/bps-specialties/
4. Hilgarth H., Wichmann D., Baehr M., Kluge S., Langebrake C. Clinical pharmacy services in critical care: results of an observational study comparing ward-based with remote pharmacy services. *Int. J. Clin. Pharm.* 2023; 45(4):847–856.
5. Borthwick M. The role of the pharmacist in the intensive care unit. *J. Intensive Care Soc.* 2019; 20(2):161–164.
6. Arredondo E., Udeani G., Horseman M., Hintze T.D., Surani S. Role of Clinical Pharmacists in Intensive Care Units. *Cureus* 2021; 13(9):e17929.
7. Jurado L.V., Steelman J.D. The role of the pharmacist in the intensive care unit. *Crit. Care Nurs. Q.* 2013; 36(4):407–414.
8. Althomali A., Altowairqi A., Alghamdi A., et al. Impact of Clinical Pharmacist Intervention on Clinical Outcomes in the Critical Care Unit, Taif City, Saudi Arabia: A Retrospective Study. *Pharmacy (Basel)* 2022; 10(5):108.
9. Bosma B.E., van den Bemt P.M.L.A., Melief P.H.G.J., van Bommel J., Tan S.S., Hunfeld N.G.M. Pharmacist interventions during patient rounds in two intensive care units: Clinical and financial impact. *Neth. J. Med.* 2018; 76(3):115–124.
10. Fideles G.M., de Alcântara-Neto J.M., Peixoto Júnior A.A., et al. Pharmacist recommendations in an intensive care unit: three-year clinical activities. *Rev. Bras. Ter. Intensiva* 2015; 27(2):149–154. doi:10.5935/0103-507X.20150026
11. Muñoz-Pichuante D., Villa-Zapata L. Benefit of incorporating clinical pharmacists in an adult intensive care unit: A cost-saving study. *J. Clin. Pharm. Ther.* 2020; 45(5):1127–1133. doi:10.1111/jcpt.13195

12. Al Dali S., Al-Badriyeh D., Gulied A., et al. Characteristics of the clinical pharmacist interventions at the National Center for Cancer Care and Research Hospital in Qatar. *J. Oncol. Pharm. Pract.* 2023; 0(0). doi:10.1177/10781552231187305
13. McClave S., DiBaise J., Mullin G., Martindale R. ACG clinical guideline: Nutrition therapy in the adult hospitalized patient. *Am. J. Gastroenterol.* 2016; 111(3):315–334.
14. National Cancer Institute. Definition of vitamins. *NCI Dictionary of Cancer Terms* [Internet]. 2024 [cited 2024 Apr 8]. Available from: https://www.cancer.gov/publications/dictionaries/cancer-terms/def/vitamin
15. Society of Critical Care Medicine and American Society for Parenteral and Enteral Nutrition. Guidelines for the provision and assessment of nutrition support therapy in the adult critically ill patient. *JPEN* 2016; 40(2):159–211.
16. Yalcin S., Gumus M., Oksuzoglu B., Ozdemir F., Evrensel T., Sarioglu A., et al. Nutritional aspect of cancer care in medical oncology patients. *Clin. Ther.* 2019; 41(11):2382–2396.
17. Sioson M., Martindale R., Abayadeera A., Abouchaleh N., Aditianingsih D., Bhurayanontachai R., et al. Nutrition therapy for critically ill patients across the Asia–Pacific and Middle East regions: A consensus statement. *Clin. Nutr. ESPEN* 2018; 24:156–164.
18. American Society for Parenteral and Enteral Nutrition (ASPEN). What is nutrition support therapy? *Nutritioncare.org* [Internet]. 2024 [Accessed: Mar 01, 2024]. Available from: https://www.nutritioncare.org/About_Clinical_Nutrition/What_is_Nutrition_Support_
19. ASPEN. What is a nutrition support professional? *Nutritioncare.org* [Internet]. 2024 [Accessed: Mar 01, 2024]. Available from: https://www.nutritioncare.org/what-is-a-NSP/
20. Value of nutrition support therapy: Impact on clinical and economic outcomes in the United States. *J. Parenter. Enteral Nutr.* 2020; 44(3):395–406.
21. Berger M.M., Shenkin A., Schweinlin A., et al. ESPEN micronutrient guideline. *Clin. Nutr.* 2022; 41(6):1357–1424. doi:10.1016/j.clnu.2022.02.015 [published correction appears in *Clin. Nutr.* 2024; 43(4):1024].
22. Dresen E., Pimiento J.M., Patel J.J., Heyland D.K., Rice T.W., Stoppe C. Overview of oxidative stress and the role of micronutrients in critical illness. *JPEN J. Parenter. Enteral Nutr.* 2023; 47(Suppl 1):S38–S49.
23. Harnett J.E., Ung C.O.L., Hu H., Sultani M., Desselle S.P. Advancing the pharmacist's role in promoting the appropriate and safe use of dietary supplements. *Complement. Ther. Med.* 2019; 44:174–181. doi:10.1016/j.ctim.2019.04.018
24. Harnett J.E., Ung C.O.L. Towards defining and supporting pharmacists' professional role associated with traditional and complementary medicines – A systematic literature review. *Res. Soc. Adm. Pharm.* 2023; 19(3):356–413. doi:10.1016/j.sapharm.2022.11.001
25. The jamovi project. jamovi (Version 2.3) [Computer software]. 2022. Available at: https://www.jamovi.org
26. R Core Team. R: A language and environment for statistical computing (Version 4.1) [Computer software]. 2021. Available at: https://cran.r-project.org (R packages retrieved from MRAN snapshot 2022-01-01).
27. Zhou X., Qiu F., Wan D., et al. Nutrition support for critically ill patients in China: role of the pharmacist. *Asia Pac J Clin Nutr*. 2019; 28(2):246–251. doi:10.6133/apjcn.201906_28(2).0006
28. Giancarelli A., Davanos E. Evaluation of nutrition support pharmacist interventions. *J. Parenter. Enteral Nutr*. 2014; 39(4):476–481.
29. Salman G., Boullata J.I. The value of nutrition support pharmacist interventions. *Crit. Care Explor*. 2022; 10(2):e0650. doi:10.1097/CCE.0000000000000650

30. Gallagher J., Byrne S., Woods N., Lynch D., McCarthy S. Cost-outcome description of clinical pharmacist interventions in a university teaching hospital. *BMC Health Serv. Res*. 2014; 14:177. doi:10.1186/1472-6963-14-177
31. Alqassieh R., Odeh M., Jirjees F. Intraoperative insulin infusion regimen versus insulin bolus regimen for glucose management during CABG surgery: A randomized clinical trial. *Jordan J. Pharm. Sci*. 2023; 16(3):487–498. doi:10.35516/jjps.v16i3.708
32. Daghash R., Al-Saaideh M.A., Itani R. Evaluation of pharmacotherapy standards during pregnancy among Jordanian pharmacy colleges graduates. *Jordan J. Pharm. Sci*. 2023; 16(3):607–620. doi:10.35516/jjps.v16i3.972
33. Jarab A.S., Al-Qerem W., Mukattash T.L., Alqudah S.G., Abu-Zaytoun L., Al-Azayzih A., Khdour M. Public perception of pharmacist's role during COVID-19 outbreak in Jordan. *Jordan J. Pharm. Sci*. 2022; 15(3):365–377.

دور خدمات الصيدلة السريرية في صرف مكملات الفيتامينات لمرضى السرطان المصابين بأمراض خطيرة: دراسة استرجاعية لمدة ثلاث سنوات في مركز شامل للسرطان

نادين عبد الهادي[1*]، الاء دبوس[2]، سعد محمد جدوعه[2]

[1] كلية الصيدلة، جامعة العقبة للتكنولوجيا، العقبة، الأردن

[2] دائرة الصيدلة، مركز الحسين للسرطان، عمان، الأردن

ملخص

الخلفية: يقدم الصيادلة الإكلينيكيون خدمات صيدلانية داعمة للتغذية، تشمل تقييم حالة المغذيات الدقيقة وإدارة استخدام الفيتامينات. من الجدير بالذكر أن عدد الدراسات حول دور الصيادلة الإكلينيكيين في إدارة مكملات الفيتامينات محدود.

الهدف: دراسة تدخلات الصيادلة الإكلينيكيين في إدارة مكملات الفيتامينات لدى مرضى السرطان ذوي الحالات الحرجة الذين دخلوا وحدات العناية المركزة.

المنهجية: هذا تحليل بأثر رجعي لـ 9949 تدخلًا صيدلانيًا سريريًا مُبلّغًا عنها إلكترونيًا لدى مرضى دخلوا وحدة العناية المركزة من يناير 2020 إلى ديسمبر 2022. تم استخراج جميع سجلات المرضى التي تتضمن تدخلات الصيادلة الإكلينيكيين المتعلقة بمكملات الفيتامينات لدى مرضى السرطان في وحدة العناية المركزة، وتم تحليلها.

النتائج: بلغ إجمالي عدد التدخلات المتعلقة بإدارة الفيتامينات 129 تدخلًا (1.30%). وكان فيتامين د أكثر مكملات الفيتامينات استخدامًا (n = 39، 30.2%). كان البدء بتقديم مكملات الفيتامينات (n = 55، 42.6%) التدخل الأكثر شيوعًا للصيادلة السريريين. وبلغ معدل قبول الأطباء 100%.

الخلاصة: للصيادلة السريريين دور في إدارة العلاج الداعم للتغذية ومكملات الفيتامينات لمرضى السرطان ذوي الحالات الحرجة. تُعد هذه التجربة الأولى من نوعها في الأردن، وتُعتبر نموذجًا يُحتذى به. هناك حاجة إلى مزيد من الدراسات لدراسة عوائق تطبيق خدمات صيدلية الدعم الغذائي ومكملات الفيتامينات في الأردن، واستكشاف تأثير هذه الخدمات على نتائج المرضى.

الكلمات الدالة: خدمات الصيدلة السريرية، صيدلية الدعم الغذائي، الفيتامينات، الرعاية الحرجة.

[*] ***المؤلف المراسل: نادين عبد الهادي***

nadine_abdelhadi@yahoo.com

تاريخ استلام البحث 2024/4/16 وتاريخ قبوله للنشر 2024/8/22.

Nano-Analytical Techniques in Pharmaceutical Analysis

C. Hima Bindu[1], T. Farmaan[1], K. Aparna[1], M. Sadan[1], T. Reshma[2*]

[1]Department of Pharmaceutical Analysis, Raghavendra Institute of Pharmaceutical Education and Research, K.R. Palli Cross, Anantapur, Chiyyedu, Andhra Pradesh-India.
[2]Department of Pharmaceutical Quality Assurance, Raghavendra Institute of Pharmaceutical Education and Research, K.R. Palli Cross, Anantapur, Chiyyedu, Andhra Pradesh-India.

ABSTRACT

Nano-analytical techniques play a pivotal role in advancing pharmaceutical analysis by providing detailed insights into drug formulations, quality control processes, nanoparticle characterization, impurity detection, and emerging trends in the field. This abstract highlights the significance of nano-analytical tools in optimizing drug delivery systems, ensuring product quality and safety, characterizing nanoparticles, and detecting trace impurities. Key points include the importance of these techniques in enhancing drug stability, enabling targeted drug delivery, and facilitating personalized medicine. Furthermore, the abstract emphasizes the evolving landscape of nano-analytical methods, such as multimodal imaging and quantum-based sensors, and their potential for breakthroughs in real-time drug monitoring and precision medicine. The abstract calls for continued research and development efforts to advance instrumentation, explore novel applications, address technical challenges, foster collaboration, and enhance education and training programs in pharmaceutical analysis. Overall, nano-analytical techniques hold promise for revolutionizing drug development, improving healthcare outcomes, and paving the way for personalized therapies tailored to individual patient needs.

Keywords: Nano-analytical techniques, Pharmaceutical analysis, Drug formulations, Quality control, Nanoparticle characterization, Impurity detection

1. INTRODUCTION:

1.1. Significance of Pharmaceutical Analysis:

Pharmaceutical analysis is a critical component of drug development, manufacturing, and quality control within the pharmaceutical industry. It encompasses a range of techniques and methods used to evaluate the identity, purity, potency, and stability of pharmaceutical substances and products. The significance of pharmaceutical analysis can be understood through several key points(1).

Ensuring Drug Safety and Efficacy: Perhaps the most crucial aspect of pharmaceutical analysis is its role in ensuring that drugs are safe and effective for patient use. Through rigorous testing, analysts can identify impurities, contaminants, or other substances that could pose risks to human health(2).

Quality Control in Manufacturing: Pharmaceutical analysis plays a pivotal role in maintaining the quality and consistency of manufactured drugs(3). By monitoring the manufacturing process and conducting quality tests on raw materials and finished products, manufacturers can meet regulatory standards and produce reliable medications(4).

Regulatory Compliance: Regulatory bodies such as the FDA (Food and Drug Administration) and EMA (European Medicines Agency) require thorough pharmaceutical analysis data as part of the drug approval process. This data helps demonstrate the safety, efficacy, and quality of new pharmaceutical products(5).

[*]***Corresponding author: T. Reshma***
shaikreshmat614@gmail.com
Received: 9/5/2024 Accepted: 22/8/2024.
DOI: https://doi.org/10.35516/jjps.v18i2.2631

Monitoring Drug Stability: Pharmaceuticals can degrade over time, affecting their potency and safety. Pharmaceutical analysis methods are used to assess the stability of drugs under various conditions, such as temperature, humidity, and light exposure, ensuring that medications remain effective throughout their shelf life(6, 7).

Detecting Counterfeit Drugs: In regions where counterfeit drugs are a concern, pharmaceutical analysis techniques are used to authenticate medications. By comparing the chemical composition of suspected counterfeit drugs to genuine products, analysts can identify fraudulent or substandard medicines(8).

Research and Development: Pharmaceutical analysis is integral to drug discovery and development processes. Researchers use analytical techniques to characterize new drug candidates, determine their chemical properties, and assess their potential for therapeutic use(9).

In summary, pharmaceutical analysis is indispensable for maintaining public health by ensuring the safety, quality, and efficacy of pharmaceutical products. It serves as a cornerstone of the pharmaceutical industry, providing the scientific foundation for drug development, manufacturing, and regulatory approval processes(10).

1.2. Introduction to Nano Analytical Techniques:

Nano analytical techniques represent a cutting-edge field in analytical chemistry, focusing on the characterization and analysis of materials at the nanometer scale(11). These techniques have revolutionized the way scientists study and manipulate matter, offering unparalleled insights into the properties of nanoscale materials. Some key points in the introduction to nano analytical techniques include(12):

Definition and Scope: Nano analytical techniques involve methods used to investigate materials at the nanoscale, typically ranging from 1 to 100 nanometers(13). This scale allows researchers to observe phenomena that are not evident at larger scales and explore the unique properties of nanomaterials(14).

Evolution from Traditional Methods: Nano analytical techniques have emerged as a response to the increasing demand for precise characterization of nanoscale materials. They build upon traditional analytical methods such as microscopy, spectroscopy, and chromatography, but with a focus on nanometer-scale resolution(15).

Focus on Nanomaterials: These techniques are particularly suited for studying nanomaterials, which exhibit novel properties due to their small size and high surface area-to-volume ratio(16). Nano analytical methods enable researchers to understand the structure, composition, and behaviour of nanomaterials in various applications(17).

Applications in Various Fields: Nano analytical techniques find applications in diverse fields such as materials science, electronics, environmental science, and, significantly, pharmaceuticals(18). In the pharmaceutical industry, these methods are invaluable for characterizing drug nanoparticles, nanocarriers, and other nano formulations(19).

Examples of Nano Analytical Techniques: Some common nano analytical techniques include Scanning Electron Microscopy (SEM), Transmission Electron Microscopy (TEM), Atomic Force Microscopy (AFM), Dynamic Light Scattering (DLS), and X-ray Photoelectron Spectroscopy (XPS)(20). Each of these techniques offers unique capabilities for analyzing nanoscale materials with high precision and resolution(21).

By providing a glimpse into the world of nano analytical techniques, this introduction sets the stage for exploring how these advanced methods are transforming pharmaceutical analysis and drug development(22, 23).

1.3. Importance of Nanotechnology in Pharmaceuticals:

Nanotechnology has emerged as a game-changer in the pharmaceutical industry, offering innovative solutions to longstanding challenges in drug delivery, formulation, and therapeutic efficacy. Here's an in-depth look at the importance of nanotechnology in pharmaceuticals(24):

Definition and Scope of Nanotechnology:

Nanotechnology involves the manipulation and control of materials at the nanometer scale. In pharmaceuticals, nanotechnology focuses on designing and developing nanoscale drug delivery systems and formulations(25).

Enhanced Drug Delivery Systems: One of the primary advantages of nanotechnology in pharmaceuticals is its ability to improve drug delivery. Nano formulations such as nanoparticles, liposomes, micelles, and dendrimers can enhance drug solubility, bioavailability, and targeted delivery to specific sites in the body(26).

Overcoming Bioavailability Challenges: Many promising drug compounds have poor solubility or stability, limiting their therapeutic effectiveness(27). Nanotechnology enables the encapsulation of these compounds into nano-sized carriers, protecting them from degradation and improving their absorption into the bloodstream(28).

Targeted Drug Delivery: Nanoscale drug carriers can be designed to selectively accumulate in diseased tissues or cells while minimizing exposure to healthy tissues. This targeted approach enhances the therapeutic effects of drugs while reducing side effects and toxicity(29).

New Therapeutic Modalities: Nanotechnology opens doors to novel therapeutic modalities such as gene therapy, RNA interference, and personalized medicine(30). Nanoparticles can deliver genetic material or therapeutic agents directly to target cells, offering tailored treatments for individual patients(31).

Improved Imaging and Diagnostics: Nanotechnology-based contrast agents and imaging probes enable more accurate diagnosis of diseases such as cancer. Nanoparticles designed for imaging applications provide high-resolution images of tissues and organs, aiding in early detection and treatment monitoring(32).

Regulatory Considerations: The introduction of nanotechnology in pharmaceuticals has prompted regulatory agencies to develop guidelines for evaluating the safety and efficacy of nanomedicines. This includes considerations for nanoparticle toxicity, pharmacokinetics, and biocompatibility(33).

Future Directions: The rapid advancements in nanotechnology continue to drive innovation in drug development. Scientists are exploring nanoscale drug delivery platforms, smart nanoparticles that respond to specific stimuli, and nanotheranostics that combine therapy and diagnostics in a single system(34).

In conclusion, nanotechnology represents a transformative force in pharmaceuticals, offering new possibilities for drug delivery, therapeutic efficacy, and personalized medicine. Its integration into pharmaceutical research and development holds promise for addressing unmet medical needs and improving patient outcomes(35).

2. Basics of Nano Analytical Techniques:

Nano analytical techniques are a set of advanced methods used to characterize and analyze materials at the nanometer scale, typically ranging from 1 to 100 nanometers(36). This scale is significant because it is at this level that materials exhibit unique and often unexpected properties due to quantum effects and increased surface area-to-volume ratios(37). The scope of nano analytical techniques encompasses a wide array of methods, each tailored to probe different aspects of nanomaterials(38):

Imaging Techniques: Nano analytical techniques include powerful imaging methods such as Scanning Electron Microscopy (SEM), Transmission Electron Microscopy (TEM), and Atomic Force Microscopy (AFM)(39). These techniques provide high-resolution images of nanoscale structures, offering insights into particle size, morphology, and surface characteristics(40).

Spectroscopic Techniques: Spectroscopy at the nanoscale involves techniques like X-ray Photoelectron Spectroscopy (XPS) and Raman Spectroscopy(41). These methods analyze the chemical composition, molecular structure, and bonding of nanomaterials, providing invaluable information for pharmaceutical analysis(42).

Particle Sizing Methods: Dynamic Light Scattering (DLS) is a common nano analytical technique used to

determine the size distribution of nanoparticles in a sample. It measures the fluctuations in the intensity of scattered light to calculate the hydrodynamic diameter of particles(43).

Surface Analysis Techniques: Nanomaterials often exhibit unique surface properties that influence their behavior. Surface analysis methods such as Scanning Probe Microscopy (SPM) and Auger Electron Spectroscopy (AES) are employed to study surface topography, composition, and reactivity at the nanoscale(44).

Chemical Mapping Methods: Techniques like Energy-Dispersive X-ray Spectroscopy (EDS) and Electron Energy Loss Spectroscopy (EELS) provide spatially resolved elemental analysis of nanomaterials. These methods are crucial for understanding the distribution of elements within a sample(45).

The significance of nano analytical techniques lies in their ability to delve into the nanoscale world, where materials behave differently than they do at larger scales(46). This enables researchers to design and optimize nanomaterials for specific pharmaceutical applications, such as drug delivery systems, nanomedicines, and diagnostic agents(47).

1.1. Comparison with Traditional Analytical Methods:

Nano analytical techniques offer several distinct advantages over traditional analytical methods, particularly when it comes to characterizing nanomaterials used in pharmaceuticals(48):

Improved Resolution: Traditional methods such as optical microscopy have limited resolution, often unable to visualize structures below the micrometer scale(49). In contrast, nano analytical techniques like TEM and AFM can achieve resolutions down to atomic levels, providing detailed insights into nanoscale features(50).

Enhanced Sensitivity: Nanomaterials often have properties that are highly sensitive to their environment. Nano analytical techniques excel in detecting subtle changes in properties such as surface charge, chemical composition, and magnetic behavior, which are crucial for pharmaceutical applications(51).

Quantitative Analysis: Many nano analytical techniques allow for precise quantitative analysis of nanomaterials(52). For example, DLS provides accurate measurements of particle size distribution, crucial for designing optimal drug delivery systems with controlled release properties(53).

Multi-Modal Analysis: Nano analytical methods often combine several analytical techniques into a single platform. This multi-modal approach allows researchers to gather comprehensive data on nanomaterials, including structural, chemical, and physical properties, in a single experiment(54).

Non-Destructive Characterization: Unlike some traditional methods that may alter or damage samples during analysis, many nano analytical techniques are non-destructive(55).Real-Time Monitoring: Some nano analytical techniques, such as AFM and certain spectroscopic methods, offer real-time monitoring capabilities. This means researchers can observe dynamic changes in nanomaterial properties, aiding in the development of responsive drug delivery systems(56).

Table 1: Comparison of Nano Analytical Techniques with Traditional Methods

Feature	Traditional Methods	Nano Analytical Techniques
Resolution	Limited to micrometer scale	Down to atomic levels
Sensitivity	Lower for subtle property changes	Higher, detects small changes in properties
Quantitative Analysis	Limited	Precise measurements possible
Multi-Modal Analysis	Rare	Common, combining multiple techniques
Non-Destructive Characterization	Often destructive	Typically non-destructive
Real-Time Monitoring	Limited	Available in some techniques

1.2. Advantages of Nano Analytical Techniques in Pharmaceutical Analysis:

Nano analytical techniques bring numerous advantages to the field of pharmaceutical analysis, offering new avenues for research, development, and quality control(57):

Characterization of Nanoformulations: Nano analytical methods are crucial for characterizing drug nanoparticles, liposomes, micelles, and other nanoformulations(58). They provide insights into particle size, shape, surface properties, and stability, which are vital for optimizing drug delivery systems(59).

Quality Control in Nanomedicines: Pharmaceutical companies rely on nano analytical techniques to ensure the quality and consistency of nanomedicines. By monitoring the characteristics of nanoparticles, manufacturers can maintain batch-to-batch uniformity and adherence to regulatory standards(60).

Assessment of Drug Release Profiles: Nano analytical techniques play a key role in studying the release kinetics of drugs from nanocarriers. Researchers can determine factors such as release rates, mechanisms, and triggers, aiding in the design of controlled and targeted drug delivery systems(61).

Detection of Impurities and Contaminants: Pharmaceutical analysis using nano analytical methods helps in detecting trace levels of impurities or contaminants in drug formulations. This ensures that pharmaceutical products meet strict purity standards, minimizing risks to patient safety(62).

Optimization of Formulation Parameters: Researchers utilize nano analytical techniques to optimize formulation parameters such as drug-to-carrier ratios, stability under physiological conditions, and interactions with biological tissues. This leads to the development of more effective and safe drug formulations(63).

Understanding Drug-Particle Interactions: Nano analytical methods provide insights into how drugs interact with nanoparticles at the molecular level(64). This knowledge helps in predicting drug behavior in vivo, including absorption, distribution, metabolism, and excretion (ADME), improving drug efficacy and bioavailability(65).

Accelerating Drug Development: By providing detailed information on nanomaterial properties, nano analytical techniques accelerate the drug development process(66). Researchers can make informed decisions about candidate selection, formulation design, and preclinical testing, leading to faster translation of discoveries into clinically viable products(67). Nano analytical techniques offer unparalleled capabilities in characterizing nanomaterials, enabling precise control over drug delivery systems and formulations. Their advantages in pharmaceutical analysis contribute to the development of safer, more effective, and targeted therapies for various diseases(68, 69).

Table 2: Applications of Nano Analytical Techniques in Pharmaceutical Analysis

Application	Technique	Example Case Study
Characterizing drug nanoparticles	TEM, SEM	Analysis of liposomal drug delivery systems
Quality control of excipients	SEM	Examination of particle size and uniformity
Studying drug-excipient interactions	TEM, AFM	Interactions in drug formulations
Detecting contaminants	SEM, TEM	Identifying impurities in final products
Analyzing drug release profiles	DLS	Release kinetics of nanoparticles

2. Common Nano Analytical Techniques:

2.1. Scanning Electron Microscopy (SEM):

Principle of Operation:

Scanning Electron Microscopy (SEM) is a powerful imaging technique used to visualize the surface morphology of samples at high magnifications and

resolutions. Unlike optical microscopes which use light, SEM employs a focused beam of electrons to interact with the sample, providing detailed images with nanoscale resolution(70).

The basic principle of SEM involves the following steps:

A beam of electrons is generated in the electron source, typically a tungsten filament(71).

These electrons are accelerated through an electron column by applying a high voltage(72).

The focused electron beam then scans across the surface of the sample in a raster pattern(73).

As the electrons interact with the atoms in the sample, signals such as secondary electrons, backscattered electrons, and characteristic X-rays are generated(74).

Detectors in the SEM measure these signals, which are then used to create an image with details of the sample's surface topography(75).

The resulting SEM images provide valuable information about the three-dimensional structure, surface features, and texture of the sample, revealing details down to the nanometer scale(76).

Application in Pharmaceutical Analysis:

SEM finds diverse applications in pharmaceutical analysis, offering insights into the structure, morphology, and quality of pharmaceutical materials. Some key applications include(77):

Particle Size and Morphology: SEM is used to characterize the size, shape, and distribution of drug particles in formulations. This information is crucial for assessing drug stability, dissolution rates, and bioavailability. For instance, in the development of inhalable pharmaceuticals, SEM helps analyze the size and shape of drug particles for optimal lung deposition(78).

Quality Control of Excipients: Pharmaceutical formulations often contain various excipients such as fillers, binders, and disintegrants. SEM enables the examination of these excipients for uniformity, particle size, and aggregation, ensuring consistency in drug manufacturing(79).

Analysis of Drug Delivery Systems: SEM is instrumental in studying nanocarriers, microspheres, and other drug delivery systems. Researchers can visualize the structure, porosity, and surface modifications of these carriers, which influence drug release profiles and targeting efficiency(80).

Contaminant Detection: SEM helps in detecting foreign particles, contaminants, or defects in pharmaceutical products. This is critical for ensuring product quality, preventing batch recalls, and maintaining regulatory compliance(81).

3.2. Transmission Electron Microscopy (TEM):

Principles:

Transmission Electron Microscopy (TEM) is a sophisticated imaging technique that utilizes a beam of electrons transmitted through an ultra-thin sample to produce high-resolution images. TEM operates on the principle of wave-particle duality, where electrons behave both as particles and waves(82).

The key principles of TEM operation are as follows:

Electron Source: TEM uses an electron gun to generate a beam of electrons(83).

Electron Lenses: These lenses focus and direct the electron beam towards the sample, similar to the function of optical lenses in light microscopy(84).

Electron Specimen Interaction: As the electrons pass through the sample, they interact with the atoms, undergoing scattering, absorption, and diffraction. This interaction provides valuable information about the sample's structure and composition(85).

Image Formation: The transmitted electrons are collected by a detector on the other side of the sample. The resulting image is formed by the varying intensity of transmitted electrons, which is influenced by the density and thickness of the sample(86).

Magnification: TEM can achieve extremely high magnifications, up to millions of times, allowing visualization of nanoscale features(87).

Resolution: The resolution of TEM is governed by the wavelength of the electrons, which is much shorter than that of visible light. This enables TEM to resolve details at the atomic and near-atomic levels(88).

In summary, TEM provides detailed images of the internal structure of materials, revealing atomic arrangements, crystal defects, grain boundaries, and other nanoscale features.

Pharmaceutical Applications

Transmission Electron Microscopy (TEM) is a valuable tool in pharmaceutical research and development, offering unique capabilities for characterizing nanomaterials and understanding their behavior(89). Some key applications of TEM in the pharmaceutical industry include:

Nanoparticle Characterization: TEM is essential for visualizing and characterizing drug nanoparticles, liposomes, dendrimers, and other nano-sized drug delivery systems. It provides insights into particle size, shape, aggregation, and internal structure, crucial for optimizing drug formulations(90).

Drug-Excipient Interactions: TEM helps in studying the interactions between drugs and excipients at the nanoscale. This includes investigating how drugs are encapsulated within carriers, the distribution of drug molecules, and the stability of the formulation over time(91).

Crystal Structure Analysis: TEM can be used to determine the crystal structure of drug compounds, especially for polymorphic forms(92). Understanding the crystal structure is vital for assessing drug stability, solubility, and bioavailability(93).

Quality Control of Pharmaceuticals: TEM is employed in quality control processes to detect and analyze contaminants, impurities, or defects in pharmaceutical products. It ensures the integrity and purity of the final drug formulations(94).

Biological Sample Analysis: In the study of drug interactions with biological tissues or cells, TEM provides detailed images of cellular uptake, intracellular localization of drugs, and drug-induced changes at the subcellular level(95).

Examples:

Analysis of Liposomal Drug Delivery Systems: TEM was used to study the morphology and structure of liposomes loaded with anticancer drugs. The images revealed the size distribution, bilayer structure, and drug encapsulation efficiency of the liposomes. This information guided researchers in optimizing the formulation for enhanced drug delivery and cellular uptake(96).

Characterization of Nanocrystals for Enhanced Dissolution: In a study on nanocrystals of poorly water-soluble drugs, TEM was employed to analyze the size, shape, and surface characteristics of the nanocrystals. The images provided insights into the crystalline structure and surface modifications, which improved the dissolution rate and bioavailability of the drugs(97).

Investigation of Protein-Nanoparticle Interactions: TEM was utilized to examine the interaction between proteins and nanoparticles in drug delivery systems(98). The images elucidated the adsorption mechanisms, complexes. This knowledge helped in designing nanoparticles with improved biocompatibility and targeted delivery(99).

These case examples demonstrate how Transmission Electron Microscopy (TEM) plays a pivotal role in pharmaceutical research, offering detailed insights into nanomaterials, drug formulations, and interactions at the molecular level(100). TEM's ability to visualize nanoscale structures is instrumental in advancing drug development, formulation optimization, and quality assurance in the pharmaceutical industry(101).

3.3. Atomic Force Microscopy (AFM):

Principles:

Atomic Force Microscopy (AFM) is a powerful imaging and probing technique used to study surfaces at the atomic and molecular levels(102). Unlike conventional

optical microscopes or electron microscopes, AFM does not rely on lenses or electron beams. Instead, it utilizes a sharp tip mounted on a flexible cantilever to scan the surface of a sample(103). The working principles of AFM are as follows:

Cantilever with Tip: The heart of an AFM system is a tiny cantilever with a sharp tip at its end. This tip is usually made of materials such as silicon or silicon nitride and has a radius of a few nanometers(104).

Intermittent Contact: In the intermittent contact mode, the AFM tip approaches the sample surface, and when it gets close enough, van der Waals forces between the tip and the surface cause the cantilever to bend. This bending is detected by a laser beam reflecting off the back of the cantilever(105).

Feedback Loop: A feedback loop constantly adjusts the height of the AFM tip to maintain a constant force or amplitude as it scans the surface. This feedback generates a topographic map of the sample surface(106).

3D Imaging: As the AFM tip scans across the sample in a raster pattern, it generates a series of height measurements. These measurements are used to construct a three-dimensional image of the surface, revealing details such as height variations, surface roughness, and molecular structures(107).

Force Spectroscopy: AFM can also be used for force spectroscopy, where the tip is used to apply controlled forces to the sample surface. This allows researchers to measure properties such as adhesion forces, elasticity, and mechanical properties of materials at the nanoscale(108).

In summary, AFM provides high-resolution imaging and precise measurements of surface topography and properties at the atomic and molecular scales, making it a versatile tool for a wide range of applications.

Pharmaceutical Analysis:

Atomic Force Microscopy (AFM) has become increasingly valuable in pharmaceutical analysis due to its ability to visualize and characterize nanoscale features of pharmaceutical materials(109).

Some key applications of AFM in the pharmaceutical industry include:

Drug Delivery Systems Characterization: AFM is used to study the morphology, size distribution, and surface properties of drug delivery systems such as nanoparticles, liposomes, and micelles. This helps in optimizing formulations for targeted drug delivery, controlled release, and stability(110).

Surface Roughness and Texture Analysis: AFM provides detailed information about the surface roughness, texture, and topography of pharmaceutical materials. This is crucial for assessing the quality of coatings, films, tablets, and other dosage forms(111).

Crystallographic Studies: AFM can be used to investigate the crystallographic properties of drug molecules, including crystal size, shape, and orientation. This information is vital for understanding drug stability, solubility, and dissolution behavior(112).

Biological Interactions: AFM enables researchers to study the interactions between drugs, nanoparticles, or biomolecules with biological surfaces such as cell membranes or tissues. This includes assessing adhesion forces, binding kinetics, and cellular uptake mechanisms(113).

Quality Control and Contaminant Detection: AFM helps in quality control processes by detecting contaminants, impurities, or defects on pharmaceutical surfaces. It ensures the purity and integrity of drug formulations(114).

Case Studies:

Nanoparticle Morphology in Drug Delivery Systems: AFM was used to characterize the morphology and size distribution of polymer-based nanoparticles designed for targeted drug delivery. The AFM images revealed uniform spherical shapes with diameters in the nanometer range. This information guided researchers in optimizing the formulation for efficient drug release and cellular uptake(115).

Surface Roughness of Coated Tablets: In a study on

tablet coatings, AFM was employed to analyze the surface roughness and texture of coated tablets. The AFM images provided detailed insights into the uniformity and integrity of the coating layers, ensuring consistent drug release profiles and stability(116).

Adhesion Forces in Nanomedicine: Researchers used AFM to measure the adhesion forces between drug-loaded nanoparticles and cancer cells. The AFM force spectroscopy revealed varying adhesion strengths, indicating differences in nanoparticle surface modifications. This study helped in designing nanoparticles with enhanced targeting and cellular uptake for improved anticancer therapy(117).

These case studies highlight the versatility of Atomic Force Microscopy (AFM) in pharmaceutical analysis, from characterizing drug delivery systems to assessing surface properties and biological interactions. AFM's ability to provide detailed, nanoscale imaging and measurements makes it a valuable tool for advancing pharmaceutical research, formulation development, and quality assurance(118).

3.4. Dynamic Light Scattering (DLS):

Overview of DLS:

Dynamic Light Scattering (DLS), also known as Photon Correlation Spectroscopy, is a technique used to measure the size distribution of particles in solution. It relies on the principle of how particles in suspension will scatter light due to Brownian motion(119). The basic working principle of DLS involves the following steps:

Laser Light Source: A laser beam is directed onto the sample containing particles in suspension(120).

Scattering of Light: The particles in the sample scatter the laser light in different directions due to their Brownian motion(121).

Detector: A detector measures the fluctuations in the intensity of the scattered light over time(122).

Correlation Function Analysis: The data collected by the detector is analyzed using correlation functions. This analysis provides information about the speed at which particles move, which is directly related to their size(123).

Size Calculation: The autocorrelation function is used to calculate the diffusion coefficient of the particles, which is then converted into particle size distribution using the Stokes-Einstein equation(124).

DLS provides information about the hydrodynamic diameter of particles in solution, which includes the size of the particles as well as the solvent molecules that are attached or associated with them. It is a rapid, non-invasive technique that requires minimal sample preparation(125).

Applications in Pharmaceuticals

Dynamic Light Scattering (DLS) has numerous applications in the pharmaceutical industry, particularly in the characterization of colloidal systems, nanoparticles, and biomolecules(126).

Some key applications include:

Nanoparticle Size Distribution: DLS is widely used to determine the size distribution of drug nanoparticles, liposomes, micelles, and other colloidal drug delivery systems. This information is crucial for assessing stability, aggregation tendencies, and drug release profiles(127).

Protein Aggregation Studies: In the development of biopharmaceuticals such as monoclonal antibodies, DLS is used to monitor protein aggregation and oligomerization. It helps in optimizing formulation conditions to prevent aggregation, which can affect drug efficacy and safety(128).

Polymer Characterization: DLS is employed to analyze the size distribution of polymer nanoparticles used in drug delivery and tissue engineering. It provides insights into the polydispersity and stability of polymer-based formulations(129).

Quality Control of Suspensions: Pharmaceutical suspensions, such as oral suspensions and injectable formulations, require precise particle size control. DLS ensures the uniformity and stability of suspended particles, preventing sedimentation or aggregation issues(130).

Microparticle Analysis: DLS can also be used to analyze larger microparticles or microspheres, providing

information on their size distribution and surface properties. This is important for the development of sustained-release formulations and inhalable drug delivery systems(131).

Examples:

Liposome Size Optimization for Drug Delivery: In a study focusing on liposomal drug delivery systems, DLS was used to optimize the size of liposomes for enhanced drug delivery(132). The DLS measurements allowed researchers to control the size distribution of liposomes, ensuring optimal stability and bioavailability of the encapsulated drug(133).

Protein Aggregation Monitoring in Biologics: DLS was employed to monitor the aggregation of therapeutic proteins during formulation development(134). By tracking changes in the size distribution of protein aggregates over time, researchers could identify optimal storage conditions and prevent aggregation-induced degradation(135).

Characterization of Polymeric Nanoparticles: In a study on polymeric nanoparticles for targeted drug delivery, DLS provided insights into the size distribution and stability of the nanoparticles. The data from DLS measurements guided the selection of polymer types and formulation parameters for efficient drug release and cellular uptake(136).

These case examples illustrate the versatility of Dynamic Light Scattering (DLS) in pharmaceutical applications, from optimizing nanoparticle size for drug delivery to monitoring protein stability in biopharmaceuticals(137). DLS's ability to provide rapid, precise measurements of particle size distribution plays a crucial role in formulation development, quality control, and ensuring the effectiveness of pharmaceutical products(138).

3.5. X-ray Photoelectron Spectroscopy (XPS):

Principles:

X-ray Photoelectron Spectroscopy (XPS), also known as Electron Spectroscopy for Chemical Analysis (ESCA), is a surface-sensitive technique used to analyze the elemental composition and chemical state of materials(139). It operates on the principle of photoelectric effect and involves the following basic principles:

X-ray Excitation: A sample is bombarded with monochromatic X-rays, typically generated by a focused X-ray source such as a monochromator(140).

Photoelectric Effect: When the X-rays strike the sample, they cause the ejection of inner-shell electrons (core electrons) from atoms in the sample(141).

Energy Analysis: The kinetic energy of the ejected photoelectrons is measured using an electron energy analyzer(142).

Spectra Generation: XPS generates a plot known as a spectrum, which shows the number of emitted electrons (intensity) as a function of their kinetic energy. Peaks in the spectrum correspond to the binding energies of the electrons, revealing information about the elements present and their chemical environments(143).

Chemical State Analysis: By analyzing the peak positions and shapes in the XPS spectrum, researchers can determine the chemical state, oxidation state, and bonding environment of elements within the sample(144).

XPS provides valuable information about the surface composition, chemical bonding, and electronic structure of materials with high sensitivity and precision(145).

Pharmaceutical Analysis

X-ray Photoelectron Spectroscopy (XPS) plays a significant role in pharmaceutical analysis by providing detailed insights into the surface properties of pharmaceutical materials(146).

Some key applications of XPS in the pharmaceutical industry include:

Surface Composition of Drug Formulations: XPS is used to analyze the surface composition of drug formulations, including tablets, powders, and coatings. It helps in identifying the presence of active pharmaceutical ingredients (APIs), excipients, and contaminants on the surface(147).

Characterization of Nanomaterials: XPS is crucial for characterizing nanomaterials used in drug delivery systems, such as nanoparticles, nanocarriers, and liposomes. It reveals the chemical composition, surface functionalization, and stability of nanoscale formulations(148).

Quality Control of Packaging Materials: XPS is employed to analyze the surface properties of packaging materials used for pharmaceutical products. It helps in assessing the composition, cleanliness, and barrier properties of packaging films, ensuring product stability and integrity(149).

Drug-Excipient Interactions: XPS studies the interactions between drugs and excipients at the molecular level. This includes investigating binding sites, chemical reactions, and stability of drug formulations, aiding in formulation optimization and compatibility studies(150).

Surface Modifications and Coatings: Pharmaceutical surfaces are often modified with coatings for controlled release or enhanced bioavailability. XPS provides insights into the composition and thickness of these coatings, ensuring desired functionalities and performance(151).

Illustrative Case Studies:

Surface Analysis of Drug Nanoparticles: In a study on polymeric nanoparticles for targeted drug delivery, XPS was used to analyze the surface composition and functional groups of the nanoparticles. The XPS spectra revealed the presence of polymer chains and surface modifications, guiding researchers in optimizing the nanoparticles for enhanced drug release and stability(152).

Identification of Surface Contaminants: XPS was employed to analyze the surface of pharmaceutical tablets for the presence of contaminants. The spectra identified trace amounts of environmental contaminants on the tablet surface, prompting investigations into manufacturing processes and storage conditions(153).

Characterization of Drug-Coated Stents: In a case involving drug-coated stents for cardiovascular applications, XPS was used to analyze the composition and uniformity of the drug coating. The XPS data confirmed the presence of the drug and its distribution on the stent surface, ensuring the efficacy and durability of the medical device(154).

These case studies demonstrate the versatility of X-ray Photoelectron Spectroscopy (XPS) in pharmaceutical analysis, from characterizing drug nanoparticles to assessing surface contaminants and analyzing drug-coated formulations. XPS's ability to provide detailed chemical information at the surface level is invaluable for formulation development, quality control, and ensuring the safety and efficacy of pharmaceutical products(155).

Table 3: Summary of Nano Analytical Techniques

Technique	Principle	Applications
Scanning Electron Microscopy (SEM)	Uses focused electron beam for surface imaging	Particle size and morphology analysis
Transmission Electron Microscopy (TEM)	Transmits electrons through thin samples for internal structure imaging	Nanoparticle characterization, crystal structure analysis
Atomic Force Microscopy (AFM)	Measures forces between a sharp probe and sample surface	Surface topography and property measurements
Dynamic Light Scattering (DLS)	Analyzes fluctuations in light scattering from particles in suspension	Particle size distribution measurement
X-ray Photoelectron Spectroscopy (XPS)	Measures kinetic energy of electrons ejected by X-rays	Chemical composition and electronic state analysis

4. Advances in Nano Analytical Techniques:

4.1. Recent Developments in Nano Analytical Tools:

Recent years have witnessed remarkable advancements in nano analytical tools, offering unprecedented capabilities for characterizing and understanding nanomaterials(156).

Some of the noteworthy developments include:

Correlative Microscopy: This emerging field combines multiple imaging techniques such as Scanning Electron Microscopy (SEM), Transmission Electron Microscopy (TEM), and Atomic Force Microscopy (AFM). Correlative microscopy allows researchers to obtain complementary information on the same sample, providing a comprehensive view of nanoscale structures and properties(157).

Super-Resolution Microscopy: Techniques like Stimulated Emission Depletion Microscopy (STED) and Single-Molecule Localization Microscopy (SMLM) have revolutionized imaging at the nanoscale. These methods surpass the diffraction limit of light, enabling visualization of molecular details within cells, nanoparticles, and biological tissues(158).

Cryo-Electron Microscopy (Cryo-EM): Cryo-EM has become a powerful tool for structural biology and nanomaterial characterization. Recent advancements in hardware and softwar(159)e have improved resolution and speed, allowing for detailed imaging of biological macromolecules, protein complexes, and synthetic nanomaterials(160).

Multi-Modal Analysis Platforms: Integrated systems combining different analytical techniques, such as AFM with Raman spectroscopy or SEM with energy-dispersive X-ray spectroscopy (EDS), are becoming more prevalent. These platforms offer synergistic insights into the chemical, structural, and mechanical properties of nanomaterials(161).

In-Situ and Operando Techniques: Real-time imaging and analysis under operando conditions provide dynamic insights into nanomaterial behavior during reactions or environmental changes. In-situ TEM, for instance, allows researchers to observe nanoscale phenomena such as phase transitions, growth processes, and catalytic reactions(162).

Machine Learning and Data Analytics: Advanced algorithms and machine learning approaches are being applied to analyze vast amounts of data generated by nano analytical tools. These tools aid in pattern recognition, image segmentation, and prediction of material properties based on complex datasets(163).

4.2. Integration with Other Analytical Methods:

The integration of nano analytical tools with complementary techniques enhances the depth and breadth of information obtained from materials characterization(164).

Some examples of integration include:

Correlative Analysis: Combining SEM with focused ion beam (FIB) milling allows for precise sample preparation followed by high-resolution imaging. This approach is invaluable for studying nanomaterials in their native state with minimal artifacts(165).

AFM-Raman Spectroscopy: AFM coupled with Raman spectroscopy provides simultaneous topographic and chemical information at the nanoscale. This integration enables the mapping of chemical compositions, molecular structures, and surface properties of samples(166).

TEM-EDS: Transmission Electron Microscopy combined with Energy-Dispersive X-ray Spectroscopy offers elemental analysis at the nanoscale. This integration is essential for identifying and mapping the distribution of elements within nanomaterials and biological specimens(167).

XPS-Depth Profiling: X-ray Photoelectron Spectroscopy with depth profiling capabilities allows for the analysis of layered structures. This integration is crucial for studying coatings, thin films, and interfaces in pharmaceutical formulations or material science applications(168).

Multi-Modal Microscopy: Integrated platforms that

combine fluorescence microscopy with AFM or SEM enable simultaneous imaging of biological samples with high spatial resolution and molecular specificity(169).

4.3. Impact on Pharmaceutical Research and Development:

The integration of advanced nano analytical tools has had a transformative impact on pharmaceutical research and development (R&D) in several ways(170):

Drug Delivery Optimization: Nano analytical tools aid in the design and optimization of drug delivery systems, including nanoparticles, liposomes, and micelles. Precise characterization of these systems ensures controlled release, enhanced bioavailability, and targeted delivery of therapeutic agents(171).

Formulation Stability and Quality Control: Pharmaceutical formulations undergo rigorous analysis using nano analytical techniques to assess stability, uniformity, and particle size distribution. This ensures product quality, shelf-life, and compliance with regulatory standards(172).

Biomolecular Interactions and Mechanisms: Advanced microscopy techniques coupled with nano analytical tools allow researchers to study drug-protein interactions, cellular uptake mechanisms, and intracellular trafficking. This knowledge is crucial for understanding drug efficacy, toxicity, and pharmacokinetics(173).

Personalized Medicine and Nanomedicine: Nano analytical tools enable the development of personalized therapies based on individual patient characteristics. Nanomedicines tailored to specific diseases or genetic profiles offer targeted treatments with reduced side effects(174).

Accelerated Drug Development: The rapid, detailed insights provided by nano analytical tools accelerate the drug discovery process. Researchers can screen and optimize drug candidates, predict formulations with desirable properties, and reduce the time-to-market for new pharmaceuticals(175).

Safety and Toxicity Assessment: Nanotoxicology studies benefit from nano analytical tools to assess the safety profiles of nanomaterials. Techniques such as TEM, AFM, and XPS aid in understanding cellular responses, potential risks, and mitigating factors for safe use in pharmaceutical applications(176).

In summary, the integration of advanced nano analytical tools with other techniques has revolutionized pharmaceutical R&D, offering precise control over drug formulations, insights into molecular mechanisms, and the development of innovative therapies. These tools continue to drive innovation in nanomedicine, personalized treatments, and the optimization of pharmaceutical products for improved patient outcomes(177).

5. Challenges and Limitations:

5.1. Technical Challenges in Nano Analytical Techniques:

Nano analytical techniques, despite their incredible capabilities, come with several technical challenges that researchers and scientists often encounter(178):

Resolution Limitations: Achieving high resolution at the nanoscale can be challenging, especially in techniques like Optical Microscopy. Diffraction limits restrict the ability to distinguish features smaller than the wavelength of light(179).

Instrumentation Complexity: Many nano analytical tools require sophisticated and specialized equipment, which can be expensive to acquire, operate, and maintain. This includes instruments like Electron Microscopes, which demand vacuum conditions and precise beam control(180).

Sample Preparation: Preparing samples for analysis is crucial but can be complex and time-consuming. Ensuring that the sample is representative, properly mounted, and free from artifacts is essential for accurate results(181).

Data Analysis and Interpretation: The vast amount of data generated by nano analytical tools requires advanced data analysis techniques. Extracting meaningful information from complex datasets and interpreting results accurately can be a significant challenge(182).

Sample Damage or Alteration: Techniques such as Electron Microscopy can potentially damage or alter the sample due to high-energy beams. Minimizing sample damage while obtaining high-quality images is a balancing act(183).

Environmental Interference: Nano analytical techniques are sensitive to environmental conditions such as temperature, humidity, and vibration. Controlling these factors to ensure stable and reproducible measurements is a constant challenge(184).

Single-Molecule Detection: In techniques like Single-Molecule Fluorescence Microscopy, detecting and tracking individual molecules in real-time poses technical hurdles due to background noise and signal-to-noise ratio challenges(185).

Quantitative Analysis: Accurately quantifying properties such as particle size, distribution, and concentration can be difficult in nano analytical techniques, especially in complex samples(186).

Instrument Alignment and Calibration: Maintaining precise alignment and calibration of instruments is crucial for obtaining reliable and reproducible results. Any misalignment or drift can introduce errors in measurements(187).

Addressing these technical challenges requires a combination of expertise in instrumentation, sample preparation techniques, data analysis, and a deep understanding of the principles underlying each nano analytical method(188).

5.2. Sample Preparation Issues:

Sample preparation is a critical aspect of nano analytical techniques, and issues in this stage can significantly impact the results(189):

Contamination and Artifacts: Improper handling or storage of samples can introduce contaminants, affecting the analysis. Artifacts such as dust particles, residues, or surface contaminants can obscure true sample features(190).

Homogeneity and Representativeness: Ensuring sample homogeneity is crucial for obtaining reliable and reproducible results. Variations in sample composition or structure can lead to misleading conclusions(191).

Size and Shape Alterations: Some sample preparation methods, such as drying techniques for Electron Microscopy, can alter the size, shape, or distribution of nanoparticles or biological specimens(192).

Embedding and Mounting: The choice of embedding media and mounting substrates can affect the interaction of the sample with the nano analytical tool. Incompatibility between the sample and substrate can lead to signal distortion or poor resolution(193).

Compatibility with Techniques: Different nano analytical techniques require specific sample preparation methods. Adapting samples to suit multiple techniques while preserving their integrity can be challenging(194).

Minimizing Surface Effects: Surface-sensitive techniques like X-ray Photoelectron Spectroscopy (XPS) are highly sensitive to surface conditions. Controlling sample exposure to air or contaminants during preparation is crucial(195).

Thin Sectioning for TEM: Samples for Transmission Electron Microscopy (TEM) often require ultra-thin sections, which can be difficult to achieve without specialized equipment and techniques. Variations in section thickness can impact image quality and analysis(196).

Biological Specimen Preservation: Preserving the native structure and function of biological samples during preparation is challenging. Cryogenic methods or chemical fixation may introduce artifacts or alter cellular structures(197).

5.3. Potential Drawbacks in Pharmaceutical Applications:

While nano analytical techniques offer significant advantages in pharmaceutical research, there are also potential drawbacks to consider(198):

Cost and Resources: Acquiring and maintaining advanced nano analytical instruments can be costly,

especially for smaller pharmaceutical companies or research institutions. This can limit accessibility to cutting-edge technologies(199).

Complexity and Training: Operating nano analytical tools requires specialized training and expertise. The complexity of instruments can pose a barrier to entry for researchers unfamiliar with the techniques(200).

Time-Consuming Processes: Sample preparation, analysis, and data interpretation in nano analytical techniques can be time-consuming. This can slow down the pace of drug development and research(201).

Limited Sample Throughput: Some techniques, such as Cryo-Electron Microscopy (Cryo-EM), may have limitations in sample throughput due to the time-intensive nature of sample preparation and imaging(202).

Interpretation Challenges: Interpreting nano analytical data, especially in complex systems like drug delivery nanoparticles or biological tissues, requires expertise in both the technique and the specific application(203).

Limited Compatibility: Not all nano analytical techniques are compatible with pharmaceutical formulations or biological samples. Ensuring compatibility and adapting methods for specific applications can be challenging(204).

Sample Size Requirements: Some techniques, such as Single-Molecule Microscopy, may require a high concentration of samples or specific conditions for optimal detection. This can limit the applicability to small sample volumes or dilute solutions(205).

Regulatory Considerations: Implementing new nano analytical methods in pharmaceutical research may require validation, standardization, and adherence to regulatory guidelines. This can add complexity and time to the development process(206).

Ethical and Safety Concerns: In the case of nanomedicine, there are ongoing discussions about the safety, toxicity, and long-term effects of nanoparticles on human health. Thorough evaluation and risk assessment are essential(207).

Despite these drawbacks, the benefits of nano analytical techniques in pharmaceutical applications often outweigh the challenges. Addressing these concerns through collaborative research efforts, standardization of protocols, and continuous technological advancements is crucial for harnessing the full potential of these powerful tools in drug development and healthcare(208).

6. Applications in Pharmaceutical Industry:

6.1. Drug Formulation Analysis:

Nano analytical techniques play a crucial role in the analysis and optimization of drug formulations, ensuring their effectiveness, stability, and targeted delivery(209):

Particle Size and Distribution: Techniques like Dynamic Light Scattering (DLS) and Laser Diffraction are used to measure the particle size distribution of drug nanoparticles or microparticles. This information is vital for controlling drug release rates, solubility, and bioavailability(210).

Surface Morphology and Coating Analysis: Scanning Electron Microscopy (SEM) and Atomic Force Microscopy (AFM) provide detailed images of the surface morphology of drug particles. This helps in assessing the effectiveness of coatings for controlled release, stability, and interaction with biological systems(211).

Chemical Composition and Bonding: X-ray Photoelectron Spectroscopy (XPS) and Fourier Transform Infrared Spectroscopy (FTIR) are utilized to analyze the chemical composition of drug formulations. These techniques reveal the presence of active pharmaceutical ingredients (APIs), excipients, and any chemical changes during formulation processes(212).

Crystallographic Studies: Transmission Electron Microscopy (TEM) and X-ray Diffraction (XRD) are employed to study the crystalline structure of drug compounds. Understanding the polymorphic forms, crystal sizes, and orientation aids in predicting stability, dissolution rates, and bioavailability of drugs(213).

Encapsulation Efficiency: Fluorescence Spectroscopy and Confocal Microscopy are used to assess the

encapsulation efficiency of drug molecules within nanocarriers such as liposomes or nanoparticles. This ensures optimal drug loading capacity and controlled release characteristics(214).

Rheological Properties: Rheology measurements using techniques like Rheometry provide insights into the flow properties and viscosity of drug formulations. This is crucial for designing injectable formulations, creams, or gels with desired application and administration properties(215).

By employing these nano analytical techniques, pharmaceutical scientists can gain a comprehensive understanding of the physical, chemical, and structural properties of drug formulations. This knowledge enables them to optimize formulations for enhanced drug stability, efficacy, and patient compliance(216).

6.2. Quality Control and Assurance:

Nano analytical tools are indispensable for maintaining the quality and consistency of pharmaceutical products throughout the manufacturing process(217):

Batch-to-Batch Variability: Techniques such as DLS and SEM help in monitoring the particle size distribution and morphology of drug formulations across different batches. Any variations can be identified early, ensuring consistent product quality(218).

Contaminant Detection: XPS and Energy-Dispersive X-ray Spectroscopy (EDS) are used to detect and analyze contaminants or impurities in pharmaceutical samples. This ensures compliance with regulatory standards and patient safety(219).

Stability Studies: Long-term stability of drug formulations is assessed using techniques like FTIR, XRD, and Differential Scanning Calorimetry (DSC). Changes in crystallinity, chemical composition, or physical properties over time are monitored to ensure product shelf-life and efficacy(220).

Uniformity of Dosage Forms: SEM and AFM are employed to examine the surface uniformity and integrity of tablets, capsules, or patches. This ensures uniform drug distribution and dissolution rates for consistent dosing(221).

Validation of Cleaning Processes: SEM and XPS are used to validate cleaning procedures for manufacturing equipment. Residual traces of previous formulations or cleaning agents can be detected and eliminated to prevent cross-contamination(222).

Trace Elemental Analysis: ICP-MS (Inductively Coupled Plasma Mass Spectrometry) is utilized for trace elemental analysis in pharmaceuticals. It helps in detecting minute levels of heavy metals or toxic elements that can pose risks to patient safety(223).

By implementing these nano analytical techniques in quality control processes, pharmaceutical companies can ensure that their products meet stringent regulatory requirements, adhere to Good Manufacturing Practices (GMP), and deliver safe and effective treatments to patients(224).

6.3. Nanoparticle Characterization for Drug Delivery Systems:

Nano analytical techniques are essential for characterizing the properties and behavior of nanoparticles used in drug delivery systems(225):

Size and Size Distribution: DLS, TEM, and SEM are employed to measure the size, size distribution, and morphology of nanoparticles. This information is crucial for designing nanoparticles with optimal drug loading capacity and controlled release profiles(226).

Surface Functionalization: XPS and FTIR spectroscopy help in analyzing the surface chemistry and functional groups of nanoparticles. Surface modifications with polymers, ligands, or targeting moieties can be characterized to enhance biocompatibility and target-specific delivery(227).

Drug Encapsulation Efficiency: Fluorescence Spectroscopy and UV-Vis Spectroscopy are used to quantify the amount of drug encapsulated within nanoparticles. This ensures efficient drug loading and controlled release kinetics(228).

In vitro Release Studies: Techniques like HPLC (High-Performance Liquid Chromatography) combined with SEM or TEM are utilized for in vitro release studies of drug-loaded nanoparticles. This provides insights into the release kinetics, stability, and mechanisms of drug release from nanoparticles(229).

Biological Interactions: AFM and Confocal Microscopy allow researchers to study the interactions of nanoparticles with biological systems. Cellular uptake, intracellular trafficking, and cytotoxicity can be assessed to optimize nanoparticles for therapeutic efficacy and safety(230).

Stability in Biological Fluids: DLS and Zeta Potential measurements are used to assess the stability of nanoparticles in biological fluids such as blood or saliva. This ensures that nanoparticles retain their integrity and drug release properties in physiological conditions(231).

Characterizing nanoparticles with these nano analytical techniques is essential for developing successful drug delivery systems with enhanced therapeutic outcomes, reduced side effects, and improved patient compliance(232).

6.4. Detection of Impurities and Contaminants:

Nano analytical tools are invaluable for detecting, identifying, and quantifying impurities or contaminants in pharmaceutical products(233):

Particle Analysis: DLS, SEM, and TEM are used to analyze the size, morphology, and composition of particulate contaminants in pharmaceutical samples. This includes foreign particles, aggregates, or crystals that may affect product quality(234).

Chemical Composition: XPS, FTIR, and Raman Spectroscopy provide information on the chemical composition and structure of contaminants. This helps in identifying the source of contamination and taking corrective actions(235).

Trace Elemental Analysis: ICP-MS and Atomic Absorption Spectroscopy (AAS) are employed for detecting trace levels of heavy metals, such as lead, arsenic, or mercury, which can be harmful if present in pharmaceutical products(236).

Organic Impurities: GC-MS (Gas Chromatography-Mass Spectrometry) and HPLC are utilized for detecting organic impurities, such as residual solvents, degradation products, or impurities from raw materials(237).

Microbial Contamination: Microbial contamination is detected using techniques like Polymerase Chain Reaction (PCR) for genetic analysis or Microbiological Assays for viable counts. These methods ensure that pharmaceutical products are free from harmful microbes(238).

Cross-Contamination Prevention: SEM and XPS are used to validate cleaning procedures to prevent cross-contamination between different drug formulations or manufacturing equipment(239).

By employing these nano analytical techniques for impurity detection, pharmaceutical manufacturers can ensure the safety, purity, and efficacy of their products, meeting regulatory standards and safeguarding patient health(240).

7. Future Perspectives:

7.1. Emerging Trends in Nano Analytical Techniques:

Nano analytical techniques continue to evolve, driven by the need for higher resolution, sensitivity, and multi-modal capabilities(241). Some emerging trends in this field include:

Multimodal Imaging and Spectroscopy: Integration of multiple imaging and spectroscopic techniques into a single platform allows researchers to obtain comprehensive information about samples. For example, combining AFM with Raman spectroscopy enables simultaneous characterization of topography and chemical composition at the nanoscale(242).

3D Tomography and Reconstruction: Techniques such as Electron Tomography and X-ray Tomography are advancing towards three-dimensional imaging of nanostructures. This allows for detailed visualization of internal structures, pores, and interfaces within materials

and biological specimens(243).

Plasmonic and Optical Sensing: Plasmonic techniques, such as Surface-Enhanced Raman Spectroscopy (SERS), offer ultra-sensitive detection of molecules at the nanoscale. These methods are being explored for label-free sensing of biomolecules, environmental pollutants, and drug interactions(244).

Single-Particle Analysis: Advancements in techniques like Single-Particle Cryo-Electron Microscopy (Cryo-EM) enable the study of individual nanoparticles or biomolecules. This provides insights into heterogeneity, conformational dynamics, and interactions at the single-molecule level(245).

In-Situ and Operando Analysis: Real-time imaging and analysis under realistic conditions are becoming more feasible with in-situ techniques. Observing reactions, phase transitions, and structural changes as they occur provides deeper insights into material behavior(246).

Machine Learning and Big Data Analytics: Integration of machine learning algorithms with nano analytical data allows for faster analysis, pattern recognition, and prediction of material properties. This facilitates data-driven decision-making and accelerates discoveries(247).

Nanopore Sensing: Nanopore-based techniques, such as Nanopore Sequencing, offer rapid, label-free analysis of biomolecules like DNA and proteins. These methods have potential applications in personalized medicine, diagnostics, and drug screening(248).

Quantum Sensing: Quantum-based sensors, such as Quantum Dots or NV Centers in diamonds, are being explored for ultra-sensitive detection of magnetic fields, biomolecules, and molecular interactions. These sensors offer high precision and low detection limits(249).

7.2. Potential Breakthroughs in Pharmaceutical Analysis:

The integration of nano analytical techniques holds promise for several potential breakthroughs in pharmaceutical analysis(250):

Real-Time Drug Monitoring: Nanosensors capable of detecting drug concentrations in the body in real-time could revolutionize personalized medicine. These sensors, possibly implanted or wearable, would allow for precise dosing adjustments and monitoring of therapeutic levels(251).

Nanomedicine Design Optimization: Advanced imaging techniques combined with computational modeling can lead to the rational design of nanocarriers for drug delivery. Tailoring nanoparticles for specific tissues, diseases, and patient profiles could enhance efficacy and reduce side effects(252).

Targeted Drug Delivery Systems: Precision targeting of diseased cells or tissues using nano analytical tools enables the development of targeted therapies. Functionalized nanoparticles with ligands or antibodies can deliver drugs directly to the site of action, minimizing systemic exposure(253).

Predictive Pharmacokinetics and Pharmacodynamics: Incorporating nanoscale imaging and modeling into drug development processes can improve predictions of drug behavior in the body. This includes understanding drug distribution, metabolism, and response in different patient populations(254).

Theranostic Nanoparticles: Nanoparticles with combined diagnostic and therapeutic capabilities offer personalized treatment options. Imaging modalities integrated into nanoparticles allow for real-time monitoring of treatment response, guiding adjustments in therapy(255).

Biosensors for Disease Biomarkers: Nanoscale biosensors capable of detecting disease biomarkers in bodily fluids could enable early diagnosis and monitoring of diseases such as cancer, diabetes, and infectious diseases(256).

Nanoparticle Vaccine Delivery: Nano analytical techniques aid in the design of efficient vaccine delivery systems. Nanoparticles carrying antigens or adjuvants can enhance immune responses, leading to improved vaccine efficacy and durability(257).

Drug-Device Combinations: Nano analytical tools contribute to the development of smart drug-device combinations. These include implantable devices, microneedle patches, and controlled-release systems designed for precise drug delivery and patient convenience(258).

7.3. Role in Personalized Medicine and Targeted Therapies:

Nano analytical techniques are at the forefront of personalized medicine, offering tailored treatments based on individual patient characteristics(259):

Patient-Specific Drug Formulations: High-resolution imaging and characterization of nanoparticles allow for customizing drug formulations to suit patient needs. Variations in particle size, coating, or drug loading can be optimized for optimal efficacy and patient tolerance(260).

Biomarker Detection and Monitoring: Nanoscale biosensors and imaging tools enable the detection of specific biomarkers indicative of disease or treatment response. This facilitates early diagnosis, treatment monitoring, and adjustment of therapies in real-time(261).

Precision Drug Delivery: Functionalized nanoparticles with targeting ligands or antibodies enable precise delivery of drugs to diseased tissues or cells. This minimizes systemic side effects and enhances the therapeutic index of medications(262).

Genomic and Proteomic Analysis: Nano analytical techniques contribute to the study of individual genetic variations and protein expression profiles. This information guides the selection of personalized therapies, predicting drug responses and potential adverse reactions(263).

Theranostics for Integrated Diagnosis and Therapy: Theranostic nanoparticles combine diagnostic imaging and therapeutic functionalities in a single platform. These nanoparticles allow for non-invasive monitoring of treatment response while delivering targeted therapies(264).

Tailored Cancer Therapies: Nanoparticles designed for targeted drug delivery to cancer cells revolutionize cancer treatment. Imaging-guided therapies, such as photodynamic therapy or magnetic hyperthermia, offer precise and localized treatment options(265).

Regenerative Medicine and Tissue Engineering: Nano analytical tools aid in the development of biomimetic scaffolds and nanoparticles for tissue regeneration. These personalized approaches facilitate the repair of damaged tissues and organs(266).

Remote Monitoring and Telemedicine: Wearable nanosensors or implantable devices provide continuous monitoring of patient health parameters. This data, transmitted remotely to healthcare providers, enables proactive interventions and personalized care plans(267).

As nano analytical techniques continue to advance, their integration into personalized medicine holds immense potential for improving patient outcomes, reducing healthcare costs, and ushering in a new era of targeted, patient-centric therapies. These developments mark a significant shift towards precision medicine, where treatments are tailored to the unique biology and needs of each individual(268).

Conclusion:

Nano analytical techniques represent a cornerstone of modern pharmaceutical analysis, offering invaluable insights that shape every stage of drug development and patient care. By delving into the intricate details of drug formulations, these techniques enable optimization for enhanced stability, bioavailability, and targeted delivery, fostering the creation of innovative therapies. Moreover, their role in stringent quality control processes ensures the production of safe and effective pharmaceutical products that comply with regulatory standards. The evolution of nano analytical tools continues to drive breakthroughs in personalized medicine, nanomedicine, and efficient drug development, promising transformative outcomes for healthcare. However, to fully harness their potential, further research and development are imperative. This

entails advancing instrumentation, exploring novel applications, overcoming technical challenges, and fostering collaborative initiatives across academia, industry, and regulatory sectors.

Moreover, emphasis on education and training programs is crucial to cultivate a skilled workforce capable of leveraging these technologies effectively. By investing in these endeavors, the pharmaceutical industry can not only advance drug discovery and formulation but also pave the way for personalized therapies tailored to individual patient needs. Ultimately, the continued advancement of nano analytical techniques holds the promise of revolutionizing healthcare, improving patient outcomes, and ushering in a new era of precision medicine. Through collective efforts, we can unlock the full potential of these tools to address the complex challenges of disease treatment and propel pharmaceutical innovation towards a brighter, healthier future.

Acknowledgement:

The authors are thankful to Raghavendra Institute of Pharmaceutical Education and Research, Ananthapur.

Conflict of interest:

The authors do not have any conflict of interest.

REFERENCES

1. Crommelin DJ, Anchordoquy TJ, Volkin DB, Jiskoot W, Mastrobattista E. Addressing the cold reality of mRNA vaccine stability. *Journal of pharmaceutical sciences*. 2021;110(3):997-1001.
2. Sardella M, Belcher G, Lungu C, Ignoni T, Camisa M, Stenver DI, et al. Monitoring the manufacturing and quality of medicines: a fundamental task of pharmacovigilance. *Therapeutic Advances in Drug Safety*. 2021;12:20420986211038436.
3. Markl D, Warman M, Dumarey M, Bergman E-L, Folestad S, Shi Z, et al. Review of real-time release testing of pharmaceutical tablets: State-of-the art, challenges and future perspective. *International journal of pharmaceutics*. 2020;582:119353.
4. Wang H, Chen Y, Wang L, Liu Q, Yang S, Wang C. Advancing herbal medicine: enhancing product quality and safety through robust quality control practices. *Frontiers in Pharmacology*. 2023;14:1265178.
5. Mofid S, Bolislis WR, Kühler TC. Real-world data in the postapproval setting as applied by the EMA and the US FDA. *Clinical Therapeutics*. 2022;44(2):306-22.
6. González-González O, Ramirez IO, Ramirez BI, O'Connell P, Ballesteros MP, Torrado JJ, et al. Drug stability: ICH versus accelerated predictive stability studies. *Pharmaceutics*. 2022;14(11):2324.
7. Al-Halaseh L, Issa R, Said R, Al-suhaimat R. Antioxidant Activity, Phytochemical Screening, and LC/MS-MS Characterization of Polyphenol Content of Jordanian Habitat of Pennisetum Setaceum Aqueous Leaf Extract. *Jordan Journal of Pharmaceutical Sciences*. 2024;17(4):706-16.
8. Bolla AS, Patel AR, Priefer R. The silent development of counterfeit medications in developing countries–A systematic review of detection technologies. *International Journal of Pharmaceutics*. 2020;587:119702.
9. Kiriiri GK, Njogu PM, Mwangi AN. Exploring different approaches to improve the success of drug discovery and development projects: a review. *Future Journal of Pharmaceutical Sciences*. 2020;6:1-12.
10. Hotez PJ, Batista C, Amor YB, Ergonul O, Figueroa JP, Gilbert S, et al. Global public health security and justice for vaccines and therapeutics in the COVID-19 pandemic. *EClinicalMedicine*. 2021;39.

11. López-Sánchez C, de Andrés F, Ríos Á. Implications of analytical nanoscience in pharmaceutical and biomedical fields: a critical view. *Journal of Pharmaceutical and Biomedical Analysis*. 2024:116118.
12. Milson S, Derrick R. Microfluidics and Nanotechnology: a Synergistic Approach for Bioengineering. *EasyChair*. 2023. Report No.: 2516-2314.
13. Liu M, Li X. Mechanical properties measurement of materials and devices at micro-and nano-scale by optical methods: A review. *Optics and Lasers in Engineering*. 2022;150:106853.
14. Chen Y, Yu B, Lu W, Wang B, Sun D, Jiao K, et al. Review on numerical simulation of boiling heat transfer from atomistic to mesoscopic and macroscopic scales. *International Journal of Heat and Mass Transfer*. 2024;225:125396.
15. Mitchell S, Qin R, Zheng N, Pérez-Ramírez J. Nanoscale engineering of catalytic materials for sustainable technologies. *Nature nanotechnology*. 2021;16(2):129-39.
16. Patel JK, Patel A, Bhatia D. Introduction to nanomaterials and nanotechnology. *Emerging technologies for nanoparticle manufacturing: Springer*; 2021. p. 3-23.
17. Roco MC, Williams RS, Alivisatos P. Nanotechnology research directions: IWGN workshop report: vision for nanotechnology in the next decade: *Springer Science & Business Media*; 2000.
18. Sajid M, Płotka-Wasylka J. Nanoparticles: Synthesis, characteristics, and applications in analytical and other sciences. *Microchemical Journal*. 2020;154:104623.
19. Zielińska A, Szalata M, Gorczyński A, Karczewski J, Eder P, Severino P, et al. Cancer nanopharmaceuticals: Physicochemical characterization and in vitro/in vivo applications. *Cancers*. 2021;13(8):1896.
20. Asafa T, Adedokun O, Dele-Afolabi T. Characterization techniques in nanotechnology: the state of the art. *Microbial Nanobiotechnology: Principles and Applications*. 2021:21-73.
21. Gault B, Chiaramonti A, Cojocaru-Mirédin O, Stender P, Dubosq R, Freysoldt C, et al. Atom probe tomography. *Nature Reviews Methods Primers*. 2021;1(1):51.
22. Betz UA, Arora L, Assal RA, Azevedo H, Baldwin J, Becker MS, et al. Game changers in science and technology-now and beyond. *Technological Forecasting and Social Change*. 2023;193:122588.
23. Fahdawi A, Shalan N, Lafi Z, Markab O. Analytical approaches for assessing curcumin and nicotinamide Co-encapsulated in liposomal formulation: UV spectrophotometry and HPLC validation. *Jordan Journal of Pharmaceutical Sciences*. 2024;17(3):468-80.
24. Mousa SA, Bawa R, Audette GF. The road from nanomedicine to precision medicine: *CRC Press*. 2020.
25. Lee Y-C, Moon J-Y, Lee Y-C, Moon J-Y. Introduction to nanotechnology and bionanotechnology. *Introduction to bionanotechnology*. 2020:1-14.
26. Sahu T, Ratre YK, Chauhan S, Bhaskar L, Nair MP, Verma HK. Nanotechnology based drug delivery system: Current strategies and emerging therapeutic potential for medical science. *Journal of Drug Delivery Science and Technology*. 2021;63:102487.
27. Verma S, Goand UK, Husain A, Katekar RA, Garg R, Gayen JR. Challenges of peptide and protein drug delivery by oral route: Current strategies to improve the bioavailability. *Drug development research*. 2021;82(7):927-44.
28. Crintea A, Dutu AG, Sovrea A, Constantin A-M, Samasca G, Masalar AL, et al. Nanocarriers for drug delivery: an overview with emphasis on vitamin D and K transportation. *Nanomaterials*. 2022;12(8):1376.
29. Raj S, Khurana S, Choudhari R, Kesari KK, Kamal MA, Garg N, et al., editors. Specific targeting cancer cells with nanoparticles and drug delivery in cancer therapy. *Seminars in cancer biology*. 2021: Elsevier.
30. Lima ES, Dos Santos D, Souza AL, Macedo ME, Bandeira ME, Junior SSS, et al. RNA combined with nanoformulation to advance therapeutic technologies. *Pharmaceuticals*. 2023;16(12):1634.

31. Chen L, Hong W, Ren W, Xu T, Qian Z, He Z. Recent progress in targeted delivery vectors based on biomimetic nanoparticles. *Signal transduction and targeted therapy*. 2021;6(1):225.
32. Nasir A, Khan A, Li J, Naeem M, Khalil AA, Khan K, et al. Nanotechnology, a tool for diagnostics and treatment of cancer. *Current topics in medicinal chemistry*. 2021;21(15):1360-76.
33. De Jong WH, Geertsma RE, Borchard G. Regulatory safety evaluation of nanomedical products: key issues to refine. *Drug Delivery and Translational Research*. 2022;12(9):2042-7.
34. Sharma A, Mittal K, Arora D, Ganti SS. A comprehensive review on strategies for new drug discovery and enhanced productivity in research and development: recent advancements and future prospectives. *Mini-Reviews in Organic Chemistry*. 2021;18(3):361-82.
35. dos Santos J, de Oliveira RS, de Oliveira TV, Velho MC, Konrad MV, da Silva GS, et al. 3D printing and nanotechnology: a multiscale alliance in personalized medicine. *Advanced functional materials*. 2021;31(16):2009691.
36. Mariano S, Tacconi S, Fidaleo M, Rossi M, Dini L. Micro and nanoplastics identification: classic methods and innovative detection techniques. *Frontiers in toxicology*. 2021;3:636640.
37. Dena ASA, Abdelaziz OA, El-Sherbiny IM. Nanomaterials: classification, composition, and recent advances in synthesis. *Immunomodulatory Effects of Nanomaterials*. 2022:1-19.
38. Andreo J, Ettlinger R, Zaremba O, Pena Q, Lächelt U, de Luis RF, et al. Reticular nanoscience: bottom-up assembly nanotechnology. *Journal of the American Chemical Society*. 2022;144(17):7531-50.
39. Falsafi SR, Rostamabadi H, Assadpour E, Jafari SM. Morphology and microstructural analysis of bioactive-loaded micro/nanocarriers via microscopy techniques; CLSM/SEM/TEM/AFM. *Advances in Colloid and Interface Science*. 2020;280:102166.
40. Chee SW, Lunkenbein T, Schlögl R, Cuenya BR. In situ and operando electron microscopy in heterogeneous catalysis—insights into multi-scale chemical dynamics. *Journal of Physics: Condensed Matter*. 2021;33(15):153001.
41. Son D, Cho S, Nam J, Lee H, Kim M. X-ray-based spectroscopic techniques for characterization of polymer nanocomposite materials at a molecular level. *Polymers*. 2020;12(5):1053.
42. Salahshoori I, Jorabchi MN, Ghasemi S, Golriz M, Wohlrab S, Khonakdar HA. An in silico study of sustainable drug pollutants removal using carboxylic acid functionalized-MOF nanostructures (MIL-53 (Al)-(COOH) 2): Towards a greener future. *Desalination*. 2023;559:116654.
43. Babick F. Dynamic light scattering (DLS). *Characterization of nanoparticles: Elsevier*. 2020: 137-72.
44. Asha AB, Narain R. Nanomaterials properties. Polymer science and nanotechnology: Elsevier. 2020: 343-59.
45. Hodoroaba V-D. Energy-dispersive X-ray spectroscopy (EDS). *Characterization of Nanoparticles: Elsevier*. 2020: 397-417.
46. Malik S, Muhammad K, Waheed Y. Nanotechnology: A revolution in modern industry. *Molecules*. 2023;28(2):661.
47. Jia L, Zhang P, Sun H, Dai Y, Liang S, Bai X, et al. Optimization of nanoparticles for smart drug delivery: a review. *Nanomaterials*. 2021;11(11):2790.
48. Catalano PN, Chaudhary RG, Desimone MF, Santo-Orihuela PL. A survey on analytical methods for the characterization of green synthesized nanomaterials. *Current Pharmaceutical Biotechnology*. 2021;22(6):823-47.
49. Möckl L, Moerner W. Super-resolution microscopy with single molecules in biology and beyond–essentials, current trends, and future challenges. *Journal of the American Chemical Society*. 2020;142(42):17828-44.

50. Shi X, Qing W, Marhaba T, Zhang W. Atomic force microscopy-Scanning electrochemical microscopy (AFM-SECM) for nanoscale topographical and electrochemical characterization: Principles, applications and perspectives. *Electrochimica Acta*. 2020;332:135472.
51. Verma A, Yadav BC. Comprehensive review on two dimensional nanomaterials for optical biosensors: Present progress and outlook. *Sustainable Materials and Technologies*. 2024:e00900.
52. Jayawardena HSN, Liyanage SH, Rathnayake K, Patel U, Yan M. Analytical methods for characterization of nanomaterial surfaces. *Analytical chemistry*. 2021;93(4):1889-911.
53. Ghezzi M, Pescina S, Padula C, Santi P, Del Favero E, Cantù L, et al. Polymeric micelles in drug delivery: An insight of the techniques for their characterization and assessment in biorelevant conditions. *Journal of Controlled Release*. 2021;332:312-36.
54. Chen-Wiegart Y-CK, Campbell SI, Yager KG, Liu Y, Frenkel AI, Yang L, et al. Multi-Modal Synchrotron Characterization: Modern Techniques and Data Analysis. HANDBOOK ON BIG DATA AND MACHINE LEARNING IN THE PHYSICAL SCIENCES: Volume 2 Advanced Analysis Solutions for Leading Experimental Techniques: *World Scientific*; 2020. p. 39-64.
55. Wang B, Zhong S, Lee T-L, Fancey KS, Mi J. Non-destructive testing and evaluation of composite materials/structures: A state-of-the-art review. *Advances in mechanical engineering*. 2020;12(4):1687814020913761.
56. Zhou Y, Su M, Yu X, Zhang Y, Wang J-G, Ren X, et al. Real-time mass spectrometric characterization of the solid–electrolyte interphase of a lithium-ion battery. *Nature nanotechnology*. 2020;15(3):224-30.
57. Frosch T, Knebl A, Frosch T. Recent advances in nano-photonic techniques for pharmaceutical drug monitoring with emphasis on Raman spectroscopy. *Nanophotonics*. 2020;9(1):19-37.
58. Salem H, Elsoud FA, Magdy A, Heshmat D, Soliman AA, Wissa K, et al. Spectroscopic methods for analysis of nano drug distribution system. *Pharm Anal Acta*. 2020;11:619.
59. Nejati S, Vadeghani EM, Khorshidi S, Karkhaneh A. Role of particle shape on efficient and organ-based drug delivery. *European Polymer Journal*. 2020;122:109353.
60. Bastogne T, Caputo F, Prina-Mello A, Borgos S, Barberi-Heyob M. A state of the art in analytical quality-by-design and perspectives in characterization of nano-enabled medicinal products. *Journal of Pharmaceutical and Biomedical Analysis*. 2022;219:114911.
61. Heredia NS, Vizuete K, Flores-Calero M, Pazmiño V K, Pilaquinga F, Kumar B, et al. Comparative statistical analysis of the release kinetics models for nanoprecipitated drug delivery systems based on poly (lactic-co-glycolic acid). *PLoS One*. 2022;17(3):e0264825.
62. Singh D, Isharani R. A Detailed Review on Analytical Methods to Manage the Impurities in Drug Substances. *Open Access Library Journal*. 2023;10(8):1-18.
63. Goel H, Saini K, Razdan K, Khurana RK, Elkordy AA, Singh KK. In vitro physicochemical characterization of nanocarriers: a road to optimization. *Nanoparticle Therapeutics: Elsevier*; 2022. p. 133-79.
64. Augustine R, Hasan A, Primavera R, Wilson RJ, Thakor AS, Kevadiya BD. Cellular uptake and retention of nanoparticles: Insights on particle properties and interaction with cellular components. *Materials Today Communications*. 2020;25:101692.
65. Pantaleão SQ, Fernandes PO, Gonçalves JE, Maltarollo VG, Honorio KM. Recent advances in the prediction of pharmacokinetics properties in drug design studies: a review. *ChemMedChem*. 2022;17(1):e202100542.
66. Valencia PM, Farokhzad OC, Karnik R, Langer R. Microfluidic technologies for accelerating the clinical translation of nanoparticles. *Nano-enabled medical applications*. 2020:93-112.

67. Dangeti A, Bynagari DG, Vydani K. Revolutionizing Drug Formulation: Harnessing Artificial Intelligence and Machine Learning for Enhanced Stability, Formulation Optimization, and Accelerated Development. 2023.
68. Alzoubi L, Aljabali AA, Tambuwala MM. Empowering precision medicine: the impact of 3d printing on personalized therapeutic. *AAPS PharmSciTech*. 2023;24(8):228.
69. Le TKN, Le N. Formulation and Evaluation of Herbal Emulsion-Based Gel Containing Combined Essential Oils from Melaleuca alternifolia and Citrus hystrix. *Jordan Journal of Pharmaceutical Sciences*. 2024;17(1):163-73.
70. Relucenti M, Familiari G, Donfrancesco O, Taurino M, Li X, Chen R, et al. Microscopy methods for biofilm imaging: focus on SEM and VP-SEM pros and cons. *Biology*. 2021;10(1):51.
71. Yampolsky N, Rybarcyk L, Henestroza E, Draganic I. Modeling of tungsten filament in gas discharge in H− ion source. *Review of Scientific Instruments*. 2021;92(11).
72. Kim HT, Pathak VB, Hojbota CI, Mirzaie M, Pae KH, Kim CM, et al. Multi-GeV laser wakefield electron acceleration with PW lasers. *Applied Sciences*. 2021;11(13):5831.
73. Shao M, Vijayan S, Nandwana P, Jinschek JR. The effect of beam scan strategies on microstructural variations in Ti-6Al-4V fabricated by electron beam powder bed fusion. *Materials & Design*. 2020;196:109165.
74. Kim H, Murata MM, Chang H, Lee SH, Kim J, Lee JH, et al. Optical and electron microscopy for analysis of nanomaterials. *Nanotechnology for Bioapplications*. 2021:277-87.
75. Nohl JF, Farr NT, Sun Y, Hughes GM, Cussen SA, Rodenburg C. Low-voltage SEM of air-sensitive powders: From sample preparation to micro/nano analysis with secondary electron hyperspectral imaging. *Micron*. 2022;156:103234.
76. Li Y, Yang J, Pan Z, Tong W. Nanoscale pore structure and mechanical property analysis of coal: An insight combining AFM and SEM images. *Fuel*. 2020;260:116352.
77. Rahamathulla M, Bhosale RR, Osmani RA, Mahima KC, Johnson AP, Hani U, et al. Carbon nanotubes: Current perspectives on diverse applications in targeted drug delivery and therapies. *Materials*. 2021;14(21):6707.
78. Witika BA, Aucamp M, Mweetwa LL, Makoni PA. Application of fundamental techniques for physicochemical characterizations to understand post-formulation performance of pharmaceutical nanocrystalline materials. *Crystals*. 2021;11(3):310.
79. Ghourichay MP, Kiaie SH, Nokhodchi A, Javadzadeh Y. Formulation and quality control of orally disintegrating tablets (ODTs): recent advances and perspectives. *BioMed Research International*. 2021;2021:1-12.
80. Espinoza MJC, Lin K-S, Weng M-T, Kunene SC, Wang SS-S. In vitro studies of Pluronic F127 coated magnetic silica nanocarriers for drug delivery system targeting liver cancer. *European Polymer Journal*. 2021;153:110504.
81. Lee W, Rho N-K, Yang E-J. Determination of hyaluronic acid dermal filler impurities using SEM/EDS analysis. *Polymers*. 2023;15(7):1649.
82. Serra-Maia R, Kumar P, Meng AC, Foucher AC, Kang Y, Karki K, et al. Nanoscale chemical and structural analysis during in situ scanning/transmission electron microscopy in liquids. *ACS nano*. 2021;15(6):10228-40.
83. Zhang H, Jimbo Y, Niwata A, Ikeda A, Yasuhara A, Ovidiu C, et al. High-endurance micro-engineered LaB6 nanowire electron source for high-resolution electron microscopy. *Nature nanotechnology*. 2022;17(1):21-6.
84. Chen Q, Dwyer C, Sheng G, Zhu C, Li X, Zheng C, et al. Imaging beam-sensitive materials by electron microscopy. *Advanced Materials*. 2020;32(16):1907619.

85. Franken LE, Grünewald K, Boekema EJ, Stuart MC. A technical introduction to transmission electron microscopy for soft-matter: Imaging, possibilities, choices, and technical developments. *Small*. 2020;16(14):1906198.
86. Savitzky BH, Zeltmann SE, Hughes LA, Brown HG, Zhao S, Pelz PM, et al. py4DSTEM: A software package for four-dimensional scanning transmission electron microscopy data analysis. *Microscopy and Microanalysis*. 2021;27(4):712-43.
87. Luo Q, Holm EA, Wang C. A transfer learning approach for improved classification of carbon nanomaterials from TEM images. *Nanoscale Advances*. 2021;3(1):206-13.
88. Egerton R, Watanabe M. Spatial resolution in transmission electron microscopy. *Micron*. 2022;160:103304.
89. Mabrouk M, Das DB, Salem ZA, Beherei HH. Nanomaterials for biomedical applications: Production, characterisations, recent trends and difficulties. *Molecules*. 2021;26(4):1077.
90. Nikezić AVV, Bondžić AM, Vasić VM. Drug delivery systems based on nanoparticles and related nanostructures. *European Journal of Pharmaceutical Sciences*. 2020;151:105412.
91. Pokharkar V, Suryawanshi S, Dhapte-Pawar V. Exploring micellar-based polymeric systems for effective nose-to-brain drug delivery as potential neurotherapeutics. *Drug Delivery and Translational Research*. 2020;10:1019-31.
92. Bernstein J. Polymorphism in Molecular Crystals 2e: International Union of Crystal; 2020.
93. Pandi P, Bulusu R, Kommineni N, Khan W, Singh M. Amorphous solid dispersions: An update for preparation, characterization, mechanism on bioavailability, stability, regulatory considerations and marketed products. *International journal of pharmaceutics*. 2020;586:119560.
94. Gawin-Mikołajewicz A, Nartowski KP, Dyba AJ, Gołkowska AM, Malec K, Karolewicz Be. Ophthalmic nanoemulsions: From composition to technological processes and quality control. *Molecular pharmaceutics*. 2021;18(10):3719-40.
95. Rane N. Transformers in Material Science: Roles, Challenges, and Future Scope. *Challenges, and Future Scope* (March 26, 2023). 2023.
96. Guimarães D, Cavaco-Paulo A, Nogueira E. Design of liposomes as drug delivery system for therapeutic applications. *International journal of pharmaceutics*. 2021;601:120571.
97. Zielińska A, Carreiró F, Oliveira AM, Neves A, Pires B, Venkatesh DN, et al. Polymeric nanoparticles: production, characterization, toxicology and ecotoxicology. *Molecules*. 2020;25(16):3731.
98. Lynch I, Dawson KA. Protein–nanoparticle interactions. *Nano-enabled medical applications*. 2020:231-50.
99. Kopac T. Protein corona, understanding the nanoparticle–protein interactions and future perspectives: A critical review. *International Journal of Biological Macromolecules*. 2021;169:290-301.
100. Salo-Ahen OM, Alanko I, Bhadane R, Bonvin AM, Honorato RV, Hossain S, et al. Molecular dynamics simulations in drug discovery and pharmaceutical development. *Processes*. 2020;9(1):71.
101. Silge A, Weber K, Cialla-May D, Müller-Bötticher L, Fischer D, Popp J. Trends in pharmaceutical analysis and quality control by modern Raman spectroscopic techniques. *TrAC Trends in Analytical Chemistry*. 2022;153:116623.
102. Bian K, Gerber C, Heinrich AJ, Müller DJ, Scheuring S, Jiang Y. Scanning probe microscopy. *Nature Reviews Methods Primers*. 2021;1(1):36.
103. Venkateshaiah A, Padil VV, Nagalakshmaiah M, Waclawek S, Černík M, Varma RS. Microscopic techniques for the analysis of micro and nanostructures of biopolymers and their derivatives. *Polymers*. 2020;12(3):512.

104. Alunda BO, Lee YJ. Cantilever-based sensors for high speed atomic force microscopy. *Sensors*. 2020;20(17):4784.
105. Burnham NA, Kulik AJ. Surface forces and adhesion. Handbook of micro/nano tribology: CRC Press. 2020:247-71.
106. Garcia R. Nanomechanical mapping of soft materials with the atomic force microscope: methods, theory and applications. *Chemical Society Reviews*. 2020;49(16):5850-84.
107. Habibullah H. 30 years of atomic force microscopy: creep, hysteresis, cross-coupling, and vibration problems of piezoelectric tube scanners. *Measurement*. 2020;159:107776.
108. Müller DJ, Dumitru AC, Lo Giudice C, Gaub HE, Hinterdorfer P, Hummer G, et al. Atomic force microscopy-based force spectroscopy and multiparametric imaging of biomolecular and cellular systems. *Chemical reviews*. 2020;121(19):11701-25.
109. Xia F, Youcef-Toumi K. Advanced atomic force microscopy modes for biomedical research. *Biosensors*. 2022;12(12):1116.
110. Zajda J, Wróblewska A, Ruzik L, Matczuk M. Methodology for characterization of platinum-based drug's targeted delivery nanosystems. *Journal of Controlled Release*. 2021;335:178-90.
111. Porojan L, Vasiliu R-D, Porojan S-D, Bîrdeanu M-I. Surface quality evaluation of removable thermoplastic dental appliances related to staining beverages and cleaning agents. *Polymers*. 2020;12(8):1736.
112. Struczyńska M, Firkowska-Boden I, Levandovsky N, Henschler R, Kassir N, Jandt KD. How Crystallographic Orientation-Induced Fibrinogen Conformation Affects Platelet Adhesion and Activation on TiO2. *Advanced Healthcare Materials*. 2023;12(13):2202508.
113. Zhang X, Ma G, Wei W. Simulation of nanoparticles interacting with a cell membrane: probing the structural basis and potential biomedical application. *NPG Asia Materials*. 2021;13(1):52.
114. Huang J, Chen H, Zheng Y, Yang Y, Zhang Y, Gao B. Microplastic pollution in soils and groundwater: Characteristics, analytical methods and impacts. *Chemical Engineering Journal*. 2021;425:131870.
115. Jha R, Mayanovic RA. A review of the preparation, characterization, and applications of chitosan nanoparticles in nanomedicine. *Nanomaterials*. 2023;13(8):1302.
116. Seo K-S, Bajracharya R, Lee SH, Han H-K. Pharmaceutical application of tablet film coating. *Pharmaceutics*. 2020;12(9):853.
117. Souri M, Soltani M, Kashkooli FM, Shahvandi MK, Chiani M, Shariati FS, et al. Towards principled design of cancer nanomedicine to accelerate clinical translation. *Materials Today Bio*. 2022;13:100208.
118. Nguyen-Tri P, Ghassemi P, Carriere P, Nanda S, Assadi AA, Nguyen DD. Recent applications of advanced atomic force microscopy in polymer science: A review. *Polymers*. 2020;12(5):1142.
119. Farkas N, Kramar JA. Dynamic light scattering distributions by any means. *Journal of Nanoparticle Research*. 2021;23(5):120.
120. Kumar S, Gunaseelan M, Vaippully R, Kumar A, Ajith M, Vaidya G, et al. Pitch-rotational manipulation of single cells and particles using single-beam thermo-optical tweezers. *Biomedical Optics Express*. 2020;11(7):3555-66.
121. Förster R, Weidlich S, Nissen M, Wieduwilt T, Kobelke J, Goldfain AM, et al. Tracking and analyzing the Brownian motion of nano-objects inside hollow core fibers. *ACS sensors*. 2020;5(3):879-86.
122. Buikema A, Cahillane C, Mansell G, Blair C, Abbott R, Adams C, et al. Sensitivity and performance of the Advanced LIGO detectors in the third observing run. *Physical Review D*. 2020;102(6):062003.
123. Zhong H-S, Deng Y-H, Qin J, Wang H, Chen M-C, Peng L-C, et al. Phase-programmable gaussian boson sampling using stimulated squeezed light. *Physical review letters*. 2021;127(18):180502.

124. Tosi MM, Ramos AP, Esposto BS, Jafari SM. Dynamic light scattering (DLS) of nanoencapsulated food ingredients. *Characterization of nanoencapsulated food ingredients: Elsevier*. 2020. p. 191-211.
125. Kurian TK, Banik S, Gopal D, Chakrabarti S, Mazumder N. Elucidating methods for isolation and quantification of exosomes: a review. *Molecular biotechnology*. 2021;63:249-66.
126. Yaraki MT, Tan YN. Recent advances in metallic nanobiosensors development: colorimetric, dynamic light scattering and fluorescence detection. *Sensors international*. 2020;1:100049.
127. Atanase LI. Micellar drug delivery systems based on natural biopolymers. *Polymers*. 2021;13(3):477.
128. Le Basle Y, Chennell P, Tokhadze N, Astier A, Sautou V. Physicochemical stability of monoclonal antibodies: a review. *Journal of Pharmaceutical Sciences*. 2020;109(1):169-90.
129. Samrot AV, Sean TC, Kudaiyappan T, Bisyarah U, Mirarmandi A, Abubakar A, et al. Production, characterization and application of nanocarriers made of polysaccharides, proteins, bio-polyesters and other biopolymers: A review. *International journal of biological macromolecules*. 2020;165:3088-105.
130. Cun D, Zhang C, Bera H, Yang M. Particle engineering principles and technologies for pharmaceutical biologics. *Advanced Drug Delivery Reviews*. 2021;174:140-67.
131. Pedroso-Santana S, Fleitas-Salazar N. Ionotropic gelation method in the synthesis of nanoparticles/microparticles for biomedical purposes. *Polymer International*. 2020;69(5):443-7.
132. Mehryab F, Rabbani S, Shahhosseini S, Shekari F, Fatahi Y, Baharvand H, et al. Exosomes as a next-generation drug delivery system: An update on drug loading approaches, characterization, and clinical application challenges. *Acta biomaterialia*. 2020;113:42-62.
133. Lombardo D, Kiselev MA. Methods of liposomes preparation: Formation and control factors of versatile nanocarriers for biomedical and nanomedicine application. *Pharmaceutics*. 2022;14(3):543.
134. Pham NB, Meng WS. Protein aggregation and immunogenicity of biotherapeutics. *International journal of pharmaceutics*. 2020;585:119523.
135. Lundahl ML, Fogli S, Colavita PE, Scanlan EM. Aggregation of protein therapeutics enhances their immunogenicity: causes and mitigation strategies. *RSC chemical biology*. 2021;2(4):1004-20.
136. Kenry, Yeo T, Manghnani PN, Middha E, Pan Y, Chen H, et al. Mechanistic understanding of the biological responses to polymeric nanoparticles. *ACS nano*. 2020;14(4):4509-22.
137. Gross-Rother J, Blech M, Preis E, Bakowsky U, Garidel P. Particle detection and characterization for biopharmaceutical applications: current principles of established and alternative techniques. *Pharmaceutics*. 2020;12(11):1112.
138. Clogston JD, Hackley VA, Prina-Mello A, Puri S, Sonzini S, Soo PL. Sizing up the next generation of nanomedicines. Pharmaceutical research. 2020;37:1-10.
139. Stevie FA, Donley CL. Introduction to x-ray photoelectron spectroscopy. *Journal of Vacuum Science & Technology A*. 2020;38(6).
140. Sedigh Rahimabadi P, Khodaei M, Koswattage KR. Review on applications of synchrotron-based X-ray techniques in materials characterization. *X-Ray Spectrometry*. 2020;49(3):348-73.
141. Santra R, Young L. Interaction of intense x-ray beams with atoms. *Synchrotron Light Sources and Free-Electron Lasers: Accelerator Physics, Instrumentation and Science Applications*. 2020:1435-62.
142. Istone WK. X-ray photoelectron spectroscopy (XPS). *Surface analysis of paper: CRC Press*. 2020: 235-68.

143. Major GH, Fairley N, Sherwood P, Linford MR, Terry J, Fernandez V, et al. Practical guide for curve fitting in x-ray photoelectron spectroscopy. *Journal of Vacuum Science & Technology A*. 2020;38(6).
144. Krishna DNG, Philip J. Review on surface-characterization applications of X-ray photoelectron spectroscopy (XPS): Recent developments and challenges. *Applied Surface Science Advances*. 2022;12:100332.
145. Greczynski G, Hultman L. X-ray photoelectron spectroscopy: towards reliable binding energy referencing. *Progress in Materials Science*. 2020;107:100591.
146. Wang Y, Jing B, Wang F, Wang S, Liu X, Ao Z, et al. Mechanism Insight into enhanced photodegradation of pharmaceuticals and personal care products in natural water matrix over crystalline graphitic carbon nitrides. *Water Research*. 2020;180:115925.
147. Chen H, Paul S, Xu H, Wang K, Mahanthappa MK, Sun CC. Reduction of punch-sticking propensity of celecoxib by spherical crystallization via polymer assisted quasi-emulsion solvent diffusion. *Molecular pharmaceutics*. 2020;17(4):1387-96.
148. Shakiba S, Astete CE, Paudel S, Sabliov CM, Rodrigues DF, Louie SM. Emerging investigator series: polymeric nanocarriers for agricultural applications: synthesis, characterization, and environmental and biological interactions. *Environmental Science: Nano*. 2020;7(1):37-67.
149. Cui H, Surendhiran D, Li C, Lin L. Biodegradable zein active film containing chitosan nanoparticle encapsulated with pomegranate peel extract for food packaging. *Food Packaging and Shelf Life*. 2020;24:100511.
150. Lu X, Li M, Huang C, Lowinger MB, Xu W, Yu L, et al. Atomic-level drug substance and polymer interaction in posaconazole amorphous solid dispersion from solid-state NMR. *Molecular pharmaceutics*. 2020;17(7):2585-98.
151. Osman N, Devnarain N, Omolo CA, Fasiku V, Jaglal Y, Govender T. Surface modification of nano-drug delivery systems for enhancing antibiotic delivery and activity. *Wiley Interdisciplinary Reviews: Nanomedicine and Nanobiotechnology*. 2022;14(1):e1758.
152. Shi L, Zhang J, Zhao M, Tang S, Cheng X, Zhang W, et al. Effects of polyethylene glycol on the surface of nanoparticles for targeted drug delivery. *Nanoscale*. 2021;13(24):10748-64.
153. Silva M, Baltrus JP, Williams C, Knopf A, Zhang L, Baltrusaitis J. Heterogeneous photo-Fenton-like degradation of emerging pharmaceutical contaminants in wastewater using Cu-doped MgO nanoparticles. *Applied Catalysis A: General*. 2022;630:118468.
154. Azar D, Lott JT, Jabbarzadeh E, Shazly T, Kolachalama VB. Surface modification using ultraviolet-ozone treatment enhances acute drug transfer in drug-coated balloon therapy. *Langmuir*. 2020;36(17):4645-53.
155. Rizzarelli P, Rapisarda M, Valenti G. Mass spectrometry in bioresorbable polymer development, degradation and drug-release tracking. *Rapid Communications in Mass Spectrometry*. 2020;34:e8697.
156. Baig N, Kammakakam I, Falath W. Nanomaterials: A review of synthesis methods, properties, recent progress, and challenges. *Materials Advances*. 2021;2(6):1821-71.
157. Kubota R, Tanaka W, Hamachi I. Microscopic imaging techniques for molecular assemblies: electron, atomic force, and confocal microscopies. *Chemical Reviews*. 2021;121(22):14281-347.
158. Valli J, Garcia-Burgos A, Rooney LM, e Oliveira BVdM, Duncan RR, Rickman C. Seeing beyond the limit: A guide to choosing the right super-resolution microscopy technique. *Journal of Biological Chemistry*. 2021;297(1).

159. Yang Y, Xiong Y, Zeng R, Lu X, Krumov M, Huang X, et al. Operando methods in electrocatalysis. *ACS Catalysis*. 2021;11(3):1136-78.
160. Luque D, Castón JR. Cryo-electron microscopy for the study of virus assembly. *Nature chemical biology*. 2020;16(3):231-9.
161. Botifoll M, Pinto-Huguet I, Arbiol J. Machine learning in electron microscopy for advanced nanocharacterization: current developments, available tools and future outlook. *Nanoscale horizons*. 2022;7(12):1427-77.
162. Boebinger MG, Lewis JA, Sandoval SE, McDowell MT. Understanding transformations in battery materials using in situ and operando experiments: progress and outlook. *ACS Energy Letters*. 2020;5:335-45.
163. Cai J, Chu X, Xu K, Li H, Wei J. Machine learning-driven new material discovery. *Nanoscale Advances*. 2020;2(8):3115-30.
164. Ali A, Chiang YW, Santos RM. X-ray diffraction techniques for mineral characterization: A review for engineers of the fundamentals, applications, and research directions. *Minerals*. 2022;12(2):205.
165. Berger C, Dumoux M, Glen T, Yee NB-y, Mitchels JM, Patáková Z, et al. Plasma FIB milling for the determination of structures in situ. *Nature communications*. 2023;14(1):629.
166. Bussetti G, Menegazzo M, Mitko S, Castiglioni C, Tommasini M, Lucotti A, et al. A Combined Raman Spectroscopy and Atomic Force Microscopy System for In Situ and Real-Time Measures in Electrochemical Cells. *Materials*. 2023;16(6):2239.
167. Xu Y, Wu H, Jia H, Zhang J-G, Xu W, Wang C. Current density regulated atomic to nanoscale process on Li deposition and solid electrolyte interphase revealed by cryogenic transmission electron microscopy. *ACS nano*. 2020;14(7):8766-75.
168. Otto S-K, Moryson Y, Krauskopf T, Peppler K, Sann J, Janek Jr, et al. In-depth characterization of lithium-metal surfaces with XPS and ToF-SIMS: toward better understanding of the passivation layer. *Chemistry of Materials*. 2021;33(3):859-67.
169. Walter A, Paul-Gilloteaux P, Plochberger B, Sefc L, Verkade P, Mannheim JG, et al. Correlated multimodal imaging in life sciences: expanding the biomedical horizon. *Frontiers in Physics*. 2020;8:47.
170. Germain M, Caputo F, Metcalfe S, Tosi G, Spring K, Åslund AK, et al. Delivering the power of nanomedicine to patients today. *Journal of Controlled Release*. 2020;326:164-71.
171. Mitchell MJ, Billingsley MM, Haley RM, Wechsler ME, Peppas NA, Langer R. Engineering precision nanoparticles for drug delivery. *Nature reviews drug discovery*. 2021;20(2):101-24.
172. Panigrahi D, Sahu PK, Swain S, Verma RK. Quality by design prospects of pharmaceuticals application of double emulsion method for PLGA loaded nanoparticles. *SN applied sciences*. 2021;3:1-21.
173. Xing Y, Cheng Z, Wang R, Lv C, James TD, Yu F. Analysis of extracellular vesicles as emerging theranostic nanoplatforms. *Coordination Chemistry Reviews*. 2020;424:213506.
174. Ho D, Quake SR, McCabe ER, Chng WJ, Chow EK, Ding X, et al. Enabling technologies for personalized and precision medicine. *Trends in biotechnology*. 2020;38(5):497-518.
175. Keith JA, Vassilev-Galindo V, Cheng B, Chmiela S, Gastegger M, Muller K-R, et al. Combining machine learning and computational chemistry for predictive insights into chemical systems. *Chemical reviews*. 2021;121(16):9816-72.
176. Zielińska A, Costa B, Ferreira MV, Miguéis D, Louros JM, Durazzo A, et al. Nanotoxicology and nanosafety: Safety-by-design and testing at a glance. *International Journal of Environmental Research and Public Health*. 2020;17(13):4657.

177. Vora LK, Gholap AD, Jetha K, Thakur RRS, Solanki HK, Chavda VP. Artificial intelligence in pharmaceutical technology and drug delivery design. *Pharmaceutics*. 2023;15(7):1916.
178. Luo Y, Abidian MR, Ahn J-H, Akinwande D, Andrews AM, Antonietti M, et al. Technology roadmap for flexible sensors. *ACS nano*. 2023;17(6):5211-95.
179. Lelek M, Gyparaki MT, Beliu G, Schueder F, Griffié J, Manley S, et al. Single-molecule localization microscopy. *Nature reviews methods primers*. 2021;1(1):39.
180. Beć KB, Grabska J, Huck CW. Principles and applications of miniaturized near-infrared (NIR) spectrometers. *Chemistry–A European Journal*. 2021;27(5):1514-32.
181. López-Lorente ÁI, Pena-Pereira F, Pedersen-Bjergaard S, Zuin VG, Ozkan SA, Psillakis E. The ten principles of green sample preparation. *TrAC Trends in Analytical Chemistry*. 2022;148:116530.
182. Züllig T, Trötzmüller M, Köfeler HC. Lipidomics from sample preparation to data analysis: a primer. *Analytical and bioanalytical chemistry*. 2020;412:2191-209.
183. Ilett M, S'ari M, Freeman H, Aslam Z, Koniuch N, Afzali M, et al. Analysis of complex, beam-sensitive materials by transmission electron microscopy and associated techniques. *Philosophical Transactions of the Royal Society A.* 2020;378(2186):20190601.
184. Kumar V, Singh E, Singh S, Pandey A, Bhargava PC. Micro-and nano-plastics (MNPs) as emerging pollutant in ground water: Environmental impact, potential risks, limitations and way forward towards sustainable management. *Chemical Engineering Journal*. 2023;459:141568.
185. Fu S, Zhang T, Jiang H, Xu Y, Chen J, Zhang L, et al. DNA nanotechnology enhanced single-molecule biosensing and imaging. *TrAC Trends in Analytical Chemistry*. 2021;140:116267.
186. Ivleva NP. Chemical analysis of microplastics and nanoplastics: challenges, advanced methods, and perspectives. *Chemical reviews*. 2021;121(19):11886-936.
187. Seidenstein A, Birmingham M, Foran J, Ogden S. Better accuracy and reproducibility of a new robotically-assisted system for total knee arthroplasty compared to conventional instrumentation: a cadaveric study. *Knee Surgery, Sports Traumatology, Arthroscopy*. 2021;29:859-66.
188. Bhalla N, Pan Y, Yang Z, Payam AF. Opportunities and challenges for biosensors and nanoscale analytical tools for pandemics: COVID-19. *ACS nano*. 2020;14(7):7783-807.
189. Allan J, Belz S, Hoeveler A, Hugas M, Okuda H, Patri A, et al. Regulatory landscape of nanotechnology and nanoplastics from a global perspective. *Regulatory Toxicology and Pharmacology*. 2021;122:104885.
190. Bellasi A, Binda G, Pozzi A, Galafassi S, Volta P, Bettinetti R. Microplastic contamination in freshwater environments: A review, focusing on interactions with sediments and benthic organisms. *Environments*. 2020;7(4):30.
191. Londhe V, Rajadhyaksha M. Opportunities and obstacles for microsampling techniques in bioanalysis: special focus on DBS and VAMS. *Journal of Pharmaceutical and Biomedical Analysis*. 2020;182:113102.
192. Saleh TA. Trends in the sample preparation and analysis of nanomaterials as environmental contaminants. *Trends in Environmental Analytical Chemistry*. 2020;28:e00101.
193. Ahmed O, Wang X, Tran M-V, Ismadi M-Z. Advancements in fiber-reinforced polymer composite materials damage detection methods: Towards achieving energy-efficient SHM systems. *Composites Part B: Engineering*. 2021;223:109136.

194. Soares da Silva Burato J, Vargas Medina DA, de Toffoli AL, Vasconcelos Soares Maciel E, Mauro Lanças F. Recent advances and trends in miniaturized sample preparation techniques. *Journal of separation science*. 2020;43(1):202-25.
195. Shard AG. X-ray photoelectron spectroscopy. *Characterization of Nanoparticles: Elsevier*; 2020. p. 349-71.
196. Peddie CJ, Genoud C, Kreshuk A, Meechan K, Micheva KD, Narayan K, et al. Volume electron microscopy. *Nature Reviews Methods Primers*. 2022;2(1):51.
197. Turk M, Baumeister W. The promise and the challenges of cryo-electron tomography. *FEBS letters*. 2020;594(20):3243-61.
198. Ahmed SF, Mofijur M, Rafa N, Chowdhury AT, Chowdhury S, Nahrin M, et al. Green approaches in synthesising nanomaterials for environmental nanobioremediation: Technological advancements, applications, benefits and challenges. *Environmental Research*. 2022;204:111967.
199. Haleem A, Javaid M, Singh RP, Suman R. Medical 4.0 technologies for healthcare: Features, capabilities, and applications. *Internet of Things and Cyber-Physical Systems*. 2022;2:12-30.
200. Wiecha PR, Arbouet A, Girard C, Muskens OL. Deep learning in nano-photonics: inverse design and beyond. *Photonics Research*. 2021;9(5):B182-B200.
201. Umapathi R, Sonwal S, Lee MJ, Rani GM, Lee E-S, Jeon T-J, et al. Colorimetric based on-site sensing strategies for the rapid detection of pesticides in agricultural foods: New horizons, perspectives, and challenges. *Coordination Chemistry Reviews*. 2021;446:214061.
202. Böhning J, Bharat TA. Towards high-throughput in situ structural biology using electron cryotomography. *Progress in biophysics and molecular biology*. 2021;160:97-103.
203. Herrmann IK, Wood MJA, Fuhrmann G. Extracellular vesicles as a next-generation drug delivery platform. *Nature nanotechnology*. 2021;16(7):748-59.
204. Safaei M, Shishehbore MR. A review on analytical methods with special reference to electroanalytical methods for the determination of some anticancer drugs in pharmaceutical and biological samples. *Talanta*. 2021;229:122247.
205. Khater IM, Nabi IR, Hamarneh G. A review of super-resolution single-molecule localization microscopy cluster analysis and quantification methods. *Patterns*. 2020;1(3).
206. Foulkes R, Man E, Thind J, Yeung S, Joy A, Hoskins C. The regulation of nanomaterials and nanomedicines for clinical application: Current and future perspectives. *Biomaterials science*. 2020;8(17):4653-64.
207. Wu L-P, Wang D, Li Z. Grand challenges in nanomedicine. *Materials Science and Engineering: C*. 2020;106:110302.
208. Sajid M, Płotka-Wasylka J. Green analytical chemistry metrics: A review. *Talanta*. 2022;238:123046.
209. Kashkooli FM, Soltani M, Souri M. Controlled anti-cancer drug release through advanced nano-drug delivery systems: Static and dynamic targeting strategies. *Journal of controlled release*. 2020;327:316-49.
210. Gowayed OY, Moosa T, Moratos AM, Hua T, Arnold S, Garetz BA. Dynamic light scattering study of a laser-induced phase-separated droplet of aqueous glycine. *The Journal of Physical Chemistry B*. 2021;125(28):7828-39.
211. Candan M, Ünal M. The effect of various asthma medications on surface roughness of pediatric dental restorative materials: An atomic force microscopy and scanning electron microscopy study. *Microscopy Research and Technique*. 2021;84(2):271-83.
212. Song Y, Cong Y, Wang B, Zhang N. Applications of Fourier transform infrared spectroscopy to pharmaceutical preparations. *Expert opinion on drug delivery*. 2020;17(4):551-71.

213. Abdelghany TM, Al-Rajhi AM, Yahya R, Bakri MM, Al Abboud MA, Yahya R, et al. Phytofabrication of zinc oxide nanoparticles with advanced characterization and its antioxidant, anticancer, and antimicrobial activity against pathogenic microorganisms. *Biomass Conversion and Biorefinery*. 2023;13(1):417-30.
214. Shah S, Famta P, Raghuvanshi RS, Singh SB, Srivastava S. Lipid polymer hybrid nanocarriers: Insights into synthesis aspects, characterization, release mechanisms, surface functionalization and potential implications. *Colloid and Interface Science Communications*. 2022;46:100570.
215. Amorim P, d'Ávila M, Anand R, Moldenaers P, Van Puyvelde P, Bloemen V. Insights on shear rheology of inks for extrusion-based 3D bioprinting. *Bioprinting*. 2021;22:e00129.
216. Li M, Xu W, Su Y. Solid-state NMR spectroscopy in pharmaceutical sciences. *TrAC Trends in Analytical Chemistry*. 2021;135:116152.
217. Operti MC, Bernhardt A, Grimm S, Engel A, Figdor CG, Tagit O. PLGA-based nanomedicines manufacturing: Technologies overview and challenges in industrial scale-up. *International Journal of Pharmaceutics*. 2021;605:120807.
218. Tomeh MA, Zhao X. Recent advances in microfluidics for the preparation of drug and gene delivery systems. *Molecular Pharmaceutics*. 2020;17(12):4421-34.
219. Melo-Agustín P, Kozak ER, de Jesús Perea-Flores M, Mendoza-Pérez JA. Identification of microplastics and associated contaminants using ultra high resolution microscopic and spectroscopic techniques. *Science of The Total Environment*. 2022;828:154434.
220. Alzahrani A, Nyavanandi D, Mandati P, Youssef AAA, Narala S, Bandari S, et al. A systematic and robust assessment of hot-melt extrusion-based amorphous solid dispersions: Theoretical prediction to practical implementation. *International Journal of Pharmaceutics*. 2022;624:121951.
221. Rahmani F, Ziyadi H, Baghali M, Luo H, Ramakrishna S. Electrospun PVP/PVA nanofiber mat as a novel potential transdermal drug-delivery system for buprenorphine: A solution needed for pain management. *Applied Sciences*. 2021;11(6):2779.
222. Dikpati A, Mohammadi F, Greffard K, Quéant C, Arnaud P, Bastiat G, et al. Residual solvents in nanomedicine and lipid-based drug delivery systems: a case study to better understand processes. *Pharmaceutical research*. 2020;37:1-11.
223. Laur N, Kinscherf R, Pomytkin K, Kaiser L, Knes O, Deigner H-P. ICP-MS trace element analysis in serum and whole blood. *PloS one*. 2020;15(5):e0233357.
224. Halwani AA. Development of pharmaceutical nanomedicines: from the bench to the market. *Pharmaceutics*. 2022;14(1):106.
225. Duan Y, Dhar A, Patel C, Khimani M, Neogi S, Sharma P, et al. A brief review on solid lipid nanoparticles: Part and parcel of contemporary drug delivery systems. *RSC advances*. 2020;10(45):26777-91.
226. Basak M, Rahman ML, Ahmed MF, Biswas B, Sharmin N. The use of X-ray diffraction peak profile analysis to determine the structural parameters of cobalt ferrite nanoparticles using Debye-Scherrer, Williamson-Hall, Halder-Wagner and Size-strain plot: Different precipitating agent approach. *Journal of Alloys and Compounds*. 2022;895:162694.
227. Riazi H, Anayee M, Hantanasirisakul K, Shamsabadi AA, Anasori B, Gogotsi Y, et al. Surface modification of a MXene by an aminosilane coupling agent. *Advanced Materials Interfaces*. 2020;7(6):1902008.
228. Shinde P, Agraval H, Srivastav AK, Yadav UC, Kumar U. Physico-chemical characterization of carvacrol loaded zein nanoparticles for enhanced anticancer activity and investigation of molecular interactions between them by molecular docking. *International Journal of Pharmaceutics*. 2020;588:119795.

229. Pouroutzidou GK, Liverani L, Theocharidou A, Tsamesidis I, Lazaridou M, Christodoulou E, et al. Synthesis and characterization of mesoporous mg-and sr-doped nanoparticles for moxifloxacin drug delivery in promising tissue engineering applications. *International Journal of Molecular Sciences*. 2021;22(2):577.
230. Ghaffari M, Dehghan G, Baradaran B, Zarebkohan A, Mansoori B, Soleymani J, et al. Co-delivery of curcumin and Bcl-2 siRNA by PAMAM dendrimers for enhancement of the therapeutic efficacy in HeLa cancer cells. *Colloids and Surfaces B: Biointerfaces*. 2020;188:110762.
231. Martins TS, Vaz M, Henriques AG. A review on comparative studies addressing exosome isolation methods from body fluids. *Analytical and Bioanalytical Chemistry*. 2023;415(7):1239-63.
232. Chandrakala V, Aruna V, Angajala G. Review on metal nanoparticles as nanocarriers: Current challenges and perspectives in drug delivery systems. *Emergent Materials*. 2022;5(6):1593-615.
233. Pena-Pereira F, Bendicho C, Pavlović DM, Martín-Esteban A, Díaz-Álvarez M, Pan Y, et al. Miniaturized analytical methods for determination of environmental contaminants of emerging concern–a review. *Analytica chimica acta*. 2021;1158:238108.
234. Shah AH, Rather MA. Effect of calcination temperature on the crystallite size, particle size and zeta potential of TiO2 nanoparticles synthesized via polyol-mediated method. *Materials Today: Proceedings*. 2021;44:482-8.
235. Jabbar ZH, Graimed BH, Okab AA, Issa MA, Ammar SH, Khadim HJ, et al. A review study summarizes the main characterization techniques of nano-composite photocatalysts and their applications in photodegradation of organic pollutants. *Environmental Nanotechnology, Monitoring & Management*. 2023;19:100765.
236. Hossain M, Karmakar D, Begum SN, Ali SY, Patra PK. Recent trends in the analysis of trace elements in the field of environmental research: A review. *Microchemical Journal*. 2021;165:106086.
237. Giménez-Campillo C, Pastor-Belda M, Campillo N, Hernández-Córdoba M, Viñas P. Development of a new methodology for the determination of N-nitrosamines impurities in ranitidine pharmaceuticals using microextraction and gas chromatography-mass spectrometry. *Talanta*. 2021;223:121659.
238. Kim SO, Kim SS. Bacterial pathogen detection by conventional culture-based and recent alternative (polymerase chain reaction, isothermal amplification, enzyme linked immunosorbent assay, bacteriophage amplification, and gold nanoparticle aggregation) methods in food samples: A review. *Journal of Food Safety*. 2021;41(1):e12870.
239. Liu S, Ulugun B, DeFlorio W, Arcot Y, Yegin Y, Salazar KS, et al. Development of durable and superhydrophobic nanodiamond coating on aluminum surfaces for improved hygiene of food contact surfaces. *Journal of Food Engineering*. 2021;298:110487.
240. Demelenne A, Servais A-C, Crommen J, Fillet M. Analytical techniques currently used in the pharmaceutical industry for the quality control of RNA-based therapeutics and ongoing developments. *Journal of Chromatography A*. 2021;1651:462283.
241. Huang H, Zheng O, Wang D, Yin J, Wang Z, Ding S, et al. ChatGPT for shaping the future of dentistry: the potential of multi-modal large language model. *International Journal of Oral Science*. 2023;15(1):29.
242. Schmid R, Heuckeroth S, Korf A, Smirnov A, Myers O, Dyrlund TS, et al. Integrative analysis of multimodal mass spectrometry data in MZmine 3. *Nature biotechnology*. 2023;41(4):447-9.
243. Witte K, Späth A, Finizio S, Donnelly C, Watts B, Sarafimov B, et al. From 2D STXM to 3D imaging: Soft X-ray laminography of thin specimens. *Nano letters*. 2020;20(2):1305-14.

244. Shvalya V, Filipič G, Zavašnik J, Abdulhalim I, Cvelbar U. Surface-enhanced Raman spectroscopy for chemical and biological sensing using nanoplasmonics: The relevance of interparticle spacing and surface morphology. *Applied Physics Reviews*. 2020;7(3).
245. Uchański T, Masiulis S, Fischer B, Kalichuk V, López-Sánchez U, Zarkadas E, et al. Megabodies expand the nanobody toolkit for protein structure determination by single-particle cryo-EM. *Nature methods*. 2021;18(1):60-8.
246. Zhu Y, Wang J, Chu H, Chu Y-C, Chen HM. In situ/operando studies for designing next-generation electrocatalysts. *ACS Energy Letters*. 2020;5(4):1281-91.
247. Guo K, Yang Z, Yu C-H, Buehler MJ. Artificial intelligence and machine learning in design of mechanical materials. *Materials Horizons*. 2021;8(4):1153-72.
248. Ying Y-L, Hu Z-L, Zhang S, Qing Y, Fragasso A, Maglia G, et al. Nanopore-based technologies beyond DNA sequencing. *Nature nanotechnology*. 2022;17(11):1136-46.
249. Xavier J, Yu D, Jones C, Zossimova E, Vollmer F. Quantum nanophotonic and nanoplasmonic sensing: towards quantum optical bioscience laboratories on chip. *Nanophotonics*. 2021;10(5):1387-435.
250. Parihar A, Ranjan P, Sanghi SK, Srivastava AK, Khan R. Point-of-care biosensor-based diagnosis of COVID-19 holds promise to combat current and future pandemics. *ACS applied bio materials*. 2020;3(11):7326-43.
251. Pollard TD, Ong JJ, Goyanes A, Orlu M, Gaisford S, Elbadawi M, et al. Electrochemical biosensors: a nexus for precision medicine. *Drug Discovery Today*. 2021;26(1):69-79.
252. Kashkooli FM, Soltani M, Souri M, Meaney C, Kohandel M. Nexus between in silico and in vivo models to enhance clinical translation of nanomedicine. *Nano Today*. 2021;36:101057.
253. Manzari MT, Shamay Y, Kiguchi H, Rosen N, Scaltriti M, Heller DA. Targeted drug delivery strategies for precision medicines. *Nature Reviews Materials*. 2021;6(4):351-70.
254. Ng TS, Garlin MA, Weissleder R, Miller MA. Improving nanotherapy delivery and action through image-guided systems pharmacology. *Theranostics*. 2020;10(3):968.
255. Indoria S, Singh V, Hsieh M-F. Recent advances in theranostic polymeric nanoparticles for cancer treatment: A review. *International journal of pharmaceutics*. 2020;582:119314.
256. Sharma A, Badea M, Tiwari S, Marty JL. Wearable biosensors: an alternative and practical approach in healthcare and disease monitoring. *Molecules*. 2021;26(3):748.
257. Kheirollahpour M, Mehrabi M, Dounighi NM, Mohammadi M, Masoudi A. Nanoparticles and vaccine development. *Pharmaceutical nanotechnology*. 2020;8(1):6-21.
258. Tian J, Song X, Wang Y, Cheng M, Lu S, Xu W, et al. Regulatory perspectives of combination products. *Bioactive Materials*. 2022;10:492-503.
259. Nehra M, Uthappa U, Kumar V, Kumar R, Dixit C, Dilbaghi N, et al. Nanobiotechnology-assisted therapies to manage brain cancer in personalized manner. *Journal of Controlled Release*. 2021;338:224-43.
260. Wallis M, Al-Dulimi Z, Tan DK, Maniruzzaman M, Nokhodchi A. 3D printing for enhanced drug delivery: current state-of-the-art and challenges. *Drug Development and Industrial Pharmacy*. 2020;46(9):1385-401.
261. Mahmudunnabi RG, Farhana FZ, Kashaninejad N, Firoz SH, Shim Y-B, Shiddiky MJ. Nanozyme-based electrochemical biosensors for disease biomarker detection. *Analyst*. 2020;145(13):4398-420.
262. Mi P, Cabral H, Kataoka K. Ligand-installed nanocarriers toward precision therapy. *Advanced Materials*. 2020;32(13):1902604.

263. Gardner L, Kostarelos K, Mallick P, Dive C, Hadjidemetriou M. Nano-omics: nanotechnology-based multidimensional harvesting of the blood-circulating cancerome. *Nature Reviews Clinical Oncology*. 2022;19(8):551-61.
264. Siafaka PI, Okur NÜ, Karantas ID, Okur ME, Gündoğdu EA. Current update on nanoplatforms as therapeutic and diagnostic tools: A review for the materials used as nanotheranostics and imaging modalities. *Asian Journal of Pharmaceutical Sciences*. 2021;16(1):24-46.
265. Sun T, Zhang YS, Pang B, Hyun DC, Yang M, Xia Y. Engineered nanoparticles for drug delivery in cancer therapy. *Nanomaterials and Neoplasms*. 2021:31-142.
266. Zhang LG, Leong K, Fisher JP. 3D bioprinting and nanotechnology in tissue engineering and regenerative medicine: academic press. 2022.
267. Mbunge E, Muchemwa B, Batani J. Sensors and healthcare 5.0: transformative shift in virtual care through emerging digital health technologies. *Global Health Journal*. 2021;5(4):169-77.
268. Johnson KB, Wei WQ, Weeraratne D, Frisse ME, Misulis K, Rhee K, et al. Precision medicine, AI, and the future of personalized health care. *Clinical and translational science*. 2021;14(1):86-93.

تقنيات التحليل النانوي في التحليل الصيدلاني

سي. هيما بندو[1]، تي. فارما كي[1]، أبارنا إم[1]، سادن ي. رشما[2]*

[1]قسم التحليل الصيدلاني، معهد راغافيندرا للتعليم والبحوث الصيدلانية، تقاطع كيه. آر. بالي، أنانتابور، تشيتيدو، أندرا براديش– الهند.

[2]قسم ضمان الجودة الصيدلانية، معهد راغافيندرا للتعليم والبحوث الصيدلانية، تقاطع كيه. آر. بالي، أنانتابور، تشيتيدو، أندرا براديش – الهند.

ملخص

تلعب التقنيات التحليلية النانوية دورًا محوريًا في تقدم التحليل الصيدلاني من خلال توفير رؤى مفصلة حول التركيبات الدوائية، وعمليات مراقبة الجودة، وتوصيف الجسيمات النانوية، واكتشاف الشوائب، والاتجاهات الناشئة في هذا المجال. يبرز هذا الملخص أهمية الأدوات التحليلية النانوية في تحسين أنظمة توصيل الأدوية، وضمان جودة المنتج وسلامته، وتوصيف الجسيمات النانوية، واكتشاف الشوائب الدقيقة. تشمل النقاط الرئيسية أهمية هذه التقنيات في تعزيز استقرار الأدوية، وتمكين توصيل الأدوية المستهدف، وتسهيل الطب الشخصي. علاوة على ذلك، يسلط الملخص الضوء على المشهد المتطور للطرق التحليلية النانوية، مثل التصوير متعدد الأوضاع وأجهزة الاستشعار القائمة على الكم، وإمكاناتها لتحقيق اختراقات في مراقبة الأدوية في الوقت الفعلي والطب الدقيق. يدعو الملخص إلى استمرار الجهود البحثية والتطويرية لتحسين الأجهزة، واستكشاف التطبيقات الجديدة، ومعالجة التحديات التقنية، وتعزيز التعاون، وتحسين برامج التعليم والتدريب في التحليل الصيدلاني. بشكل عام، تعد التقنيات التحليلية النانوية بإحداث ثورة في تطوير الأدوية، وتحسين نتائج الرعاية الصحية، وتمهيد الطريق للعلاجات الشخصية المخصصة لتلبية احتياجات المرضى الفردية.

الكلمات الدالة: تقنيات التحليل النانوية، التحليل الصيدلاني، التركيبات الدوائية، مراقبة الجودة، توصيف الجسيمات النانوية، اكتشاف الشوائب.

* ***المؤلف المراسل: ت. رشمة***

shaikreshmat614@gmail.com

تاريخ استلام البحث 2024/5/9 وتاريخ قبوله للنشر 2024/8/22.

Effect of Mannitol on Renal Function during Cardiac Surgery and Immediate Post-Operative in Selected Private Hospitals in Nablus City/ Palestine

Belal Rahhal[1*], Heba Salah[1], Leen Abu Abdoh[2], Noor Almasri[2], Shahd Al-Tarsha[2], Shoroq Bsharat[2], Jumana Najjar[2]

[1] Department of Biomedical Sciences, Faculty of Medicine and Health Sciences, An-Najah National University, Nablus, Palestine.
[2] Division of cardiac perfusion technology, Department of Medical Allied sciences, Faculty of Medicine and Health Sciences, An-Najah National University, Nablus, Palestine.

ABSTRACT

Background: Cardiopulmonary bypass (CPB) is a common technique in cardiac surgery, however, it is associated with acute kidney injury. The type of solution in the CPB circuit can potentially affect surgery outcome through affecting several organs and body homeostasis. The optimal prime solution for the CPB) circuit in adult cardiac surgery has not yet been defined. Mannitol is widely used in the priming solution for CPB even though there is no clear consensus on the role of mannitol in cardiac surgery.

Purpose: The purpose of this study was to investigate the effect of mannitol in the CPB prime solution on renal function during cardiac surgery and post-operative in selected private hospitals in Nablus City

Design and method: prospective cohort study design conducted at An-Najah National University Hospital and specialized Arab hospital. A sample of 120 patients was studied. The patients had cardiac surgery and they had preoperative normal renal function.

Results: The use of mannitol in the CPB prime solution was associated with a decrease in creatinine and BUN readings levels in the postoperative period (postoperative period mean =0.7692 ± 0.26068, and 18.3917 ± 7.56629mg/dl, respectively; p-value<0.001) and an increase in GFR levels in the postoperative period (postoperative period mean = 112.27861 ± 1.43604, p-value<0.001) indicating and improvement in renal function following cardiac surgery.

Keywords: creatinine, mannitol, cardiopulmonary bypass, cardiac surgery, Renal function.

1.INTRODUCTION

Cardiopulmonary bypass (CPB) is a required circulatory support during cardiac surgery. CPS is (1). often associated with the risk of postoperative renal dysfunction, and thus it needs careful management strategies to recover this complication (2) especially to maintain acid-base balance and normal electrolyte levels. The CPB circuit prime solution can potentially affect post-surgical outcomes through affecting various organ systems and homeostasis, such as the central nervous, renal systems, coagulation, osmolality, and electrolyte levels (1-6). previous studies examined the effect of using mannitol in the prime solution for CPB to protect renal system during and post cardiac surgery with the aim of preserving renal function during and after cardiac surgery (7).

However, the selection of CPB prime typically relies on individual preferences and practices (6). There is a debate within medical community on mannitol impact on renal function during cardiac surgery and immediate postoperative period (7). Recent surveys have revealed

[*]***Corresponding author: Belal Rahhal***
belalrahhal@najah.edu
Received: 12/5/2024 Accepted: 22/8/2024.
DOI: https://doi.org/10.35516/jjps.v18i2.2640

significant global disparities in CPB techniques and priming, yet the reasons behind such variations and their clinical ramifications remain vague (8). Currently, no standardized guidelines exist regarding the choice or customization of CPB prime solutions to suit specific patient characteristics or conditions.

CPB prime solutions commonly consist of crystalloid fluids, often supplemented with mannitol, a 6-carbon natural alditol. Mannitol serves as a volume expander with osmotic diuretic properties and thus has potential effects on various organ systems (1,8, 9). Several studies reported conflicting results regarding mannitol use. Some of these studies raised concerns about potential adverse effects on renal function, while others suggested a protective effect of mannitol (10-14).

Notably, one study found no significant clinical impact following the removal of mannitol from the priming solution, identifying only economic benefits (15). Consequently, consensus regarding mannitol's role during cardiac surgery remains elusive, with limited studies investigating its effects in CPB prime solutions (16).

2.MANNITOL AND RENAL FUNCTION

Emerging studies are exploring various renal protective strategies during cardiac surgery. These strategies include pharmacological interventions, modifications in surgical techniques, and advancements in perfusion strategies, aiming to optimize renal outcomes (25).

Mannitol, a well-established osmotic diuretic, has been a subject of significant interest in cardiac surgery field. It increases intratubular osmotic pressure, thus enhancing free water excretion. Furthermore, mannitol was reported to induce renal vasodilatation by decreasing renal vascular resistance and thus increasing renal blood flow although it may not affect glomerular filtration rates (GFR).

Research had focused on the possible effects of mannitol in cardiac surgery, focusing on its potential Reno-protective effects and implications for patient outcomes. For instance, Mannitol is studied for its potential ability to alleviate renal ischemia and perfusion related injuries during cardiac surgery. In addition, as an osmotic diuresis, mannitol could protect renal function through maintaining renal blood flow and reducing tubular obstruction (24, 26).

Many studies especially randomized controlled trials have been conducted to check and evaluate the effectiveness of mannitol in protecting the renal function during and after cardiac surgery. These studies often assess the special parameters and tests such as creatinine serum level, Blood urea nitrogen (BUN), and GFR (27).

Variable effects have been reported for the possible outcomes for mannitol use during cardiac surgery. These Conflicting findings highlight the need for a better understanding, taking into account factors such as patient populations, surgical techniques, and study designs (28).

In conclusion, mannitol holds promise as a reno-protective agent in the context of cardiac surgery. However, ongoing research is essential to address existing controversies and to refine guidelines for its optimal use. As cardiac surgery evolves, the role of mannitol and its potential synergies with emerging therapies will continue to shape the landscape of renal protection strategies.

3. METHODS

Study Design and Settings:

This study is an observational prospective cohort study that is designed to evaluate whether mannitol given during cardiac surgery are associated with the changes in renal functions among patients underwent cardiac surgery. The study was conducted in Palestine at An-Najah National University Hospital and specialized Arab hospital. A sample of 120 patients were studies. Data collection started in October 2023 and was completed by March 2024.

Ethical approval:

Ethical approval for our study entitled " Effect of Mannitol on renal function during cardiac surgery and immediate post-operative in selected private hospitals in

Nablus City/ Palestine" was obtained from An–Najah National University IRB committee on 9th of October 2023 (C.P.T. Oct. 2023/40) and all methods were carried out in accordance with relevant guidelines and regulations.

Patient Recruitment:

The study included adult patients scheduled for cardiac surgery The Patients were recruited from the cardiac surgery unit, and informed consent was obtained prior to participation.

Inclusion and exclusion Criteria:

Patients aged 18 years and older undergoing elective cardiac surgery (e.g., CABG, valve replacement) and received intraoperative Mannitol administration and not complaining of renal failure were included in this study. .

Patients with pre-existing renal impairment (e.g., chronic kidney disease), undergoing emergency surgery, , patients weight less than 50 kg, patients with preoperative hematocrit less than 24% and previous history of cardiac surgery and patients who had contraindications to Mannitol were excluded from the study.

Study Tool:

Data were collected from the patients' medical records. The studied data includes demographic information (age, gender, BMI, smoking status), Preoperative medical history (e.g., hypertension, diabetes) and Laboratory results (creatinine, BUN, hemoglobin, GFR) measured preoperatively and postoperatively.

The study primary outcome variable was postoperative renal function, which was assessed through serum creatinine levels, blood urea nitrogen (BUN) levels. These variables were measured using standard laboratory procedures preoperatively and postoperatively. Glomerular filtration rate (GFR) was calculated based on serum creatinine levels.

Data Analysis:

Statistical analyses were performed using SPSS. Paired sample t-tests were used to compare preoperative and postoperative values for creatinine, BUN, hemoglobin, and GFR. A p value of 0.05 was adopted as a threshold for significance.

Associations between demographic factors (e.g., age, gender) and postoperative renal function were analyzed through chi square and linear regression, with p-values reported to indicate statistical significance.

4. RESULTS

A sample of 120 patients who underwent cardiac surgery during the time period of the study were enrolled. All patients enrolled in the study used heart lung machine with mannitol used in the cardiopulmonary bypass. All of the enrolled patients had normal renal function in the preoperative period. Table 1 shows the demographic data of the participants.

Table1. Demographic characteristics of the study sample

Variable	Frequency (%) N= 120
Age category (years)	
<30	3 (2.5)
30-45	10 (8.3)
45.1-60	58 (48.3)
>60	49 (40.8)
Age scale	Mean: 56 ± 0.06
Gender	
Male	80 (66.7)
Female	40 (33.3)
BMI category(kg/m^2)	
<18.5 underweight	0
18.5-24.9 normal	43 (35.8)
25-29.9 overweight	53 (44.2)
30-34.9 obese	14 (11.7)
≥35 extremely obese	10 (8.3)
Smoking	
No	71(59.2)
Yes	49 (40.8)
past medical history	
Hypertension	79 (65.8)
Diabetes Meletus	70 (58.3)

4.1 preoperative measurements

The distribution of preoperative creatinine serum levels showed that the majority of patients (66.7%) had a

creatinine level within the normal range (0.7-1.2 mg/dl), while small proportion of patients have higher or lower levels (>1.2 mg/dL or <0.7 mg/dL). Similarly, the majority of patients (84%) had BUN levels within the normal range (7-30 mg/dL), with a smaller proportion exhibiting either lower (<7 mg/dL) or higher (>30 mg/dL) levels. Furthermore, the mean preoperative GFR was 84.64 ± 30.6 ml/min/1.73m² which reflects the overall renal function of the study population.

The distribution of preoperative hemoglobin levels showed that most patients had either mild anemia (8-11.9 g/dL) or normal levels (12-17 g/dL). In addition, most of the study participants (97.5%) did not receive blood transfusions preoperatively, indicating overall stable hemodynamics and adequate preoperative preparation.

4.2. intraoperative measurements

All participants enrolled in the study received mannitol intraoperatively. The majority of study participants (65%) underwent coronary artery bypass grafting (CABG), while a smaller number underwent valve replacement (17.5%) or other cardiac surgeries (17.5%)

In addition, the use of hemofiltration and intraoperative blood transfusion was studied. Our results showed that a small proportion of patients (1.7%) underwent hemofiltration intraoperatively, while 26.7% of patients received blood transfusions intraoperatively, either as whole blood or packed red blood cells (RBCs).

In order to evaluate the potentially mitigation effect of mannitol on renal ischemia-reperfusion injury, the volume of mannitol used intraoperatively were studied. The mean volume of mannitol administered intraoperatively was 156.17 ± 64.9mLThis variability in volume suggests differences in clinical practice or patient-specific considerations.

Regarding the cross-clamp time; the mean duration of aortic cross-clamping was 102 ± 43.91 minutes with the mean duration of cardiopulmonary bypass (CPB) of 150.21 ± 67.736 minutes. During bypass temperature maintained as low as possible; the analyzed data showed that the mean minimum intraoperative temperature was 33.17° ± 2.85C.

4.3. Post operation measurements

The majority of study participants (60%) had postoperative creatinine levels within the normal range (0.7-1.2 mg/dL), while smaller proportions had either lower (<0.7 mg/dL) or higher (>1.2 mg/dL) levels. The mean postoperative creatinine level was 0.76 ± 0.260 mg/dL. In addition, the majority of participants (90.8%) had postoperative BUN levels within the normal range (7-30 mg/dL), with a smaller proportion of participants had either lower (<7 mg/dL) or higher (>30 mg/dL) levels.

Postoperative hemoglobin level showed mild anemia (8-11.9 g/dL), for most of the patients (80%) while smaller proportions having either moderate (6-7 g/dL) or normal (12-17 g/dL) hemoglobin levels. The mean postoperative hemoglobin level was 10.7021 ± 1.436g/dL, while the mean postoperative GFR was 112.27 ± 58.52mL/min/1.73m². The mean postoperative GFR suggests preserved renal function overall. The analyzed data showed that the majority of patients (93.3%) did not receive blood transfusions postoperatively, while a smaller proportion (6.7%) received red blood cell (RBC) transfusions table 2.

4.4. Effect of mannitol administration on renal function (pre-op and post-op)

In order to study the effect of mannitol administration on renal function, creatinine and BUN levels were studied before and after cardiac surgery. Our study showed a significant difference ($p < 0.001$) between preoperative creatinine level (mean= 0.9365 ± 0.27097mg/dl, Fig. 1A) postoperative creatinine level (mean =0.7692 ± 0.26068 mg/dl, Fig. 1A). In addition, a significant difference ($p < 0.001$) was observed between preoperative and postoperative BUN levels (Fig. 1B).

The paired sample t-test demonstrated a statistically significant difference ($p < 0.001$) between preoperative and postoperative hemoglobin levels, also, there was a statistically significant difference ($p < 0.001$) between

preoperative and postoperative hemoglobin levels (fig.1C). The means and standard deviations for preoperative and postoperative levels of creatinine, BUN and hemoglobin are presented in table 2.

Table 5: the differences between preoperative and postoperative lab results according to the paired sample t test.

Variable	N	Mean	Standard deviation	P value
Creatinine				
Pre op	120	.9365	.27097	<0.001
Post op	120	.7692	.26068	
BUN				
Pre op	120	22.5000	7.80971	<0.001
Post op	120	18.3917	7.56629	
HGB				
Pre op	120	11.8978	30.68077	<0.001
Post op	120	10.7021	58.52910	
GFR				
Pre op	120	84.6463	2.14284	<0.001
Post op	120	112.2786	1.43604	

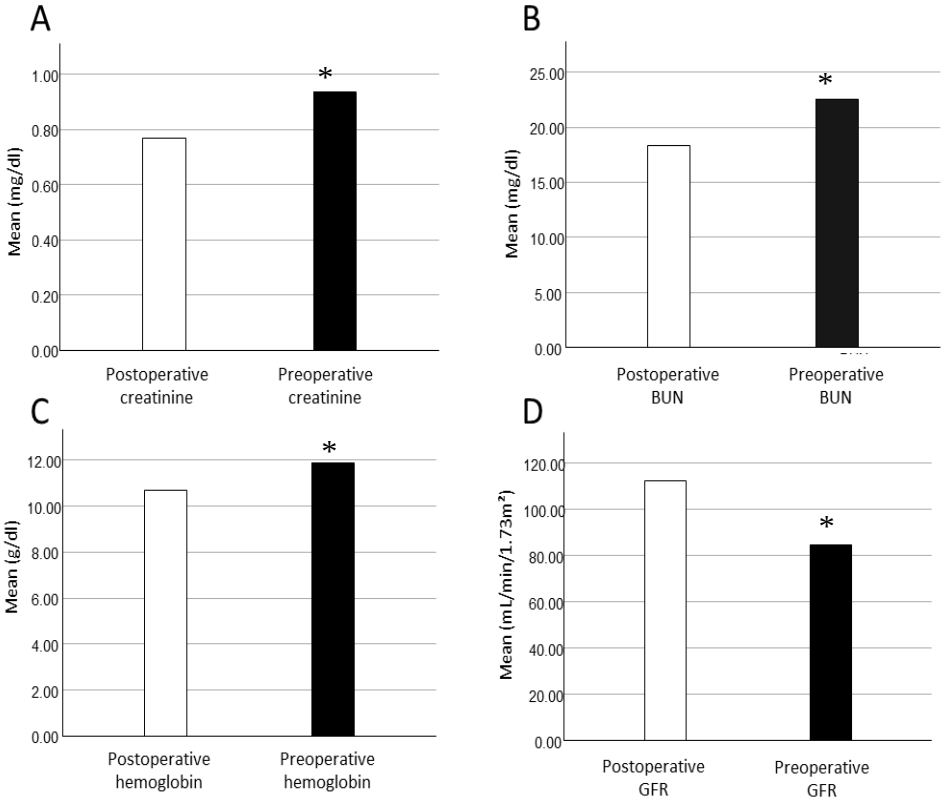

Figure 1: preoperative and post-operative levels of creatinine, BUN, hemoglobin and GFR. Black columns represent the preoperative levels of creatinine (A), BUN (B), hemoglobin (C) and GFR (D). White columns represent the postoperative levels of creatinine (A), BUN (B), hemoglobin (C) and GFR (D). * represents a p-value less than 0.05

4.5. Effect of mannitol volume on renal function

The effect of mannitol volume on renal function was also studied through the measured postoperative levels of creatinine, BUN and GFR. Our results showed that there was no significant effect for mannitol volume on postoperative creatinine level (0.769 ± 0.0260 mg/dl). In addition, no significant effect was observed for the mannitol volume on postoperative BUN levels (18.39 ± 7.566 mg/dl) and postoperative GFR (112.27 ± 58.529 mL/min/1.73m², Table 3).

Table 3: Effect of mannitol volume on renal function

Variable	N	Mean	Standard deviation	P value
Mannitol volume	120	156.17	64.900	0.809
Post op creatinine	120	0.769	0.260	
Mannitol volume	120	156.17	64.900	0.149
Post op BUN	120	18.39	7.566	
Mannitol volume	120	156.17	64.900	0.255
Post op GFR	120	112.27	58.529	

4.6. Association between socio-demographic data and post operation renal function

The association Between different socio-demographic variable and postoperational renal function was studied using the postoperative levels of creatinine and GFR using linear regression analysis. Different postoperative creatinine levels were obtained for variable age groups. The mean postoperative creatinine levels were 0.5400 ± 0.052 , 0.7200 ± 0.204 ,0.7047 ± 0.241 and0.8698 ± 0.268 mg/dl for patients aged 30, 30-45, 45-60 and >60 years, respectively. These results shows that there is a statistically significant association between age and postoperative creatinine levels (p = 0.002). Specifically, older age (>60) is associated with higher postoperative creatinine levels.

Furthermore, GFR levels were 96.6272 ± 19.41, 101.0786 ± 32.50, 91.8801 ± 30.004 and 71.9969 ± 27.54 for patients aged below 30, 30-45, 45-60 and patients above 60 years old, respectively. The analyzed data revealed that there is a statistically significant association between age and postoperative GFR (p < 0.001). Specifically, older age (>60) is associated with lower postoperative GFR.

The association Between Surgery Type and Postoperative Renal Function was also evaluated in this study. The results showed that for patients undergoing CABG surgery, the mean postoperative creatinine level was 0.7442 ± 0.232, and for patients undergoing valve replacement, the mean postoperative creatinine level was 0.6862 ± 0.266. Patients undergoing other types of surgery had a mean postoperative creatinine level of 0.9452 ± 0.288. These results showed that there is a statistically significant association between surgery type and postoperative creatinine levels (p = 0.005). Specifically, patients undergoing other types of surgery had higher postoperative creatinine levels compared to those undergoing CABG or valve replacement.

In addition, the association between postoperative GFR and the type of surgery was analyzed. Our results showed that the mean postoperative GFR was 87.6369 ± 30.6 for patient undergoing CABG surgery, while the mean postoperative GFR was 83.1737 ± 26.12 for patients undergoing valve replacement and 75.0112 ± 34.21 for patients undergoing other type of surgery. Our analysis showed a statistically significant association between surgery type and postoperative GFR (p = 0.034). Specifically, patients undergoing other types of surgery had lower postoperative GFR compared to those undergoing CABG or valve replacement.

Finally, the association between smoking and postoperative GFR was analyzed. The analyzed data showed that the mean postoperative GFR was 77.9104 ± 29.5 for non-smokers, while the mean postoperative GFR was 94.4066 ± 29.9 for smokers indicating that smokers had higher postoperative GFR (p = 0.003, Table 4).

Table 4: Association between socio-demographic data and post operation renal function

Independent Variable	Dependent variable	P value
Age	**Post op Creatinine mean**	
<30	.5400 ± 0.052	0.002
(30-45)	.7200 ± 0.204	
(45.1-60)	.7047 ±0.241	
>60	.8698 ±0.268	
Surgery type	Post op creatinine mean	0.005
CABG	.7442 ±0.232	
valve replacement	.6862± 0.266	
Other	.9452 ± 0.288	
Age	Post op GFR	<0.001
<30	96.6272 ± 19.41	
(30-45)	101.0786 ± 32.50	
(45.1-60)	91.8801 ± 30.004	
>60	71.9969 ± 27.54	
Smoking	Post op GFR	0.003
No	77.9104 ± 29.5	
Yes	94.4066 ± 29.9	
Surgery type	Post op GFR	0.034
CABG	87.6369 ±30.6	
valve replacement	83.1737 ± 26.12	
Other	75.0112 ± 34.21	

5. DISCUSSION

The best solution for the CPB circuit during cardiac surgery is still under evaluation. Our study focused on the beneficial effects of using mannitol in the prime solution for CPB. The results showed a decrease in creatinine and BUN levels and an increase in GFR in the postoperative period, indicating an improvement in renal function following cardiac surgery (48). Additionally, our results showed a decrease in hemoglobin postoperatively, indicating a decline in red blood cell mass, potentially due to surgical blood loss or hemodilution (42).

Our study also evaluated the effects of using different volumes of mannitol in the prime solution for CPB. There was no significant effect of mannitol volume on postoperative creatinine levels, BUN levels, or GFR. Furthermore, the association between socio-demographic data and postoperative renal function was studied. There was a statistically significant association between age and postoperative creatinine levels and GFR: older age was associated with higher postoperative creatinine levels and lower GFR.

Finally, our results showed that different types of surgery affect postoperative renal function. For instance, patients undergoing other types of surgery had higher postoperative creatinine levels and lower GFR compared to those undergoing CABG or valve replacement.

Findings concerning the relationship between mannitol and socio-demographic characteristics are limited and inconsistent. The gender distribution in the sample population showed a significant skew towards males, with 66.6% being male and 33.3% female. Some previous studies have also noted gender differences in health research (49–51). The gender imbalance in our study may have implications for understanding health outcomes within the population. For instance, a study found a similar trend of male predominance in their sample of cardiovascular disease patients, suggesting a need for gender-sensitive approaches in healthcare research.

While gender distribution might not directly relate to the effect of mannitol on renal function, it is essential to consider potential gender differences in response to treatments (34). Other studies have highlighted gender-specific differences in renal outcomes post-cardiac surgery, suggesting the need for gender-stratified analyses in future research (13, 34).

In our study, the notable gender imbalance within the sample may influence how mannitol affects renal function post-cardiac surgery. While there is limited direct research on gender-specific responses to mannitol in this context, some studies have suggested that gender differences may influence renal outcomes following cardiac surgery, possibly due to variations in renal physiology and response to medications (35).

In addition, in our study older age was associated with higher postoperative creatinine levels and lower GFR. The age-distribution in the sample was skewed towards older individuals, with a predominant presence of middle-aged to elderly individuals, and thus, may impact how mannitol affects renal function post-cardiac surgery. Elderly patients are often more susceptible to renal complications post-surgery (35). Studies have shown that advanced age is a significant risk factor for acute kidney injury (AKI) after cardiac surgery, potentially affecting the efficacy and safety of mannitol administration (36).

On the other hand, the varied BMI distribution, with a substantial proportion of individuals classified as overweight, obese, or extremely obese, may also influence the impact of mannitol on renal function post-cardiac surgery (36). Obesity is a known risk factor for postoperative complications, including AKI. While specific studies on the interaction between BMI and mannitol in cardiac surgery are scarce; research has highlighted the increased risk of AKI in obese patients undergoing cardiac surgery (37).

The high prevalence of smoking within the sample population (40.8%) may also be a factor to consider in assessing the effects of mannitol on renal function post-cardiac surgery. Smoking is associated with various cardiovascular and renal complications, which may interact with mannitol's effects. While direct studies on the interaction between smoking and mannitol in this context are limited, research has demonstrated the adverse effects of smoking on postoperative renal function in cardiac surgery patients (38). In addition, the high prevalence of hypertension (65.8%) and diabetes mellitus (58.3%) within the sample population underscores the importance of considering comorbidities when assessing the effects of mannitol on renal function post-cardiac surgery. Both hypertension and diabetes are risk factors for AKI and may interact with mannitol's renal effects. While direct studies on the interaction between these comorbidities and mannitol in cardiac surgery are limited, research has demonstrated the impact of hypertension and diabetes on postoperative renal outcomes (39).

We observed a decrease in creatinine levels in the postoperative period indicating an improvement in renal function or clearance of creatinine following cardiac surgery (48). Also, we found a decrease in hemoglobin postoperatively indicating a decline in red blood cell mass, potentially due to surgical blood loss or hemodilution (42).

Our study showed that the amount of mannitol administered intraoperatively did not have a statistically significant effect on postoperative renal function, as assessed by creatinine levels, BUN levels, or GFR. These findings indicates that factors other than mannitol volume may have a greater influence on postoperative renal outcomes in patients undergoing cardiac surgery. Studies suggest that mannitol is commonly used as a renal protective agent during cardiac surgery, its impact on postoperative renal function may be influenced by various patient-specific factors and surgical variables beyond the volume administered (46).

We found significant differences between preoperative and postoperative levels of creatinine, BUN, hemoglobin, and GFR. The decrease in creatinine and BUN levels and the increase in GFR postoperatively indicate improvements in renal function following cardiac surgery. Also, the decrease in hemoglobin levels postoperatively may reflect surgical blood loss or hemodilution, which is commonly observed after cardiac surgery (39). Overall, these findings suggest favorable outcomes in terms of renal function and hemodynamic stability following cardiac surgery, as evidenced by the changes in laboratory parameters from preoperative to postoperative measurements.

6. LIMITATIONS OF THE STUDY

The application of our results is limited to two private hospitals, which may reduce the generalizability of the study. In addition, the sample size was 120 participants, and broader generalizability may require a larger sample size.

7. CONCLUSIONS

This prospective cohort study revealed no effect of the volume of mannitol administered during cardiac surgery on postoperative renal function in patients with normal preoperative renal function. However, the use of mannitol in the prime solution resulted in a significant decrease in creatinine and BUN levels in the postoperative period. We therefore conclude that the role of mannitol and the effect of its volume in cardiac surgery require further research to support the generalizability of these findings.

REFERENCES

1. Shann K.G., Likosky D.S., Murkin J.M., et al. An evidence-based review of the practice of cardiopulmonary bypass in adults: A focus on neurologic injury, glycemic control, hemodilution, and the inflammatory response. *J. Thorac. Cardiovasc. Surg.* 2006; 132:283–290.
2. Poullis M. Mannitol and cardiac surgery. *Thorac. Cardiovasc. Surg.* 1999; 47:58–62.
3. Liskaser F.J., Bellomo R., Hayhoe M., et al. Role of pump prime in the etiology and pathogenesis of cardiopulmonary bypass-associated acidosis. *Anesthesiology* 2000; 93:1170–1173.
4. Hosseinzadeh Maleki M., Derakhshan P., Rahmanian Sharifabad A., Amouzeshi A. Comparing the effects of 5% Albumin and 6% Hydroxyethyl Starch 130/0.4 (Voluven) on renal function as priming solutions for cardiopulmonary bypass: A randomized double-blind clinical trial. *Anesth. Pain Med.* 2016; 6:e30326.
5. Russell J.A., Navickis R.J., Wilkes M.M. Albumin versus crystalloid for pump priming in cardiac surgery: Meta-analysis of controlled trials. *J. Cardiothorac. Vasc. Anesth.* 2004; 18:429–437.
6. Liskaser F., Story D.A., Hayhoe M., Poustie S.J., Bailey M.J., Bellomo R. Effect of pump prime on acidosis, strong-ion-difference and unmeasured ions during cardiopulmonary bypass. *Anaesth. Intensive Care* 2009; 37:767–772.
7. Lilley A. The selection of priming fluids for cardiopulmonary bypass in the UK and Ireland. *Perfusion* 2002; 17:315–319.
8. Miles L.F., Coulson T.G., Galhardo C., Falter F. Pump priming practices and anticoagulation in cardiac surgery: Results from the global cardiopulmonary bypass survey. *Anesth. Analg.* 2017; 125:1871–1877.
9. Himpe D. Colloids versus crystalloids as priming solutions for cardiopulmonary bypass: A meta-analysis of prospective, randomized clinical trials. *Acta Anaesthesiol. Belg.* 2003; 54:207–215.
10. Bragadottir G., Redfors B., Ricksten S.E. Mannitol increases renal blood flow and maintains filtration fraction and oxygenation in postoperative acute kidney injury: A prospective interventional study. *Crit. Care* 2012; 16:R159.
11. Fisher A.R., Jones P., Barlow P., et al. The influence of mannitol on renal function during and after open-heart surgery. *Perfusion* 1998; 13:181–186.
12. Kim M.Y., Park J.H., Kang N.R., et al. Increased risk of acute kidney injury associated with higher infusion rate of mannitol in patients with intracranial hemorrhage. *J. Neurosurg.* 2014; 120:1340–1348.
13. Fang L., You H., Chen B., et al. Mannitol is an independent risk factor of acute kidney injury after cerebral trauma: A case-control study. *Ren. Fail.* 2010; 32:673–679.
14. Lin S.Y., Tang S.C., Tsai L.K., et al. Incidence and risk factors for acute kidney injury following mannitol infusion in patients with acute stroke: A retrospective cohort study. *Med. (Baltimore)* 2015; 94:e2032.

15. Haydock M.D., Kruger C., Willcox T., Haydock D.A. Does removing Mannitol and Voluven from the priming fluid of the cardiopulmonary bypass circuit have clinical effects? *J. Extra-Corporeal Technol.* 2014; 46:77–83.
16. Yallop K.G., Sheppard S.V., Smith D.C. The effect of mannitol on renal function following cardio-pulmonary bypass in patients with normal pre-operative creatinine. *Anesthesia* 2008; 63:576–582.
17. Malmqvist G., Claesson Lingehall H., Appelblad M., Svenmarker S. Cardiopulmonary bypass prime composition: Beyond crystalloids versus colloids. *Perfusion* 2018; 34:130–135.
18. Martin-Calderon J.L., Bustos F., Tuesta-Reina L.R., Varona J.M., Caballero L., Solano F. Choice of the best equation for plasma osmolality calculation: Comparison of fourteen formulae. *Clin. Biochem.* 2015; 48:529–533.
19. Kishimoto N., Watanabe T., Hiraoka H., Kobayashi Y. Postoperative fluid management in cardiac surgery: a narrative review. *J. Anesthesia* 2018; 32:109–117.
20. Inomata T., Ikeda Y., Kida K., Shibagaki Y., Sato N., Kumagai Y., Shinagawa H., Ako J., Izumi T., Kanagawa Aquaresis Investigators. Effects of additive tolvaptan vs. increased furosemide on heart failure with diuretic resistance and renal impairment—Results from the K-STAR study. *Circ. J.* 2017; 82:159–167. https://doi.org/10.1253/circj.CJ-17-0179
21. Ranucci M., Ballotta A., Castelvecchio S., Baryshnikova E., Brozzi S.; Surgical and Clinical Outcome REsearch (SCORE) Group. Acute kidney injury and hemodilution during cardiopulmonary bypass: a changing scenario. *Ann. Thorac. Surg.* 2018; 105:605–612.
22. Chertow G.M., Lazarus J.M., Christiansen C.L., Cook E.F., Hammermeister K.E. Preoperative renal risk stratification. *Circulation* 1997; 95:878–884.
23. Dorje C., Sharma V., Kamath U. Acute kidney injury following cardiac surgery: The journey so far. *J. Clin. Diagn. Res.* 2017; 11:OC01.
24. Zhong Z., Wang Y., Guo H., Sagittal A., He F. Effects of mannitol on renal ischemia-reperfusion injury: a narrative review. *J. Transl. Intern. Med.* 2018; 6:32–39.
25. Garg A.X., Kurz A., Sessler D.I., Cuerden M., Robinson A., Mrkobrada M., Parikh C.R. Perioperative aspirin and clonidine and risk of acute kidney injury: A randomized clinical trial. *JAMA Surg.* 2020; 155:986–993.
26. Bove T., Calabrò M.G., Landoni G., Aletti G., Marino G., Crescenzi G., Zangrillo A. The incidence and risk of acute renal failure after cardiac surgery. *J. Cardiothorac. Vasc. Anesth.* 2007; 21:853–856.
27. Zarbock A., Kellum J.A., Schmidt C., Van Aken H., Wempe C., Pavenstädt H. Effect of early vs delayed initiation of renal replacement therapy on mortality in critically ill patients with acute kidney injury: the ELAIN randomized clinical trial. *JAMA* 2016; 315:2190–2199.
28. Belley-Cote E.P., Lamy A., Devereaux P.J., Bhandari M. A systematic review and meta-analysis of randomized controlled trials of adjunctive therapies for postoperative atrial fibrillation after cardiac surgery. *Eur. J. Cardiothorac. Surg.* 2019; 56:411–420.
29. Karthik S., Grayson A.D., McCarron E.E. Reexploration for bleeding after coronary artery bypass surgery: risk factors, outcomes, and the effect of time delay. *Ann. Thorac. Surg.* 2012; 94:434–439.
30. Brown J.R., Venner T.A. Renoprotection: What are the key components. *J. Extra-Corporeal Technol.* 2018; 50:165–173.
31. Munsch C.M., Mammen E., Kollmeyer K.R. Advances in cardiopulmonary bypass technology. *Anesthesiol. Clin.* 2020; 38:277–287.
32. Seicean A., Seicean S., Alan N., Plunkett A., Schiltz N.K., Rosenbaum B.P., Jones D.R. Short-term versus long-term mortality in patients undergoing coronary artery bypass surgery and postoperative bleeding. *J. Thorac. Cardiovasc. Surg.* 2013; 146:323–330.
33. Setia M.S. Methodology Series Module 1: Cohort Studies. *Indian J. Dermatol.* 2016; 61:21–25.

34. Smith J., et al. Gender disparities in cardiovascular disease: A review of the current literature. *J. Cardiol.* 2019; 10:87–94.
35. Luciani R., et al. Gender differences in cardiac surgery. *J. Cardiovasc. Med.* 2017; 18:201–207.
36. Han S., et al. Age-related risk factors for acute kidney injury after cardiac surgery. *J. Thorac. Dis.* 2019; 11:2018–2028.
37. Reddy S., et al. Obesity and acute kidney injury in cardiac surgery: A retrospective cohort study. *J. Cardiothorac. Vasc. Anesth.* 2018; 32:1752–1758.
38. Liu J., et al. Impact of smoking on acute kidney injury following cardiac surgery. *J. Card. Surg.* 2020; 35:1918–1924.
39. Zhang H., et al. Impact of hypertension and diabetes on acute kidney injury after cardiac surgery. *J. Cardiothorac. Vasc. Anesth.* 2019; 33:1597–1603.
40. Hogue C.W. Jr, Palin C.A., Arrowsmith J.E., Cardiopulmonary Bypass Neurologic Outcome Research Group. Cardiopulmonary bypass management and neurologic outcomes: an evidence-based appraisal of current practices. *Anesth. Analg.* 2018; 126:419–431.
41. Kishimoto Y., Nakamura Y., Harada S., Onohara T., Kishimoto S., Kurashiki T., Fujiwara Y., Nishimura M. Can Tolvaptan Protect Renal Function in the Early Postoperative Period of Cardiac Surgery? Results of a Single-Center Randomized Controlled Study. *Circ. J.* 2018; 82:999–1007.
42. Ranucci M., De Toffol B., Isgro G., Romitti F., Conti D., Vicentini M., Brozzi S. Hyperlactatemia during cardiopulmonary bypass: determinants and impact on postoperative outcome. *Crit. Care.* 2006; 10:R167.
43. Wang B., et al. Trends in age distribution among patients with chronic conditions: A systematic review. *J. Epidemiol. Community Health.* 2020; 25:312–321.
44. Johnson D., et al. Prevalence of smoking among adults: A meta-analysis. *Tob. Control.* 2016; 30:112–120.
45. Lee S., et al. Smoking and health outcomes: A systematic review and meta-analysis. *J. Smoking Cessat.* 2021; 18:87–95.
46. Patel R., et al. Prevalence of hypertension among adults: A systematic review and meta-analysis. *J. Hypertens.* 2018; 22:301–310.
47. Kim S., et al. Epidemiology of diabetes mellitus: A global perspective. *Diabetes Res. Clin. Pract.* 2020; 15:112–120.
48. Malmqvist G., Claesson Lingehall H., Appelblad M., Svenmarker S. Cardiopulmonary bypass prime composition: beyond crystalloids versus colloids. *Perfusion.* 2018; 34:130–135.
49. Humza A.U., Ghousia Baig S., Ali A., Ahmed I., Yousuf J.B. Assessment of QTc-interval prolonging medication utilization and associated potential drug-drug interactions in hospitalized cardiac patients: A cross-sectional study in cardiology. *Jordan J. Pharm. Sci.* 2024; 17:3.
50. Abazid H., Abu Farha R., Jaffal S., Alkaddah D., Al Jomaa E.E. Substance abuse among university students: Assessing prevalence, risk and preventive measures. *Jordan J. Pharm. Sci.* 2023; 16:2.
51. Alqassieh R., Omar M., Jirjees F. Intraoperative insulin infusion regimen versus insulin bolus regimen for glucose management during CABG surgery: A randomized clinical trial. *Jordan J. Pharm. Sci.* 2023; 16:3.

تأثير المانيتول على وظائف الكلى أثناء جراحة القلب وبعدها مباشرة في مستشفيات خاصة مختارة في مدينة نابلس/ فلسطين.

بلال رحال[1*]، هبة صلاح[1]، لين ابو عبده [2]، نور المصري[2]، شهد الطرشة[2]، شروق بشارات[2]، جمانة نجار[2]

[1]دائرة العلوم الطبية الحيوية، كلية الطب وعلوم الصحة، جامعة النجاح الوطنية، نابلس، فلسطين

[2]دائرة العلوم الطبية المساندة، كلية الطب وعلوم الصحة، جامعة النجاح الوطنية، نابلس، فلسطين

ملخص

الخلفية: تُعد مجازة القلب والرئة (CPB) تقنية شائعة في جراحة القلب، إلا أنها ترتبط بإصابة كلوية حادة. يمكن أن يؤثر نوع المحلول في دائرة مجازة القلب والرئة على نتائج الجراحة من خلال التأثير على العديد من الأعضاء وتوازن الجسم. لم يُحدد بعد المحلول الأولي الأمثل لدائرة مجازة القلب والرئة في جراحة القلب للبالغين. يُستخدم المانيتول على نطاق واسع في محلول التحضير لمجازة القلب والرئة، على الرغم من عدم وجود إجماع واضح على دوره في جراحة القلب.

الغرض: هدفت هذه الدراسة إلى دراسة تأثير المانيتول في محلول مجازة القلب والرئة الأولي على وظائف الكلى أثناء جراحة القلب وبعدها في مستشفيات خاصة مختارة في مدينة نابلس.

التصميم والمنهجية: تصميم دراسة أترابية مستقبلية أُجريت في مستشفى النجاح الوطني الجامعي ومستشفى العربي التخصصي. دُرست عينة من 120 مريضًا. خضع المرضى لجراحة قلب، وكانت وظائف الكلى لديهم طبيعية قبل الجراحة.

النتائج: ارتبط استخدام المانيتول في محلول CPB الرئيسي بانخفاض مستويات قراءات الكرياتينين والنيتروجين في الدم خلال فترة ما بعد الجراحة (متوسط فترة ما بعد الجراحة = 0.7692 ± 0.26068، و 18.3917 ± 7.56629 ملغ/ديسيلتر، على التوالي؛ قيمة p <0.001) وزيادة في مستويات معدل الترشيح الكبيبي خلال فترة ما بعد الجراحة (متوسط فترة ما بعد الجراحة = 112.27861 ± 1.43604، قيمة p <0.001) مما يشير إلى تحسن في وظائف الكلى بعد جراحة القلب.

الكلمات الدالة: الكرياتينين، المانيتول، مجازة القلب والرئة، جراحة القلب، وظائف الكلى.

[*] ***المؤلف المراسل: بلال رحال***

belalrahhal@najah.edu

تاريخ استلام البحث 2024/5/12 وتاريخ قبوله للنشر 2024/8/22.

Community Pharmacists' Attitudes Toward the Implementation of Good Pharmacy Practice Guidelines in Jordan: A Cross-Sectional Survey

Tahani Alwidyan[1*], Rawan Abudalo[1], Mohannad Odeh PhD[1], May Tayyem[2], Aya Banat[1]

[1]Department of Clinical Pharmacy and Pharmacy Practice, Faculty of Pharmaceutical Sciences, The Hashemite University, Zarqa, Jordan
[2]Department of Pharmaceutical Technology and Cosmetics, Faculty of Pharmacy, Middle East University, Amman, Jordan

ABSTRACT

Good Pharmacy Practice (GPP) guidelines have been adopted in many countries around the globe to improve the quality of services. However, there is a lack of evidence regarding the extent to which community pharmacists (CPs) adhere to the implementation of GPP guidelines, as reported in the literature. This study aimed to assess CPs' attitudes toward the implementation of GPP guidelines in Jordan. A probabilistic stratified random sampling approach was used to recruit eligible CPs. A validated Good Pharmacy Practice among Community Pharmacists (GPP-CP) questionnaire was administered to evaluate participants' attitudes toward GPP implementation. A total of 241 participants completed the GPP-CP questionnaire (response rate: 68.1%). Of these, 65.1% were females, and 91.7% reported having knowledge about GPP. The study findings demonstrated that good knowledge of GPP significantly influenced CPs' attitudes toward adherence to the profession's essentials and requirements (φc = 0.16, P = 0.047), administrative professional performance (φc = 0.20, P = 0.015), and patient counseling practices (φc = 0.22, P = 0.003). Among participants, the lowest level of agreement (52.3%) was reported regarding the documentation process of dispensed medications to patients. This study highlights the imperative need for establishing structured indicators to monitor the implementation of GPP in community pharmacy settings. Documentation of pharmaceutical care should also be prioritized. Educational programs and workshops are recommended to enhance pharmacists' practice in community settings. However, since these research findings on pharmacists' attitudes were gathered from Jordanian respondents within Arab society, they may not be generalizable to pharmacists in non-Arab societies where GPP guidelines could differ.

Keywords: social and administrative sciences, community settings, pharmacy practice, Good Pharmacy Practice, cross-sectional.

INTRODUCTION

Community pharmacists (CPs) are the primary contact point for people to fulfill their daily healthcare needs (1). In recent years, the role of CPs has expanded from dispensing and compounding medications to embracing patient-centered services (2-5). To adapt the growing health needs of people, CPs should enforce their structured knowledge of medications-related issues (for example, safety, efficacy, and monitoring outcomes) to provide optimal pharmaceutical care (6). In addition, CPs should ensure the appropriate delivery of pharmaceutical care services (7). National and international health practice standards and guidelines play an integral role in the best delivery of pharmaceutical care (8,9). The development of community pharmacy standards has been the subject of much research in social health science (10-12). In 1992, the World Health Organization (WHO) and the

[*]***Corresponding author: Tahani Alwidyan***
alwidyantahani@hu.edu.jo
Received: 13/5/2024 Accepted: 22/8/2024.
DOI: https://doi.org/10.35516/jjps.v18i2.2643

International Pharmaceutical Federation (FIP) developed the Good Pharmacy Practice (GPP) (13), an international standards for pharmacy profession aimed at guiding pharmacists on specific roles, functions, and activities to respond to the health needs of the people through optimal, evidence-based care in line with the mission of pharmacy practice in the new era (14).

Many countries including Jordan have adopted the international GPP guidelines by WHO/FIP in the development of their national guidelines (12). A wide range of services provided by a CP were reported in many studies (15-27). For example, improvement in lipid, blood glucose and blood pressure levels were reported in 59 diabetic patients in the United Kingdom following the application of pharmaceutical care model (i.e., drug therapy problems identification and patients' education about their hypoglycemic agents) by CPs (15). However, only few studies assessed CPs' attitude toward implementation of GPP guidelines in providing the pharmaceutical care services (28-32) or evaluated CPs ' familiarity with GPP elements (33) have been conducted. This study aimed to understand pharmacists' attitudes toward implementation of GPP guidelines in routine practice in community settings.

METHODS

Design

This cross-sectional survey study consisted of two phases; firstly, the data collection tool was developed and validated. Secondly, the validated Good Pharmacy Practice among Community Pharmacists (GPP-CP) questionnaire was administered (online and paper-based) to eligible participants between June and August 2023.

Participants and settings

Eligible participants included in this study were pharmacists who have a minimum qualification of BSc. in Pharmacy or Doctor of Pharmacy, were working in a community pharmacy and were able to consent. This study was conducted in community pharmacies in Jordan, either pharmacist-owned (independent pharmacy) or within pharmacy chains.

Data collection and sampling

The psychometric properties of the GPP-CP questionnaire indicate the questionnaire had good reliability based on the results from both the Cronbach's alpha (0.932) and composite reliability (0.972) tests, demonstrating a high level of internal consistency for the questionnaire. The GPP-CP questionnaire included two sections. The first section included sociodemographic and general information of pharmacists' knowledge about the GPP. The second section consists of 33 attitudinal items organized into five themes. The themes are profession's essentials and requirements (five items), organization management (eight items), administrative professional performance (five items), prescription management (seven items) and patient education (eight items). The sample size had been estimated based on sample size estimation for a finite population (N). The following formula was used for the calculation of sample size (n) considering population size from the Jordanian Pharmacists Association (JPA) website, 95% confidence interval (z = 1.96) and 5% margin of error (e = 0.05) (Equation 1).

$$Sample\ size\ (n) = \left[\frac{\left(\frac{z^2 p(1-p)}{e^2} \right) N}{\left(\frac{z^2 p(1-p)}{e^2} \right) + (N-1)} \right] \quad (Equation\ 1)$$

Where:

n = Required sample size

N = Population size

z = Z-score (based on confidence level)

p = Estimated proportion of population

e = Margin of error

The number of community pharmacies was determined from the JPA website, which stated that 4437 CPs were distributed through Jordan until the mid of January 2023. It was estimated that each community pharmacy should

have a minimum of one pharmacist. Thus, the population size of CPs was estimated to be 4437. Therefore, the required sample size was chosen to be 354.

A probabilistic stratified random sampling approach (34) was applied to identify community pharmacies for inclusion in this study. The researcher, AB, contacted potential participants, introduced herself, provided a brief description of the study, and confirmed the eligibility and willingness of the community pharmacists (CPs) to participate. On the day of the face-to-face administration of the hard copy of the GPP-CP questionnaire, participants were given time to review the consent form and provide written informed consent before completing the questionnaire. For those who preferred to complete the GPP-CP questionnaire electronically via email, telephone, Microsoft Teams, Skype, or WhatsApp, a weblink to the online version of the questionnaire—including online consent—was sent.

Statistical analysis

All data were coded and entered into a customized database developed using IBM SPSS® V28.0 (IBM, New York, USA) for statistical analysis. Descriptive statistics were reported for participant characteristics (e.g., age, gender, and type of pharmacy) as well as for responses to the questionnaire items (i.e., Likert scale responses). To evaluate pharmacists' attitudes toward Good Pharmacy Practice (GPP) in community settings, respondents indicated their level of agreement or disagreement on a five-point Likert scale: "Strongly agree," "Agree," "Neutral," "Disagree," and "Strongly disagree," scored from 5 to 1, respectively. Based on the number of questions within each theme, the total possible scores were: 25 points for the "Profession's Essentials and Requirements" and "Administrative Professional Performance" themes, 35 points for the "Prescription Management" theme, and 40 points for the "Organization Management" and "Patient Counselling" themes. The overall attitude level was categorized according to Bloom's cut-off point reference (35,36), as a "positive attitude" if the score was 80–100% (20– 25 points for profession's essentials and requirements and administrative professional performance themes; 28-35 points for prescription management theme and 32-40 points for organization management and patient counselling themes), "neutral attitude" if the score was 60– 79% (15–19.9 points for profession's essentials and requirements and administrative professional performance themes; 21-27.9 points for prescription management theme and 24-31.9 points for organization management and patient counselling themes) and "negative attitude" if the score was less than 60% (< 15 points for profession's essentials and requirements and administrative professional performance themes; < 21 points for prescription management theme and < 24 points for organization management and patient counselling themes). The Kolmogorov-Smirnov test was used to assess variables' normality of distribution. To identify association between participant's demographics and participants' level of attitude toward GPP within each theme, Pearson Chi-square or Fischer's Exact test as appropriate was used at $p<0.05$. To determine the strength of these associations, Cramer's v (φc) test was used. The strength of associations was interpreted as follows: a (φc) value of "1" indicated a complete association, ">0.25" represented a very strong association, ">0.15" indicated a strong association, ">0.1" suggested a moderate association, and ">0.05" implied a weak association, while "0" denoted no association (37).

Ethical approvals

Ethical approval was obtained for this study from the Hashemite University Institutional Review Board (reference number: 17/4/2022/2023) on 15th January 2023. Electronic or written informed consent was obtained from all participants.

RESULTS

Demographics

A total of 241 participants completed the GPP-CP questionnaire (response rate of 68.1%). The sample consisted of 34.9% (n=157) males and 65.1% females (n=84). Regarding the age of pharmacy building, pharmacies with less than 10 years, accounted for 61.8% (n=149) of the total sample. Just over three quarters

(75.5%, n=182) of participants worked in independent pharmacies. Chain pharmacies represented a smaller proportion of the sample, constituting 24.5% (n=59). The minority of participated pharmacies were located near hospitals, accounting for 9.5% (n=23). The majority of participated pharmacies have an employee's area (90%, n=217) whereas less than three-quarters (73%, n=176) have a counseling area (Table 1).

Table 1. Demographics and community pharmacy related information (n=241)

Variable	Categories	Frequency	Percent
Participant's age	21-25 years	65	27.0
	26-30 years	80	33.2
	31-35 years	46	19.1
	36-40 years	14	5.8
	41-45 years	17	7.1
	46-50 years	7	2.9
	More than 50 years	12	5.0
Participant's gender	Male	84	34.9
	Female	157	65.1
Age of pharmacy building	Less than 5 years	87	36.1
	5-9 years	62	25.7
	10-14 years	45	18.7
	15 years or more	47	19.5
Type of pharmacy	Independent pharmacy	182	75.5
	Chain pharmacy	59	24.5
Pharmacy's location	Near hospital	23	9.5
	Near medical center	76	31.5
	No hospital or medical center	87	36.1
	Near private doctor clinic	55	22.8
Presence of counselling area in the pharmacy	Yes	176	73.0
	No	65	27.0
Presence of an employee's area in the pharmacy	Yes	217	90.0
	No	2	10.0

In terms of familiarity with GPP, 91.7% (n=221) of participants indicated their knowledge of GPP. Less than half of the participants (43.6%, n=105) reported attending workshops about GPP, whereas 56.4% (n=136) indicated they had not participated in any. Furthermore, the data highlight the nearly equal division between those who actively participated in research and continuing education courses and those who did not (Table 2).

Table 2. Knowledge about GPP (n=241)

Variable	Categories	Frequency	Percent
Having knowledge about GPP	Yes	221	91.7
	No	20	8.3
Workshops about the GPP	Yes	105	43.6
	No	136	56.4
Participate in research and continuing education courses	Yes	119	49.4
	No	122	50.6
GPP, Good Pharmacy Practice			

Responses to the GPP-CP questionnaire items

Figure 1 presents the participants' responses to statements categorized into five themes: profession's essentials and requirements, organization management, administrative

professional performance, prescription management and patient counselling. It is noteworthy that a majority of participants agreed with almost all the questions, with the highest percentage being associated with the statement *" O3. The pharmacy has the necessary equipment to store medicines (e.g., refrigerator)"* (organization management) at 98.3% (n=237). This was closely trailed by *" A3. I ensure that medicines and other pharmaceutical products are provided from reliable sources and ensure their availability in the pharmacy store consistently"* (administrative professional performance) at 97.9% (n=236). Interestingly, almost all statements received zero to less than 4% of responses indicating disagreement, except for three statements within the organization management theme. These statements were *" O5. The pharmacy has systems for documenting possible side effects that may occur with healthcare seekers"* with 24.9% (n=60) of participants indicating disagreement, closely followed by the statement *" O7. The pharmacy has documentation systems for patient profile and therapeutic interventions"* with 25.3% (n=61) disagreement. The statement *" O6. The medication dispensed to the patient is recorded and the patient's drug data is constantly updated"* has a slightly higher percentage of 28.6% (n=61) disagreement (Figure 1).

Participants' attitude

A higher mean score of each theme in the GPP-CP questionnaire indicates a good level of attitude of CPs toward implementation of GPP guidelines. As shown in Table 3 below, more than fifty of participants had a positive attitude toward all themes included in the GPP-CP questionnaire. The vast majority (94.6%, n=228) were seen toward the administrative professional performance theme and the lowest proportion (66.0%, n=159) were seen toward the organization management theme. However, zero to 1.2% of participants had a negative attitude toward each theme included in the GPP-CP questionnaire. Participants have good compliance with the national professional obligations of the law to permit pharmacists to work in community settings, such as familiarization with the code of ethics, legislations, and regulations that enhance implementation of GPP in community pharmacy settings (Profession's essentials and requirements). More than three-quarters (78.8%, n=190) of participants adhered positively to these guidelines, whereas only 0.8% (n=2) had a negative attitude toward compliance with the national law and regulations (Table 3). Just below two-thirds (66.0%, n=159) of participants showed a positive fulfillment of GPP's requirement in managing their community pharmacies' facilities and resources (Organization management). For example, consideration of product's storage conditions, provision of Standard Operating Procedures and documentation systems for patients' data and medical prescriptions. Others either had a negative (0.8%, n=2) or neutral attitude (33.2%, n=80) toward the fulfilment of management requirements in the community pharmacy (Table 3). Regarding the administrative professional performance, the majority of participants (94.6%, n=228) showed a positive attitude regarding good communication and consideration of coworkers' ideas and skills and purchasing pharmaceutical products from reliable sources to ensure the quality of medicines. Further, the use of distinct files to keep the dispensed prescriptions and the invoices of purchased medicines, in which the documents are arranged according to the dates and for the period specified by the laws (Table 3). More than ninety percent of participants (92.5%, n=223) showed a positive level of adherence to the component of GPP in medical prescription management. Before dispensing the prescription medications, they ensure that each medication in the prescription is administered to the right patient, at the right time, in the right dose, by the right route, and that there is no duplication. Only 1.2% (n=3) of participants had a negative attitude toward prescription management (Table 3). Patient counselling was perceived to be an integral part of GPP according to the mean score of this theme (35.8± 4.1). Just below ninety percent (88.8%, n=214) of participated CPs tend positively to engage with patients and educate them about their medications and lifestyle. They also follow up with the patient to ensure the treatment appropriateness (Table 3).

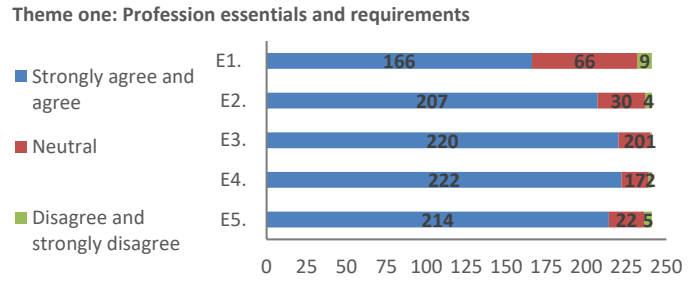

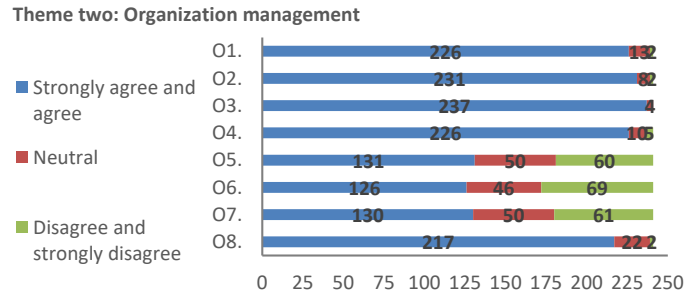

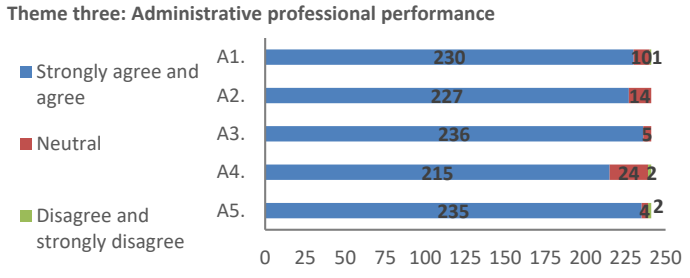

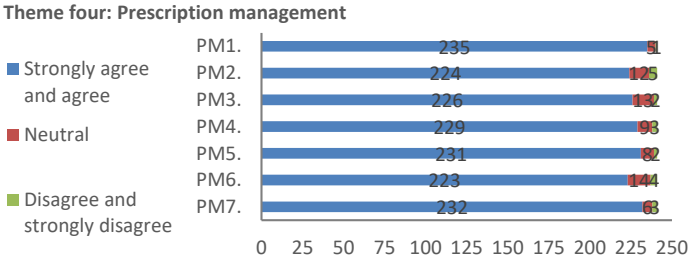

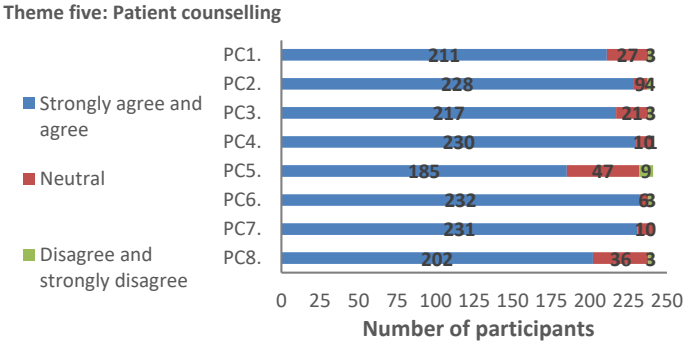

KEY OF ITEMS DESCRIPTION

Theme one: Profession essentials and requirements

E1. I am familiar with all national laws and regulations of the pharmacy profession.

E2. I apply all national laws and regulations of the pharmacy profession.

E3. I adhere to the national code of ethics and apply it in routine practice.

E4. It is my responsibility to inform the patient and health care providers (pharmacists and/or doctors) of any circumstances that may delay the provision of treatment.

E5. I know my rights, duties, and professional responsibilities of a pharmacist towards pharmaceutical care seekers according to the national laws and regulations.

Theme two: Organization management

O1. The pharmacy has decent appearance and good hygiene.

O2. The storage conditions of each product are considered as stated on the product packaging or its internal leaflet.

O3. The pharmacy has the necessary equipment to store medicines (e.g., refrigerator).

O4. Pharmacy Standard Operating Systems (SOPs) are available at the pharmacy.

O5. The pharmacy has systems for documenting possible side effects that may occur with health care seekers.

O6. The medication dispensed to the patient is recorded and the patient's drug data is constantly updated.

O7. The pharmacy has documentation systems for patient profile and therapeutic interventions.

O8. All documents and prescriptions are kept until destroyed by the inspecting pharmacists.

Theme three: Administrative professional performance

A1. In the communication with the pharmacy staff, I respect their opinion and decisions.

A2. Attention is given to what staff raise and respond to their ideas.

A3. I ensure that medicines and other pharmaceutical products are provided from reliable sources and ensure their availability in the pharmacy store consistently.

A4. The prescriptions that are dispensed and the invoices of medicines and other pharmaceutical products are kept in a special file in which the documents are arranged according to the dates and for the period specified by the laws.

A5. I do not deal with agents that provide medicine or other pharmaceutical products that are counterfeit or smuggled.

Theme four: Prescription management

PM1. Regarding the prescription, I check its clarity and the identity of the prescriber who wrote it.

PM2. I re-check the conformity between the label on the dispensed medicine and the prescription information (dose, frequency, duration of treatment) and that the correct medicine has been dispensed to the correct patient.

PM3. I review the medications included in the prescription to ensure that the patient's complaint matches the indications of the prescribed medications.

PM4. I review the medications included in the prescription to ensure that there is no duplication of medications.

PM5. I review the prescribed medications to ensure that the dosage form is appropriate for the patient.

PM6. In case of doubt about the prescription, or if I have a recommendation on the medicine, dosage, or alternative, I refer to the prescriber to check.

PM7. I do not dispense forged and illegal prescriptions and return them to the patient.

Theme five: Patient counselling

PC1. I check with the patients their lifestyle, dietary habits, allergy to food or medicine, smoking, alcohol intake to ensure there is no interferences with prescribed medications.

PC2. I give information to patients about the form and content of their medications.

PC3. I explain to patients the proper storage conditions of their medications.

PC4. I explain to patients the instructions of how to take their medications, correct dose, route, frequency and when to stop their using these medications (i.e., duration of treatment).

PC5. I review laboratory tests, if patients bring them with the prescription and educate patients about monitoring.

PC6. I explain any information I deem necessary to patients.

PC7. I make sure that patients understand the information by asking them to explain what they understood in their own languages.

PC8. I follow up the patient to ensure that the treatment results are achieved or to suggest the necessary modifications to the treatment plan if the wanted outcome is not achieved.

Table 3. The level of attitude of community pharmacists toward the five themes of the GPP-CP questionnaire

Theme	level of attitude	Score	N (%)
Profession's essentials and requirements	Positive	20-25	190 (78.8)
	Neutral	15-19.9	49 (20.3)
	Negative	<15	2 (0.8)
Minimum score =13; maximum score =25; mean score =21.5; SD =2.9.			
Organization management	Positive	32-40	159 (66.0)
	Neutral	24-31.9	80 (33.2)
	Negative	<24	2 (0.8)
Minimum score =23; maximum score =40; mean score =33.8; SD =4.5.			
Administrative professional performance	Positive	20-25	228 (94.6)
	Neutral	15-19.9	13 (5.4)
	Negative	<15	0 (0)
Minimum score =20; maximum score =35; mean score =32.4; SD =3.4.			
Prescription management	Positive	28-35	223 (92.5)
	Neutral	21-27.9	15 (6.2)
	Negative	<21	3 (1.2)
Minimum score =20; maximum score =35; mean score =32.4; SD =3.4.			
Patient counselling	Positive	32-40	214 (88.8)
	Neutral	24-31.9	26 (10.8)
	Negative	<24	1 (0.4)
Minimum score =18; maximum score =40; mean score =35.8; SD =4.1.			
The overall level of attitude was categorized using bloom's cut-off point, as a "positive attitude" if the score was 80–100% (20– 25 points for profession essentials and requirements and administrative professional performance themes ; 28-35 points for prescription management theme and 32-40 points for organization management and patient counselling themes), "neutral attitude" if the score was 60– 79% (15–19.9 points for profession essentials and requirements and administrative professional performance themes; 21-27.9 points for prescription management theme and 24-31.9 points for organization management and patient counselling themes) and "negative attitude" if the score was less than 60% (< 15 points for profession essentials and requirements and administrative professional performance themes; < 21 points for prescription management theme and < 24 points for organization management and patient counselling themes).			

Determinants of CPs' attitude

Participant's age, type of pharmacy and pharmacy's location did not statistically influence any level of participants' attitude toward implementation of GPP guidelines (P>0.05). The highest impact was seen for the determinant "knowledge about the GPP" which have strong and significant association with the positive attitudes of the majority of participants toward the profession's essentials and requirements (n=177 (73.4%); φc=0.16; P=0.047), administrative professional performance (n=212 (88%); φc=0.20, P=0.015), and patient counselling practices (n=198 (82.2%); φc=0.22, P=0.003); Tables 4, 6 and 8, respectively. Also, female participants were strongly and significantly perceived to be more responsible for administrative professional performance (φc=0.17, P=0.010; Table 6) and prescription management (φc=0.23, P=0.001; Table 7) than male participants. Statistically significant influences were seen

for GPP-related workshops attendance and research participation on participants' attitudes toward their adherence to the pharmacy profession's essentials and requirements (*P*=0.026 and 0.013, respectively; Table 4). Further, participants who attended GPP-related workshops had a positive attitude toward prescription management than others who did not attend (*P*=0.026; Table 7). The presence of counselling area within the community pharmacy influences the positive attitude of participants toward organizational issues of the community pharmacy (*P*=0.021; Table 5) while the presence of employee's area influences the positive attitude of participants toward patient counselling practice (*P*=0.010; Table 8).

Table 4. Determinants that are associated with the pharmacists' attitude toward the implementation of GPP guidelines in community settings (Theme: Profession's essentials and requirements) (n=241)

		Level of attitude			X^2	*P*-value	Cramer's phi (φc)
Variable	**Category**	**Positive**	**Neutral**	**Negative**			
Participant's age	21-25 years	52	12	1	8.20	0.769	0.13
		21.6%	5.0%	0.4%			
	26-30 years	63	16	1			
		26.1%	6.6%	0.4%			
	31-35 years	38	8	0			
		15.8%	3.3%	0 %			
	36-40 years	8	6	0			
		3.3%	2.5%	0 %			
	41-45 years	12	5	0			
		5%	2.1%	0 %			
	46-50 years	6	1	0			
		2.5%	0.4%	0 %			
	More than 50 years	11	1	0			
		4.6%	0.4%	0 %			
Participant gender	Male	64	19	1	0.65	0.723	0.05
		26.6%	7.9%	0.4%			
	Female	126	30	1			
		52.3%	12.4%	0.4%			
Pharmacy type	Independent pharmacy	147	34	1	2.10	0.358	0.09
		61%	14.1%	0.4%			
	Chain pharmacy	43	15	1			
		17.8%	6.2%	0.4%			
Location	Near hospital	17	6	0	7.50	0.279	0.13
		7.1%	2.5%	0 %			
	Near medical center	62	14	0			
		25.7%	5.8%	0 %			
	No hospital or medical center	69	18	0			
		28.6%	7.5%	0 %			
	Near private doctor clinic	42	11	2			
		17.4%	4.6%	0.8%			
Counselling area	Yes	138	36	2	0.76	0.684	0.06
		57.3%	14.9%	0.8%			
	No	52	13	0			
		21.65	5.4%	0 %			
Employee's area	Yes	175	40	2	5.00	0.083	0.14

		Level of attitude			X^2	*P*-value	Cramer's phi (φc)
Variable	**Category**	**Positive**	**Neutral**	**Negative**			
		72.6%	16.6%	0.8%			
	No	15	9	0			
		6.2%	3.7%	0 %			
knowledge about GPP	Yes	177	43	1	6.10	**0.047**	0.16
		73.4%	17.8%	0.4%			
	No	13	6	1			
		5.4%	2.5%	0.4%			
GPP related workshops	Yes	91	13	1	7.27	**0.026**	0.17
		37.8%	5.4%	0.4%			
	No	99	36	1			
		41.1%	14.9%	0.4%			
Research	Yes	103	15	1	8.68	**0.013**	0.19
		42.7%	6.2%	0.4%			
	No	87	34	1			
		36.1%	14.1%	0.4%			
GPP, Good Pharmacy Practice; *Fischer's Exact test was used for the analysis.							

Table 5. Determinants that are associated with the pharmacists' attitude toward the implementation of GPP guidelines in community settings (Theme: Organization management) (n=241)

		Level of attitude			X^2	*P*-value	Cramer's phi (φc)
Variable	**Category**	**Positive**	**Neutral**	**Negative**			
Participant's age	21-25 years	48	16	1	10.8	0.543	0.05
		19.9%	6.6%	0.4%			
	26-30 years	54	25	1			
		22.4%	10.4%	0.4%			
	31-35 years	31	15	0			
		12.9%	6.2%	0%			
	36-40 years	8	6	0			
		3.3%	2.5%	0%			
	41-45 years	10	7	0			
		4.1%	2.9%	0%			
	46-50 years	4	3	0			
		1.7%	1.2%	0%			
	More than 50 years	4	8	0			
		1.7%	3.3%	0%			
Participant gender	Male	58	25	1	0.84	0.656	0.06
		24.1%	10.4%	0.4%			
	Female	101	55	1			
		41.9%	22.8%	0.4%			
Pharmacy type	Independent pharmacy	122	58	2	1.12	0.557	0.07
		50.6%	24.1%	0.8%			
	Chain pharmacy	37	22	0			
		15.4%	9.1%	0%			

Variable	Category	Level of attitude			X^2	*P*-value	Cramer's phi (φc)
		Positive	Neutral	Negative			
Location	Near hospital	15	8	0	5.80	0.447	0.11
		6.2%	3.3%	0%			
	Near medical center	56	19	1			
		23.2%	7.9%	0.4%			
	No hospital or medical center	57	29	1			
		23.7%	12%	0.4%			
	Near private doctor clinic	31	24	0			
		12.9%	10%	0%			
Counselling area	Yes	122	54	0	7.76	**0.021**	0.18
		50.6%	22.4%	0%			
	No	37	26	2			
		15.4%	10.8%	0.8%			
Employee's area	Yes	145	71	1	3.96	0.138	0.13
		60.2%	29.5%	0.4%			
	No	14	9	1			
		5.8%	3.7%	0.4%			
knowledge about GPP	Yes	148	71	2	1.50	0.474	0.08
		61.4%	29.5%	0.8%			
	No	11	9	0			
		4.6%	3.7%	0%			
GPP related workshops	Yes	75	29	1	2.62	0.270	0.10
		31.1%	12%	0.4%			
	No	84	51	1			
		34.9%	21.2%	0.4%			
Research	Yes	83	34	2	4.10	0.131	0.13
		34.4%	14.1%	0.8%			
	No	76	46	0			
		31.5%	19.1%	0%			

GPP, Good Pharmacy Practice; *Fischer's Exact test was used for the analysis.

Table 6. Determinants that are associated with the pharmacists' attitude toward the implementation of GPP guidelines in community settings (Theme: Administrative professional performance) (n=241)

		Level of attitude			X^2	*P*-value	Cramer's phi (φc)
Variable	**Category**	**Positive**	**Neutral**	**Negative**			
Participant's age	21-25 years	62	3	0	0.96	0.986	0.06
		25.7%	1.2%	0%			
	26-30 years	75	5	0			
		31.1%	2.1%	0%			
	31-35 years	44	2	0			
		18.3%	0.8%	0%			
	36-40 years	13	1	0			
		5.4%	0.4%	0%			
	41-45 years	16	1	0			
		6.6%	0.4%	0%			
	46-50 years	7	0	0			
		2.9%	0%	0%			
	More than 50 years	11	1	0			
		4.6%	0.4%	0%			
Participant gender	Male	75	9	0	7.15	**0.010***	0.17
		31.1%	3.7%	0%			
	Female	153	4	0			
		63.5%	1.7%	0%			
Pharmacy type	Independent pharmacy	172	10	0	0.02	0.602*	0.01
		71.4%	4.1%	0%			
	Chain pharmacy	56	3	0			
		23.2%	1.2%	0%			
Location	Near hospital	21	2	0	2.01	0.570	0.09
		8.7%	0.8%	0%			
	Near medical center	74	2	0			
		30.7%	0.8%	0%			
	No hospital or medical center	81	6	0			
		33.6%	2.5%	0%			
	Near private doctor clinic	52	3	0			
		21.6%	1.2%	0%			
Counselling area	Yes	166	10	0	0.12	0.517*	0.02
		68.9%	4.1%	0%			
	No	62	3	0			
		25.7%	1.2%	0%			
Employee's area	Yes	207	10	0	2.06	0.127*	0.11
		85.9%	4.1%	0%			

Variable	Category	Level of attitude			X^2	*P*-value	Cramer's phi (φc)
		Positive	Neutral	Negative			
	No	21	3	0			
		8.7%	1.2%	0%			
knowledge about GPP	Yes	212	9	0	9.12	**0.015***	0.20
		88%	3.7%	0%			
	No	16	4	0			
		6.6%	1.7%	0%			
GPP related workshops	Yes	100	5	0	0.15	0.467*	0.03
		41.5%	2.1%	0%			
	No	128	8	0			
		53.1%	3.3%	0%			
Research	Yes	115	4	0	1.90	0.137*	0.09
		47.7%	1.7%	0%			
	No	113	9	0			
		46.9%	3.7%	0%			

GPP, Good Pharmacy Practice; *Fischer's Exact test was used for the analysis.

Table 7. Determinants that are associated with the pharmacists' attitude toward the implementation of GPP guidelines in community settings (Theme: Prescription management) (n=241)

Variable	Category	Level of attitude			X^2	*P*-value	Cramer's phi (φc)
		Positive	Neutral	Negative			
Participant's age	21-25 years	58	6	1	9.21	0.685	0.14
		24.1%	2.5%	0.4%			
	26-30 years	76	4	0			
		31.5%	1.7%	0%			
	31-35 years	42	3	1			
		17.4%	1.2%	0.4%			
	36-40 years	13	1	0			
		5.4%	0.4%	0%			
	41-45 years	16	1	0			
		6.6%	0.4%	0%			
	46-50 years	7	0	0			
		2.9%	0%	0%			
	More than 50 years	11	0	1			
		4.6%	0%	0.4%			
Participant gender	Male	71	10	3	13.19	**0.001**	0.23
		29.5%	4.1%	1.2%			
	Female	152	5	0			
		63.1%	2.1%	0%			

		Level of attitude			X^2	*P*-value	Cramer's phi (φc)
Variable	**Category**	**Positive**	**Neutral**	**Negative**			
Pharmacy type	Independent pharmacy	170	10	2	0.82	0.662	0.06
		70.5%	4.1%	0.8%			
	Chain pharmacy	53	5	1			
		22%	2.1%	0.4%			
Location	Near hospital	22	1	0	7.76	0.256	0.13
		9.1%	0.4%	0%			
	Near medical center	73	3	0			
		30.3%	1.2%	0%			
	No hospital or medical center	76	8	3			
		31.5%	3.3%	1.2%			
	Near private doctor clinic	52	3	0			
		21.6%	1.2%	0%			
Counselling area	Yes	162	12	2	0.45	0.799	0.04
		67.2%	5%	0.8%			
	No	61	3	1			
		25.3%	1.2%	0.4%			
Employee's area	Yes	201	14	2	2.01	0.366	0.09
		83.4%	5.8%	0.8%			
	No	22	1	1			
		9.1%	0.4%	0.4%			
knowledge about GPP	Yes	207	12	2	5.54	0.063	0.15
		85.9%	5%	0.8%			
	No	16	3	1			
		6.6%	1.2%	0.4%			
GPP related workshops	Yes	99	3	3	7.34	**0.026**	0.17
		41.1%	1.2%	1.2%			
	No	124	12	0			
		51.5%	5%	0%			
Research	Yes	111	7	1	0.34	0.832	0.04
		46.1%	2.9%	0.4%			
	No	112	8	2			
		46.5%	3.3%	0.8%			

GPP, Good Pharmacy Practice; *Fischer's Exact test was used for the analysis.

Table 8. Determinants that are associated with the pharmacists' attitude toward the implementation of GPP guidelines in community settings (Theme: Patient counselling) (n=241)

		Level of attitude			X^2	*P*-value	Cramer's phi (φc)
Variable	**Category**	**Positive**	**Neutral**	**Negative**			
Participant's age	21-25 years	60	5	0	8.25	0.765	0.13
		24.9%	2.1%	0%			
	26-30 years	73	7	0			
		30.3%	2.9%	0%			
	31-35 years	40	5	1			
		16.6%	2.1%	0.4%			
	36-40 years	11	3	0			
		4.6%	1.2%	0%			
	41-45 years	14	3	0			
		5.8%	1.2%	0%			
	46-50 years	6	1	0			
		2.5%	0.4%	0%			
	More than 50 years	10	2	1			
		4.1%	0.8%	0.4%			
Participant gender	Male	72	11	1	2.64	0.267	0.12
		29.9%	4.6%	0.4%			
	Female	142	15	0			
		58.9%	6.2%	0%			
Pharmacy type	Independent pharmacy	164	18	0	3.79	0.151	0.13
		68%	7.5%	0%			
	Chain pharmacy	50	80	1			
		20.7%	33.2%	0.4%			
Location	Near hospital	18	5	0	6.56	0.363	0.12
		7.5%	2.1%	0%			
	Near medical center	71	5	0			
		29.5%	2.1%	0%			
	No hospital or medical center	75	11	1			
		31.1%	4.6%	0%			
	Near private doctor clinic	50	5	0			
		20.7%	2.1%	0%			
Counselling area	Yes	156	19	1	0.34	0.831	0.04
		64.7%	7.9%	0.4%			
	No	58	7	0			
		24.1%	2.9%	0%			
Employee's area	Yes	193	24	0	9.20	**0.010**	0.20
		80.1%	10%	0%			
	No	21	2	1			

		Level of attitude			X^2	*P*-value	Cramer's phi (φc)
Variable	**Category**	**Positive**	**Neutral**	**Negative**			
		8.7%	0.8%	0.4%			
knowledge about GPP	Yes	198	23	0	11.60	**0.003**	0.22
		82.2%	9.5%	0%			
	No	16	3	1			
		6.6%	1.2%	0.4%			
GPP related workshops	Yes	92	12	1	1.40	0.498	0.08
		38.2%	5%	0.4%			
	No	122	14	0			
		50.6%	5.8%	0%			
Research	Yes	106	13	0	1.00	0.612	0.06
		44%	5.4%	0%			
	No	108	13	1			
		44.8%	5.4%	0.4%			
GPP, Good Pharmacy Practice; *Fischer's Exact test was used for the analysis.							

DISCUSSION

Main findings

In this study, a 33-item GPP-CP questionnaire was developed and validated to assess the attitudes of CPs toward GPP guidelines. The psychometric properties of the questionnaire were established in the Jordanian context and showed good reliability (Cronbach's alpha = 0.932). While limited continuous learning activity was identified, CPs were perceived to have a good level of knowledge about GPP (91.7%). The findings suggest that CPs fulfill various functions in compliance with GPP guidelines (38,39). These functions can be categorized into five essential roles of a CP: (a) obey national professional laws, legislation, and guidelines; (b) maintain pharmacy organization; (c) manage administrative aspects of professional performance; (d) provide effective prescription management; and (e) provide effective medication therapy management and counseling.

In the present study, the lack of a documentation system in pharmacies—which would allow CPs to formally record dispensed medications, medication side effects, and therapeutic interventions—among a significant proportion of CPs (organization management theme) may be linked to limited attendance at workshops and continuing education courses. Therefore, there may be opportunities to increase awareness and documentation activities among CPs in routine practice. However, the extent to which this is feasible and acceptable is still unknown. Future research should explore the barriers and enablers for pharmacists to increase proactive documentation activity in community settings.

Interpretation and implications of practice

GPP is an essential practice to provide optimal and evidence-based pharmaceutical care in community settings. While many countries worldwide adopted their national GPP guidelines, the impact of pharmacists' adherence to these guidelines in providing pharmaceutical care services in community settings is still being examined in the literature. This study sought to assess the level of adherence of pharmacists to GPP guidelines in community settings. The highest agreement level detected was for the presence of essential requirement for the storage of

medications in the pharmacy (98.3%). Importantly, this level was not associated to the pharmacy or the pharmacists' characteristics. These findings were in line with what was found in a cross-sectional study conducted among 250 CPs in Lebanon which reported that 88% of pharmacies have been equipped with cooling and heating systems to properly store medications (30). It is highly recommended that pharmacists should supervise storage conditions on a regular basis to safeguard compliance with the manufacturer's instructions, thus ensuring sought medication safety and efficacy. Our findings reported a good attitude toward prescription management among more than 90% of CPs. They review the dose, dosage form, indication, and duplication of medications. Interprofessional collaboration with prescribers was reported by participants in case of recommending any modification about the medicines or information related to them. A similar trend was seen in one cross-sectional postal survey among 112 general practitioners and 163 CPs to assess their role in medication review and medication management programs in clinical practice in Germany. Although not restricted to community settings. Most CPs revealed that they check the storage conditions of medications (n = 154, 94.5%), initial compilation of the patient's medication (n = 148, 90.8%), clinical parameters (n = 144, 88.3%), administration times (n = 118, 72.4%) and medication overuse and underuse (n = 100, 61.3%) either alone or in collaboration with general practitioners. Few pharmacists revealed that they check the dose of medications (n = 64, 39.3%), side effects (n = 61, 37.4%) and non-adherence (n = 52, 31.9%) (40). In the current study, more than three-quarters of the respondents agreed that they provide comprehensive information to patients about their medications (for example, dosing, duration of treatment, instructions about the appropriate use, storage conditions) and ensure that patients understand pharmacists' educational information. This may be linked to the shift of CPs ' role toward a patient-centric approach to meet patient's health-related needs. Though not limited to the operationalization of GPP guidelines and conducted in heterogeneous healthcare settings in different countries, several studies have assessed the role of pharmacists in patient counselling to provide effective medication therapy management (41-47). A retrospective longitudinal study of 1,572 patients who received medication management interventions from CPs in British Columbia reported that all patients were educated about their medications during pharmacy visits. Furthermore, pharmacists identified 2,133 drug-related problems, including the need for additional therapy 61.8% (n = 1319); unnecessary drug therapy 11.4% (n = 243); poor adherence 10.8% (n = 231); adverse drug reaction 4.8% (n = 103); dosage too low 4.8% (n = 103); dosage too high 4.2% (n = 90); and recommend alternative drug 2.1% (n = 44) (47). Particular emphasis should be given to the key elements of pharmaceutical care process such as patients' medication review, medication monitoring and treatment follow-up that should be adopted into day-to-day activities. Documentation of pharmaceutical care process should also be prioritized.

Determinants related to good attitudes of CPs towards the implementation of GPP guidelines in routine practice are also explored in this study. The findings revealed that CPs' knowledge about the GPP and the attendance of GPP workshops positively impact CPs' attitudes toward the implementation of GPP guidelines. These findings provide insights that participants who have better attitudes might have better opportunities to access updated information, which would help them to improve their knowledge of GPP; consequently, improve their attitude and practice. Educational programs and workshops are recommended for pharmacists to enhance their practice in community settings. Regular audits could assist the national health authorities in ensuring that the pharmacies are following GPP guidelines. Incentives would be to optimize patient care. Future research should focus on the development of structured indicators to monitor implementation of GPP in community pharmacy settings.

Strength and limitations

The assessment of the GPP-CP questionnaire's validity and reliability enhanced the quality and accuracy of the data collected. Notwithstanding the existence of positive attitude of pharmacists toward implementation to most of GPP guidelines, the current findings identified areas for improvement, such as the adoption of documentation of the pharmaceutical care process in routine practice. Some limitations need to be considered when interpreting the results. First, the cross-sectional design of this research makes it difficult to determine causal inferences from the data. Second, the self-reported method of data collection exerts the possibility of recall bias; pharmacists may have altered their answers to meet GPP guidelines. Third, for the accurate assessment of pharmacists' adherence to GPP guidelines specifically those of critical importance for patients' health, we should use specific measurement outcomes such as patient satisfaction; this should be the aim of future work. Finally, Hence, the research findings on pharmacists' attitudes garnered from Jordanian respondents in Arab society, findings may not generalize to pharmacists in non-Arab societies, where the GPP guidelines could be different.

CONCLUSIONS

This study highlighted that most GPP guidelines in community pharmacy settings are being met by pharmacists—for example, maintaining proper storage conditions and ensuring appropriate patient education to maximize medication safety and efficacy. However, documentation of the pharmaceutical care process was found to be lacking to a lesser extent. Future interventional research should focus on changing pharmacists' behavior toward documentation activities and aim to identify the most relevant and feasible measures and outcomes for implementation in routine practice.

ACKNOWLEDGEMENTS

The authors would like to thank CPs who agreed to take part either in the validation stage of the questionnaire or in the main study phase. The authors would also like to thank Dr Ola Alnatsheh, Dr Nedaa Radwan, Dr Rania Obidat, Dr Alaa Habib, and Dr Ayman Shaheen for assisting with piloting the questionnaire.

DECLARATION OF CONFLICT OF INTEREST

The author(s) declare that there are no conflicts of interest.

FUNDING

This research did not receive any specific grant from funding agencies in the public, commercial, or not-for-profit sectors.

REFERENCES

1. Agomo CO. The role of community pharmacists in public health: a scoping review of the literature. *Journal of Pharmaceutical Health Services Research*. 2012;3(1):25-33.
2. Wheeler JS, Chisholm-Burns M. The benefit of continuing professional development for continuing pharmacy education. *American journal of pharmaceutical education*. 2018;82(3).
3. Kusynová Z, van den Ham HA, Leufkens HG, Mantel-Teeuwisse AK. Longitudinal study of Good Pharmacy Practice roles covered at the annual world pharmacy congresses 2003–2019. *Journal of Pharmaceutical Policy and Practice*. 2022;15(1):1-14.
4. Amara N, Naser AY, Esra'O T. Patient satisfaction with pharmaceutical services in Jordan: A cross-sectional study. *Jordan Journal of Pharmaceutical Sciences*. 2023;16(1):1-10.

5. Mea'ad MH, Mukattash TL, Al-Shatnawi S, Abu-Farha R, Abuhammad S, Jarab A, et al. Community Pharmacists' Perceptions of the most Important Interventions Implemented in Supporting Breastfeeding Women During Maternal Life: A Cross-Sectional Study in Jordan. *Jordan Journal of Pharmaceutical Sciences*. 2024;17(1):144-50.
6. Zekan L, Mestrovic A, Perisin AS, Bukic J, Leskur D, Rusic D, et al. Improving community pharmacists' clinical knowledge to detect and resolve drug-related problems in Croatia: a before/after survey study investigating the efficacy of an educational intervention. *BMJ open*. 2020;10(6):e034674.
7. Kho BP, Hassali MA, Lim CJ, Saleem F. Challenges in the management of community pharmacies in Malaysia. *Pharmacy Practice (Granada)*. 2017;15(2).
8. Chertes A, Crişan O. Standards for good pharmacy practice–a comparative analysis. *Farmacia*. 2019;67(3):545-50.
9. Grimshaw JM, Russell IT. Effect of clinical guidelines on medical practice: a systematic review of rigorous evaluations. *The Lancet*. 1993;342(8883):1317-22.
10. Parinyarux P, Dhippayom T, Wongpoowarak P, Kitikannakorn N. Development of community pharmacy competencies. *Journal of Pharmacy Technology*. 2022;38(3):183-90. doi: https://doi.org/10.1177/87551225221081370.
11. Alenezi S, Alanazi M, Aljazaeri R, Almuzaini M, Alrasheidi S, Shamlan WB, et al. Community Pharmacies in the *Asian Countries of Developing Health System: Formation, Regulation, and Implication. Pharmacy*. 2023;11(4):127.
12. Hallit S, Sacre H, Sarkis H, Dalloul N, Abou Jaoude C, Nahhas Z, et al. Good pharmacy practice standardized for community pharmacists: the Lebanese order of pharmacists initiative. *Journal of Research in Pharmacy Practice*. 2019;8(1):29.
13. Pearson GJ. Evolution in the practice of pharmacy—not a revolution! *Cmaj*. 2007;176(9):1295-6.
14. Unhurian L, Bielyaieva O, Vyshnytska I, Suschuk N, Petkova I. Implementation of standards of good pharmacy practice in the world: a review. 2018.
15. Wermeille J, Bennie M, Brown I, McKnight J. Pharmaceutical care model for patients with type 2 diabetes: Integration of the community pharmacist into the diabetes team - A pilot study. *Pharmacy World and Science*. 2004;26(1):18-25. doi: 10.1023/B:PHAR.0000013465.24857.a8.
16. Burns A. Medication therapy management services: A critical review. *Journal of the American Pharmacists Association*. 2005;45(5):580-7. doi: 10.1331/1544345055001328.
17. Murphy AL, MacKinnon NJ, Flanagan PS, Bowles SK, Sketris IS. Pharmacists' participation in an inhaled respiratory medication program: Reimbursement of professional fees. *Annals of Pharmacotherapy*. 2005;39(4):655-61. doi: 10.1345/aph.1E286.
18. Schulke DG, Krantzberg E, Grant J. Introduction: Medicare quality improvement organizations - Activities and partnerships. *Journal of Managed Care Pharmacy*. 2007;13(6 SUPPL. B):S3-S44.
19. Layson-Wolf C, Morgan JA. Pharmacy continuity of care: What do community pharmacists need from an acute care hospital to improve continuity of pharmaceutical care? *Disease Management and Health Outcomes*. 2008;16(4):199-203. doi: 10.2165/00115677-200816040-00001.
20. Moczygemba LR, Barner JC, Lawson KA, Brown CM, Gabrillo ER, Godley P, et al. Impact of telephone medication therapy management on medication and health-related problems, medication adherence, and medicare part D drug costs: A 6-month follow up. *American Journal Geriatric Pharmacotherapy*. 2011;9(5):328-38. doi: 10.1016/j.amjopharm.2011.08.001.

21. Steele KM, Ruisinger JF, Bates J, Prohaska ES, Melton BL, Hipp S. Home-based comprehensive medication reviews: Pharmacist's impact on drug therapy problems in geriatric patients. *Consultant Pharmacist*. 2016;31(10):598-605. doi: 10.4140/TCP.n.2016.598.
22. Jackson DL, Michaels NM, Melson B, Bruder E, Rhodes LA, Marciniak MW. Evaluation of the economic and clinical impact of community pharmacist-driven pharmacy benefit management services. *Journal of the American Pharmacists Association*. 2019;59(4):S91-S4. doi: 10.1016/j.japh.2019.03.016.
23. Moszczyński AA, Makarewicz-Wujec M, Kozłowska-Wojciechowska M. Community Pharmacy services available in United Kingdom. *Farmacja Polska*. 2019;75(10):542-8. doi: 10.32383/FARMPOL/115155.
24. Peláez Bejarano A, Villar Santos P, Robustillo-Cortés MDLA, Sánchez Gómez E, Santos Rubio MD. Implementation of a novel home delivery service during pandemic. *European Journal of Hospital Pharmacy*. 2021;28(e1):E120-E3. doi: 10.1136/ejhpharm-2020-002500.
25. Ramakrishnan M, Poojari PG, Rashid M, Nair S, Pulikkel Chandran V, Thunga G. Impact of COVID-19 pandemic on medicine supply chain for patients with chronic diseases: Experiences of the community pharmacists. *Clinical Epidemiology and Global Health*. 2023;20. doi: 10.1016/j.cegh.2023.101243.
26. Pantasri T. Expanded roles of community pharmacists in COVID-19: A scoping literature review. *Journal of the American Pharmacists Association*. 2022;62(3):649-57. doi: 10.1016/j.japh.2021.12.013.
27. Saadeh A, Jarab AS, Jaradat Ra, Al Daqqa R. Community Pharmacists' Attitudes, Preferences and Barriers toward Continuing Pharmaceutical Education: A Cross Sectional Study in Jordan. *Jordan Journal of Pharmaceutical Sciences*. 2023:245-57.
28. Wijesinghe PR, Jayakody RL, Seneviratne RDA. An assessment of the compliance with good pharmacy practice in an urban and rural district in Sri Lanka. *Pharmacoepidemiology and Drug Safety*. 2007;16(2):197-206. doi: 10.1002/pds.1277.
29. Gokcekus L, Toklu HZ, Demirdamar R, Gumusel B. Dispensing practice in the community pharmacies in the Turkish Republic of Northern Cyprus. *International Journal of Clinical Pharmacy*. 2012;34(2):312-24. doi: 10.1007/s11096-011-9605-z.
30. Badro DA, Sacre H, Hallit S, Amhaz A, Salameh P. Good pharmacy practice assessment among community pharmacies in Lebanon. *Pharmacy Practice*. 2020;18(1). doi: 10.18549/PharmPract.2020.1.1745.
31. Pizarro AMVPDA, Martins MRO, Simões JA. Exploring the Policies Applied to Pharmaceutical Care Practice for Type 2 Diabetes over the Last Decade in European Community Pharmacies. *Portuguese Journal of Public Health*. 2021;39(2):103-18. doi: 10.1159/000519498.
32. Bou-Saba AW, Kassak KM, Salameh PR. The current trends and challenges towards good community pharmacy practice and the way forward. *Exploratory Research in Clinical and Social Pharmacy*. 2022;6. doi: 10.1016/j.rcsop.2022.100152.
33. Hanafi S, Poormalek F, Torkamandi H, Hajimiri M, Esmaeili M, Khooie SH, et al. Evaluation of community pharmacists' knowledge, attitude and practice towards good pharmacy practice in Iran. *Journal of pharmaceutical* care. 2013:19-24.
34. Levy PS, Lemeshow S. Sampling of populations: methods and applications: John Wiley & Sons; 2013.
35. Alzahrani MM, Alghamdi AA, Alghamdi SA, Alotaibi RK. Knowledge and attitude of dentists towards obstructive sleep apnea. *International Dental Journal*. 2022;72(3):315-21.

36. Chand D, Mohammadnezhad M, Khan S. Levels and Predictors of Knowledge, Attitude, and Practice Regarding the Health Hazards Associated With Barber's Profession in Fiji. *INQUIRY: The Journal of Health Care Organization, Provision, and Financing*. 2022;59:00469580221100148.
37. Akoglu H. User's guide to correlation coefficients. Turkish journal of emergency medicine. 2018;18(3):91-3. doi: https://doi.org/10.1016/j.tjem.2018.08.001.
38. Organization WHO. Joint FIP/WHO guidelines on good pharmacy practice: standards for quality of pharmacy services 2011. Available from: https://www.who.int/docs/default-source/medicines/norms-and-standards/guidelines/distribution/trs961-annex8-fipwhoguidelinesgoodpharmacypractice.pdf.
39. Association JPA. Jordan Pharmaceutical Association/ Standards of good pharmacy practice 2022. Available from: https://jpa.org.jo/almmarsh-aljydt-llsydlt.
40. Moecker R, Weissenborn M, Klingenberg A, Wirbka L, Fuchs A, Eickhoff C, et al. Task sharing in an interprofessional medication management program–a survey of general practitioners and community pharmacists. *BMC Health Services Research*. 2022;22(1):1005.
41. Kimberlin CL, Jamison AN, Linden S, Winterstein AG. Patient counseling practices in US pharmacies: Effects of having pharmacists hand the medication to the patient and state regulations on pharmacist counseling. *Journal of the American Pharmacists Association*. 2011;51(4):527-34. doi: 10.1331/JAPhA.2011.10012. PubMed PMID: WOS:000297755800011.
42. Adepu R, Nagavi BG. Attitudes and Behaviors of Practicing Community Pharmacists Towards Patient Counselling. *Indian Journal of Pharmaceutical Sciences*. 2009;71(3):285-9. doi: 10.4103/0250-474x.56029. PubMed PMID: WOS:000270549400008.
43. Jimmy B, Jose J, Rao PGM. Patient Medication Counseling in Chronic Diseases - Pharmacists Role. *Indian Journal of Pharmaceutical Education and Research*. 2008;42(3):301-9. PubMed PMID: WOS:000268896200016.
44. Okumura LM, Rotta I, Correr CJ. Assessment of pharmacist-led patient counseling in randomized controlled trials: a systematic review. *International Journal of Clinical Pharmacy*. 2014;36(5):882-91. doi: 10.1007/s11096-014-9982-1. PubMed PMID: WOS:000343647000005.
45. Hilsenrath P, Woelfel J, Shek A, Ordanza K. Redefining the Role of the Pharmacist: Medication Therapy Management. *Journal of Rural Health*. 2012;28(4):425-30. doi: 10.1111/j.1748-0361.2012.00417.x. PubMed PMID: WOS:000310346400012.
46. Moczygemba LR, Berner JC, Roberson K. Texas pharmacists' opinions about and plans for provision of medication therapy management services. *Journal of the American Pharmacists Association*. 2008;48(1):38-45. doi: 10.1331/JAPhA.2008.07015. PubMed PMID: WOS:000253164700007.
47. Salmasi S, Tsao NW, Li K, Shaske JN, Marra CA, Lynd LD. Characterization of pharmacist-based medication management services in a community pharmacy. *Research in Social & Administrative Pharmacy*. 2020;16(2):178-82. doi: 10.1016/j.sapharm.2019.04.051. PubMed PMID: WOS:000507925300007.

سلوكيات الصيادلة تجاه تطبيق معايير الممارسة الصيدلانية الجيدة في صيدليات المجتمع: دراسة مسحية مقطعية

تهاني الوديان*[1]، روان أبودلو[1]، مهند عودة[1]، مي تيم[2]، آية بنات[1]

[1] قسم الصيدلة السريرية والممارسة الصيدلانية، كلية العلوم الصيدلانية، الجامعة الهاشمية، الزرقاء، الأردن

[2] قسم التكنولوجيا الصيدلانية ومستحضرات التجميل، كلية الصيدلة، جامعة الشرق الأوسط، عمّان، الأردن

ملخص

لتحسين جودة الخدمات، تم تطوير إرشادات الممارسات الصيدلانية الجيدة في العديد من البلدان حول العالم. بالإشارة إلى الأبحاث التي تمت دراستها عن موضوع الممارسة الصيدلانية الجيدة، فإنّه لا زال هناك نقص في الأدلة حول مدى التزام صيادلة المجتمع باتباع إرشادات الممارسة الصيدلانية الجيدة. تهدف هذه الدراسة إلى تقييم مواقف الصيادلة تجاه هذه الممارسات في الأردن. تم استخدام نهج أخذ العينات العشوائية الطبقية الاحتمالية لتوظيف الصيادلة المؤهلين. تمت إدارة استبيان الممارسة الصيدلانية الجيدة بين صيادلة المجتمع (GPP-C) وتم تقييم مستوى موقف المشاركين تجاه الالتزام بمعايير الممارسة الصيدلانية الجيدة. شارك في هذه الدراسة 241 صيدلانيًا (معامل الاستجابة 68.1%). من المشاركين، كان هناك ما نسبته 65.1% من الإناث و91.7% أشاروا إلى معرفتهم عن الممارسة الصيدلانية الجيدة. أظهرت نتائج الدراسة أن وجود مستوى معرفي حول الممارسة الصيدلانية الجيدة عند المشارك أثّر بشكل كبير على توجه المشاركين نحو الالتزام بأساسيات المهنة ومتطلباتها $P = 0.047$، والأداء المهني الإداري $P = 0.015$، وممارسات تقديم المشورة للمرضى $P = 0.003$، كما أظهرت الدراسة أن هناك ممارسة قليلة بشأن عملية توثيق الأدوية المصروفة للمرضى (52.3٪). تسلط هذه الدراسة الضوء على الحاجة الملحة لإنشاء مؤشرات منظمة لرصد تنفيذ الممارسة الصيدلانية الجيدة في قطاع صيدليات المجتمع. ينبغي أيضًا إعطاء الأولوية لتوثيق عملية الرعاية الصيدلانية. لتحقيق ذلك، يُوصى بالبرامج التعليمية وورش العمل التي تهدف إلى تعزيز الممارسة الجيدة للصيادلة في قطاع صيدليات المجتمع. لا بد من الإشارة إلى أن نتائج البحث حول مواقف الصيادلة تم الحصول عليها من مشاركين أردنيين في مجتمع عربي وقد لا تنعكس هذه النتائج على الصيادلة في المجتمعات غير العربية، حيث يمكن أن تكون مبادئ الممارسة الصيدلانية الجيدة هناك مختلفة.

الكلمات الدالة: العلوم الاجتماعية والإدارية، الصيدليات المجتمعية، ممارسة مهنة الصيدلة، ممارسات الصيدلة الجيدة، دراسة مقطعية.

* ***المؤلف المراسل: تهاني الوديان***

alwidyantahani@hu.edu.jo

تاريخ استلام البحث 2024/5/13 وتاريخ قبوله للنشر 2024/8/22.

Evaluation of Health-Related Quality of Life in Patients with Type 2 Diabetes Mellitus through EQ-5D-3L: in public sector hospitals of Quetta, Pakistan

Hamad Haider Khan [1], Faiz Ullah Khan [2], Tawseef Ahmad [3], Hui Guo [1], and Bingyin Shi[1]*

[1]Department of Endocrinology, First Affiliated Hospital of Xian Jiaotong University, Xi'an, China
[2]Department of Pharmacy Administration and Clinical Pharmacy, Xi'an Jiaotong University, Xi'an, China
[3]Department of Clinical Pharmacy, Faculty of Pharmaceutical Sciences, Prince of Songkla University, Hat-Yai, Thailand

ABSTRACT

Background: Diabetes mellitus (DM) is a chronic metabolic illness associated with substantial morbidity and mortality worldwide. It affects physical activity, social life, and mental health. In our country, most diabetes research has focused on morbidity and mortality. This study assessed the quality of life (QOL) of type 2 diabetes mellitus (DMT-2) patients in Quetta, Pakistan.

Methods*:* This cross-sectional study examined 440 DMT-2 patients from public hospitals in Quetta between July and November 2021. The EuroQoL 5-Dimension 3-Level (EQ-5D-3L) scale was used to assess the health-related quality of life (HRQoL) of DMT-2 patients. Inferential statistical analyses were performed using SPSS version 22.

Results: Most participants (73%) were aged between 35 and 55 years, with 246 (55.9%) males. The largest group of respondents (30.3%) had completed secondary school. Most patients (79.4%) reported no mobility issues, and 61.8% reported no difficulties with self-care. However, a substantial proportion (41.8%) experienced some difficulties with their usual activities. Additionally, 46.3% of patients reported moderate pain and discomfort. Significant correlations were found between HRQoL scores and gender (p=0.016), marital status (p=0.003), age (p=0.001), unemployment (p=0.001), and education (p=0.001). The time trade-off (TTO) and visual analog scale (VAS) scores were 0.496 and 0.555, respectively.

Conclusion: The quality of life of DMT-2 patients depends on education, occupation, gender, and marital status. Therefore, these key factors influencing HRQoL should be prioritized when designing and implementing strategies to improve diabetes treatment and the quality of life of diabetic patients in this region.

Keywords: Quality of life; QoL; DMT-2; Quetta; Pakistan; EQ-5D-3 L

1. Introduction

Diabetes mellitus (DM) is caused by a high level of blood glucose disrupting normal cellular functions and disrupting cellular metabolism on each level to such an extent that damaging almost any organ in the body. Diabetes impairs functional capacities and quality of life, resulting in substantial morbidity and premature mortality. Recent concerns highlight that over one-third of diabetes-related deaths occur in individuals under the age of 60 [1]. Diabetes accounts for over 1 million deaths annually, positioning it as the ninth leading cause of mortality, diabetes was estimated to have caused four million deaths worldwide in 2017 [2]. The global burden of diabetes mellitus is increasing, particularly rapidly in developed regions such as Western Europe. The condition affects men and women equally, with incidence peaking around 55 years of age. The global prevalence of type 2 diabetes is projected to rise to 7,079 per 100,000 individuals by 2030, indicating a continued increase worldwide[3].

****Corresponding author: Bingyin Shi***
shibingy@126.com.com
Received: 23/5/2024 Accepted: 22/8/2024.
DOI: https://doi.org/10.35516/jjps.v18i2.2614

According to the International Diabetics Federation (IDF), DM affects 415 million people globally in 2015 and will reach to affect 642 million people with DM by 2040 [4]. In Pakistan, some regional diabetes surveys have been conducted through the associations formed in the country, one such is the Diabetic Association of Pakistan (DAP) which was established in 1966 and became associated with the International Diabetes Federation (IDF) in 1967. DAP, since its inception, Pakistan has worked to enhance diabetes care and prevention. The first four National Diabetes Action Plans were established by DAP between 1996 and 1998, 1999–2001, 2001–2004, and 2005–2009, even though its field operations are primarily limited to the city of Karachi and Sind province [5]. DAP stated the prevalence of diabetes is between 0.95% and 32.9% [6]. DM, like any other chronic illness, is linked to several personal, familial, societal, and economical problems, and an even higher risk of mortality [7]. Poor food choices, elevated glucose levels in the blood and activity restrictions, the need for insulin injections daily, musculoskeletal movement difficulties and disorders, physical limitations, sexual dysfunction, and vascular abnormalities are just a few of the issues that individuals with DM can face [8]. Loss of employment, recurring hospitalization, continued increased the need for medical and clinical outcomes, economic impacts associated with early mortality, deterioration in developing and maintaining social relationships and relationships with the family, and a decline in the standard of living of individuals are just a few of the main challenges confronting these patients' familial, social, and financial situations [9].

Health-related quality of life (HRQoL) is among the most extensively and thoroughly studied clinical outcomes and analyzes the physical, cognitive, and interpersonal aspects of human health to self-assess the impact of chronic illness management on individual health and its outcome on living standards [10]. A reliable instrument for assessing the overall impact of health on an individual's well-being is the HRQoL scale. The HRQoL measure offers numerous strengths that make it particularly advantageous for use in various research contexts, especially when compared to other scales such as the SF-36, EQ-5D, and WHOQOL. In research settings, the HRQoL scale stands out as a more appropriate tool for evaluating health-related quality of life. Its comprehensive yet efficient methodology ensures that it encompasses all relevant health domains, making it valuable to both researchers and respondents. This makes the HRQoL scale highly pertinent and significant for studies aiming to understand and improve quality of life outcomes. Expectations, beliefs, perceptions, and experiences of individuals all have an impact on a person's standard of living and coping with day-to-day stressors. DM patients have a worse quality of life than healthy persons, according to studies, the variables influencing this are unknown. Some factors, such as diabetes type including other types, insulin usage and its availability, age, DM-related complications, socioeconomic status, psychological disorders leading to adherence and multiple problems, ethnicity, and educational level to one which could a considerable understanding of the depth of disease, knowledge of the condition and coping with it, and the type of care they received from others, may influence these patients' outcomes QoL [11].

The EQ-5D is amongst the most often practical instruments for assessing people's quality of life, it evaluates their physical condition, psychological perception, and social capabilities [12]. Several research have examined QoL in chronic illnesses like diabetes mellitus, its comorbidities, chronic lung disease, cerebrovascular disease, and chronic mental disorders. EQ-5D comes in three dimensions: 5L, 3L, and y. The 3L has been thoroughly tested in many settings and groups [13].

The general quality of life questionnaire has been supplanted in epidemiological research and clinical assessments of diabetes patients by the EQ-5D-3L, a concise and user-friendly instrument. Assessing the standard of living and its contributing factors can help

diabetes mellitus (DM) patients improve their quality of life (QoL). Due to the geographic and cultural context of the region, patients' QoL and its influencing factors may vary significantly. Therefore, a shorter, validated questionnaire that can be quickly administered is essential for assessing patients' QoL. Health professionals can evaluate DM-related metabolic abnormalities and physiological dysfunctions, but patients' health perceptions and well-being are influenced by more than just symptoms, functional limitations, and physiological and pathological conditions. Psychological, social, and cultural factors also moderate the effects of biological disorders on HRQoL. Consequently, this study evaluated type 2 diabetes mellitus (DMT-2) patients in Quetta, Pakistan, using the EQ-5D-3L questionnaire.

2. MATERIALS AND METHODS

2.1 Study population and study settings

A total of 440 individuals diagnosed with type 2 diabetes mellitus (DMT-2) from two public hospitals in Quetta, Baluchistan, were selected to participate in this cross-sectional study. The steps of selection are presented in the flow chart (figure 01). The Sandeman Provincial Hospital (SPH) in Quetta, Pakistan, has a capacity of 780 beds. Founded in 1939, it is located in the heart of Quetta. SPH is the preferred healthcare facility for local residents as it is a public healthcare institution providing quality medical services. Another setting involved Bolan Medical Complex Hospital (BMCH) with a capacity of 1,062 beds. Verbal and written consent was obtained from the subjects, who were assured that their responses would be kept confidential and that they could withdraw from the study at any time without any impact on their healthcare services.

2.2 Study Instrument

The EQ-5D (EQ-5D-3L) form was utilised in this research study due to its simplicity and the brief time required for participants to complete it. In 1990, as the European association expanded to a broader audience, the EuroQol group released the EQ-5D-3L questionnaire, a three-level version of the earlier EQ-5D. The EQ-5D-3L is divided into two main pages: a descriptive system called EQ-5D and a visual analog scale called EQ-5D-3L (EQ-VAS). The EQ-5D-3L descriptive system comprises five key dimensions: mobility, self-care, usual activities, pain/discomfort, and anxiety/depression. Each dimension is categorized into three levels: no problems, moderate problems, and severe problems. The questionnaire was self-administered. After obtaining permission, we utilized the questionnaire for data collection. The questionnaire was in English, and if participants encountered any difficulties, the data collector translated the specific questions for them. The patient is asked to tick the box next to the most appropriate statement in each of the five dimensions to describe their health state. Each selection corresponds to a single-digit number representing the level chosen for that dimension. These five scores can be combined to produce a five-digit value representing the patient's overall condition. The EQ visual analog scale (VAS) is used to assess the participant's health on a linear scale with endpoints labeled 'Best imaginable health state' and 'Worst imaginable health state.' The VAS provides a numerical measure of health status, reflecting the patient's subjective evaluation.

2.3 Inclusion and Exclusion criteria

Participants were assessed according to departmental protocols, which included a comprehensive medical history and physical examinations. Individuals under 18 years of age, pregnant women, those planning to become pregnant, individuals with known psychiatric conditions, and those with communication barriers (e.g., hearing impairments, cognitive disabilities, severe psychiatric disorders, or chronic renal failure) were excluded from the study. All eligible participants who met the criteria were invited to participate, and informed consent was obtained from them prior to data collection.

2.4 Scoring the EQ-5D-3 L descriptive system

The EQ-5D-3L, developed by the European Association, encompasses five dimensions: mobility, self-care, usual activities, pain/discomfort, and

anxiety/depression. Each dimension is rated on a scale with three levels: no problems (1), mild problems (2), and severe problems (3). Patients were instructed to select the most accurate descriptor for each of the five dimensions to represent their health status. The health status codes are represented by five-digit numbers. The combined scores from the five dimensions generate a five-digit code that reflects the patient's condition. For instance, a code of 11,111 indicates no problems in any of the five dimensions, while a code of 12,233 signifies no issues with mobility, mild difficulties with self-care, significant pain or discomfort, and severe anxiety or distress. A value set is required to convert an individual EQ-5D health state into a composite index. Due to the absence of a locally relevant value set, the EQ-5D score was calculated using threshold values provided by the EuroQol Group's standardized valuation technology (EQ-VT), where 1 represents the highest quality of life (1 = highest QoL) and 0 represents the lowest (0 = lowest QoL). According to the EQ-5D-3L instruction booklet, data is typically presented in a table format to illustrate the health profile. The EQ-5D-3L categories are divided into "no issues" (level 1) and "difficulties" (levels 2–5), forming a profile that reflects the frequency of problems. We have converted the profile into frequency distributions for data reporting.

2.5 Scoring the EQ-5D-3 L VAS

The EQ visual analog scale (VAS) measures subjects' self-reported health on a linear scale ranging from 0 to 100, with endpoints labeled 'The best health you can imagine' and 'The worst health you can conceive'. Specifically, on the EQ-VAS, a score of "100" represents the highest possible health status, while a score of "0" indicates the most severe health condition.

2.6 Statistical analysis

Data were entered into SPSS version 22 and analyzed using various tests. After the confirmation of normal distribution, ANOVA, Chi-Square, independent sample t-tests, and logistic regression were performed. A p-value of 0.05 was considered statistically significant. For each classification of the EQ-5D-3L, the dependent variable (QoL) was divided into two groups: 'no difficulties' (level 1) and 'having varying degrees of difficulties' (levels 2–3) in the regression analysis model. Independent variables such as age, sexual identity, educational status, profession, duration of DMT-2, HbA1c levels, medication, renal dysfunction, diabetic retinopathy, and diabetic peripheral neuropathy were included in the regression model. Only variables strongly associated with EQ-5D-3L categories were included in the final summary of the data.

RESULTS

2.2 Sociodemographic characteristics

A total number of 440 patients with a confirmed diagnosis of DMT-2 between the age range of 30-80 years participated in this research. The majority of respondents were male, accounting for 246 individuals (55.9%). Moreover, a significant portion of the participants were married, with 414 individuals (94%) reporting marital status. In terms of residency, 248 respondents (56.3%) were from rural areas shown in Table 1. Additionally, the age group of 41-50 represented 132 individuals (30.4%) of the total respondents. Patients with a family history of DM included 140 (31.8%) of the study participants. Of most of the patients 164 (37.25%), we're taking at least two different medications as anti-diabetic treatment. Exercise control of DM was noticed in 45.4% of the patients, the majority of patients (47.2) had their blood glucose levels between 150-200mg/dl as shown in Table 2. The box plot (Figure 01) shows the differences in the readings of the patient's sugar levels in response to age and gender. The sugar level differences are visible.

Table 1: Patients' Sociodemographic (n= 440)

Demographic Characteristics	n (%)
Age group (Years)	
30 – 40	120 (27.6)
41 –50	131 (30.4)
51 – 60	120 (27.6)
61 – 70	53 (11.5)
71 – 80	14 (2.8)
Gender	
Male	246 (55.9)
Female	194 (44.1)
Marital Status	
Married	414 (94.0)
Single	26 (5.9)
Locality	
Urban	192 (43.6)
Rural	248 (56.3)
Qualification	
No formal education	100 (22.7)
Religious education	52 (11.9)
Primary	54 (12.5)
Matric	132 (30.3)
Intermediate	58 (13.3)
B.A\B.S.C	22 (5.0)
Graduation	16 (3.7)
Occupation	
Unemployed	112 (25.7)
Government Employed	36 (8.3)
Private Employed	108 (24.8)
Self Employed	178 (40.8)

Table 2: Patients' Clinical data (n= 440)

Variables	n (%)
Family History	
Yes	140 (31.8)
No	300 (68)
Is there any diet change due to diabetes?	
Yes	178 (39)
No	262 (59.9)
Do you exercise to control diabetes?	
Yes	200 (45.4)
No	240 (54.5)
In your opinion your diabetes is	
Controlled	242 (55)
Uncontrolled	198 (45)
Is current treatment your first consultation?	
Yes	50 (11.3)

Variables	n (%)
No	376 (85.4)
Don't know	14 (3.1)
On average how much capital (in PKR) do you spend on your medication?	
1000 – 1500	250 (56.8)
1600 – 2400	190 (43.1)
On average how much capital (in PKR) do you spend on lab/home tests?	
1000 – 1500	140 (31.3)
1600 – 2400	300 (68.1)
Three last readings of blood glucose (mg/dl)	
70 – 140	112 (25.4)
141 -190	160 (36.3)
191 -280	168 (38.1)
Current blood glucose readings (mg/dl)	
70 – 150	100 (22.7)
151 – 200	208 (47.2)
<200	132 (30)

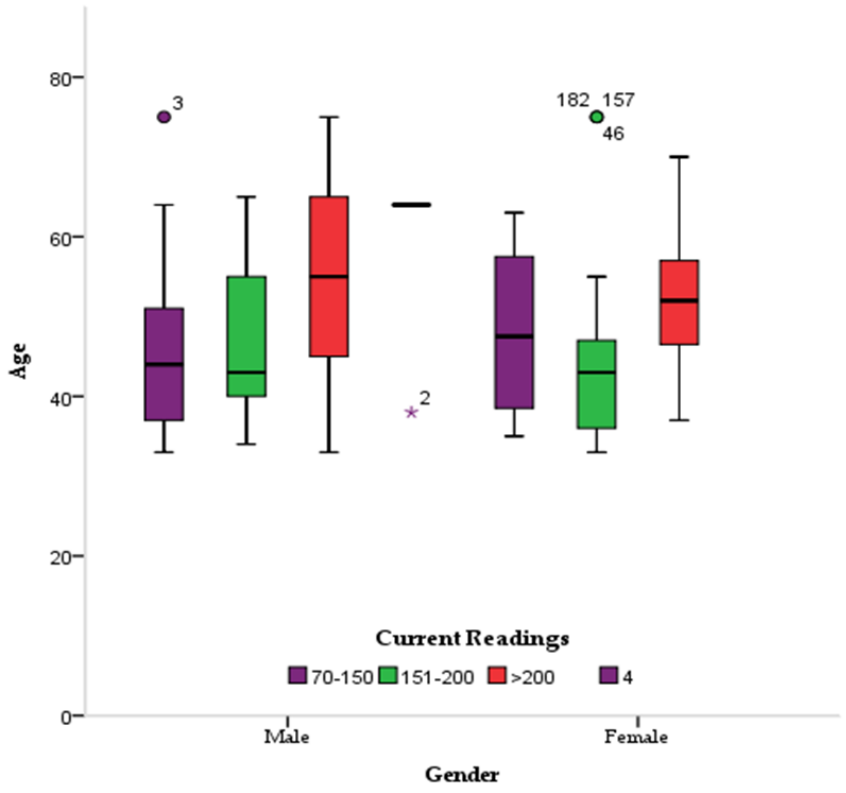

Figure 02: Current sugar level measurements in diabetic patients, including age and gender disparities.

The majority of patients (79.4%) reported no issues with mobility. Among the study participants, 61.8% experienced no difficulties with self-care. A substantial proportion (41.8%) had some degree of difficulty with usual activities. Additionally, moderate pain and discomfort were observed in 46.3% of the patients. As illustrated in Tables 3, each patient's reported issue was assessed based on both clinical and demographic parameters. Regarding mobility, the age group of 35–65 years exhibited the highest incidence of difficulties. Specifically, 71 individuals (17.2%), females (18.8%), married subjects (18.4%), those with education beyond the intermediate level (22.8%), unemployed individuals (24.8%), persons with a monthly income of ≤10,000 PKR (88.8%), and those residing in urban areas (20.2%) reported significant mobility challenges. In the anxiety dimension, a higher prevalence of problems was observed among females (95%), individuals aged 35–65 years (93.5%), and urban residents (96.1%). Increased issues in the self-care category were noted within the 35–65 age range. The majority of this population included males (24.3%), unmarried individuals (40.9%), those with education beyond the intermediate level (31.7%), unemployed individuals (33.9%), those with monthly incomes under 10,000 PKR (28%), and urban residents (26.4%)—amounting to 71 individuals (17.2%). In the pain/discomfort dimension, a higher incidence of problems was observed among individuals aged 66–80 years (96.3%), education greater than Intermediate (66.7%), unemployed (71.6%), individuals with monthly income less than or equal to 10,000 PKR (66.7%), females (67.4%), a higher prevalence of issues was noted among unmarried individuals (90.9%) and those residing in urban areas (66.9%). In the term of regular activities, more difficulties were reported by females (56.9%), individuals aged 66–80 (59.3%), urban inhabitants (52.2%), those with education above the intermediate level (54%), the unemployed (55%), and individuals with a monthly income of less than 10,000 PKR were (58.5%). Additionally, anxiety and depression levels related to type 2 diabetes mellitus (DMT-2) were higher in males (Figure 2).

Table 3: The abundance of problems (percentage) reported by the patients in terms of their demographic and clinical characteristics

Variables	Mobility n (%)		LOS	Anxiety n (%)		LOS	Self-care n (%)		LOS
	Yes	No		Yes	No		Yes	No	
Gender									
Male	212 (81.9)	47 (18.1)	0.865	18 (6.9)	241 (93.1)	0.395	196 (75.7)	63 (24.3)	0.339
Female	147 (81.2)	34 (18.8)		9 (5)	172 (95)		144 (79.6)	37 (20.4)	
Age (years)									
35-65	342 (82.8)	71 (17.2)	0.010	25 (6.1)	388 (93.9)	0.776	324 (78.5)	89 (21.5)	0.021
66-80	17 (63.0)	10 (37)		2 (7.4)	25 (92.6)		16 (59.3)	11 (40.7)	
Marital status									
Married	341 (81.6)	77 (18.4)	0.977	27 (6.5)	391 (93.5)	0.219	327 (78.2)	91 (21.8)	0.037
Unmarried	18 (81.8)	4 (18.2)		0 (0)	22 (100)		13 (59.1)	9 (40.9)	
Education									

Variables	Mobility n (%)		LOS	Anxiety n (%)		LOS	Self-care n (%)		LOS
≤ Intermediate	213 (84.9)	38 (15.1)	0.041	9 (3.6)	242 (96.4)	0.010	211 (84.1)	40 (15.9)	<0.001
>Intermediate	146 (77.2)	43 (22.8)		18 (9.5)	171 (90.5)		129 (68.3)	60 (31.7)	
Employment									
Unemployed	82 (75.2)	27 (24.8)	0.048	14 (12.8)	95 (87.2)	0.001	72 (66.1)	37 (33.9)	0.001
Employed	277 (83.7)	54 (16.3)		13 (3.9)	318 (96.1)		268 (81)	63 (19)	
Income									
≤10,000 PKR	182 (74)	198 (88.8)	<0.001	22 (8.9)	224 (91.1)	0.006	177 (72)	69 (28)	0.003
>10,000PKR	177 (91.2)	11 (78.6)		5 (2.6)	189 (97.4)		163 (84)	31 (16)	
Residency									
Urban	142 (79.8)	36 (20.2)	0.418	7 (3.9)	171 (96.1)	0.112	131 (73.6)	47 (26.4)	0.129
Rural	217 (82.8)	45 (17.2)		20 (7.6)	242 (92.4)		209 (79.8)	53 (20.2)	
LOS: level of significance (P<0.05);									

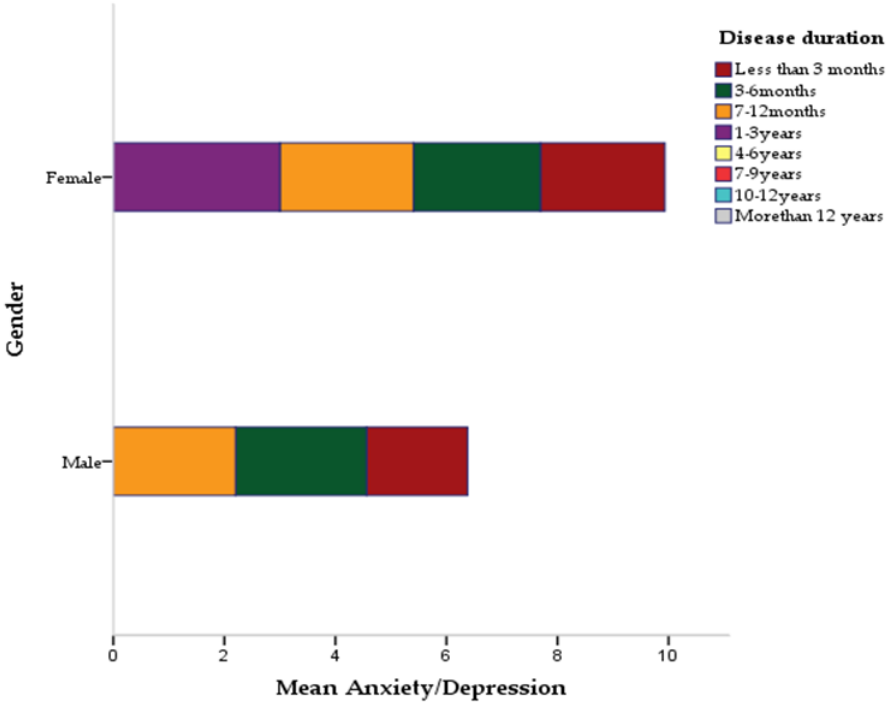

Figure 03: The mean anxiety/depression scores in males and females as per the duration of the disease.

3. Discussion

HRQoL is a key indicator of how long-term illness treatment affects health. To the best of our knowledge, this is the first Quetta study to use the EQ-5D-3L tool to assess DMT-2 patients' health-related quality of life. EQ-5D-3L, Visual analogue scale, and socio-demographic disparities in health-related quality of life in DMT-2 patients were examined. The majority of participants were aged between 35 and 55 years, with 55.9% being male. Most respondents had completed secondary school. The majority of patients reported no mobility issues, while 61.8% experienced no difficulties with self-care. However, 41.8% of participants faced some difficulties with usual activities, and 46.3% reported moderate pain and discomfort. The EQ-5D was used to assess diabetics' health-related quality of life. [14,15]. For this project, we selected the EQ-5D-3L questionnaire due to its ease of use and shorter completion time compared to other similar tools used in this type of research. [16]. Several socio-demographic factors also affect the health-related life quality of DMT-2 individuals. There was a striking difference in health-related life quality comparing males and females in our studies. Female patients had a substantially lower EQ-5D-3L score than male patients. This is in line with the result of earlier research, which found that men with diabetes have superior HRQoL than women [14,17]. Additionally, there was better control of diabetes in males as compared to females with lesser exposure to depression or anxiety [18].

A significant association was observed in the age group 65 and above. Increased age with lower HRQoL was quoted in several scientific studies previously as well [17,19]. Age-related physical and mental decline negatively impacts HRQoL scores. Marital status also influences HRQoL, with married individuals demonstrating better HRQoL in our study. This finding is consistent with the results observed by Amer et al. [20].

Studies conducted in Adama and Gondar cities in Ethiopia also reported a clear association between health-related quality of life and the level of education of the subjects [4,21]. Level of academic education was directly and positively associated with diabetic education i.e., those with higher education were more aware of diabetic care as compared to subjects with lower education, and increased education in any field increases health literacy as well [22]. Other significant variables in this context included unemployment and monthly income, both of which exhibited a positive association with HRQoL. Previous studies have also reported similar findings [4,23]. HRQoL and employment status are linked because unemployment causes financial hardship. Patients can't afford medicine, nutrition, or lifestyle. All these causes will lower HRQoL. This study was conducted in Pakistan, a developing nation. Our findings contrast with those from developed countries. In England, patients with type 2 diabetes mellitus (DMT-2) and renal disease experienced the greatest reduction in health utility, while in Sweden, patients with DMT-2 and cerebrovascular disease faced the largest increase in health costs [24]. Patients with the diagnosis of DMT-2 who were using medications taken orally were studied in a cross-sectional survey in a city in Bangladesh, where outpatient clinics depicting to have high rates of hypertension, obesity, and dyslipidemia [25]. Eye difficulties were the most common consequence, followed by long-term diseases such as chronic renal failure and chronic diseases mostly involving heart failure, congestive heart failure, and cerebrovascular accidents.

Despite our research participants being individuals diagnosed with type 2 diabetes mellitus (DMT-2) who were receiving continuous oral medication in outpatient clinics, the most prevalent comorbidity was hypertension, followed by dyslipidemia and heart disease, as reported by Zhang et al. [26]. In the United States, healthcare providers have observed that diabetes control is compromised by sequelae such as coronary artery disease, painless peripheral neuropathy, cardiomyopathy, and neuropathic pain, which collectively diminish health-related quality of life. Zhang et al. reported similar findings in Singapore [26]. Comorbidities include cardiac illness, high glucose-

induced nephropathy, nerve damage from blood supply reduction, and serious eye difficulties like blindness had significantly poorer physical component assessments. In an Australian study, cerebrovascular accidents, eyesight loss, and kidney illness were substantially associated to health-related quality of life [27].

Limitations

4. This study had several notable limitations. As an observational cross-sectional analysis, it highlighted the complex temporal relationship between diabetes and HRQoL. To enhance generalizability, a more rigorous sampling approach should be employed to gather data from a diverse range of respondents, as the convenience sampling method used may have omitted critical aspects. Additionally, self-reported questionnaires may potentially overestimate HRQoL values. Finally, the study, conducted at a few public hospitals in Quetta, does not represent the entire country and would benefit from a larger sample size and inclusion of more healthcare settings.

5. Conclusions

To improve diabetes management and patient outcomes in Pakistan, it is essential for policymakers to address factors such as education, career, gender, and marital status that significantly impact the quality of life for individuals with type 2 diabetes mellitus. This involves integrating HRQoL factors into diabetes care, including the management of complications, promotion of physical activity, and encouragement of proper nutrition and foot hygiene practices. Rigorous lifestyle coaching should be implemented, with a focus on older adults and rural populations who face additional challenges. Regular HRQoL assessments should be incorporated into routine care to monitor and enhance patient well-being. Furthermore, policies should support the integration of HRQoL factors into diabetes management programs and ensure that healthcare systems are equipped to provide necessary resources and support for effective interventions. By adopting these measures, policymakers can significantly enhance diabetes care and improve the overall quality of life for patients.

Author Contributions: The study concept and design: HHK. Writing of the manuscript: FUK and TA , Data analysis: HG, Obtaining data: HHK and TA. Interpretation of results: HG**,** FUK and HHK. Critical revisions of the manuscript: BS and FUK. All authors approved the version for submission.

Funding: Nill

Institutional Review Board Statement: The study was approved by the Institutional Review Broad (IRB) Committee of Post-graduate Medical Institute (BMCH)Quetta, Pakistan with Reference number; NO/PGMI-47/2021.

Informed Consent Statement: An oral and written informed consent was obtained from the study participants.

Data Availability Statement: Data related to this manuscript can be provided upon reasonable request.

Acknowledgments: The authors would like to acknowledge all the research team members and their support throughout the project.

Conflicts of Interest: The authors declare no conflict of interest.

REFERENCES

1. Al-Rahamneh H, Habees AA, Baqleh R, Eston R. Quality of life in disabled versus able-bodied individuals during COVID-19 pandemic. *Jordan Journal of Pharmaceutical Sciences*. 2022;15(2):227-238.
2. Lisni I, Lestari K, Andalusia LR. Polypharmacy in Type 2 Diabetes Patients of the PROLANIS Program in Indonesia: Identification of Potential Drug-Drug Interaction. *Jordan Journal of Pharmaceutical Sciences*. 2025;18(1):245-257.
3. Mohtasham-Amiri Z, Barzigar A, Kolamroudi HR, et al. Prevalence, awareness and control of diabetes in urban area of north of Iran, 2009. *International Journal of Diabetes in Developing Countries*. 2015;35:346-350.
4. Aschalew AY, Yitayal M, Minyihun A. Health-related quality of life and associated factors among patients with diabetes mellitus at the University of Gondar referral hospital. *Health and quality of life outcomes*. 2020;18(1):1-8.
5. Sherin A. National diabetes action plan of Pakistan: need and challenges. *Khyber Medical University Journal*. 2015;7(1):1-2.
6. Adnan M, Aasim M. Prevalence of type 2 diabetes mellitus in adult population of Pakistan: a meta-analysis of prospective cross-sectional surveys. *Annals of global health*. 2020;86(1)
7. Yosef B, Kaddar N, Boubou A. Evaluation of the Effect of Dapagliflozin on CRP Levels in Type 2 Diabetes Patients. *Jordan Journal of Pharmaceutical Sciences*. 2023:313-321.
8. Koliaki C, Tentolouris A, Eleftheriadou I, Melidonis A, Dimitriadis G, Tentolouris N. Clinical management of diabetes mellitus in the era of COVID-19: practical issues, peculiarities and concerns. *Journal of clinical medicine*. 2020;9(7):2288.
9. Mukona DM. Diabetes mellitus and depression amid the COVID-19 pandemic: Possible solutions for resource limited settings. *African Journal of Diabetes medicine*. 2020;28(1):1-3.
10. Kim Y-J, Jeong I-K, Kim S-G, et al. Changes in the quality of life in patients with type 2 diabetes mellitus according to physician and patient behaviors. *Diabetes & metabolism journal*. 2020;44(1):91-102.
11. Woon LS-C, Sidi HB, Ravindran A, et al. Depression, anxiety, and associated factors in patients with diabetes: evidence from the anxiety, depression, and personality traits in diabetes mellitus (ADAPT-DM) study. *BMC psychiatry*. 2020;20(1):1-14.
12. Thompson AJ, Turner AJ. A comparison of the EQ-5D-3L and EQ-5D-5L. *Pharmacoeconomics*. 2020;38:575-591.
13. Mahesh P, Gunathunga M, Jayasinghe S, et al. Construct validity and reliability of EQ-5D-3L for stroke survivors in a lower middle income setting. *Ceylon Medical Journal*. 2019;64(2):52-58.
14. Lee WJ, Song K-H, Noh JH, Choi YJ, Jo M-W. Health-related quality of life using the EuroQol 5D questionnaire in Korean patients with type 2 diabetes. *Journal of Korean medical science*. 2012;27(3):255-260.
15. Solli O, Stavem K, Kristiansen IS. Health-related quality of life in diabetes: The associations of complications with EQ-5D scores. *Health and quality of life outcomes*. 2010;8(1):1-8.
16. Glasziou P, Alexander J, Beller E, Clarke P, Group AC. Which health-related quality of life score? A comparison of alternative utility measures in patients with Type 2 diabetes in the ADVANCE trial. *Health and quality of life outcomes*. 2007;5:1-11.

17. Quah JH, Luo N, Ng WY, How CH, Tay EG. Health-related quality of life is associated with diabetic complications, but not with short-term diabetic control in primary care. *Annals of the Academy of Medicine-Singapore*. 2011;40(6):276.
18. Peyrot M, Rubin RR. Persistence of depressive symptoms in diabetic adults. *Diabetes care*. 1999;22(3):448-452.
19. Javanbakht M, Abolhasani F, Mashayekhi A, Baradaran HR, Jahangiri noudeh Y. Health related quality of life in patients with type 2 diabetes mellitus in Iran: a national survey. 2012;
20. Al-Shehri AH, Taha AZ, Bahnassy AA, Salah M. Health-related quality of life in type 2 diabetic patients. *Ann Saudi Med*. Sep-Oct 2008;28(5):352-60. doi:10.5144/0256-4947.2008.352
21. Tusa BS, Geremew BM, Tefera MA. Heath related quality of life and associated factors among adults with and without diabetes in Adama city East Shewa, Ethiopia 2019; using generalized structural equation modeling. *Health and Quality of Life Outcomes*. 2020/03/30 2020;18(1):83. doi:10.1186/s12955-020-01337-9
22. Walters R, Leslie SJ, Polson R, Cusack T, Gorely T. Establishing the efficacy of interventions to improve health literacy and health behaviours: a systematic review. *BMC public health*. 2020;20(1):1-17.
23. Dedefo MG, Abate SK, Ejeta BM, Korsa AT. Predictors of poor glycemic control and level of glycemic control among diabetic patients in west Ethiopia. *Annals of Medicine and Surgery*. 2020;55:238-243.
24. Kiadaliri AA, Gerdtham U-G, Eliasson B, Gudbjörnsdottir S, Svensson A-M, Steen Carlsson K. Health utilities of type 2 diabetes-related complications: a cross-sectional study in Sweden. *International journal of environmental research and public health*. 2014;11(5):4939-4952.
25. Islam SMS, Alam DS, Wahiduzzaman M, et al. Clinical characteristics and complications of patients with type 2 diabetes attending an urban hospital in Bangladesh. *Diabetes & Metabolic Syndrome: Clinical Research & Reviews*. 2015;9(1):7-13.
26. Zhang P, Brown MB, Bilik D, Ackermann RT, Li R, Herman WH. Health utility scores for people with type 2 diabetes in US managed care health plans: results from Translating Research Into Action for Diabetes (TRIAD). *Diabetes care*. 2012;35(11):2250-2256.
27. Hayes A, Arima H, Woodward M, et al. Changes in quality of life associated with complications of diabetes: results from the ADVANCE study. *Value in health*. 2016;19(1):36-41.

تقييم جودة الحياة المتعلقة بالصحة لدى مرضى السكري من النوع الثاني من خلال أداة :EQ-5D-3L في مستشفيات القطاع العام في كويته، باكستان

حمد حيدر خان [1]، فايز الله خان [2]، توسيف أحمد [3]، هوي قوه [1]، وبينغيين شي [1]*

[1]قسم الغدد الصماء، المستشفى الأول التابع لجامعة شيان جياوتونغ، شيان، الصين

[2]قسم إدارة الصيدلة والصيدلة السريرية، جامعة شيان جياوتونغ، شيان، الصين

[3]قسم الصيدلة السريرية، كلية العلوم الصيدلانية، جامعة برنس أوف سونغكلا، هات–ياي، تايلاند

ملخص

الخلفية: داء السكري هو مرض استقلابي مزمن يسبب معدلات عالية من المراضة والوفيات على مستوى العالم. يؤثر المرض على النشاط البدني، والحياة الاجتماعية، والصحة النفسية. في باكستان، ركزت معظم الدراسات المتعلقة بداء السكري على المراضة والوفيات، بينما تهدف هذه الدراسة إلى تقييم جودة الحياة لدى مرضى السكري من النوع الثاني في مدينة كويته.

المنهجية: أجريت دراسة مقطعية شملت 440 مريضاً بالسكري من النوع الثاني في مستشفيات القطاع العام في كويته خلال الفترة من يوليو إلى نوفمبر 2021. تم استخدام مقياس EQ-5D-3L (أداة يوروكوال ذات الأبعاد الخمسة والمستويات الثلاثة) لتقييم جودة الحياة المرتبطة بالصحة لدى المرضى. تم استخدام برنامج SPSS الإصدار 22 لإجراء التحليل الإحصائي الاستنتاجي لمتغيرات الدراسة.

النتائج: كان أغلب المشاركين (73%) تتراوح أعمارهم بين 35 و55 سنة، وبلغ عدد الذكور 246 (55.9%). أتم 30.3% من المشاركين المرحلة الثانوية، و79.4% منهم لم يعانوا من مشاكل في الحركة. وذكر 61.8% من المرضى أنهم لا يواجهون صعوبات في العناية الذاتية، بينما أبلغ 41.8% عن وجود بعض الصعوبات في أداء الأنشطة اليومية المعتادة. كما أفاد 46.3% من المرضى أنهم يعانون من ألم وانزعاج بدرجة متوسطة. لوحظت علاقات ذات دلالة إحصائية بين درجات جودة الحياة المتعلقة بالصحة وكل من الجنس(p=0.016) ، والحالة الاجتماعية(p=0.003) ، والعمر (p=0.001)، والبطالة(p=0.001) ، والتعليم .(p=0.001) بلغ متوسط درجات أسلوب مبادلة الوقت0.496 (TTO) ، ودرجة مقياس التماثل البصري.0.555 (VAS)

الاستنتاج: تعتمد جودة حياة مرضى السكري من النوع الثاني على التعليم، والمهنة، والجنس، والحالة الاجتماعية. لذا يجب التركيز على العوامل المؤثرة الرئيسية في جودة الحياة عند تصميم وتنفيذ استراتيجيات لتحسين علاج السكري وجودة حياة المرضى في هذه المنطقة.

الكلمات الدالة: جودة الحياة؛ QoL؛ السكري من النوع الثاني؛ كويته؛ باكستان؛ EQ-5D-3L.

---

* ***المؤلف المراسل: بينغيين شي***

shibingy@126.com

تاريخ استلام البحث 2024/5/23 وتاريخ قبوله للنشر 2024/8/22.

Formulation and Characterization of Methyldopa Floating Tablets Using Polymeric Excipients: A Study on Gastroretentive Drug Delivery System

Amaresh Prusty[1*], Chinmaya Keshari Sahoo[2], Sanjit Kumar Senapati[1], Priyanka Singh[1], Gyanranjan Behera[1]

[1]Department of Pharmaceutics, Royal College of Pharmacy & Health Sciences, Berhampur, Odisha, India
[2]Department of Pharmaceutics, College of Pharmaceutical Sciences, Puri, Bidyaniketan, Baliguali, Puri, Odisha, India

ABSTRACT

This research aims to develop a novel gastro retentive drug delivery system (GRDDS) that can prolong the drug release of methyldopa. In the present research tablets are prepared by direct compression method using carbapol 934 and HPMC K100M polymer, by the use effervescent (for Formulations F1, F2, F3, and F4) and non-effervescent (F5) technology. One of the medications used to treat hypertension is methyldopa, a sympatholytic drug that acts centrally having short half-life of 2 h. Sedation, nausea, and vomiting are some of the drug's side effects that occur as a result of its frequency of its administration (250 mg two to three times day). Therefore, it would be far more effective to prepare GRDDS of methyldopa to release drug in the gastric environment for an extended duration. F3 is the most effective formulation batch because the combination of polymers HPMC K 100M and carbopol 934 in methyldopa effervescent tablets significantly prolongs the drug release in 0.1N HCl for more than 12 hours with a floating lag time of 60 seconds. The drug release mechanism reveals a new approach to treat hypertension with methyldopa floating tablets by utilising a mixture of HPMC K 100 M and carbopol 934 polymers.

Keywords: Methyldopa, HPMC K 100 M, Carbopol 934, Floating Tablets, Floating Lag Time.

INTRODUCTION

The oral route of medication delivery is often considered the best and most convenient choice among the available dosage form. Depending on the physicochemical properties of a dosage forms, they are absorbed after dissolving in stomach or intestinal fluids. Drugs that are unstable in the intestinal pH can have their gastric residence duration greatly prolonged using gastro-retentive systems because of their ability to remain in the stomach region for lengthy periods (1). Improving bioavailability (2-4), decreasing drug wastage, and extending drug release over a longer duration are just a few of the advantages of prolonging gastric retention. Localised medication distribution to the stomach and upper section of the small intestines is another area where gastro-retentive systems are effective. Innovative therapeutic opportunities and substantial patient advantages can be realised through the creation of novel products made possible by enhanced gastro retention. A number of mechanisms, including mucoadhesion (5), flotation (6), expansion, changed shape systems (7-8), or the concurrent administration of pharmacological drugs that delay stomach emptying, can be employed to control the gastric retention of solid dosage forms.

The use of a GRDDS allows for the prolonged oral administration of medications that are absorbed in particular sections of the gastrointestinal tract, as they are

[*]***Corresponding author: Amaresh Prusty***
amareshprusty@gmail.com
Received: 1/6/2024 Accepted: 22/8/2024.
DOI: https://doi.org/10.35516/jjps.v18i2.2718

kept in the stomach. Floating drug delivery systems, expanding and swelling systems, high-density systems, polymeric bio adhesive systems, and other devices are utilised to extend stomach retention time (9). An easy and successful way to prolong the gastric residence duration of dose forms is to prepare it in Floating Drug Delivery form (10). These systems have bulk density lower than that of gastric fluids, allowing them to remain buoyant in the stomach for extended periods without being affected by the gastric emptying rate.

Drug delivery systems that float in the stomach are able to evade the effects of the stomach's natural gastric emptying rate because their bulk density is lower than that of gastric fluids. The floating system releases the drug at a controlled rate in stomach. The generation and entrapment of carbon dioxide within the polymeric gel cause the dosage form to swell, reducing its bulk density to less than. As a result, the system floats in the stomach acid (11).

Methyldopa, an antihypertensive medication and the drug of choice for treating hypertension during pregnancy is selected for this investigation. Only methyldopa has undergone comprehensive safety testing for the mother, neonate, and infant (12). The half-life of methyldopa is just about two hours; thus, it needs to be taken three or four times a day. Because of its side effects due to frequent administration, it is an ideal candidate to be formulating in GRDDS by using HPMC K 100 m and carbopol 934 polymers. No research publications have been found that utilize the specified combination of polymers to prolong the release of methyldopa in the acidic pH of the stomach. However, it has been observed that when selected polymers are used to release drugs in the alkaline pH of the intestine, tablets disintegrate and develop a red tint within the first few minutes. As the reaction progresses, the dissolution media becomes dark due to protonation, indicating the drug's instability in an alkaline environment. This study entails the formulation and evaluation of methyldopa gastroretentive floating tablets.

MATERIALS AND METHODS

Materials

The pharmaceutical company Pfizer India Healthcare Limited supplied the methyldopa. Carbopol 934 and HPMC K 100 M were purchased from Rolex Pharmaceuticals in Bhubaneswar, Odisha. From S.D. Fine chemicals in Mumbai, we obtained the additional components talc and magnesium stearate.

Methods

Compatibility study

FT-Infrared spectroscopy (FTIR) study

In FTIR study, 10 milligrammes of the sample and four hundred milligrammes of potassium bromide (KBr) were triturated in a mortar. Next, a tiny amount of the triturated mixture was put into a pellet maker and compacted with a hydraulic press at a pressure of 10 kg/cm². A Shimadzu FTIR Spectrophotometer was used to scan the resultant pellet from 4000 cm^{-1} to 400 cm^{-1} after it was placed on the sample holder.

DSC Study

In order to examine the significant changes in the thermal behavior of either a drug or a polymer can be measured by DSC (Schimadzu, DSC-60, Japan). Samples weighing 5mg were sealed in aluminum pans and heated to 300ºC at a rate of 40ºC per minute.

Isothermal stress testing

The compatibility of drug-excipients is evaluated using the isothermal stress testing method (13). The medicine and various excipients were measured, mixed thoroughly in a vortex mixer for 2 minutes, and then transferred to 4 ml glass vials (n = 2) according to the authors' protocol (14). After that, 10% (w/w) water was added to each vial before the drug-excipients mixture was further blended using a heat-sealed glass capillary. Capillary was broken and kept within the vial to avoid material loss. Using a hot air oven, each vial was sealed and kept at a temperature of 50^0C. At the end of the first, second, and third weeks of storage under the aforementioned conditions, as well as after the third week, the samples were quantitatively

analysed using a UV-visible spectrophotometer to determine the drug-excipients compatibility by calculating the percentage assay.

Preparation of Gastro Retentive Floating tablets

Composition of tablets for five best formulations is shown in table 1. All the ingredients except magnesium stearate were taken as per prescribed weight and mixed properly for sufficient time to form a uniform mixing. Magnesium stearate was added and stirred for an extra 2-3 minutes. Then the prepared powder mixtures were compressed using 12 mm Karnavati tablet punching machine. Each batch of tablets maintained the same weight of 620 mg.

Table 1: Formula for the preparation of Methyldopa tablets

Ingredients amount (mg)	**F1**	**F2**	**F3**	**F4**	**F5**
Methyldopa	250	250	250	250	250
HPMC K100M	200	-----	180	150	250
Carbapol 934	----	200	20	50	60
Sodium bicarbonate	70	70	70	70	-----
Citric acid	40	40	40	40	-----
Starch 1500	50	50	50	50	50
Magnesium stearate	5	5	5	5	5
Talc	5	5	5	5	5
Total weight (mg)	**620**	**620**	**620**	**620**	**620**

Calibration curve of Methyldopa

A quantity of 100 mg of the drug was precisely weighed and transferred into a 100 ml volumetric flask. The drug was dissolved and the volume was adjusted to 100 ml using 0.1N HCl to prepare stock solution A. From this stock solution A, different concentrations like 5 µg/ml, 10 µg/ml, 15 µg/ml, 20 µg/ml, 25 µg/ml, up to 40 µg/ml were prepared. By UV-Spectrophotometer at λ_{max} of 282 nm solutions are analysed and absorbance and standard graph is represented in **Figure 1**.

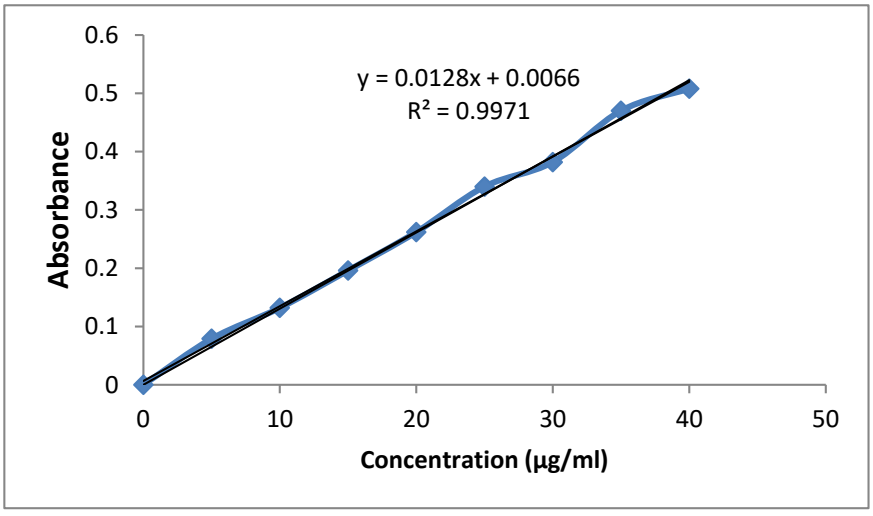

Figure 1: Calibration curve of Methyldopa in 0.1N HCl

Characterization of pre compression parameters of tablets

Pre-compression parameters like bulk density, tapped density, angle of repose and Compressibility index and percentage porosity were calculated (15).

Bulk density

In Bulk density determination, volume occupied is determined by transferring 25 gm powder samples into 100 ml graduated cylinder and the ratio between weight of sample to volume gives bulk density value.

Tapped density

In tapped density, 25 gm of powder samples transferred to a 100 ml graduated cylinder and tapped to get tapped volume reading and ratio between weigh to tapped volume gives tapped density.

Compressibility Index

It is determined by using following formula.

Compressibility Index= $(\rho_t - \rho_0)/(\rho_t)x\ 100$

ρ_t =tapped density, ρ_0=bulk density

Percentage Porosity

It was determined by liquid displacement method by applying formula

% Porosity= (True Density-Bulk Density)/True Density X 100

Angle of repose

Angle of repose was calculated by following funnel method using the equation.

$\theta = \tan^{-1} h/r$,

Where h and r are the height of pile and radius of the pile.

Characterization of post compression parameters of tablets

Characterization of Methyldopa tablets:

Tablets parameters like thickness, hardness (measured with Pfizer hardness tester and units in Kg/cm²) and percentage friability were determined. Roche Friabilator (Labindia) was used to determine friability, where 10 tablets were weighed initially by placing in the friabilator for 4 min giving 100 rpm and after that final tablets weight was measured. The percent friability (PF) = (Initial Weight – Final Weight) / Initial Weight X 100.

Weight variation test is performed as per USP guidelines to calculate average weight which compared with % deviation.

Drug content

To determine drug content of methyldopa tablets, five tablets of each formulation were weighed and finely powdered. About 0.1 gm equivalents were accurately weighed, completely dissolved in buffer and was filtered. About 1ml of the filtrate was further diluted to 100ml with buffer. The solution's absorbance was measured at 282 nm using a UV-visible spectrophotometer.

Floating property study

In floating property parameters like floating lag time (FLT) and total floating time (TFT) are evaluated. FLT is the amount of time tablets takes to reach the surface of the medium, and TFT is the amount of time tablets float on the surface. The tablets from each batch of formulation were added to 900 ml of 0.1 N HCl (pH 1.2) in USP type II dissolution equipment (Disso 2000, Labindia). While keeping the medium at a constant temperature, the speed of paddle maintained at 100 revolutions per minute and FLT and TFT are determined (16). Tablets showing faster hydration improve their floating ability in GRDDS of the effervescent type of floating system, which is caused by a gas-forming mixture of sodium bicarbonate ($NaHCO_3$) and citric acid. This mixture induces effervescence, which in turn leads to the creation of pores.

Methyldopa Swelling Property Study

Swelling behaviour confirms how the tablet absorbs fluids, which causes it to grow in size and weight. The extent of swelling is measured by difference in weight gain between before and after immersion of the tablet weight to the tablet weight before immersion in media and is expressed as a percentage weight gain by the tablet. Tablets from each formulation batch were weighed and placed in a beaker containing 200 ml of 0.1 N HCl with a

pH of 1.2. At hourly intervals, the tablets were removed, reweighed, and the percentage weight gain by the tablet was calculated.

***In vitro* dissolution studies**

It was carried out by USP Type II paddle type dissolution apparatus (Disso 2000, Labindia) by taking 900 ml of 0.1 N HCl (pH 1.2) media by maintaining temperature at 37±0.5°C. Methyldopa floating tablets are immersed in medium by setting the paddle to rotate at 100 rpm. At regular intervals 10 ml samples were removed and replaced with same media of the same volume. The samples were examined for drug concentration using a double beam UV-Visible spectrophotometer (Genesis-2, USA) at a wavelength of 282 nm, to calculate the percentage of cumulative drug release.

Drug release Kinetics

The release kinetics can be found by fitting the data to the various kinetic equations and to explain how the floating tablets release their drugs; the most appropriate model will be the one that correlates best with the experimental data (17). A coefficient of determination (R^2) value closer to 1 indicates a better match, which was used to select the optimal model. The release can be described as either Fickian diffusion ($n \leq 0.5$), anomalous diffusion ($0.5< n< 1$), or zero-order release ($n = 1$) depending on the value of (n).

Zero-Order Kinetics

In zero-order kinetics, the concentration has no effect on the rate of drug release. Here is the zero-order equation:

$Q_t = k_0 t$

First-Order Kinetics

The First-order kinetics model describes a system where the drug release rate is concentration-dependent. The First-order equation is given by:

$Q_t = Q_\infty (1-e^{-k1t})$

Higuchi Model

The Higuchi model describes drug release as a diffusion process based on Fick's law, primarily applicable to matrix systems. The Higuchi equation is given by:

$Q_t = K_H t^{1/2}$

Where k_0, k1, K_H is rate constant for zero order, first order kinetic constant and Higuchi rate constant respectively and Q_∞ being the total amount of drug in the tablet.

Stability study

As per ICH guidelines accelerated stability study was conducted at 40±2°C/75±5% relative humidity for 3month. Ten tablets were wrapped individually using aluminium foil and put at above specified condition and after each month tablet sample was analyzed for the *in vitro* drug release.

RESULTS AND DISCUSSION:

FTIR study

Figures 2 and 3 illustrate the results of the infrared spectroscopy approach used to determine drug compatibility. The IR spectrum clearly shows peaks at 1400 and 1600 cm^{-1}, which correspond to the benzene ring, at 3400 cm^{-1}, which indicates the OH vibration of the phenol, and peak at 3200 and 3400 cm^{-1}, which indicate the N−H vibrations. Similarly in figure 3 for FTIR of physical mixture of Methyldopa, HPMC K 100 M and Carbopol 934, there was no deviation or extra peak observed in the combinations of methyldopa, HPMC K 100 M, and carbopol 934. Although there is an additional peak at 3600 cm^{-1}, this might be because carbopol 934 is able to make hydrogen bonds with the O-H of methyldopa. It suggests that the excipients along with selected polymers used are completely compatible with the active pharmaceutical ingredient (API), methyldopa.

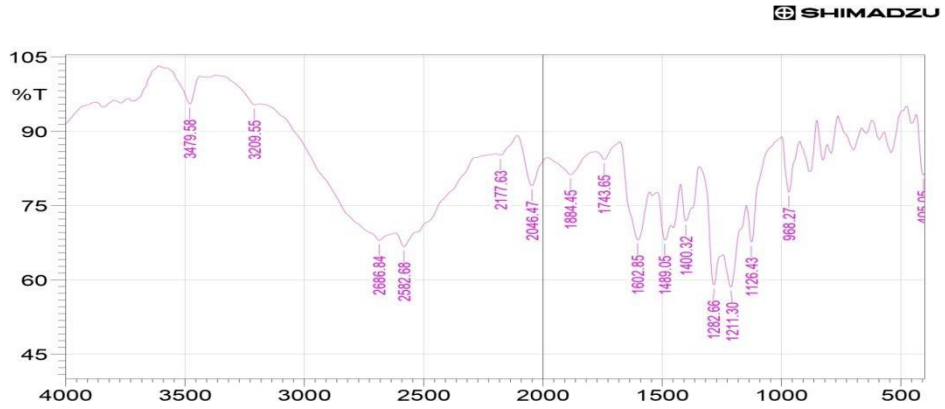

Figure 2: FTIR Spectrum of Methyldopa

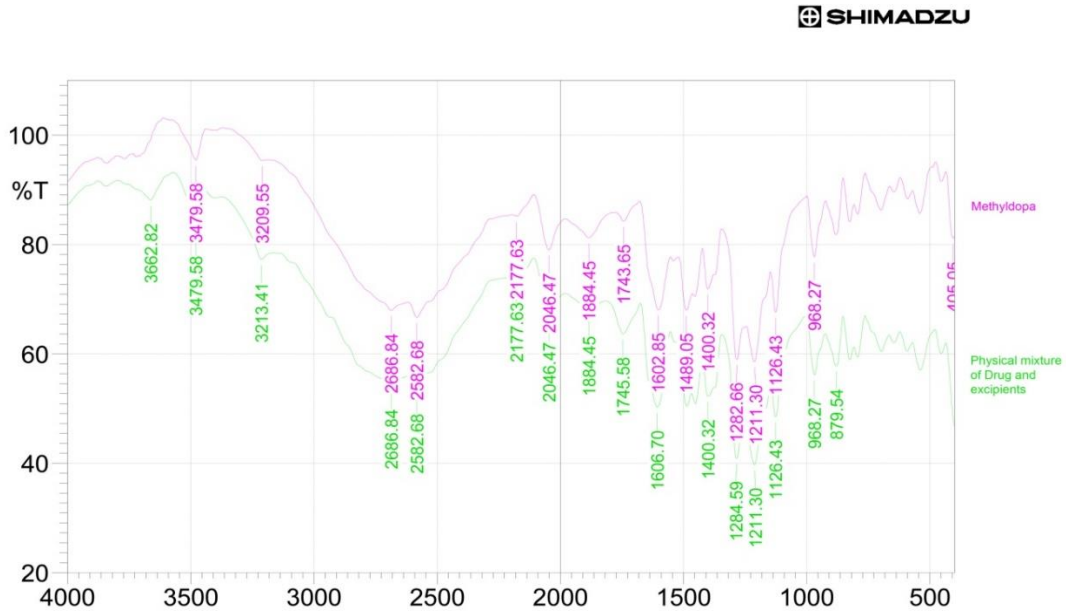

Figure3: FTIR Spectrum of physical mixture of Methyldopa, HPMC K 100 M and Carbopol 934

DSC Study

Figure 4 displays the DSC thermogram of the physical mixture of excipients utilised in the formulations as well as the drug methyldopa. When it comes to the samples' physical features, such as their thermal behaviour and possible interactions between the drug and excipients, DSC is invaluable. At its melting point of 140.05°C, the pure drug showed an endothermic peak in its DSC thermogram. The tablet formulation's DSC thermogram, on the other hand, displayed an endothermic peak at 141.85°C. There was no significant change in the endothermic peak between drug and formulation**.** Since the polymer HPMC K 100 M is compatible with the formulation and does not affect the stability of the drug, it can be attributed to the additional peak at 103.12°C, but this peak has no interaction with optimal formulation F3. Hence from the above DSC study, it was observed the formulation is still thermodynamically stable.

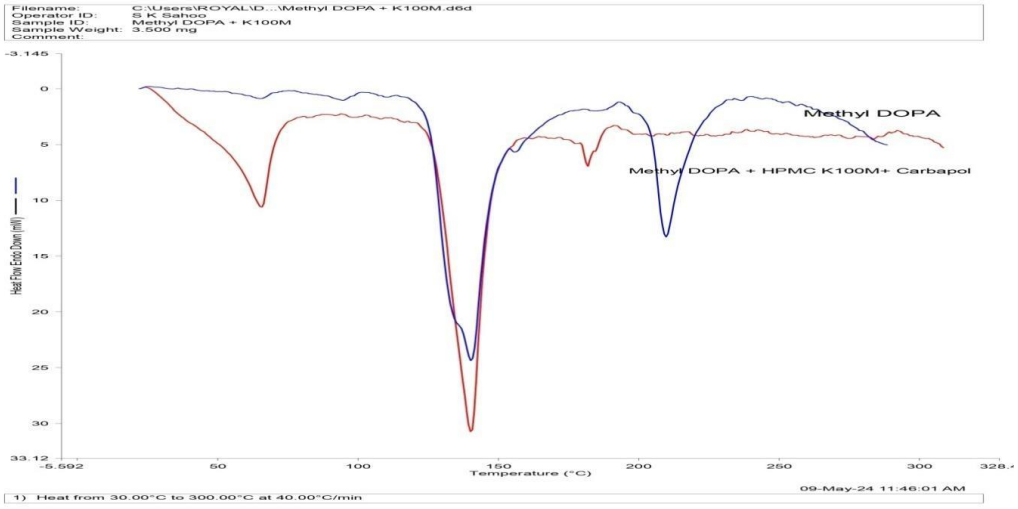

Figure 4: DSC of pure drug Methyldopa and F3 batch

Isothermal stress testing

In isothermal stress testing, there was no significant changes (colour and appearance) occur after storage of drug–excipients blend under stressed conditions Results shown in Table 2 shows their compatibility.

Table 2: Results of Isothermal Testing

Week	(drug excipients mixture)	% Assay	
		Control samples	Stressed samples
1	No significant changes in colour	100.81 ± 0.72	100.27 ± 1.65
2	No significant changes in colour	100.46 ± 0.86	99.27 ± 2.04
3	No significant changes in colour	101.8 ± 1.48	99.27 ± 2.04

Pre-compression parameters of powder mixtures

Pre-compression parameters like bulk density, tapped density, angle of repose and Carr's index results are shown in Table 3. Angle of repose value for all batches is less than 30 ^{0} indicated powder showing excellent flow property. Similarly, compressibility index values for all batches shows good flow ability**.** Percentage porosity of powder samples of all batches comes in the range of 20-25%. In floating tablets presence of polymers, delays penetration of the dissolution medium into the tablets in decreasing the drug release makes powder mixture particles more close to each other which reduces porosity percentage values.

Table 3: Pre-compression evaluation parameters of powder mixtures

Formulations	Angle of repose(θ)	Bulk density (g/ml)	Tapped density (g/ml)	Compressibility index (%)
F1	27.04±0.61	0.364±0.07	0.561±0.07	12.12±0.07
F2	26.01±0.37	0.329±0.59	0.312±0.09	13.94±0.07
F3	27.24±0.61	0.301±0.03	0.561±0.59	13.07±0.07
F4	26.01±0.37	0.329±0.59	0.312±0.08	12.12±0.07
F5	27.24±0.63	0.301±0.03	0.561±0.07	13.94±0.07

n= 6; SD-standard deviation

Post compression parameters

The prepared methyldopa floating tablets were white in colour, with an average diameter of 10.0 ± 0.0 mm and a mean thickness ranging from 3.384 ± 0.05 mm across all batches. The results of various post-compression parameters—such as weight variation, tablet hardness, and percentage friability—are presented in Table 4. All values fall within the acceptable limits specified by the applicable official compendia.

Table 4: Post compression parameters of different tablet batches

Batches	Weight variation test [a](mg) ±S.D	Hardness (kg/cm^2) ±S.D	Thickness (mm) ±S.D	%Friability (%) ± S.D	Floating lag time (sec) ± S.D	Total floating time (h) ± S.D
F1	620±0.016	5.50±0.36	3.384±0.05	0.48±0.02	60	>11h
F2	620±0.016	7.79±0.24	3.384±0.05	0.32±0.02	180	>9h
F3	620±0.016	5.50±0.24	3.384±0.05	0.65±0.02	60	>12h
F4	620±0.016	5.80±0.26	3.384±0.05	0.58±0.02	90	>12h
F5	620±0.016	6.19±0.20	3.384±0.05	0.53±0.02	1200	>9h

a, d (n=3**±S.D**) ; b(n=5±S.D) and c (n=20±S.D)

Floating property Study

The results are presented in Table 4. The presence of HPMC K100M alone in batch F1, or in combination with Carbopol 934 in batches F3 and F4, resulted in faster hydration. This led to the formation of a viscous gelatinous layer upon exposure to an aqueous medium, causing shorter floating lag time (FLT) and total floating time (TFT), as shown in Table 4. These findings are consistent with previous studies (18). In contrast, formulation F2, which contained Carbopol 934 alone at high concentrations, demonstrated greater moisture absorption compared to HPMC. This increased moisture uptake raised the tablet density, made the tablets sticky, and resulted in an increased FLT (19). Similarly, formulation F5, which lacked gas-forming agents, exhibited variable lag and floating times (20).

Swelling Study

In addition to facilitating drug disintegration, the carbon dioxide bubbles generated by sodium bicarbonate may obstruct the diffusion pathway through the hydrated gel layer (21). This explains the differences in swelling and drug release characteristics between effervescent and non-effervescent tablet formulations. One possible reason for the lower mean drug release in non-effervescent formulations is that their swelling indices—such as those observed in formulation F5—are higher compared to those of the corresponding effervescent formulations. The findings are presented in Table 5.

Table 5: Swelling Index of different tablet batches

Time (h)	F1	F2	F3	F4	F5
0.5	64.13 ±0.15	78.38±0.11	45.22 ±0.02	31.85 ±0.06	80.19 ±0.19
1	89.3 ±0.01	110.4±0.05	60.34 ±0.14	40.64 ±0.17	116.3 ±0.29
2	119.4±0.06	134.5±0.08	89.65 ±0.12	60.71 ±0.09	143.2 ±0.06
3	169.1±0.16	166.6±0.14	108.9 ±0.13	94.31 ±0.07	176.8 ±0.07
4	184.2±0.11	189.7±0.15	148.1 ±0.14	132.1 ±0.05	199.1 ±0.14
5	213.4±0.19	217.9±0.13	174.4 ±0.12	141.7 ±0.01	227.3 ±0.13

***In vitro* dissolution study**

In vitro drug release data and comparative dissolution profiles of tablet batch F1 to F5 h is shown in figure 5. According to this study, the concentration of the polymer

is responsible to prolong the drug release. In F1, due to increased chain entanglement caused by the presence of HPMC K 100 M, the side chains inflate more rapidly to create a strong gel. This gel demonstrates a stronger ability to withstand drug diffusion and gel erosion, which in turn decreases the drug release rate. In F1 around 27.27±1.46% release of methyldopa takes place in the initial half-hour. But with increase in time, the release was at a slower rate because the polymer swelled, and the release might last up to 11h hours with 98.87±1.13 % drug release (22).

Higher concentration of carbopol 934 polymer in formulation F2 makes tablets to a sticky mass upon contact with media. When carbopol polymers used in higher concentration in tablets increases crushing strength and have good binding characteristic resulting in increase in hardness as we have observed in F2 batch which shows hardness of 7.79±0.24 kg/cm ^{2}, but in dissolution media carbopol are almost completely non-ionized at pH 1.2 and do not completely swell at lower pH values; hence, solvent can permeate the glassy core deeply and swiftly, leading to faster drug release within 7 hours where more than 98% drug released. This property of carbopol was in agreement with various previous studies (23). But that at higher pH levels, the swelling caused by the ionisation of the carboxylic acid groups causes fewer and smaller regions of microviscosity, leading to a longer release of the drug (24-25).

Formulations F3 and F4, which contain a mixture of HPMC K100M and Carbopol 934, releases drug at a rate of 17.68±1.87 % and 33.85±3.02 %, respectively after 30 minutes. While HPMC K100M hydrates to produce a protective gel layer, the fast drug dissolution from the tablet surface may be responsible for the initial burst effect for F1 which contain only HPMC K 100 M (26). However, the first burst impact was diminished due to the inclusion of carbopol 934 which is an anionic polymer, which formed an insoluble mass that acted as a barrier to drug diffusion and lowered the drug release in the acidic medium in F3 (27). The fact that the carbopol 934 polymer has an adverse effect on floating behaviour and is only used for its drug release retardant properties which are extremely effective at low concentrations to achieve extended release characteristics and may be another reason why F3 has better control over drug release and takes 12 hr to release 99.09±0.13 % drug release (28).

But in F4 the increase in amount of Carbopol demonstrates 98% drug release in 8 hours. This is because the less viscous polymer, carbopol, replaces the more viscous HPMC K 100 M to increase drug release (29). In order to check the effect of gas forming agents in drug release of methyldopa GRDS tablets, authors have designed the non-effervescent formula F5 and have observed tablets of this batch have the slowest release rate and drug release pattern and similar to F3, but with a longer floating lag period. This might be because as there are no gas-forming agents, which means there is no effervescence and no pore development. This resulted in a slower rate of drug release since the tablets were hydrated more slowly. However, tablets having both HPMC K 100 M and carbopol 934, the addition of sodium bicarbonate increased the hydration volume, leading to a larger volume expansion in the former scenario (30).

So from this research finding it may confirm polymer viscosity responsible for cumulative drug release from methyldopa tablets. Formulation F3 tablets with HPMC K 100 M and carbopol 934 showed that the drug was released in the gastric pH more slowly which extends more than 12 h, with a floating lag time of 60 seconds indicating the most suitable tablet batch.

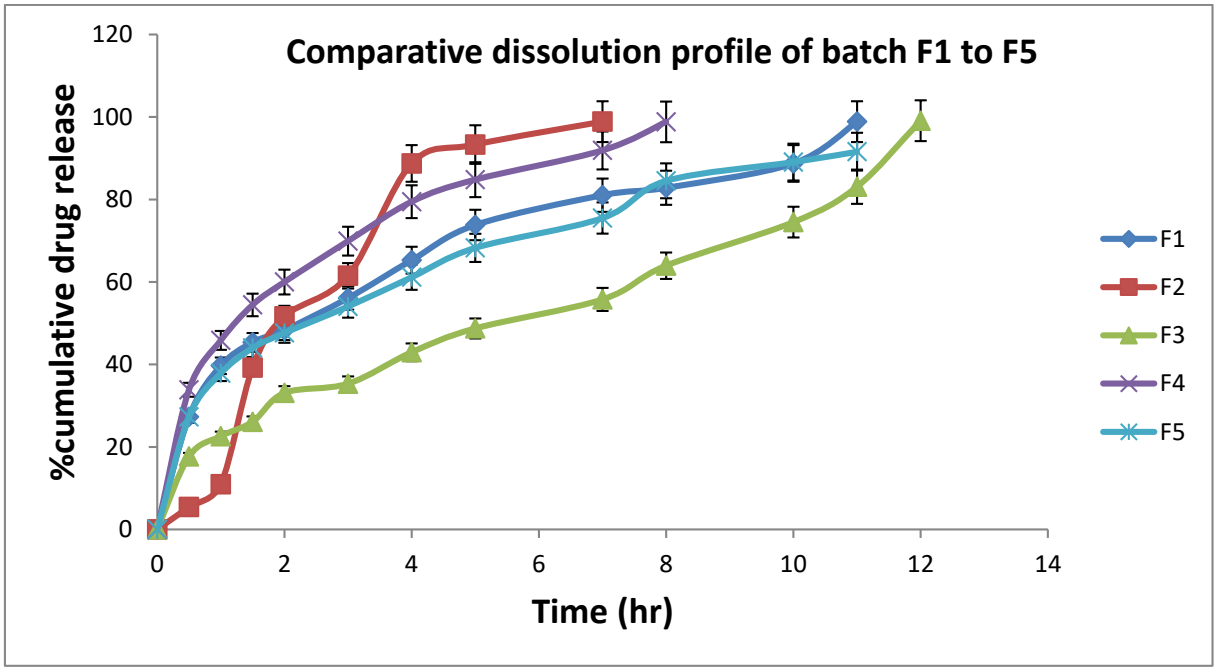

Figure 5: Comparative dissolution profiles of Tablet Batch F1 to F5

Drug Release Mechanism

Table 6 presents the results of the drug release mechanism, showing an R^2 value of 0.998 for the F3 tablet and an n value of 0.720 (within the range of 0.89–1) based on the Peppas equation. These values suggest that the drug release follows a diffusion–erosion mechanism, driven by the swelling and hydration behavior of the combined polymers HPMC K 100 M and Carbopol 934.

Table 6: The results of kinetic treatment applied to dissolution profile of tablet of each batch were as shown.

Batches	Zero order (R^2)	Higuchi (R^2)
F1	0.969	0.991
F2	0.973	0.997
F3	0.974	0.998
F4	0.959	0.992
F5	0.963	0.994

***In vitro* drug release comparison of the batch F3 with the marketed methyldopa tablets (Aldopam Tabs)**

The in vitro release study compared the optimized formula F3 with the commercially available Aldopam tablets. The marketed tablets demonstrated complete drug release within 6 hours, whereas the F3 batch exhibited a sustained drug release over 12 hours, with a floating lag time of 60 seconds and a total floating duration exceeding 24 hours. The comparative dissolution profile results are presented in Figure 6.

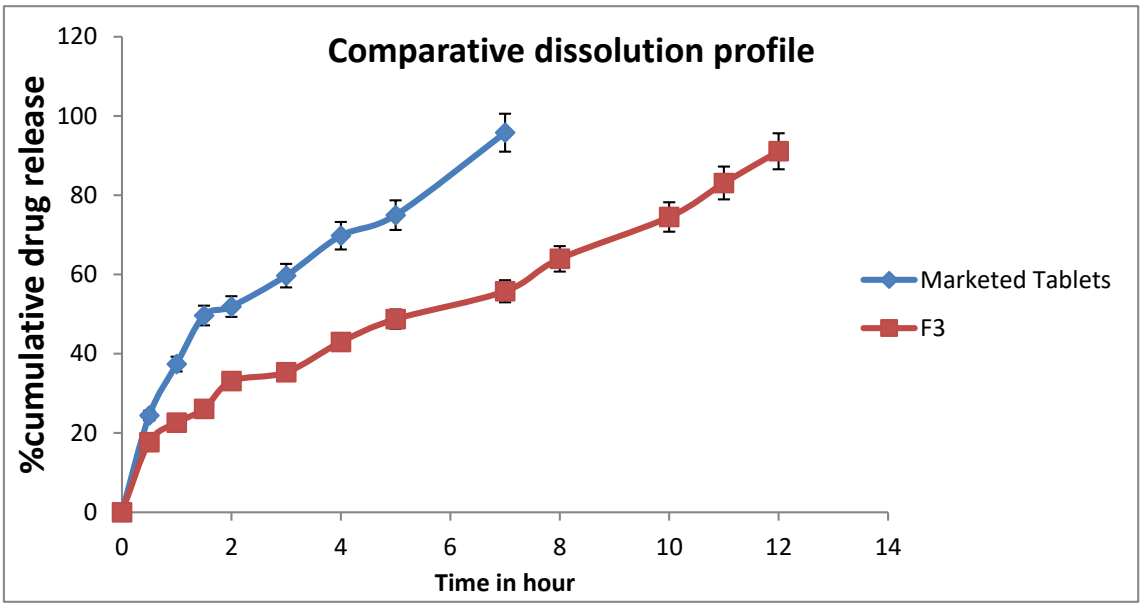

Figure 6: *In vitro* dissolution study of Marketed Tablets and F3

Stability Study

Throughout the storage period, no colour or appearance changes were observed and results are shown in table 7.

Table 7: Stability data of F3 formulation after 3 month accelerated stability study

Parameters	Initial	After 1Month	After 2M	After 3M
Physical appearance	Tablets are pale white, convex smooth surface without any cracks	No change	No change	No change
Thickness(mm) ± S.D	3.384±0.05	3.384±0.05	3.384±0.05	3.384±0.05
Hardness(kg/cm^2) ± S.D	5.50±0.24	5.50±0.24	5.50±0.24	5.50±0.24
Friability(%) ± S.D	0.65±0.02	0.65±0.02	0.65±0.02	0.65±0.02
% cumulative Drug release	99.09±0.13	99.32±0.79	99.1±0.09	98.19±0.79

CONCLUSION

In this research, the authors successfully formulated GRDDS floating tablets of methyldopa using HPMC K100M and carbopol 934 polymers. Out of different formulation batches, F3 is the most ideal batch tablet, which extends drug release for more than 12 hours with a floating lag time of 60 seconds. The drug is released through diffusion-erosion mechanisms, which are caused by the swelling and hydration behavior of the combination polymers of HPMC K 100 M and carbopol 934. Swelling studies indicate significant water uptake, which contributed to drug release and could be important in gastric retention. Isothermal stress testing shows that no significant changes (color and appearance) occurred after the storage of drug-excipients blends under stressed conditions. Similarly, FTIR suggests that the excipients

and selected polymers used are completely compatible with the active pharmaceutical ingredient (API), methyldopa, and from the DSC study, it was observed that the formulation is still thermodynamically stable. The prepared methyldopa floating tablets of the F3 batch in the accelerated storage conditions study remain stable, indicating the stability of the formulation.

ACKNOWLEDGMENT

The authors are thankful to the Department of Pharmaceutics, Royal College of Pharmacy and Health Sciences, for their help in providing the necessary resources and facilities for this study.

FINANCIAL SUPPORT

There is no funding to report.

CONFLICTS OF INTEREST

The authors declare no conflict of interest.

ETHICAL APPROVALS

The study does not involve experiments on humans or animals.

REFERENCES

1. Prusty A, Ray D. Designing and in vitro studies of gastric floating tablets of tramadol hydrochloride. *Int J Appl Pharm*. 2009; 2(4):12–16.
2. Sreelekha S, Kumar KV, Mahammed N, Reshma T, Sree GU, Basha SS, Bhuvaneswari M. Quality by design approaches in pharmaceutical development and solid dosage forms production: a narrative overview. *Jordan J Pharm Sci*. 2023; 16(4):770–784. https://doi.org/10.35516/jjps.v16i4.908
3. Raut S, Hajare A, Chougale R, Kamble S, Patil K. Formulation, development, and evaluation of bosentan monohydrate spray dried-solid dispersion tablets for improved dissolution profile. *Jordan J Pharm Sci*. 2023; 16(4):714–733. https://doi.org/10.35516/jjps.v16i4.514
4. Khanfar M, Salem MS. Dissolution enhancement of poorly water-soluble drugs by co-precipitation in the presence of additives and stabilizers. *Jordan J Pharm Sci*. 2009; 2(1):32–40.
5. Lenaerts VM, Gurny R. Gastrointestinal tract—physiological variables affecting the performance of oral sustained release dosage forms. In: Lenaerts V, Gurny R, eds. *Bioadhesive Drug Delivery Systems*. Boca Raton, FL: CRC Press; 1990. p.281–283.
6. Deshpande AA, Shah NH, Rhodes CT, Malick W. Development of a novel controlled-release system for gastric retention. *Pharm Res*. 1997; 14:815–819.
7. Mali AD, Bathe RS. Development and evaluation of gastroretentive floating tablets of a quinapril HCl by direct compression technique. *Int J Pharm Pharm Sci*. 2017; 9(8):35–46.
8. Yeole PG, Khan S, Patel VF. Floating drug delivery systems: need and development. *Indian J Pharm Sci*. 2005; 67:265–272.
9. Arora S, Ali J, Ahuja A, Khar RK, Baboota S. Floating drug delivery systems: a review. *AAPS PharmSciTech*. 2005; 6:E372–E390.
10. Patel M, Shelke S, Surti N, Panzade P, Al-Keridis LA, Upadhyay TK, Alshammari N, Saeed M. Design, preparation, and in vitro evaluation of gastroretentive floating matrix tablet of mitiglinide. *Front Pharmacol*. 2023; 14:1140351.
11. Sharma S, Prashar M, Sahu RK. Floating drug delivery system: incredible revolution. *Pharmacologyonline*. 2011; 3:1039–1054.
12. Ibrahim IAA, Shahzad N, Al-Joudi FS, Al-Ghamdi SS, Alshagga MA. In vitro and in vivo study of effect of α-adrenergic agonist-methyldopa on the serum biochemical laboratory findings. *J Clin Exp Pharmacol*. 2013; 3:136.
13. Liltorp K, Larsen TG, Willumsen B, Holm R. Solid state compatibility studies with tablet excipients using non-thermal methods. *J Pharm Biomed Anal*. 2011; 55(3):424–428.

14. Pani NR, Nath LK, Bhunia B. Formulation, development and optimization of immediate release tablet of nateglinide by factorial designs. *Drug Discov Ther*. 2010; 4:453–458.
15. Prusty A, Patra A. Formulation and evaluation of ciprofloxacin colon targeted tablets by compression coating technique using guar gum and hydroxy propyl methylcellulose. *J Res Pharm*. 2022; 26(6):1593–1607.
16. Jadi RK, Bomma R, Sellappan V. Development of a new single unit dosage form of propranolol HCl extended-release non-effervescent floating matrix tablets: in vitro and in vivo evaluation. *J Appl Pharm Sci*. 2016; 6:112–118.
17. Higuchi T. Mechanism of sustained action medication: theoretical analysis of rate of release of solid drugs dispersed in solid matrices. *J Pharm Sci*. 1963; 52:1145–1148.
18. Basak S, Reddy JB. Formulation and release behaviour of sustained release ambroxol hydrochloride HPMC matrix tablet. *Indian J Pharm Sci*. 2006; 68:594–598.
19. Li S, Lin S, Daggy BP, Mirchandani HL, Chien YW. Effect of HPMC and Carbopol on the release and floating properties of gastric floating drug delivery system using factorial design. *Int J Pharm*. 2003; 253:13–22.
20. Shah SH, Patel JK, Patel NV. Formulation and evaluation of effervescent floating tablet of levofloxacin against *H. pylori* infection. *Der Pharm Sin*. 2010; 1:232–244.
21. Sambanni P, Reddy V, Walikar A, Marapur SC, Patil RG. Formulation and evaluation of atorvastatin calcium floating tablets. *Int J Appl Pharm*. 2018; 22(12):1543–1556.
22. Li L, et al. Optimization of sustained release matrix tablet of metoprolol succinate using central composite design. *Pak J Pharm Sci*. 2013; 26(5):929–937.
23. Noveon. Controlled release formulations using Carbopol polymers. In: *Carbopol – Pharmaceutical Applications*. Cleveland: Noveon Inc.; 1999. p. 1–59.
24. Mohamed F, Mahrous G, Mohamed I, Adel S. Influence of Carbopol 71G-NF on the release of dextromethorphan hydrobromide from extended-release matrix tablets. *Pharm Dev Technol*. 2011; 18. doi:10.3109/10837450.2011.586037.
25. Bulut-Oner F, Capan Y, Kas S, Oner L, Hincal AA. Sustained release isoniazid tablets. I—Formulation and in vitro evaluation. *Farmaco*. 1989; 44(7–8):739–752. PMID: 2590371.
26. Tiwari SB, Rajabi-Siahboomi AR. Applications of complementary polymers in HPMC hydrophilic extended release matrices. *Drug Deliv Technol*. 2009; 9:20–27.
27. Tatavarti A, Mehta K, Augsburger L, Hoag S. Influence of methacrylic and acrylic acid polymers on the release performance of weakly basic drugs from sustained release hydrophilic matrices. *J Pharm Sci*. 2004; 93:2319–2331.
28. Loh ZC, Elkordy AA. Formulation and evaluation of different floating tablets containing metronidazole to target stomach. *Curr Drug Deliv*. 2015; 12(4):425–443.
29. El-Zahaby SA, Kassem A, El-Kamel AH. Design and evaluation of gastroretentive levofloxacin floating mini-tablets-in-capsule system for eradication of *Helicobacter pylori*. *Saudi Pharm J*. 2014; 22:570–579.
30. Tadros MI. Controlled-release effervescent floating matrix tablets of ciprofloxacin hydrochloride: development, optimization and in vitro–in vivo evaluation in healthy human volunteers. *Eur J Pharm Biopharm*. 2010; 74:332–339.

صياغة وتوصيف أقراص ميثيل دوبا العائمة باستخدام سواغات بوليمرزية: دراسة حول نظام توصيل الأدوية المضبوطة في الجهاز الهضمي

أماريش بروستي[1] * ، تشينمايا كيشاري ساهو [2] ، سانجيت كومار سيناباتي [1] ، بريانكا سينغ [1] ، جيانرانجان بيهيرا [1]

[1] قسم الصيدلانيات، الكلية الملكية للصيدلة والعلوم الصحية، بيرهامبور، أوديشا، الهند

[2] قسم الصيدلانيات، كلية العلوم الصيدلانية، بوري، بيديانيكتان، باليغوالي، بوري، أوديشا ,.الهند

ملخص

يهدف هذا البحث إلى تطوير نظام جديد لتوصيل الأدوية للاحتفاظ بالجهاز الهضمي (GRDDS) يمكنه إطالة إفراز دواء ميثيل دوبا .في هذا البحث ، يتم تحضير الأقراص بطريقة الضغط المباشر باستخدام كاربابول 934وبوليمر HPMC K100M، باستخدام تقنية الفوار)للتركيبات F1و F2و F3و (F4وغير الفوارة .(F5)أحد الأدوية المستخدمة لعلاج ارتفاع ضغط الدم هو methyldopa، وهو دواء ود يعمل مركزيا له عمر نصف قصير يبلغ 2ساعة .التخدير ,الغثيان , والقيء هي بعض الآثار الجانبية للدواء التي تحدث نتيجة لتكرار إعطائه 250)ملغ مرتين إلى ثلاث مرات في اليوم .(لذلك ، سيكون من الأكثر فعالية تحضير GRDDSمن methyldopaلإطلاق الدواء في بيئة المعدة لفترة طويلة F3 . هي دفعة التركيبة الأكثر فعالية لأن مزيج البوليمرات HPMC K 100Mو carbopol 934في أقراص ميثيل دوبا الفوارة يطيل بشكل كبير من إطلاق الدواء في 0.1N HClل ...

الكلمات الدالة: ميثيل دوبا ، HPMC K 100 M، Carbopol 934 ، أقراص عائمة ، وقت تأخر عائم.

* ***المؤلف المراسل: أماريش بروستي***

amareshprusty@gmail.com

تاريخ استلام البحث 2024/6/1 وتاريخ قبوله للنشر 2024/8/22.

Jordan Journal of Pharmaceutical Sciences, Volume 18, No. 2, 2025

In-silico Innovative mRNA Vaccine Development Using Multi-Epitopes of SopD Protein for Enteric Fever Caused by *Salmonella enterica*

Aaiza Mumtaz[1*], Muhammad Umair[1], Hadia Hussain[1], Wasla Ali[1], Muhammad Sajid[1]

[1]Department of Biotechnology, University of Okara, Pakistan.

ABSTRACT

An increase in antibiotic resistance has created significant challenges in treating *Salmonella enterica* infections. Consequently, various vaccines have been developed as practical alternatives to antibiotics for preventing *S. enterica* infections. mRNA vaccine technology is rapidly advancing as a replacement for conventional methods due to its high efficiency, low cost, and ability to elicit a strong humoral immune response. This research aims to develop a novel mRNA vaccine against *S. enterica* using immunoinformatics approaches. The protein SopD was selected, and its suitable epitopes were identified. These epitopes were evaluated to ensure they are antigenic, non-allergenic, and non-toxic. Subsequently, the epitopes were linked using appropriate linkers to create a vaccine construct. This construct was further analyzed and subjected to molecular docking with the Toll-like receptor TLR3 using the HDock server. Molecular dynamics (MD) simulations showed that the vaccine construct is stable based on RMSD and RMSF parameters. Immune simulation indicated the vaccine's efficacy, and it was successfully cloned using the SnapGene tool. Finally, a multi-epitope protein was modeled and optimized. The results demonstrated that the vaccine construct is effective, non-allergenic, non-toxic, and successfully cloned. Overall, the findings suggest that the designed mRNA vaccine construct could be a promising candidate for *S. enterica* treatment, pending validation through in vitro techniques such as ELISA and in vivo testing in animal models.

Keywords: Enteric fever, Epitopes, Gastroenteritis, *S. enterica*, Septicemia.

1. INTRODUCTION

Typhoid fever is commonly known as enteric fever which is caused by the food or water which is contaminated with bacteria. It is characterized by a prolonged high fever lasting for weeks. It affect majorly to your small intestine and shows symptoms like high fever, chills, cough, muscle aches and rose spots like rash [1].

Salmonella enterica can easily be transmitted from person to person through objects and surfaces contaminated with the bacteria. It is considered a serious health concern, especially in children, due to their weaker immune systems. Enteric fever, if left untreated, can be fatal [2]. Moreover, it is more common in people that travel from one place to another [3]. Symptoms typically do not appear within the first week, but after 7 to 14 days, a high fever develops and can become severe. In infants and children, diagnosis may be delayed until serious complications arise beyond just the fever. Diagnosis is usually made clinically based on physical examination and the patient's history of exposure [4].

Three major types of diseases are involved in typhoid i.e. gastroenteritis, septicemia, and enteric fever. Gastroenteritis is the inflammation of digestive system which may result in infection. It is considered as short-term illness and includes symptoms like diarrhea, abdominal cramps and vomiting condition. Virus, parasites, bacterial toxins, various chemicals and drugs are

[*]***Corresponding author: Aaiza Mumtaz***
aaizamumtaz07@gmail.com
Received: 23/6/2024 Accepted: 22/8/2024.
DOI: https://doi.org/10.35516/jjps.v18i2.2819

the reason behind the cause of gastroenteritis. Good hygiene is necessary for the prevention from the spread of disease in other people [5]. Septicemia is also known as sepsis which is the utmost response to infection in the human body. It is considered as the blood poisoning by the contamination of microorganisms like bacteria, fungi, and viruses [6]. It can cause various types of infections i.e. infection in intestine, lungs, urinary tract, and responsible for the skin infection. It may also cause organ failure, damage of tissues, and death of the patient. It can be treated with the antibiotics, avoiding the source that is the cause of infection. Enteric fever is also been a health problem in public, and can be fatal if it is not treated [7].

Enteric fever or typhoid fever symptoms swiftly develop in four stages, these stages are as stage 1 is the initial stage of typhoid which occur within five to fourteen days after getting in contact with the bacteria. The symptom of this is fever which gets higher and higher over days and is known as stepwise [8]. At this stage, bacteria keep on moving in the blood of the patient. In stage 2, which is the second week of the fever, bacteria began to multiply in the part of human body immune system that is responsible for the identification of the harmful invaders known as Peyer's patches. At this point, patient start facing symptoms like stomach pain leading to diarrhea. Moreover, rashes or red spots appear on the body [9]. Stage 3 is the point at which no antibiotic will work to prevent the bacterial infection and can cause serious damage. This stage is the third week of the infection and symptoms like internal bleeding or inflammation in your brain which is encephalitis appears in the patient [10]. Final stage is the 4^{th} stage, in which patient began to recover and fever gradually decreases. However, the bacteria may remain in your gallbladder without causing any symptoms.

Healthcare providers suggests the patient to take tests for the diagnosis of the disease by taking samples of your blood, urine, stool, or bone marrow [11]. X-ray can also be taken to look deeper changes in your lungs. Furthermore, it can be treated with antibiotics but some types of bacteria cannot be treated with antibiotics which include medicines like levoflaxin, cephalosporins, azithromycin, and cefixime [12, 13]. If the patient is severely ill, it might be given additional treatment like being admitted into the hospital for proper care and treatment. To reduce risk of being in contact with enteric fever, vaccination should be taken if you travel or live in the area where there are chances of getting in contact with the bacteria *Salmonella enterica* [14, 15]. Till now, there are two types of vaccines that were being used for the prevention of enteric fever but they do not helped in complete prevention and protection which included oral vaccine for typhoid in which four pills were taken after every few days but in December 2020, it was no more available in the market from the manufacturers [16]. Second type of vaccine is injectable vaccine that is needed almost two weeks before arriving in an area where *S. enterica* is common. This vaccine will develop your immunity by making it able to resist or fight with the bacteria and it is needed to build up immunity after every two years to stay protected from the infection. The children with the age of 2 years can also get this vaccination [17].

S. enterica is a gram-negative, motile, rod shaped pathogenic and harmful bacteria. There are further six subspecies and have 2,600 serotypes that are responsible for the cause of various infections in humans and animals [18]. According to various studies, *S. enterica* on biotic and abiotic surfaces forms biofilms such as glass surfaces, cabbage, polystyrene, stainless steels etc. The various qualities of *S. enterica* control the statement of cell parts during the development of biofilm. The ycfR is a profoundly managed quality which shows articulation under the pressure of chlorine and shows high harmfulness [19]. It assists the *S. enterica* with framing biofilms for the most part on the outer layer of glass and polystyrene. In contain proteins like, CsgD which is the transcriptional administrative protein which manages the outflow of curli protein and cellulose that aides in surface grip [20]. The fliL in *S. enterica* controls the development and course of

flagella which helps in the micro-colonies' arrangement. This bacteria is responsible for enteric fever which is more common in those areas where there is more contamination and sanitation condition is poor [21].

The significance of the research is to identify the new and more efficient vaccine for the prevention of bacteria *S. enterica* that is responsible for the cause of enteric fever. Furthermore, mRNA vaccine is considered to be more significant as compared to the other vaccines because they are used for early treatment before getting in contact with the bacteria and should be subjected to further in vitro and in vivo testing.

2. MATERIALS AND METHODS

2.1 Sequence retrieval, prediction and evaluation of B-cells and T-cells epitopes:

For the preparation and designing of vaccine, SopD protein sequence of *Salmonella enterica* in the form of FASTA format was retrieved from UniProt (https://www.uniprot.org/) using its advance feature of finding protein along with the organism [22]. An IEDB tool (http://tools.iedb.org/main/) was utilized for the epitope prediction of B-cells and T-cells on the basis of sequence obtained from Knowledge based Database (UniProt).

B-cells epitopes were taken from portion of IEBD tool for B-cell epitope prediction (http://tools.iedb.org/main/bcell/) which explained number of B-cells epitopes present in the sequence along with each epitope sequence, their starting and ending point [23, 24]. It also provides graphical representation on the basis of peaks to distinguish between epitopes and remaining sequence. T-cells epitopes on the other hand can be obtained from (http://tools.iedb.org/main/tcell/) having two parts of MHC-I and MHC-II for CD8+ and CD4+ [25]. All the epitopes of the protein were validated for antigenicity using Vexijen (https://www.ddg-pharmfac.net/vaxijen/VaxiJen/VaxiJen.html) and its non-allergenicity was checked by utilization of Allertop v. 2.0 (https://www.ddg-pharmfac.net/AllerTOP/) [26, 27].

2.2 Population coverage of the predicted epitopes worldwide:

Population coverage potential of MHC-I and MHC-II was studied by using IEDB analysis resource (http://tools.iedb.org/population/) which reveals about the worldwide coverage of the predicted epitopes of Class-I and Class-II. This population coverage should be greater than 60% [28].

2.3 Vaccine Construction using epitopes obtained from SopD protein:

The mRNA vaccine construct was proposed to be arranged in the form starting from N-terminal to C-terminal in the following arrangement: An adjuvant-EAAAK linker- linker-B-cells Predicted epitopes-CPGPG linker-T-Cells predicted epitopes for MHC-I-AAY linker-T-Cells predicted epitopes for MHC-II-HHHHH tag which is Histidine tag.

2.4 Evaluation of toxicity and physiochemical properties of the vaccine construct:

To evaluate the harmfulness and toxicity of the antibody build, the computational device ToxinPred (http://crdd.osdd.net/raghava/toxinpred/) server was used. It additionally divulged about the atomic weight, its charge, hydrophobicity, hydropathicity and change position in each linker and anticipated epitopes [29]. The outcome made sense of that there is no transformation and all the peptide arrangements are non-toxic [30].

The compositional examination and physiochemical properties of SopD protein were estimated by using Expasy's Protparam server (https://web.expasy.org/protparam/). It additionally made sense of about the amino corrosive creation and nuclear arrangement which makes sense of about the quantity of amino acids and number of molecules individually to concentrate on the SopD protein of *Salmonella enterica* [31].

2.5 Prediction of secondary structure for the vaccine construct:

To dissect the underlying organization of protein based on alpha helix, beta sheets, and loops utilizing optional construction forecast instrument PsiPred

(http://bioinf.cs.ucl.ac.uk/psipred/). PsiPred is accessible as both web server and programming. The grouping of the protein is placed into the server and it gives us optional construction based on its essential design. This apparatus additionally tells about the certainty score of the protein anticipated structure [32].

2.6 Prediction and validation of tertiary structure of the vaccine construct:

trRosseta (https://yanglab.qd.sdu.edu.cn/trRosetta/) was utilized for the homology displaying and modeling of the protein tertiary structure. For approval of the construction got from saves server (https://saves.mbi.ucla.edu/) instruments like ERRAT and ProCheck, and Molprobity (http://molprobity.biochem.duke.edu/) were used to find generally quality element, Ramachandran leaned toward locales, Z-score value and different boundaries of each anticipated design from the above utilized servers. ERRAT tells about the general quality component of the protein. Procheck makes sense of exhaustively about the Ramachandran plot and its mistakes in the SopD [33]. Molprobity distinguishes issues in the 3D construction of the protein which was anticipated by utilizing different protein structure forecast servers. After validation of the predicted structures, it was revealed that the trRosseta web tool provides a fast and precise evaluation of protein models, as well as an efficient assessment of model accuracy.

2.7 Vaccine construct and suitable ligand docking:

An online bioinformatics tool HDock (http://hdock.phys.hust.edu.cn/) was utilized for the docking of vaccine construct with any specific ligand. In this tool, PDB file of the predicted structure and ligand was utilized will shows interaction with each other [34]. It take 20 to 30 minutes to compute the results of docking and the whole process is fast. It provides top 10 models after docking run and the best results are further utilized. The lower the docking score, the greater will be the interaction.

2.8 Protein in water simulation of vaccine construct:

To verify the vaccine construct of SopD protein Simlab (https://simlab.uams.edu/ProteinInWater/index.html) which is an accurate computational tool for the simulation was utilized in which different parameters are set to compute the results like number of frames per simulation, time and duration of the simulation, and number of energy minimization steps [35].

2.9 Visualization of predicted epitopes in the vaccine construct:

The visualization of the epitopes which were available in the vaccine construct especially B-cells epitopes can be visualized with the help of a computational tool known as ElliPro (http://tools.iedb.org/ellipro/) which is used for the linear or discontinuous antibody epitopes prediction available in the given sequence. A PDB file of the sequence based structure is provided to the server which is used for the visualization of the epitopes [36].

2.10 Analysis of receptor-ligand interaction in vaccine-SopD:

PDBSum (https://www.ebi.ac.uk/thornton-srv/databases/pdbsum/) is used for the analysis of interactions between the receptor and ligand that is present in the vaccine construct. The ligand in the protein can be easily seen and amino acids present in the ligand can also be visualized. It also explains about the interactions between the A, B, C, and D chains of the vaccine construct and tells about the maximum interactions between them [37, 38].

2.11 Codon optimization of the vaccine construct:

The vaccine construct was as amino acids which was changed over into the nucleotide framework by the utilization of online server known as Emboss (https://www.ebi.ac.uk/jdispatcher/st/emboss_backtranseq) server in which the grouping of the antibody develop is used. To upgrade the interpretation of the mRNA vaccine develop inside have cells, codon optimization tool were used which bring about the better DNA grouping. The JCat (https://www.jcat.de/) Codon Optimization tool (G.S.) was utilized to enhance the antibody grouping for effective articulation in human cells [39].

2.12 Prediction of the secondary structure of the

mRNA constructed vaccine:

For RNA structure prediction of the protein RNAfold (https://rna.tbi.univie.ac.at/cgi-bin/RNAWebSuite/RNAfold.cgi) webserver was utilized which shows the secondary structure. In this webserver, the improved DNA sequence was input into the server and resulted secondary structure is obtained having nucleotide Guanine, Adenine, Cytosine, and Uracil. These discoveries will recommend that the mRNA vaccine construct can be proficiently produced and is fundamentally steady, possibly upgrading its viability as an antibody [40].

2.13 In silico immune response simulation against vaccine:

To ensure effectiveness of vaccine was further validated on the basis of the immune response and for this immune simulation tool C-immsim (https://kraken.iac.rm.cnr.it/C-IMMSIM/index.php) was utilized in which sequence of the vaccine was used as input and the results were obtained on the basis of antigen, antibody, B-cells, T-cells, and other responses that are essential for human immunity [41].

2.14 Cloning of the mRNA vaccine construct:

SnapGene is a software which is used for the cloning of the SopD vaccine. In this software, a vector and fragment of DNA sequence are converted into product and further prepared for cloning. The major purpose of SnapGene is the visualization and documentation of DNA cloning and PCR.

3. RESULTS

3.1 Prediction and estimation of B-cells and T-cells epitopes:

The FASTA sequence of selected protein SopD obtained from bacterial specie *Salmonella enterica* was retrieved from UniProt (https://www.uniprot.org/) that can cause enteric fever and was used to predict the b-cells and t-cells epitopes [42]. The IEDB tool was utilized to obtain the epitopes of B-cells. The tool displayed the length, sequence, and beginning and ending points of each peptide or epitope. This tool is also used to identify the epitopes of its two classes of T-cells.

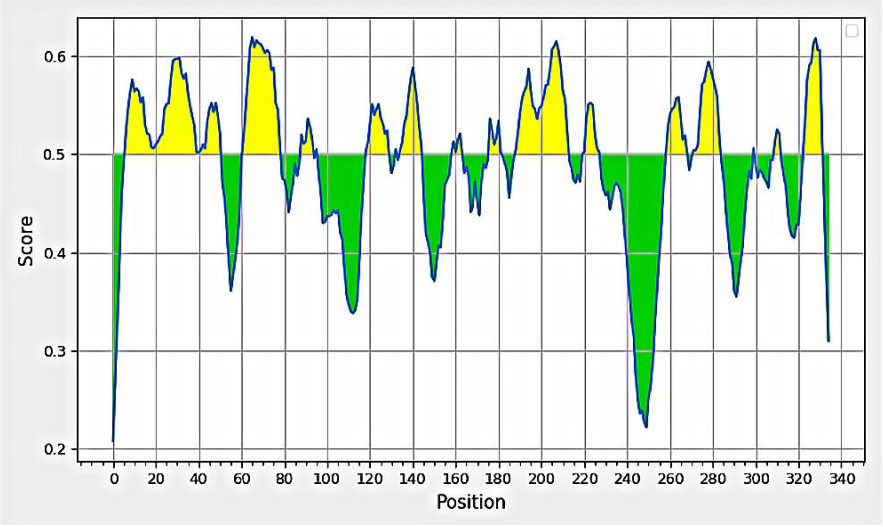

Figure 1. The figure shows the epitope position according to its score which should be above than 0.5. The yellow-colored peaks having score above than 0.5 are constituted as epitopes from the sequence.

The epitopes of MHC I and MHC II binding results were also taken from the IEDB tool. The predicted epitopes were on the basis of the alleles and resultant epitopes were sorted on the basis of its ic50 value which should be less than 100.

Table 1. Predicted epitopes of MHC I with their sequences and ic50 values

Allele	Seq_Num	Start	End	length	Epitopes	ic50	Rank
HLA-B*44:03	1	151	160	10	CEVIGATITW	37.71	0.03
HLA-B*44:02	1	151	160	10		38.52	0.06
HLA-B*15:01	1	243	252	10	FSMMHPCISY	8.31	0.03
HLA-A*01:01	1	243	252	10		57.16	0.12
HLA-B*35:01	1	243	252	10		89.81	0.21
HLA-B*40:01	1	101	110	10	IEMDASQTQL	37.99	0.09
HLA-B*44:02	1	101	110	10		71.39	0.11
HLA-A*30:01	1	39	48	10	KVRDHFRSEK	4.22	0.03
HLA-A*31:01	1	39	48	10		35.7	0.39
HLA-A*03:01	1	39	48	10		36.92	0.13
HLA-A*33:01	1	286	294	9	MFIDVILER	9.84	0.02
HLA-A*68:01	1	286	294	9		12.51	0.09
HLA-A*31:01	1	286	294	9		51.22	0.55
HLA-A*02:01	1	145	153	9	QLFLQICEV	24.52	0.22
HLA-A*02:03	1	145	153	9		37.82	0.61
HLA-A*02:06	1	145	153	9		48.12	0.49
HLA-A*31:01	1	55	63	9	VLYAIIHGR	11.85	0.11
HLA-A*03:01	1	55	63	9		55.97	0.22
HLA-A*68:01	1	55	63	9		56	0.49
HLA-B*15:01	1	234	243	10	YQEVEGEVAF	12.41	0.06
HLA-A*02:06	1	234	243	10		78.47	0.7

Allegenicity and antigenicity of these epitopes was checked by using AllerTop and Vexijen Tools respectively which reveals about the protein to be useful for making vaccine if it is a probable antigen and non-allergen [43]. If antigenicity score of the epitopes is greater than 0.5000 than it is called probable antigen that have ability to fight against diseases.

Table 2. Predicted epitopes of MHC II along with their sequence, ic50 value, and adjusted rank

Allele	Seq_Num	Start	End	Length	Core_peptide	Epitopes	ic50	Rank
HLA-DRB1*01:01	1	147	161	15	CEVIGATIT	FLQICEVIGATITWH	46.3	15
HLA-DRB1*01:01	1	146	160	15		LFLQICEVIGATITW	51	16
HLA-DRB1*01:01	1	148	162	15		LQICEVIGATITWHP	65.1	20
HLA-DRB1*01:01	1	149	163	15		QICEVIGATITWHPE	88.5	24
HLA-DRB4*01:01	1	95	109	15	DLFKIEMDA	HQDLFKIEMDASQTQ	41.7	2
HLA-DRB4*01:01	1	96	110	15		QDLFKIEMDASQTQL	44.6	2.2
HLA-DRB4*01:01	1	94	108	15		AHQDLFKIEMDASQT	50.1	2.6
HLA-DRB4*01:01	1	93	107	15		PAHQDLFKIEMDASQ	65.8	3.6
HLA-DRB1*04:01	1	96	110	15	FKIEMDASQ	QDLFKIEMDASQTQL	51.1	1.8
HLA-DRB1*04:01	1	97	111	15		DLFKIEMDASQTQLL	51.6	1.8

Allele	Seq_Num	Start	End	Length	Core_peptide	Epitopes	ic50	Rank
HLA-DRB1*04:01	1	95	109	15		HQDLFKIEMDASQTQ	67.2	2.6
HLA-DRB1*07:01	1	10	24	15	LNETRLAHL	HQNYTLNETRLAHLL	48.6	5.7
HLA-DRB1*07:01	1	9	23	15		NHQNYTLNETRLAHL	59.1	7
HLA-DRB1*07:01	1	11	25	15		QNYTLNETRLAHLLS	61	7.2
HLA-DRB1*07:01	1	12	26	15		NYTLNETRLAHLLSA	84.2	9.6
HLA-DRB1*13:02	1	125	139	15	LNTSDNVVV	QDILNTSDNVVVESM	27.7	3.7
HLA-DRB1*13:02	1	126	140	15		DILNTSDNVVVESMS	58.1	6.8
HLA-DRB5*01:01	1	162	176	15	LQGSVSTLR	PELLQGSVSTLRKEV	64.6	9
HLA-DRB5*01:01	1	163	177	15		ELLQGSVSTLRKEVT	69.7	9.5
HLA-DRB5*01:01	1	161	175	15		HPELLQGSVSTLRKE	86.7	12
HLA-DRB1*11:01	1	53	67	15	LYAIIHGRG	LEVLYAIIHGRGPGE	88.8	8.1
HLA-DRB1*11:01	1	54	68	15		EVLYAIIHGRGPGEP	89.1	8.2
HLA-DRB1*11:01	1	52	66	15		ALEVLYAIIHGRGPG	98.2	8.7
HLA-DRB1*03:01	1	283	297	15	MFIDVILER	KNKMFIDVILERIYL	27	0.92
HLA-DRB1*03:01	1	282	296	15		HKNKMFIDVILERIY	30.2	1.1
HLA-DRB1*03:01	1	284	298	15		NKMFIDVILERIYLA	33.9	1.2
HLA-DRB1*03:01	1	281	295	15		YHKNKMFIDVILERI	42.9	1.7
HLA-DRB1*03:01	1	285	299	15		KMFIDVILERIYLAH	46.8	1.9
HLA-DRB1*03:01	1	280	294	15		GYHKNKMFIDVILER	87.5	3.7
HLA-DPA1*03:01/DPB1*04:02	1	283	297	15		KNKMFIDVILERIYL	28.2	0.53
HLA-DPA1*03:01/DPB1*04:02	1	284	298	15		NKMFIDVILERIYLA	28.2	0.53
HLA-DPA1*03:01/DPB1*04:02	1	282	296	15		HKNKMFIDVILERIY	31.4	0.67
HLA-DPA1*03:01/DPB1*04:02	1	285	299	15		KMFIDVILERIYLAH	34.4	0.84
HLA-DPA1*03:01/DPB1*04:02	1	281	295	15		YHKNKMFIDVILERI	40.2	1.2
HLA-DPA1*02:01/DPB1*01:01	1	281	295	15		YHKNKMFIDVILERI	50.3	0.47
HLA-DPA1*02:01/DPB1*01:01	1	282	296	15		HKNKMFIDVILERIY	51	0.51
HLA-DPA1*02:01/DPB1*01:01	1	283	297	15		KNKMFIDVILERIYL	51.1	0.51
HLA-DPA1*02:01/DPB1*01:01	1	284	298	15		NKMFIDVILERIYLA	65.9	0.84
HLA-DPA1*02:01/DPB1*01:01	1	285	299	15		KMFIDVILERIYLAH	91.4	1.7
HLA-DPA1*03:01/DPB1*04:02	1	12	26	15	TLNETRLAH	NYTLNETRLAHLLSA	91.5	4
HLA-DPA1*02:01/DPB1*01:01	1	11	25	15		QNYTLNETRLAHLLS	79.3	1.3
HLA-DPA1*02:01/DPB1*01:01	1	12	26	15		NYTLNETRLAHLLSA	92.7	1.7
HLA-DRB4*01:01	1	291	305	15	YLAHEHSLH	ILERIYLAHEHSLHI	89.9	5.3
HLA-DRB4*01:01	1	292	306	15		LERIYLAHEHSLHIG	98.1	5.8

Allele	Seq_Num	Start	End	Length	Core_peptide	Epitopes	ic50	Rank
HLA-DPA1*03:01/DPB1*04:02	1	291	305	15		ILERIYLAHEHSLHI	87.5	3.8
HLA-DRB1*01:01	1	232	246	15	YQEVEGEVA	IGYQEVEGEVAFSMM	82.2	23
HLA-DRB1*01:01	1	231	245	15		KIGYQEVEGEVAFSM	93.4	25
HLA-DQA1*05:01/DQB1*02:01	1	231	245	15		KIGYQEVEGEVAFSM	89.3	2
HLA-DQA1*05:01/DQB1*02:01	1	232	246	15		IGYQEVEGEVAFSMM	91.6	2.1

All the epitopes are selected on the basis of their antigenicity using Vexijen server. These epitopes are further checked by the tools to find if they are toxic or may cause allergen to the body. MHC I epitopes and MHC II epitopes are non-allergen and non-toxic [44]. If the vaccine has allergenicity then the epitopes of the vaccine cannot be used because they can also produce harmful effects to the human body when taken.

3.2 Population coverage of the predicted epitopes worldwide:

The population coverage tool provides three different metrics: the average number of epitope hits, the minimum number of epitope hits, and the projected population coverage. The predicted epitopes showed a population coverage potential of 83.75% for MHC class I and 63.36% for MHC class II worldwide. Additionally, the average number of epitope hits was 1.83 for MHC class I and 0.88 for MHC class II. This population coverage analysis was conducted because MHC class I and II alleles specifically bind to the predicted epitopes from the protein used in vaccine construction [45].

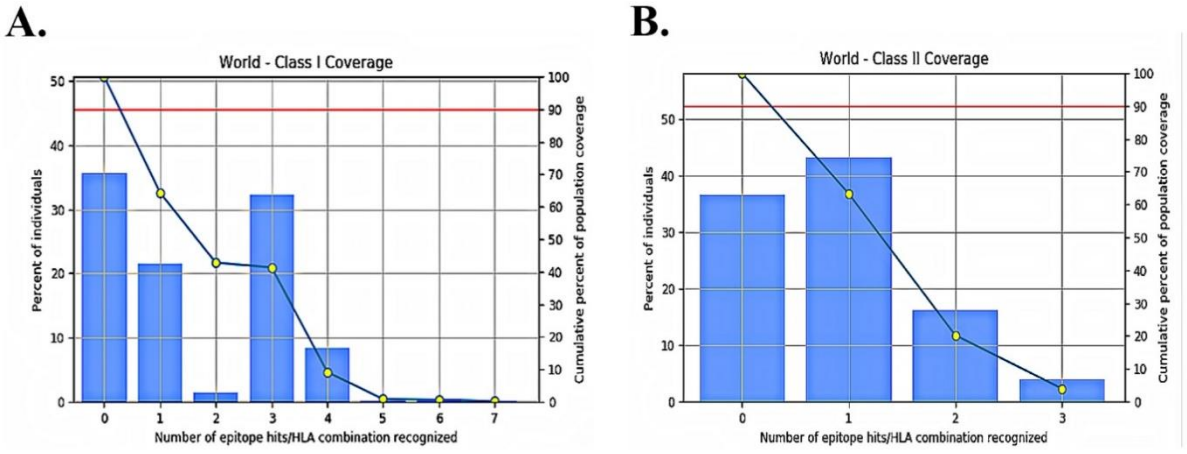

Figure 2. Graphical representation of the population coverage in the world (A) Population coverage of World-Class I is shown along with its number of epitope hits (B) Population coverage of World-Class II is shown along with its number of epitope hits

3.3 Vaccine Construction using epitopes obtained from SopD protein:

The mRNA vaccine construct was proposed to be arranged in the form starting from N-terminal to C-terminal in the following order: A 50s ribosomal adjuvant-EAAAKlinker-GRGPGEPGEMEVNVEDMS-VVESMSREERO-MMRPAEAPDHQLVEWQDSLTENEKS-TDLKSGSLP-CPGPGlinker-CEVIGATITW-FSMMHPCISY-IEMDASQTQL-KVRDHFRSEK-MFIDVILER-QLFLQICEV-VLYAIIHGR-YQEVEGEVAF-AAYlinker-CEVIGATIT-DLFKIEMDA-FKIEMDASQ-LNETRLAHL-LNTSDNVVVLQGSVSTLR-TLNETRLAH-YLAHEHSLH-YQEVEGEVA-HHHHH tag.

3.4 Evaluation of toxicity, solubility and physiochemical properties of the vaccine construct:

To assess the toxicity of the vaccine construct, the computational tool ToxinPred server was utilized which is shown in the **Table 3.** It also unveiled about the molecular weight, its charge, hydrophobicity, hydropathicity and mutation position in each linker and predicted epitopes [44]. The result explained that there is no mutation, and all the peptide sequences are non-toxin. Solubility score of the vaccine construct was 0.617 (towards green color) which indicates its soluble expression in *E.coli*. Therefore, we can use it as vaccine for the protection of disease enteric fever.

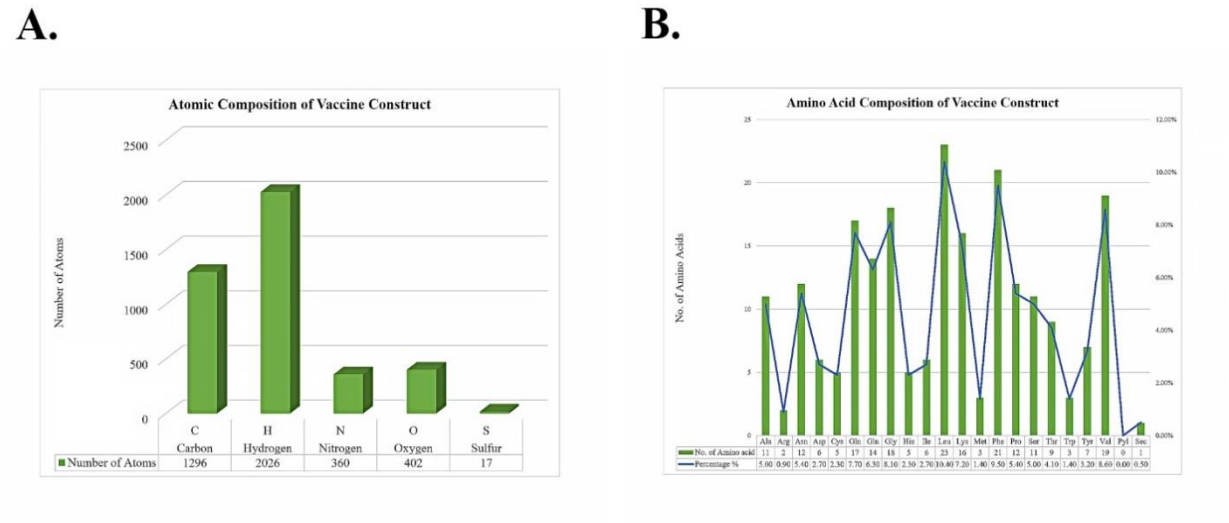

Figure 3. (A) The figure explains about graphical representation of atomic number present in the vaccine construct (B) The figure shows the bar graph of amino acids composition of vaccine construct shows the highest number of amino acids present in it is Glutamic acid having 11.10 % for its composition

The physiochemical parameters were explained by utilizing Protparam tool of Expasy [31]. These parameters revealed that the number of amino acids in vaccine construct is 261, the molecular weight is 29627.53, Theoretical pI is 4.97 and have Grand average of hydropathicity (GRAVY) is -0.264. It contains 4101 atoms in its composition and hydrogen is most abundant in it [46].

The composition of atoms in protein SopD obtained from *S. enterica* sequence shows that the hydrogen atoms are more than the other atoms in the protein structure. According to this compositional analysis, number of atoms of Carbon (C), Hydrogen (H), Nitrogen (N), Oxygen (O), and Sulfur (S) are 1296, 2026, 360, 402, and 17 respectively as shown in **Figure 3**. Vaccine construct

prepared by using SopD protein of *S. enterica* is a combination of 261 amino acids which are as follow, Ala, Arg, Asn, Asp, Cys, Gln, Glw, Gly, His, Ile, Leu, Lys, Met, Phe, Tro, Ser, Trp, Tyr, Bal, Pyl, and Sec.

Table 3. Toxicity prediction of the vaccine construct SopD obtained from *S. enterica*

Peptide Sequence	SVM score	Prediction	Hydrophobicity	Hydropathicity	Hydrophilicity	Charge	Mol wt
EAAAK	-0.93	Non-Toxin	-0.19	-0.4	0.9	0	488.59
GRGPGEPGEMEVNVEDMS	-1.05	Non-Toxin	-0.21	-1.05	0.72	-4	1890.3
VVESMSREERQ	-0.67	Non-Toxin	-0.48	-1.3	1.05	-1	1349.6
MMRPAEAPDHQLVEWQDSLTENEKS	-1.88	Non-Toxin	-0.28	-1.21	0.49	-3.5	2942.6
TDLKSGSLP	-1.14	Non-Toxin	-0.15	-0.46	0.29	0	917.15
CPGPG	-0.74	Non-Toxin	0.04	-0.3	-0.2	0	429.55
CEVIGATITW	-0.51	Non-Toxin	0.18	1.13	-0.78	-1	1092.4
FSMMHPCISY	-0.14	Non-Toxin	0.09	0.59	-1.01	0.5	1215.6
IEMDASQTQL	-1.42	Non-Toxin	-0.14	-0.35	0.09	-2	1135.4
KVRDHFRSEK	-1.24	Non-Toxin	-0.66	-2.08	1.38	2.5	1301.6
MFIDVILER	-1.22	Non-Toxin	0.03	1.13	-0.19	-1	1135.5
QLFLQICEV	-0.55	Non-Toxin	0.11	1.23	-0.78	-1	1092.5
VLYAIIHGR	-0.92	Non-Toxin	0.09	1.04	-0.8	1.5	1041.4
YQEVEGEVAF	-0.92	Non-Toxin	-0.04	-0.27	0.09	-3	1170.4
AAY	-0.84	Non-Toxin	0.17	0.77	-1.1	0	323.37
CEVIGATIT	-0.49	Non-Toxin	0.16	1.36	-0.49	-1	906.19
DLFKIEMDA	-0.81	Non-Toxin	-0.09	0.04	0.46	-2	1081.4
FKIEMDASQ	-0.97	Non-Toxin	-0.17	-0.47	0.38	-1	1068.3
LNETRLAHL	-0.8	Non-Toxin	-0.2	-0.24	-0.07	0.5	1066.4
LNTSDNVVV	-0.94	Non-Toxin	-0.03	0.49	-0.33	-1	960.18
LQGSVSTLR	-1.11	Non-Toxin	-0.15	0.12	-0.19	1	960.23
LYAIIHGRG	-0.86	Non-Toxin	0.05	0.53	-0.63	1.5	999.32
MFIDVILER	-1.22	Non-Toxin	0.03	1.13	-0.19	-1	1135.5
TLNETRLAH	-1.04	Non-Toxin	-0.27	-0.74	0.09	0.5	1054.3
YLAHEHSLH	-0.92	Non-Toxin	-0.08	-0.64	-0.51	0.5	1106.3
YQEVEGEVA	-0.85	Non-Toxin	-0.12	-0.61	0.38	-3	1023.2

3.5 Secondary structure prediction of the vaccine construct:

The prediction of secondary structure is usually authentic and is based on the consensus from PsiPred in **Figure 4.** Its cartoonic two dimensional structure shows the confidence level of the protein structure predicted and showed α-helix, β-sheets and coils in the structure [32]. The secondary structure of the protein has alpha sheets, beta helix and coils that provide shape and structure to the protein.

PsiPred tool reveals that the structure obtained for this protein have good confidence on the basis of its amino acid sequence. In the **figure 4**, straight line shows coils, yellow bars show alpha strands while pink bars show beta helix in the secondary structure of the protein SopD obtained from the bacteria *S. enterica*.

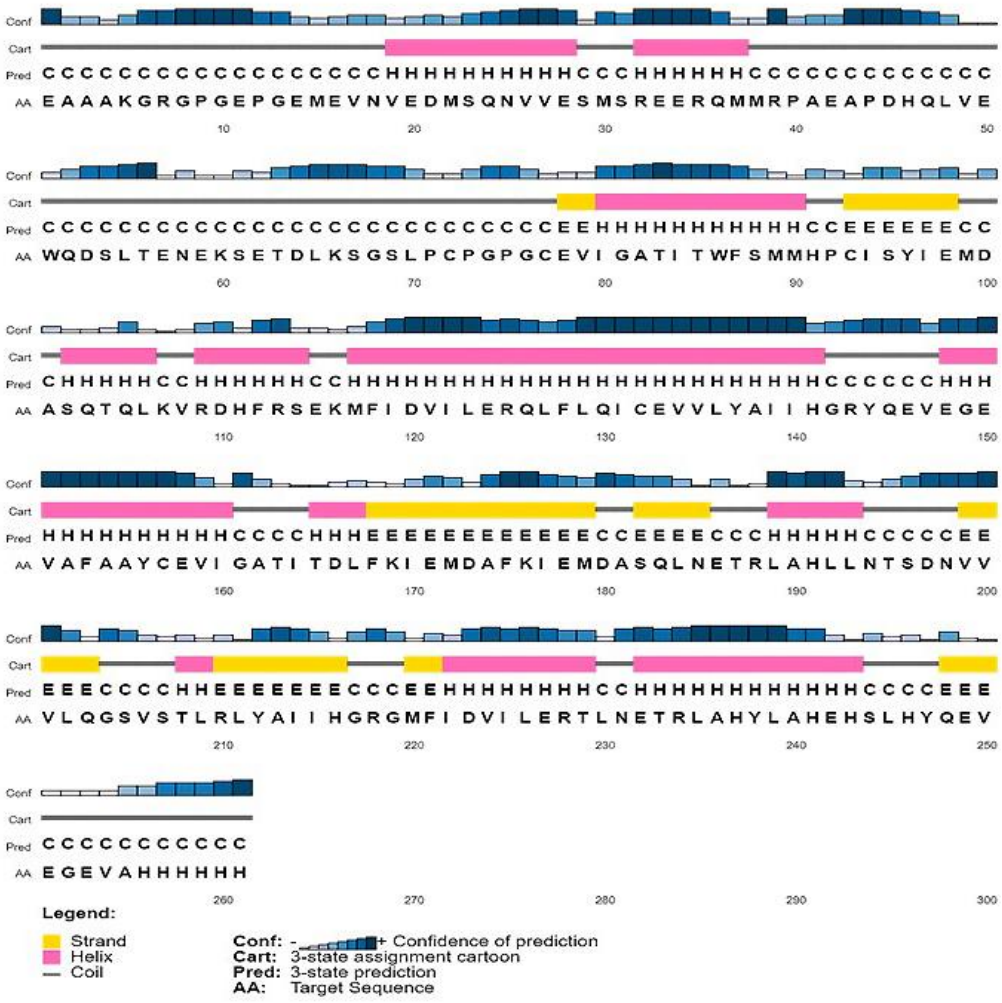

Figure 4. The figure shows the predicted cartoon secondary structure along with its confidence score for vaccine construct

3.6 Tertiary structure prediction and its validation in the vaccine construct:

The tertiary structure (3D) structure of the vaccine construct was also predicted using online computation tool known as 3D pro which predicts the structure on the basis of homology modelling [47].

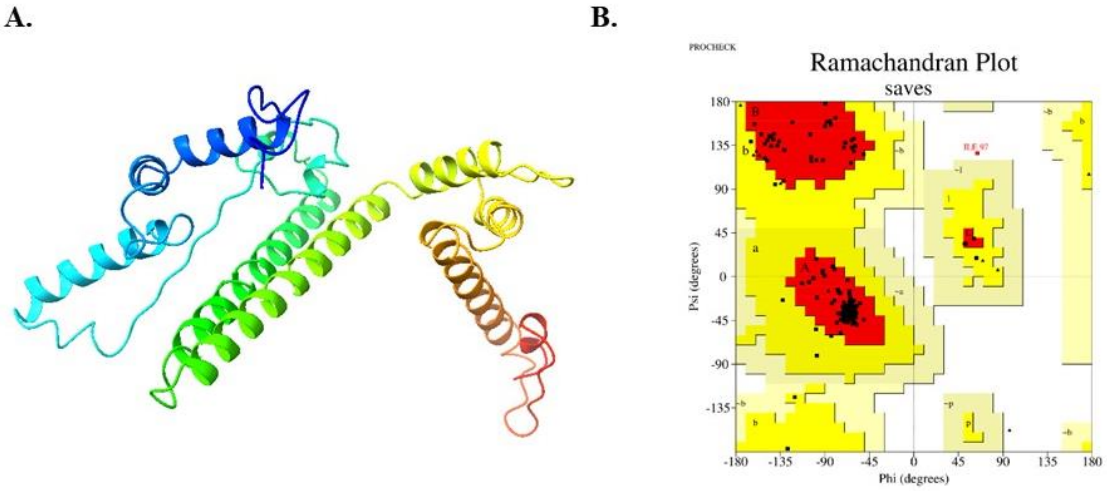

Figure 5. (A) Cartoon presentation of Three-dimensional modeled structures using trRosseta server (B) Ramachandran plot constructed based on Psi (degree) and Phi (degree) after being refined using GalaxyWEB server

The predicted structure is refined by utilizing GalaxyWEB (https://galaxy.seoklab.org/) [48]. The tool used for refinement showed 5 top refined structures that had better results as compared to the initial one.

The favored region in the Ramachandran plot was increased from 91.1% to 95.8%, residues in additional allowed regions were 4.2%, and residues in disallowed regions were only 0.4%. Its clash score was also reduced from 159.4 to 19.0. The poor rotamers of the structure also reduced to 0.9 which is shown in **Table 4**. Ramachandran plot after refinement, explained that the three dimensional structure of vaccine construct is valid because most of its residues are present in the favored region [49].

Table 4. Summary of structure refinement of initial 3D dimensional structure and 5 refined models

Model	GDT-HA	RMSD	MolProbity	Clash score	Poor rotamers	Rama favored
Initial	1.0000	0.000	3.825	159.4	7.1	91.1
MODEL 1	0.8841	0.576	2.070	19.0	0.9	95.8
MODEL 2	0.8812	0.558	2.082	18.3	0.9	95.4
MODEL 3	0.8956	0.534	2.093	18.8	0.9	95.4
MODEL 4	0.9004	0.525	2.027	17.1	0.4	95.8
MODEL 5	0.8784	0.585	2.130	16.4	1.3	95.4

3.7 Vaccine construct and suitable ligand docking:

HDock server was utilized for the docking of the vaccine construct. In docking a receptor and ligand is utilized It showed docking with top 10 models out of which model 1 was selected for further research [34]. Models generated after docking should have docking score very low [50]. Model 1 had docking score -318.45 with 0.9667 confidence score and ligand root mean square deviation (RMSD) 83.91 which is selected for further simulation and validation is explained in **Table 5**.

Table 5. Summary of the top 10 models obtained using HDock server

Rank	1	2	3	4	5	6	7	8	9	10
Docking Score	-325.6	-323.5	-321.2	-319.7	-313.6	-312.5	-311.6	-309.4	-308.4	-299.99
Confidence Score	0.971	0.969	0.968	0.967	0.9635	0.9627	0.9621	0.9604	0.9596	0.9525
Ligand rmsd (Å)	54.0	64.5	51.8	67.0	93.85	61.74	62.38	73.92	67.56	80.46
Interface residues	model_1	model_2	model_3	model_4	model_5	model_6	model_7	model_8	model_9	model_10

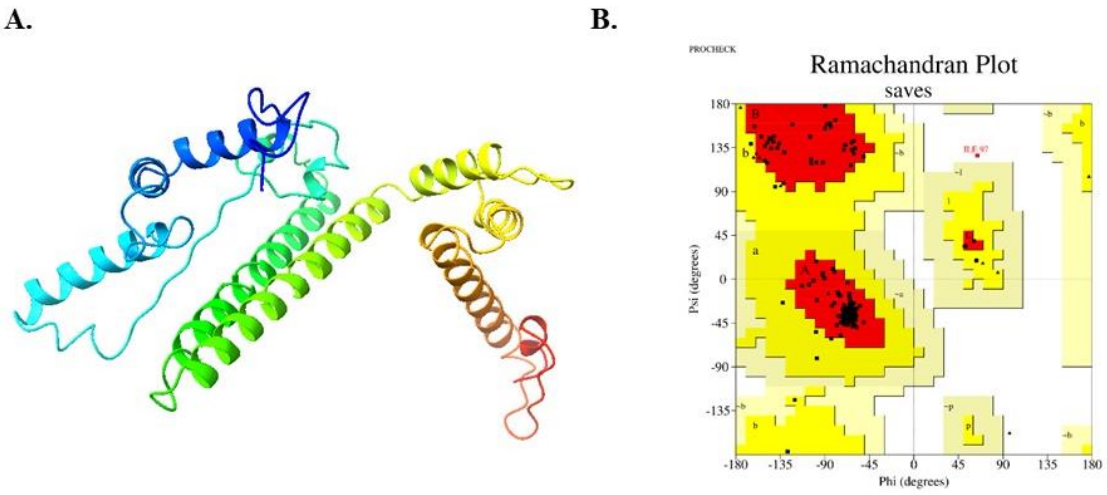

Figure 6. (A) Cartoon structure obtained from HDock and visualized by ChimeraX (B) Surface structure obtained from HDock by the docking analysis of receptor and ligand

The resultant cartoon and surface structure of vaccine construct of SopD protein and ligand that is utilized in the docking using HDock server [51], the structure which is represented in yellow color in our vaccine construct obtained from utilization of SopD protein of *S. enterica* is shown in the **Figure 5**.

3.8 Protein in water simulation of vaccine construct:

The **Figure 7** explain about the water simulation of the vaccine construct on the basis of its radius of gyration, Root mean square deviation RMSD, hydrogen bonding, RMSD fluctuations, and solvent accessible surface. Simlab webserver was utilized for this protein in water simulation [35].

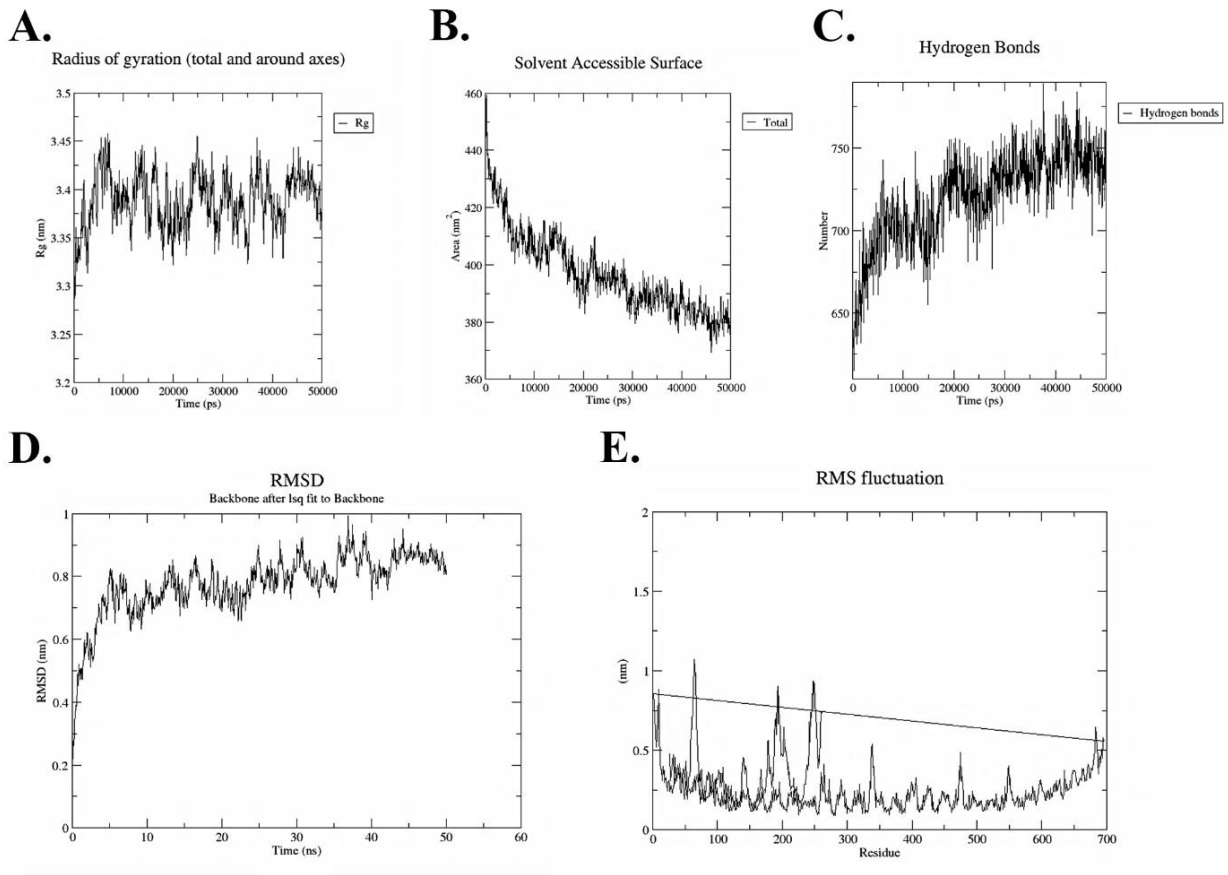

Figure 8. The figure explains graphical representation of protein in water simulation (A) Graphical representation of the Radius of gyration with respect to time (B) Area of solvent accessible surface (C) Number of hydrogen bonds obtained in water simulation (D) Graphical representation of Root mean square deviation (RMSD) w.r.t time (ns) (E) Fluctuations of root mean square along with the residues

3.9 Visualization of predicted epitopes in the vaccine construct:

Ellipro tool was utilized to visualize the antibody predicted epitopes which were present in A or B chain of the mRNA vaccine-SopD. These epitopes are visualized in yellow color in the **Figure 9**.

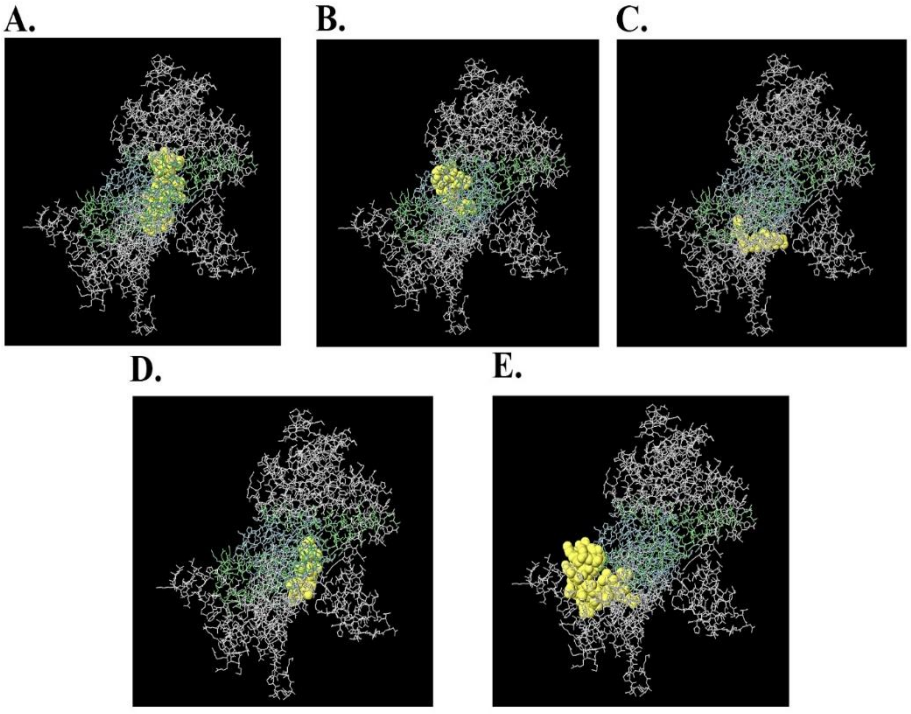

Figure 9. The figure contains the graphical representation of the discontinuous epitopes constructed from the Ellipro server.

1.1 Analysis of receptor-ligand interaction in vaccine-SopD:

Receptor and ligand both are examined using the PDBsum Web which provide comprehensive explanation of its interactions on the basis of bonding and chains. This server showed that ligand which is interaction is GNP. Furthermore, the interacting chains are joined by lines drawn by different colors having salt bridges and hydrogen bonding between them. Every color represents its specific interaction with the other one [52].

3.10 Codon optimization of the vaccine construct:

The vaccine construct was in the form of amino acids, which the EMBOSS server transformed into a nucleotide sequence [53]. Codon optimization tools were used to improve the mRNA vaccine construct's translation within host cells. The vaccine sequence was optimized using the JCat Codon Optimization tool (G.S.) to ensure effective expression in human cells. It was discovered that in order to ensure effective expression in the human host, the ideal percentage of G.C. content should be between 30 and 70%. As a result of codon optimization, the GC content of the nucleotide sequence was increased to 66.28% and improved DNA sequence is obtained.

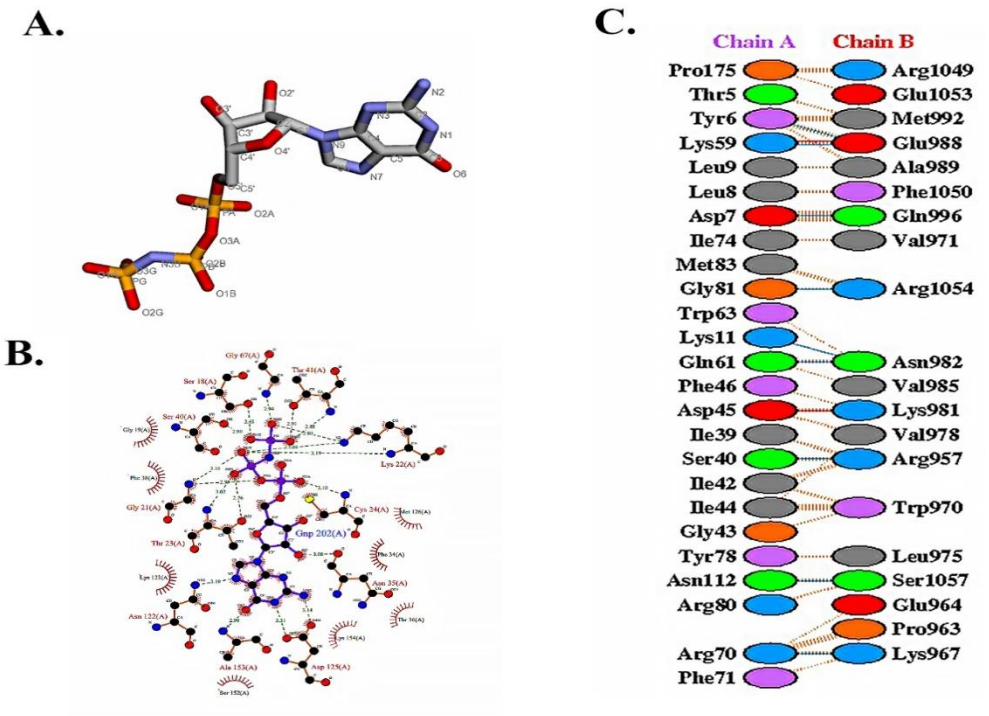

Figure 10. The figure explains about (A) Structure of ligand GNL (B) Interaction of ligand GNL with the other amino acids (C) Receptor-ligand interaction using PDBsum Webserver

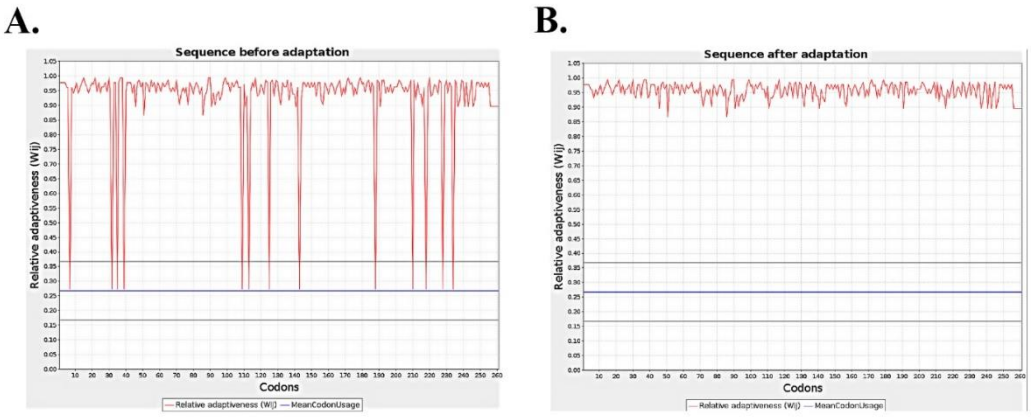

Figure 11. (A) Graphical representation of sequence before adaptation (B) Sequence after adaptation by using JCat codon optimization tool.

3.11 Prediction of the secondary structure of the mRNA constructed vaccine:

The RNAfold server was used to predict the structure of the mRNA vaccine construct. The optimized codons of the construct were used as input, and the free energies of the structure were assessed using the server. These findings suggest that the mRNA vaccine construct can be efficiently manufactured and is structurally stable, potentially enhancing its efficacy as a vaccine.

According to the predicted structure of mRNA, the free energy of the thermodynamic ensemble was -335.79 Kcal/mol, ensemble diversity is 229.65, and free energy of centroid secondary structure was -203.32 Kcal/mol.

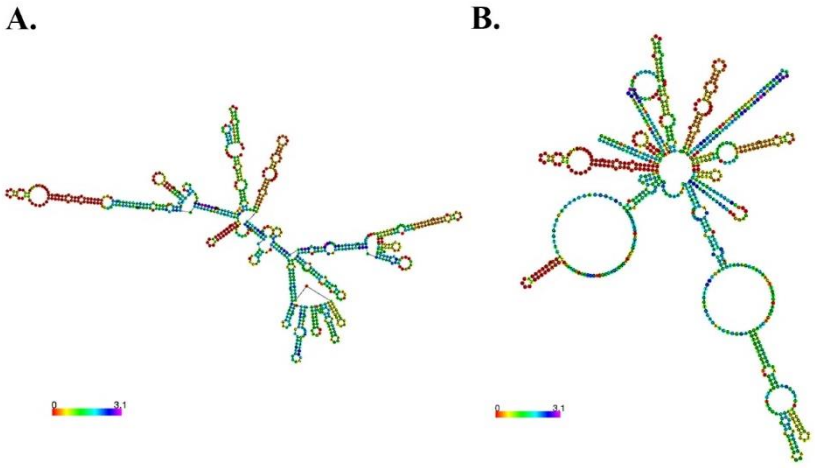

Figure 12. The figure explains mRNA vaccine structure (A) MFE optimal secondary structure (B) centroid secondary structure of the vaccine mRNA retrieved using RNAfold webserver

3.12 In silico immune response simulation against vaccine:

C-immsim tool was utilized which showed the immunoglobin production after antigen injection, B-cell population and T-cell population in the immune response [41]. Immune simulation of the vaccine-SopD is shown in the form of graphs in **Figure 13**. In this research study, administration of three vaccine injection was done for the stimulation of immune response. The second and third administered injections elicited higher immune responses in comparison to the primary injection. Immunoglobin M levels in the simulation were higher than immunoglobin G levels. Formation of memory and isotype switching to the B-cell population were also examined, in presence with the persisting B-cell isotypes for a longer duration. In addition to increase in MHC-I and MHC-II with generation of memory was also examined. Furthermore, macrophage activity was modified.

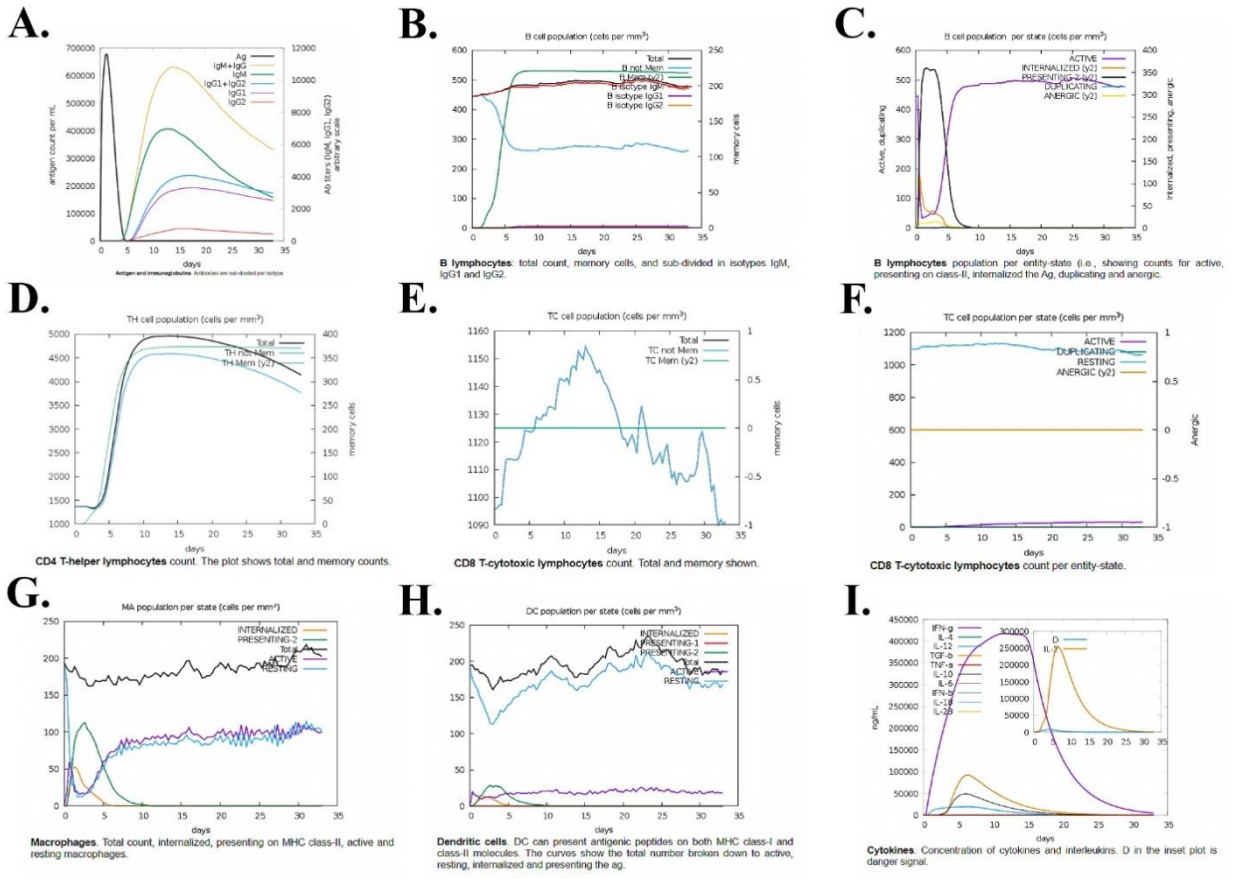

Figure 13. In silico immune simulation against the mRNA vaccine retrieved from the C-ImmSim server (https://kraken.iac.rm.cnr.it/C-IMMSIM/). (A) Production of immunoglobin after injection of antigen (B) The B-cell population after 3 different injections (C) The B-cell population at each state (D) The helper T-cell population after 3 different injections (E) The helper T-cell population at each state (F) The cytotoxic T-cell population at each state (G) Macrophage population at each state (H) Dendritic cell population at each state (I) Cytokine and interleukin production with immune response Simpson Index

1.2 Cloning of the mRNA vaccine construct:

SnapGene software was utilized for this purpose in which the vaccine construct DNA fragment and vector (pET-28a) was attached together using restriction sites [54]. The product obtained after cloning was of 3894 bps which is shown in **Figure**

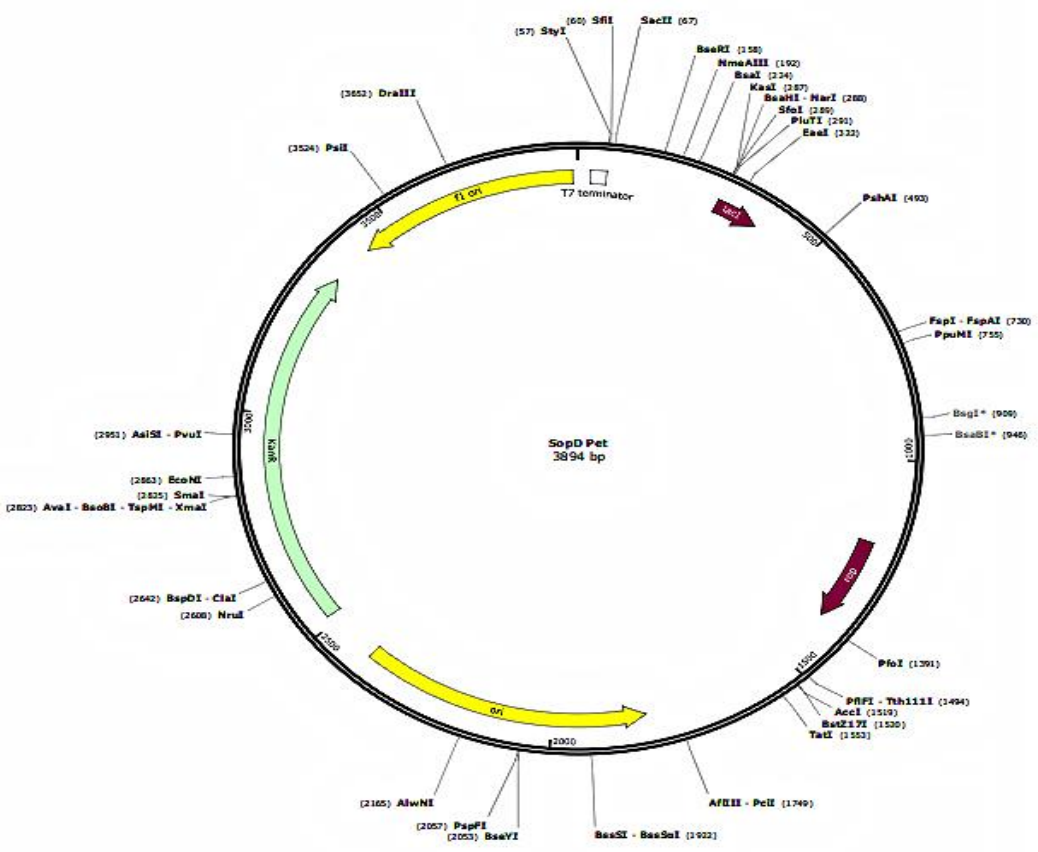

Figure 14. Cloned vaccine construct having 3894 bps with f1 origin, T7 terminator, lac operator, and promoter region.

4 DISCUSSION

Salmonella enterica is a challenging pathogen that can be used for the development of efficient vaccine because of its ability of antibiotic resistance. Many studies are being done on the production of antibiotics, but they are not much efficient for use, and some does not support till date. Various factors are responsible for the production of *S. enterica* vaccine which includes a large variety of serotypes that work as a barrier in the production of a powerful vaccine [55]. In the treatment of bacterial infection caused by *S. enterica* both innate and adaptive immune responses play crucial role. Various vaccines are also designed for the poultry to make the chicken less contaminated and resulting in the reduction of food borne diseases that are harmful for human health [56].

In present time, Commercially there are variety of vaccines that are available for chickens which include killed vaccines, live attenuated vaccines, as well as subunit vaccines that can reduce the risk of causing disease [57]. For human use, different vaccines were designed and got rejected because of their high incidence of local reactions and were considered unsafe for public use. However, there are two vaccines that have been developed in the last 15 years and are considered safe for the use against typhoid fever. First vaccine was parental capsular polysaccharide vaccine, and the other one was oral live attenuated vaccine. Both of these are not only licensed and have been used for immunizing against enteric fever successfully but they may have complications as well [58].

To reduce these complications, scientists need to

develop more effective vaccines to face the challenge of this critical health issue. A novel mRNA vaccine is developed by utilization of immunoinformatic approaches that is efficient, modified and safe. This messenger RNA vaccine is proved to be more efficient and effective against different viral and bacterial infections. Currently, various clinical human trials are conducting worldwide, these trials for mRNA vaccines are now the indication of safe and effective alternative of the variety of therapies which are in the form of vaccination.

One of the advantages of mRNA-based vaccine is its ability for accumulation of antigen selected in the cytoplasm which targets pathogen and triggers an immune response against it. This approach for the development of vaccine may offer variety of advantages over conventional vaccine strategies which include the quick and rapid development, improved efficiency, and easy production [59].

In this study, a novel mRNA multi epitope vaccine which is in silico based, has been proposed to fight against the infection and enteric fever caused by *S. enterica*. The vaccine is proposed on the basis of proteins that contribute in the binding of cell and bacterium attachment in *S. enterica* [60]. Furthermore, this approach offer solution to the challenges that occur due to the enteric fever, and relatively further research and study is needed for the safety and evaluation of this multi epitope mRNA vaccine. For the identification of target epitopes web-based tools like IEDB databases are utilized, which can predict epitopes of B-cell, MHC-I and MHC-II based on the determination of immune epitopes. The epitopes are then further evaluated by the utilization of web servers for the determination of antigenicity, allergenicity, and their toxicity. Only those epitopes were further examined that were antigens, non-allergen, and non-toxic. Moreover, specific linkers were also used for combining the epitopes.

For further refinement of the vaccine design, conduction of immune simulation was done to validate responses of the vaccine. Targeted epitopes of the vaccine construct had 19 corresponding MHC alleles. Furthermore, it is necessary to understand that vaccine may be not effective in those individuals with a specific or particular allele which has ability to bind with the epitope. For this reason, prediction of population coverage in the world for proposed design using IEDB tool revealed that this vaccine would cover 83.75 % of the world's overall population on the basis of alleles and epitopes obtained and was considered to be widely effective vaccine [28, 61]. As, docking interaction is necessary, the vaccine construct that resulted by the linkage of epitopes was later subjected to molecular docking analysis. This docking analysis was done with the help of Toll-like receptor TLR3 by the computational tool known as HDock to ensure the maximum efficacy of vaccine design [51]. The outcomes of molecular docking showed strong binding affinity between the epitopes and their alleles of MHC-I and MHC-II that indicated the efficacy of the designed vaccine.

Moreover, a variety of computational tools were used for the prediction and evaluation of epitopes and further MD simulation in which RMSD and RMSF parameters were evaluated which revealed that vaccine is stable with them and immune simulations were also performed for the validation of safety and effectiveness of the vaccine in which three injections were utilized. Resultant immune simulation of vaccine construct revealed that the vaccine had great ability to stimulate immune response. The results obtained from these tools indicated that all epitopes used in the construction of vaccine were antigenic and non-allergen and can be used for the process of vaccination [43, 62]. Overall, the research provides valuable response into the designing of efficient mRNA vaccine against *S. enterica* and marks the effectiveness and potential of in silico computational approaches for vaccine development.

In future, multivalent mRNA vaccines against multiple enteric fever-causing pathogens should be developed. Furthermore, vaccine and immunotherapies should be investigated. mRNA vaccine may become a better option for the prevention of viral and bacterial infection along

with its related diseases due to the ongoing research, preclinical and clinical trials.

5 CONCLUSION

To sum up the whole discussion, this study provides that mRNA vaccination can be very effective against bacterium *S. enterica* and provides a favorable framework for coming times. However, it is necessary to note that more in vitro along with in vivo studies are important to authenticate the findings for the research taken and to validate and evaluate the potential, safety and limitations of vaccine in worldwide scenarios. Development of successful and effective vaccine against *S. enterica* could have important applications for health of public by reducing infection risk associated with the disease-causing pathogen. The high population coverage prediction and its strong affinity suggest that it may be useful and authentic vaccine to deal with *S. enterica* infections. Altogether, this study marks the computational approaches for vaccine design's potential and provides esteemed insights into the designing of effective mRNA multi-epitope vaccines against *S. enterica*.

ACKNOWLEDGMENT: Especially thankful to my respective supervisor and co. supervisor for providing all the necessary facilities for carrying out this research project.

Conflicts of interest: The authors declare no conflicts of interest

Funding: This study received no external funding

REFERENCES

1. House D., et al. Typhoid fever: pathogenesis and disease. *Current Opin. Infect. Dis.* 2001; 14(5):573-578.
2. Crump J.A., Luby S.P., Mintz E.D. The global burden of typhoid fever. *Bull. World Health Organ.* 2004; 82(5):346-353.
3. Greenaway C., et al. Typhoid: summary of the statement on international travellers and typhoid by the committee to advise on tropical medicine and travel (CATMAT). *Canada Communicable Dis. Rep.* 2014; 40(4):60.
4. Raffatellu M., et al. Clinical pathogenesis of typhoid fever. *J. Infect. Dev. Ctries.* 2008; 2(4):260-266.
5. Bányai K., et al. Viral gastroenteritis. *Lancet* 2018; 392(10142):175-186.
6. Schaefer K., et al. Septicemia due to Listeria monocytogenes infection: A systematic review and meta-analysis. *Foodborne Pathog. Dis.* 2022; 19(2):104-114.
7. Neupane D.P., Dulal H.P., Song J. Enteric fever diagnosis: current challenges and future directions. *Pathogens* 2021; 10(4):410.
8. Wain J., Hosoglu S. The laboratory diagnosis of enteric fever. *J. Infect. Dev. Ctries.* 2008; 2(6):421-425.
9. Azmatullah A., et al. Systematic review of the global epidemiology, clinical and laboratory profile of enteric fever. *J. Glob. Health* 2015; 5(2).
10. Adesegun O.A., et al. Current trends in the epidemiology and management of enteric fever in Africa: a literature review. *Asian Pac. J. Trop. Med.* 2020; 13(5):204-213.
11. Saha T., et al. Enteric fever: diagnostic challenges and the importance of early intervention. *Cureus* 2023; 15(7).
12. Dahiya S., et al. Current antibiotic use in the treatment of enteric fever in children. *Indian J. Med. Res.* 2019; 149(2):263-269.
13. Kuehn R., et al. Treatment of enteric fever (typhoid and paratyphoid fever) with cephalosporins. *Cochrane Database Syst. Rev.* 2022;(11).
14. Parry C.M., et al. What should we be recommending for the treatment of enteric fever? *Open Forum Infect. Dis.* 2023; Oxford University Press US.

15. Qamar F.N., Hussain W., Qureshi S. Salmonellosis including enteric fever. *Pediatr. Clin.* 2022; 69(1):65-77.
16. Soulier A., et al. Engineering a novel bivalent oral vaccine against enteric fever. *Int. J. Mol. Sci.* 2021; 22(6):3287.
17. Masuet-Aumatell C., Atouguia J. Typhoid fever infection–antibiotic resistance and vaccination strategies: A narrative review. *Travel Med. Infect. Dis.* 2021; 40:101946.
18. Knodler L.A., Elfenbein J.R. *Salmonella enterica. Trends Microbiol.* 2019; 27(11):964-965.
19. Andino A., Hanning I. *Salmonella enterica*: survival, colonization, and virulence differences among serovars. *Sci. World J.* 2015; 2015:520179.
20. Brombacher E., et al. Gene expression regulation by the curli activator CsgD protein: modulation of cellulose biosynthesis and control of negative determinants for microbial adhesion. *J. Bacteriol.* 2006; 188(6):2027-2037.
21. Attmannspacher U., Scharf B.E., Harshey R.M. FliL is essential for swarming: motor rotation in absence of FliL fractures the flagellar rod in swarmer cells of *Salmonella enterica. Mol. Microbiol.* 2008; 68(2):328-341.
22. Zaru R., Orchard S., U. Consortium. UniProt tools: BLAST, align, peptide search, and ID mapping. *Curr. Protoc.* 2023; 3(3):e697.
23. Dhanda S.K., et al. IEDB-AR: immune epitope database—analysis resource in 2019. *Nucleic Acids Res.* 2019; 47(W1):W502-W506.
24. Aqsha Z.M., et al. Reverse vaccinology analysis of B-cell epitope against Nipah virus using fusion protein. *Jordan J. Pharm. Sci.* 2023; 16(3):499-507.
25. Kim Y., Sette A., Peters B. Applications for T-cell epitope queries and tools in the Immune Epitope Database and Analysis Resource. *J. Immunol. Methods* 2011; 374(1-2):62-69.
26. Kumar S., Hasija Y. Immunoinformatics tools: a boon in vaccine development against COVID-19. In: *IEEE Delhi Section Conference (DELCON)*. IEEE; 2022.
27. Dimitrov I., Flower D.R., Doytchinova I. AllerTOP—a server for in silico prediction of allergens. In: *BMC Bioinformatics*. Springer; 2013.
28. Fleri W., et al. The immune epitope database and analysis resource in epitope discovery and synthetic vaccine design. *Front. Immunol.* 2017; 8:2503.
29. Gupta S., et al. In silico approach for predicting toxicity of peptides and proteins. *PLoS One* 2013; 8(9):e73957.
30. Rajendhiran N., Bhattacharyya S. Preparation and evaluation of nanolipid carriers of bedaquiline—in vitro evaluation and in silico prediction. *Jordan J. Pharm. Sci.* 2024; 17(3):450-467.
31. Gasteiger E., et al. Protein identification and analysis tools on the ExPASy server. Springer; 2005.
32. McGuffin L.J., Bryson K., Jones D.T. The PSIPRED protein structure prediction server. *Bioinformatics* 2000; 16(4):404-405.
33. Dym O., Eisenberg D., Yeates T. ERRAT. 2012.
34. Yan Y., et al. The HDOCK server for integrated protein–protein docking. *Nat. Protoc.* 2020; 15(5):1829-1852.
35. Tarantola S., Becker W. SIMLAB software for uncertainty and sensitivity analysis. In: Ghanem R., Higdon D., Owhadi H., editors. *Handbook of Uncertainty Quantification*. 2016; p. 1979-1999.
36. Ponomarenko J., et al. ElliPro: a new structure-based tool for the prediction of antibody epitopes. *BMC Bioinformatics* 2008; 9:1-8.
37. Laskowski R.A., et al. PDBsum: structural summaries of PDB entries. *Protein Sci.* 2018; 27(1):129-134.
38. Laskowski R.A., et al. PDBsum: a web-based database of summaries and analyses of all PDB structures. *Trends Biochem. Sci.* 1997; 22(12):488-490.
39. Grote A., et al. JCat: a novel tool to adapt codon usage of a target gene to its potential expression host. *Nucleic Acids Res.* 2005; 33(suppl_2):W526-W531.
40. Taneda A., Sato K. A web server for designing molecular switches composed of two interacting RNAs. *Int. J. Mol. Sci.* 2021; 22(5):2720.

41. Castiglione F., Bernaschi M. C-immsim: playing with the immune response. In: Proceedings of the Sixteenth International Symposium on Mathematical Theory of Networks and Systems (MTNS2004). Katholieke Universiteit Leuven, Belgium; 2004.
42. Consortium U. UniProt: a hub for protein information. *Nucleic Acids Res.* 2015; 43(D1):D204-D212.
43. Doytchinova I.A., Flower D.R. VaxiJen: a server for prediction of protective antigens, tumour antigens and subunit vaccines. *BMC Bioinformatics* 2007; 8:1-7.
44. Rathore A.S., et al. ToxinPred 3.0: an improved method for predicting the toxicity of peptides. *bioRxiv* 2023; 2023.08.11.552911.
45. Bui H.-H., et al. Predicting population coverage of T-cell epitope-based diagnostics and vaccines. *BMC Bioinformatics* 2006; 7:1-5.
46. Babnigg G., Joachimiak A. Predicting protein crystallization propensity from protein sequence. *J. Struct. Funct. Genomics* 2010; 11:71-80.
47. Teng D., et al. 3DPro: querying complex three-dimensional data with progressive compression and refinement. In: *Advances in Database Technology: Proceedings of the International Conference on Extending Database Technology*. NIH Public Access; 2022.
48. Ko J., et al. GalaxyWEB server for protein structure prediction and refinement. *Nucleic Acids Res.* 2012; 40(W1):W294-W297.
49. Sheik S., et al. Ramachandran plot on the web. *Bioinformatics* 2002; 18(11):1548-1549.
50. Maslov O., et al. Evaluation of anti-inflammatory, antioxidant activities and molecular docking analysis of *Rubus idaeus* leaf extract. *Jordan J. Pharm. Sci.* 2024; 17(1):105-122.
51. Yan Y., et al. HDOCK: a web server for protein–protein and protein–DNA/RNA docking based on a hybrid strategy. *Nucleic Acids Res.* 2017; 45(W1):W365-W373.
52. Laskowski R.A. PDBsum: summaries and analyses of PDB structures. *Nucleic Acids Res.* 2001; 29(1):221-222.
53. Olson S.A. EMBOSS opens up sequence analysis. *Brief. Bioinform.* 2002; 3(1):87-91.
54. Al-Kanany F.N., Othman R.M. Cloning and expression of *Pseudomonas aeruginosa* AlkB gene in *E. coli*. *J. Pure Appl. Microbiol.* 2020; 14(1).
55. Hegazy W.A.H., Hensel M. *Salmonella enterica* as a vaccine carrier. *Future Microbiol.* 2012; 7(1):111-127.
56. Crouch C.F., et al. Safety and efficacy of a novel inactivated trivalent *Salmonella enterica* vaccine in chickens. *Vaccine* 2020; 38(43):6741-6750.
57. Wisner A.L., et al. Immunization of chickens with *Salmonella enterica* subspecies enterica serovar Enteritidis pathogenicity island-2 proteins. *Vet. Microbiol.* 2011; 153(3-4):274-284.
58. Garmory H.S., Brown K.A., Titball R.W. *Salmonella* vaccines for use in humans: present and future perspectives. *FEMS Microbiol. Rev.* 2002; 26(4):339-353.
59. Jawalagatti V., Kirthika P., Lee J.H. Oral mRNA vaccines against infectious diseases—A bacterial perspective. *Front. Immunol.* 2022; 13:884862.
60. Abadi M.H.J.N., et al. In silico design and immunoinformatics analysis of a chimeric vaccine construct based on *Salmonella* pathogenesis factors. *Microb. Pathog.* 2023; 180:106130.
61. Oyarzun P., Kobe B. Computer-aided design of T-cell epitope-based vaccines: addressing population coverage. *Int. J. Immunogenet.* 2015; 42(5):313-321.
62. Mallik B., Morikis D. Applications of molecular dynamics simulations in immunology: a useful computational method in aiding vaccine design. *Curr. Proteomics* 2006; 3(4):259-270.

تطوير لقاح mRNA مبتكر باستخدام الحاسوب باستخدام عدة أنماط من بروتين SopD للحمى المعوية التي تسببها السالمونيلا المعوية

آئزة ممتاز [1]*، محمد عمير [1]، هادية حسين [1]، وصلة علي [1]، محمد ساجد [1]

[1] قسم التكنولوجيا الحيوية، جامعة أوكارا، باكستان.

ملخص

أدى تزايد مشكلة مقاومة المضادات الحيوية إلى تحديات في علاج عدوى السالمونيلا المعوية. وبناءً على ذلك، طُوّرت مجموعة متنوعة من اللقاحات كبديل عملي للمضادات الحيوية للوقاية من عدوى السالمونيلا المعوية لدى المرضى. وتشهد تقنية لقاح الرنا المرسال (mRNA) ازديادًا سريعًا في استبدالها بالطرق التقليدية نظرًا لكفاءتها العالية وتكلفتها المنخفضة واستجابتها المناعية الخلطية. يهدف هذا البحث إلى تطوير لقاح جديد قائم على الرنا المرسال (mRNA) باستخدام مناهج المعلوماتية المناعية ضد السالمونيلا المعوية. تم اختيار بروتين SopD والحصول على مستضداته المناسبة. دُرست هذه المستضدات للتحقق مما إذا كانت مستضدات، وغير مسببة للحساسية، وغير سامة. علاوة على ذلك، تم ربط هذه المستضدات باستخدام روابط لتحويلها إلى تركيبة لقاح. خضعت تركيبة اللقاح هذه لمزيد من التحليل، وخضعت للالتحام الجزيئي مع مستقبلات محددة تُعرف باسم مستقبلات Toll-like receptors TLR3 باستخدام خادم HDock. أظهرت محاكاة MD أن اللقاح مستقر مع معايير RMSD وRMSF، وكشفت المحاكاة المناعية للقاح أنه فعال، وتم استنساخه باستخدام أداة SnapGene. في النهاية، تم نمذجة بروتين متعدد النُسَخ وتحسينه. أظهرت النتائج أن تركيبة اللقاح كانت فعالة، وغير مُسببة للحساسية، وغير سامة، وتم استنساخها بنجاح. في النهاية، اتضح من النتائج أن بنية mRNA المُصممة يمكن أن تكون لقاحًا فعالًا وواعدًا للعلاج بعد التحقق من صحتها باستخدام تقنيات مُختبرية مثل ELISA والاختبارات الحيوية باستخدام نماذج حيوانية.

الكلمات الدالة: الحمى المعوية، النمط الظاهري، التهاب المعدة والأمعاء، المكورات العنقودية المعوية، تسمم الدم.

* ***المؤلف المراسل: آئزة ممتاز***

aaizamumtaz07@gmail.com

تاريخ استلام البحث 2024/6/23 وتاريخ قبوله للنشر 2024/8/22.

Jordan Journal of Pharmaceutical Sciences, Volume 18, No. 2, 2025

Single Nucleotide Pleomorphisms of Different Cytokines among Jordanian Patients with Lupus Nephritis: A Pilot Study

Sawsan I. Khdair[1,a]*, Seham Zarour[1], May Almajawleh[1,a], Feras A. Khudeir[2]

[1] Department of Pharmacy, Faculty of Pharmacy, Al-Zaytoonah University of Jordan, Amman, Jordan.
[2] Faculty of Medicine, Jordan University of Science and Technology, Irbid, Jordan.

ABSTRACT

Lupus nephritis (LN) is one of the most common clinical manifestations of systemic lupus erythematosus (SLE) and significantly affects the morbidity and mortality associated with SLE. Both environmental and genetic factors contribute to the development of SLE. There is growing interest in identifying genetic markers, particularly cytokine-related variants, that may indicate susceptibility to SLE, predict future organ involvement, and monitor changes in disease activity. This study aims to examine a wide array of cytokine genetic variants and their association with LN in a cohort of 83 Jordanian samples. Genotyping was performed using the Polymerase Chain Reaction/Sequence Specific Primer (PCR/SSP) technique. Our results show an increased frequency of the G allele at the promoter region (-1082 A/G) of interleukin-10 (IL-10) in LN samples ($p = 0.001$) compared to controls, whereas the A allele predominated in the control group ($p = 0.001$). At the genotype level for the -1082 A/G promoter region of IL-10, the GG genotype was significantly associated with LN ($p < 0.001$), while the GA genotype predominated in controls ($p = 0.027$). No significant associations were observed between other cytokine SNPs (IFN-γ, IL-6, TNF-α) and LN in Jordanian SLE patients. Our pilot study suggests that the G allele and GG genotype at the IL-10 promoter region (-1082 A/G) increase the risk of developing LN in Jordanian SLE patients, while the A allele and GA genotype are more common in controls.

Keywords: lupus nephritis, cytokines, SNPs, Jordan.

INTRODUCTION

The autoimmune disease known as systemic lupus erythematosus (SLE) is heterogeneous, inflammatory, and characterized by excessive synthesis of autoantibodies against a variety of auto-antigens, primarily nuclear components, and the creation of immune complexes [1, 2]. SLE, which can cause symptoms like nephritis, leukopenia, arthritis, skin rashes, and neurological inflammation, is nine times more common in women than in men [3, 4]. As with other inflammatory autoimmune diseases, the exact etiology of SLE remains mysterious. But, environmental, epigenetic, and genetic factors are believed to be crucial in its development[5, 6, 7]. Genome-wide association studies (GWAS) have significantly improved our comprehension of the inherent origins of SLE over the past ten years [8]. Approximately one hundred SLE genetic loci have been found thus far, predominantly in Asian and European populations, and they can explain up to 3 percent of the heritability of SLE [9]. The human leukocyte antigen (HLA), specifically HLA class II genes, have by far the highest link with vulnerability to SLE [10, 11]. In addition, a recent study conducted among Jordanian SLE patients showed that the class II alleles of HLA

[a] have equal contribution
[*]Corresponding author: Sawsan I. Khdair
sawsan.khdair@zuj.edu.jo
Received: 26/6/2024 Accepted: 22/8/2024.
DOI: https://doi.org/10.35516/jjps.v18i2.2833

namely DRB1: *0301 and *1501 and DQB1*0601 elevated the risk of developing SLE [12]. Moreover, several meta-analysis studies and review articles encompassing studies across diverse populations and ethnicities support the implication of different cytokines in the pathogenesis of SLE. These cytokines play pivotal roles as mediators of inflammatory and immune responses and are associated with various levels of cytokines produced, being as high, intermediate, or low [2, 13-16]. While the genes responsible for producing these cytokines differ, multiple studies have highlighted the notable influence of single nucleotide pleomorphisms (SNPs) in diverse cytokines on predisposition to SLE. Notably, interleukin-6 (IL-6) and tumor necrosis factor-alpha (TNF-α) are pro-inflammatory cytokines that have a fundamental role in regulating humoral and cellular responses, in which both play an essential role in inflammation [14, 17-19]. In addition, several studies showed that SNPs of interleukin-10 (IL-10) which have immunosuppressive properties, along with SNPs of interferon-γ (IFN-γ), both are key T helper-1 cytokines involved in immune cell activation [13, 20-24].

Lupus nephritis (LN), a severe and prevalent clinical feature of SLE that reached 50.4% in Arab countries including Jordan, as well as for African Americans, Hispanics, and Europeans LN was estimated to reach 68.9%, 60.6%, and 29.1% respectively[25-27]. Our study aims to examine a wide array of cytokine SNPs among Jordanian LN patients in the promoter areas of the following cytokine DNA segment: TNF-α (−308 A/G) (rs1800629) and IL-6 (−174 G/C) (rs1800795), three polymorphic regions of IL-10: (−1082 A/G) (rs1800896), (−819 C/T) (rs1800871) and (−592 A/C) (rs1800872), as well as IFN-γ +874 (rs62559044) in comparison with healthy controls.

Sample collection

A total of eighty-three individuals took part in this study, 39 LN patients (36 females, 3 males,) and 44 healthy controls (27 females, 17 males) (Figure 1). All the patients were Jordanians who were enrolled at the Jordan University Hospital in Amman with IRB approval number (146/2021). As well as the control group was collected from Al-Zaytoonah University Health Center with IRB approval number (4/2/2020-2021). The patients diagnosed with LN had a mean age of 25.15 with a standard deviation (SD) of ±10.78 years, while the control group had a mean age of 24.25 with SD ± 6.15 years. The inclusion criteria for all participants were as follows: they had to be between the ages of 22 and 50, all participants had to be of Jordanian nationality with no relative degree among them. In this study, healthy volunteers with a family member affected by SLE or any other autoimmune disorder were excluded. However, patients with SLE and LN were selected based on the standards outlined by the American College of Rheumatology (ACR) [28]. Following the volunteer's agreement by signing a consent document, 3 ml of blood was gathered using EDTA tubes.

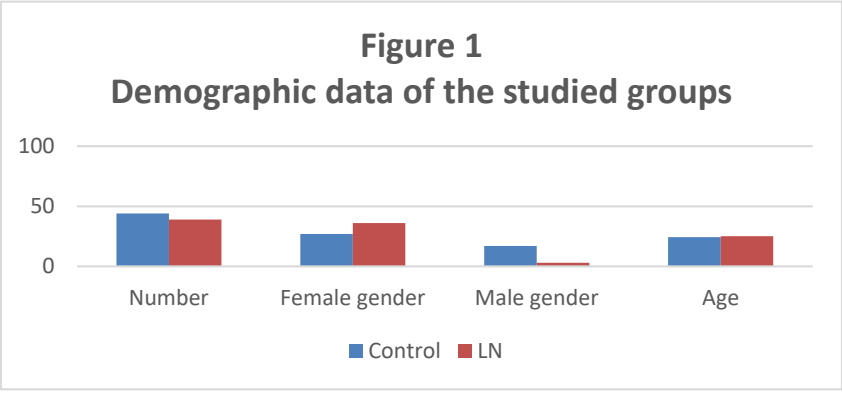

DNA extraction and cytokine SNPs genotyping

After collecting a three-milliliter complete blood sample, the DNA was extracted by the Wizard® Genomic DNA extraction Kit by Promega, USA, according to the previously outlined protocol [29]. The cytokine SNPs detection of IL-6 (−174G/C), TNF-α (−308A/G), three polymorphic regions of IL-10: (−1082A/G), (−819C/T), (−592A/C), and IFN-γ (+874) was carried out through polymerase chain reaction/sequence-specific primers (PCR/SSP) technique of One Lambda, USA Genotyping Tray following the manufactures' protocol.

Statistical analysis

The Statistical Package for Social Sciences (SPSS) program (IBM SPSS Statistics 22, USA) was used for statistical analysis of the data in the current study. Alleles, genotypes, and haplotypes frequency were calculated according to the rate of recurrence of each allele, genotype, and haplotype among the total number of alleles, genotypes, and haplotypes for each SNPs loci, and the categorical variables were presented as frequency (%). Cross-tabulation analysis was used evaluate the link among various cytokines alleles, genotypes and haplotypes and LN in comparison to controls. Statistical significance within the two studied groups was calculated by using Chi-square (X^2) test with P-value less than 0.05[30].

To assess the variables linked to LN, a two-step binary regression analysis (LN vs. control) was used to estimate the 95% Confidence Interval (CI) odds and ratio (OR). Genotypes for TNF-*α*, IL-6, IFN-γ, and IL-10 were used as independent factors in the regressions. Results were considered significant if the P value was less than 0.05.

Results

TNF-α (-308A/G) gene pleomorphism

The TNF-α (-308A/G) allele and genotype occurrences are shown in Table 1 for both the control and LN patient groups. The results showed that the frequency of the G allele was 78.4% in the control group while 88.5% in LN patients without any statistical significance. The frequency of A allele was 21.6% and 11.5% among control group and LN patients respectively. Additionally, at the genotype level, the most frequent genotype was GG with frequency of 63.6% and 82.1% among control group and LN patients respectively, followed by GA genotype with frequency of 29.5% and 12.8% among control group and LN patients respectively. Overall, the TNF-α (-308A/G) allele and genotype polymorphisms did not vary significantly between the two groups (Table 1).

Table 1: The allele and genotype occurrence of the TNF-α (-308A/G) SNPs.

TNF-α (-308A/G) SNPs			
Allele	**Control N=88 (Frequency %)**	**LN N=78 (Frequency %)**	**P Value**
G	69 (78.4%)	69 (88.5%)	ref
A	19 (21.6%)	9 (11.5%)	0.084
Genotype	N=44 (Frequency %)	N=39 (Frequency %)	
G/G	28 (63.6%)	32 (82.1%)	0.061
G/A	13 (29.5%)	5 (12.8%)	0.065
A/A	3 (6.8%)	2 (5.1%)	0.747

N: Number, LN: lupus Nephritis, (P value <0.05).

IL-6 (-174 G/C) gene pleomorphisms

The IL-6 (-174 G/C) allele and genotype occurrences are shown in Table 2 for both the control and LN patient groups. The results showed that the frequency of the G allele was 79.5% in the control group and 80.8% in LN patients without any statistical significance. While the frequency of C allele was 20.5% and 19.2% among control group and LN patients respectively. Additionally, at the

genotype level, the most frequent genotype was GG with frequency of 68.2% and 76.9% among control group and LN patients respectively. Our findings revealed that the occurrence of allele and genotype polymorphisms of the promotor IL-6 (-174 G/C) did not significantly vary between the LN and control groups. (Table 2).

Table 2: The allele and genotype occurrence of IL-6 (-174 G/C) SNPs.

FIL-6 (-174 G/C) SNPs			
Allele	**Control N=88 (Frequency %)**	**LN N=78 (Frequency %)**	**P Value**
G	70 (79.5%)	63 (80.8%)	ref
C	18 (20.5%)	15 (19.2%)	0.844
Genotype	N=44 (Frequency %)	N=39 (Frequency %)	
G/G	30 (68.2%)	30 (76.9%)	0.375
G/C	10 (22.7%)	3 (7.7%)	0.060
C/C	4 (9.1%)	6 (15.4%)	0.379

N: Number, LN: lupus Nephritis, (P value <0.05).

IFN-γ (+874 T/A) gene pleomorphisms

The **IFN-γ (+874 T/A)** allele and genotype occurrences are shown in Table 3 for both the control and LN patient groups. The results showed that the frequency of the T allele was 58% in the control group and 69.2% in LN patients while the frequency of the A allele was 42% and 30.8% among control group and LN patients, respectively. While at the genotype level, the most frequent genotype was TT with frequency of 34.1% and 51.3% among control group and LN patients respectively, followed by TA genotype with frequency of 47.7% and 35.9% among control group and LN patients respectively. Our results show that the two groups did not differ significantly at the allele or genotype level of the IFN-γ +874 T/A polymorphisms (Table 3).

Table 3: The allele and genotype occurrence of IFN-γ (+874 T/A) SNPs.

IFN-γ (+874 T/A) SNPs			
Allele	**Control N=88 (Frequency %)**	**LN N=78 (Frequency %)**	**P Value**
			Control-LN
T	51 (58%)	54 (69.2%)	ref
A	37 (42%)	24 (30.8%)	0.133
Genotype	N=44 (Frequency %)	N=39 (Frequency %)	
T/T	15 (34.1%)	20 (51.3%)	0.113
T/A	21 (47.7%)	14 (35.9%)	0.276
A/A	8 (18.2%)	5 (12.8%)	0.502

N: Number, LN: lupus Nephritis, (P value <0.05).

IL-10 gene pleomorphisms

The three SNPs promoter regions for IL-10, namely (-1082 A/G), (-819 C/T), and (-592 A/C), exhibit genotype and allele frequencies, as presented in Table 4. Our findings showed a significant difference in IL-10 allele frequency at -1082 G to A region between the control group and LN patients. With a frequency of (61.8%) in LN compared to controls (34.1%) and a P value (P<0.001), the occurrence of IL-10-1082 G allele was noticed in LN patients rather than in controls. In contrast, the IL-10 (-1082 A) allele variants were more predominant in controls, with a frequency of (65.9%) compared to LN (38.2%) and a P value (P<0.001). Furthermore, concerning the genotype level of IL-10 position -1082, our findings

revealed a statistically significant variation in the occurrence of the G/G genotype, which was found to be in frequency of 52.6%) in LN as opposed to a frequency of 13.6%) in the control group with a P value of (P<0.001), and the G/A genotype, which was found to be in frequency of 18.4% in LN as opposed to a frequency of (40.9%) in the control group with a P value of (P=0.02). Conversely, no differences were observed between the LN and control group in the allele and genotype occurrence of IL-10 at the two positions (-819 C/T, -592 A/C).

Additionally, there were noticeable changes in the genotype frequencies of IL-10 (-1082 AG, -819 CT, -592 AC), the genotype GCC/GCC was more frequent in LN (52.6%) in comparison to the control group (13.6%) with P value (P<0.001), and GCC/ACC was more commonly observed in the control group (25%) compared to LN (2.6%) with P value (P=0.027) (Table 4). As well as, our results revealed a significant difference at the haplotype level between controls and LN patients in IL10 GCC to be predominate in LN patients with a frequency of (61.8%) compared to the control group (34.1%) with P value (P<0.001) while the ACC haplotype was found in higher frequency in controls (37.5%) compared with a frequency of (22.4%) LN patients with P value (P=0.036).

Table 4: The allele, genotype, and haplotype occurrence of IL-10 (-1082 A/G), (-819 C/T), (-592 A/C) SNPs.

IL-10: (-1082 A/G), (-819 C/T), (-592 A/C) SNPs			
Allele	**Control N=88 (Frequency %)**	**LN N=76 (Frequency %)**	**P Value Control-LN**
−1082			
G	**30 (34.1%)**	**47 (61.8%)**	**0.001**
A	**58 (65.9%)**	**29 (38.2%)**	**0.001**
−819			
C	63 (71.6%)	64 (84.2%)	0.054
T	25 (28.4%)	12 (15.8%)	0.35
−592			
A	25 (28.4%)	12 (15.8%)	0.054
C	63 (71.6%)	64 (84.2%)	0.054
Genotype	N=44 (Frequency %)	N=38 (Frequency %)	
−1082			
G/G	**6 (13.6%)**	**20 (52.6%)**	**0.001**
G/A	**18 (40.9%)**	**7 (18.4%)**	**0.027**
A/A	20 (45.5%)	11 (28.9%)	0.124
−819			
C/C	26 (59.1%)	28 (73.7%)	0.165
C/T	11 (25%)	8 (21.1%)	0.673
T/T	7 (15.9%)	2 (5.3%)	0.124
−592			
A/A	7 (15.9%)	2 (5.3%)	0.124
C/A	11 (25%)	8 (21.1%)	0.673
C/C	26 (59.1%)	28 (73.7%)	0.165
Genotype	N=44 (Frequency %)	N=38 (Frequency %)	
GCC/GCC	**6 (13.6%)**	**20 (52.6%)**	**0.001**
GCC/ACC	**11 (25%)**	**1 (2.6%)**	**0.004**
GCC/ATA	7 (15.9%)	6 (15.8%)	0.988
ACC/ACC	9 (20.5%)	7 (18.4%)	0.817

IL-10: (-1082 A/G), (-819 C/T), (-592 A/C) SNPs			
Allele	**Control N=88 (Frequency %)**	**LN N=76 (Frequency %)**	**P Value Control-LN**
ACC/ATA	4 (9.1%)	2 (5.3%)	0.507
ATA/ATA	7 (15.9%)	2 (5.3%)	0.124
Haplotype	N=88 (Frequency %)	N=76 (Frequency %)	
GCC	**30 (34.1%)**	**47 (61.8%)**	**0.001**
ACC	**33 (37.5%)**	**17 (22.4%)**	**0.036**
ATA	25 (28.4%)	12 (15.8%)	0.054

N= number, LN: Lupus Nephritis. (P value <0.05).

4.2 Discussion

Systemic lupus erythematosus (SLE) is a complicated autoimmune disorder. Although the precise etiology of SLE is still unknown, it is broadly recognized that both genetic susceptibility and ecological factors are protagonists in disease development [31]. The genetic components of SLE have been clarified by recent research, which has focused in particular on the IL-10 gene and its variations [32]. IL-10 gene, which is located on chromosome number one at the (1q31-1q32) locus is considered an important factor in the pathogenesis of SLE [33]. Research has shown that patients with SLE often exhibit elevated levels of IL-10, which can impact the production of autoantibodies and contribute to disease progression [34]. Indeed, lowering IL-10 expression with focused therapies has shown promise in ameliorating clinical symptoms in SLE patients, highlighting the reputation of IL-10 in the disease process [13].

The IL-10 (-1082 A/G) SNPs is the most genetic variant found in the IL-10 gene that has gained significant attention from researchers[21]. However, different studies have suggested a potential link between the IL-10 (-1082 G) variant and the likelihood of developing SLE [32, 35]. To explain the complexity of genetic factors influencing SLE risk, a meta-analysis found that the IL-10 promoter (-1082 G) variant is associated with SLE in Asian populations but not in Caucasians [34].

Our current study focuses on genetic variations in large panel cytokines among LN patients compared to a control group, investigating the role of cytokine SNPs in LN pathogenesis. This study examined SNPs for: TNF-α (−308A/G), IL-6 (−174G/C), three polymorphic regions of IL-10: (−1082A/G), (−819C/T) and (−592A/C), in addition to IFN-γ (+874 T/A**)** using advanced genotyping techniques. A significant increase in the IL-10 (-1082 G) allele variants was observed in LN patients, indicating a potential genetic susceptibility among Jordanian SLE patients. In contrast, the IL-10 (-1082 A) allele variant was more common in controls, suggesting a protective genetic factor against SLE and LN. Our results are compatible with the results obtained from a meta-analysis study conducted on seventeen populations including Europeans and Asians. The study presented that the IL-10 (-1082 G) allele was associated with both European and Asian SLE patients [25]. In addition, at the genotype level, the IL-10 genotype at the position (-1082 G/G) was linked to LN with (P<0.001), so it may be considered a susceptible genotype for LN development among Jordanian SLE patients; while the IL-10 (-1082 G/A) genotype is thought to be protective, since it was much more common in the control group than in the LN group with (P=0.027). On the other hand, our findings align with the results from diverse populations, including Egyptians, Bulgarians, and Iranians, all of which demonstrated a significant increase in the occurrence of the IL-10 (-1082 G/G) genotype in patients with LN [3, 20, 36]. From the other side, some studies in various ethnic populations (Asians, Europeans, Brazilians and Chinese) showed that IL-10 (-1082 G/A) genotype frequencies are related to SLE development but not LN, since these studies are not linked with any clinical manifestation of SLE disease, while our

study was focused on SLE patients with LN manifestation[21, 32, 37, 38]. Moreover, in this study, the homozygous (GCC/GCC) genotype in the IL-10 promoter region was found to be significantly correlated with LN (P<0.001), whereas the frequency of heterozygous (GCC/ACC) genotype was significantly related to controls (P=0.004), so it may be suggested as a protective genotype since it was much more frequent in the control groups. Additionally, the IL-10 haplotype of ACC was also marked as a protective haplotype (P=0.036), whereas the IL-10 haplotype of GCC is associated with LN disease (P<0.001). Furthermore, consistent with our findings, a study conducted on LN patients demonstrated a link between the GCC haplotype and LN in Iranian and European populations [15, 36]. Notably, associations between specific IL-10 genotypes and haplotypes with LN disease severity further emphasize the intricate genetic landscape underlying SLE pathogenesis. Additionally, our study did not identify significant associations between certain cytokine SNPs (TNF-α, IL-6, IFN-γ) and LN among Jordanian SLE patients, consistent with findings from other populations like Mexican, Thai, and Polish groups [16, 39, 40]. Overall, the results from different ethnicities are debatable but, these collective insights highlight the intricate genetic interplay in LN susceptibility and highpoint. However, these collective insights highlight the intricate genetic interplay in LN susceptibility and highlight the importance of considering diverse populations to unravel the complexities of SLE genetics.

CONCLUSION

This study highlights (for the first time) the link between large panels of cytokine SNPs. Our finding showed that IL-10 (-1082) G allele variants, IL-10 (-1082) GG genotype, homozygous (GCC/GCC) genotype, and IL-10 haplotype of GCC are linked as risk factors for the vulnerability to LN. Therefore, these SNPs might be used as potential predictive markers for early LN risk assessment. It would be simpler for those susceptible to LN to take the required steps to stall the onset of the illness. Additionally, knowing how these cytokines work may help in the development of more potent strategies for treating LN and its related complications. It is also essential to understand the origin and course of LN to diagnose, prevent, intervene with, and manage these conditions. However, additional genetic markers that are considered as potential risk genes for developing LN in Jordanian patients should be examined to uncover all possible risk genes influencing LN pathogenesis.

Declaration of competing interest

The authors confirmed that none of their personal or financial ties could be interpreted as having an impact on the work presented in this paper.

REFERENCES

1. Su, D. L., Lu Z. M., Shen M. N., Li X. and Sun L. Y. Roles of pro- and anti-inflammatory cytokines in the pathogenesis of SLE. *J Biomed Biotechnol.* 2012; 2012: 347141.
2. Goulielmos, G. N., Zervou M. I., Vazgiourakis V. M., Ghodke-Puranik Y., Garyfallos A. and Niewold T. B. The genetics and molecular pathogenesis of systemic lupus erythematosus (SLE) in populations of different ancestry. *Gene.* 2018; 668: 59-72.
3. Talaat, R. M., Alrefaey S. A., Bassyouni I. H., Ashour M. E. and Raouf A. A. Genetic polymorphisms of interleukin 6 and interleukin 10 in Egyptian patients with systemic lupus eythematosus. *Lupus.* 2016; 25(3): 255-64.
4. Davis, L. S., Hutcheson J. and Mohan C. The role of cytokines in the pathogenesis and treatment of systemic lupus erythematosus. *J Interferon Cytokine Res.* 2011; 31(10): 781-9.
5. Alabbadi, Ibrahim, Massad Eman, Taani Nashaat,

Dababneh Safwan, Shersheer Qasem, Nimri Omar, Mahmoud Refqi, Hijazeen Rami and Ishaq Adnan. Exploring the Economic Aspects of β-Thalassemia in Jordan in 2019. *Jordan Journal of Pharmaceutical Sciences.* 2022; 15(3): 390-404.

6. Alhawamdeh, Ebtesam, Bulatova Nailya R., Yousef Al Motassem F., AlAbbadi Mohammed A. and Omer Ethar A. A Cross-sectional Study of the Catalase Genetic Polymorphism (-262 cytosine/ thymine) and Blood Catalase Activity among Jordanian Vitiligo Patients. *Jordan Journal of Pharmaceutical Sciences.* 2023; 16(2): 330-344.
7. Nelson, P., Rylance P., Roden D., Trela M. and Tugnet N. Viruses as potential pathogenic agents in systemic lupus erythematosus. *Lupus.* 2014; 23(6): 596-605.
8. Buniello, A., MacArthur J. A. L., Cerezo M., Harris L. W., Hayhurst J., Malangone C., McMahon A., Morales J., Mountjoy E., Sollis E., Suveges D., Vrousgou O., Whetzel P. L., Amode R., Guillen J. A., Riat H. S., Trevanion S. J., Hall P., Junkins H., Flicek P., Burdett T., Hindorff L. A., Cunningham F. and Parkinson H. The NHGRI-EBI GWAS Catalog of published genome-wide association studies, targeted arrays and summary statistics 201 .*9Nucleic Acids Res.* 2019; 47(D1): D1005-d1012.
9. Kwon, Y. C., Chun S., Kim K. and Mak A. Update on the Genetics of Systemic Lupus Erythematosus: Genome-Wide Association Studies and Beyond. *Cells.* 2019; 8(10).
10. Chai, H. C., Phipps M. E. and Chua K. H. Genetic risk factors of systemic lupus erythematosus in the Malaysian population: a minireview. *Clin Dev Immunol.* 2012; 2012: 963730.
11. Lewis, M. J. and Jawad A. S. The effect of ethnicity and genetic ancestry on the epidemiology, clinical features and outcome of systemic lupus erythematosus. *Rheumatology (Oxford).* 2017; 56(suppl_1): i67-i77.
12. Khdair, S. I., Al-Bdour R., Jarrar W., Hammad A., Al-Jayeh A., Masa'deh M., Adwan M. and Farah R. Immunogenetic Profiling of SLE and LN among Jordanian Patients. *J Pers Med.* 2022; 12(12).
13. López, P., Gutiérrez C. and Suárez A. IL-10 and TNFalpha genotypes in SLE. *J Biomed Biotechnol.* 2010; 2010: 838390.
14. Liu, J., Liao M. Q., Cao D. F., Yang Y., Yang Y., Liu Y. H., Zeng F. F. and Chen X .H. The Association between Interleukin-6 Gene Polymorphisms and Risk of Systemic Lupus Erythematosus: A Meta-analysis with Trial Sequential Analysis. *Immunol Invest.* 2021; 50(2-3): 259-272.
15. Song, G. G., Choi S. J., Ji J. D. and Lee Y. H. Associations between interleukin-10 polymorphisms and susceptibility to systemic lupus erythematosus: a meta-analysis. *Hum Immunol.* 2013; 74(3): 364-70.
16. Paradowska-Gorycka, A., Roszak M., Stypinska B., Lutkowska A., Walczyk M., Olesinska M., Wajda A., Piotrowski P., Puszczewicz M., Majewski D. and Jagodzinski P. P. IL-6 and TGF-β gene polymorphisms, their serum levels, as well as HLA profile, in patients with systemic lupus erythematosus. *Clin Exp Rheumatol.* 2019; 37(6): 963-975.
17. Umare, V. D., Pradhan V. D., Rajadhyaksha A. G., Patwardhan M. M., Ghosh K. and Nadkarni A. H. Impact of TNF-α and LTα gene polymorphisms on genetic susceptibility in Indian SLE patients. *Hum Immunol.* 2017; 78(2): 201-208.
18. Umare, V., Pradhan V., Dadheech S., Rajadhyaksha A., Ghosh K. and Nadkarni A. Cytokine genes multi-locus analysis reveals synergistic influence on genetic susceptibility in Indian SLE - A multifactor-dimensionality reduction approach. *Cytokine.* 2020; 135: 155240.
19. Asano, N. M., Angelo H .D., da Silva H. A., Maia M. M., Lins O. G. and Souza P. E. Interleukin-6 promoter polymorphisms -174 G/C in Brazilian patients with systemic lupus erythematosus. *Hum Immunol.* 2013; 74(9): 1153-6.
20. Manolova, I., Miteva L., Ivanova M., Kundurzhiev T ,. Stoilov R. and Stanilova S. The Synergistic Effect of TNFA and IL10 Promoter Polymorphisms on Genetic

Predisposition to Systemic Lupus Erythematosus. *Genet Test Mol Biomarkers.* 2018; 22(2): 135-140.

21. Yuan, Y., Wang X., Ren L., Kong Y., Bai J. and Yan Y. Associations between interleukin-10 gene polymorphisms and systemic lupus erythematosus risk: a meta-analysis with trial sequential analysis. *Clin Exp Rheumatol.* 2019; 37(2): 242-253.
22. Rosado, S., Rua-Figueroa I., Vargas J. A., Garcia-Laorden M. I., Losada-Fernandez I., Martin-Donaire T., Perez-Chacon G., Rodriguez-Gallego C., Naranjo-Hernandez A., Ojeda-Bruno S., Citores M. J. and Perez-Aciego P. Interleukin-10 promoter polymorphisms in patients with systemic lupus erythematosus from the Canary Islands. *Int J Immunogenet.* 2008; 35(3): 235-42.
23. Hee, Chee Seng, Gun Suk Chyn, Naidu Rakesh, Somnath Sushela Devi and Radhakrishnan Ammu Kutty %J International Journal of Rheumatic Diseases. The relationship between single nucleotide polymorphisms of the interleukin-10 gene promoter in systemic lupus erythematosus patients in Malaysia: a pilot study. 2008; 11(2): 148-154.
24. Lee, Y. H. and Bae S. C. Association between interferon-γ +874 T/A polymorphism and susceptibility to autoimmune diseases: a meta-analysis. *Lupus.* 2016; 25(7): 710-8.
25. Adwan, M. Clinical and Serologic Characteristics of Systemic Lupus Erythematosus in the Arab World: A Pooled Analysis of 3,273 Patients. *Arch Rheumatol.* 2018; 33(4): 455-463.
26. Bastian ,H. M., Roseman J. M., McGwin G., Jr., Alarcón G. S., Friedman A. W., Fessler B. J., Baethge B. A. and Reveille J. D. Systemic lupus erythematosus in three ethnic groups. XII. Risk factors for lupus nephritis after diagnosis. *Lupus.* 2002; 11(3): 152-60.
27. Webber, D., Cao J., Dominguez D., Gladman D. D., Levy D. M., Ng L., Paterson A. D., Touma Z., Urowitz M. B., Wither J. E., Silverman E. D. and Hiraki L. T. Association of systemic lupus erythematosus (SLE) genetic susceptibility loci with lupus nephritis in childhood-onset and adult-onset SLE. *Rheumatology (Oxford).* 2020; 59(1): 90-98.
28. Aringer, M., Costenbader K., Daikh D., Brinks R., Mosca M., Ramsey-Goldman R., Smolen J. S., Wofsy D., Boumpas D. T., Kamen D. L., Jayne D., Cervera R., Costedoat-Chalumeau N., Diamond B., Gladman D. D., Hahn B., Hiepe F., Jacobsen S., Khanna D., Lerstrøm K., Massarotti E., McCune J., Ruiz-Irastorza G., Sanchez-Guerrero J., Schneider M., Urowitz M., Bertsias G., Hoyer B. F., Leuchten N., Tani C., Tedeschi S. K ,.Touma Z., Schmajuk G., Anic B., Assan F., Chan T. M., Clarke A. E., Crow M. K., Czirják L., Doria A., Graninger W., Halda-Kiss B., Hasni S., Izmirly P. M., Jung M., Kumánovics G., Mariette X., Padjen I., Pego-Reigosa J. M., Romero-Diaz J., Rúa-Figueroa Fernández Í, Seror R., Stummvoll G. H., Tanaka Y., Tektonidou M. G., Vasconcelos C., Vital E. M., Wallace D. J., Yavuz S., Meroni P. L., Fritzler M. J., Naden R., Dörner T. and Johnson S. R. 2019 European League Against Rheumatism/American College of Rheumatology classification criteria for systemic lupus erythematosus. *Ann Rheum Dis.* 2019; 78(9): 1151-1159.
29. Jarrar, Y. B. and Ghishan M. The Nudix Hydrolase 15 (NUDT15) Gene Variants among Jordanian Arab Population. *Asian Pac J Cancer Prev.* 2019; 20(3): 801-808.
30. Al-Qerem, Walid, Safar Mohammad, Safar Ibrahim and Al-Ibadah Mahmood. Identifying factors associated with increased rate of mortality of COVID-19 patients among Jordanian population: A multicenter case-controlled retrospective study .*Jordan Journal of Pharmaceutical Sciences.* 2023; 16(2): 483.
31. Ameer, M. A., Chaudhry H., Mushtaq J., Khan O. S., Babar M., Hashim T., Zeb S., Tariq M. A., Patlolla S. R., Ali J., Hashim S. N. and Hashim S. An Overview of Systemic Lupus Erythematosus (SLE) Pathogenesis, Classification, and Management. *Cureus.* 2022; 14(10): e30330.
32. Zhou, M., Ding L., Peng H., Wang B., Huang F., Xu W.

D., Li J. H., Ye X. R., Pan H. F. and Ye D. Q. Association of the interleukin-10 gene polymorphism (-1082A/G (with systemic lupus erythematosus: a meta-analysis. *Lupus.* 2013; 22(2): 128-35.

33. Johanneson, B., Lima G., von Salomé J., Alarcón-Segovia D. and Alarcón-Riquelme M. E. A major susceptibility locus for systemic lupus erythemathosus maps to chromosome 1q31. *Am J Hum Genet.* 2002; 71(5): 1060-71.
34. Nath, S. K., Harley J. B. and Lee Y. H. Polymorphisms of complement receptor 1 and interleukin-10 genes and systemic lupus erythematosus: a meta-analysis. *Hum Genet.* 2005; 118(2): 225-34.
35. Rees ,L. E., Wood N. A., Gillespie K. M., Lai K. N., Gaston K. and Mathieson P. W. The interleukin-10-1082 G/A polymorphism: allele frequency in different populations and functional significance. *Cell Mol Life Sci.* 2002; 59(3): 560-9.
36. Mohammadi, S., Saghaeian Jazi M., Zare Ebrahimabad M., Eghbalpour F., Abdolahi N., Tabarraei A. and Yazdani Y. Interleukin 10 gene promoter polymorphisms (rs1800896, rs1800871 and rs1800872) and haplotypes are associated with the activity of systemic lupus erythematosus and IL10 levels in an Iranian population. *Int J Immunogenet.* 2019; 46(1): 20-30.
37. da Silva, H. D., da Silva A. P., da Silva H. A., Asano N. M., Maia Mde M. and de Souza P. R. Interferon gamma and Interleukin 10 polymorphisms in Brazilian patients with systemic lupus erythematosus. *Mol Biol Rep.* 2014; 41(4): 2493-500.
38. Liu, P., Song J., Su H., Li L., Lu N., Yang R. and Peng Z. IL-10 gene polymorphisms and susceptibility to systemic lupus erythematosus: a meta-analysis. *PLoS One.* 2013; 8(7): e69547.
39. Ramírez-Bello, J., Cadena-Sandoval D., Mendoza-Rincón J. F., Barbosa-Cobos R. E., Sánchez-Muñoz F., Amezcua-Guerra L. M., Sierra-Martínez M. and Jiménez-Morales S. Tumor necrosis factor gene polymorphisms are associated with systemic lupus erythematosus susceptibility or lupus nephritis in Mexican patients. *Immunol Res.* 2018; 66(3): 348-354.
40. Tangwattanachuleeporn, M., Sodsai P., Avihingsanon Y., Wongpiyabovorn J., Wongchinsri J. and Hirankarn N. Association of interferon-gamma gene polymorphism (+874A) with arthritis manifestation in SLE. *Clin Rheumatol.* 2007; 26(11): 1921-4.

تعدد أشكال النوكليوتيدات المفردة للسيتوكاينز المختلفة بين المرضى الأردنيين المصابين بالتهاب الكلية الذئبي: دراسة تجريبية

سوسن خضير[1*] ، سهام زعرور[1]، مي المجاولة[1]، فراس خضير[2]

[1]كلية الصيدلة، قسم الصيدلة، جامعة الزيتونة الأردنية، الأردن

[2] كلية الطب، جامعة العلوم والتكنولوجيا الأردنية، الأردن

ملخص

يعد التهاب الكلية الذئبي (LN)أحد العلامات السريرية الأكثر شيوعًا في مرض الذئبة الحمراء (SLE) وله تأثير ملحوظ على معدلات الامراض والوفيات المرتبطة بمرض الذئبة الحمراء. تشارك العوامل البيئية والوراثية في تطور مرض الذئبة الحمامية. ومع ذلك، هناك اهتمام متزايد بتحديد العلامات الجينية، وخاصة السيتوكينات، التي قد تشير إلى القابلية للإصابة بمرض الذئبة الحمراء، والتنبؤ بدور الأعضاء الوشيكة للإصابة بالمرض، وتتبع التغيرات في نشاط المرض. الهدف من هذه الدراسة هو فحص مجموعة واسعة من المتغيرات الوراثية للسيتوكاينز وارتباطها بالتهاب الكلية الذئبي LN في إجمالي 83 عينة من الأردن. تم إجراء النمط الجيني للسيتوكاينز باستخدام تقنية .(PCR/SSP) تشير نتائجنا إلى وجود زيادة في الشكل الجيني G في النمط الجيني −1082 (A/G لـ IL-10) في عينات مرضى LN (P = 0.001) مقارنة بالأشخاص الأصحاء في حين كان الشكل الجيني A هو السائد (P = 0.001) عند الأشخاص الأصحاء. وعلى مستوى النمط الجيني لمنطقة (−1082 A/G لـ IL-10، ارتبط النمط الجيني GG بـ (P <0.001) LN، بينما النمط الجيني G/A كان هو السائد عند الأشخاص الأصحاء (P = 0.027). علاوة على ذلك، لم تتم ملاحظة أي ارتباطات مهمة في تعدد الأشكال الجينية السيتوكينية الأخرى (IFN-γ، IL-6، TNF-α LN) لدى مرضى التهاب الكلية الذئبي في الأردن. بشكل عام، تشير دراستنا التجريبية إلى أن الشكل الجينيG والنمط الجيني GG في المنطقة (−1082 A/G لـ IL-10 تزيد من خطر الإصابة بالتهاب الكلية الذئبي لدى المرضى الأردنيين المصابين بمرض الذئبة الحمامية. بينما تسود المتغيرات A والنمط الوراثي GA عند الأشخاص الأصحاء.

الكلمات الدالة: التهاب الكلية الذئبي، السيتوكاينز، الأردن.

[*] ***المؤلف المراسل: سوسن خضير***

sawsan.khdair@zuj.edu.jo

تاريخ استلام البحث 2024/6/26 وتاريخ قبوله للنشر 2024/8/22.

Jordan Journal of Pharmaceutical Sciences, Volume 18, No. 2, 2025

Pre treatment Neutrophil to Lymphocyte Ratio and Total Cholesterol Levels as Biomarkers for Breast Cancer

Razan Hasan[1]*, Nader Abdalla[2], Maram Bilal[1]

[1]Department of biochemistry and microbiology, Faculty of pharmacy, Tishreen University, Lattakia, Syria
[2]Department of oncology, Faculty of medicine, Tishreen University, Lattakia, Syria

ABSTRACT

Background: Breast cancer is one of the most common cancers worldwide. The effectiveness of treatment in different breast cancer types depends on clinicopathological characteristics. Several factors can influence tumor aggressiveness, with the neutrophil-to-lymphocyte ratio (NLR) and total cholesterol (TC) being among the most prevalent. Due to the limited number of studies evaluating the relationship between these markers and tumor stage, this study aimed to investigate the role of NLR and total cholesterol as biomarkers in relation to breast cancer stage.

Methods: We evaluated 101 newly diagnosed breast cancer patients and analyzed NLR and total cholesterol (TC) in relation to clinicopathological parameters, based on cut-off values determined using the Receiver Operating Characteristic (ROC) curve.

Results: Breast cancer stage was significantly associated with NLR, total cholesterol, neutrophil count, and white blood cell (WBC) count ($p < 0.05$). Based on tumor stage, cut-off values were determined to be 2 for NLR and 194 mg/dL for total cholesterol, considering the optimal points of sensitivity and specificity from the ROC curve. Higher NLR was significantly associated with increased tumor size ($p = 0.004$) and lymph node metastasis ($p = 0.021$). Higher total cholesterol was associated with increased BMI ($p = 0.002$), tumor size ($p = 0.04$), lymph node metastasis ($p = 0.001$), and tumor grade ($p = 0.013$). Additionally, higher NLR was significantly associated with increased total cholesterol levels ($p = 0.004$).

Conclusions: Pretreatment NLR and total cholesterol may serve as useful predictors of breast cancer stage. Elevated levels of NLR and total cholesterol were associated with more advanced tumor characteristics. Further large-scale studies are recommended to explore their association with survival and recurrence rates.

Keywords: breast cancer, NLR, total cholesterol.

INTRODUCTION

Breast cancer is considered one of the most common cancers among women around the world [1],[2]. It is estimated that about 2.3 million cases were diagnosed worldwide in 2020, especially in industrial countries, with an increasing number of new cases diagnosed globally [3],[4]. It occurs and develops due to various factors including genetic and environmental factors. Many associated risk factors such as hormonal, physiological, and nutritional factors are related to lifestyle [4]. Clinical outcomes in breast cancer differ significantly from one patient to another depending on several variables and clinicopathological factors [5],[6]. According to different studies, the impairment in inflammatory response plays a crucial role in tumor development. For this purpose, many markers can reflect the systemic inflammatory response. One of these markers is neutrophils to lymphocytes ratio

***Corresponding author: Razan Hasan**
razanhasan98@gmail.com
Received: 22/8/2024 Accepted: 18/7/2024.
DOI: https://doi.org/10.35516/jjps.v18i2.2989

(NLR) [7]. Recent studies evaluated the NLR correlation with clinical characteristics among breast cancer patients such as(stage, grade, tumor size, and metastasis…) and they reported equivocal results with many findings showing no correlation, while others indicated a positive relationship [8],[9]. several tumor- derived molecules affect inflammatory cells in the tumor microenvironment; Cholesterol and its metabolites are common examples [10]. Many studies reported that serum total cholesterol was a risk factor for breast cancer. These studies demonstrated that its metabolite 27Hydroxy cholesterol (27HC) is important in tumor progression and metastasis [11],[12]. The relationship between NLR and total cholesterol levels among breast cancer patients was assessed by Dominguez *et al.* ; they found a significant statistical correlation between NLR values and total cholesterol levels.[13]

NLR and total cholesterol (TC) are inexpensive, affordable, and widely applicable in clinical practice. However, due to the shortage of studies evaluating the association between the previous markers and breast cancer stage in Syria, we aimed in this study to assess the pretreatment NLR and total cholesterol. We also evaluated their relationship with some clinicopathological parameters such as (grade, tumor size, lymph node metastasis, distant metastasis, hormonal receptors, histological and molecular subtypes) in a group of breast cancer patients using optimal cutoff values determined depending on tumor stage. This can help us predict breast cancer progression.

Materials And Methods

This study was conducted at Tishreen University Hospital (TUH) in Lattakia City, Syria from December 2022 to January 2024. It was confirmed by the institution's ethics board of Tishreen University and formal acceptance was obtained from all participants.

Study design and exclusion criteria:

This study evaluated 101 newly diagnosed breast cancer patients before receiving any treatment, who were admitted to the chemotherapy and radiotherapy center at TUH. All patients' complete demographical, medical, and pathological data were ensured before including them in the study sample. Clinical stages were classified into early stage (1-2) and advanced stage (3-4) [14].

We excluded patients with infections or inflammatory diseases, autoimmune diseases, steroid administration, and statin therapy.

Analytical methods:

Venous blood samples were assembled from each participant. A Complete blood count (CBC) was performed using an auto hematology analyzer to obtain the absolute count of white blood cells, neutrophils and lymphocytes. NLR ratio was determined by dividing the absolute neutrophil count by the absolute lymphocyte count. While total cholesterol was measured using the enzymatic method by Mindray BS-380 analyzer (China), serum total cholesterol less than 200mg/dl was considered normal.

Statistical analysis:

The study was tested using the statistical package for social science (SPSS V22). The Kolmogrov Smirnov test (KS-test) determined the normality of distribution. Data were introduced as mean± standard deviation for continuous variables and percentages for categorical variables.

Student *t*-test and Mann Whitney test were used for comparing means between two groups depending on variables' distribution and the Chi-square or Fisher exact test was used for categorical data. Cut-off points for the two variables were determined using the ROC curve (receiver operating characteristic curve) by considering the sensitivity and specificity value. A P-value less than 0.05 was considered statistically significant.

Results:

1- Patient characteristics:

The study included 101 breast cancer patients divided according to tumor stage into early stage 1-2 (48 patients)

and advanced stage 3-4 (53 patients).The patients were staged clinically according to tumor, node, and metastasis (TNM) staging issued by the American Joint Committee on Cancer (AJCC), 8th edition [15].

There were no significant differences in age, menopause, BMI, and tumor grade between the two groups. However, when comparing the hematological parameters and total cholesterol, we found that both groups differ significantly in WBC count (p=0.016), neutrophil count (p=0.003), NLR(p=0.001) and serum total cholesterol (p=0.001) whereas there was no significant difference in lymphocyte count(p>0.05).

Table 1 compares early and advanced-stage groups' demographical, pathological, and hematological parameters.

Table1: Patients characteristics and blood parameters according to tumor stage

characteristic	**Early(n=48)**	**Advanced(n=53)**	**p-value**
Age(years)	49.73±9.55	53.72±12.73	0.076
Menopause(%)			
Premenopause	22(45.8%)	18(34%)	0.22
Postmenopause	26(54.2%)	35(66%)	
BMI(%)			
Normal weight(<25kg/m²)	18(37.5%)	15(28.3%)	
Over-weight(25-29.9 kg/m²)	19(39.6%)	24(45.3%)	
Obesity(≥30kg/m²)	11(22.9%)	14(26.4%)	0.61
Grade(%)			
Grade1	5(10.4%)	4(7.5%)	
Grade2	29(60.4%)	21(39.7%)	0.054
Grade3	14(29.2%)	28(52.8%)	
Blood parameters			
White blood cells(10^6/µl)	7.01±1.97	7.89±2.27	**0.016***
Neutrophils(10^6/µl)	4.35±1.42	5.31±1.86	**0.003***
Lymphocytes(10^6/µl)	2.24±0.77	2.13±0.84	0.21
NLR	1.90±0.59	2.77±1.26	**0.001***
Total cholesterol(mg/dl)	170±31.02	219±47.15	**0.001***

P<0.05*

2- ROC curve, sensitivity, and specificity of NLR and total cholesterol (TC) as predictive markers of breast cancer stage:

ROC analysis was carried out to determine the optimal cutoff points for NLR and total cholesterol. It has been found that AUC (Area Under Curve) was >0.70 which indicated that both NLR and total cholesterol could be used as predictive markers for the advanced stage of breast cancer. NLR had 73.6% sensitivity, and 70.8% specificity with a cut-off value of 2 while total cholesterol had 75.5% sensitivity, and81.2% specificity with a cut-off value of 194 mg/dl. Table 2 performs ROC analysis details.

Table 2: AUC, cut-off values, sensitivity, and specificity of NLR and total cholesterol for predicting the advanced stage of breast cancer:

parameter	**AUC**	**95%Cl**	**Cut-off value**	**Sensitivity%**	**Specifity%**	**p-value**
NLR	0.74	0.643-0.838	2	73.6%	70.8%	0.001*
TC	0.82	0.744-0.906	194	75.5%	81.2%	0.001*

*P<0.05

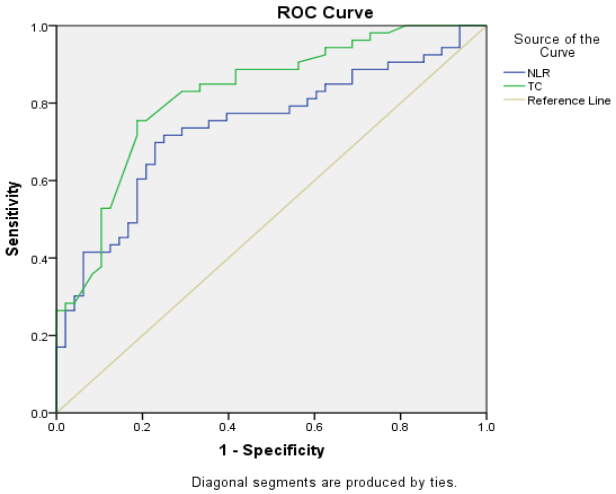

Figure 1: ROC curve of NLR and TC as predictive values of the advanced stage of breast cancer

3- Comparison of clinicopathological characteristics of breast cancer patients according to the high and low NLR:

Among 101 breast cancer ,45 patients had low NLR(NLR<2) , while 56 patients had high NLR(NLR≥2). High NLR values were significantly associated with increased tumor size(p=0.005) and lymph node metastasis (p=0.021). High NLR values were not associated with age, menopause, BMI, distant metastasis, hormonal status, histological and molecular subtypes. Baseline clinicopathological factors and the comparison according to NLR values are summarized in Table3:

Table3: Comparison of clinicopathological factors of breast cancer patients between high NLR and low NLR groups

Variables	Category	N	Low NLR (<2) (N=45)	High NLR (≥2) (N=56)	P-Value
Age (years)	< 40	15	6 (13.3%)	9(16.1%)	0.72
	40-60	63	30(66.7%)	33(58.9%)	
	>60	23	9(20%)	14(25%)	
Menopause	Premenopause	61	27(60%)	34(60.7%)	0.94
	Postmenopause	40	18(40%)	22(39.3%)	
BMI (Kg/m²)	Normal weight (<25)	33	14(13.1%)	19(33.9%)	0.45
	Over-weight (25-29.9)	43	22(48.9%)	21(37.5%)	
	Obesity (≥30)	25	9(20%)	16(28.6%)	
Grade	Grade1	9	5(11.1%)	4(7.1%)	0.15
	Grade2	50	26(57.8%)	24(42.9%)	
	Grade3	42	14(31.1%)	28(50%)	
Tumor size	T1(Tumor size<2cm)	9	5(11.1%)	4(7.1%)	**0.004***
	T2 (2cm<Tumor size≤5cm)	62	34(75.6%)	28(50%)	
	T3 (Tumor size>5cm) + T4 (Tumor of any size growing into chest wall and skin)	30	6(13.3%)	24(42.9%)	

Variables	Category	N	Low NLR (<2) (N=45)	High NLR (≥2) (N=56)	P-Value
Lymph node metastasis	N0(No involved lymph nodes)	43	26(57.8%)	17(30.4%)	**0.021***
	N1(1-3 involved lymph nodes)	23	8(17.8%)	15(26.8%)	
	N2(4-9 involved lymph nodes) +N3(≥10 involved lymph nodes)	35	11(24.4%)	24(42.9%)	
Distant metastasis	M0	97	44(97.8%)	53(94.6%)	
	M1	4	1(2.2%)	3(5.4%)	0.62
ER (Estrogen receptors)	Negative	34	13(28.9%)	21(37.5%)	
	Positive	67	32(71.1%)	35(62.5%)	0.36
PR (Progesteron receptors)	Negative	52	22(48.9%)	30(53.6%)	0.64
	Positive	49	23(51.1%)	26(46.4%)	
HER2(Human epidermal growth factor receptor-2)	Negative	71	31(68.9%)	40(71.4%)	0.78
	Positive	30	14(31.1%)	16(28.6%)	
Histological types	IDC (Invasive Ductal Carcinoma)	87	36(80%)	51(91.1%)	0.27
	ILC (Invasive Lobular Carcinoma)	9	6(13.3%)	3(5.4%)	
	Others	5	3(6.7%)	2(3.6%)	
Molecular subtypes	Luminal A	51	22(48.9%)	29(51.8%)	
	Luminal B	20	10(22.2%)	10(17.9%)	
	HER2-overexpression	10	4(8.9%)	6(10.7%)	0.95
	TNBC (Triple negative breast cancer)	20	9(20%)	11(19.6%)	

*P<0.05

4- Comparison of clinicopathological characteristics of breast cancer patients according to the high and low TC:

Using the total cholesterol cut-off value (194 mg/dL), the patients were divided into two groups: 50 patients with high TC (TC ≥ 194 mg/dL) and 51 patients with low TC (TC < 194 mg/dL). High total cholesterol was significantly associated with increased BMI, tumor size, lymph node metastasis, and tumor grade. However, no significant correlation was observed with age, menopausal status, distant metastasis, hormonal status, histological subtype, or molecular subtype. Table 4 summarizes the comparison of clinicopathological factors according to TC levels:

Table 4: Comparison of clinicopathological factors of breast cancer patients between high TC and low TC groups:

Variables	Category	N	Low TC (<194) (N=50)	High TC (≥194) (N=51)	P-Value
Age (years)	< 40	15	6 (11.8 %)	9(18%)	
	40-60	63	37 (72.5%)	26 (52%)	0.09
	>60	23	8 (15.7%)	15 (30%)	
Menopause	Premenopause	61	28 (54.9%)	33 (66%)	0.25
	Postmenopause	40	23 (45.1%)	17 (34%)	

Variables	Category	N	Low TC (<194) (N=50)	High TC (≥194) (N=51)	P-Value
BMI (Kg/m²)	Normal weight (<25)	33	25 (49%)	8 (16%)	**0.002***
	Over-weight (25-29.9)	43	17 (33.3%)	26 (52%)	
	Obesity (≥30)	25	9(17.7%)	16(32%)	
Grade	Grade1	9	6 (11.7 %)	3(6%)	**0.013***
	Grade2	50	31 (60.8%)	19 (38%)	
	Grade3	42	14(27.5%)	28(56%)	
Tumor size	T1	9	7 (13.7%)	2 (4%)	**0.04***
	T2	62	34(66.7%)	28(56%)	
	T3+T4	30	10 (19.6%)	20 (40%)	
Lymph nodes metastasis	N0	43	31 (60.8%)	12 (24%)	**0.001***
	N1	23	13 (25.5%)	10(20%)	
	N2+N3	35	7 (13.7%)	28 (56%)	
Distant metastasis	M0	97	49 (96.1%)	48 (96%)	0.98
	M1	4	2 (3.9%)	2 (4%)	
ER	Negative	34	16 (31.4%)	18 (36%)	0.62
	Positive	67	35 (68.6%)	32 (64%)	
PR	Negative	52	26 (51%)	26 (52%)	0.91
	Positive	49	25 (49%)	24 (48%)	
HER2	Negative	71	39 (76.5%)	32 (64%)	0.17
	Positive	30	12 (23.5%)	18 (36%)	
Histological types	IDC	87	46 (90.2%)	41 (82%)	0.47
	ILC	9	3 (5.9%)	6 (12%)	
	Others	5	2 (3.9%)	3 (6%)	
Molecular subtypes	Luminal A	51	28 (54.9%)	23 (46%)	0.47
	Luminal B	20	7 (13.7%)	13 (26%)	
	HER2-overexpression	10	5(9.8%)	5 (10%)	
	TNBC	20	11(21.6%)	9 (18%)	

5- Association between NLR and total cholesterol in breast cancer patients:

We evaluated the correlation between total cholesterol levels and NLR using cut-off values. We found that high total serum cholesterol was significantly associated with high NLR in breast cancer patients(**p=0.004**), as shown in Table 5:

Table 5: The association between NLR and total cholesterol in breast cancer patients:

			TC levels		p-value
NLR	Value	N	TC<194 (N=51)	TC≥194 (N=50)	**0.004***
	NLR<2	45	30(58.8%)	15(30%)	
	NLR≥2	56	21(41.2%)	35(70%)	

*P<0.05

6- Association of elevated values of both NLR and total cholesterol with some clinicopathological factors:

We also assessed the correlation between elevated values of the studied markers (NLR ≥ 2 and TC ≥ 194 mg/dL) and clinicopathological parameters. The patient cohort (N = 101) was divided into two groups: Group 1 (N = 35), which included patients with both NLR ≥ 2 and TC ≥ 194 mg/dL, and Group 2 (N = 66), which included the

remaining patients. A statistically significant correlation was found with tumor size (p = 0.01) and lymph node metastasis (p = 0.001). However, no significant correlation was observed with tumor grade or distant metastasis (p > 0.05), as illustrated in Table 6:

Table 6: association between high NLR and total cholesterol with some clinicopathological characteristics in breast cancer patients

Tumor characteristics		Patient group(N=101)		*P*-Value
		Group1(N=35)	Group2(N=66)	0.01*
Tumor size	T1	2(5.7%)	7(10.6%)	
	T2	16(45.7%)	46(69.7%)	
	T3+T4	17(48.6%)	13(19.7%)	
Lymph nodes metastasis	N0	7(20%)	36(54.6 %)	0.001*
	N1	8(22.9%)	15(22.7%)	
	N2+N3	20(57.1%)	15(22.7 %)	
Distant metastasis	M0	33(94.3%)	64(97%)	0.51
	M1	2(5.7%)	2(3%)	
Tumor grade	Grade1	3(8.6%)	6(9.1%)	0.06
	Grade2	12(34.3%)	38(57.6%)	
	Grade3	20(57.1%)	22(33.3%)	

*P<0.05

DISCUSSION

This study evaluated NLR (Neutrophils to Lymphocytes ratio) and total cholesterol in Syrian breast cancer patients. We also assessed WBC, neutrophil, and lymphocyte count. We found significant differences between early-stage and advanced-stage patients. The values were higher in the advanced stage except for lymphocyte count. These findings are consistent with other studies that evaluated the predictive value of NLR in breast cancer. Wiranta *et al.* and Phillip *et al*. found a significant correlation between NLR and breast cancer staging [14][16]. Gong et al. also found an association between high neutrophil count and tumor progression in patients with breast cancer[17]. Lymphocyte count was higher in the early stage similar to the findings of Rana et al. [18].

The inflammatory response has a major role in acerbating different cancers, including breast cancer, by detecting many infilitrating immune cells in malignant tissues[19]. Neutrophils activate tumor progression and invasion through several mechanisms. For example, neutrophils can produce pro-inflammatory cytokines including interleukin-6 (IL-6), IL-7, and IL-8, which induce tumor invasion. They also can secrete circulating vascular endothelial growth factor (VEGF), promoting tumor development. High neutrophil count was associated with poor survival and advanced TNM stage [20][16]. On the other hand, lymphocytic response is considered an important component for controlling cancer progression by producing cytokines such as IFN-ƛ ,which are effective against tumor growth and metastasis [21]. In addition, lymphopenia is associated with adverse consequences in advanced malignancies [22]. All these effects could lead to increasing NLR in peripheral blood. Elevated NLR among breast cancer patients was suggested to be correlated with advanced stage and increasing tumor aggressiveness [23].

Furthermore, our study found an increase of serum total cholesterol in the advanced stage compared to the early stage, which could result from cholesterol composition of tumor cells. According to previous studies, cholesterol synthesis is linked with cancer stem cells, which are cancer cells correlated with tumor progression

and metastasis[24]. Ehmsen et al. showed an augmenting of *de novo* cholesterol synthesis from breast cancer stem cells [25].

We evaluated the clinicopathological characteristics of patients according to NLR and total cholesterol obtained using the ROC curve. High NLR values were significantly associated with increased tumor size and lymph node metastasis. These findings were by Elyasina et al. and Sokmen et al. [26][27]. High neutrophil count induces secreting cytokines and growth factors that promote tumor invasion and angiogenesis[20]. Breast cancer cells also activate the secretion of IL-1β, IL-17, and G-CSF inhibiting CD8 T cells and promoting metastasis[28].In addition, high serum levels of total cholesterol were significantly associated with increased tumor size, lymph node metastasis, tumor grade, and BMI. These results were consistent with previous studies.

Ahmed et al. demonstrated a gradual increase in serum cholesterol levels with increasing tumor size [29]. Jin et al. showed that patients with abnormal blood lipids had a higher rate of positive lymph nodes than patients with normal lipids[30]. Cholesterol has been shown to increase cancer cell development and proliferation through activating AKT phosphorylation[31]. Moreover, 27 hydroxy cholesterol has been found to increase the expression of matrix metalloproteinase9 (MMP9) and activate migration and epithelial-to-mesenchymal transition (EMT) in breast cancer cells [24]. Pandag et al. demonstrated a significant correlation between cholesterol levels and the grade of breast cancer. It has been found that changes in cholesterol levels could affect tumor grading. It could influence the expression of proteins related to advanced tumors in mammals [32]. In addition, 27HC, by activating EMT, could increase tumor grade. Feng et al. showed that the expression of EMT markers had increased with higher tumor grade [33].

There was also a significant correlation between cholesterol levels and BMI in line with Owiredu et al. and Mina et al.[34],[35]. That could result from increasing its synthesis by adipose tissues [36].

High levels of serum total cholesterol were significantly associated with high NLR similar to the finding of Dominguez *et al*. [13]. Also, high values of both were associated with increased tumor size and lymph node metastasis. The alterations in lipid levels, including total cholesterol, can affect immune cell activation. Cholesterol metabolites, such as oxysterols, induce neutrophil recruitment through activating CXC receptor 2(CXCR2). Recruited neutrophils have been found to promote angiogenesis and tumor growth. Furthermore, elevated total cholesterol levels can inhibit T-cell receptor signaling, impairing T-cell proliferation, cytokine production and decreasing anti-tumor immune response [37][10].

CONCLUSIONS

We found a statistically significant difference in NLR and total cholesterol values between patient groups stratified by tumor stage. Higher NLR and total cholesterol levels were associated with more advanced stages of breast cancer. Furthermore, based on the cut-off values determined for both markers using ROC curve analysis (maximizing sensitivity and specificity), a significant correlation was observed with tumor size and lymph node metastasis. Therefore, pretreatment NLR and total cholesterol may serve as predictive markers for breast cancer stage. However, further studies with larger sample sizes are needed to evaluate the prognostic value of these markers, particularly in relation to survival and recurrence rates.

REFERENCES

1. Kzar H.H., Al-Gazally M.E. and Wtwt M.A. Everolimus loaded NPs with FOL targeting: preparation, characterization and study of its cytotoxicity action on MCF-7 breast cancer cell lines. *Jordan J. Pharm. Sci.* 2022; 15(1):25–39. doi:10.35516/JJPS.V15I1.286.
2. Abu Msafer B.A., Abbas M.A., Al Shaer W. and Arafat S. Enhanced Platelet Activation Induced by Palbociclib Treatment in MCF-7 Breast Cancer Cells. *Jordan J. Pharm. Sci.* 2025; 18(1):10–20. doi:10.35516/JJPS.V18I1.2459.
3. Inasu M. and Lunds universitet. Cholesterol metabolism in breast cancer: Prognostic factors and optimizing treatment. *[Online]*. Accessed: Jul. 12, 2024; pp.14–59.
4. Smolarz B., Nowak A.Z. and Romanowicz H. Breast cancer—epidemiology, classification, pathogenesis and treatment (Review of literature). *Cancers (Basel)* 2022; 14(10). doi:10.3390/cancers14102569.
5. van 't Veer L.J., et al. Gene expression profiling predicts clinical outcome of breast cancer. *Nature* 2002; 415(6871):530–536. doi:10.1038/415530a.
6. Manimaran D., Elangovan N. and Palanisamy V. Anti-tumorgenic impact of nano-formulated peptide HIF-Alpha therapy by DMBA induced mammary carcinoma in rodent type. *Jordan J. Pharm. Sci.* 2024; 17(4):783–793. doi:10.35516/jjps.v17i4.2482.
7. Gonzalez H., Hagerling C. and Werb Z. Roles of the immune system in cancer: from tumor initiation to metastatic progression. *Genes Dev.* 2018; 32(19–20):1267–1284. doi:10.1101/gad.314617.118.
8. Dirican A., et al. Do the derived neutrophil to lymphocyte ratio and the neutrophil to lymphocyte ratio predict prognosis in breast cancer? *Int. J. Clin. Oncol.* 2015; 20(1):70–81. doi:10.1007/s10147-014-0672-8.
9. Rayan N.A., Zaky A.H., Eltyb H.A., Zeidan A. and Zahran A.M. The prognostic significance of pre- and post-treatment neutrophil to lymphocyte ratio in breast cancer patients. *J. Cancer Ther.* 2019; 10(7):525–536. doi:10.4236/JCT.2019.107044.
10. Zhang H., Zhao W., Li X. and He Y. Cholesterol metabolism as a potential therapeutic target and a prognostic biomarker for cancer immunotherapy. *Onco. Targets. Ther.* 2021; 14:3803–3812. doi:10.2147/OTT.S315998.
11. Stadler S.C., Hacker U. and Burkhardt R. Cholesterol metabolism and breast cancer. *Curr. Opin. Lipidol.* 2016; 27(2):200–201. doi:10.1097/MOL.0000000000000285.
12. Nelson E.R., Chang C. and McDonnell D.P. Cholesterol and breast cancer pathophysiology. *Trends Endocrinol. Metab.* 2014; 25(12):649–655. doi:10.1016/j.tem.2014.10.001.
13. Gago-Dominguez M., et al. Neutrophil to lymphocyte ratio and breast cancer risk: analysis by subtype and potential interactions. *Sci. Rep.* 2020; 10(1):13203. doi:10.1038/s41598-020-70077-z.
14. Wiranata S., et al. Pretreatment neutrophil-to-lymphocyte ratio and platelet-to-lymphocyte ratio as a stage determination in breast cancer. *Open Access Maced. J. Med. Sci.* 2020; 8(B):1058–1063. doi:10.3889/OAMJMS.2020.5336.
15. American Joint Committee on Cancer. Breast. In: *AJCC Cancer Staging Manual*. 2017; p.589.
16. Philip A., Jose M., Jose W.M., Vijaykumar D.K. and Pavithran K. Pretreatment neutrophil-to-lymphocyte ratio predicts lymph node metastasis in triple-negative breast cancer. *Indian J. Cancer* 2022; 59(4):469–473. doi:10.4103/ijc.IJC_914_19.
17. Gong Y.T., et al. Neutrophils as potential therapeutic targets for breast cancer. *Pharmacol. Res.* 2023; 198:106996. doi:10.1016/J.PHRS.2023.106996.
18. Rana A.P.S., Kaur M., Zonunsanga B., Puri A. and Kuka A.S. Preoperative peripheral blood count in breast carcinoma: predictor of prognosis or a routine test. *Int. J. Breast Cancer* 2015; 2015:964392. doi:10.1155/2015/964392.
19. Okuturlar Y., et al. Utility of peripheral blood parameters in predicting breast cancer risk. *Asian Pac. J. Cancer Prev.* 2015; 16(6):2409–2412. doi:10.7314/apjcp.2015.16.6.2409.

20. Gong W., Yang S., Yang X. and Guo F. Blood preoperative neutrophil-to-lymphocyte ratio is correlated with TNM stage in patients with papillary thyroid cancer. *Clinics (Sao Paulo)* 2016; 71(6):311–314. doi:10.6061/clinics/2016(06)04.
21. Ozyalvacli G., Yesil C., Kargi E., Kizildag B., Kilitci A. and Yilmaz F. Diagnostic and prognostic importance of the neutrophil lymphocyte ratio in breast cancer. *Asian Pac. J. Cancer Prev.* 2014; 15(23):10363–10366. doi:10.7314/apjcp.2014.15.23.10363.
22. Fogar P., et al. Decreased total lymphocyte counts in pancreatic cancer: an index of adverse outcome. *Pancreas* 2006; 32(1):22–28. doi:10.1097/01.mpa.0000188305.90290.50.
23. Guthrie G.J.K., Charles K.A., Roxburgh C.S.D., Horgan P.G., McMillan D.C. and Clarke S.J. The systemic inflammation-based neutrophil-lymphocyte ratio: experience in patients with cancer. *Crit. Rev. Oncol. Hematol.* 2013; 88(1):218–230. doi:10.1016/j.critrevonc.2013.03.010.
24. Halimi H. and Farjadian S. Cholesterol: an important actor on the cancer immune scene. *Front. Immunol.* 2022; 13:1057546. doi:10.3389/fimmu.2022.1057546.
25. Ehmsen S., et al. Increased cholesterol biosynthesis is a key characteristic of breast cancer stem cells influencing patient outcome. *Cell Rep.* 2019; 27(13):3927–3938.e6. doi:10.1016/j.celrep.2019.05.104.
26. Sökmen F.C. and Karacin C. The role of peripheral blood inflammatory markers in the staging of breast cancer. *East J. Med.* 2021; 26(1):171–174. doi:10.5505/ejm.2021.71542.
27. Elyasinia F., et al. Neutrophil-lymphocyte ratio in different stages of breast cancer. *Acta Med. Iran.* 2017; 55(4):228–232. Available: http://www.ncbi.nlm.nih.gov/pubmed/28532133
28. Anwar S.L., Cahyono R., Avanti W.S., Budiman H.Y., Harahap W.A. and Aryandono T. Pre-treatment neutrophil-lymphocyte and platelet-lymphocyte ratios as additional markers for breast cancer progression: a retrospective cohort study. *Ann. Med. Surg.* 2021; 63:102144. doi:10.1016/j.amsu.2021.01.092.
29. Ahmad S.S., Ashraf S., Jamal A. and Akhtar K. Total serum cholesterol level in cases of carcinoma breast—a correlative study. *[Online]*. Accessed: Mar. 02, 2024. Available: www.sospublication.co.in
30. Jin W., et al. The correlation between blood lipids and clinicopathological features of breast cancer in young females. *Gland Surg.* 2020; 9(5):1443–1449. doi:10.21037/gs-20-616.
31. Ben Hassen C., et al. Is cholesterol a risk factor for breast cancer incidence and outcome? *J. Steroid Biochem. Mol. Biol.* 2023; 232:106346. doi:10.1016/j.jsbmb.2023.106346.
32. García-Estévez L., Cortés J., Pérez S., Calvo I., Gallegos I. and Moreno-Bueno G. Obesity and breast cancer: a paradoxical and controversial relationship influenced by menopausal status. *Front. Oncol.* 2021; 11:705911. doi:10.3389/fonc.2021.705911.
33. Feng X., et al. Expression of EMT markers and mode of surgery are prognostic in phyllodes tumors of the breast. *Oncotarget* 2017; 8(20):33365–33374. doi:10.18632/oncotarget.16497.
34. Owiredu W.K.B.A., Donkor S., Addai B.W. and Amidu N. Serum lipid profile of breast cancer patients. *Pakistan J. Biol. Sci.* 2009; 12(4):332–338. doi:10.3923/pjbs.2009.332.338.
35. Ha M., Sung J. and Song Y.-M. Serum total cholesterol and the risk of breast cancer in postmenopausal Korean women. *Cancer Causes Control* 2009; 20(7):1055–1060. doi:10.1007/s10552-009-9301-7.
36. Mc Auley M.T. Effects of obesity on cholesterol metabolism and its implications for healthy ageing. *Nutr. Res. Rev.* 2020; 33(1):121–133. doi:10.1017/S0954422419000258.
37. Zipinotti Dos Santos D., et al. The impact of lipid metabolism on breast cancer: a review about its role in tumorigenesis and immune escape. *Cell Commun. Signal.* 2023; 21(1):161. doi:10.1186/s12964-023-01178-1.

نسبة العدلات إلى اللمفاويات ومستويات الكوليسترول الكلي قبل العلاج كواسمات حيوية للتنبؤ بعدوانية سرطان الثدي

***رزان حسن*[1]، نادر عبدالله[2]، مرام بلال[1]**

[1]قسم الكيمياء الحيوية والأحياء الدقيقة، كلية الصيدلة، جامعة تشرين، سوريا

[2]قسم الأورام، كلية الطب البشري، جامعة تشرين، سوريا

ملخص

يعتبر سرطان الثدي من أكثر السرطانات شيوعاً لدى النساء حول العالم. تتواجد مجموعة من العوامل لتي بإمكانها التأثير على عدوانية الورم, من بين هذه العوامل نسبة العدلات إلى اللمفاويات (NLR) ومستويات الكوليسترول الكلي. نتيجة قلة الدراسات التي تقيم العلاقة بين الواسمات السابقة ومرحلة الورم, هدفت هذه الدراسة إلى تقصي دور كل من النسبة NLR ومستويات الكوليسترول الكلي كواسمات حيوية للتنبؤ بمرحلة الورم في سرطان الثدي. قمنا بتقييم 101 من المريضات المُشخصات حديثاً ودراسة علاقة كل من العوامل السابقة مع بعض الخصائص السريرية للمريضات بالاعتماد على القيم الحدية التي تم تحديدها باستخدام منحنى خصائص تشغيل المستقبل ROC curve. أظهرت نتائجنا وجود ارتباط هام بين مرحلة الورم وكل من نسبة العدلات إلى اللمفاويات, الكوليسترول الكلي, الكريات البيض والعدلات ($p<0.05$). بالاعتماد على مرحلة الورم, تم تحديد القيم الحدية 2 لنسبة العدلات إلى اللمفاويات و 194mg/dl للكوليسترول الكلي .ترافق ارتفاع نسبة العدلات إلى اللمفاويات مع تزايد حجم الورم($p=0.004$) ونقائل العقد اللمفية($p=0.021$) بينما ترافق ارتفاع مستويات الكوليسترول الكلي مع ازدياد مشعر كتلة الجسم($p=0.002$) , حجم الورم($p=0.04$), نقائل العقد اللمفية ($p=0.001$) ودرجة الورم($p=0.013$) كما ترافق ارتفاع النسبة NLR مع ارتفاع مستويات الكوليسترول الكلي لدى المريضات, وبالتالي, نسبة العدلات إلى اللمفاويات ومستويات الكوليسترول الكلي قبل العلاج قد تكون عوامل مساعدة للتنبؤ بمرحلة الورم في سرطان الثدي.

الكلمات الدالة: سرطان الثدي، نسبة العدلات إلى اللمفاويات، الكوليسترول الكلي.

* ***المؤلف المراسل: رزان حسن***

razanhasan98@gmail.com

تاريخ استلام البحث 2024/8/22 وتاريخ قبوله للنشر 2024/7/18.

Jordan Journal of Pharmaceutical Sciences, Volume 18, No. 2, 2025

The Remedial Effect of *Ziziphus lotus* Extract against Oxidative Stress Induced by Deltamethrin Pesticide in Rats

Djahra Ali Boutlelis[1]*, Benkaddour Mounia[1], Benkherara Salah[2], Laib Ibtissam[1], Benine Chaima[1], Chrait Sabrina[1]

[1]Laboratory of Biology, Environment, and Health, Faculty of natural and life sciences, University of El Oued, Algeria.
[2]Department of Biology, Faculty of natural and life sciences and Earth Sciences, University of Ghardaia, Algeria.

ABSTRACT

This study investigated the antioxidant properties of natural compounds derived from the medicinal plant *Ziziphus lotus*, traditionally used for treating liver disorders. The research focused on its potential to mitigate biochemical alterations induced by the pesticide Deltamethrin in rats. Thirty male Wistar albino rats were exposed to Deltamethrin (7 µl/kg/day), after which they received aqueous extract of *Ziziphus lotus* at three different doses (100, 200, and 400 mg/kg/day) via oral gavage. After 33 days of treatment, the animals were sacrificed, and blood samples were collected for serum biochemical analysis. Liver tissues were preserved for assessment of antioxidant activity. The extraction process yielded 20%, with a high polyphenol content of 12.04 ± 0.142 mg AGE/mL (Gallic Acid Equivalents per millilitre of extract). The DPPH assay confirmed strong antioxidant potential of the extract, with an IC_{50} value of 0.62 ± 0.146 µg/mL. In vivo results showed that Deltamethrin exposure led to significant reductions in body weight and increases in serum levels of Aspartate Transaminase (AST), Alanine Transaminase (ALT), Alkaline Phosphatase (ALP), alpha-amylase, cholesterol, creatinine, and urea ($p < 0.05$ vs. control), indicating hepatotoxicity and nephrotoxicity. Additionally, antioxidant defence markers such as reduced glutathione (GSH) were diminished, while malondialdehyde (MDA) levels increased, reflecting enhanced lipid peroxidation. Treatment with *Ziziphus lotus* extract at all three doses ameliorated several liver and kidney function markers and restored body weight. The presence of bioactive secondary metabolites in the extract contributed to its significant biological activities, notably its potent antioxidant effects demonstrated both in vitro and in vivo.

Keywords: Natural products, *Ziziphus lotus*, Biochemical alterations, Deltamethrin, Oxidative stress.

INTRODUCTION

Deltamethrin is a modern insecticide that protects vegetables, fruits, and crops from pests such as ants, mites, beetles, and weevils. Its applications include nurseries, golf courses, urban landscaping, residential homes, construction sites, and garden pest management. Additionally, it is utilized as an ectoparasiticide in veterinary practice to reduce vector-borne infections by eliminating mites, flies, fleas, and ticks. Deltamethrin belongs to the synthetic pyrethroid group and is promoted as an alternative to organophosphate chemicals due to its persistent and effective properties [1,2].

However, excessive use, improper application, and mishandling in various fields have accumulated significant amounts of Deltamethrin in water sources and soil [3]. This accumulation results in toxic contamination and causes harm to non-target organisms, including humans. Acute Deltamethrin poisoning manifests with

Corresponding author: Djahra Ali Boutlelis
djahra_ab@yahoo.fr
Received: 28/2/2024 Accepted: 19/9/2024.
DOI: https://doi.org/10.35516/jjps.v18i2.2445

clinical symptoms similar to those observed in organophosphorus insecticide poisoning, such as abdominal pain, dizziness, headache, nausea, pulmonary oedema, bronchospasm, fatigue, increased secretions in body tissues, muscle twitching, and vomiting [4].

The toxicity of Deltamethrin is attributed to various mechanisms, including the generation of free radicals. Research predominantly indicates that oxidative stress is a central factor in the toxic effects of Deltamethrin [5]. One study revealed that Deltamethrin exposure significantly increases hepatic lipid peroxidation and weakens the antioxidant defense system, producing oxygen-free radicals and subsequent liver injury [6]. Another study found that Deltamethrin exposure causes kidney damage by modulating apoptotic activity and oxidative stress response [7].

Natural products, particularly those of plant origin, have long been regarded as a significant source of medicinal compounds. Currently, between 25% and 30% of medications used to treat illnesses are derived from natural sources (plants, animals, microbes, and fungi) or are obtained from these sources [8]. Furthermore, current data from the drug industry show that natural products remain an essential source for developing new chemical entities to treat complex diseases, as their structures have been refined over millions of years of evolution to be highly effective [9].

Among these potentially promising natural products, antioxidants like polyphenols have been extensively studied due to their applications in various pharmaceutical fields, such as antibacterial [10], antifungal [11], antidiabetic [12], hepatoprotective [13], and hematoprotective [14], uses as well as in cosmetics and food for their health benefits [15]. Recently, there has been growing interest in the potential of antioxidants to enhance food preservation due to concerns that certain synthetic antioxidants may pose carcinogenic risks [16]. Numerous plants, whether used as food or medicine, contain antioxidant components. Regular consumption of phytonutrients with significant antioxidant properties is associated with a lower incidence of disorders linked to oxidative stress, such as cancers, cardiovascular diseases, and atherosclerosis [17] as well as reduced mortality rates [18].

Considering these beneficial properties of natural products, this study aimed to investigate the remedial effect of **Ziziphus lotus** extract against oxidative stress induced by the Deltamethrin pesticide in rats.

MATERIAL AND METHODS

Reagents and chemicals:

Sigma-Aldrich from the USA was used to purchase all chemicals and was of analytical quality. Deltamethrin pesticide was obtained from Bayer laboratory, and a commercial kit from Spinreact, Spain, was used for biochemical parameter determinations.

Plant material:

Aerial parts (Branches, Leaves, Thorns) of **Ziziphus lotus** were collected from Hamraya, El-Oued state, Algeria, and the plant was identified by Prof. Dr. Atef Chouikh (Faculty of Natural and Life Sciences, El-Oued University, Algeria). The aerial parts of the medicinal herb Ziziphus lotus were cleaned, dried, and powdered, then kept at ambient temperature.

Plant extract preparation:

Two hundred grams of Ziziphus lotus were macerated in 2000 mL of distilled water for 24 hours with continuous agitation at room temperature and protected from light. The solvent was then removed using a rotary evaporator, and the remaining extract was incubated at 40°C until completely dry. The dried extract was weighed and stored at 4°C for subsequent analyses [19]. The extraction yield was 20% w/w based on the initial raw plant material.

Total phenolic content estimation:

The total phenolic content was determined using the Folin–Ciocalteu method. Briefly, 0.1 mL of Ziziphus lotus extract was mixed with 0.2 mL of Folin–Ciocalteu reagent and diluted with 3.16 mL of distilled water. Then, 0.6 mL of

20% sodium carbonate solution was added. After incubating the mixture for 120 minutes at room temperature, the absorbance was measured at 765 nm. The assay was performed in triplicate to ensure data consistency. The phenolic content was expressed as milligrams of gallic acid equivalents per milliliter of extract [20].

DPPH free radical scavenging assay:

2.4 mg of DPPH• is dissolved in 100 ml of methanol to make the 1,1-diphenyl-2-picrylhydrazyl solution. 50 µl of extract (or ascorbic acid as a control) is added to 1.950 ml of the DPPH• solution previously produced. The reaction mixture is quickly agitated and then maintained at ambient temperature for 30 minutes in the dark to complete the reaction. The absorbance of the reaction medium is measured at 515 nm [21].

Liver protective effect of Ziziphus lotus **extract estimation:**

Acute toxicity of Ziziphus lotus extract:

The median lethal dose (LD_{50}) of *Ziziphus lotus* extract was determined following the procedure described by Litchfield and Wilcoxon (1949) [22]. Thirty male Albino rats were divided into five groups of six animals each and administered different oral doses of the extract (25, 250, 500, 1000, and 2000 mg/kg). A control group received distilled water only. The rats were monitored for signs of toxicity and mortality over a 14-day period.

Animals and experiment design:

Thirty adult Wistar albino rats, weighing 352.44 ± 8.77 g, were obtained from the Pasteur Institute of Algiers. They were housed in the Department of Molecular and Cellular Biology at El-Oued University, Algeria, under controlled conditions: temperature 24 ± 1 °C, a 12-hour light/12-hour dark photoperiod, with free access to standard food and water throughout the study. The rats were acclimated to these laboratory conditions for 15 days prior to the experiment. All animal experiments and protocols were approved by the Institutional Animal Ethical Committee (IAEC) of El-Oued University. The rats were then randomly divided into five groups of six animals each and subjected to the following treatments for 33 days:

Group 1: Control group.

Group 2: Received daily Deltamethrin (7 µl/kg/J in oral gavage). [23]

Group 3: Received daily Deltamethrin (7 µl/kg/J in oral gavage) than **Ziziphus lotus** extract (100 µl/kg/J in oral gavage).

Group 4: Received daily Deltamethrin (7 µl/kg/J in oral gavage) than **Ziziphus lotus** extract (200 µl/kg/J in oral gavage).

Group 5: Received daily Deltamethrin (7 µl/kg/J in oral gavage) than **Ziziphus lotus** extract (200 µl/kg/J in oral gavage).

Throughout the weeks of the study, body weight was frequently monitored.

Relative liver weight estimation:

After the rats were sacrificed, the liver was removed, cleaned with physiological saline, and weighed to calculate the relative liver weight using the formula: Relative liver weight = (Liver weight / Body weight) * 100% [24].

Blood collection for biochemical parameters analyses:

After 16 hours of feeding, the rats were sacrificed by decapitation following anaesthesia with chloroform. Blood was then drawn, and the samples were placed into serum-separating tubes and centrifuged for 10 minutes at 3000 rpm to prepare them for biochemical analysis.

Biochemical parameters analyses:

(AST): Serum Aspartate Transaminase (ALT): Alanine Transaminase (ALP): Alkaline Phosphatase, Alpha-amylase, Protein, Glycaemia, Cholesterol, Triglycerides, Creatinine, and Urea.

Liver homogenate parameters:

- Post mitochondrial supernatant preparation

To reduce nuclear debris, 0.5 g of liver from the sacrificed animals was homogenized in a cold phosphate buffer solution (0.1 M, pH 7.4) containing potassium

chloride (1.17%). The resulting homogenate was centrifuged at 9600 rpm for 45 minutes at 4°C to produce a post-mitochondrial supernatant (PMS), which served as the enzyme source.

- Total protein, Glutathione (GSH), and Malondialdehyde (MDA) estimation

Total protein content in liver homogenates was measured using the Coomassie Brilliant Blue G-250 assay, with bovine serum albumin as the standard reference (Bradford, 1976) [25]. Glutathione (GSH) and malondialdehyde (MDA) levels were determined following the methods described by Weckbecker and Cory (1988) [26] and Quintanilha (1981) [27], respectively.

Statistical analysis:

To analyze the obtained data, a student t-test (using Minitab® 13 software) was conducted. P-values of 0.05 or below were considered significant. The results of each experiment were presented as the mean and standard deviation (SD).

Total phenol content:

The total phenol content of **Ziziphus lotus** extract was estimated using the equation (y = 0.00116 x + 0.0375, r2 = 0.09985) and expressed as Gallic Acid Equivalents (GAE). It was 12.04 ± 0.142 mg GAE/ml of the **Ziziphus lotus** aerial part extract.

DPPH free radical scavenging assay:

The antioxidant activity of **Ziziphus lotus aerial** parts extract was tested using the DPPH free radical scavenging assay. The results are summarized in Table 1. The DPPH free radical scavenging activity of the plant extract was compared to that of the standard (ascorbic acid).

Table 01: DPPH free radical scavenging of *Ziziphus lotus* aerial parts extract.

IC_{50}	Ascorbic acid (µg/mL)	*Ziziphus lotus* extract (µg/mL)
	0.43 ±0.102	0.62 ±0.146

Data are expressed as mean±SE (Standard Error), (n=3).

Liver protective effect of Ziziphus lotus extract:

Acute toxicity of Ziziphus lotus extract:

The acute toxicity study, based on the method of Litchfield and Wilcoxon (1949) [22], is a standard preliminary screening test for evaluating new chemical substances. After administering Ziziphus lotus extract at five different doses over a 14-day period, none of the rats in any group showed clinical or behavioral changes, and no mortality was observed (Table 2).

Table 02: Rat's acute toxicity analyses treated by *Ziziphus lotus* aerial parts extract.

Group	Doses (mg/kg)	Mortality rate	Mortality ratio	Mortality (%)
Group 1	25	0	0/5	0
Group 2	250	0	0/5	0
Group 3	500	0	0/5	0
Group 4	1000	0	0/5	0
Group 5	2000	0	0/5	0

Relative liver weight:

The results of relative liver weight show that body weight was affected by the Deltamethrin pesticide and the plant extract. Additionally, Group 2 (treated with Deltamethrin) showed liver hypertrophy. In contrast, the extract of **Ziziphus lotus**, when administered at different doses in combination with Deltamethrin pesticide, reduced the elevated liver weight. The results of relative liver weight are summarized in Table 3.

Table 03: Rats' relative liver weight treated by *Ziziphus lotus* aerial parts extract.

Groups	Body weight (g)	Liver weight (g)	Relative liver weight (%)
Group 1	367.35 ± 3.9	12.1±0.74	2.600 ±0.1
Group 2	351.66□± □□□□ ***	10.38 ±0.75***	□□□□□± □□□□□***
Group 3	354.5□□± □□□*	9.35 ±0.44**	2.500 ±0.0816***
Group 4	361.90 ±3.8**	9.97 ±0.12*	2.650 ±0.191***
Group 5	365.4□□±□□□□□□□	10.32 ±0.58Ns	2.725 ±0.097**

Results are presented as the mean ± S.E. (Standard Error) (n = 5). (*) p≤0.05, (**)p≤0.01 and (***)p≤0.001. (NS)p > 0.05 as compared with Deltamethrin pesticide. Model group. bp < 0.05 as compared with a normal control group.

Biochemical parameters analyses:

- Serum enzyme activity

Figure 1 illustrates the effect of Ziziphus lotus aerial parts extract on serum enzyme activities (ALT, AST, ALP, and alpha-amylase). Exposure to the pesticide Deltamethrin caused a significant increase in serum enzyme activities. However, rats pretreated with Ziziphus lotus extract at various doses showed a notable reduction in these enzyme levels.

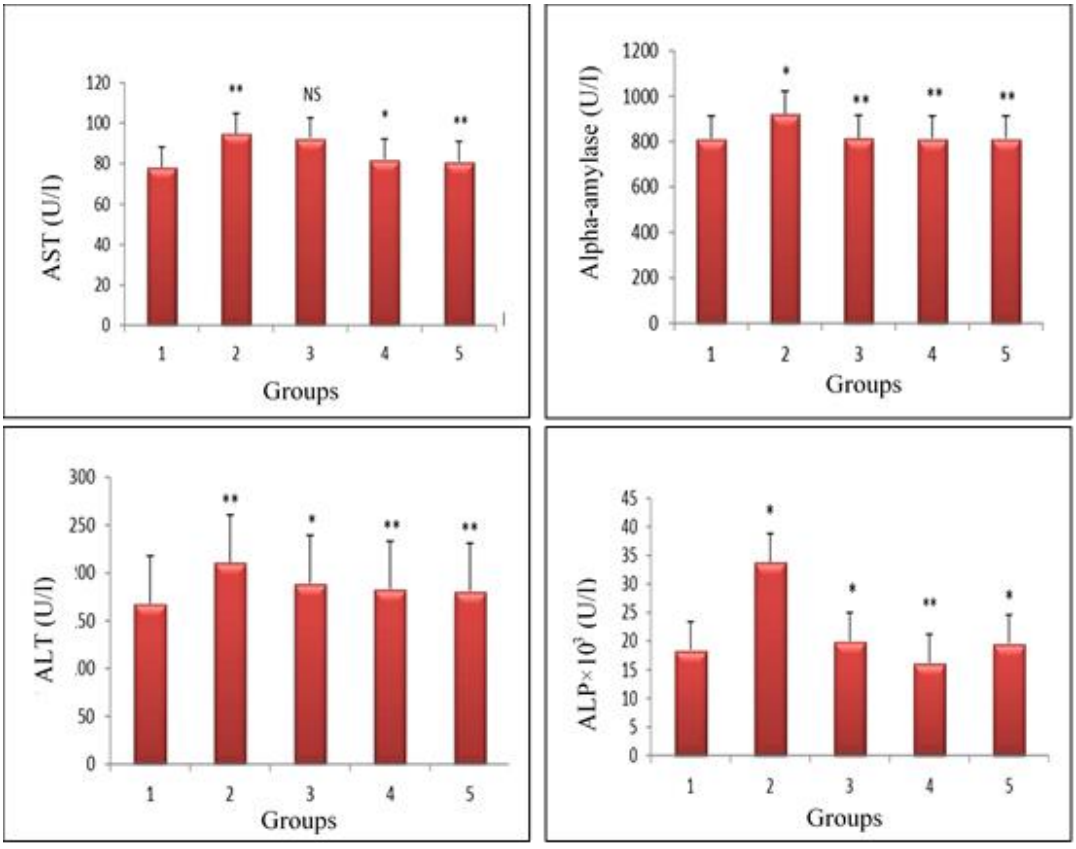

Figure 1: Effect of *Ziziphus lotus* aerial parts extract on serum enzyme activity.

(AST): Serum Aspartate Transaminase, (ALT): Alanine Transaminase, (ALP): Alkaline Phosphatase, Results are presented as the mean ± S.E. (Standard Error) (n = 5). (*) p≤0.05, (**) p≤0.01 and (***) p≤0.001. (NS) p > 0.05 as compared with Deltamethrin pesticide. Model group. bp < 0.05 as compared with a normal control group.

- Serum biochemical parameters

Administration of the pesticide Deltamethrin caused a significant increase in the analyzed serum biochemical parameters. The mitigating effects of Ziziphus lotus aerial parts against Deltamethrin-induced damage are shown in Figure 2.

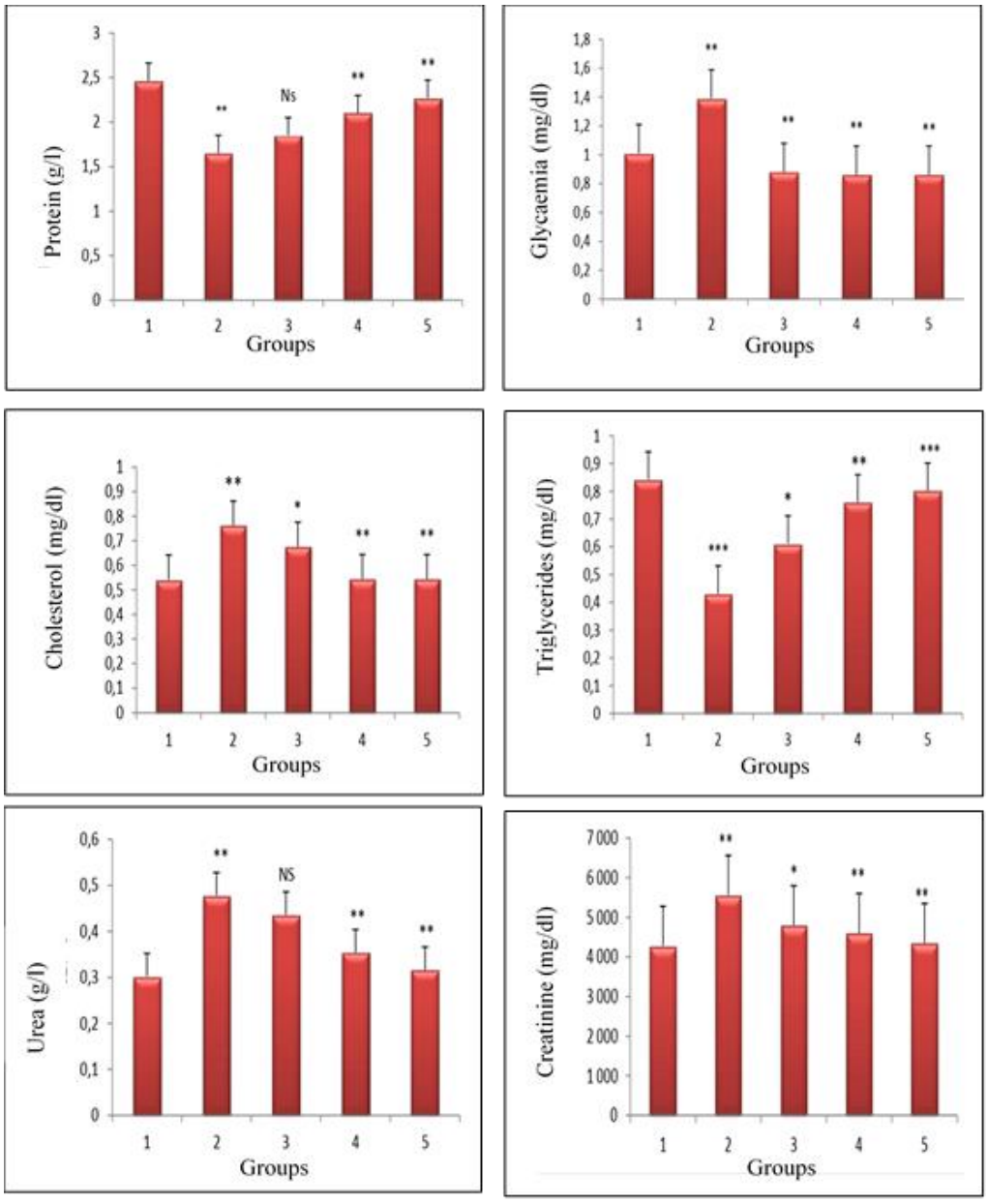

Figure 2: Effect of *Ziziphus lotus* aerial parts extract on biochemical parameters.

Results are presented as the mean ± S.E. (Standard Error) (n = 5). (*) p≤0.05, (**) p≤0.01 and (***) p≤0.001. (NS) p > 0.05 as compared with Deltamethrin pesticide. Model group. bp < 0.05 as compared with a normal control group.

-Liver enzyme activity (GSH and MDA):

The administration of the pesticide Deltamethrin caused alterations in liver oxidative stress markers, specifically Glutathione (GSH) and Malondialdehyde (MDA) levels. Figure 3 summarizes the protective effects of *Ziziphus lotus* aerial parts against Deltamethrin-induced liver damage.

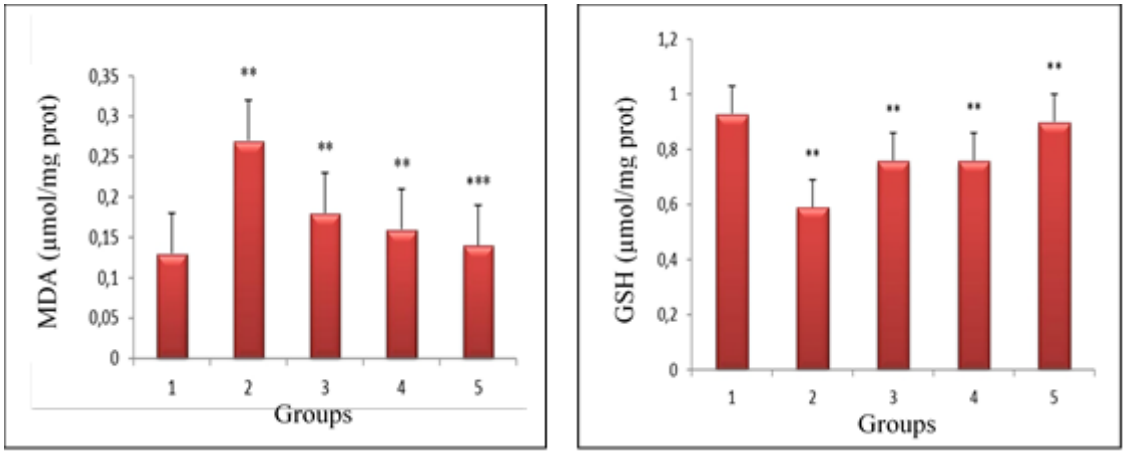

Figure 3: Effect of *Ziziphus lotus* aerial parts extract on liver enzymes activity.

(GSH): Glutathione. (MDA): Malondialdehyde. Results are presented as the mean ± S.E. (Standard Error) (n = 5). (*) $p \leq 0.05$, (**) $p \leq 0.01$ and (***) $p \leq 0.001$. (NS) $p > 0.05$ as compared with Deltamethrin pesticide. Model group. bp < 0.05 as compared with a normal control group.

DISCUSSION

This series of tests was conducted to evaluate the antioxidant capacity of *Ziziphus lotus* extract both in vitro, using the DPPH assay, and in vivo against Deltamethrin pesticide poisoning. The results are, in several respects, quite promising. Overall, the tests demonstrated consistency for extracts of similar nature, with plant extracts consistently exhibiting strong antioxidant potency. Based on these findings, a strong correlation can be established between the abundance of secondary metabolites (polyphenolics) in the aerial parts of *Ziziphus lotus*, including its aqueous extract, and the high level of antioxidant activity observed.

In this study, the maceration method with agitation accelerated the extraction process by minimizing the contact time between solvent and plant material while preserving the bioactivity of the constituents. Furthermore, extracting at room temperature and removing the solvent under reduced pressure enabled maximum recovery of compounds and prevented potential denaturation or modification due to high temperatures [28]. Approximately 4 g of aqueous extract was obtained from the water extraction of *Ziziphus lotus* aerial parts, corresponding to a 20% yield. Generally, concentrations in crude extracts vary among plants within the same family, depending on factors such as solid-liquid extraction conditions, extraction solvent, particle size, and solvent diffusion coefficient [29].

According to the results, the aqueous extract of *Ziziphus lotus* aerial parts contained a remarkably high amount of total polyphenols, measured at 12.04 ± 0.142 mg GAE/ml. In contrast, our findings differ from those of Djemai Zoughlache (2009) [30], who reported lower total polyphenol levels in raw extracts prepared with polar solvents (methanolic and aqueous) from *Ziziphus lotus* fruits collected in the Batna region of Algeria. In

Zoughlache's study, the total polyphenol content was 5.8 ± 1.24 µg GAE/mg.

The DPPH free radical scavenging assay results demonstrate the promising effect of polyphenolic substances in plant extracts, which act as primary antioxidants [31,32]. Generally, our results indicate that the aqueous extract of Ziziphus lotus exhibits strong activity in scavenging DPPH free radicals, with an IC50 of 0.43 ± 0.102 µg/mL. The efficacy of these antioxidants is attributed to their ability to donate hydrogen atoms or electrons, primarily from hydroxyl groups in flavonoids [20]. Indeed, polyphenolic compounds, especially flavonoids, are recognized as potent antioxidants capable of scavenging radical species and reactive forms of oxygen [33]. The scavenging effect of flavonoids is due to their low redox potential, which enables them to reduce free radicals by transferring hydrogen atoms from hydroxyl groups [34].

Male rats were orally administered different doses (25, 250, 500, 1000, and 2000 mg/kg) of Ziziphus lotus aerial parts extract and observed for 14 days in the acute toxicity study. These findings are consistent with earlier research demonstrating that extracts from medicinal plants can be safe even at high doses, such as Marrubium vulgare (2000 mg/kg) [23], Euphorbia hirta (5000 mg/kg) [35], and Lactuca serriola (6000 mg/kg) [56]. Moreover, to ensure greater confidence in the safety of natural products intended for human use—especially in pharmaceutical applications—data from acute toxicity studies of medicinal plants should be thoroughly evaluated [36].

Many xenobiotics, especially pesticides, are believed to produce reactive oxygen species (ROS) or even free radicals that cause oxidative stress in biological systems [37]. A significant reduction in mean body weight indicates general health deterioration in rats, which a decrease in daily food intake could explain. Previous studies on adult rats treated with pesticides also showed decreased body weight [38,39]. Moreover, rats given pesticide treatments exhibited a significant increase in their relative organ weights, particularly in the liver, showing hepatic hypertrophy (hepatomegaly). Numerous authors have described this anomaly as a consequence of the aggressive effects of various chemicals and pesticides [40].

Similarly, Prieto-Simón et al. (2006) [41] observed that a biomarker of pesticide cytotoxicity is a decrease in the relative weights of several animal organs. In contrast, the relative liver weights of intoxicated rats decreased following the oral administration of **Ziziphus lotus** plant extract. This improvement is attributed to the protective effects of the bioactive components in the plant extract against Deltamethrin pesticide toxicity.

Decreased levels of serum enzymes AST, ALT, ALP, and alpha-amylase were observed in rats treated with different doses of Ziziphus lotus plant extract following intoxication with Deltamethrin pesticide. Serum enzymes TGO (AST) and TGP (ALT) are synthesized in the cytoplasm of cells and are released into circulation when cellular damage occurs [42,43]. These enzymes serve as reliable indicators of liver cytolysis. Additionally, ALP reflects pathological changes in biliary flow [44]. Conversely, elevated levels of the pancreatic enzyme alpha-amylase were observed. The results showed that Deltamethrin pesticide increased alpha-amylase levels (Group 2), potentially impairing pancreatic function and reducing insulin secretion [45]. In contrast, rats treated with Ziziphus lotus extract demonstrated improved pancreatic function, as indicated by normalized alpha-amylase levels, which play a role in glucose regulation [46].

Results for biochemical metabolites such as triglycerides and cholesterol, along with renal indicators including creatinine and urea, demonstrate that these parameters are adversely affected by cytotoxic agents like the Deltamethrin pesticide. Elevated levels of renal markers, lipids (cholesterol), and proteins were observed. Since the kidneys are responsible for excreting harmful by-products of protein metabolism—such as creatinine and urea—[47], the

increased blood levels of these substances in this study suggest impaired kidney function. This impairment was also accompanied by a significant decrease in serum protein levels [48]. Additionally, some studies propose that synthetic chemicals, including pesticides, may negatively impact thyroid function [49,50,51]. Hyperlipidemia has been linked by some researchers to hypothyroidism or reduced lipase activity [52]. Treatment with various doses of *Ziziphus lotus* extract helped restore these metabolite levels to normal.

Toxic effects often originate from alterations in the endoplasmic reticulum, resulting in the loss of intracellular components such as metabolic enzymes [53]. A healthy organism possesses a robust defense system to prevent and neutralize damage caused by free radicals. Endogenous antioxidant enzymes, including glutathione (GSH) and malondialdehyde (MDA), play vital roles in protecting cells against reactive oxygen species [54]. In this study, the intoxicated group exhibited decreased GSH levels alongside excessive hepatic MDA production. Similar findings were reported by Djahra et al. (2020b) [13], who observed these changes following oral exposure to the insecticide Lambda-cyhalothrin at 62.5 mg/L per day. The normalization of hepatic function after administration of *Ziziphus lotus* extract underscores the extract's beneficial antioxidant properties, consistent with findings by Zeghib and Djahra (2019) [55].

CONCLUSION

This study reaffirmed the protective potential of natural compounds, particularly polyphenolics, present in Ziziphus lotus extract. The extract exhibited a significant modulatory effect on biochemical parameters commonly disrupted by oxidative damage following intoxication with the Deltamethrin pesticide.

ACKNOWLEDGMENTS

The authors express their gratitude to the Faculty of Sciences of Nature and Life, University of El-Oued, Algeria, and the Laboratory of Biology, Environment, and Health (LBEH) at El Oued University for providing the necessary facilities. This research was conducted as part of the D01N01UN390120230004 project, funded by the Algerian Ministry of Higher Education and the Directorate General for Scientific Research and Technological Development.

Conflicts of interest

The authors declare no conflicts of interest.

REFERENCES

1. Hassan R R., Micheal M, W., Badr A M., Hassan M E. and Abdel-Wahhab M A., Impact of sub chronic administration of deltamethrin on autoimmune activity in rat. *Pestic Biochem Physiol*. 2024; 203: 106008.
2. Lindsay S W., Thomas M B. and Kleinschmidt I. Threats to the effectiveness of insecticide-treated bednets for malaria control: thinking beyond insecticide resistance. *Lancet Glob. Health* 2021; 9:325-1331.
3. Deng F., Sun J., Dou R., Yu X., Wei Z., Yang C., Zeng X. and Zhu L. Contamination of pyrethroids in agricultural soils from the yangtze river delta, China. *Sci. Total Environ*. 2020; 731: 139181.
4. Ilyas W M., Chavan G. and Gadkari C. Deltamethrin poisoning mimicking organophosphate poisoning: a case report. *Cureus*. 2023; 15(1): e34303.
5. Lu Q., Sun Y., Ares I., Anadón A., Martínez M., Martínez-Larrañaga M R., Yuan Z, Wang X. and Martínez M A. Deltamethrin toxicity: A review of oxidative stress and metabolism. *Envi Res*. 2019; 170: 260-281.

6. Tuzmen N., Candan N., Kaya E. and Demiryas N. Biochemical effects of chlorpyrifos and deltamethrin on altered antioxidative defense mechanisms and lipid peroxidation in rat liver. *Cell Biochem. Funct.* 2008; 26:119-124.
7. Kumar A., Sasmal D. and Sharma. Mechanism of deltamethrin induced thymic and splenic toxicity in mice and its protection by piperine and curcumin: in vivo study. *Drug Chem. Toxicol*. 2018; 41(1):33-41.
8. Boldi A M. Libraries from natural product-like scaffolds. *Curr Opin Chem Biol.* 2004; 8: 281-286.
9. Newman D J., Cragg G M. and Snader K M. Natural products as sources of new drugs over the period 1981−2002. *J. Nat. Prod*. 2003; 66: 1022-1037.
10. Djahra A B., Benkaddour M. and Benkherara S. Evaluation of antimicrobial activity of medicinal plant Cotula cinerea against pathogenic strains. *Ponte J*, 2020a; 76(4):316-322.
11. Djahra, A B., Benkaddour M., Zeghib K., Benkherara S., Shaieb I., Ghania A. and Bdida S. Biofungicide activity of Datura stramonium leaf extract against phytopathogenic fungi. *Int. J. Bio. Agric. Res*. 2019; 2(1):1-5.
12. Benkherara S., Bordjiba O., Harrat S. and Djahra A B. Antidiabetic potential and chemical constituents of *Haloxylon scoparium* aerial part, an endemic plant from Southeastern Algeria. Int. j**.** *second. metab*. 2021; 8:398-413.
13. Djahra A B., Benkaddour M., Benkherara S. and Ouahiba B. Antioxidant and hepatoprotective Potential of Coriandrum sativum L. against hepatic injury by Lambda-cyhalothrin insecticide. *J. Drug Deliv. Ther*. 2020b; 10:182-188.
14. Zeghib K. and Boutlelis D. A. Food additive (sodium benzoate)-induced damage on renal function and glomerular cells in rats; modulating effect of aqueous extract of Atriplex halimus L. *Iran J Pharm Res*. 2021; 20:296.
15. Chebil L., Acylation des flavonoïdes par les lipases de *Candida antarctica* et de *Pseudomonas cepacia*: études cinétique, structurale et conformationnelle. Ph.D. Thesis. National Polytechnic Institute of Lorraine. Franch. 2006: 230.
16. Velioglu Y., Mazza G., Gao L. and Oomah B. Antioxidant activity and total phenolics in selected fruits, vegetables, and grain products. *J. Agric. Food Chem.* 1998; 46: 4113-4117.
17. Bravo L., Polyphenols: chemistry, dietary sources, metabolism, and nutritional significance. *Nutr rev.*1998; 56**:**317-333.
18. Anderson K J., Teuber S S., Gobeille A., Cremin P., Waterhouse A L. and Steinberg FM. Walnut polyphenolics inhibit in vitro human plasma and LDL oxidation. *J Nutr*. 2001; 131**:** 2837-2842.
19. [19] Matkowski A. and Piotrowska M. Antioxidant and free radical scavenging activities of some medicinal plants from the Lamiaceae. *Fitoterapia*, 2006; 77:346-353.
20. Li H B., Cheng K W., Wong C C., Fan K W., Chen F. and Jiang Y. Evaluation of antioxidant capacity and total phenolic content of different fractions of selected microalgae. *Food Chem.*, 2007; 102:771-776.
21. Benhammou N., Bekkara F A. and Panovska T K. Antiradical capacity of the phenolic compounds of *Pistacia lentiscus* L. and *Pistacia atlantica* desf. *Adv. Food Sci.* 2007; 29**:**155-161.
22. Litchfield J. and Wilcoxon F. A simplified method of evaluating dose-effect experiments. *J Pharmacol Exp Ther*. 1949; 96**:**99-113.
23. Boutlelis D A. 2014. Etude phytochimique et activité antimicrobienne, antioxydante, antihépatotoxique du Marrube blanc ou *Marrubium vulgare* L. Ph.D. Thesis, Annaba University Algeria, 2014, p 114.

24. Djahra A B., Zoubiri F., Benkaddour M. and Gouasmia S. Antioxidant and Hepatoprotective Activity of *Ephedra alata* Extracts against Intoxication with Deltamethrin Pesticide in Male Rats. *Pharmacophore*. 2023; 14(1):19-24.
25. Bradford, M. M., A rapid and sensitive method for the quantitation of microgram quantities of protein utilizing the principle of protein-dye binding. *Anal Biochem.* 1976; 72**:** 248-254.
26. Weckbecker G. and Cory J G. Ribonucleotide reductase activity and growth of glutathione-depleted mouse leukemia L1210 cells in vitro. *Can lett.* 1988; 40**:**257-264.
27. Quintanilha A T. Membrane effects of vitamin E deficiency: bioenergetic and surface charge density studies of skeletal muscle and liver mitochondria. 1981. University of California.
28. Lee K W., Kim Y J., Lee H J. and Lee C Y. Cocoa has more phenolic phytochemicals and a higher antioxidant capacity than teas and red wine. *J. Agric. Food Chem.* 2003; 51:7292-7295.
29. Salah B. Aspect Phytochimique et Activités Antibactérienne, Antioxydante ,Antihépatotoxique et Antinéphrotoxique de la plante *Hammada scoparia* (Pomel) Iljin de la région de Biskra (Sud-Est Algérien). Ph.D. Thesis. University of Annaba. Algeria. 2019. 143p.
30. Djemai Zoughlache S., Etude de l'activité biologique des extraits du fruit de *Zizyphus lotus* L. Ph.D. Thesis. University of Batna. Algeria. 2009: 196.
31. Djahra, A B., Benkaddour M., Benkherara S., Oualabi K., Ghania A. and Jdidi K. Evaluation of total phenolic contents and antioxidant potentials of ten medicinal plants from Algerian Sahara. *Int. J. Bio. Agric. Res.* 2018; 1(2):28-36.
32. Ibtissam L. and Djahra A. B. Phytochemical investigation of *Helianthemum lippii* L. aerial Dum. Cours part and evaluation for its antioxidant activities. *Int. j. second. metab.* 2022; 9:229-237.
33. Jovanovic S V., Steenken S., Tosic M., Marjanovic B. and Simic M G. Flavonoids as antioxidants. *J. Am. Chem. Soc.* 1994; 116**:**4846-4851.
34. Siddhuraju P. and Becker K. The antioxidant and free radical scavenging activities of processed cowpea (*Vigna unguiculata* (L.) Walp.) seed extracts. *Food chem.* 2007; 101**:**10-19.
35. Yuet Ping K., Darah I., Chen Y., Sreeramanan S. and Sasidharan S. Acute and subchronic toxicity study of Euphorbia hirta L. methanol extract in rats. *BioMed research international*. 2013; Vol 2013: 1-14
36. Ukwuani A., Abubakar M., Hassan S. and Agaie B. Toxicological studies of hydromethanolic leaves extract of Grewia crenata. *Int J Pharm Sci Drug Res.* 2012; 4**:**245-249.
37. Kehrer J P. Free radicals as mediators of tissue injury and disease. *Crit. Rev. Toxicol.* 1993; 23**:**21-48.
38. Mongi S., Mahfoud M., Amel B. and Kamel J. Protective effects of vitamin C against haematological and biochemical toxicity induced by deltamethrin in male Wistar rats. *Ecotoxicol Environ Saf.* 2011; 74**:**1765-1769.
39. Mossa A T H., Heikal T M. and Omara E A A. Liver damage associated with exposure to aspirin and diazinon in male rats and the ameliorative effect of selenium. *Biomedicine & Aging Pathology*. 2014; 4**:**137-145.
40. Boutlelis D A., Mounia B., Salah B., Hakim B., Rebiai A., Laib I., Chaima B., Djemaa F. and Islam R. Bio-Synthesis of Zinc Nanoparticle Using *Helianthemum Lippii* L. Extract and Improving in Rats Their Hepatoprotective Effects against Carbon Tetrachloride Induced Liver Damage. *Ann Rom Soc Cell Biol*. 2022; 26**:**1949-1963.
41. Prieto-Simón B., Campàs M., Andreescu S. and Marty J.L. Trends in flow-based biosensing systems for pesticide assessment. *Sens.* 2006; 6**:**1161-1186.

42. Singh B., Saxena A., Chandan B., Anand K., Suri O., Suri K. and Satti N. Hepatoprotective activity of verbenalin on experimental liver damage in rodents. *Fitoterapia.* 1998; 69**:**135-140.
43. Drotman R. and Lawhorn G. Serum enzymes as indicators of chemically induced liver damage. *Drug Chem. Toxicol*. 1978; 1:163-171.
44. Hayes, A W., and Kruger C L. (Eds.). Hayes' Principles and Methods of Toxicology (6e éd.). CRC Press. 2014: 2184.
45. Ettinger S J. Pocket companion to the fourth edition of Textbook of veterinary internal medicine. WB Saunders Company, Philadelphia. 1995: 877.
46. AL-Zorri S G A. Some Physiological And Histological Effect Of Alcoholic Extract *Tribulus Terrestris* In Diabetic Female Rabbits. Ph.D. Thesis. Baghdad University. 2006: 180.
47. Abd Ali A R S. and Ismail H. The protective effect of honey against amikacin-induced nephrotoxicity in rats. *Iraqi J Pharm Sci.* 2012; 21**:** 85-93.
48. Zeghib K., Boutlelis D A., Menai S. and Debouba M. Protective effect of *Atriplex halimus* extract against benzene-induced haematotoxicity in rats. *Ukr Bioch J.* 2021; 93**:**66-76.
49. Gatseva P D. and Argirova M D. High-nitrate levels in drinking water may be a risk factor for thyroid dysfunction in children and pregnant women living in rural Bulgarian areas. *Int J Hyg Environ Health.* 2008; 211**:**555-559.
50. Jublanc C. and Bruckert E. Hypothyroidism and cardiovascular disease: role of new risk factors and coagulation parameters. In *Seminars in Vascular Medicine*, 2004: 145-151.
51. Pearce E N. Hypothyroidism and dyslipidemia: modern concepts and approaches. *Curr. Cardiol. Rep.* 2004; 6**:**451-456.
52. Jahn C E., Schaefer E J., Taam L A., Hoofnagle J H., Lindgren F T., Albers J J., Jones E A. and Brewer H. B. Lipoprotein abnormalities in primary biliary cirrhosis: association with hepatic lipase inhibition as well as altered cholesterol esterification. *World J Gastroenterol.* 1985; 89**:** 1266-1278.
53. James G. and Pickering R. The protective effect of a novel compound RU 18492, on galactosamine-induced hepatotoxicity in the rat. *Arzneimittel-forschung.* 1976; 26**:** 2197-2199.
54. Venukumar M. and Latha M. Antioxidant activity of curculigo orchioides in carbon tetrachloride—induced hepatopathy in rats. *Int J Clin Biochem Res.* 2002; 17**:**80-87.
55. Zeghib K. and Djahra A. Protective role of aqueous extract of *Atriplex halimus* L. Against benzene-induced damage on renal function and glomerular cells in rats. *Asian J Pharm Clin Res.* 2019; 12**:**387-392.
56. Sayyah M., Hadidi N. and Kamalinejad M. Analgesic and anti-inflammatory activity of Lactuca sativa seed extract in rats. *J. Ethnopharmacol.* 2004; 92**:**325-329.
57. Qanwil, T., Malik, A., Mushtaq, A., Alamgeer, Muhamad Fayyaz Ur Rehman, M., & Gohar, U. F. Hypolipidemic and Vasoprotective Potential of *Caralluma edulis*: A Histological and Biochemical Study. *Jordan Journal of Pharmaceutical Sciences*. 2025; 18(1): 21–35.
58. Shrestha, M., K.C., S., Sah, B. S., Kumar Jha, P., Khaitu, S., Pandey, B., Kishor Yadav, R., Gautam, A., & Yadav, B. Hydroethanolic Leaf Extract of *Murraya Koenigii*: Phytochemical Constituents and Biological Evaluation of its Toxicity and Antipyretic Activity in Wistar Albino Rats. *Jordan Journal of Pharmaceutical Sciences.* 2024; 17(4): 811–817.
59. AlMallah, B., Al Laham, S., Alkhatib, R., & Al-Manadili, A. Evaluation of the Therapeutic Effect of Cardamom Extract on Nephropathy Induced by Aspirin in Rats Model. *Jordan Journal of Pharmaceutical Sciences*. 2025; 18(1): 146–159.

الأثر العلاجي لمستخلص نبات *Ziziphus lotus* ضد الاجهاد التأكسدي الناتج عن مبيد Deltamethrin على الفئران

جهرة علي بوتليليس[1*]، بن قدور منية[1]، بن خرارة صالح[2]، العايب ابتسام[1]، بنين شيماء[1]، شريط صبرينة[1]

[1] مخبر البيولوجيا المحيط والصحة كلية علوم الطبيعة والحياة، جامعة الوادي، الجزائر

[2] قسم البيولوجيا، كلية علوم الطبيعة والحياة وعلوم الأرض، جامعة غرداية، الجزائر

ملخص

اختبرت هذه الدراسة الخصائص المضادة للأكسدة للمركبات الطبيعية المستخلصة من نبات السدر (Ziziphus lotus) الطبي، الذي استُخدم تقليديًا لعلاج اضطرابات الكبد ومقاومة التغيرات البيوكيميائية التي يُحدثها مبيد الحشرات دلتامثرين في الجرذان. شملت التجربة 30 جرذًا ذكرًا من نوع ويستر ألبينو، تم تعريضهم لمبيد دلتامثرين (7 ميكرولتر/كغ/يوم). بعد ذلك، تم إعطاء الجرذان مستخلصًا مائيًا من نبات السدر بثلاث جرعات مختلفة (100، 200، و400 مغ/كغ/يوم) عبر التغذية الأنبوبية. بعد 33 يومًا من العلاج، تم التضحية بالجرذان وجمع عينات الدم لتحليل المصل البيوكيميائي. كما تم حفظ أنسجة الكبد لتقييم التأثيرات مضادات الأكسدة. أظهرت النتائج أن عملية الاستخلاص المائي أنتجت 20%، مع تركيز عالٍ من البوليفينولات بلغ 0.142± 12.04 مغ مكافئ حمض الجاليك لكل ملليلتر من المستخلص. علاوة على ذلك، أظهر اختبار DPPH أن مستخلص السدر أبدى نشاطًا مضادًا للأكسدة بشكل كبير، حيث بلغت قيمة 0.146 ± IC50=0.62 ميكروغرام/ملل. أظهرت نتائج النشاط المضاد للأكسدة في الجسم الحي أنه في المجموعة المعرضة لدلتامثرين، انخفض وزن الجسم، بينما زادت مستويات أنزيمات الأسبارتات ترانساميناز (AST) والألانين ترانساميناز (ALT) والفوسفاتاز القلوي (ALP) والأميليز ألفا والكوليسترول والكرياتينين واليوريا ($p < 0.05$ مقابل مجموعة الشاهد)، مما يشير إلى وجود سمية كلوية وكبدية. كما انخفضت مستويات بيروكسيد الدهون (GSH) للدفاعات المضادة للأكسدة وزادت تركيزات المالونديالديهيد (MDA). أدى العلاج بمستخلص السدر بجرعاته الثلاثة إلى تحسين بعض وظائف الكبد والكلى وزيادة وزن الجسم. كما أثبتت وجود المركبات الثانوية في مستخلص السدر أن لها أنشطة بيولوجية كبيرة ومثيرة للاهتمام، بما في ذلك خصائص مضادة للأكسدة قوية في الاختبارات المخبرية وفي الجسم الحي.

الكلمات الدالة: المنتجات الطبيعية، *Ziziphus lotus* ، التغيرات البيوكيميائية، دلتامثرين، الإجهاد التأكسدي.

[*] ***المؤلف المراسل: جهرة علي بوتليليس***

djahra_ab@yahoo.fr

تاريخ استلام البحث 2024/2/28 وتاريخ قبوله للنشر 2024/9/19.

A Review on the Application of Electrospun Herbal Extract-Loaded Metallized Nanofiber Composites as Wound Healing Promoter: Fabrication, Efficacy, and Safety

Hebah Ayash[1], Muhammed Hamitoğlu[1], Soodabeh Davaran[1,2], Ahmet Aydin[1*]

[1]Institute of Health Sciences, Department of Pharmaceutical Toxicology, Yeditepe University, Istanbul, Türkiye.
[2]Department of Medicinal Chemistry, Faculty of Pharmacy, Tabriz University of Medical Sciences, Tabriz, Iran.

ABSTRACT

Electrospinning is a promising technique for wound healing applications, as it enables the fabrication of nanostructures that closely mimic the natural extracellular matrix. This review highlights the potential of electrospun nanofiber composites loaded with herbal extracts and metal nanoparticles as effective wound healing agents. Herbal extracts, known for their antioxidant, anti-inflammatory, and antibacterial properties, contribute significantly to therapeutic outcomes. The incorporation of metal nanoparticles further enhances antimicrobial activity and accelerates the healing process. This review provides a comprehensive overview of the fabrication methods, efficacy, and safety of electrospun herbal extract-loaded metallized nanofiber composites in wound healing applications.

Keywords: Nanofibers; electrospinning; Multimodal nanostructure; Wound healing.

1. INTRODUCTION

Wound dressing is essential for healing, providing a protective barrier and supporting recovery. The global demand for wound care is increasing, with millions suffering from burns and chronic skin ulcers. In the U.S. alone, records show 1.25 million burn patients and 6.5 million with chronic ulcers [1]. In 2021, A survey from 470 hospitals in the U.S. showed that 398,000 patients with burn injuries and 368,000 patients with other inflammatory conditions of skin and subcutaneous tissue received medical treatment [2]. The WHO forecasts 180,000 annual burn deaths and over 640 million diabetic ulcer cases by 2030 [3,4].

There isn't a single dressing that universally suits every condition; instead, clinicians should evaluate each wound individually and choose the appropriate dressing accordingly. Plain gauze, despite its affordability, has limitations, leading to the development of various wound dressings such as films, foams, sponges, hydrogel, and nanofiber dressings. Ideally, a dressing for a specific wound should absorb fluid, protect against microbes, allow gas exchange, maintain a moist environment, be non-toxic, biocompatible, degradable, and promote angiogenesis and tissue regeneration while being easy to replace and remove without sticking to the wound [5,6].

Nanofiber dressings, particularly created through electrospinning, offer advantages over conventional options by mimicking tissue and providing an optimal wound repair environment. They excel in meeting diverse requirements and can incorporate therapeutic or antimicrobial agents for added functionality [1]. Wang et al. (2022) prepared a structurally stable Poly (DL-Lactic-co-caprolactone) (PLCL) scaffold as an

[*]***Corresponding author: Ahmet Aydin***
ahmet.aydin@yeditepe.edu.tr
Received: 24/3/2024 Accepted: 19/9/2024.
DOI: https://doi.org/10.35516/jjps.v18i2.2506

"electronic skin" that transmits endogenous bioelectricity by absorbing wound exudates, thereby promoting the treatment of diabetic wounds [7]. Hu et al. (2023) designed an ultra-thin, breathable, and flexible Janus nanofiber dressing using polyvinylidene fluoride (PVDF) and polycaprolactone (PCL), which can unidirectionally drain excess exudate and kill local bacteria [8]. Lee et al. (2015) developed a nanofibrous membrane using collagen (Col) and Poly Lactic-co-Glycolic Acid (PLGA) to enhance diabetic wound healing. The PLGA/Col nanofiber membrane exhibited sustained release of high concentrations of glucophage for over three weeks, indicating its capacity for prolonged drug delivery. Experimental results showed that Col/PLGA membranes incorporated with glucophage were highly effective in promoting early-stage diabetic wound healing [9]. Anand et al. (2022) prepared multifunctional nanofiber scaffolds based on polyvinyl alcohol/sodium alginate/silk fibroin and loaded with *Centella asiatica*, demonstrating good antibacterial effects against *Pseudomonas aeruginosa* and *Staphylococcus aureus* and promoting wound healing in diabetic rats [10]. Poornima and Korrapati (2017) developed a nanofiber wound dressing consisting of chitosan (CS) and PCL using coaxial electrospinning technology. The dressing loaded with ferulic acid and resveratrol, exhibited antioxidant activity, high compatibility, with epidermal keratinocytes (HaCaT) *in vitro*, and accelerated wound cuts healing *in vivo* [11].

Electrospinning, a cost-effective and straightforward process, is employed to create nanofibers suitable for bandages. These nanofibers, with their extensive surface area and porous nature, can accommodate various substances, including medicines, vitamins, minerals, and herbal extracts, allowing controlled drug release by adjusting fiber structure and morphology [12,13].

This review explores the wound healing process, the concept of electrospinning to produce nanofiber mats for wound dressing, and the potential role of herbal-loaded metallized electrospun nanofibers in promoting wound healing while ensuring safety.

2. WOUND HEALING

Wounds, classified as acute or chronic, disrupt normal skin structure and function. The ideal wound healing process involves organized cell migration and angiogenesis, progressing through hemostasis, inflammation, proliferation, and maturation phases. Local wound treatment aims to address pain, itching, infection, and bleeding, with chronic wounds presenting additional challenges like managing excess exudate and unpleasant odor. Figure 1 illustrates the different phases of wound healing.

The wound healing process begins with events focused on achieving hemostasis, involving a cascade of serine protease events preventing blood loss and leading to the formation of a fibrin clot. The inflammation phase, starting 72 hours post-injury, includes molecular signals facilitating immune cell infiltration and pathogen elimination. The proliferation phase, post-tissue injury, involves angiogenesis and re-epithelialization, driven by various signals. Remodeling, commencing two to three weeks after the injury, focuses on achieving maximum tensile strength through ECM reorganization, resulting in less vascular scar tissue and tissue structure recovery [1,14–16].

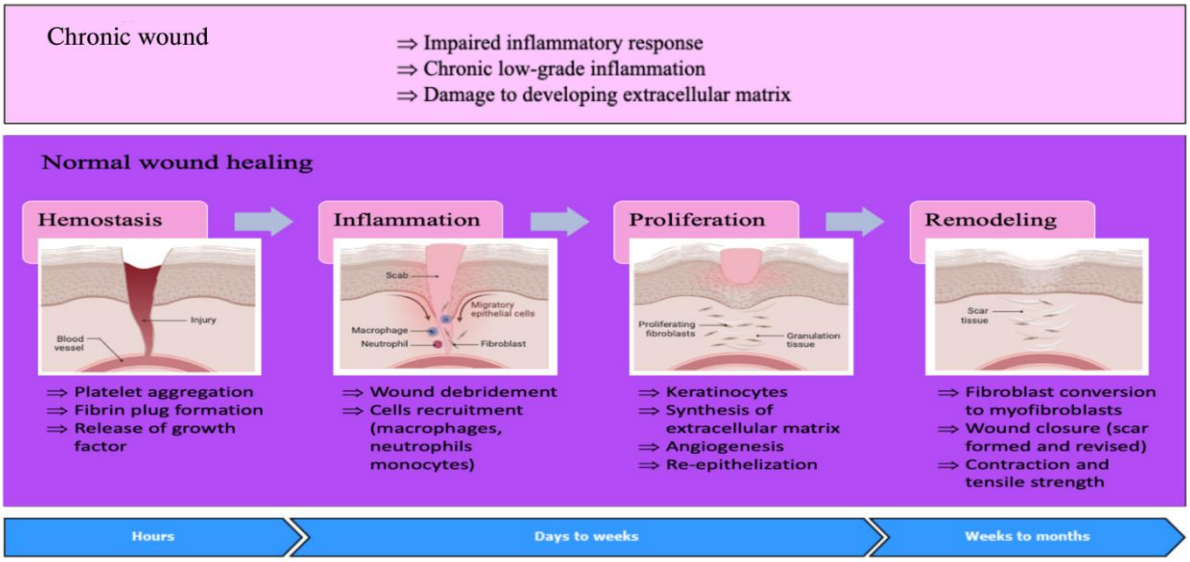

Figure 1. Wound healing phases

Therapeutic options such as coagulants, local anesthetics, anti-inflammatories, and antimicrobial agents can be employed to promote wound healing. However, it's important to note that no single treatment modality can address all aspects of the healing process [16].

The speed at which a wound heals, the strength and function of the healed skin, and the aesthetic appearance of the resulting scar can all be significantly influenced by the proper application and replacement of a dressing. While a moderately moist wound bed can facilitate healing, excessive moisture can lead to maceration. Ideally, a dressing for a specific wound should absorb excess drainage while maintaining an optimal level of moisture. In addition to these primary functions, certain dressings may also offer secondary benefits such as reduced pain during changes, odor control, anti-inflammatory or mild debridement properties, and local antibacterial actions [6,16].

3. ELECTROSPUN NANOFIBERS FOR WOUND HEALING

Nanofiber dressings have garnered attention for their superior qualities compared to traditional options, offering improved anti-inflammatory and antimicrobial properties, better exudate absorption, prolonged dressing lifespan, and enhanced mechanical strength [14]. Nanotechnology advancements are crucial for overcoming the limitations of conventional dressings and enhancing wound healing outcomes. Nanofiber mats, with their high porosity and efficient gas permeation, address these limitations by promoting hemostasis, exudate management, moisture retention, skin regeneration, and cellular respiration [17]. Additionally, electrospun mats with added functionality can serve as personalized bandages [18]. These advantages not only improve patient comfort by reducing dressing changes but also contribute to cost-effective treatment [12]. This review discusses various approaches to achieving these benefits.

3.1. Basic Principles of Electrospinning

Electrospinning is an electrohydrodynamic process where electrically charged fluids are set in motion by applied electric fields. In this process, a liquid droplet is electrified to generate a jet, which then undergoes

stretching and elongation to form fibers. The electrospinning apparatus includes a high-voltage power supply, a collector, and a spinneret. As voltage is applied, the electrospinning fluid is injected into the spinneret, gradually changing its morphology until it reaches the critical voltage. At this point, the droplet at the tip, supported by surface tension, forms a Taylor cone. The liquid jet must evaporate before fibers collect on the collector, reaching a specific distance and entering the bending and whiplash stage [1,5,12,14].

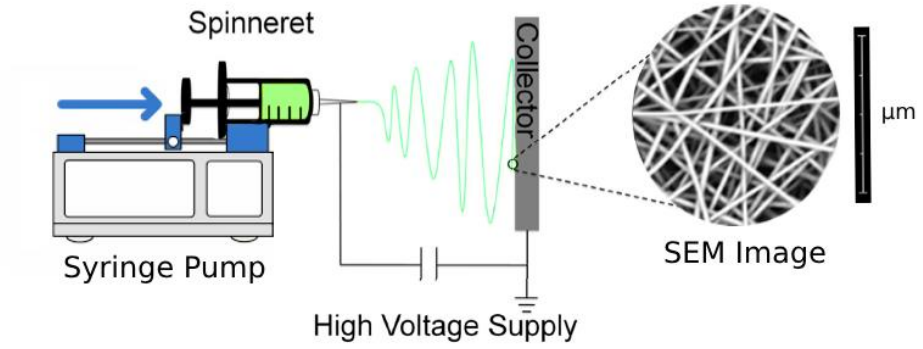

Figure 2. Elcectospinning basic principle

Several factors influence electrospinning and can be categorized into three main groups: apparatus, precursor solution, and environmental conditions. Apparatus-related variables include the setup type, collector type (stationary or rotating), and parameters such as voltage, spinneret-to-collector distance, and flow rate. The properties of the precursor solution—such as conductivity, surface tension, viscosity, and concentration—depend on the choice of polymer and solvent. The polymer concentration must be adjusted to a critical value to produce uniform nanofibers without beads. When the polymer concentration is too low, the entangled polymer chains may break into fragments before reaching the collector, resulting in bead formation. Conversely, if the polymer concentration exceeds a critical threshold, it may disrupt the solution flow through the needle tip, leading to defective or beaded nanofibers. Environmental conditions, particularly temperature and humidity, also influence fiber synthesis and should be carefully controlled. Higher temperatures reduce solution viscosity, leading to a decrease in average fiber diameter. In contrast, high humidity can induce polymer swelling, which increases the average fiber diameter [19].

Precursor solution is usually made of polymer solutions or polymer melts. The polymer matrix can be synthetic, natural, or a sensible blend of polymers to produce the required properties of the nanofiber. The most commonly used polymers are summarized in Table 1.

To create wound healing scaffolds, biopolymers are often mixed with synthetic polymers to alter the porous fiber mat's degradative, mechanical, and/or morphological properties to meet the individual needs of each patient [5].

Table 1: Most commonly used polymers' types and applications [5,20,21]

Category		Polymer Examples		Applications
Synthetic	Biocompatible	• Poly(vinyl alcohol) (PVA) • Poly(lactic acid) (PLA) • Poly(glycolic acid) (PGA) • Poly(lactic-co-glycolic acid) (PLGA) • Poly(ethylene oxide) (PEO) • Polycaprolactone (PCL) • Poly(hydroxybutyrate) (PHB)		• Tissue engineering • Drug delivery • Wound healing • Scaffolds for cell growth • Filtration
Natural	Polysaccharide	Plant	• Alginate • Dextran • Cellulose	• Wound healing • Drug delivery • Tissue engineering • Enzyme immobilization • Scaffolds for cell growth • Cosmetics
		Animal	• Chitosan (CS) • Hyaluronic acid	
	Protein	• Gelatine • Collagen • Silk fibroin		

3.1.2. Incorporation of bioactive agent into electrospun nanofibers

Loading an active agent into nanofiber mats can be achieved through various methods, depending on the desired properties of the final product [5]. For burst release, the active agent is suspended in the electrospinning blend to distribute it throughout or on the fiber's surface. Coaxial electrospinning is employed when abrupt release is undesirable or when the active agent is solvent-labile, forming core/shell fibers using a concentric needle configuration. Another approach involves using an emulsion as the feeding solution, with a surfactant added during electrospinning to create a core/shell structure. This technique protects proteins, DNA, and peptides from harsh solvents, enabling their incorporation. Finally, dip-coating imparts desired qualities to electrospun mats by immersing them in a solution [17].

Loading efficacy and release profiles can be assessed using appropriate analytical methods, such as spectroscopy or high-performance liquid chromatography [22]. Various active agents—including antibacterial particles, growth factors, stem cells, vitamins, and other effective wound-healing factors—can be incorporated into electrospun nanofibers.

In one study, lemon oil was used as a highly antibacterial active agent to create cellulose acetate nanofiber membranes. The investigation examined various properties and demonstrated that lemon oil-loaded cellulose acetate nanofibers maintained antibacterial efficacy, eliminating *Escherichia coli* and *Staphylococcus aureus* even at low lemon oil concentrations. The nanofiber structure retained its antibacterial properties after two months, suggesting its potential as a long-lasting bioactive wound dressing [23].

4. MEDICINAL PLANTS IN WOUND HEALING

Throughout history, herbal remedies have been valued for their healing properties, with many plants used in traditional medicine for treating burns, wounds, and cuts. These remedies often offer antioxidant, antibacterial, and anti-inflammatory benefits. Illustrative examples include *Sphagneticola trilobata*, *Aloe vera*, *Panax ginseng*, and *Hypericum perforatum*. Extracts from plants like *Centella asiatica* and *Curcuma longa* have shown support for key wound healing processes like angiogenesis and collagen formation [24,25]. Researchers are now exploring new formulations and dressings to create stable, sustainable,

and cost-effective wound care treatments. The use of innovative materials and advancements in nanotechnology have led to improved wound management, focusing more on patients' needs [26].

5. METALLIC AND INORGANIC NANOPARTICLES IN WOUND HEALING

Metallized nanmaterials, featuring unique physicochemical characteristics like a large specific surface area and excellent surface properties, play a crucial role in biomedicine. Nanoparticles like gold, silver, iron, silicon, germanium, and cadmium selenide possess antibacterial properties, aiding wound healing and combating antibiotic resistance. These nanoparticles are increasingly utilized in medical applications for drug delivery, imaging, diagnostics, and tissue engineering [27,28]. In addition, incorporating inorganic nanoparticles into nanofibers offers a promising approach to regulate release kinetics from biomaterials.

Gold nanoparticles applied topically speed up wound healing by boosting the production of growth factors, cytokines, and collagen [29]. Silver nanoparticles fight bacteria and are useful for treating wounds [30]. Zinc oxide nanoparticles help tissues regenerate by promoting processes like tissue granulation and collagen deposition [31]. Mesoporous silica nanoparticles (MSNs) are versatile in medical applications and aid wound healing by helping blood clot [32–34].

6. COMBINATION OF HERBAL EXTRACT AND METALLIC/INORGANIC NANOPARTICLES IN THE FABRICATION OF NANOFIBROUS WOUND DRESSING

There are several parameters depending on the application of nanofibers. The water absorption capacity of electrospun nanofibers plays an important role in wound healing. Nanofibers can retain moisture and nutrients in the wound area and also increase cell adhesion and proliferation with a higher swelling ratio. Adequate mechanical properties of engineered electrospun nanofibers are another important parameter for the formation of new skin tissue and resistance to biological degradation during the wound healing process. Plant extracts may act as a reinforcing agent and increase the tensile strength of nanofibers, leading to enhanced wound healing. On the other hand, the solubility of plant extracts is important in choosing the type of nanofibers, and depending on the type of plant extract, suitable biomaterials are selected for making nanofibers[26]. Utilizing nanotechnology for improved phytochemical delivery involves incorporating plant-derived substances into nanomaterials like nanoparticles and nanofibers. These environmentally friendly and non-toxic nanocarriers provide controlled release of active plant materials in wound treatment. Plant extract-loaded nanofibers, with unique properties, exhibit antimicrobial, anti-inflammatory, antioxidant, antiseptic, and antiviral effects, showcasing their potential in wound healing [35,36].

In a study, St. John's Wort infused oil was incorporated into a CS cryogel for use as a wound dressing material. The investigation revealed antimicrobial activity, particularly against *E. coli* and *L. pneumophila*. Additionally, the presence of free radical scavenging activity makes it a promising candidate for wound healing [37].

Another study introduced a silk fibroin-curcumin-based nanofiber in combination with PCL and PVA for sustained drug release and oxygen delivery to diabetic wounds. *In vivo* studies on diabetes-induced mice demonstrated a higher wound healing rate compared to the control group, highlighting the potential of the nanofibrous tissue formulation with no dermal irritation [38]

Metal nanoparticles can be immobilized on nanofibers, which brings a new generation of nanomaterials that have potential applications in a wide range of fields such as electronics, medicine, sensors. As a result, many efforts have been made to synthesize, identify and use metal nanofiber composites with well-controlled dimensions and properties. this modified fiber can be called metallized nanofibers or composite nanofibers with metallic nanoparticles.

Metallic nanofiber-based composites, created through electrospinning, involve the integration of metal nanoparticles into polymer nanofibers. This combination, known as metallized nanofibers, can be achieved through *in situ* reactions of metallic precursors during electrospinning. Alternatively, precursor metal nanoparticles can be added to the polymer solution, and their nanofibers can be prepared through electrospinning [39]. These nanocomposites offer a unique combination of nanofiber qualities and metallic nanoparticle properties, including formability, stability, and conductivity. Metallized nanofibers find applications in tissue engineering due to their exceptional antimicrobial properties and plasticity [40–43]. They boast strong mechanical properties, providing a non-toxic and antibacterial foundation for constructing drug-loaded wound healing platforms. Metallized nanofibers are new biomaterials obtained by combining metals or metal nanoparticles with nanofibers. Due to their unique physical and chemical properties, metallized nanofibers are rapidly developing in the fields of physical chemistry, materials science, and biomedical applications.

Silver nanoparticles dispersed in a CS matrix are electrospun, resulting in immobilized cubic-structured silver nanofibers [44]. Researchers incorporated MSNs into CS, forming porous CS-silica composite microspheres with hemostatic properties for controlling traumatic hemorrhaging. Positive results were observed in a rat liver laceration model, with no adverse effects in cytotoxicity and histological analysis [45]. Additionally, gentamicin-loaded MSNs-PCL nanofibers were produced, demonstrating sustained antibiotic release to prevent post-surgery wound infections. MSNs played a crucial role in drug delivery, acting as release modifiers and bioactivity protectors. The antimicrobial activity of the fibers was confirmed, with 50% drug release after 40 hours and complete release after 136 hours [22].

Herbal extract-loaded metallized nanofibers have garnered research attention. In a study, MSNs were incorporated into PCL/Curcumin nanofibers. Antibacterial studies encompassing both gram-positive and gram-negative bacteria, in vitro experiments with Swiss 3T6 cell lines, and in vivo studies on female Wister rats were conducted. Results indicated enhancements in the zone of inhibition, tissue re-epithelization, collagen deposition, and granulation tissue formation. Using the fabricated nanofibers on rats demonstrated 99% scar-less wound healing within 3 weeks [46].

7. SAFETY OF HERBAL EXTRACT-LOADED MULTIMODAL NANOFIBERS

Ensuring the safety of nanofibers loaded with various active ingredients requires comprehensive toxicity testing. Key assessments, such as in vitro cytotoxicity, irritation, and sensitization, form the forefront of toxicity evaluations. Additionally, genotoxicity serves as a crucial endpoint, underscoring the necessity of its application to novel materials.

7.1. Genotoxicity evaluation of nanomaterials

Genotoxicity from nanomaterial exposure can induce transient or permanent genetic changes through direct or indirect mechanisms. Direct mechanisms involve physical contact between nanomaterials and the nucleus, leading to DNA damage like chromosomal breaks. Indirect mechanisms occur when nanomaterials dissolve, releasing harmful ions or reactive oxygen species (ROS), inducing oxidative stress. Additionally, molecules released by nanomaterials can interfere with DNA replication and cell division, further contributing to genotoxic effects.

The genotoxicity of nanomaterials depend on factors like dose, exposure duration, size, surface characteristics, chemical composition, and shape. The genotoxicity mechanism is primarily influenced by the uptake method. Smaller nanomaterials (<10nm) have a higher chance of entering the nucleus directly through nuclear pores, while larger ones (>10nm) may enter through endocytosis or during mitosis when the nuclear membrane dissolves. Indirect damage is more common, triggering inflammation

and chronic immune cell responses [47–49].

Genotoxicity biomarkers include gene mutations, chromosomal damage, and DNA damage. In the genotoxic risk assessment of nanomaterials, three commonly employed *in vitro* methodologies are: (a) Tests for mammalian gene mutation, utilizing Thymidine kinase (Tk) and hypoxanthine phosphoribosyltransferase (Hprt) as a basis for gene mutation, (b) Chromosomal damage tests, with clastogenicity (structural chromosome damage) and aneugenicity (numerical chromosome alterations) as key endpoints, employing assays such as the micronucleus test, and (c) the comet test for assessing DNA damage, serving as the preferred technique for evaluating DNA strand breakage and quantifying damage to cellular DNA [47,48].

It is worthy to note that, before introducing nanomaterial stock solutions to cultured cells in *in vitro* genotoxicity testing systems, they are typically diluted in a cell culture medium. The interactions of nanomaterials, whether particle-particle or particle-cell, undergo alterations when suspended in cell culture medium or other biological fluids. These changes may affect the nanomaterials size, shape, composition, surface chemistry, as well as the temperature, pH, ionic strength, and protein content of the surrounding fluid. Techniques such as dynamic light scattering (DLS) and nanoparticle tracking analysis (NTA) determine nanomaterial size and distribution, while microscopic methods like atomic force microscopy (AFM), scanning electron microscopy (SEM), and transmission electron microscopy (TEM) directly observe nanomaterials. Zeta potential, measuring the electrostatic potential of the electrical double layer where nanomaterials are suspended and describing their surface charge.

7.2. Cytotoxicity testing

Various cytotoxicity assessment techniques exist, with viability tests being common. These tests, following OECD Test Guidelines 476 and 490, measure cell proliferation, survival, and colony formation. Methods like Trypan blue exclusion or dual staining with fluorescent dyes indicate damaged cell membranes. Intracellular material leakage, detected by LDH assays like Alamar Blue or MTT tests, identifies dead cells. Studies evaluating nanofiber safety include one examining composite CS microspheres loaded with mesoporous silica. Using the MTT method on mouse embryonic fibroblast cells, it demonstrated good biocompatibility and non-cytotoxicity, suggesting their safety for medical use [47,48].

7.3. Irritation

Historically, skin irritation and corrosion experiments often relied on animal testing, specifically involving rabbits following OECD Test Guideline (TG 404). Ethical considerations have led to the exploration of alternative in vitro methods to assess skin irritation and corrosion, seeking to replace animal-based approaches [50]. Several three-dimensional (3D) human skin models, such as SkinEthic™, EpiDerm™, and EpiSkin™, serve as substitutes for in vivo tests, utilizing reconstructed human epidermis closely mimicking histological, morphological, biochemical, and physiological characteristics of human skin [51,52]. *In vitro* testing with cultivated skin-derived cell lines has assessed the skin irritation potential of nanomaterials. For instance, titanium nanoparticles and quantum dot nanoparticles exhibited reduced viability in cultured HaCaT human keratinocytes but showed no effect on a human skin equivalent model [53,54] Conversely, nano silica nanoparticles induced cell death in cultured human keratinocytes but demonstrated no cytotoxicity in a human skin equivalent model [55]. Exposure of EpiDerm™ to TiO_2 nanoparticles did not cause skin irritation symptoms in one study [56]. Furthermore, the application of TiO_2 nanoparticles and ZnO nanoparticles, either alone or in combination, did not induce irritation or corrosion on undamaged rabbit skin or KeraSkin, a 3D human skin model [57].

7.4. Sensitization

While many studies have explored skin sensitization caused by certain chemicals, limited research exists on the potential sensitization effects of nanomaterials. The skin sensitization process involves the covalent interaction of

electrophilic substances with primary amines in skin proteins and nucleophilic thiol as the initial step. Subsequently, inflammatory reactions and modifications in gene expression occur in keratinocytes, involving cell signaling pathways like the antioxidant/electrophile response element (ARE) [58]. The ARE-Nrf$_2$ Luciferase KeratinoSens™ test is a tool representative of these events, capable of distinguishing between skin sensitizers and non-sensitizers in line with the United Nations Globally Harmonized System of Classification and Labelling of Chemicals standards [53].

In a study by Kim et al., the ARE-Nrf2 Luciferase KeratinoSens™ test assessed skin sensitization induced by seven different metal oxide nanoparticles, including nickel oxide, titanium oxide, copper oxide, cobalt oxide, zinc oxide, iron oxide, and cerium oxide on KeratinoSens™ cells. Notably, copper oxide nanoparticles produced a positive response, while the other nanoparticles exhibited no response [59].

8. CONCLUSION

Electrospinning technology finds applications in medicine, including tissue engineering scaffolds, drug delivery, and wound dressings. Simultaneous production of nanofibers with natural and mixed polymers enhances biocompatibility, biodegradability, and physical characteristics. The nanofibers, with high surface area and extracellular matrix -like properties, offer a unique delivery method for herbal medicine extracts and bioactive components. As genotoxicity is a main concern of nanomaterials, more studies for a better understanding of the mechanism of toxicity and the development of more robust *in vitro* toxicity assay methods. Further studies are needed to explore herbal loaded metallized nanofiber efficacy, safety, co-encapsulation with inorganic materials, synergistic activity, controlled release, and scalability.

REFERENCES

1. Rieger K.A., Birch N.P. and Schiffman J.D. Designing electrospun nanofiber mats to promote wound healing—a review. *J. Mater. Chem. B.* 2013; 1:4531–4541.
2. Center for Health Statistics N. National Hospital Ambulatory Medical Care Survey: 2021 Emergency Department Summary Tables. *Centers for Disease Control and Prevention.* 2021. Available from: https://ftp.cdc.gov/pub/Health_
3. WHO. Burns. *WHO Newsroom* n.d. Available from: https://www.who.int/news-room/fact-sheets/detail/burns
4. WHO. Director-General's live speech at Maria Holder Diabetes Center for the Caribbean—"Early Detection for Better Outcomes with Diabetes". *WHO Speeches* n.d. Available from: https://www.who.int/director-general/speeches/detail/who-director-general-s-live-speech-at-maria-holder-diabetes-center-for-the-caribbean---early-detection-for-
5. Liu X., Xu H., Zhang M. and Yu D.G. Electrospun medicated nanofibers for wound healing: Review. *Membranes (Basel).* 2021; 11(9):770.
6. Yaşayan G., Alarçin E., Bal-Öztürk A. and Avci-Adali M. Natural polymers for wound dressing applications. *Stud. Nat. Prod. Chem.* 2022; 75:367–441.
7. Wang J., Lin J., Chen L., Deng L. and Cui W. Endogenous electric-field-coupled electrospun short fiber via collecting wound exudation. *Adv. Mater.* 2022; 34:2108325. Available from: https://onlinelibrary.wiley.com/doi/full/10.1002/adma.202108325
8. Hu Q., Wan X., Wang S., Huang T., Zhao X., Tang C., et al. Ultrathin, flexible, and piezoelectric Janus nanofibrous dressing for wound healing. *Sci. China Mater.* 2023; 66:3347–3360.

9. Lee C.H., Chang S.H., Chen W.J., Hung K.C., Lin Y.H., Liu S.J., et al. Augmentation of diabetic wound healing and enhancement of collagen content using nanofibrous glucophage-loaded collagen/PLGA scaffold membranes. *J. Colloid Interface Sci.* 2015; 439:88–97.
10. Anand S., Rajinikanth P.S., Arya D.K., Pandey P., Gupta R.K., Sankhwar R., et al. Multifunctional biomimetic nanofibrous scaffold loaded with Asiaticoside for rapid diabetic wound healing. *Pharmaceutics.* 2022; 14. Available from: https://pubmed.ncbi.nlm.nih.gov/35214006/
11. Poornima B. and Korrapati P.S. Fabrication of chitosan-polycaprolactone composite nanofibrous scaffold for simultaneous delivery of ferulic acid and resveratrol. *Carbohydr. Polym.* 2017; 157:1741–1749.
12. Croitoru A.M., Ficai D., Ficai A., Mihailescu N., Andronescu E. and Turculet C.F. Nanostructured fibers containing natural or synthetic bioactive compounds in wound dressing applications. *Materials.* 2020; 13(24):5765.
13. Aljamal S., Sotari S., Tarawneh O., Al-Hashimi N., Hamed S., Al-Hussein M., et al. Preparation and characterization of drug-loaded, electrospun nanofiber mats formulated with zein or zein-based mixtures for wound healing applications. *Jordan J. Pharm. Sci.* 2023; 16:475.
14. Mbese Z., Alven S. and Aderibigbe B.A. Collagen-based nanofibers for skin regeneration and wound dressing applications. *Polymers (Basel).* 2021; 13(11):1884.
15. *Basic principles of wound healing*. UpToDate.
16. *Basic principles of wound management*. UpToDate.
17. Patel Z., Gharat S., Al-Tabakha M.M., Ashames A., Boddu S.H.S. and Momin M. Recent advancements in electrospun nanofibers for wound healing: Polymers, clinical and regulatory perspective. *Crit. Rev. Ther. Drug Carrier Syst.* 2022. Available from: www.begellhouse.com
18. Behere I. and Ingavle G. In vitro and in vivo advancement of multifunctional electrospun nanofiber scaffolds in wound healing applications: Innovative nanofiber designs, stem cell approaches, and future perspectives. *J. Biomed. Mater. Res. A* 2022; 110:443–461.
19. Haider A., Haider S. and Kang I.K. A comprehensive review summarizing the effect of electrospinning parameters and potential applications of nanofibers in biomedical and biotechnology. *Arab. J. Chem.* 2018; 11:1165–1188.
20. Islam M.S., Ang B.C., Andriyana A. and Afifi A.M. A review on fabrication of nanofibers via electrospinning and their applications. *SN Appl. Sci.* 2019; 1:1248.
21. Hiwrale A., Bharati S., Pingale P. and Rajput A. Nanofibers: A current era in drug delivery system. *Heliyon.* 2023; 9:e15350.
22. Chen X., Xu C. and He H. Electrospinning of silica nanoparticles-entrapped nanofibers for sustained gentamicin release. *Biochem. Biophys. Res. Commun.* 2019; 516:1085–1089.
23. Beikzadeh S., Akbarinejad A., Swift S., Perera J., Kilmartin P.A. and Travas-Sejdic J. Cellulose acetate electrospun nanofibers encapsulating Lemon Myrtle essential oil as active agent with potent and sustainable antimicrobial activity. *React. Funct. Polym.* 2020; 157:104770.
24. Sharma A., Khanna S., Kaur G. and Singh I. Medicinal plants and their components for wound healing applications. *Futur. J. Pharm. Sci.* 2021; 7:88.
25. Sardi V.F., Astika, Jalius I.M. and Ismed F. Quantification of mangiferin from the bioactive fraction of mango leaves (*Mangifera indica* L.) and evaluation of wound-healing potential. *Jordan J. Pharm. Sci.* 2023; 16:595–606.
26. Liu H., Bai Y., Huang C., Wang Y., Ji Y., Du Y. *et al.* Recent progress of electrospun herbal medicine nanofibers. *Biomolecules.* 2023; 13:1225.
27. Lu Z., Yu D., Nie F., Wang Y. and Chong Y. Iron nanoparticles open up new directions for promoting healing in chronic wounds in the context of bacterial infection. *Pharmaceutics.* 2023; 15:2327.

28. Ibraheem L.M. and Khattabi A.M. Studying the effect of functional group and size of silica nanoparticles loaded with quercetin on their *in vitro* characteristics. *Jordan J. Pharm. Sci.* 2022; 15:569–582.
29. Grant S.A., Spradling C.S., Grant D.N., Fox D.B., Jimenez L., Grant D.A. *et al.* Assessment of the biocompatibility and stability of a gold nanoparticle collagen bioscaffold. *J. Biomed. Mater. Res. A* 2014; 102:332–339.
30. Wang L., Wu Y., Xie J., Wu S. and Wu Z. Characterization, antioxidant and antimicrobial activities of green synthesized silver nanoparticles from *Psidium guajava* L. leaf aqueous extracts. *Mater. Sci. Eng. C.* 2018; 86:1–8.
31. Mendes C., Thirupathi A., Corrêa M.E.A.B., Gu Y. and Silveira P.C.L. The use of metallic nanoparticles in wound healing: New perspectives. *Int. J. Mol. Sci.* 2022; 23:7559.
32. Ahmed H., Gomte S.S., Prathyusha E., A P. and Agrawal M. Biomedical applications of mesoporous silica nanoparticles as a drug delivery carrier. *J. Drug Deliv. Sci. Technol.* 2022; 69:103093.
33. Gryshchuk V. and Galagan N. Silica nanoparticles effects on blood coagulation proteins and platelets. *Biochem. Res. Int.* 2016; 2016:1–8.
34. Wu H., Li F., Wang S., Lu J., Li J., Du Y. *et al.* Ceria nanocrystals decorated mesoporous silica nanoparticle-based ROS-scavenging tissue adhesive for highly efficient regenerative wound healing. *Biomaterials.* 2018; 151:66–77.
35. Hajialyani M., Tewari D., Sobarzo-Sánchez E., Nabavi S.M., Farzaei M.H. and Abdollahi M. Natural product-based nanomedicines for wound healing purposes: Therapeutic targets and drug delivery systems. *Int. J. Nanomedicine.* 2018; 13:5023–5043.
36. Huesca-Urióstegui K., García-Valderrama E.J., Gutierrez-Uribe J.A., Antunes-Ricardo M. and Guajardo-Flores D. Nanofiber systems as herbal bioactive compounds carriers: Current applications in healthcare. *Pharmaceutics.* 2022; 14:2582.
37. Bölgen N., Demir D., Yalçın M.S. and Özdemir S. Development of *Hypericum perforatum* oil incorporated antimicrobial and antioxidant chitosan cryogel as a wound dressing material. *Int. J. Biol. Macromol.* 2020; 161:1581–1590.
38. Agarwal Y., Rajinikanth P.S., Ranjan S., Tiwari U., Balasubramaniam J., Pandey P. *et al.* Curcumin-loaded polycaprolactone/polyvinyl alcohol–silk fibroin-based electrospun nanofibrous mat for rapid healing of diabetic wound: *In vitro* and *in vivo* studies. *Int. J. Biol. Macromol.* 2021; 176:376–386.
39. Mohanty S., Maity T.N., Mukhopadhyay S., Sarkar S., Gurao N.P. and Bhowmick S. *et al.* Powder metallurgical processing of equiatomic AlCoCrFeNi high entropy alloy: Microstructure and mechanical properties. *Mater. Sci. Eng. A.* 2017; 679:299–313.
40. Alven S. and Aderibigbe B.A. Hyaluronic acid-based scaffolds as potential bioactive wound dressings. *Polymers (Basel).* 2021; 13:2102.
41. Yan J., Li W., Tian H., Li B., Yu X., Wang G. *et al.* Metal-phenolic nanomedicines regulate T-cell antitumor function for sono-metabolic cancer therapy. *ACS Nano.* 2023; 17:14667–14677. Available from: https://pubs.acs.org/doi/full/10.1021/acsnano.3c02428
42. Zhu C. and Kaldis P. Retraction: Metallic ions encapsulated in electrospun nanofiber for antibacterial and angiogenesis function to promote wound repair. *Front. Cell Dev. Biol.* 2021; 9:1058556.
43. Bhadauriya P., Mamtani H., Ashfaq M., Raghav A., Teotia A.K., Kumar A. *et al.* Synthesis of yeast-immobilized and copper nanoparticle-dispersed carbon nanofiber-based diabetic wound dressing material: Simultaneous control of glucose and bacterial infections. *ACS Appl. Bio Mater.* 2018; 1:246–258.
44. Santiago-Castillo K., Torres-Huerta A.M., Del Ángel-López D., Domínguez-Crespo M.A., Dorantes-Rosales H., Palma-Ramírez D. *et al.* In situ growth of silver nanoparticles on chitosan matrix for the synthesis of hybrid electrospun fibers: Analysis of microstructural and mechanical properties. *Polymers (Basel).* 2022; 14:4127.

45. Sun X., Fang Y., Tang Z., Wang Z., Liu X. and Liu H. Mesoporous silica nanoparticles carried on chitosan microspheres for traumatic bleeding control. *Int. J. Biol. Macromol.* 2019; 127:311–319.
46. Rathinavel S., Korrapati P.S., Kalaiselvi P. and Dharmalingam S. Mesoporous silica incorporated PCL/Curcumin nanofiber for wound healing application. *Eur. J. Pharm. Sci.* 2021; 167:106012.
47. Kirsch-Volders M., Decordier I., Elhajouji A., Plas G., Aardema M.J. and Fenech M. *In vitro* genotoxicity testing using the micronucleus assay in cell lines, human lymphocytes and 3D human skin models. *Mutagenesis.* 2011; 26:177–184.
48. Kohl Y., Rundén-Pran E., Mariussen E., Hesler M., Yamani N. El, Longhin E.M. *et al.* Genotoxicity of nanomaterials: Advanced *in vitro* models and high throughput methods for human hazard assessment—A review. *Nanomaterials.* 2020; 10:1919.
49. Barua S. and Mitragotri S. Challenges associated with penetration of nanoparticles across cell and tissue barriers: A review of current status and future prospects. *Nano Today.* 2014; 9:223–243.
50. Kim H., Choi J., Lee H., Park J., Yoon B. I., Jin S.M. *et al.* Skin corrosion and irritation test of nanoparticles using reconstructed three-dimensional human skin model, EpiDerm™. *Toxicol. Res.* 2016; 32:311–316.
51. OECD. Test No. 439: In Vitro Skin Irritation: Reconstructed Human Epidermis Test Method [Internet]. OECD; 2021 [cited 2024 Mar 13]. Available from: https://www.oecd-ilibrary.org/environment/test-no-439-in-vitro-skin-irritation-reconstructed-human-epidermis-test-method_9789264242845-en
52. OECD. Test No. 431: In vitro skin corrosion: reconstructed human epidermis (RHE) test method [Internet]. OECD; 2015 [cited 2024 Mar 13]. Available from: https://www.oecd-ilibrary.org/environment/test-no-431-in-vitro-skin-corrosion-reconstructed-human-epidermis-rhe-test-method_9789264242753-en
53. Park Y.H., Jeong S.H., Yi S.M., Choi B.H., Kim Y.R., Kim I.K. *et al.* Analysis for the potential of polystyrene and TiO_2 nanoparticles to induce skin irritation, phototoxicity, and sensitization. *Toxicol. In Vitro.* 2011; 25:1863–1869.
54. Jeong S.H., Park Y.H., Choi B.H., Kim J.H., Sohn K.H., Park K.L., Kim M.K. and Son S.W. Assessment of the skin irritation potential of quantum dot nanoparticles using a human skin equivalent model. *J. Dermatol. Sci.* 2010; 59:147–148.
55. Park Y.H., Kim J.N., Jeong S.H., Choi J.E., Lee S.H., Choi B.H. *et al.* Assessment of dermal toxicity of nanosilica using cultured keratinocytes, a human skin equivalent model and an *in vivo* model. *Toxicology.* 2010; 267:178–181.
56. Miyani V.A. and Hughes M.F. Assessment of the *in vitro* dermal irritation potential of cerium, silver, and titanium nanoparticles in a human skin equivalent model. *Cutan. Ocul. Toxicol.* 2017; 36:145–151.
57. Choi J., Kim H., Choi J., Oh S.M., Park J., Park K. Skin corrosion and irritation test of sunscreen nanoparticles using reconstructed 3D human skin model. *Environ. Health Toxicol.* 2014; 29:e2014004.
58. OECD. The Adverse Outcome Pathway for Skin Sensitisation Initiated by Covalent Binding to Proteins [Internet]. OECD; 2014 [cited 2024 Mar 13]. Available from: https://www.oecd-ilibrary.org/environment/the-adverse-outcome-pathway-for-skin-sensitisation-initiated-by-covalent-binding-to-proteins_9789264221444-en
59. Kim S.H., Lee D.H., Lee J.H., Yang J.Y., Seok J.H., Jung K., et al. Evaluation of the skin sensitization potential of metal oxide nanoparticles using the ARE-Nrf2 Luciferase KeratinoSens™ assay. *Toxicol. Res.* 2021; 37:277–284.

مراجعة لتطبيق مركبات الألياف النانوية المعدنية المحملة بمستخلصات الأعشاب المغزولة كهربائيًا كمحفز لالتئام الجروح: التصنيع، الفعالية، والسلامة

هبه عياش[1]، محمد حميد أوغلو[1]، سودابه دافاران[2،1]، أحمد أيدن*[1]

[1]معهد العلوم الصحية، قسم السموم الدوائية، جامعة يدي تبة، إسطنبول، تركيا.

[2]قسم الكيمياء الطبية، كلية الصيدلة، جامعة تبريز للعلوم الطبية، تبريز، إيران.

ملخص

يُعد الغزل الكهربائي تقنية واعدة لتطبيقات التئام الجروح، حيث يُنتج هياكل نانوية تُشبه النّسيج خارج الخليّة الطبيعية. تُركز هذه المراجعة على مركبات الألياف النانوية المعدنية المُحمَّلة بمستخلصات عشبية مُغزولة كهربائيًا كمُحفِّزات لالتئام الجروح. تُعزز المستخلصات العشبية، المعروفة بخصائصها العلاجية كمضادات الأكسدة والعوامل المضادة للبكتيريا، العناية بالجروح. كما يُعزز دمج الجسيمات النانوية المعدنية الوقاية من العدوى وتعزيز التئام الجروح. تهدف هذه المراجعة إلى تقديم لمحة عامة عن مركبات الألياف النانوية المعدنية المُحمَّلة بمستخلصات عشبية مُغزولة كهربائيًا، وتصنيعها، وفعاليتها، وسلامتها في تطبيقات التئام الجروح.

الكلمات الدالة: الألياف النانوية؛ الغزل الكهربائي؛ بنية نانوية متعددة الوسائط؛ التئام الجروح.

* ***المؤلف المراسل: أحمد أيدن***

ahmet.aydin@yeditepe.edu.tr

تاريخ استلام البحث 2024/3/24 وتاريخ قبوله للنشر 2024/9/19.

Jordan Journal of Pharmaceutical Sciences, Volume 18, No. 2, 2025

Unveiling the Phytochemical Profiling, hypolipidemic, hypoglycemic and antioxidant effects of different extracts from *Lavandula stoechas* L. (French lavender) grown in Palestine

Belal Rahhal[1, *], Nidal Jaradat[2, *], Linda Issa[2] , Fatimah Hussein[2], Gidaa Amara[2], Leen Gazawi[2], Sahar Alheen[2], Waed Jbara[2], Zan Baransi[2] and Zena keadan[2]

[1] Department of Biomedical Sciences, Faculty of Medicine and Health Sciences, An-Najah National University, Nablus, Palestine.
[2] Department of Pharmacy, Faculty of Medicine and Health Sciences, An-Najah National University, Nablus, Palestine.

ABSTRACT

Background: *Lavandula stoechas* L. (French lavender; Lamiaceae) is a well-known Lavender species in the Mediterranean Sea Basin. It is widely used in traditional medicine owing to its wound healing, antispasmodic, and expectorant properties. As a result, the current study was the first to investigate the phytochemical composition, phenol, tannin, flavonoid contents, DPPH free radicals, porcine pancreatic lipase, and α-amylase inhibitory capacities of *L. stoechas* various polarities fractions from Palestine.

Methods: Specific coloring and precipitation procedures were used for phytochemical screening. Total phenolic content was quantified using the colorimetric technique Folin-Ciocalteu. The aluminum chloride technique was used to determine the total flavonoid level, while the vanillin approach was used to determine tannins. The antioxidant value was determined using the DPPH technique. At the same time, porcine pancreatic lipase and α-amylase inhibitory effects were estimated by p-nitrophenyl butyrate (PNPB) and 3,5-dinitrosalicylic acid (DNSA) approaches, respectively.

Results: The results indicate that *L. stoechas* methanol fraction exhibited the highest total flavonoid content (18.028 ±1.51 mg of QUE/g) and notable total phenol contents of 127.13 ±2.07 mg of GAE/g. While acetone fraction yielded the highest total tannin content (94.01±1.08 mg of CAE/g). Moreover, among the *L. stoechas* fractions, the aqueous one has a higher antioxidant (IC_{50}= 47.86±0.08 µg/ml) compared to methanol (IC_{50}= 66.06±0.06 µg/ml), acetone (IC_{50}= 63.09±0.29 µg/ml), and hexane (IC_{50}= 79.43±0.1 µg/ml) fractions. All plant fractions showed weak porcine pancreatic lipase and α-amylase inhibitory effects compared with the employed positive controls.

Conclusions: The present study has provided valuable insights into the phytochemical composition and bioactivity of different fractions obtained from *L. stoechas*. Based on the results obtained, it is recommended that the specific bioactive compounds responsible for the observed effects be explored and identified.

Keywords: *Lavandulastoechas*; Phytochemical composition; Phenol; Tannin; Flavonoid; DPPH Free Radicals; Porcine pancreatic lipase; α-Amylase.

[*] ***Corresponding author:***
Belal Rahhal **:** belalrahhal@najah.edu
Nidal Jaradat: nidaljaradat@najah.edu
Received: 1/5/2024 Accepted: 19/9/2024.
DOI: https://doi.org/10.35516/jjps.v18i2.2611

INTRODUCTION

Lavandula stoechas L. (French lavender; Lamiaceae)is an evergreen shrub and is considered one of the most commonly known Lavender species, especially in the Mediterranean Sea Basin regions. It is utilized broadly in folk medicine due to its wound healing, carminative, antispasmodic, and expectorant characteristics. *L. stoechas* volatile oil also treats headaches, chest colds, and colics (1). Some investigations have reported the antioxidant (2), antifungal (3), anti-leishmanial (4), anti-inflammatory (5), and antibacterial activities of the plant (6, 7).

The World Health Organization (WHO) reports that the global incidence of obesity has nearly quadrupled since 1975. Moreover, in 2016, about 1.9 billion people aged 18 and older were diagnosed as overweight, with more than 650 million of them classified as obese. These figures demonstrate the enormous and rising global problem of obesity. Obesity has multiple complications that can influence various elements of health. Obesity is associated with a higher risk of cardiovascular illnesses such as stroke and heart disease, respiratory issues such as sleep apnea, musculoskeletal disorders such as osteoarthritis, diabetes, and certain forms of cancer, among other things (8).

According to the WHO, the number of people with diabetes has been rising globally. In 2014, there were 422 million individuals with diabetes, compared to 108 million in 1980. The prevalence of diabetes has been increasing more rapidly in low- and middle-income countries compared to high-income countries. Diabetes is associated with various complications. It is a major cause of blindness, kidney failure, heart attacks, stroke, and lower limb amputation. These complications significantly impact the health and quality of life of individuals with diabetes (9).

Respiratory illnesses, neurological disorders, cardiovascular diseases, atherosclerosis, metabolic disorders, diabetes, and cancer have all been linked to oxidative stress. It is characterized by excess reactive oxygen species (ROS), which can cause cellular damage and malfunction (10).

Natural products have been an important source of therapeutic molecules for various medical disorders, including diabetes, obesity, and illnesses caused by oxidative stress (11). Many antidiabetic, anti-obesity, and antioxidative stress pharmaceuticals have their origins in compounds derived from plants, marine organisms, bacteria, fungi, and other natural sources. For example, metformin isolated from *Galega officinalis*, berberine found in Berberis species, and Quercetin (found in various fruits and vegetables) (12). Orlistat is a drug used to treat obesity, developed from the lipase inhibitor lipstatin discovered in the *Streptomyces toxytricini* bacteria (13). Furthermore, the catechin Epigallocatechin gallate (EGCG) present in green tea has been researched for its potential to assist in weight control. Moreover, curcumin, generated from turmeric, has potent antioxidative stress (14-16).

Hence, the present research aims to explore the total phenol, tannin, and flavonoid amounts and pancreatic lipase, α-amylase, and free radicals inhibitory effect by *L. stoechas* four extracts.

MATERIAL AND METHODS

Plant material collection, identification, and drying conditions

L. stoechas plant material collection, identification, and drying conditions were followed according to the WHO guidelines on good agricultural and collection practices [GACP] for medicinal herbals (17). However, the plant materials, including the leaves, stems, branches, and flowers of *L. stoechas* shrubs, were collected during the flowering period in May 2023 from the Nablus governorate of Palestine. The taxonomical characteristics were performed in the Department of Pharmacy, Faculty of Medicine and Health Sciences, An-Najah National University. The plant was deposited in the Pharmacognosy Laboratory with a voucher number of Pharm-PCT-2802.

The collected plant materials were extensively washed and dried in shady conditions with ordinary humidity for about three weeks. After drying, the dried material was coarsely powdered and kept in glass jars for further experiments.

Instrumentations

Cryo-Desiccator (Mill-rock technology, BT85, Kingston, USA) A Spectrophotometer-UV/Visible (Jenway® 7135, Staffordshire, UK), filter papers (Whitman no.1, Washington, USA), Shaker device (Memmert 531-25-1, Stockholm, Germany), rotavap apparatus (Heidolph-VV 2000, Schwabach, Germany), grinder (Aero Plus 500W Mixer Grinder, I01, Wan Chai, China), and balance-electronic (Radwag, AS 220/c/2, Toruńska, Poland) were used.

Chemicals

Acarbose, p-nitrophenyl butyrate, Orlistat, tris-HCl buffer, and porcine pancreatic lipase type II were sourced from Sigma (St. Louis, USA). Magnesium ribbon, acetic acid, ferric chloride, and DMSO (Dimethyl sulfoxide) were acquired from Riedel De Haen (Teningen, Germany). Folin-Ciocalteu's reagent, hydrochloric acid, aluminum chloride, potassium acetate, chloroform, and 2,2-Diphenyl-1-picrylhydrazyl (DPPH) were obtained from Sigma-Aldrich (Steinheim, Germany).

Furthermore, iodine solution, Sulfuric acid, and Molisch's reagent were sourced from Alfa-Aesar (Lancaster, UK). Ninhydrin solution and Benedict's and Millon's reagents were acquired from Alfa Agar (Binfield, UK). Methanol, n-hexane, acetone, and sodium hydroxide were procured from LobaChemie (Mumbai, India),

Extraction method

The powdered material of the *L. stoechas* plant was sequentially fractionated by adding four solvents of increasing polarity: hexane (non-polar), acetone (polar-aprotic), methanol, and water (polar-protic solvents). About 50 g of the powdered plant material was steeped in 1000 ml of acetone, n-hexane, methanol, and water separately, and each fraction was placed in a shaker for 96 h at room temperature, with 80 rounds per min. Then, each fraction was kept in a refrigerator for seven days. After that, the hexane, acetone, and methanol fractions were filter-evaporated using a rotavapor under certain vacuum conditions. The aqueous fraction was lyophilized utilizing a Cryo-Desiccator. Finally, all crude plant fractions were stored in the refrigerator at 4 ºC until further use (18).

Preliminary phytochemical assessment

The *L. stoechas* plant methanol, water, n-hexane, and acetone fractions were screened for the presence of major natural phytochemical classes by utilizing the phytochemical tests of Trease and Evans (19). They were performed on the organic and aqueous fractions. The alkaloids were highlighted by the reagents of Mayer, Dragendorff, and by the Reagent of Wagner, tannins by ferric chloride, terpenes by the reaction of Liebermann, saponins were determined based on their foam-forming abilities, polyphenolic substances by $FeCl_3$, and the revelation of flavonoids by the reaction with cyanidin.

Quantification of phenol

The quantifications of phenolic matter in the *L. stoechas* plant fractions were evaluated using the Folin-Ciocalteu reagent method described previously (20). Using a 100 mL volumetric flask, a 7.5% sodium carbonate (Na_2CO_3) solution was prepared by dissolving 7.5 g of Na_2CO_3 in less than 100 mL of distilled water, and then distilled water was used to bring the volume up to 100 mL. Like sodium carbonate solution, a stock solution of the standard solution (Gallic acid solution) was prepared by dissolving 100 mg of gallic acid and adding up to 100 mL of distilled water. The reaction mixture was prepared by mixing 0.5 mL of each extract solution, 2.5 mL of 10% Folin-Ciocalteu's reagent dissolved in water, and 2.5 mL of 7.5% sodium carbonate (Na_2CO_3) in a test tube for each sample. The sample tubes were incubated for 45 min at 45 ºC. The absorbance was determined using a spectrophotometer at wavelength 765 nm. The samples were prepared in triplicate for each analytic trial to obtain the mean and standard deviation values.

Quantification of flavonoids

The quantifications of flavonoids in the *L. stoechas* plant

fractions were estimated using the aluminum chloride colorimetric method described previously (21). Quercetin was used to make the standard calibration curve for total flavonoid determination. Stock Quercetin solution was prepared by dissolving 5.0 mg Quercetin in 1.0 mL methanol, then the standard solutions of Quercetin were prepared by serial dilutions using methanol (10–100 mg/mL). An amount of 0.6 mL diluted standard Quercetin solutions or extracts was separately mixed with 0.6 mL of 2% aluminum chloride. After mixing, the solution was incubated for 60 min at room temperature. The absorbance of the reaction mixtures was measured against a blank at 420 nm wavelength with UV-Vis spectrophotometer.

Antioxidant assay

The 2,2-di-phenyl-1-picrylhydrazyl (DPPH) free radical scavenging ability was evaluated following the previously described method (22). Each plant extract stock solution was serially diluted to achieve 2-100 µg/mL concentrations using methanol as solvent. Each test tube contained 1 mL of each concentration and was appropriately marked. One mL of 0.002% methanolic DPPH solution was added to each test tube, and 1 mL of methanol was added to each test tube to bring the final volume up to 3 mL (caution: DPPH is light sensitive, so preparation of working test tubes should be performed with minimum light exposure).

The samples were incubated for 30 minutes in a dark place, and then their optical densities were determined using spectrophotometric measurements at a wavelength of 517 nm. The equation used in this analytical study to calculate the inhibition percentage is shown below:

% DPPH inhibition = (AB−AS)/AB×100%

A_B is the recorded absorbance of the blank solution; A_s is the recorded absorbance of the sample solution.

Quantifications of tannin

The condensed tannin contents of four *L. stoechas* fractions were assessed according to Sun *et al*.'s procedure (23). 4% methanolic vanillin solution was prepared freshly. 100 µg/mL stock solution from each plant extract fraction was prepared using methanol as a solvent. For the working solution, each test tube contained 0.5 mL from each extract mixed with 3 mL of vanillin solution and 1.5 mL of concentrated HCl. The mixture was allowed to stand for 15 min, and then the absorption was measured at 500 nm against methanolic vanillin as a blank. All working samples were analyzed in triplicate. The total tannin in each fraction was expressed as catechin equivalents (mg of CAE/g of plant fraction).

Lipase inhibition assay

The anti-lipase assay was conducted according to Bustanji*et al.*'s studies (24). A stock solution of 500 µg/mL from each plant fraction, in 10% DMSO, was used to prepare five different solutions with the following concentrations: 50, 100, 200, 300, and 400 µg/mL. A 1 mg/mL stock solution of porcine pancreatic lipase enzyme was freshly prepared in Tris–HCl buffer before be used. The substrate used for this study, *p*-nitrophenyl butyrate (PNPB), was prepared by dissolving 20.9 mg in 2 mL of acetonitrile. For each working test tube, 0.1 mL of porcine pancreatic lipase (1 mg/mL) was mixed with 0.2 mL of each diluted solution series for each plant fraction. The resulting mixture was then brought to a total volume of 1 mL, by adding Tri-HCl solution and incubated at 37 °C for 15 min. Following incubation, 0.1 mL of PNPB solution was added to each test tube. The mixture was incubated for 30 min at 37 °C. Pancreatic lipase activity was determined by measuring the hydrolysis of the PNPB compound into *p*-nitrophenolate ions at 410 nm using a UV spectrophotometer. The same procedure was repeated for Orlistat, which was used as a standard reference compound. The equation used in this analytical study is shown below:

% Lipase inhibition = (AB−AS)/AB×100%

A_B is the recorded absorbance of the blank solution; A_s is the recorded absorbance of the sample solution.

α-Amylase inhibitory assay

This method was carried out by utilizing the procedure of McCue and Shetty (25). For working solutions, a volume of 0.2 mL of enzyme solution was mixed with 0.2 mL of each plant extract fraction and was incubated for

10 min at 30 °C. After the incubation period, 0.2 mL of a freshly prepared 1% starch aqueous solution was added to each working solution, followed by an incubation period of at least 3 min. The reaction was stopped by the addition of 0.2 mL dinitrosalicylic acid (DNSA) yellow color reagent. Each working solution was then diluted with 5 mL of distilled water and then boiled for 10 min in a water bath at 90 °C. The mixture was cooled to room temperature, and the absorbance was taken at 540 nm. The blank was prepared following the steps above, but the plant fraction was replaced with 0.2 mL of the previously described buffer. Acarbose was used as the standard reference, following the same steps used for plant extract.

Statistical analysis

All of the obtained results of the four studied plant fractions (quantifications of tannin, phenols, and flavonoids, in addition to the antioxidant, anti-lipase, and anti-amylase activities) were repeated three times for each experiment and expressed as means ± SD standard deviation. When the *p-value* was <0.05, the outcomes were considered significant. Data were compared using unpaired *t*-tests.

RESULTS

Phytochemical screening

The results of the phytochemical preliminary tests on the *L. stoechas* aqueous fractions revealed the presence of cardiac glycosides, phenols, and flavonoids. Meanwhile, phenols, tannins, and flavonoids were observed in the methanol fraction. At the same time, tannin, phenols, flavonoids, steroids, and volatile oils were identified in the acetone fractions. Moreover, phenols, flavonoids, steroids, carbohydrates, and volatile oils were found in the plant hexane fraction, as depicted in Table 1, and the fractionation yields are shown in Table 2.

Table 1 Phytochemical screening assessment of *L. stoechas* four solvents fractions

Phytochemical Classes	Aqueous fraction	Methanol fraction	Acetone fraction	Hexane fraction
Cardiac glycosides	+ve	-ve	-ve	-ve
Saponin glycoside	-ve	-ve	-ve	-ve
Alkaloids	-ve	-ve	-ve	-ve
Protein	-ve	-ve	-ve	-ve
Starch	-ve	-ve	-ve	-ve
Phenols	+ve	+ve	+ve	+ve
Volatile oil	-ve	-ve	+ve	+ve
Tannins	-ve	+ve	+ve	-ve
Steroids	-ve	-ve	+ve	+ve
Reducing sugar	-ve	-ve	-ve	-ve
Carbohydrate	-ve	-ve	-ve	+ve
Flavonoids	+ve	+ve	+ve	+ve

Positive (+ve); Negative (-ve)

Table 2 The yield percentage of *L. stoechas* fractions

Fractions	Plant extract, (g)	Dried plant, (g)	Yields, (%)
Hexane	4.55	50	9.10
Acetone	2.71	50	5.42
Methanol	3.82	50	7.64
Aqueous	3.11	50	6.22

Quantitative analysis of phenols

To determine the total phenol content in the *L. stoechas* plant, Table 3 displays the absorbance values for various concentrations of the Gallic acid standard.

Table 3. Absorption values of several concentrations of the standard Gallic acid

Gallic acid concentrations (mg/ml)	Absorption at λmax =765 nm
0	0.00
10	0.14
40	0.50
50	0.56
70	0.80

From the calibration curve of Gallic acid, the following equation was calculated to estimate the total phenol content in the four *L. stoechas* plant fractions.

$y = 0.0112x + 0.0176$, $R^2 = 0.9956$

Where y is the absorbance at 765nm, and x is the total phenol content of the *L. stoechas* plant fraction.

Absorbance values from various concentrations were employed to determine the total flavonoid contents in four fractions of *L. stoechas*. A standard calibration curve was constructed to quantify the total flavonoid content in these fractions. Table 4 presents the absorbance values for different concentrations of the standard Quercetin.

Table 4. Absorption values of several concentrations of the standard Quercetin

Concentration of quercetin (mg/mL)	Absorption at λ_{max} =510 nm
0	0
10	0.01
30	0.01
50	0.02
70	0.03
100	0.04

Using the standard calibration curve of Quercetin, the equation $y = 0.0004x + 0.0011$ with an R^2 value of 0.995 was applied to determine the total flavonoid contents in the four fractions of the *L. stoechas* plant.

Where Y is the absorbance at 510 nm, and X is the total flavonoids in the plant fractions. Furthermore, to assess the total tannin contents in the four fractions of the *L. stoechas* plant, the absorbance values of various concentrations of the standard Catechin were examined and are detailed in Table 5.

Table 5. Absorption values of several concentrations of the standard Catechin

Concentration of Catechin (µg/mL)	Absorption at 500 nm λ_{max}
0	0
10	0.08
30	0.11
50	0.15
70	0.18
100	0.29

Utilizing the standard calibration curve of Catechin, the equation $y = 0.0025x + 0.0232$ with an R^2 value of 0.9569 was employed to estimate the total condensed tannin contents in the four fractions of the *L. stoechas* plant. Here, Y represents the absorbance at 500 nm, and X denotes the total tannin contents in the four fractions of the *L. stoechas* plant.

The investigation into the phytochemical composition

of different *L. stoechas* plant fractions, extracted using varying solvents, revealed distinct profiles regarding total flavonoids, phenols, and tannins. The data, presented as mean values with standard deviations (±SD), are summarized in Table 6.

Table 6. Total flavonoids, tannins, and phenols of *L. stoechas* the aqueous, methanol, hexane, and acetone fractions.

Fractions	Total flavonoids contents, mg of QUE/g of plant fraction, ±SD	Total phenol contents, mg of GAE/g of plant fraction, ±SD	Total Tannin contents, mg of CAE/g of plant fraction, ±SD
Hexane	10.01±1.22	36.04±1.01	-
Acetone	11.011±1.18	73.07±2.02	94.01±1.08
Methanol	18.028±1.51	127.13±2.07	37.04±1.11
Aqueous	16.02±0.61	88.09±2.04	-

The experiment was repeated in triplicate. P-value less than 0.05

The results indicate that the methanol fraction exhibited the highest total flavonoid content (18.028 ±1.51 mg of QUE/g), suggesting its effectiveness in extracting flavonoids from *L. stoechas*. The aqueous fractions showed a relatively lower value of 16.02 mg of QUE/g.

In addition, *L. stoechas* methanol fraction demonstrated notable total phenol contents of 127.13 ±2.07 mg of GAE/g, followed by aqueous and acetone plant fractions (88.09±2.04 and 73.07±2.02 mg of GAE/g, respectively). Hexane exhibited the lowest phenolic content, with 36.04±1.01 mg of GAE/g values.

Moreover, *L. stoechas* acetone extraction yielded the highest total tannin content (94.01±1.08 mg of CAE/g), followed by methanol (37.04 ±1.11 mg of CAE/g). Meanwhile, hexane and aqueous fractions did not show detectable tannin content.

The variations observed in the phytochemical composition across the fractions highlight the solvent-dependent extraction efficiency. Water and methanol appear to be effective solvents for extracting phenolic and acetone, and methanol seems to be effective solvents for extracting tannin compounds. In contrast, methanol is particularly efficient in extracting flavonoids. These findings contribute valuable insights for the strategic selection of solvents in future studies focusing on the medicinal properties of *L. stoechas*.

Antioxidant effect

Thus, the DPPH technique was utilized in this study to examine the in vitro antioxidant activity of the *L. stoechas* hexane, acetone, methanol, and aqueous fractions. The DPPH (2,2-diphenyl-1-picrylhydrazyl) assay is widely used in antioxidant research to evaluate compounds' free radical scavenging activity. The advantages of the DPPH technique include being widely adopted and standardized, broad applicability, and low cost (26). In addition, the DPPH assay provides quantitative results, allowing researchers to compare the antioxidant activity of different compounds or samples. Moreover, this assay is sensitive to both hydrophilic and lipophilic antioxidants, allowing for the assessment of the total antioxidant capacity of a sample. Also, DPPH is a stable free radical, which contributes to the reproducibility of the assay and can be applied to a wide range of samples, including natural extracts, synthetic compounds, and even food samples. Most importantly, the DPPH assay is a simple and rapid method that can be easily conducted in a laboratory setting (27, 28).

The DPPH percentage of inhibition and IC_{50} doses were determined. The antioxidant IC_{50} values, % DPPH inhibition of *L. stoechas* four fractions, and positive control (Trolox) are presented in Fig. 4 and Table 7.

Table 7. DPPH inhibition percentages and IC_{50} values (µg/mL) of *L. stoechas* different fractions and Trolox

Conc.	Trolox, ±SD	Aqueous fraction, ±SD	Methanol fraction, ±SD	Acetone fraction, ±SD	Hexane fraction, ±SD
0	0±0.00	0±0.00	0±0.00	0±0.00	0±0.00
5	70.2±0.29	20.25±0.05	25.3±0.2	13.855±0.05	6.49±0.05
7	83.95±0.58	25.85±0.1	29.35±0.05	19.08±0.03	9.55±0.1
10	95.99±1.22	28.17±0.05	31.13±0.04	34.6±0.01	13.4±0.15
20	96±1.62	38.1±0.12	38.85±0.05	39.85±0.025	13.89±0.05
50	97.15±2.1	44.2±0.15	56.2±0.09	47.39±0.21	14.75±0.15
80	97.33±1.52	47.19±0.05	56.65±0.09	51.7±0.7	18.65±0.12
100	99.71±2.2	64.94±0.05	57.59±0.05	53.02±0.22	22.09±0.05
IC_{50}, ±SD	2.81±1.54	47.86±0.08	66.06±0.06	63.09±0.29	79.43±0.1

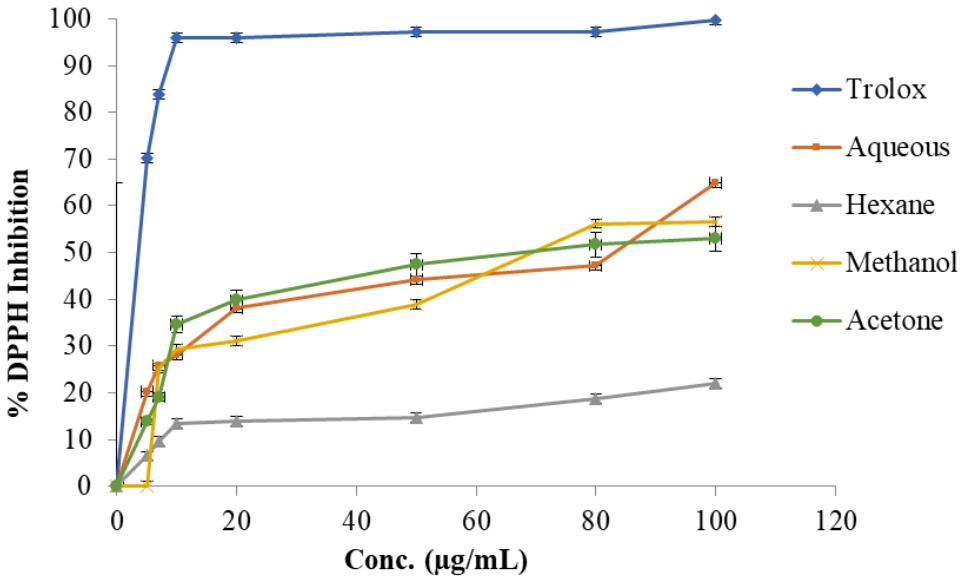

Figure 4. DPPH radical scavenging activity of *L. stoechas* plant fractions and Trolox. The experiment was repeated in triplicate. P-value less than 0.05

Trolox, a standard antioxidant, demonstrated a concentration-dependent increase in DPPH radical scavenging activity. At the highest concentration (100 µg/ml), Trolox exhibited a remarkable inhibition percentage of 99.71±2.2%, indicating potent antioxidant capacity.

Among the fractions of *L. stoechas*, the aqueous fraction showed a progressive increase in antioxidant activity with concentration. The methanol and acetone fractions also exhibited concentration-dependent activities, reaching inhibition percentages of 57.59±0.05% and 66.06±0.06%, respectively, at the highest concentration. While demonstrating lower activity at lower concentrations, the hexane fraction substantially increased at higher concentrations.

The IC_{50} values represent the concentration at which

50% inhibition of DPPH radicals occurs. Trolox had the lowest IC_{50} (2.81±1.54 µg/ml), suggesting its superior efficacy. Among the fractions, the aqueous fraction had a higher IC_{50} (47.86±0.08 µg/mL) compared to methanol (66.06±0.06 µg/ml), acetone (63.09±0.29 µg/ml), and hexane (79.43±0.1 µg/ml) fractions.

α-Amylase inhibition assay

An *in vitro* assay of α-amylase inhibitory activity using starch as a substrate and Acarbose as a positive control was conducted on four *L. stoechas* plant fractions. The α-amylase inhibitory activity of Acarbose and *L. stoechas* fractions was assessed at various concentrations (0, 10, 50, 70, 100, and 500 µg/ml) using different solvents (Aqueous, Methanol, Acetone, and Hexane). The results of IC_{50} α-amylase inhibitory activity values for the four fractions of *L. stoechas* and Acarbose are illustrated in Table 8 and were obtained from Figure 5.

Table 8. α-Amylase inhibitory activity of Acarbose and *L. stoechas* fractions

Conc.	Acarbose±SD	Aqueous±SD	Methanol±SD	Acetone±SD	Hexane±SD
0	0±0.00	0±0.00	0±0.00	0±0.00	0±0.00
10	53.22±0.29	6.6±0.1	2.36±0.02	8.85±0.02	8.86±0.02
50	54.91±0.58	8.66±0.14	8.85±0.02	9.5±0.03	9.51±0.02
70	66.1±1.22	9.715±0.025	31.4±0.2	17.83±0.13	15.87±0.08
100	66.1±1.62	33.47±0.07	33.76±0.00	24.1±0.1	27.94±0.03
500	72.54±2.1	34.61±0.02	36.95±0.06	32.85±0.02	34.08±0.15
IC_{50} (µg/mL), ±SD	28.18±0.38	12.5×10^3±0.07	11.7×10^3±0.07	19.5×10^3±0.06	19.9×10^3±0.07

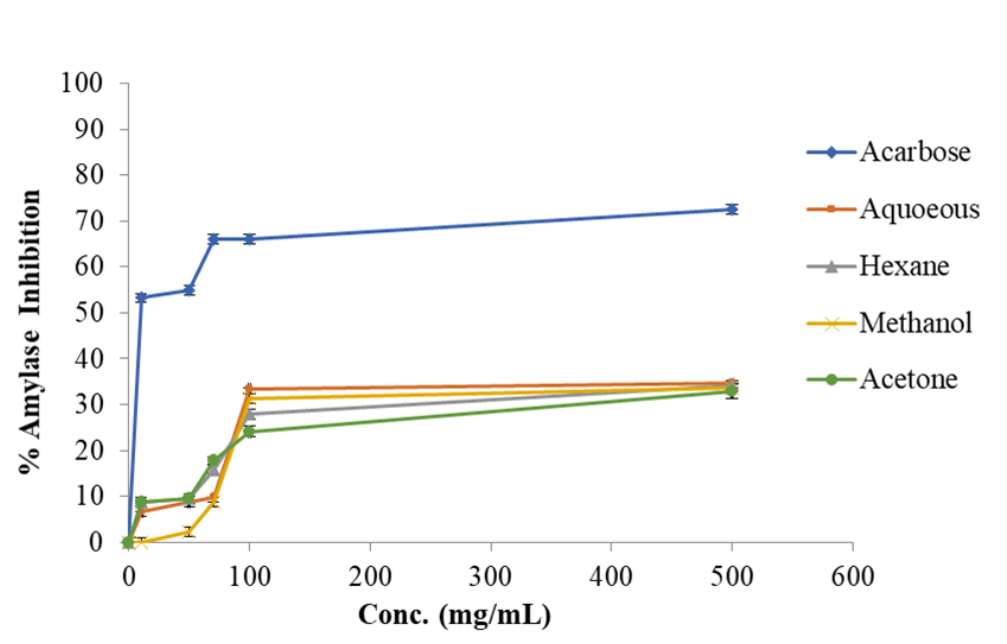

Fig. 5 α-Amylase inhibitory activity values of Acarbose and *L. stoechas* fractions. The experiment was repeated in triplicate. P-value less than 0.05

Both Acarbose and *L. stoechas* fractions exhibited concentration-dependent α-amylase inhibitory activity. As the concentration increased, the inhibitory activity also increased, reaching its maximum at the highest

concentration (500 µg/mL). Acarbose demonstrated substantial inhibitory activity at all concentrations, with a notable increase at higher concentrations. *L. stoechas* fractions also showed inhibitory effects, albeit generally lower than Acarbose.

The choice of solvent significantly affected the α-amylase inhibitory activity. Among the solvents used, methanol and aqueous extracts of *L. stoechas* displayed higher inhibitory potential (IC_{50}=11.7× 10^3±0.07 and 12.5 × 10^3±0.07, respectively) compared to acetone and hexane extracts (IC_{50}=19.5× 10^3±0.06 and 19.9 × 10^3±0.07, respectively).

Porcine pancreatic lipase enzyme inhibition activity

The hydrolysis of *p*-nitrophenyl butyrate to *p*-nitrophenol was used to measure the influence of the four *L. stoechas* fractions on the porcine pancreatic lipase enzyme. The assay worked by comparing a strong lipase inhibitory agent to Orlistat. The lipase enzyme inhibitory activity of four *L. stoechas* fractions and Orlistat. The lipase inhibitory results of four *L. stoechas* fractions and Orlistat in their IC_{50} values are shown in Table 9 and Figure 6.

Table 9. Lipase inhibition activity and IC_{50} (µg/ml) doses of *L. stoechas* four fractions and Orlistat

Conc.	Orlistat	Aqueous	Methanol	Acetone	Hexane
0	0±0.00	0±0.00	0±0.00	0±0.00	0±0.00
10	62.5±0.8	7.3±0.01	4.33±0.54	4.86±0.01	2.14±0.03
50	66±0.58	11.66±0.01	15.89±0.09	11.66±0.015	7.56±0.02
100	94.45±1.5	23.04±0.02	43.8±0.1	15.845±0.14	10.45±0.03
500	97.3±1.22	43.8±0.1	43.81±0.1	19.23±0.01	15.66±0.06
700	98.25±0.58	45.75±0.03	44.51±0.00	26.83±0.27	17.77±0.13
IC_{50} (µg/mL), ±SD	12.3±0.97	1.5×10^3±0.05	3.16×10^3±0.07	79×10^3±0.14	15.8×10^3±0.06

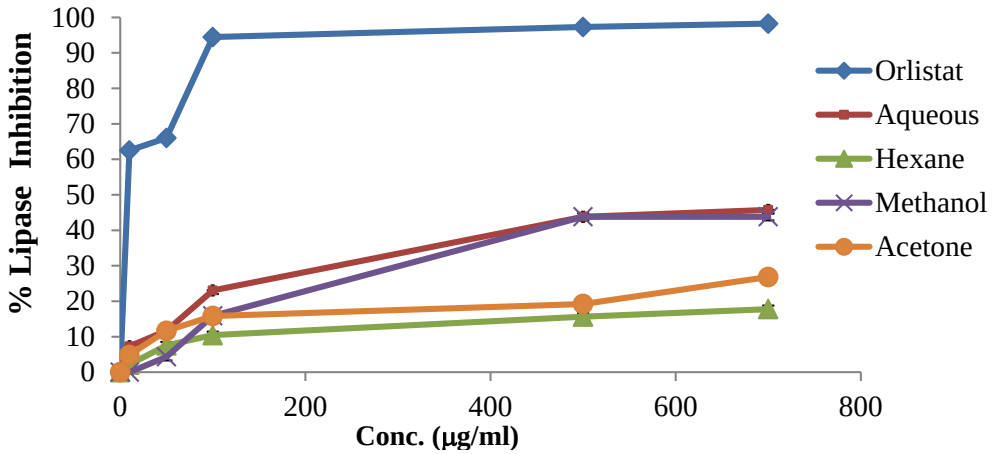

Fig. 6. Porcine pancreatic lipase inhibition activity of Orlistat and *L. stoechas* fractions. The experiment was repeated in triplicate. P-value less than 0.05

The lipase inhibition activity of the fractions obtained from *L. stoechas* was compared with the standard lipase inhibitor, Orlistat. The results indicate that all fractions of *L. stoechas* exhibited dose-dependent lipase inhibition. As

the concentration increased, a corresponding increase in inhibitory activity was observed for each fraction.

Among the fractions, the aqueous fraction demonstrated the highest lipase inhibition activity, especially at higher concentrations. The IC_{50} values further highlight the potency of the aqueous fraction, with a notably lower IC_{50} than the other fractions. This suggests that the aqueous fraction of *L. stoechas* may contain bioactive compounds with strong lipase inhibitory properties.

DISCUSSION

The phytochemical screening for *L. stoechas* in our study agrees with the study of Baptista et al. concerning polyphenols and flavonoids (25), with Ezzoubi et al. for tannins, catechin tannins, Flavonoids, and sterols (26), Teixeira et al. for polyphenols, flavonoids and terpenes (27). Moreover, the phytochemical screening of L. stoechas reveals that these plant extracts are rich in bioactive compounds that contribute to their medicinal properties (28-29). Advanced analytical techniques further enhance our understanding of *L. stoechas* chemical composition, paving the way for harnessing its therapeutic benefits in various health and wellness products.

Ceylan et al. stated that S. stoechas methanol extract from Turkey had DPPH free radical scavenging inhibitory activity by 84.45 ± 5.1% (29).

In addition, Zoubi et al. investigated the DPPH scavenging activity of *L. stoechas* from Morrocco and found that its hexane extract had potent antioxidant activity with an IC_{50} value of 1.2 µg/mL (30).

In 2012, Robu et al. performed a comparative study of antioxidant activity for different L. angustifolia and L. hybrida cultivars. The highest result was obtained for *L. hybrida* followed by *L. angustifolia* (30). On the other hand, Blazeković et al. found a slightly higher antioxidant activity was observed for *L. angustifolia* extracts than L. intermedia extracts, possibly due to their higher polyphenolic contents (31). Ahn et al. found that the aqueous-methanolic leaf extract of *L. angustifolia* afforded over twice as high DPPH value as the *L. latifolia* extract) (32). The antioxidant, antidiabetic, and antilipase effects of *L. stoechas* are consistent with other studies on medicinal plants in Palestine. For example, Rahhal et al. 2022 found that the *A. scoparia* aqueous extracts had promising antioxidant, anti-lipase, and anti-α-amylase effects (33).

CONCLUSION

This study is the first one in Palestine, and the results indicate that the *L. stoechas* methanol fraction exhibited the highest total flavonoid and phenol contents. At the same time, the acetone fraction yielded the highest total tannin content. Moreover, among the *L. stoechas* fractions, the aqueous one has a higher antioxidant capacity. All plant fractions showed weak anti-lipase and α-amylase inhibitory effects compared with the employed positive controls. This study has provided valuable insights into the phytochemical composition and bioactivity of different fractions obtained from *L. stoechas*. Based on the results obtained, it is recommended that the specific bioactive compounds responsible for the observed effects need to be isolated, purified, and identified. Further studies involving *in vivo* models and clinical trials are warranted to validate the potential health benefits of *L. stoechas* fractions. Legal procedures by the stakeholders in the country are required to start research for the application of medicinal plants in complementary medicine.

Statements and Declaration

Availability of data and materials

This published article and its supplementary information files include all data generated or analyzed during this study.

Ethics approval and consent to participate

Not applicable.

Consent for publication

Not applicable.

Competing interest

The authors declare that they have no competing interests.

Funding

None

Authors' contributions

B. R.: Conceptualization, Validation, Investigation, writing – original draft, Writing - review & editing, Visualization, Supervision, Project administration. **N. J**.: Conceptualization, Validation, Investigation, writing – original draft, Writing - review & editing, Visualization, Supervision, Project administration**. L. I.**.: Validation, Investigation, Writing - review & editing, Visualization, Supervision. **F. H**.: Validation, Investigation, Writing - review & editing, Visualization. **L. G.**: Validation, Investigation, Writing - review & editing, Visualization. **S. A.:** Validation, Investigation, Writing - review & editing. **W. J**.: Validation, Investigation, Writing - review & editing. **Z. B**.: Validation, Investigation, Writing - review & editing. **Z. H**.: Validation, Investigation, Writing - review & editing. **Z. H**.: Validation, Writing - review & editing. All authors read and approved the final manuscript.

Acknowledgments

The authors would like to thank An-Najah National University (www.najah.edu)

REFERENCES

1. Zuzarte M, Gonçalves M, Cavaleiro C, Cruz M, Benzarti A, Marongiu B, et al. Antifungal and anti-inflammatory potential of Lavandula stoechas and Thymus herba-barona essential oils. *Industrial Crops and Products*. 2013;44:97-103.
2. Messaoud C, Chograni H, Boussaid M. Chemical composition and antioxidant activities of essential oils and methanol extracts of three wild Lavandula L. species. *Natural product research*. 2012;26(21):1976-84.
3. Angioni A, Barra A, Coroneo V, Dessi S, Cabras P. Chemical composition, seasonal variability, and antifungal activity of Lavandula stoechas L. ssp. stoechas essential oils from stem/leaves and flowers. *Journal of agricultural and food chemistry*. 2006;54(12):4364-70.
4. Bouyahya A, Et-Touys A, Abrini J, Talbaoui A, Fellah H, Bakri Y, et al. Lavandula stoechas essential oil from Morocco as novel source of antileishmanial, antibacterial and antioxidant activities. *Biocatalysis and Agricultural Biotechnology*. 2017;12:179-84.
5. Algieri F, Rodriguez-Nogales A, Vezza T, Garrido-Mesa J, Garrido-Mesa N, Utrilla MP, et al. Anti-inflammatory activity of hydroalcoholic extracts of Lavandula dentata L. and Lavandula stoechas L. *Journal of ethnopharmacology*. 2016;190:142-58.
6. Benabdelkader T, Zitouni A, Guitton Y, Jullien F, Maitre D, Casabianca H, et al. Essential oils from wild populations of Algerian Lavandula stoechas L.: composition, chemical variability, and in vitro biological properties. *Chemistry & biodiversity*. 2011;8(5):937-53.
7. Zhaleh M, Sohrabi N, Zangeneh MM, Zangeneh A, Moradi R, Zhaleh H. Chemical composition and antibacterial effects of essential oil of Rhus coriaria fruits in the west of Iran (Kermanshah). *Journal of essential oil bearing plants*. 2018;21(2):493-501.
8. World Health Organization. Obesity and overweight Geneva: WHO; 2021 [Available from: https://www.who.int/news-room/fact-sheets/detail/obesity-and-overweight.
9. World Health Organization. Diabetes Geneva: WHO; 2023 [Available from: https://www.who.int/news-room/fact-sheets/detail/diabetes.

10. Pizzino G, Irrera N, Cucinotta M, Pallio G, Mannino F, Arcoraci V, et al. Oxidative stress: harms and benefits for human health. *Oxidative medicine and cellular longevity*. 2017;2017.
11. Eid AM, Jaradat N. Public knowledge, attitude, and practice on herbal remedies used during pregnancy and lactation in West Bank Palestine. *Frontiers in pharmacology*. 2020;11:46.
12. Qneibi M, Jaradat N, Hawash M, Olgac A, Emwas N. Ortho versus meta chlorophenyl-2, 3-benzodiazepine analogues: synthesis, molecular modeling, and biological activity as AMPAR antagonists. *ACS omega*. 2020;5(7):3588-95.
13. Sweileh WM, Arafat RT, Al-Khyat LS, Al-Masri DM, Jaradat NA. A pilot study to investigate over-the-counter drug abuse and misuse in Palestine. 2004.
14. Khutami C, Sumiwi SA, Khairul Ikram NK, Muchtaridi M. The effects of antioxidants from natural products on obesity, dyslipidemia, diabetes and their molecular signaling mechanism. *International Journal of Molecular Sciences*. 2022;23(4):2056.
15. Rahman MM, Dhar PS, Anika F, Ahmed L, Islam MR, Sultana NA, et al. Exploring the plant-derived bioactive substances as antidiabetic agent: an extensive review. *Biomedicine & Pharmacotherapy*. 2022;152:113217.
16. Unuofin JO, Lebelo SL. Antioxidant effects and mechanisms of medicinal plants and their bioactive compounds for the prevention and treatment of type 2 diabetes: an updated review. *Oxidative medicine and cellular longevity*. 2020;2020.
17. Organization WH. WHO guidelines on good agricultural and collection practices [GACP] for medicinal plants. *Geneva: World Health Organization*; 2003.
18. Qneibi M, Hanania M, Jaradat N, Emwas N, Radwan S. Inula viscosa (L.) Greuter, phytochemical composition, antioxidant, total phenolic content, total flavonoids content and neuroprotective effects. *European Journal of Integrative Medicine*. 2021;42:101291.
19. Trease G, Evans W. Pharmacognosy. *London: Baillier Tindall*; 1983. 256-7.
20. Cheung L, Cheung PC, Ooi VE. Antioxidant activity and total phenolics of edible mushroom extracts. *Food chemistry*. 2003;81(2):249-55.
21. Jaradat N, Hussen F, Al Ali A. Preliminary phytochemical screening, quantitative estimation of total flavonoids, total phenols and antioxidant activity of *Ephedra alata* Decne. *J Mater Environ Sci*. 2015;6(6):1771-8.
22. Jaradat N, Adwan L, K'aibni S, Shraim N, Zaid AN. Chemical composition, anthelmintic, antibacterial and antioxidant effects of Thymus bovei essential oil. *BMC Complement Altern Med*. 2016;16(1):418-24.
23. Sun B, Ricardo-da-Silva JM, Spranger I. Critical factors of vanillin assay for catechins and proanthocyanidins. *Journal of agricultural and food chemistry*. 1998;46(10):4267-74.
24. Bustanji Y, Issa A, Mohammad M, Hudaib M, Tawah K, Alkhatib H, et al. Inhibition of hormone sensitive lipase and pancreatic lipase by Rosmarinus officinalis extract and selected phenolic constituents. *J Med Plants Res*. 2010;4(21):2235-42.
25. McCue PP, Shetty K. Inhibitory effects of rosmarinic acid extracts on porcine pancreatic amylase in vitro. *Asia Pac J Clin Nutr*. 2004;13(1):12-20.
26. Baliyan S, Mukherjee R, Priyadarshini A, Vibhuti A, Gupta A, Pandey RP, et al. Determination of antioxidants by DPPH radical scavenging activity and quantitative phytochemical analysis of Ficus religiosa. *Molecules*. 2022;27(4):1326.
27. Kandi S, Charles AL. Statistical comparative study between the conventional DPPH spectrophotometric and dropping DPPH analytical method without spectrophotometer: Evaluation for the advancement of antioxidant activity analysis. *Food chemistry*. 2019;287:338-45.

28. Pyrzynska K, Pękal A. Application of free radical diphenylpicrylhydrazyl (DPPH) to estimate the antioxidant capacity of food samples. *Analytical Methods*. 2013;5(17):4288-95.
29. Ceylan Y, Usta K, Usta A, Maltas E, Yildiz S. Evaluation of antioxidant activity, phytochemicals and ESR analysis of Lavandula stoechas. *Acta Physica Polonica A*. 2015;128(2B).
30. Ezzoubi Y, Bousta D, Lachkar M, Farah A. Antioxidant and anti-inflammatory properties of ethanolic extract of Lavandula stoechas L. from Taounate region in Morocco. *Int J Phytopharm*. 2014;5(1):21-6.
31. Amer, J., Ghanim, M., Salhab, A., Jaradat, N., Alqub, M., Rabayaa, M., Hallak, L., Abdulhai, T., Dwayat, S., Issa, L., & Dwikat, M. In vitro Analysis of the Anticancer and Antidiabetic Effects of Teucrium orientale Leaf Hydrophilic Extract Grown in Two Palestinian Geographic Areas. *Jordan Journal of Pharmaceutical Sciences*. 2025;18(1): 77–89. https://doi.org/10.35516/jjps.v18i1.2492
32. Karki, D., Pandey, B., Jha, P., Acharya, A., Khanal, D. P., Raut, B., & Panthi, S. Senna alata: Phytochemistry, Antioxidant, Thrombolytic, Anti-inflammatory, Cytotoxicity, Antibacterial activity, and GC-MS analysis. *Jordan Journal of Pharmaceutical Sciences*. 2024; 17(3): 549–566. https://doi.org/10.35516/jjps.v17i3.2406
33. Al-Halaseh, L., Issa, R., Said, R., & Al-suhaimat, R. Antioxidant Activity, Phytochemical Screening, and LC/MS-MS Characterization of Polyphenol Content of Jordanian Habitat of Pennisetum Setaceum Aqueous Leaf Extract. *Jordan Journal of Pharmaceutical Sciences*. 2024;17(4): 706–716. https://doi.org/10.35516/jjps.v17i4.2442

دراسة المحتوى الكيميائي، وتأثيرات خفض مستوى الدهون و مستوى السكر في الدم، ومضادات الأكسدة لمستخلصات مختلفة من نبات اللافندر الفرنسي (*Lavandula stoechas* L) المزروع في فلسطين

بلال رحال*[1*]، نضال جرادات[2]، ليندا عيسى[2]، فاطمة حسين[2]، غيداء امارة[2]، لين غزاوي[2]، سحر الحين[2]، وعد جبارة[2]، زين برانسة[2]، زينة قعدان[2]

[1]دائرة العلوم الطبية الحيوية– كلية الطب وعلوم الصحة –جامعة النجاح الوطنية – نابلس – فلسطين

[2]دائرة الصيدلة – كلية الطب وعلوم الصحة– جامعة النجاح الوطنية – نابلس – فلسطين

ملخص

Lavandula stoechas L. (الخزامى الفرنسي؛ Lamiaceae) نوعٌ معروف من الخزامى في حوض البحر الأبيض المتوسط. يُستخدم على نطاق واسع في الطب التقليدي نظرًا لخصائصه في التئام الجروح، وخصائصه المضادة للتشنج، وخصائصه المقشّعة. ونتيجةً لذلك، تُعدّ هذه الدراسة الأولى التي تبحث في التركيب الكيميائي النباتي، ومحتويات الفينول، والتانين، والفلافونويد، والجذور الحرة DPPH، والليباز البنكرياسي الخنزيري، والقدرات المثبطة لـ α-amylase لأجزاء مختلفة من L. stoechas من فلسطين.

الطريقة: استُخدمت أساليب تلوين وترسيب محددة للفحص الكيميائي النباتي. حُدد محتوى الفينول الكلي باستخدام تقنية قياس الألوان Folin-Ciocalteu. واستُخدمت تقنية كلوريد الألومنيوم لتحديد مستوى الفلافونويد الكلي، بينما استُخدمت طريقة الفانيلين لتحديد العفص. وحُددت القيمة المضادة للأكسدة باستخدام تقنية DPPH. وفي الوقت نفسه، قُدِّرت التأثيرات المثبطة لليباز البنكرياسي الخنزيري وألفا أميليز باستخدام طريقتي بارا–نيتروفينيل بوتيرات (PNPB) وحمض 3،5– داينيتروساليسيليك (DNSA)، على التوالي.

النتائج: تشير النتائج إلى أن نسبة الميثانول في L. stoechas أظهرت أعلى محتوى إجمالي من الفلافونويد (18.028 ± 1.51 ملغ من QUE/غ) ومحتوى إجمالي ملحوظ من الفينول بلغ 127.13 ± 2.07 ملغ من GAE/غ، بينما أظهرت نسبة الأسيتون أعلى محتوى إجمالي من التانين (94.01 ± 1.08 ملغ من CAE/غ). علاوة على ذلك، من بين نسب L. stoechas، تتميز النسبة المائية بـ IC50 أعلى (47.86 ± 0.08 ميكروغرام/مل) مقارنةً بنسب الميثانول (66.06 ± 0.06 ميكروغرام/مل) والأسيتون (63.09 ± 0.29 ميكروغرام/مل) والهكسان (79.43 ± 0.1 ميكروغرام/مل). أظهرت جميع أجزاء النبات تأثيرات ضعيفة في تثبيط الليباز البنكرياسي الخنزيري وألفا أميليز مقارنةً بالضوابط الإيجابية المستخدمة.

الخلاصة: قدمت هذه الدراسة رؤى قيّمة حول التركيب الكيميائي النباتي والنشاط الحيوي لأجزاء مختلفة من L. stoechas. بناءً على النتائج المُحصل عليها، يُوصى باستكشاف وتحديد المركبات النشطة بيولوجيًا المسؤولة عن التأثيرات الملحوظة.

الكلمات الدالة: لافاندولاستويكاس؛ التركيب الكيميائي النباتي؛ الفينول؛ التانين؛ الفلافونويد؛ الجذور الحرة DPPH؛ الليباز البنكرياسي الخنزيري؛ ألفا أميليز.

المؤلف المراسل:

بلال رحال: belalrahhal@najah.edu

نضال جرادات: nidaljaradat@najah.edu

تاريخ استلام البحث 2024/5/1 وتاريخ قبوله للنشر 2024/9/19.

Jordan Journal of Pharmaceutical Sciences, Volume 18, No. 2, 2025

Evaluation of Cytotoxicity and Antibacterial Activity of Green Synthesized Silver Nanoparticles using *Hedera helix* extract.

Ahmed Naji Alfalahi [1], Sina M. Matalqah [1*], Reem Issa [2], Hala I. AL-Daghistani[3], Anas Abed [4]

[1] Department of pharmaceutics and technology, Faculty of pharmacy, Pharmacological and Diagnostics Research Center (PDRC), Faculty of Pharmacy, AL-Ahliyya Amman University.
[2] Department of pharmaceutical Science, Faculty of pharmacy, Pharmacological and Diagnostics Research Center (PDRC), Faculty of Pharmacy, AL-Ahliyya Amman University.
[3] Department of Medical Laboratory Science, Faculty of Allied Medical Science, Amman Jordan.
[4] Department of biopharmaceutics and clinical pharmacy, Faculty of pharmacy, Pharmacological and Diagnostics Research Center (PDRC), Faculty of Pharmacy, AL-Ahliyya Amman University.

ABSTRACT

Nowadays, silver nanoparticles (AgNPs) have drawn significant interest due to their unique properties, making them advantageous in biomedical applications, sensors, antimicrobial agents, catalysts, and optical fibers. Green synthesis is the safest and easiest method for producing silver nanoparticles (AgNPs). This study aimed to investigate the antibacterial and cytotoxic activities of silver nanoparticles synthesized using aqueous extracts of *Hedera helix* (AHE) against *S. aureus*, *P. aeruginosa*, and A549 lung cancer cell lines. Silver nanoparticles (Hh-AgNPs) were synthesized using the aqueous extracts of *Hedera helix* (AHE) as a reducing agent and polyvinylpyrrolidone (PVP) as a stabilizer and characterized by UV-visible spectrophotometry and particle size analysis via dynamic light scattering (DLS). The silver nanoparticles (Hh-AgNPs) were successfully synthesized, showing maximum absorption at 448 nm, with enhanced cytotoxic activity against A549 lung cancer cell lines (IC_{50} = 15.16 µg/ml) and antibacterial activity against *S. aureus* (MIC = 0.156 mg/ml) and *P. aeruginosa* (MIC = 0.3125 mg/ml), compared to AHE alone. Biological methods are cost-effective and eco-friendly and thus can serve as an economical and efficient alternative for the large-scale synthesis of silver nanoparticles.

Keywords: *Hedera helix*, Silver Nanoparticles, Green synthesis, *S. aureus*, *P. aeruginosa*, A549 lung cancer cell lines.

1. INTRODUCTION

Nanotechnology is a multidisciplinary scientific field that deals with designing, synthesizing, and manipulating particle structures with sizes ranging from about 1 to 100 nm. Applications for nanoparticles (NPs) are numerous and include many areas such as biomedical sciences, agric *Hedera helix* ulture, cosmetics, food technology, catalysis, drug delivery, drug-gene delivery, energy science, single electron transistors, chemical industries, light emitters, nonlinear optical devices, electronics, drug delivery, and photo-electrochemical applications [1,2].

Nowadays many researchers focus on silver nanoparticles (AgNPs) due to their unique characteristics (e.g., size and shape depending on optical, antimicrobial, and electrical properties). There have been reports of several preparation methods for the synthesis of silver nanoparticles: namely physical, chemical, and biological synthesis [3-5]. Nowadays biosynthetic methods, i.e., green chemistry, using natural reducing agents such as polysaccharides, biological micro-organisms such as bacteria and fungus or plant extracts have emerged as simple and viable alternatives to the chemical and physical

[*]***Corresponding author: Sina M. Matalqah***
S.matalqah@ammanu.edu.jo
Received: 6/5/2024 Accepted: 91/9/2024.
DOI: https://doi.org/10.35516/jjps.v18i2.2620

synthetic procedures to obtain AgNPs to overcome their drawbacks including the use of toxic chemicals, high temperature, pressure, and yielding of hazardous by-products[6]. Recently AgNPs were synthesized by using different plant extracts as a potential reducing agent [7].

Hedera helix L. (Araliaceae Juss.), commonly known as Ivy, is an evergreen perennial plant native to the Northern Hemisphere zones [8,9]. Extract of *H. helix* is utilized for treating respiratory tract ailments characterized by excessive mucus production, respiratory tract infections, and persistent cough associated with the common cold. The aqueous extraction of Ivy leaves has been utilized in traditional medicine to treat respiratory diseases since the 19th century [10]. Several controlled clinical investigations have shown the effectiveness and safety of medications containing Ivy leaf extract [10-12]. Today, the use of Ivy leaf extract in medicines has been standardized by a Commission monograph of the "German regulatory authority" since 1988. These formulations include syrup, tablets, drops, and suppositories [10, 12], and can be used to treat the symptoms of chronic and acute inflammatory bronchial diseases, as well as the common cold with cough [13]. The primary bioactive compounds responsible for Ivy leaf extract therapeutic properties are triterpene, phenols and saponins. It possesses a range of beneficial effects, including spasmolytic/antispasmodic properties, anti-inflammatory actions, antimicrobial activity, pain relief, anthelmintic properties (against parasitic worms), antitrypanosomal and antileishmanial effects (against specific parasites), antitumor activity, antimutagenic properties, molluscicide activity (against mollusks), antioxidant effects, and antithrombin activity [14,15].

This study aimed to synthesize Hh-AgNps stabilized by PVP without using any chemical reducing agent and to evaluate their antimicrobial and cytotoxic. There are studies in the literature concerning the antibacterial activity of AgNps synthesized by using extracts of *Hedera helix* against *Bacillus subtilis* and *Klebsiella pneumoniae* [16]. Moreover, there is no published data in the literature concerning the evaluation of the antibacterial and cytotoxic activity of Hh-AgNPs stabilized by PVP against *S. aureus*, *P. aeruginosa* and A549 lung cancer cell lines.

2. MATERIALS AND METHODS

2.1 Chemicals and Reagents

Different reagents and chemicals were employed in this study including : Silver nitrate 99.8 % purity (AgNO3), Mueller-Hinton agar and Mueller-Hinton broth(Oxoid Ltd., UK) and 3-(4,5 – dimethylthiazol-2-yl)- 2,5. diphenyltetrazolium bromide (MTT)(Promega kit, USA), Dulbecco's Modified Eagle Medium (DMEM), Clarithromycin (CLR-15 µg), Ciprofloxacin (CIP-5 µg), Clindamycin (DA-2 µg), Metronidazole (MET-5 µg), Doxycycline (DO-30 µg) , all antimicrobial disks were supplied by (Bioanalyse, Turkey), standard strain of *P. aeruginosa* ATCC 9027 and *S. aureus* ATCC 9027(Manassas,VA,USA), Folin-Ciocalteu reagent, Aluminum chloride ≥ 99% purity(AZ chem for chemicals, South Africa), 2,2-Diphenyl-1-picrylhydrazyl Radical (DPPH) free radial 95% purity (Sisco Research Laboratories, India), 2,2'-azinobis-(3-ethylbenzothiazoline-6-sulfonic acid) (ABTS) free radical ≥ %98 purity (Sigma Aldrich, USA), Dimethyl sulfoxide (DMSO) 98% purity, Gallic acid 98% purity, Sodium carbonate anhydrous 99.5-100.5 % purity, Sodium acetate trihydrate 99% purity, Polyvinylpyrrolidone (PVP) (Joswee medical, Jordan), Trypsin enzyme(Euroclone, Italy), Quercetine (Santa Cruz Biotechnology, USA), Absolute Ethanol and methanol , Potassium persulfate(Sigma Aldrich, USA), Phosphate buffered saline (Euroclone, Italy) and Deionized water.

2.2 Collection of plants

The *H. helix* leaves has been collected during spring period year 2022, from local plants nursery allocated in Jerash, Jordan. A specimen sample was authenticated and prepared by Dr. Hatem Tayfour at the Royal Botanical Garden, Jordan and kept at Al-Aliya Amman University

research laboratory. Fresh leaves were immediately cleaned and air dried to remove the moisture, grinded and kept until used. Followed by grinding the dried leaves into fine powder.

2.3 Preparation of Aqueous Leaf Extract (AHE)

Aqueous extract of *H. helix* (AHE) was prepared by placing a 25 g of dried *H. helix* plant (Collected and dried previously by our research group) inside a Soxhlet extractor with 400 mL of distilled water for 4 hrs. the resultant extract was then dried using Rotary evaporator for 24 hrs. and left inside fume hood for 48 hrs. to dry completely. The dried Aqueous extract is then stored at 4 ^{o}C for further tests.

2.4 Extraction yield calculation

The extraction yield is calculated to determine the relative amount of the extarct inside raw plant material. After the extract is dried and weighed, the weight of the extarct is divided on the total weight of raw plant material as per equation : Extraction yeild %= (weight of Extraction / weight of raw plant material) * 100%

All measurements were measured in triplicates. The average and standard deviations were used for further calculations.

2.5 Qualitative Phytochemical tests

2.5.1 Detection of saponins

Qualitative phytochemical analysis of the AHE was performed using the standard experimental procedures to detect the extract phytoconstituents. Among these phytoconstituents are saponins that have been analyzed by foam formation [17] and hemolysis tests [18]. The findings of these tests were indicated qualitatively as positive (+) or negative (-) indicating the presence or absence of saponins, respectively.

2.6 Quantitative Phytochemical Analysis and Antioxidant Properties

2.6.1Total Phenolic Content (TPC) Determination

The folin-Ciocalteu method was used to calculate the total phenolic content of AHE. All experiment setups were made in triplicate. The total phenolic content (TPC) of each extract was expressed as mg equivalent to gallic acid/ g of AHE (mg GAE/g AHE) [19]. All measurements were measured in triplicates. The average and standard deviations were used for further calculations.

2.6.2 Total Flavonoid Content (TFC) Determination

To determine the total flavonoid content, the Aluminum chloride test was utilized with some minor modifications according to the method described by Chang et al. [20]. The total flavonoid content (TFC) in the extract was expressed as mg equivalent to quercetin/ g of AHE (mg Qr/g AHE). All measurements were measured in triplicate]. The average and standard deviations were used for further calculations.

2.6.3 Quantification of Radical Scavenging activity (DPPH)

To determine the half inhibitory concentration (IC_{50}) of AHE, it is needed to scavenge 50% of the 2,2-Diphenyl-1-picrylhydrazyl Radical (DPPH) DPPH• free radical in a solution, as described by Matusiewicz et al. [21] with some modifications. DPPH solution (0.2Mm) in absolute methanol was mixed vigorously with AHE (1:1, v/v). After 30 minutes of incubation, the mixture was centrifuged (15,000 x g, 10 minutes) and the absorbance of the supernatant was recorded at 517nm, using UV -Vis spectrophotometer (Shimadzu, Japan). The IC_{50} of AHE was compared to the IC_{50} of Vitamin C, which was used as a standard antioxidant. All measurements were measured in triplicates. The average and standard deviations were used for further calculations.

2.6.4 Scavenging Activity of 2.2′-Azino-bis (3-ethylbenzthiazoline-6-sulfonic Acid) Radical Cation (ABTS•+)

The total antioxidant capacity was determined using the 2.2′-Azino-bis (3-ethylbenzthiazoline-6-sulfonic Acid) Radical Cation (ABTS) scavenging activity as described by Re et al., (1999) [22] with some modifications.7mM stock solution of ABTS with 2.45mM potassium persulfate solution was prepared and diluted with methanol until it

reached an absorbance value of 0.7 at 734nm. 1 ml samples of AHE and Hh-AgNPs within a concentration range of (64 to 4.06 µg/ml) were prepared. These samples were added to 2ml of ABTS•+solution. After exactly 1hr, the final absorbance was measured at 734nm. Ascorbic acid (Vitamin C) was used as a reference compound for comparison (Re et al., 1999) [22].

2.7 Preparation of Silver Nanoparticles (Hh-AgNPs)

Silver nanoparticles (Hh-AgNPs) were synthesized using different concentrations of Polyvinylpyrrolidone (PVP) as a stabilizer, and compared by means of particle size, surface charge, and polydispersity index (PDI) as described by Zein et al., [23], with slight modifications.

A stock solution of (PVP) was prepared in de-ionized water at concentrations of (0,10, 15, 20 mg/mL). A stock solution of $AgNO_3$ in de-ionized water was prepared at concentration of (3.5 mg/mL). 20 mL of each solution was mixed and stirred for 15 minutes at room temperature using a magnetic stirrer. A 4 mL of *H. helix* extract (30 mg/mL) was then added to the mixture and was further stirred for 24 hours. After the time elapsed, the color of the resultant nanoparticle suspension turned brownish yellow. The probe sonicator (Sonopulus ultrasonic homogenizer model HD 4000, Bandelin,Germany) was used at 80% amplitude for 2 hours to uniform the size of the NPs, followed by centrifugation for 5 minutes at 10,000 RPM and 25 ºC, the supernatant was discarded. The remaining powder was then deep frozen for 24 hours and lyophilized using freeze dryer (Zirbus, Germany) for another 24 hours. The resultant powder was then stored at 4 ºC for further examination.

2.8 Characterization of the prepared Hh-AgNPs

2.8.1 Ultraviolet -Visible Absorbance Spectroscopy

According to the method described by Zein et al., [23] the bioproduction of silver ion (Ag^+) into silver NPs (Ag^0) was monitored in aqueous solution prepared by dissolving 7 mg sample of the prepared Hh-AgNPs in 10 mL de-ionized water. Then, 1ml of the solution was scanned using Shimadzu UV-Vis spectrophotometer at regular intervals within wavelength ranges (200 to 800 nm). The formation of peak spectra confirms the formation of the expected nanoparticles. This assay was performed in triplicates.

2.8.2 Dynamic Light Scattering (DLS)

According to the method described by Zein et al.,[23], the particle size, surface charge (Zeta potential), and polydispersity index (PDI) of the prepared Hh-AgNPs was measured for 11 times over a duration of 2 weeks (excluding the nonworking days) using Malvern Zetasizer Nano-Z® device (Malvern, Model ZEN-3600).

A 7 mg sample of the prepared Hh-AgNPs was weighed and dissolved in 10 mL de-ionized water. A 10 µL of the prepared suspension was then diluted with 990 µL De-ionized water in an Eppendorf tube and vortexed for one minute to ensure homogeneous distribution of Hh-AgNPs in the vehicle. The sample was then transferred into a Zeta sizer Quartz cuvette to measure the above-mentioned parameters (Size, Charge, and PDI).

All measurements were measured in triplicates. The average and standard deviations were used for further calculations.

2.9 Determination of Antibacterial Activity of Biosynthesized Hh-AgNPs

2.9.1 Agar well diffusion method

The biosynthesized Hh-AgNPs were tested for their antibacterial potential under sterile conditions, and according to guidelines of the Clinical and Laboratory Standards Institute [24] using *Staphylococcus aureus* (Gram-positive bacteria) and *Pseudomonas aeruginosa* (Gram-negative bacteria). For testing, the desired bacteria were inoculated in Mueller–Hinton broth and incubated 2-6h in the incubator shaker at 37 °C, and the turbidity of the bacterial culture was standardized at OD_{600}=0.1 (contrast to 0.5 McFarland) to get $1.5x10^8$ CFU/mL before swabbing the agar plates.

A sterile borer was used to make wells of 8mm diameter into the Mueller–Hinton agar plates (Oxoid Ltd., UK). A cotton swab was immersed in the previously standardized broth culture of the bacteria and swabbed

uniformly on the agar plates. An aliquot of 100 µL of AHE, AgNO3, and Hh-AgNPs at concertation of 10 mg/ml was transferred into each well to measure the antibacterial activity, while the negative control well had distilled water [24].

2.9.2 Minimal inhibitory concentration (MIC)

The MIC was performed to determine the lowest concentration needed that prevent visible bacterial growth. Serial descending dilutions were prepared from Hh-AgNPs, AHE, and AgNO3 (range of 5 - 0.078 mg/ml). A 100µL of each dilution was placed in a well and plates were streaked with the desired previously standardized bacterial inoculum of *P. aeruginosa* and *S. aureus*. Plates were incubated at 37 °C overnight, and the inhibition zones were recorded in millimeters (mm)[25].

2.9.3 Antibiotics Susceptibility Test

To determine the potency of Hh-AgNPs and AHE, the antimicrobial activity was compared to the antibacterial activity of selective standard antibiotics against the tested bacteria. According to the Handbook of Performance Standards for antimicrobial susceptibility testing, (M100S, 26th edition) [26], sterile plates of Mueller–Hinton agar were streaked with a bacterial culture using a sterile cotton applicator dipped into the standardized bacterial inoculum (0.5M McFarland equivalence). The agar plates were left to dry for a few minutes before distributing the discs of selected antibiotics on the surface. The plates were incubated at 37 °C for 24hrs., then inhibition zones were measured millimeter (mm). For *P. aeruginosa*, Doxycycline (DO-30 µg), Metronidazole (MET-5 µg), and Ciprofloxacin (CIP-5 µg) were used as a positive control. Similarly, for *S. aureus*, Clarithromycin (CLR-15 µg), Clindamycin (DA-2 µg), and Ciprofloxacin (CIP-5 µg), were used.

2.10 Determination of Anticancer activity of the prepared Hh-AgNPs against Lung cancer cell line (A549)

2.10.1 Splitting of A549 lung cancer cell line

According to the method described by Mosmann et al., [27]. Splitting of the A549 cells was carried out by aspirating and removing old Dulbecco's Modified Eagle Medium (DMEM) media from the T-75 flask, and the cells were washed with sterile phosphate-buffered saline (PBS). Next, a trypsin solution was applied to the flask to release the cells from the surface, and the flask was then placed in a humid environment with 5% CO2 at a temperature of 37°C for 3-5 minutes. The cells were gently agitated to facilitate detachment and then neutralized with fresh a DMEM culture medium. The resulting cell suspension was moved to a sterile centrifuge tube and centrifuged.

Then, the supernatant was drawn off, leaving the cells to be resuspended in a new medium. After counting the cells, they were placed into a new tissue culture flask and incubated until they reached a coverage level of approximately 70-80%. This process was repeated to continue the expansion of the cells. A sterile environment was maintained throughout the procedure and were checked for possible cells contamination regularly.

2.10.2 Counting of A549 lung cancer cell line

According to the method described by Maurya et al. in 2010,[26] the cells were obtained as a cell suspension through trypsinization. This suspension was then diluted in a buffer to reach a concentration of 1-2 x 10^6 cell/ml. A trypan blue solution was created by dissolving 0.4 g of trypan blue powder in 100 mL of phosphate-buffered saline. The cell suspension was combined with the trypan blue solution and left to incubate for 3-5 minutes to allow the dye to enter the cells. The trypan blue-stained cell suspension was then placed onto the Hemo-cytometer Automated Cell Counter following the manufacturer's instructions for counting the cells.

The cell concentration was determined by dividing the number of viable cells by the volume of the cell suspension loaded onto the Hemo-cytometer. To ensure accuracy, the counting procedure was repeated several times, and the average cell concentration was calculated. Throughout the process, aseptic conditions were maintained to prevent contamination of the cell suspension, and suitable

protective equipment was used to avoid exposure to hazardous materials.

2.10.3 Treatment of A549 lung cancer cell line

To examine the effects of AHE, Hh-AgNPs, and $AgNO_3$ on A549 lung cancer cell lines, a 96-well microtiter plate was used. The cells were seeded into the wells at a density of 2000 cells per well and allowed to attach overnight. On the next day, the old medium was replaced with fresh medium containing varying concentrations of the drug, with the concentration range being from 1000 µg/ml to 15.62 µg/ml. The plate was then placed in a humid environment with 5% CO_2 and incubated at 37°C for 24, 48, and 72 hours. Control wells containing only the solvent (DMSO) without the drug were also included as described by Mosmann in 1983 [27].

After the incubation period, MTT assay was used to assess cell viability. The absorbance measurements at 570 nm were obtained using an ELISA microplate reader, and the data was analyzed to determine the half-maximal inhibitory concentration (IC_{50}) of each treatment.

3. RESULTS AND DISCUSSION

The phytochemical analysis of AHE reveals the presence of saponins, phenolic compounds and flavonoids. The presence of these compounds not only reduce Ag+ ions to AgNPs but also acted as capping/stabilizing agents which prevent aggregation of NPs[27] .In this regard, phenolic compounds were confirmed by measuring their content in AHE, it was found that the total phenolic content (TPC) was (43.98 ± 1mg/ g equivalent to gallic acid), and the total flavonoid content was (28.81 ± 0.076 mg /g equivalent to quercetin). The results of a recent study on the antioxidant potential of *H.helix* provides support for a theory regarding the role that antioxidant molecules from aqueous leaf extract may play in the biogenic synthesis of silver nanoparticles. Previous studies have shown that plants contain phenolic compounds and flavonoids, which have strong antioxidant properties and so promote the biosynthesis of nanoparticles [28-31].

Hh-AgNP showed an enhanced antioxidant activity compared with AHE, the antioxidant activity of synthesized Hh-AgNPs and AHE was evaluated by DPPH radical scavenging assay. Ascorbic acid was used as a positive control. The IC_{50} of AHE and Hh-AgNPs were 39.03 ± 0.557 µg/ml and 13.19±0.13 µg/mL respectively. Also, their antioxidant activity was evaluated by ABTS assay, it was found that IC_{50} of AHE and Hh-AgNPs were 24.81± 0.74 and 8.66± 0.64 respectively. According to previous literature obtained by Mishra et al., in 2012 [32], there are differences between the antioxidant activity of a compound when tested using DPPH or ABTS free radical's assays. Differences were because of variations in the chemical properties, reaction conditions, and the principle of the DPPH and ABTS assays, resulting in variations in the IC_{50} values obtained for the tested extract [32].

Kharat and Mendahulkar [33] studied the antioxidant activity of synthesized NPs using DPPH assay and observed their antioxidant potential. They suggested that these photosynthesized NPs can be used as a potential free radical scavenger. Divya, K. S et al in 2019 studied *In vitro* antioxidant activity of methanol and silver nanoparticles extract from *Trigonella foenum-graecum* and found significant free radical scavenging potential [34]. The results strongly recommended the application of AgNPs as useful natural antioxidants against different oxidative stress.

In a current study, NPs of *H. helix* crude extract was synthesized and evaluated for their cytotoxic effect and antimicrobial activity. Synthesis of Hh-AgNPs through bio-green method was identified when the color was changed to brownish upon adding AHE in $AgNO_3$ solutions (Fig 1. A). The intensity of the color was increased with increasing the incubation time. Collective oscillation of free electrons of reduced Hh-AgNPs were responsible for change in color of the reaction mixture [35]. Further, UV-visible spectrometric analysis of nanoparticles showed the maximum absorption of nanoparticles at a wavelength of at λ= 448 nm (Fig 1.B).

Previous study reported that AgNPs give absorption peak at 420- 450nm because of its plasma resonance (SPR) character [31,36]

Dynamic Light Scattering (DLS) demonstrated the size and surface charge distribution of biosynthesized Hh-AgNPs. It has been found that the average size and charge of Hh-AgNPs were125.1nm and -10 mv respectively (Fig 2. A). The size was 90.1nm with charge -16.0mv when 15%mg/ml pf PVP was used (Fig 2. B).

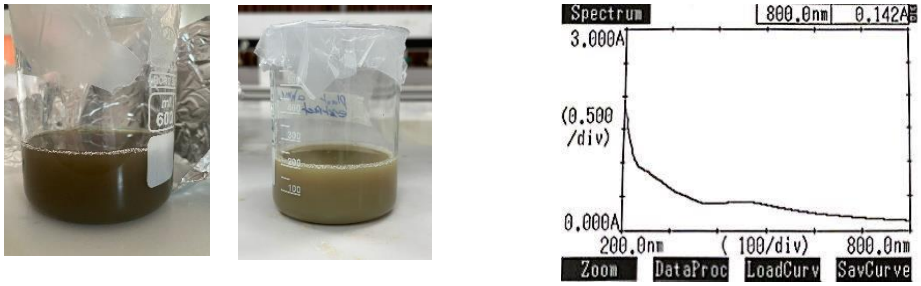

A **B**

Fig 1. A) Color changes from yellow to brown upon synthesis of AgNPs. B) UV/visible spectra of Hh-AgNPs.

AgNPs synthesized by plant extract most often are negatively charged [37,38]. This highly negative zeta potential value describes the presence of the bioactive compounds with a negative charge on the surface of AgNPs as a capping agent [39]. As we know, the zeta potential of AgNPs is one of the essential factors in preventing additional NP aggregation and stabilizing NPs by generating electronic repulsion [40]. On the other ha the negative zeta potential leads to increased cellular uptake and subsequent cytotoxicity observed from the positive-charge AgNPs [41].

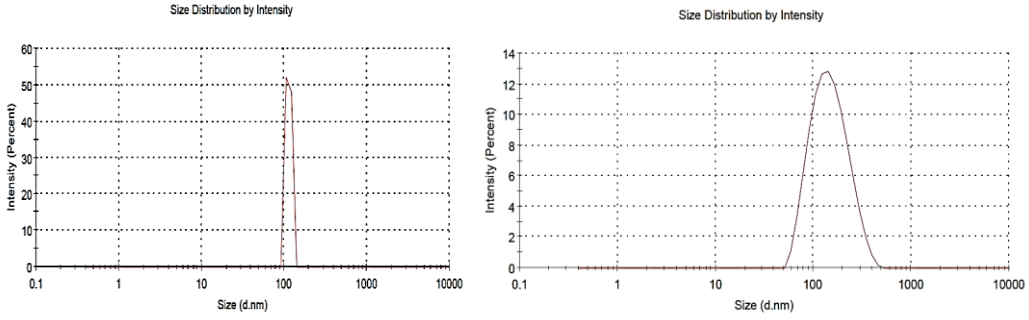

A **B**

Fig 2. DLS spectra A) Hydrodynamic size distribution of Hh-AgNPs without PVP B) Hydrodynamic size distribution of Hh-AgNPs with 15% mg/ml PVP

Broad spectrum antibacterial activity of AHE has been reported [42, 43]. The antibacterial activity of Hh-AgNPs against *S. aureus* and *P. aeruginosa* were determined by measuring the zone of growth inhibition (mm). The diameter of inhibition zone for both genus using Hh-AgNPs is slightly higher than that for AHE at all tested concentrations (Figure 3, and 4).

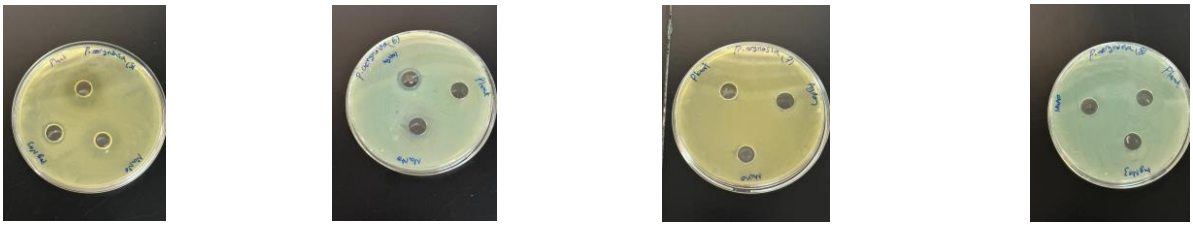

(A) (B) (C) (D)

Figure 3 Diameter of the inhibition zone after treatment of *P. aeruginosa* with various concentrations of Hh-AgNPs, AHE. and silver nitrate. (A: 0.625mg/ml, B: 0.3125mg/ml, C: 0.156mg/ml, D: 0.078mg/ml)

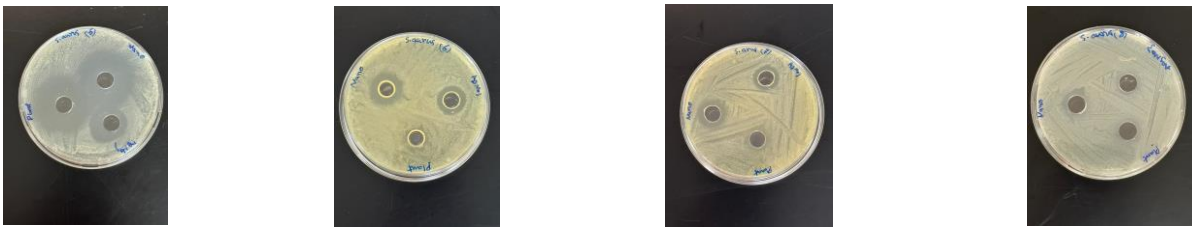

(A) (B) (C) (D)

Figure 4 Diameter of the inhibition zone after treatment of *S. aureus* with various concentrations of Hh-AgNPs, AHE. and silver nitrate. (A: 0.625mg/ml, B: 0.3125mg/ml, C: 0.156mg/ml, D: 0.078mg/ml)

The MIC of Hh-AgNPs against *S. aureus* was determined to be 0.156mg/ml, while the MIC of Hh-AgNPs, and AHE against *P. aeruginosa* was determined to be 0.3125 and 0625mg/ml, respectively. In the present study Hh-AgNPs were found to have a higher antibacterial activity compared to AHE (table 1). Reddy et al. reported that the enhanced antibacterial activity of biosynthesized NPs using *Piper longum* compared to the extract supports our results [44]. Inhibition of DNA replication and hindrance of protein synthesis are the mechanisms behind the antibacterial activity of metallic NPs [45].

Table 1: Antibacterial activity measured as zones of inhibition (mm) of Hh-AgNPs, AgNO3 and AHE against *S. aureus* and *P. aeruginosa*.

Concentration mg/mL	Diameter of inhibition zone (mm) *S. aureus*			Diameter of inhibition zone (mm) *P. aeruginosa*		
	Hh-AgNPs	AHE	$AgNO_3$	Hh-AgNPs	AHE	$AgNO_3$
10	44±2.51	38±2.30	20±4.05	39±3.05	36±5.60	17±1.20
5	42±4.00	37±6.50	19±3.51	35±2.64	30±2.08	16±1.10
2.5	40±2.49	34±4.01	18±3.42	27±1.52	29±2.00	15±0.57
1.25	39±5.01	34±0.57	16±1.15	24±5.20	22±0.57	14±0.58
0.625	36±4.20	32±4.35	16±4.10	18±1.12	20±1.15	12±0.57
0.3125	21±4.05	13±3.51	14±2.20	10±0.57	R	R
0.156	19±2.51	12±2.51	12±1.00	R	R	R
0.078	R	R	R	R	R	R

Hh-AgNPs and AHE were more effective than some standard antibiotics used for treatment of *P. aeruginosa* and *S. aureus* (table 2). Bacterial resistance to drugs is one the major global health issue, so there is a need to anticipate and develop potent antibiotic agents against multidrug resistance microbes. The use of AgNPs as antibacterial agent can be traced from ancient Greece [46].

Table 2: Inhibition zone diameter (mm) of several standard antibiotics' controls against *P. aeruginosa* and *S. aureus*

Antibiotic	Zone of inhibition (mm)	
	P. aeruginosa	***S. aureus***
Doxycycline (30µg)	R	R
Metronidazole (5µg)	R	R
Ciprofloxacin (5µg)	35± 0.23	35± 0.55
Clarithromycin (15µg)	R	40± 1.02
Clindamycin (2µg)	R	36± 0.88

R, resistant

The biomedical applications of AgNPs are promising with their tremendous effects in the fields of medicine, drug delivery and anti-angiogenic property of cancer [47-49]. In the present study the cytotoxic effect of AHE, Hh-AgNPs and AgNO3 was tested against A549 cell lines by using MTT assay. The viability of the A549 cell lines was observed after 24hr, 48hr and 72hr of treatment with AHE, Hh-AgNPs and AgNO3. Table 3 shows the IC_{50} value against A549 cell line.

The IC_{50} values after 24hr were determined to be 73.57, 15.16 and 395.5 µg/ml for AHE, Hh-AgNPs and AgNO3 respectively. The Hh-AgNPs showed excellent anticancer activity against A549 cell compared with AHE. This study strongly revealed the significant antiproliferative activity of biosynthesized silver nanoparticles. However, such activity may be due to the synergistic effect of both nanosized silver and bioactive phytocompounds attached on the surfaces of the NPs. These days much attention is being given to metallic NPs and their anticancer activity.

Table 3: Cytotoxic activity evaluation against A549 cell line

Sample	Anticancer activity against A549 lung cancer cell line (IC_{50}values)		
	24hr	**48hr**	**72hr**
AHE	73.57 µg/ml	87.96 µg/ml	103.7 µg/ml
AgNO3	395.5 µg/ml	341.3 µg/ml	542.5 µg/ml
Hh-AgNPs	15.16 µg/ml	18.61 µg/ml	25.55 µg/ml

4. CONCLUSION

In this study, stable bioactive silver nanoparticles were synthesized successfully using **H. helix** extract by bio-green method as a cost-effective manner. The nanoparticles possessed the added advantage of active phytoconstituents incorporated in them. Further, these nanoparticles were evaluated for their activities and showed higher antioxidant, antibacterial and cytotoxic activities compared with extract. The outcomes of this study illustrate a broad range of applications of bioactive silver nanoparticles synthesized by bio-green method.

Conflicts of interest

There are no conflicts to declare.

Author Contributions

Reem Issa and Sina M. Matalqah conceptualization, methodology, analyse and discuss the results, drafting and editing the final manuscript. Ahmad Alfalahi prepared silver nanoparticles and characterised them and participated in performance of antimicrobial and cytotoxicity tests. Hala .AL-Dagestani designed and conducted the antimicrobial activity test while Anas abed designed and conducted the cytotoxicity activity test.

Graphic Abstract:

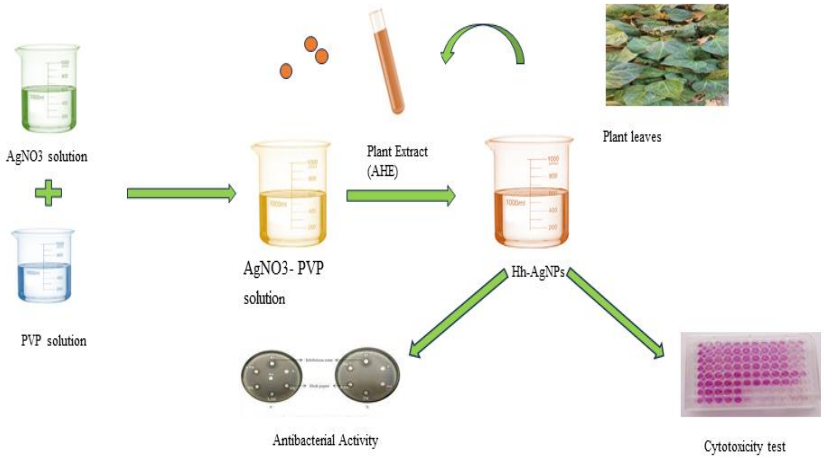

REFERENCES

1. Khan I., Saeed K. and Khan I. Nanoparticles: Properties, applications and toxicities. *Arabian J. Chem.* 2019; 12(7):908-931.
2. Matalqah S., Lafi Z. and Al-Kabariti A.Y. A recent review of PLGA-PEG hybrid nanoparticles for anticancer and anti-inflammatory applications. *Jordan J. Pharm. Sci.* 2025; 18(1):180-195.
3. Iravani S., Korbekandi H., Mirmohammadi S.V. and Zolfaghari B. Synthesis of silver nanoparticles: chemical, physical and biological methods. *Res. Pharm. Sci.* 2014; 9(6):385-406.
4. Ghorbani H.R., Safekordi A.A., Attar H. and Sorkhabadi S.M. Biological and non-biological methods for silver nanoparticles synthesis. *Chem. Biochem. Eng. Q.* 2011; 25(3):317-326.
5. Vithiya K. and Sen S. Biosynthesis of nanoparticles. *Int. J. Pharm. Sci. Res.* 2011; 2(11):2781.
6. Patel S. A review on synthesis of silver nanoparticles-a green expertise. *Life Sci. Leaflets.* 2021; 132.
7. Ahmed S., Ahmad M., Swami B.L. and Ikram S. A review on plants extracts mediated synthesis of silver nanoparticles for antimicrobial applications: a green expertise. *J. Adv. Res.* 2016; 7(1):17-28.
8. Metcalfe D.J. Hedera helix L. *J. Ecol.* 2005; 93(3):632-648.
9. Al-Snafi A.E. Pharmacological and therapeutic activities of Hedera helix—a review. *J. Pharm.* 2018; 8(5):41-53.
10. Stauss-Grabo M., Atiye S., Warnke A., Wedemeyer R.S., Donath F. and Blume H.H. Observational study on the tolerability and safety of film-coated tablets containing ivy extract (Prospan® Cough Tablets) in the treatment of colds accompanied by coughing. *Phytomedicine.* 2011; 18(6):433-436.
11. Fazio S., Pouso J., Dolinsky D., Fernandez A., Hernandez M., Clavier G. and Hecker M. Tolerance, safety and efficacy of Hedera helix extract in inflammatory bronchial diseases under clinical practice conditions: a prospective, open, multicentre postmarketing study in 9657 patients. *Phytomedicine.* 2009; 16(1):17-24.

12. Cwientzek U., Ottillinger B. and Arenberger P. Acute bronchitis therapy with ivy leaves extracts in a two-arm study. A double-blind, randomised study vs. another ivy leaves extract. *Phytomedicine.* 2011; 18(13):1105-1109.
13. Khan M.F., Akram M., Akhter N., Mukhtiar M., Zahid R., Khan F.S., et al. The evaluation of efficacy and safety of Cough (EMA) granules used for upper respiratory disorders. *Pak. J. Pharm. Sci.* 2018; 31(6):2617-2622.
14. Lutsenko Y.U.L.I.A., Bylka W.I.E.S.Ł.A.W.A., Matlawska I. and Darmohray R.O.M.A.N. Hedera helix as a medicinal plant. *Herba Polonica.* 2010; 56(1):83-96.
15. Mukattash H.K., Issa R., Hajleh M.N.A. and Al-Daghistani H. Inhibitory effects of polyphenols from Equisetum ramosissimum and Moringa peregrina extracts on Staphylococcus aureus, collagenase, and tyrosinase enzymes: in vitro studies. *Jordan J. Pharm. Sci.* 2024; 17(3):530-548.
16. Abbasifar A., Ghani S., Irvani M.A., Rafiee B., Kaji B.V. and Akbari A. Antibacterial activity of silver nanoparticles synthesized by using extracts of Hedera helix. *Zahedan J. Res. Med. Sci.* 2017; 19(1).
17. El Aziz M.M.A., Ashour A.S. and Melad A.S.G. A review on saponins from medicinal plants: chemistry, isolation, and determination. *J. Nanomed. Res.* 2019; 8(1):282-288.
18. Bissinger R., Modicano P., Alzoubi K., Honisch S., Faggio C., Abed M. and Lang F. Effect of saponin on erythrocytes. *Int. J. Hematol.* 2014; 100:51-59.
19. Lohvina H., Sándor M. and Wink M. Effect of ethanol solvents on total phenolic content and antioxidant properties of seed extracts of Fenugreek (Trigonella foenum-graecum L.) varieties and determination of phenolic composition by HPLC-ESI-MS. *Diversity.* 2021; 14(1):7.
20. Chang C.C., Yang M.H., Wen H.M. and Chern J.C. Estimation of total flavonoid content in propolis by two complementary colorimetric methods. *J. Food Drug Anal.* 2002; 10(3).
21. Matusiewicz M., Kosieradzka I., Niemiec T., Grodzik M., Antushevich H., Strojny B. and Gołębiewska M. In vitro influence of extracts from snail Helix aspersa Müller on the colon cancer cell line Caco-2. *Int. J. Mol. Sci.* 2018; 19(4):1064.
22. Re R., Pellegrini N., Proteggente A., Pannala A., Yang M. and Rice-Evans C. Antioxidant activity applying an improved ABTS radical cation decolorization assay. *Free Radic. Biol. Med.* 1999; 26(9-10):1231-1237.
23. Zein R., Alghoraibi I., Soukkarieh C., Ismail M.T. and Alahmad A. Influence of polyvinylpyrrolidone concentration on properties and anti-bacterial activity of green synthesized silver nanoparticles. *Micromachines.* 2022; 13(5):777.
24. Cockerill F.R., Wikler M., Bush K., Dudley M., Eliopoulos G. and Hardy D. Clinical and laboratory standards institute. Performance standards for antimicrobial susceptibility testing: twenty-second informational supplement. 2012.
25. Abu-Niaaj L.F., Al-Daghistani H.I., Katampe I., Abu-Irmaileh B. and Bustanji Y.K. Pomegranate peel: Bioactivities as antimicrobial and cytotoxic agents. *Food Sci. Nutr.* 2024; 12(4):2818-2832.
26. Biemer J.J. Antimicrobial susceptibility testing by the Kirby-Bauer disc diffusion method. *Ann. Clin. Lab. Sci.* 1973; 3(2):135-140.
27. Mosmann T. Rapid colorimetric assay for cellular growth and survival: application to proliferation and cytotoxicity assays. *J. Immunol. Methods.* 1983; 65(1-2):55-63.
28. Maurya D.K., Nandakumar N. and Devasagayam T.P.A. Anticancer property of gallic acid in A549, a human lung adenocarcinoma cell line, and possible mechanisms. *J. Clin. Biochem. Nutr.* 2010; 48(1):85-90.
29. Guta T. and Jemal K. Antioxidant and antimicrobial potentials of Nicotiana glauca Graham leaves extracts and synthesized silver nanoparticles: a phytochemical approach. *Jordan J. Pharm. Sci.* 2025; 18(1):57-76.

30. Jalilian F., Chahardoli A., Sadrjavadi K., Fattahi A. and Shokoohinia Y. Green synthesized silver nanoparticle from Allium ampeloprasum aqueous extract: characterization, antioxidant activities, antibacterial and cytotoxicity effects. *Adv. Powder Technol.* 2020; 31(3):1323-1332.
31. Mohanta Y.K., Panda S.K., Biswas K., Tamang A., Bandyopadhyay J., De D., et al. Biogenic synthesis of silver nanoparticles from Cassia fistula (Linn.): in vitro assessment of their antioxidant, antimicrobial and cytotoxic activities. *IET Nanobiotechnol.* 2016; 10(6):438-444.
32. Mishra K., Ojha H. and Chaudhury N.K. Estimation of antiradical properties of antioxidants using DPPH assay: a critical review and results. *Food Chem.* 2012; 130(4):1036-1043.
33. Kharat S.N. and Mendhulkar V.D. Synthesis, characterization and studies on antioxidant activity of silver nanoparticles using Elephantopus scaber leaf extract. *Mater. Sci. Eng. C* 2016; 62:719-724.
34. Divya K.S., Harshitha B.S., Kumar D. and Chauhan J.B. In vitro investigation of antioxidant potentiality of methanol and silver nanoparticles extract from *Trigonella foenum-graecum*. *J. Pharmacogn. Phytochem.* 2019; 8(3):2213-2221.
35. Noginov M.A., Zhu G., Bahoura M., Adegoke J., Small C., Ritzo B.A., et al. The effect of gain and absorption on surface plasmons in metal nanoparticles. *Appl. Phys. B* 2007; 86:455-460.
36. Nayak D., Ashe S., Rauta P.R., Kumari M. and Nayak B. Bark extract mediated green synthesis of silver nanoparticles: evaluation of antimicrobial activity and antiproliferative response against osteosarcoma. *Mater. Sci. Eng. C* 2016; 58:44-52.
37. Raja S., Ramesh V. and Thivaharan V. Green biosynthesis of silver nanoparticles using *Calliandra haematocephala* leaf extract, their antibacterial activity and hydrogen peroxide sensing capability. *Arab. J. Chem.* 2017; 10(2):253-261.
38. Rivera-Rangel R.D., González-Muñoz M.P., Avila-Rodriguez M., Razo-Lazcano T.A. and Solans C. Green synthesis of silver nanoparticles in oil-in-water microemulsion and nano-emulsion using geranium leaf aqueous extract as a reducing agent. *Colloids Surf. A Physicochem. Eng. Asp.* 2018; 536:60-67.
39. Khoshnamvand M., Huo C. and Liu J. Silver nanoparticles synthesized using *Allium ampeloprasum* L. leaf extract: characterization and performance in catalytic reduction of 4-nitrophenol and antioxidant activity. *J. Mol. Struct.* 2019; 1175:90-96.
40. Lam V.P., Beomseon L., Anh V.K., Loi D.N., Kim S., Kwang-Ya L. and Park J. Effectiveness of silver nitrate application on plant growth and bioactive compounds in *Agastache rugosa* (Fisch. & CA Mey.) kuntze. *Heliyon.* 2023; 9(9).
41. Kim S.T., Saha K., Kim C. and Rotello V.M. The role of surface functionality in determining nanoparticle cytotoxicity. *Acc. Chem. Res.* 2013; 46(3):681-691.
42. Zazharskyi V.V., Davydenko P., Kulishenko O., Borovik I.V., Zazharska N.M. and Brygadyrenko V.V. Antibacterial and fungicidal activities of ethanol extracts of 38 species of plants. *Biosyst. Divers.* 2020; 28(3):281-289.
43. Zazharskyi V.V., Davydenko P.O., Kulishenko O.M., Borovik I.V. and Brygadyrenko V.V. Antibacterial and fungicidal activities of ethanol extracts from *Cotinus coggygria*, *Rhus typhina*, *R. trilobata*, *Toxicodendron orientale*, *Hedera helix*, *Aralia elata*, *Leptopus chinensis* and *Mahonia aquifolium*. *Regul. Mech. Biosyst.* 2020; 11(2).
44. Reddy N.J., Vali D.N., Rani M. and Rani S.S. Evaluation of antioxidant, antibacterial and cytotoxic effects of green synthesized silver nanoparticles by *Piper longum* fruit. *Mater. Sci. Eng. C.* 2014; 34:115-122.
45. Feng Q.L., Wu J., Chen G.Q., Cui F.Z., Kim T.N. and Kim J.O. A mechanistic study of the antibacterial effect of silver ions on *Escherichia coli* and *Staphylococcus aureus*. *J. Biomed. Mater. Res.* 2000; 52(4):662-668.

46. Medici S., Peana M., Nurchi V.M. and Zoroddu M.A. Medical uses of silver: history, myths, and scientific evidence. *J. Med. Chem.* 2019; 62(13):5923-5943.
47. Zhang X.F., Liu Z.G., Shen W. and Gurunathan S. Silver nanoparticles: synthesis, characterization, properties, applications, and therapeutic approaches. *Int. J. Mol. Sci.* 2016; 17(9):1534.
48. Abdalla A.M., Xiao L., Ullah M.W., Yu M., Ouyang C. and Yang G. Current challenges of cancer anti-angiogenic therapy and the promise of nanotherapeutics. *Theranostics.* 2018; 8(2):533.
49. Simon S., Sibuyi N.R.S., Fadaka A.O., Meyer S., Josephs J., Onani M.O., et al. Biomedical applications of plant extract-synthesized silver nanoparticles. *Biomedicines.* 2022; 10(11):2792.

تقييم السمية الخلوية والنشاط المضاد للبكتيريا لجسيمات الفضة النانونية المصنعة بالتكنولوجيا الخضراء باستخدام مستخلص نبات اللبلاب

أحمد ناجي الفلاحي[1]، سيناء مطالقة*[1]، ريم العيسى[2]، هالة الداغستاني[3]، أنس العبد[4]

[1] قسم الصيدلانيات والتقنية الصيدلانية، كلية الصيدلة، مركز الأبحاث الدوائية والتشخيصية، جامعة عمان الأهلية.

[2] قسم العلوم الصيدلانية، كلية الصيدلة، مركز الأبحاث الدوائية والتشخيصية، جامعة عمان الأهلية.

[3] قسم العلوم الطبية المخبرية، كلية العلوم الطبية المساندة، جامعة عمان الأهلية.

[4]قسم الصيدلة الحيوية والسريرية، مركز الأبحاث الدوائية والتشخيصية، جامعة عمان الأهلية.

ملخص

في الوقت الحاضر جذبت جسيمات الفضة النانوية اهتمامًا كبيرًا نظرًا لخصائصها الفريدة التي تجعلها مفيدة في الطب الحيوي وأجهزة الاستشعار ومضادات الميكروبات، والمحفزات، وتطبيقات الألياف الضوئية. يعتبر التوليف الأخضر هو الطريقة الأكثر أمانًا وأسهل لإنتاج جسيمات الفضة النانوية. هدفت الدراسة إلى التحقق من النشاط المضاد للبكتيريا والسمية الخلوية لجسيمات الفضة النانوية المحضرة باستخدام المستخلص المائي لنبات اللبلاب ضد أنواع بكتيريا وخلايا سرطان الرئة. تم تصنيع جزيئات الفضة النانوية باستخدام المستخلص المائي لنبات اللبلاب كعامل اختزال والبولي فينايل بيروليدين كمثبت. ومن ثم تشخيص جزئيات الفضة النانوية المصنعة بواسطة مقياس الطيف الضوئي للأشعة فوق البنفسجية ومحلل حجم الجسيمات بطريقة تشتت الضوء الديناميكي. تم تصنيع هذه الجزئيات بنجاح وأظهرت أقصى امتصاص عند 448 نانوميتر مع تحسن في نشاطها السام لخلايا الرئة السرطانية بقيمة 15.16 ميكروغرام /مل كأدنى تركيز مثبط. وتحسن في نشاط هذه الجزئيات النانونية كمضاد للبكتيريا (المكورات العنقودية الذهبية) مقارنه مع المستخلص المائي. تعتبر الطرق البيولوجية فعالة من حيث التكلفة وصديقة للبيئة، وبالتالي يمكن أن تكون بديلاً اقتصاديًا وفعالاً لتخليق جسيمات الفضة النانوية على نطاق واسع.

الكلمات الدالة: اللبلاب (Hedera helix)، الجسيمات النانوية الفضية، التخليق الأخضر، المكورات العنقودية الذهبية، الزائفة الزنجاري، خلايا سرطان الرئة .A549.

* ***المؤلف المراسل: سيناء مطالقة***

S.matalqah@ammanu.edu.jo

تاريخ استلام البحث 2024/5/6 وتاريخ قبوله للنشر 2024/9/91.

Stability Indicating Rp-Hplc for Method Development and Validation for Simultaneous Estimation of Empagliflozin and Nateglinide in Bulk Drug

Kajol, Aditi Kaushik*[1], Nikhil Sharma [1]

[1] Department of Pharmaceutical Analysis & Quality Assurance, Laureate Institute of Pharmacy, Kathog, Kangra, India.

ABSTRACT

A simple, accurate, and precise stability-indicating RP-HPLC method was developed and validated for the simultaneous estimation of Empagliflozin and Nateglinide in bulk drug form. Chromatographic separation was performed on a Shim-pack C-18 column (250 × 4.6 mm, 5 µm) using a mobile phase of Acetonitrile: Water (90:10, v/v) adjusted to pH 3. The UV detection wavelength was set at 216 nm, the flow rate was maintained at 1 mL/min, and the injection volume was 20 µL. The retention times for Empagliflozin and Nateglinide were found to be 2.770 and 3.682 minutes, respectively. This method was validated according to ICH Q2(R1) guidelines for linearity, accuracy, precision, limit of detection (LOD), limit of quantification (LOQ), and robustness. A linear response was observed in the concentration range of 5–25 µg/mL for Empagliflozin and 10–50 µg/mL for Nateglinide. The LOD and LOQ for Empagliflozin were found to be 14.0502 µg/mL and 42.576 µg/mL, respectively, while for Nateglinide, they were 6.5398 µg/mL and 19.8178 µg/mL. Stress studies were performed in accordance with ICH Q1A(R2) guidelines. The drugs were subjected to stress conditions including photolytic, oxidative, thermal degradation, and acid/base hydrolysis to develop a stability-indicating method. The degraded products were effectively extracted and analyzed from the sample.

Keywords: Empagliflozin, RP-HPLC, Method validation, Stability indicating method, Nateglinide.

1. INTRODUCTION

Diabetes Mellitus (DM) is a chronic disease that affects protein, lipid and carbohydrate metabolism [1]. Diabetes Mellitus is characterized by a poor or inadequate insulin secretory response, causing hyperglycemia as well as inadequate utilization of carbohydrates (glucose). Diabetes Mellitus (DM), sometimes called "diabetes", is a common endocrine disease [2]. It is usually caused by a deficiency or deficiency of insulin or, in some cases, by a bad product of insulin (insulin resistance) [3]. Diabetes Mellitus (DM) is a disease that causes abnormal blood sugar levels, which is the main cause of prolonged hyperglycemic state in addition to recurrence of hypoglycaemia [4]. This disease is divided into groups 1 and 2, but there are other subtypes that can be caused by endocrine disorders, medications, diseases, immunity, genetics, or pancreatic disease [1,2]. These metabolic diseases lead to loss of life and can cause the decline of living beings by causing many problems affecting the heart, kidneys, blood vessels, eyes and nervous system [5].Approximately 20% of glucose in the body is controlled primarily by the hypothalamus through coordination with various hormones that influence food intake, energy, insulin utilization, hepatic glucose production, and glucose/fatty acid metabolism in adipose tissue and bone marrow2% of total body weight. Specifically for this purpose, the brain requires glucose to provide the energy needed by neurotransmitters to maintain the proper functioning of cells [6]. In addition to being involved in the pathogenesis of neurological diseases, glucose

[*] ***Corresponding author: Kajol, Aditi Kaushik***
kajolrana060@gmail.com
Received: 15/5/2024 Accepted: 19/9/2024.
DOI: https://doi.org/10.35516/jjps.v18i2.2648

also plays an important role in regulatory pathways associated with oxidative stress, cell death, hypothalamic circuit disorders, and glucose and insulin sensitivity [7]. Therefore, blood sugar control is important. More than 400 million people worldwide suffer from diabetes (DM), a major public health problem. These metabolic diseases are increasingly associated with life-threatening micro vascular, europathic consequences [8]. These metabolic diseases are increasingly associated with life-threatening micro vascular, macro vascular and neuropathic consequences. Diabetes Mellitus is caused by insulin resistance resulting from inadequate insulin secretion, damage to pancreatic beta cells, or lack of insulin use [9]. A sedentary lifestyle may be a factor in the rise of diabetes worldwide. The elderly population (>65 years old) is expected to reach 366 million by 2030[10]. Many problems associated with diabetes include kidney disease, neuropathy, heart and kidney problems, retinopathy, and eating disorders and other problems [11]. There are two types of diabetes: type 1 and type 2. Type 1 diabetes is an autoimmune disease that affects cells in the pancreas, reducing or interfering with insulin [12]. Many hormones are responsible for maintaining the body's glucose homeostasis. On the other hand, glucagon and insulin are two hormones that control glucose homeostasis [13]. As blood sugar rises, beta cells secrete insulin. Insulin increases glucose production by the liver, muscle, and fatty tissue or inhibits the liver's ability to produce glucose through the processes of glycolysis and gluconeogenesis [14]. Diabetes risk is increased by a number of factors. The following is a list of the main factors:

If a child or adolescent has type 1 diabetes, they are more likely to develop the disease if a parent or sibling has the disease. Risk factors for developing type 2 diabetes include being overweight, following a special diet, being over age 45, having a family history of the disease, being physically inactive, having diabetes or pregnancy, having high cholesterol or triglycerides, and having diabetes story [15]. Your risk of developing gestational diabetes is increased if you are overweight and over the age of 25, have gestational diabetes, have given birth to a baby weighing more than 30 pounds, or have a family history of type 2 diabetes or polycystic ovary syndrome [16]. According to the World Health Organization (WHO) Diabetes Global Report, the disease affects 422 million people worldwide. This figure is almost four times higher than in 1980[17]. According to the International Diabetes Federation (IDF), 40.9 million people in India currently suffer from diabetes, and this number is expected to increase to 69.9 million by 2025[18]. The hormones glucagon and insulin are secreted by the pancreas. Beta and alpha cells are located in the pancreatic islets and secrete insulin and glucagon, respectively [19]. Insulin lowers blood sugar levels by transporting glucose to the muscles, liver, and fatty tissues and producing glycogen. Although red blood cells and arteries can use glucose without insulin, alpha cells play an important role in blood sugar control because they produce glucagon, which accelerates glycogen in the liver and raises blood sugar levels. Additionally, after birth, the foetus may be at increased risk for obesity, metabolic and cardiovascular disease and cancer 80-90% have type 2 diabetes [20].

1.1 EMPAGLIFLOZIN

Empagliflozin (Figure 1), a sodium glucose cotransporter 2 (SGLT2) inhibitor, is a new class of oral medications used to treat type 2 diabetes (T2DM) [21]. Empagliflozin has a unique non-insulin-dependent mechanism of action that increases glucose release and lowers blood sugar and has the advantage of not producing hypoglycaemic effects due to its non-insulin-dependent properties. Additionally, Empagliflozin is very slightly soluble in water (pH 1-7.4) [22]. Empagliflozin is also used in adults with heart failure to reduce the risk of hospitalization and death from heart disease and stroke. It is also used in adults with kidney disease to reduce the risk of kidney failure, the need for hospitalization, and the risk of death from heart disease [23]. Chemically it is (2S, 3R, 4R, 5S, 6R)-2-[4-chloro-3-[[4-[(3S)-oxolan-3-yl] ox phenyl] methyl [Hydroxy]phenyl]-6 (hydroxy-methyl) oxane-3,4,5-triol [21].

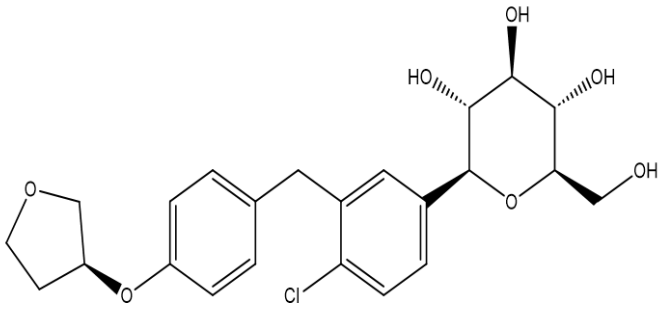

(2S,3R,4R,5S,6R)-2-[4-chloro-3-[[4-[(3S)-oxolan-3-yl]oxyphenyl]methyl]phenyl]-6-(hydroxymethyl)oxane-3,4,5-triol

Fig. 1. Chemical structure of Empagliflozin

1.2 NATEGINIDE

Nateglinide (NTG) [N(trans-4-isopropylcyclohexylcarbonyl)-d-phenylalanine] is a d-phenylalanine derivative without a sulfonylurea or amphetamine moiety and is a novel oral prandial glycaemic agent recently approved for the treatment of type 2 diabetes [24]. This meglitinide derivative works as follows: It stimulates insulin release from the beta cell membrane of the pancreas by closing ATP-dependent potassium channels, which leads to the opening of calcium channels [25]. The result of calcium influx causes insulin secretion. It is rapidly absorbed from the gastrointestinal tract, with blood concentration reaching peak in 0.5 to 1.0 hours. It is metabolized by the cytochrome P-450 system to inactive metabolites and eliminated with a half-life of 1.4 hours. Inactive metabolites and eliminated with a half-life of 1.4 hours [26].

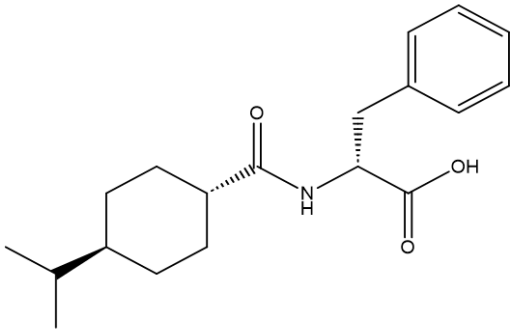

(2R)-2-({[trans-4-(1-methylethyl)cyclohexyl]carbonyl}amino)-3-phenylpropanoic acid

Fig. 2. Chemical structure of Nateglinide

2. MATERIALS AND METHOD:

2.1 Chemicals and reagents:

Empagliflozin and Nateglinide is a gift sample from Yarrow Chem product, Mumbai, India. HPLC grade chemicals: Acetonitrile and Water were preferred for the development of the method, this was obtained from CDH (Central drug house) (P) Ltd.

2.2 Instruments:

Chromatography was performed on High performance Liquid Chromatography (Shimadzu), manual sampler,

software Win chrome and detector (UV- visible). The chromatographic separation was performed using Column C-18 (Shim-pack) 250 X 4.6 mm, particle size 5µm.

Selection of Wavelength: Wavelength was fixed at 216 nm by performing UV spectroscopy.

2.3 CHROMATOGRAPHIC CONDITION:

The method development for analysis of Empagliflozin and Nateglinide was performed using various solvents finally the separation was achieved using a mobile phase consisting of Acetonitrile: water [90:10 v/v] pH=3, pumped at a flow rate of 1 ml/min, and Rheodyne injector with 20µl loop was used for injecting sample. The eluent was monitored at using a UV- detector at a wavelength of 216 nm. Before being used, the mobile phase was filtered through a 0.22 µm nylon membrane filter and then degassed in an ultrasonic bath.

2.4 Preparation of Mobile phase: 450 ml of HPLC grade acetonitrile are added to 50 ml of water in a mobile phase reservoir then adjust the PH 3 by OPA and the mixture is kept for sonication for 10 minutes

2.5 Preparation of standard stock solution:

Standard stock solution was prepared by dissolving 10mg of Empagliflozin and Nateglinide in 100mL acetonitrile and water that gives the concentration of 100 µg/ml. this solution was diluted with mobile phase as needed to produce several standard solutions.

2.6 Method Validation:

The optimized analytical method was validated for system suitability, linearity, accuracy, precision, limit of detection and limit of quantification and robustness in accordance with ICH guidelines for analytical procedure Q2 [R1] [27].

2.6.1 Linearity and range:

The linearity was evaluated at five concentration levels in the range between 5- 25µg/ml for Empagliflozin and 10-50µg/ml for Nateglinide. A calibration curve was plotted by plotting concentration against corresponding peak area and linearity was using least square regression analysis. The analytical range formed by the highest and lowest conc. of analyte was acceptable linearity obtained.

2.6.2 Precision

Precision, as defined by ICH rules, includes both repeatability and intermediate precision. Six replicates of the sample injection were used to assess repeatability. To determine intraday precision, three different doses of Empagliflozin (5, 10, and 15 µg/mL) and Nateglinide (10, 20, and 30 µg/mL) were tested three times on the same day. The three concentrations indicated above were tested on three consecutive days for inter-day precision in order to assess day-to-day variability.

2.6.3 Accuracy:

Accuracy was determined by calculating recovery of the analyte of interest. A fixed amount of pre-analysed sample was taken, and the standard drug was added and 80%, 100% and 120% levels. The standard concentration was fixed as 15µg/ml of Empagliflozin and 20µg/ml for Nateglinide, and three concentration levels of 10µg/ml, 15µg/ml and 20µg/mL for Empagliflozin and 10µg/ml, 20µg/ml and 30µg/mL for Nateglinide were added to the standard concentration. Each level was repeated three times. The percentage recovery standard deviation [% RSD] were taken into consideration for testing accuracy.

2.6.4 Limit of detection:

The term "limit of detection" refers to the lowest concentration of an analyte in a sample that can be identified but is not usually defined as a precise value (LOD). The standard deviation of response and slope were used to calculate the LOD.

$$\text{LOD} = \frac{3.3\ X\ \sigma}{S}$$

The linearity curve was used to compute the slope and standard deviation for Empagliflozin and Nateglinide concentrations ranging from 5 to 25µg/mL and 10 to50µg/mL.

2.6.5 Limit of quantitation (LOQ):

LOQ is the smallest amount of analyte in a sample that can be quantitatively measured with sufficient precision

and accuracy. LOQ is determined using the standard deviation of the response and the slope. The data was derived from the linearity curve, and the LOQ was determined.

$$\text{LOD} = \frac{10X\,\sigma}{S}$$

The linearity curve was used to compute the slope and standard deviation for Empagliflozin and Nateglinide concentrations ranging from 5 to 25µg/mL and 10 to50µg/mL.

2.6.6 Robustness:

The robustness of the study was examined by purposefully changing a few factors slightly, in accordance with ICH recommendations. The capacity of the drug to stay unaffected by minute variations in parameters such as temperature, detecting wavelength, flow rate, and mobile phase composition is mostly associated with resilience. Little adjustments to the chromatographic settings, such as changes to the detection wavelength, and flow rate, can be used to assess how resilient the approach is. At a concentration of 10µg/mL, robustness was evaluated.

3. FORCE DEGRADATION STUDIES:

Forced degradation studies include subjecting the drug substance to various stress condition to observe the extent of degradation and rate of degradation which is likely to occur in the course of storage. The degradation pathways studied are acid hydrolysis, basic hydrolysis, and oxidative degradation, thermal and photolytic degradation [28-31].

3.1 Acid Hydrolysis: Acid hydrolysis was done by adding accurately weighed 10mg of Empagliflozin and Nateglinide into a clean and dry round bottom flask. 50ml of freshly prepared Acetonitrile and water (90:10) 0.1 N HCl solution transfer to it and it was refluxed in a water bath for 6 hours by maintaining the temperature at 60℃. After refluxing the solution 1ml sample withdraw at different intervals for 6 h which was neutralized and dilute to 10ml with acetonitrile and water (90:10). The 20 µL of the resulting solution (20 µg/ ml) was injected and analysed.

3.2 Basic Hydrolysis: To a clean and dry round bottom flask accurately weighed 10mg of Empagliflozin and Nateglinidewas transferred. 50ml of freshly preparedAcetonitrile and water (90:10) 0.1 NaOH was added to it and it was refluxed in a water bath for 6 hours by maintain the temperature at 60℃. After refluxing the solution 1ml sample withdraw at different intervals for 6 h which was neutralized and dilute to 10ml with solvent combination of Acetonitrile and water 90:10. The 20 µL of the resulting solution (20 µg/ ml) was injected and analysed.

3.3 Photolytic degradation: Photolytic degradation studies was carried out by taking 10mg of Empagliflozin and Nateglinidedrug into a clean and dry petri dish which is covered with a glass lid. The drugs are kept under UV light for 12h and then, 10 mg of Empagliflozin and Nateglinideadded in 50 mL of solvent combination (Acetonitrile: water 90:10). After extracting the solution (1 mL), solvent combination (Acetonitrile: water 90:10) was added to dilute it to 10 mL. After 20 µL of the resultant solution (20 µg/ml) was injected, it was examined.

3.4 Oxidation degradation: To a clean and dry round volumetric flask accurately weigh 10mg of Empagliflozin and Nateglinidedrug was taken to this 50 mL of solvent combination (Acetonitrile: water 90:10) (v/v) hydrogen peroxide solution was added & was kept in the dark for 6h. the solution (1ml) was diluted to 10mL with solvent. The 20 µL of resulting solutions (20 µg/ ml) was injected and analysed.

3.5 Thermal degradation: Photolytic degradation studies was carried out by taking 10mg of Empagliflozin and Nateglinide drug into a clean and dry petri dish which is covered with a glass lid. The drugs are kept under oven for 12h at 100^0 C and then, 10 mg of Empagliflozin and Nateglinideadded in 50 mL of solvent combination (Acetonitrile: water 90:10). After extracting the solution (1 mL), solvent combination (Acetonitrile: water 90:10) was added to dilute it to 10 mL. After 20 µL of the resultant solution (20 µg/ml) was injected, it was examined.

4. RESULTS AND DISCUSSION:

A stability-indicating and reverse-phase high-performance liquid chromatography (RP-HPLC) method were developed and validated for the accurate and precise estimation of Empagliflozin and Nateglinide in bulk. Various validation parameters, including stressed samples and different mobile phase compositions and flow rates, were explored to establish the method. Through multiple iterations and adjustments of chromatographic conditions, optimal parameters were identified and confirmed. Empagliflozin and Nateglinide exhibited well-defined peaks with excellent symmetry and a stable baseline using a mobile phase composed of Acetonitrile: Water (90:10 v/v) at a flow rate of 1.0 ml/min. The retention times for Empagliflozin and Nateglinide were determined to be 2.770 and 3.682, respectively, with distinct peaks observed at 216 nm.

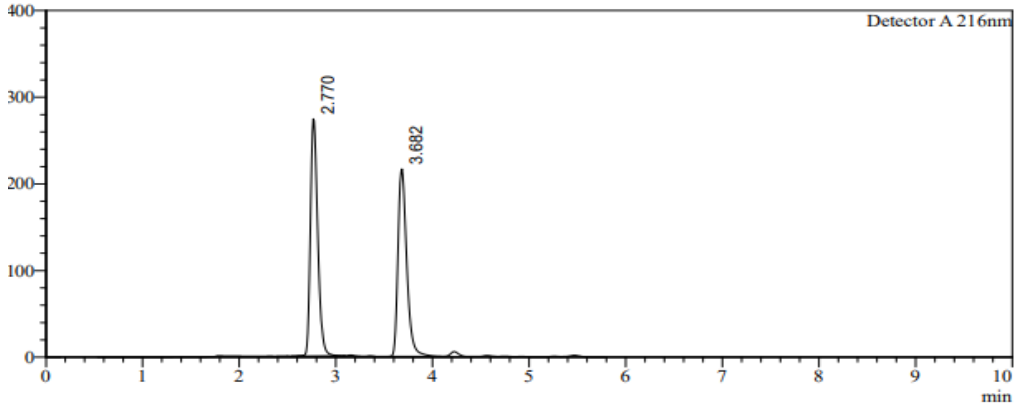

Fig.3. Chromatogram of Empagliflozin and Nateglinide

4.1 Linearity and range:

For linearity of Five-point concentration curve was obtained in concentration ranges 5 µg/mL- 25 µg/mL for Empagliflozin and 10 µg/mL- 50 µg/mL for Nateglinide. The response of the drugs was found to linear in the selected concentration range, the regression equation Y=172802x +110348, Y= 619704x - 352451 for Empagliflozin and Nateglinide and, the correlation coefficient (r^2) for Empagliflozin and Nateglinide were 0.9993 and 0.9992 respectively

Table 1. Linearity and Range data for Empagliflozin

Sr no.	Concentration µg/mL	Peak Area (mv)
1.	5 µg/mL	1012327
2.	10 µg/mL	1799519
3.	15 µg/mL	2699465
4.	20 µg/mL	3536841
5.	25 µg/mL	4463705
Average Area		2702371
Slope		172802
Y – intercept		110348
Correlation Coefficient		0.9993

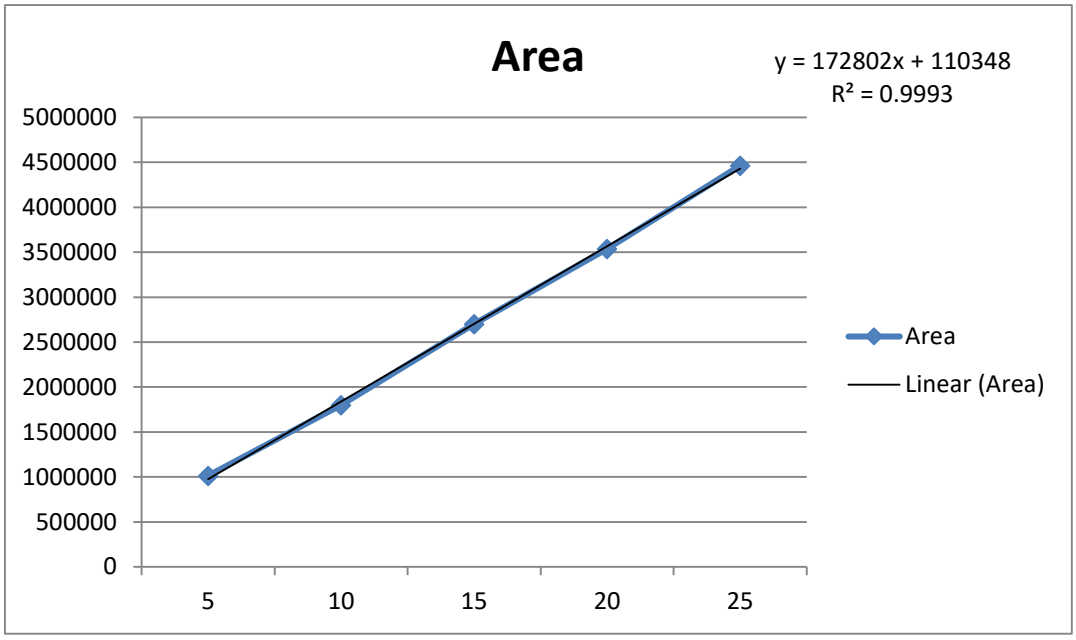

Fig.4. Calibration curve of Empagliflozin Y = 172802x + 110348Slope = 172802, Intercept = 110348, Correlation coefficient = 0.9993.

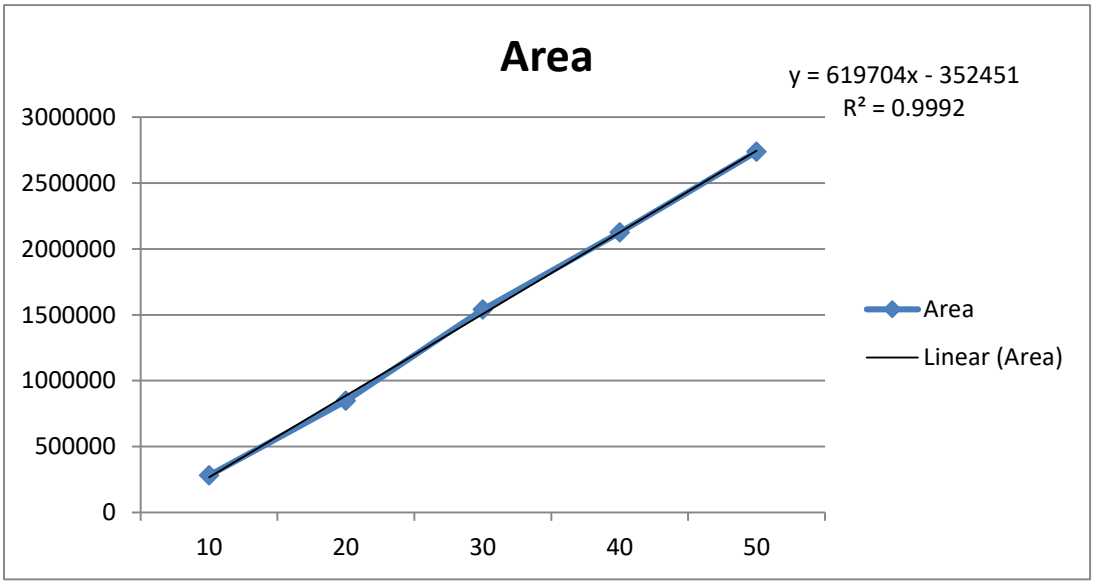

Fig.5. Calibration curve of Nateglinide. Y= 619704x - 352451Slope= 619704, Intercept = 352451, Correlation Coefficient = 0.9992

Table 2. Linearity and Range data for Nateglinide

Sr no.	Concentration µg/mL	Peak Area (mv)
1.	10 µg/mL	280427
2.	20 µg/mL	847141
3.	30 µg/mL	1540315
4.	40 µg/mL	2125807
5.	50 µg/mL	2739613
Average Area		1506661
Slope		619704
Y – intercept		352451
Correlation Coefficient		0.9992

4.2 Precision:

The analytical method's precision is characterized by the concordance level among individual test outcomes derived from applying the method across various samples. Precision assessments of the proposed method were conducted, encompassing evaluations for repeatability and intermediate precision (both within and between days). The performance of the HPLC instrument was assessed under chromatographic conditions by repetitively injecting 10 µg/mL of Empagliflozin and Nateglinide. The Relative Standard Deviation (RSD) was ascertained to be within acceptable limits, signifying the enhanced accuracy of the proposed methodology. Precision results are shown in Tables 3, 4, and 5.

Table.3. Interday precision of the developed method for Empagliflozin and Nateglinide

Interday precision										
Empagliflozin						**Nateglinide**				
Sr.no.	**Conc. (µg/ml)**	**Peak Area**	**Mean**	**S. D**	**%RSD**	**Conc. (µg/ml)**	**Peak Area**	**Mean**	**S. D**	**%RSD**
1.	**5**	1012327 1012445 1012352	1012375	62.179895	0.006142	**10**	280427 281154 280957	280846	375.996	0.13388
2.	**10**	1799519 1785491 1776497	1787169	11602.37	0.649204	**20**	847141 836549 859642	847777.3	11559.64	1.363524
3.	**15**	2699465 2697257 2683581	2693434	8604.356	0.319457	**30**	1540315 1542698 1541263	1541425	1199.765	0.077835

Table.4. Intraday precision of the developed method for Empagliflozin and Nateglinude

Intraday precision										
Empagliflozin						**Nateglinide**				
Sr.no.	**Conc. (µg/ml)**	**Peak Area**	**Mean**	**S. D**	**%RSD**	**Conc. (µg/ml)**	**Peak Area**	**Mean**	**S. D**	**%RSD**
1.	**5**	1012698 1025612 1010256	1016189	8251.682	0.812023	**10**	296554 295345 263216	285038.3	18908.36	6.63362
2.	**10**	1885649 1895478 1883654	1888260	6329.774	0.335217	**20**	877638 854412 884569	872206.3	15795.2	1.810948
3.	**15**	2597212 2696882 2696892	2663662	57547.39	2.160461	**30**	1890264 1865493 1890246	1882001	14296.35	0.759636

Table.5. Repeatability of the developed method for Empagliflozin and Nateglinide

Empagliflozin			**Nateglinide**	
Sr.no	**(Conc.(ug/ml)**	**Peak Area**	**(Conc.(ug/ml)**	**Peak Area**
1	5	1012327	10	280427
2.	5	1012341	10	280425
3.	5	1012356	10	280431
4.	5	1012356	10	280451
5.	5	1012356	10	280451
6.	5	1012351	10	280429
7.	**Mean**	1012348	**Mean**	280435.7
8.	**S. D**	11.75443	**S. D**	12.04436
9.	**%RSD**	0.001161	**%RSD**	0.004295

4.3 Accuracy:

The percentage recovery of the spiked sample was with 100±2% which ensures the accuracy of the developed method. Result of accuracy shown in Table.6,

Table.6. Accuracy of the developed method for Empagliflozin

Empagliflozin							
Sr. no.	**Unfortified sample**			**Fortified sample**			**%Recovery**
	Conc. (ug/ml)	**Area**	**Mean (Area)**	**Conc. (ug/ml)**	Area	**Mean (Area.)**	
1.	**10**	2065996	2066353	**10+15**	4935826	4935713	**100.02%**
		2066521			4934659		
		2066541			4936654		
2.	**15**	3085466	3088801	**15+15**	5546712	5551106	**100.07%**
		3085475			5547125		
		3095462			5559482		
3.	**20**	3954841	3886503	**20+15**	5016984	5019012	**99.88%**
		3859432			5024571		
		3845236			5015482		

Table.7. Accuracy of the developed method for Nateglinide

Nateglinide							
Sr. no.	**Unfortified sample**			**Fortified sample**			**%Recovery**
	Conc. (ug/ml)	**Area**	**Mean (Area)**	**Conc. (ug/ml)**	**Area**	**Mean (Area.)**	
1.	**10**	311549	316328	**10+20**	1825841	1803014	**102.64%**
		312694			1756621		
		324741			1826581		
2.	**20**	874695	879354.7	**20+20**	2468741	2469894	**99.40%**
		889821			2484561		
		873548			2456379		
3.	**30**	1736951	1730263	**30+20**	3015941	3020099	**100.04%**
					3018743		
					3025613		
		1725694					
		1728143					

4.4 Limit of detection and Limit of Quantification

Limit of detection (LOD) and limit of quantification (LOQ) was estimated from the standard deviation of the y-intercepts and slope of the calibration curve of Empagliflozin and Nateglinide. The LOD were found to be for Empagliflozin14.0502, for Nateglinide 6.539873 µg/ml and LOQ were found to be forEmpagliflozin42.57638, for Nateglinide 19.8178 µg/ml. This showed that developed method can detect and quantify at lower concentration was highly sensitive and other less sensitive.

4.5 Robustness:

Robustness of Empagliflozin and Nateglinide was determined by studying the small changes in chromatographic condition as change in flow rate (± 2mL/ min), wavelength detection (±2 nm) respectively. Robustness was assessed at concentration 5 µg/ ml and 10 µg/ ml. The standard deviation of response was calculated for each parameter and % RSD was found to less than 2% indicating that the method is robust as shown in Table.8,9

Table.8. Robustness results of the proposed RP- HPLC method for Empagliflozin

Sr.no	Parameters			Peak Area	RT	USP	
	Optimized		Used			Plate Count	Tailing factor
1.	Flow Rate (±2)	1ml/min	0.8ml/min 1.2ml/min	957654 112365	2.423 3.894	5239 5843	1.085 1.272
2.	Wavelength detection (±2)	216nm	214 nm 218 nm	1254789 1156984	2.751 2.512	5088 5120	1.380 1.375

Table.9. Robustness results of the proposed RP- HPLC method for Nateglinide

Sr.no	Parameters			Peak Area	RT	USP	
	Optimized		Used			Plate Count	Tailing factor
1.	Flow Rate (±2)	1ml/min	0.8ml/min 1.2ml/min	260569 309161	3.657 2.397	3654 2569	1.005 0.954
2.	Wavelength detection (±2)	216nm	214 nm 218 nm	275632 293741	3.156 3.178	1209 1141	0.678 0.459

4.6 Force Degradation:

The chromatograms obtained from samples exposed to be acidic, basic, oxidative, thermal and photo degradation depicted well- separated peaks of Empagliflozin and Nateglinide, its having retention time 2.770, 3.682 and some additional peaks at different values. Acid degradation for empagliflozin show 1 extra peak and for Nateglinide show additional peaks. In base degradation for empagliflozin show two additional peaks and for Nateglinide show additional peaks. In case of oxidative, photodegradation and thermal degradation, they show 2 additional peaks for Empagliflozin, and for Nateglinide, it shows additional peaks. The percentage of degradation product is listed in Table 10. Results of force degradation are shown in Fig.6,7,8,9,10,11,12,13,14,15.

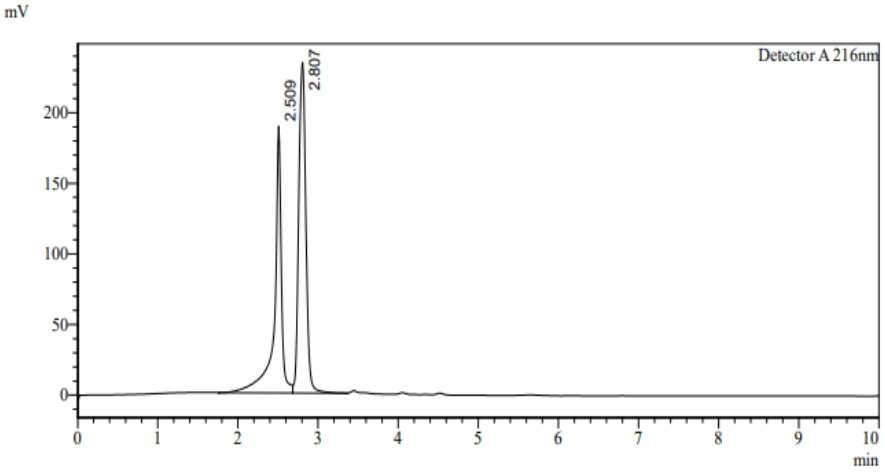

Fig. 6 Acid degradation of Empagliflozin

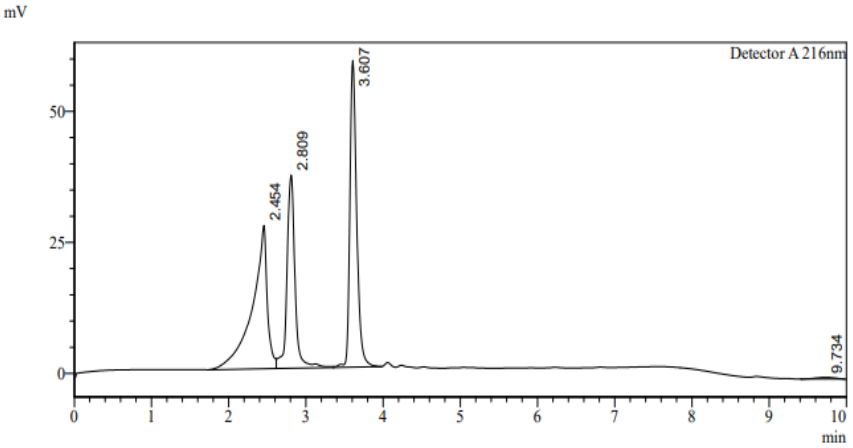

Fig. 7 Base degradation of Empagliflozin

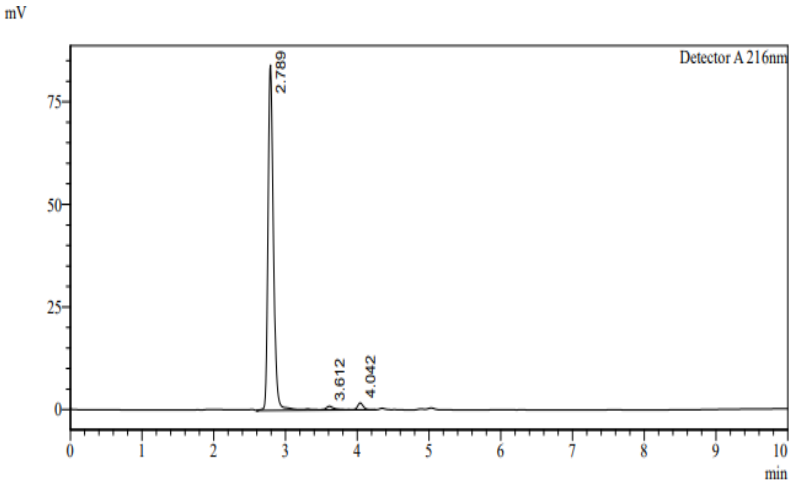

Fig. 8 Photo degradation of Empagliflozin

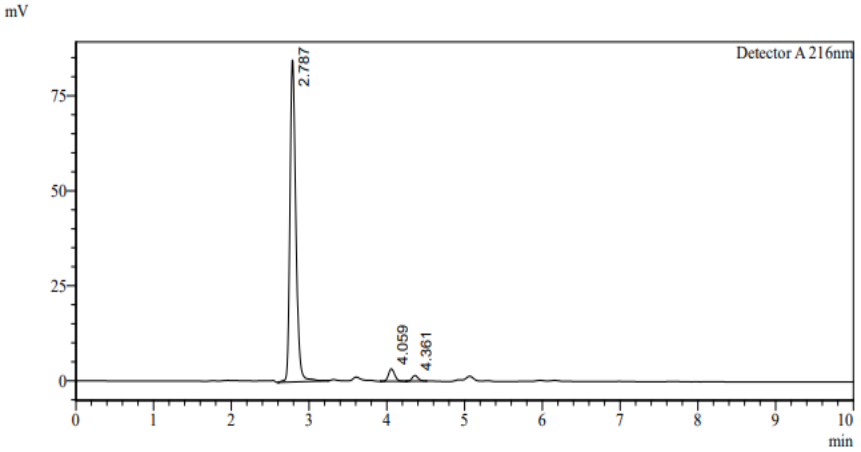

Fig. 9 Thermal degradation of Empagliflozin

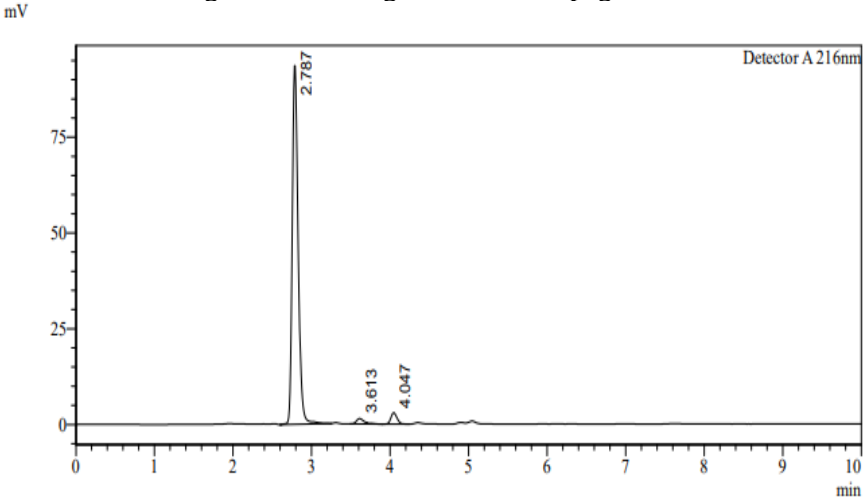

Fig. 10 Oxidative degradation of Empagliflozin

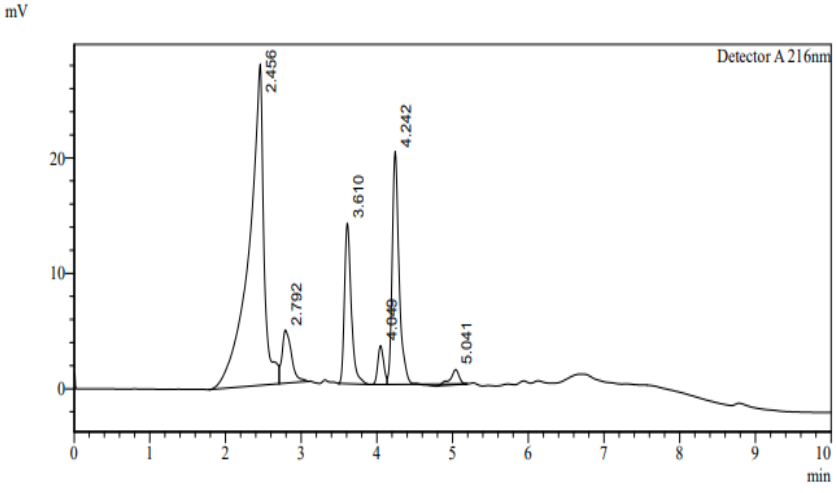

Fig. 11 Acid degradation of Nateglinide

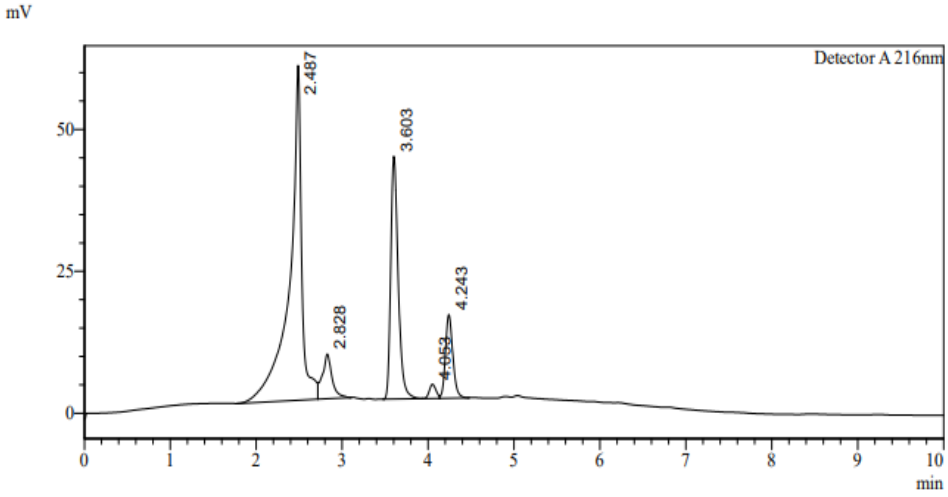

Fig. 12 Base degradation of Nateglinide

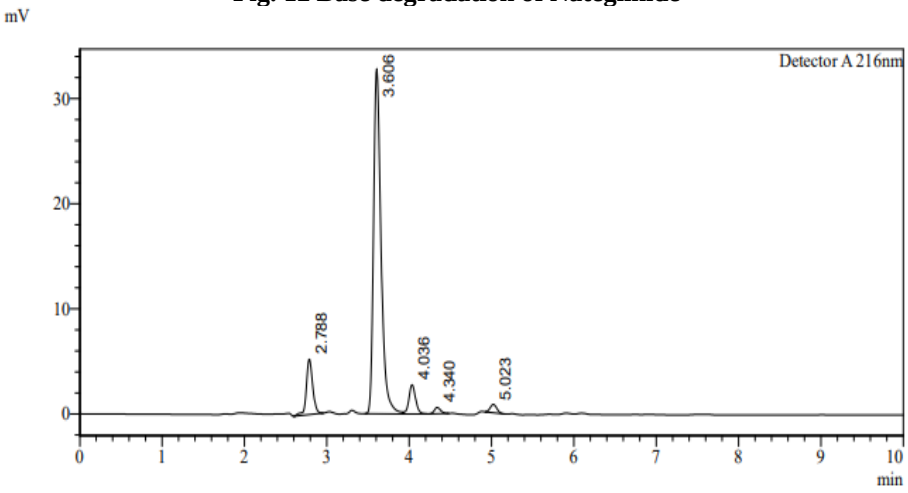

Fig. 13 Photo degradation of Nateglinide

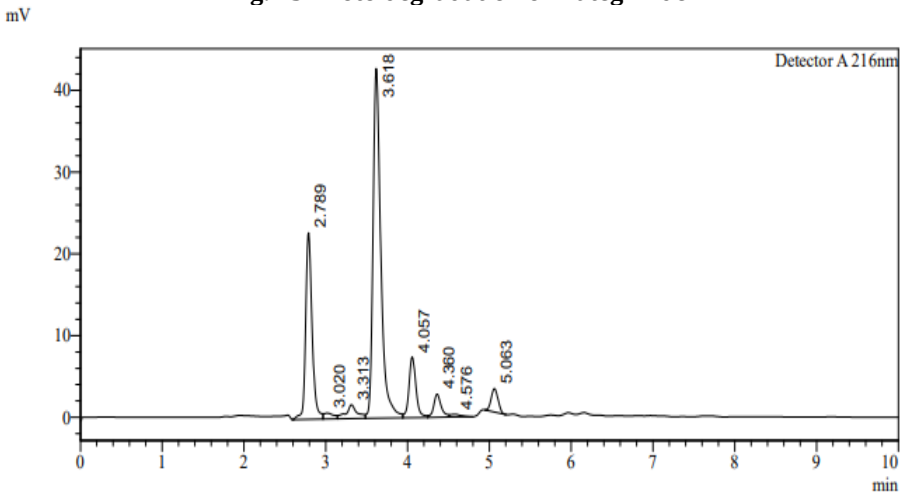

Fig. 14 Thermal degradation of Nateglinide

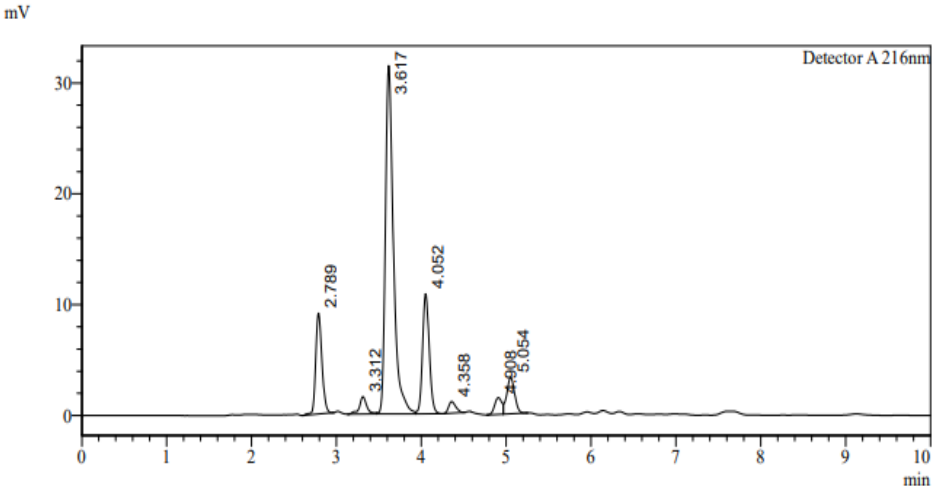

Fig. 15 Oxidative degradation of Nateglinide

Table.10. Force degradation study data of Empagliflozin and Nateglinide

	Empagliflozin			Nateglinide		
Type of degradation	**Area**	**% Recovered**	**%Degradation**	**Area**	**% Recovered**	**%Degradation**
Acid	1449208	44	**56%**	86794	87	**13%**
Base	265973	74	**26%**	259043	74	**26%**
Oxidation	490651	6	**94%**	20741	43	**57%**
Photo degradation	445996	4	**96%**	207411	20	**80%**
Thermal degradation	449292	6	**94%**	282913	45	**55%**

5. CONCLUSION

The study shows that the developed RP-HPLC method is fast precise, accurate, specific and stability. The proposed method applied for the simultaneous estimation of both the drugs in bulk form. These are within short analysis time and the low value of % RSD indicate that the proposed method is highly precise. The stability indicating method was developed and validated according to the ICH guidelines for simultaneous estimation of Empagliflozin and Nateglinide in bulk drug by RP-HPLC. Finally, concluded that the method is suitable for user in routine quality control analysis of Empagliflozin and Nateglinide in active pharmaceutical ingredient.

REFERENCES

1. Athyros V.G., Doumas M., Imprialos K.P., Stavropoulos K., Georgianou E., Katsimardou A., and Karagiannis A. Diabetes and lipid metabolism. *Hormones*. 2018; 17:61–67.
2. Sarkar B.K., Akter R., Das J., Das A., Modak P., Halder S., Sarkar A.P., and Kundu S.K. Diabetes mellitus: A comprehensive review. *Journal of Pharmacognosy and Phytochemistry*. 2019; 8(6):2362–2371.
3. Kahn B.B. Type 2 diabetes: when insulin secretion fails to compensate for insulin resistance. *Cell*. 1998; 92(5):593–596.

4. Mukhtar Y., Galalain A., and Yunusa U. A modern overview on diabetes mellitus: a chronic endocrine disorder. *European Journal of Biology*. 2020; 5(2):1–14.
5. Soumya D., and Srilatha B. Late stage complications of diabetes and insulin resistance. *J Diabetes Metab*. 2011; 2(9):1000167.
6. Cusi K. The epidemic of type 2 diabetes mellitus: its links to obesity, insulin resistance, and lipotoxicity. *Diabetes and Exercise*. 2009; pp.3–54.
7. Soares E., Nunes S., Reis F., and Pereira F.C. Diabetic encephalopathy: the role of oxidative stress and inflammation in type 2 diabetes. *International Journal of Interferon, Cytokine and Mediator Research*. 2012; 75–85.
8. Khursheed R., Singh S.K., Wadhwa S., Kapoor B., Gulati M., Kumar R., Ramanunny A.K., Awasthi A., and Dua K. Treatment strategies against diabetes: Success so far and challenges ahead. *European Journal of Pharmacology*. 2019; 862:172625.
9. Ahmed K.A.A., Muniandy S., and Ismail I.S. Type 2 diabetes and vascular complications: A pathophysiologic view. *Biomedical Research-India*. 2010; 21(2):147–155.
10. Wild S., Roglic G., Green A., Sicree R., and King H. Global prevalence of diabetes: estimates for the year 2000 and projections for 2030. *Diabetes Care*. 2004; 27(5):1047–1053.
11. Shahi A., Prasad V.S., Imam S.S., Muheem A., and Jahangir M.A. Pathophysiological ramifications of diabetic condition: a review. *Asian Journal of Biomedical and Pharmaceutical Sciences*. 2018; 8:28–38.
12. Ozougwu J.C., Obimba K.C., Belonwu C.D., and Unakalamba C.B. The pathogenesis and pathophysiology of type 1 and type 2 diabetes mellitus. *J Physiol Pathophysiol*. 2013; 4(4):46–57.
13. Quesada I., Tudurí E., Ripoll C., and Nadal A. Physiology of the pancreatic α-cell and glucagon secretion: role in glucose homeostasis and diabetes. *Journal of Endocrinology*. 2008; 199(1):5–19.
14. Sharabi K., Tavares C.D., Rines A.K., and Puigserver P. Molecular pathophysiology of hepatic glucose production. *Molecular Aspects of Medicine*. 2015; 46:21–33.
15. Larsson K., Elding-Larsson H., Cederwall E., Kockum K., Neiderud J., Sjöblad S., Lindberg B., Lernmark B., Cilio C., Ivarsson S.A., and Lernmark Å. Genetic and perinatal factors as risk for childhood type 1 diabetes. *Diabetes/Metabolism Research and Reviews*. 2004; 20(6):429–437.
16. Yong H.Y., Mohd Shariff Z., Mohd Yusof B.N., Rejali Z., Tee Y.Y.S., Bindels J., and van Der Beek E.M. Independent and combined effects of age, body mass index and gestational weight gain on the risk of gestational diabetes mellitus. *Scientific Reports*. 2020; 10(1):8486.
17. World Health Organization. WHO Global report on diabetes. *World Health Organization*. 2016.
18. Shukla M., Khanna R.S., Shukla M., Mishra A., Singh A., Gupta B., Shukla M., Shukla S.M., Singh N.P., Chaterjee R., and Srivastava P. *The Indian Journal of Research*.
19. Gromada J., Franklin I., and Wollheim C.B. α-Cells of the endocrine pancreas: 35 years of research but the enigma remains. *Endocrine Reviews*. 2007; 28(1):84–116.
20. Norton L., Shannon C., Gastaldelli A., and DeFronzo R.A. Insulin: The master regulator of glucose metabolism. *Metabolism*. 2022; 129:155142.
21. Neumiller J.J. Empagliflozin: a new sodium-glucose co-transporter 2 (SGLT2) inhibitor for the treatment of type 2 diabetes. *Drugs in Context*. 2014; 3.
22. Ndefo U.A., Anidiobi N.O., Basheer E., and Eaton A.T. Empagliflozin (Jardiance): a novel SGLT2 inhibitor for the treatment of type-2 diabetes. *Pharmacy and Therapeutics*. 2015; 40(6):364.
23. Kowalska K., Walczak J., Femlak J., Młynarska E., Franczyk B., and Rysz J. Empagliflozin—A new chance for patients with chronic heart failure. *Pharmaceuticals*. 2021; 15(1):47.

24. Tentolouris N., Voulgari C., and Katsilambros N. A review of nateglinide in the management of patients with type 2 diabetes. *Vascular Health and Risk Management*. 2007; 3(6):797–807.
25. Ashcroft F.M., and Gribble F.M. ATP-sensitive K^+ channels and insulin secretion: their role in health and disease. *Diabetologia*. 1999; 42(8):903.
26. Weaver M.L., Orwig B.A., Rodriguez L.C., Graham E.D., Chin J.A., Shapiro M.J., McLeod J.F., and Mangold J.B. Pharmacokinetics and metabolism of nateglinide in humans. *Drug Metabolism and Disposition*. 2001; 29(4):415–421.
27. ICH Guideline. Validation of analytical procedures: text and methodology. *Q2 (R1)*. 2005; 1(20):05.
28. Rignall A. ICHQ1A (R2) stability testing of new drug substance and product and ICHQ1C stability testing of new dosage forms. *ICH Quality Guidelines: An Implementation Guide*. 2017; 3–44.
29. Alzweiri M., Sweidan K., and Aqel Q. Investigation of the chemical stability of lenalidomide in methanol/ethanol solvents using RP-HPLC-UV and LC-MS. *Jordan Journal of Pharmaceutical Sciences*. 2022; 15(3):305–314.
30. Bharti A.A., and Jeyaseelan C. Quantification of potential impurities present in testosterone undecanoate active pharmaceutical ingredient by stability indicating HPLC method using UV detector. *Jordan Journal of Pharmaceutical Sciences*. 2019; 12(1):1–15.
31. Sonawane S.S., Joshi G.J., and Kshirsagar S.J. Development and validation of HPLC method for quantification of zonisamide in spiked human plasma. *Jordan Journal of Pharmaceutical Sciences*. 2022; 15(1):40–50.

التطوير والتحقق من طريقة RP-HPLC المؤشرة على الثبات للتقدير المتزامن للإمباغليفلوزين والناتيغلينيد في المادة الدوائية الخام

كاجول، أديتي كوشيك[1]*، نيكيل شارما[1]

[1]قسم تحليل الأدوية وضمان الجودة، معهد لوريات للصيدلة، كاثوغ، كانغرا، هيماشال براديش، الهند.

ملخص

تم تطوير وتحقق طريقة RP-HPLC بسيطة ودقيقة ومؤشرة على الثبات للتقدير المتزامن للإمباغليفلوزين والناتيغلينيد في المادة الدوائية الخام. تم إجراء الفصل الكروماتوغرافي على عمود) Shim-pack C-18بأبعاد 250 × 4.6 مم، 5 ميكرومتر)، باستخدام الطور المتحرك أسيتونتريل: ماء (90:10 (v/vبدرجة حموضة 3 لتطوير هذه الطريقة. تم ضبط طول موجة الكشف بالأشعة فوق البنفسجية عند 216 نانومتر، ومعدل التدفق عند 1 مل/دقيقة، وحجم الحقن عند 20 ميكرولتر. تم العثور على زمن الاحتجاز للإمباغليفلوزين والناتيغلينيد ليكون 2.770 و 3.682 دقيقة على التوالي. تم التحقق من هذه الطريقة وفقًا لإرشادات ICH Q2 R1 من حيث الخطية، الدقة، التكرارية، حد الكشف ((LOD، حد التقدير ((LOQ، والمتانة. تم ملاحظة استجابة خطية في نطاق تركيز 5–25 ميكروغرام/مل للإمباغليفلوزين و10–50 ميكروغرام/مل للناتيغلينيد. كانت حدود الكشف والتقدير للإمباغليفلوزين 14.0502 و 42.576 ميكروغرام/مل، وللناتيغلينيد 6.5398 و 19.8178 ميكروغرام/مل على التوالي. تم إجراء دراسات الإجهاد وفقًا لإرشادات ICH Q1A R2، حيث تعرضت الأدوية لظروف إجهاد تشمل التحلل الضوئي، الأكسدة، التحلل الحراري، التحلل الحمضي والقلوي، وذلك لتطوير نهج مؤشِّر على الثبات. تم استخراج المنتجات المتدهورة بفعالية من العينة.

الكلمات الدالة: إمباغليفلوزين، RP-HPLC، التحقق من الطريقة، طريقة مؤشرة على الثبات، ناتيغلينيد.

* ***المؤلف المراسل: كاجول، أديتي كوشيك***

kajolrana060@gmail.com

تاريخ استلام البحث 2024/5/15 وتاريخ قبوله للنشر 2024/9/19.

Phytochemical Constituents and in-vitro antioxidant Activity of *Aleuritopteris bicolor* Leaves, *Crinum amoenum* Bulbs, and *Drynaria coronans* Rhizomes of Nepal

Sindhu K.C[1], Atisammodavardhana Kaundinnyayana[1*], Prabhat Kumar Jha[1], Sandesh Poudel[1], Rajib Tiwari[1], Ram Kishor Yadav[1], Sistu K.C.[2], Kushal Subedi [1]

[1]School of Health and Allied Sciences, Faculty of Health Sciences, Pokhara University, Pokhara, Nepal
[2]Patan Academy of Health Sciences, Lalitpur, Kathmandu University Nepal

ABSTRACT

Background: Due to plant derived chemicals's potential as antioxidant agents, there has been a growing interest in using them to cure or prevent diseases. Similarly plant species like *Aleuritopteris bicolor(*AB) leaves,*Crinum amoenum*(CA) bulbs and *Drynaria coronans (*DC) rhizomes are used as traditional herbal medicine in Nepal.

Aims: This study aims to assess the qualitative and quantitative phytochemical constituents along with the antioxidant potency of extracts from the leaves of AB, bulbs of CA, and rhizomes of DC.

Methods and Materials: The qualitative phytochemical profile was assessed using thin-layer chromatography (TLC) and standard phytochemical tests. TLC was performed on silica gel 60 F254 plates (20×20 cm, layer thickness: 0.2 mm) using a solvent system of chloroform: methanol: water at (6:4:1) ratio. Plates were visualized under UV light (254 nm and 365 nm) and further developed using 1% $FeCl_3$, 10% H_2SO_4, and DPPH for antioxidant activity. Quantitative analysis of total flavonoid and phenol content was conducted using aluminum chloride and Folin-Ciocalteu reagents, respectively. The antioxidant activity was measured through the DPPH free radical scavenging assay.

Results: The selected species were found to contain flavonoid, phenol, saponin and tannin. Higher flavonoid and phenol content was found in the leaves of AB (398.861 ± 6.94 mg quercetin/ g dry extract) and rhizomes of CA (172.97 ± 1.777 gallic acid/ g dry extract) respectively whereas leaves of AB had the most potent antioxidant activity (IC_{50}= 3.233 µg/ml).

Conclusions: All the selected plant species were found to have significant constituents. Among them, the leaves of AB extract had the highest flavonoid concentration and the higher antioxidant activity, highlighting its potential for further medicinal use.

Keywords: Phytochemical screening, antioxidant, *Aleuritopteris bicolor* leaves, *Crinum amoenum* bulbs, *Drynaria coronans* rhizomes

Key Messages: This is a novel study which shows the importance of TLC evaluation of selected species from Nepal. This study could act as a basis for biological studies depending upon the different phytochemical estimation and antioxidant activity.

INTRODUCTION

Phytochemicals are the metabolites of plant species that have the potential to fight against diseases. These phytochemical constituents show antioxidant effects through which various diseases are inhibited (1,2). Since the beginning of human history, herbal plants have been a component of alternative treatment plans for various ailments (3). It is estimated that 70–80% of Asia's rural population uses medicinal herbs to treat medical conditions (4). Despite established ethno-medicinal uses of plants, a large array of herbal species around the world

[*]***Corresponding author:*** ***Atisammodavardhana Kaundinnyayana***
gurusbliss@gmail.com
Received: 22/5/2024 Accepted: 19/9/2024.
DOI: https://doi.org/10.35516/jjps.v18i2.2691

still have not been scientifically investigated (5).

Nepal, which ranks ninth among Asian nations for its floral richness, hosts 1792 to 2331 species of beneficial medicinal and aromatic plants. Among them some of this includes *Aleuritopteris bicolor* (AB) leaves, *Crinum amoenum* (CA) bulbs, and *Drynaria coronans* (DC) rhizomes (Table 1). However, only a small fraction of the plant of Nepal has been scientifically studied for their medicinal properties (3). Given the rich ethnomedicinal tradition and the potential health benefits of these plants, scientific research should prioritize the study of herbal plants. Thus, scientific studies should be concentrated on herbal plants. Following this, the current study was conducted to evaluate the phytochemical makeup of species and their response toward oxidative stress in order to determine its scientific validity. The evaluation involves thin-layer chromatography (TLC) for qualitative analysis and specific assays to determine flavonoid and phenol content, as well as antioxidant activity of the Nepalese species, to establish the scientific validity of these traditional herbal medicines from Nepal.

Figure A*: Aleuritopteris bicolor*

Figure B*: Crinum amoenum*

Figure C*: Drynaria coronans*

Table 1. Selected Nepalese plant species

SN	Species Name	Family	Local Name	Traditional Uses
1	*Aleuritopteris bicolor* (Roxb.) Fraser.Jnek	Pteridaceae	Dankernu(6)	Diarrhea,Dysentery, Gastritis (6), Cuts, fever, sinusitis(7)
2	*Crinum amoenum*	Amaryllidaceae	Hade Lasun (8)	Cholera(8)
3	*Drynariacoronans*(Wall.ex Mett.) J.Sm.exT.Moore	Pteridaceae	Kamaru(9)	Diarrhea, Constipation(9)

METHODS AND MATERIAL:

Plant Materials Collection

Under the guidance of a traditional healer, plants were gathered from Lekhnath region, Kaski district, Nepal. Species AB and DC were identified and authenticated by the taxonomist Mr. Dhan Raj Kandel (Reference No. 74) of the National Herbarium and Plant Laboratories, Godavari, Lalitpur, Nepal while the species CA was identified and authenticated by Mr. Dharmaraj Koirala (Reference No. 11) of Department of Plant Resources, Raniban, Pokhara, Nepal. The species were then registered and preserved at the Crude drug museum of Pharmacognosy laboratory, School of Health and Allied Sciences, Pokhara University under voucher numbers PUH-2022-39 (for AB), PUH-2022-41 (for CA), and PUH-2022-40 (for DC). Fresh and disease-free plants were chosen for the experiments. The leaves of

AB, bulbs of CA, and rhizomes of DC were used for the estimation of phytochemical constituents and evaluation of in-vitro antioxidant activity.

Preparation of Extract of Plant Species

Into labeled conical flasks, 80 grams of powdered dried samples from each species were poured. The samples were then cold-macerated in 70% ethanol in a 1: 10 w:v ratio. Maceration was carried out for three days with intermittent shaking. Filtration was carried out using Whatman No. 1 filter paper. The filtrates were concentrated at reduced pressure at 40°C using a rotary evaporator to obtain extracts which were further dried in a vacuum desiccators (10).

Thin Layer Chromatography (TLC) Profiling

One grams of the each dried extract from the leaves of **Aleuritopteris bicolor** (AB), bulbs of **Crinum amoenum** (CA), and rhizomes of **Drynaria coronans** (DC) was dissolved in 2 mL of methanol as sample solutions. The TLC profiling was conducted on Merck Silica Gel 60 F254 plates (analytical grade, silica gel with fluorescent indicator, aluminum backing, 20×20 cm size, 0.2 mm layer thickness, 10-12 µm particle size). The sample solution was applied to the TLC plats as spots where solvent mixture used for development was chloroform, methanol, and water in a ratio of 6:4:1. The plates were then developed for approximately 30 minutes and observed under UV light at 254 nm and 365 nm. After visualization, the plates were sprayed separately with 1% aqueous $FeCl_3$, 10% H_2SO_4 (followed by heating), and slightly submerged in a 60 mM methanolic solution of 2,2-diphenyl-1-picrylhydrazyl (DPPH). The TLC profile revealed spots corresponding to different phytochemicals: polar compounds appeared in the upper layer of the plate, observed under UV light; flavonoids (yellow spots) and saccharides (black spots) were visible after treatment with 10% H_2SO_4 and heating; and phenols were detected as brown spots after spraying with 10% $FeCl_3$ (11).

Phytochemical Analysis

Alkaloids, carbohydrates, flavonoids, glycosides, phenols, saponins and tannins were evaluated qualitatively by wagner, fehling, Alkaline reagent, salkowski's, sodium hydroxide, lead acetate, and ferric chloride test respectively. Wagner's reagent (Loba Chemie Pvt. Ltd., Mumbai, India), Fehling's solution (Central Drug House (P) Ltd., New Delhi, India), alkaline reagent (Nice Chemicals Pvt. Ltd., Cochin, India), Salkowski's reagent (Himedia Laboratories Pvt. Ltd., Mumbai, India), Sodium hydroxide (Qualigens Fine Chemicals ,Thermo Fisher Scientific), Mumbai, India), Lead acetate (Thomas Baker (Chemicals) Pvt. Ltd., Mumbai, India) and ferric chloride (Nice Chemicals Pvt. Ltd., Cochin, India)(12).

Determination of Total Flavonoid Contents

With few modifications, the aluminum chloride colorimetric approach was employed to determine the presence of flavonoids. In brief, 4 ml of distilled water was added to 1 ml of extract (1000 µg/mL in ethanol) and then 0.3 ml of sodium nitrite (5% w/v in distilled water) was added. After 5 minutes, 0.3 ml of aluminum chloride (20% w/v in distilled water) was added, and the mixture was let to stand for 6 minutes. 2 ml of sodium hydroxide (1M in distilled water) was then added. The mixture was vortexed and the absorbance was recorded at 510 nm against a blank using single beam UV-visible spectrophotometer (Agilent Cary-60, Malaysia). A calibration curve was drawn using quercetin (25µg /ml-500 µg /ml in ethanol) as standard, the total flavonoid concentration was reported as mg quercetin equivalent per gram dry extract (13).

Determination of Total Phenol content

According to the method,(14) with some modifications, the Folin Ciocalteu method was employed to determine total phenols. In brief, 5 ml of distilled water, 1 ml of Folin reagent (2N in distilled water), and 1 ml of test solution (1000 µg/mL) were combined. After 5 minutes of standing, 1 ml of 10% sodium carbonate was added and mixed. The mixture was incubated for an hour at room temperature, after which the absorbance at 725 nm was measured in comparison to a blank. The total phenol content was calculated using the Gallic acid (12.5 µg/mL

- 500 µg/mL) standard instead of test solution to draw a calibration curve and was represented as milligrams of Gallic acid equivalent per gram dry extract.

Antioxidant activity

A 0.1 mM DPPH (2,2-diphenyl-1-picrylhydrazyl) solution was freshly prepared by dissolving DPPH in methanol to evaluate the free-radical scavenging activity of the extracts. The plant extracts were diluted in methanol to concentrations ranging from 1.56 to 25 µg/mL, and ascorbic acid was used as a positive control within the same concentration range. In the assay procedure, 1 mL of each extract or control solution was mixed with 1 mL of the DPPH solution in a cuvette. The mixture was then incubated in the dark at room temperature for 30 minutes to facilitate the reaction. Following incubation, the absorbance of the solution was measured at 517 nm using a UV-visible spectrophotometer to determine the scavenging activity (15).

Scavenging activity (%) = $\frac{A-B}{A} \times 100\%$

Where A represents the absorbance of the control (DPPH solution without the sample) and B represents the absorbance of the DPPH solution in the presence of the sample (extracts/ascorbic acid).

Statistical analysis

Antioxidant activity was assessed in triplicate for accuracy and reproducibility. Data analysis using Microsoft Excel 2021 included calculating the mean and standard deviation. Results were reported as mean ± standard deviation to facilitate comparisons and validate findings.

RESULTS

Extraction Yield Value

The extractive values (% yield) of plant species using 70 % ethanol was found to be higher in bulbs of CA followed by leaves of AB and rhizomes of DC yielded the least amount of extract (Table 2).

Table 2. % Yield of extract in 70% ethanol solvent

Plant species	Parts used	% Yield by solvent
AB	Leaves	**11.23%**
CA	Bulbs	**13.55%**
DC	Rhizomes	**5.22%**

TLC Profiling

Figure 1 and Figure 2 show the TLC profiling of three separate extracts using three different sprays in the solvent system of chloroform, methanol, and water (6:4:1). The spot codes for the three different species are depicted as 1 (CA bulbs), 2 (AB leaves), and 3 (DC rhizomes).

$CHCl_3$: MeOH: H_2O (6:4:1)

From the Figure 1of the TLC profile, spots can be detected in the upper layer of the TLC plate as a result of the solvents being more polar, when observed at 254 nm and 365 nm.

10% (v/v) H_2SO_4 / heat

The majority of the plant extract demonstrated the presence of flavonoids (yellow-colored spots) and saccharides (black colored spots) on the TLC plate after spraying 10% $H_2SO_4$and heating. (Figure 2).

10% (w/v) aqueous Ferric chloride

The pre Figure 1 sence of phenols was detected as brown colored spots on TLC plate after spraying with 10% $FeCl_3$ (Figure 2).

DPPH Solution

After dipping in DPPH solution in the dark, observation of pale yellow or no colour on the TLC plate suggested the presence of potent antioxidants in AB leaves extract, CA bulb extract as represented by Figure 2.

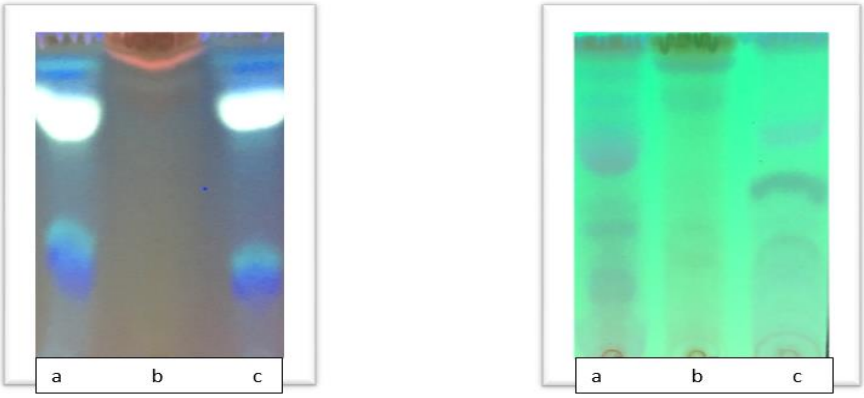

Figure 1. TLC plate with three different spots from three different species a) CA bulbs b) AB leaves c) DC rhizome observed in UV 365 nm and s UV 254 nm respectively

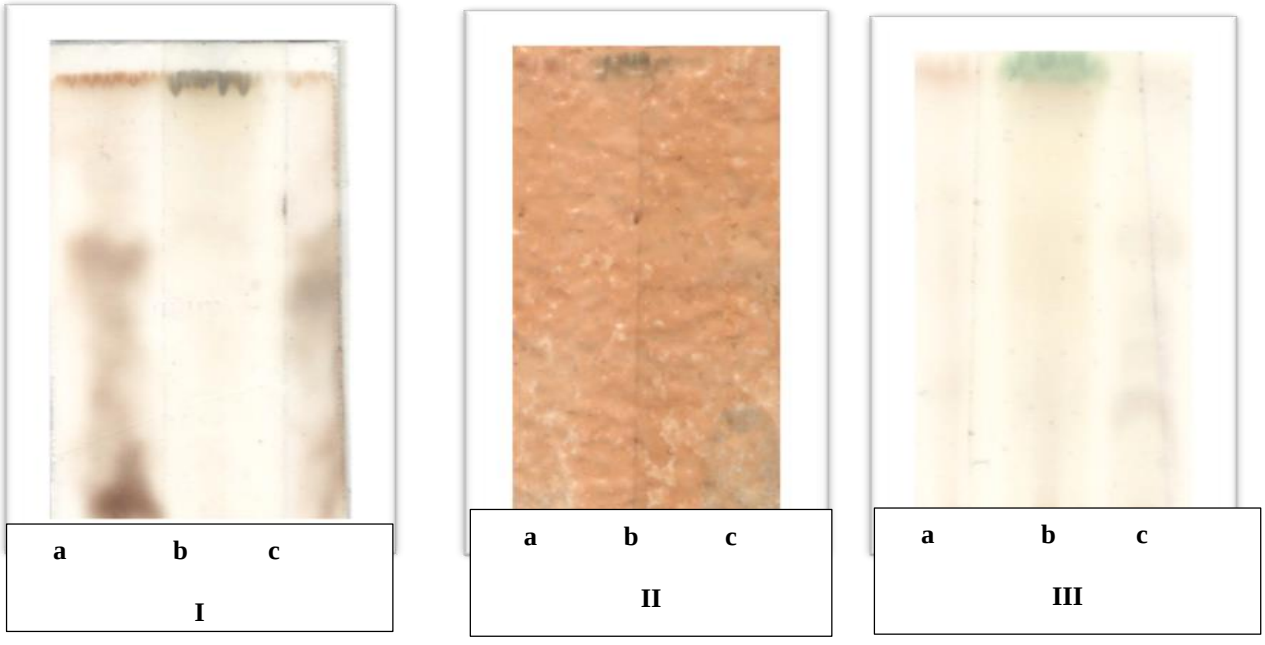

Figure 2. TLC plate with three different spots from three different species a) CA, bulbs b) AB, leaves c) DC, rhizomes sprayed with (I) 10% H_2SO_4 /Heat, (II) 10% $FeCl_3$, (III) DPPH

Phytochemical test

The extracts from the plant species AB, CA, and DC were subjected to various phytochemical tests and the tests revelaed the presence of flavonoids, phenols, saponins, and tannins as indicated in Table 3.

Table 3. Qualitative phytochemical data of plant species extract

Phytochemical Constituent	Test Conducted	Results of Different Plant species extract		
		AB leaves	CA bulbs	DC rhizomes
Alkaloids	Wagner test	-	+	+
Flavonoids	Alkaline reagent test	+	+	+
Phenols	Sodium hydroxide test	+	+	+
Tannins	Ferric chloride test	+	+	+
Glycosides	Salkowski's test	-	+	+
Saponins	Lead acetate test	+	+	+
Carbohydrates	Fehling test	-	+	+

Note: + present, - absent

Total flavonoids content

The total amount of flavonoids, which is expressed as mg quercetin equivalent (GAE)/g of dry weight of extract, was calculated using Quercetin. The table provides quantitative data regarding the flavonoids content in the extract of AB leaves, CA bulbs, and DC rhizomes. The results show that the leaves of AB had the highest content of flavonoids in the ethanolic extract as shown in Table 4.

Table 4. Total flavonoids content expressed as mg Quercetin equivalents per gram dry weight of extract

	Sample Plant	Parts used	Total flavonoid content mg QE/g dry weight of extract
1	Aleuritopteris bicolor	Leaves	398.86±6.94
2	Crinum amoenum	Bulbs	260.16±5.05
3	Drynaria coronans	Rhizomes	178.60±0.57

Note: Data expressed as mean ± standard deviation (n=3).

Total Phenolic Content

The total amount of phenol, which is expressed as mg Gallic acid equivalent (GAE)/g of dry weight of extract, was calculated using Gallic acid. The Table 5 provides quantitative data regarding the phenol content in the extract of AB leaves, CA bulbs, and DC rhizomes in which the ethanol extract from CA bulb was found to have the highest phenol content.

Table 5. Total phenol content expressed as mg phenol equivalent per gram dry weight of extract

	Sample Plant	Parts used	Total phenol content mg GAE/g dry weight of extract
1	Aleuritopteris bicolor	Leaves	28.13±0.57
2	Crinum amoenum	Bulbs	172.9± 1.77
3	Drynaria coronans	Rhizomes	52.41± 0.47

Note: Data expressed as mean ± standard deviation (n=3).

DPPH Free Radical Scavenging Analysis

Through DPPH scavenging activity, the antioxidant activity of the plant extract was assessed. Five concentrations (25 µg/ml, 12.5 µg/ml, 6.25 µg/ml, 3.125 µg/ml, and 1.56 µg/ml) were used for the computation of the IC_{50} value of the extract and ascorbic acid, as shown in Table 6. When compared to other extracts (CA bulbs extract 21.3 µg/ml, DC rhizomes extract.>25 µg/ml), the extract of AB leaves was shown to have stronger antioxidant activity with an IC_{50} value of 3.233 µg/ml, which was even potent than ascorbic acid (8.94 µg/ml).

Table 6. DPPH radical scavenging activity of the extract and ascorbic acid at different concentration

(%) DPPH Scavenging Activity of Ethanol extract						IC_{50} value
Sample	1.56 µg/ml	3.125 µg/ml	6.25 µg/ml	12.5 µg/ml	25 µg/ml	**µg/ml**
Ascorbic acid	12.26±0.049	21.93±0.2	40.27±1.36	66.05±0.48	81.51±1.51	8.94
AB leaves extract	41.26±0.20	50.79±0.178	63.80±0.54	85.95±0.05	88.78±0.21	3.23
CA bulbs extract	29.27±0.129	32.97±0.32	36.71±0.34	42.53±0.17	52.79±0.16	21.33
DC rhizomes extract	3.59±0.13	8.33±0.045	14.60±0.182	23.37±0.09	34.37±0.16	>25

Note: Data expressed as mean ± standard deviation (n=3)

DISCUSSION

In the present investigation, qualitative phytochemical test, total flavonoid and phenolic content, antioxidant activity of the chosen plant extracts was evaluated. Due to their low cost, easy accessibility, and few side effects, herbal plants have played a significant role as alternate sources for the management of numerous illnesses and conditions (16). The pharmacological effectiveness of many of these plants has not been scientifically studied, despite the widespread use of herbal plants for the treatment of various illness problems (5).

Secondary plant metabolites play a crucial role in defensive mechanisms of plants against microbes, prey, stress, and interspecies protection. Saponins, flavonoids, tannins, terpenoids, steroids, and alkaloids are secondary metabolites present in plants, that give herbal medicines their anti-diabetic, anti-parasitic, anti-diarrheal, anti-inflammatory, anti-ulcer, anti-malarial, anticancer, nephroprotective, and hepatoprotective activities (17).

The presence of components in the mixture, their purity, and the identity of the compounds are all revealed by the TLC profile of the herbal species (18). Similarly, phytochemical tests determine the types of secondary metabolite found in a species (12). Figure 1 Figure 1 of the extract and their numerous colored spots showed the presence of a variety of compounds like presence of saccharides, represented by black spot, brown and light yellow represent presence of phenol and flavonoids respectively (11). Similarly the current study on CA bulb and DC rhizome extract shows black spot that represent the saccharides whereas the leaves of AB shows the light yellow which represent the flavonoids in Figure 1 and Figure 2. Additional phytochemical testing reveals presence of phenols, flavonoids, alkaloids, tannins, and saponins in all of species extract and the absence of carbohydrates in the leaves of AB Table 3. These findings are consistent with previous reports and demonstrate the diversity of secondary metabolites presents in these plants extracts, thus indicating the widespread occurrence of these bioactive compounds in medicinal plants (19) (20) (21). The presence of phenols, flavonoids, alkaloids, tannins and saponins in the extracts underscores their potential pharmacological activities, including antioxidant, anti-inflammatory and antimicrobial properties (22) (2). These finding further support the traditional use of herbal plants for medicinal purposes and highlight the importance of exploring their therapeutic through scientific investigation. Quantitative analysis of flavonoids and phenols content in selected extract of plant shows that AB has the highest flavonoid content Table 4 consistent with previous report (21) 429.16 ± 7.21 µg QE/mg of extract, signifying its potential therapeutic significance and this continuity in flavonoid content underscores the reliability and reproducibility of our analytical methods . However, the phenol content of CA extract in present study Table 5, significantly contrasts with previous finding (21) 25.22 ± 2.41 µg GAE /mg of extract indicating a notable increase.

The ability of plant extract to scavenge free radicals was evaluated using the DPPH model. This is a common method used to assess the antioxidant activity of plant extracts, especially when phenolic chemicals are included (22). Half-maximal inhibitory concentration, or IC_{50}, is one of the parameters used to interpret the results of DPPH

scavenging activity. This is described as the amount of medication or inhibitor required to completely stop a biological response (23).

In the current investigation, the IC50 was determined by plotting the percentage of radical scavenging activity against the concentration of the investigated plant extract using the linear regression approach. As shown in Table 6, selected plant extracts demonstrated positive response as antioxidant activity against free radical. The leaves extract of AB demonstrated the highest DPPH scavenging activity when compared to other plant extracts which was greater than that Ascorbic acid (8.94 µg/ml). This highlights the potent antioxidant potential of AB leaves, which could be attributed to the presence of high levels of flavonoids, as indicated in our previous discussion. Comparing our present results with previous studies (21) (20), significant variations emerge. In the earlier studies, AB demonstrated an IC_{50} value of 46.76 µg/ml, significantly lower than the current finding. Additionally, CA exhibited a substantially lower IC_{50} value of 661.76 µg/ml in the previous study, contrasting with present observations as shown in Table 6. Remarkably, DC displayed the lowest antioxidant activity in present study: > 25µg/ml and previous study: 93.30± 5.19 µg/ml (21) when compared with others species. These differences may arise from several factors, including differences in plant material preparations, extraction technique, geographical variations and assay conditions.

The potent antioxidant activity of AB leaves in our present study underscores their potential for pharmaceutical and nutraceutical applications, particularly in combating oxidative stress-related diseases. As reported flavonoids, flavonol O-glycosides, petrosins, sitosterols are present in Pteris family which shows the potent role as antioxidant activity(24) and might be there is also a presence of some flavonoid compound along with some other secondary metabolites in AB like *Cheilanthes tenuifolia* which consists of quercetin and rutin that is also responsible to show higher DPPH scavenging activity.(25) The finding of this study align with previous study (26) introducing new insights and emphasizing the need for further research to explore the therapeutic application of these plant species.

CONCLUSION

Each of the three extracts from AB leaves, CA bulbs, and DC rhizomes shows the presence of different phytochemical components as well as potent DPPH radical scavenging activity. Among them, AB leaves extract exhibited the highest flavonoid content which might correlate with the highest antioxidant activity. Additionally, more in vivo research is needed to confirm the extract's precise efficacy of these species. Therefore, additional isolation and purification of the extract's constituents is needed in order to analyze the chemical that is in charge of the biological effects.

Abbreviations

AB - *Aleuritopteris bicolor*
CA - Crinum amoenum
DC - Drynaria coronans
TLC - Thin Layer Chromatography
UV - Ultraviolet
FeCl3 - Ferric Chloride
DPPH - 2,2-diphenyl-1-picrylhydrazyl
GAE - Gallic Acid Equivalent
QE - Quercetin Equivalent
IC50 - Half-maximal inhibitory concentration

Acknowledgement

We would like to appreciate the tremendous contributions made by Dr. Khem Raj Joshi, Dr. Hari Devkota, Nabin Pathak, whose cooperation and participation were crucial to the accomplishment of this study and the School of Health and Allied Sciences at Pokhara University, Nepal for letting us utilize their pharmacy facilities so we could conduct an in vitro investigation.

Conflict of Interest

We declare that we don't have conflict of interest.

Funding

This study has received no outside funds**.**

REFERENCES

1. Ohikhena F.U., Wintola O.A., and Afolayan A.J. Quantitative phytochemical constituents and antioxidant activities of the mistletoe, *Phragmanthera capitata* (Sprengel) Balle extracted with different solvents. *Pharmacognosy Res.* 2018; 10(1):16–23.
2. Zhang Y.J., Gan R.Y., Li S., Zhou Y., Li A.N., Xu D.P., et al. Antioxidant phytochemicals for the prevention and treatment of chronic diseases. *Molecules.* 2015; 20(12):21138–21156.
3. Kunwar R.M., Mahat L., Acharya R.P., and Bussmann R.W. Medicinal plants, traditional medicine, markets and management in far-west Nepal. *J. Ethnobiol. Ethnomed.* 2013; 9(1):24.
4. Oyebode O., Kandala N.B., Chilton P.J., and Lilford R.J. Use of traditional medicine in middle-income countries: a WHO-SAGE study. *Health Policy Plan.* 2016; 31(8):984–991.
5. Jemal K., Sandeep B.V., and Pola S. Phytochemical screening and in vitro antioxidant activity analysis of leaf and callus extracts of *Allophylus serratus* (ROXB) KURZ. *Jordan J. Pharm. Sci.* 2022; 15(1):51–69.
6. Ekor M. The growing use of herbal medicines: issues relating to adverse reactions and challenges in monitoring safety. *Front. Pharmacol.* 2014; 4:177.
7. Adhikari M., Thapa R., Kunwar R.M., Devkota H.P., and Poudel P. Ethnomedicinal uses of plant resources in the Machhapuchchhre Rural Municipality of Kaski District, Nepal. *Medicines (Basel).* 2019; 6(2):69.
8. Ojha R. and Devkota H. Edible and medicinal pteridophytes of Nepal: a review. *Ethnobot. Res. Appl.* 2021; 22:1–16.
9. Rai R. and Singh N.B. Medico-ethnobiology in Rai community: a case study from Baikunthe Village Development Committee, Bhojpur, Eastern Nepal. *J. Inst. Sci. Technol.* 2015; 20:127.
10. Subba B., Srivastav C., and Kandel R.C. Scientific validation of medicinal plants used by Yakkha community of Chanuwa VDC, Dhankuta, Nepal. *SpringerPlus.* 2016; 5(1):155.
11. Kediso T.E., Tolessa T., Getachew F., Makonnen E., and Seifu D. Effect of 70% ethanol extract and its solvent fractions of *Artemisia afra* (Jacq. Ex Willd.) against pentylenetetrazole-induced seizure in mice. *Evid. Based Complement. Alternat. Med.* 2021; 2021:6690965.
12. Giri S., Giri U., Subedi K., Magar K.T., Pant S., and Joshi K.R. Thin Layer Chromatography (TLC) based chemical profiling and antioxidant activity of selected Nepalese medicinal plants. *J. Health Allied Sci.* 2020; 10(2):15–22.
13. Pant D.R., Pant N.D., Saru D.B., Yadav U.N., and Khanal D.P. Phytochemical screening and study of antioxidant, antimicrobial, antidiabetic, anti-inflammatory and analgesic activities of extracts from stem wood of *Pterocarpus marsupium* Roxburgh. *J. Intercult. Ethnopharmacol.* 2017; 6(2):170–176.
14. Pękal A. Evaluation of aluminium complexation reaction for flavonoid content assay. *Food Anal. Methods.* 2014; 7:1776–1782.
15. Blainski A., Lopes G.C., and de Mello J.C.P. Application and analysis of the Folin Ciocalteu method for the determination of the total phenolic content from *Limonium brasiliense* L. *Molecules.* 2013; 18(6):6852–6865.
16. Sowndhararajan K. and Kang S.C. Free radical scavenging activity from different extracts of leaves of *Bauhinia vahlii* Wight & Arn. *Saudi J. Biol. Sci.* 2013; 20(4):319–325.
17. Sofowora A., Ogunbodede E. and Onayade A. The role and place of medicinal plants in the strategies for disease prevention. *Afr. J. Tradit. Complement. Altern. Med.* 2013; 10(5):210–229.

18. Ikram L., Laiche A.T. and Tlili M.L. Medicinal plants used by traditional healers in the treatment of gastrointestinal disorders in Oued Souf Region (southeast of Algeria). *Jordan J. Pharm. Sci.* 2024; 17(2):225–241.
19. Yeshi K., Crayn D., Ritmejerytė E. and Wangchuk P. Plant secondary metabolites produced in response to abiotic stresses have potential application in pharmaceutical product development. *Molecules.* 2022; 27(1):313.
20. Kagan I.A. and Flythe M.D. Thin-layer chromatographic (TLC) separations and bioassays of plant extracts to identify antimicrobial compounds. *J. Vis. Exp.* 2014; (85):51411.
21. Sardi V.F., Astika A., Jalius I.M. and Ismed F. Quantification of mangiferin from the bioactive fraction of mango leaves (*Mangifera indica* L.) and evaluation of wound-healing potential. *Jordan J. Pharm. Sci.* 2023; 16(3):595–606.
22. Khanal L.N., Sharma K.R., Pokharel Y.R. and Kalauni S.K. Assessment of phytochemical, antioxidant and antimicrobial activities of some medicinal plants from Kaski District of Nepal. *Am. J. Plant Sci.* 2020; 11(9):1383–1397.
23. Pandey L.K. and Sharma K.R. Analysis of phenolic and flavonoid content, α-amylase inhibitory and free radical scavenging activities of some medicinal plants. *Sci. World J.* 2022; 2022:4000707.
24. Tiwari R., Parajuli N., Pahari A., Gurung S., Baral R., Shrestha R. et al. Phytochemical screening, free radical scavenging and in-vitro antibacterial activity of ethanolic extracts of selected medicinal plants of Nepal and effort towards formulation of antibacterial cream from the extracts. *Int. J. Herb. Med.* 2021; 9:39–47.
25. Rahman M.M., Islam M.B., Biswas M. and Khurshid Alam A.H.M. In vitro antioxidant and free radical scavenging activity of different parts of *Tabebuia pallida* growing in Bangladesh. *BMC Res. Notes.* 2015; 8(1):621.
26. Aykul S. and Martinez-Hackert E. Determination of half-maximal inhibitory concentration using biosensor-based protein interaction analysis. *Anal. Biochem.* 2016; 508:97–103.
27. Cao H., Chai T.T., Wang X., Morais-Braga M.F.B., Yang J.H., Wong F.C. et al. Phytochemicals from fern species: potential for medicine applications. *Phytochem. Rev.* 2017; 16(3):379–440.
28. Jarial R., Shard A., Thakur S., Sakinah M., Zularisam A.W., Rezania S. et al. Characterization of flavonoids from fern *Cheilanthes tenuifolia* and evaluation of antioxidant, antimicrobial and anticancer activities. *J. King Saud Univ. Sci.* 2018; 30(4):425–432.

تقييم المكونات الكيميائية النباتية النوعية والكمية والنشاط المضاد للأكسدة في المختبر لمستخلصات أوراق Aleuritopteris bicolor ودرنات Crinum amoenum وجذور Drynaria coronans

سيندهو كيه سي [1]، أتيسامودافاردهانا كاوندينيايانا [1*]، برابهات كومار جها [1]، سانديش بوديل [1]، رجيب تيواري [1]، رام كيشور ياداف [1]، سيستو كيه سي [2]، كوشال سوبيدي [1]

[1]كلية الصحة والعلوم المرتبطة بها، كلية العلوم الصحية، جامعة بوخارا، بوخارا، نيبال

[2] أكاديمية باتان للعلوم الصحية، لاليتبور، جامعة كاتماندو نيبال

ملخص

نظرًا للإمكانات العلاجية لمركبات النباتات كمضادات للأكسدة، هناك اهتمام متزايد باستخدامها في علاج أو الوقاية من الأمراض. يتم استخدام نباتات مثل *Aleuritopteris bicolor* (AB)، و*Crinum amoenum* (CA)، و *Drynaria coronans* (DC)في الطب العشبي التقليدي في نيبال. تهدف هذه الدراسة إلى تقييم المكونات الكيميائية النباتية النوعية والكمية إلى جانب فعالية مضادات الأكسدة في مستخلصات أوراق AB ودرنات CA وجذور DC. تم تقييم التحليل الكيميائي النوعي باستخدام تقنية كروماتوغرافيا الطبقة الرقيقة (TLC) والاختبارات الكيميائية القياسية، وتم إجراء TLC على صفائح سيليكا جل F254 باستخدام نظام مذيب من الكلوروفورم:ميثانول:ماء (6:4:1)، وتمت ملاحظة الصفائح تحت الأشعة فوق البنفسجية (254 و365 نانومتر) وتطويرها باستخدام كلوريد الحديديك 1%، حمض الكبريتيك 10%، ومحلول DPPHلنشاط مضادات الأكسدة. أُجري التحليل الكمي لمحتوى الفلافونويد والفينولات باستخدام كاشف كلوريد الألمنيوم وكاشف فولين–سيوكالتي، على التوالي. تم قياس نشاط مضادات الأكسدة باستخدام اختبار DPPH للجذور الحرة. أظهرت النتائج أن الأنواع المختارة تحتوي على مركبات الفلافونويد والفينولات والصابونين والعفص، وكان لأوراق ABأعلى محتوى من الفلافونويد (398.861 ± 6.94 ملغم كيرسيتين/غرام من المستخلص الجاف) وأظهرت أيضًا أقوى نشاط مضاد للأكسدة (IC50 = 3.233 ميكروغرام/مل).تُبرز النتائج إمكانات مستخلص أوراق ABللاستخدام الطبي المستقبلي.

الكلمات الدالة: تحليل كيميائي نباتي، مضادات الأكسدة، أوراق Aleuritopteris bicolor، درنات Crinum amoenum، جذور Drynaria coronans.

المؤلف المراسل: أتيسامودافاردهانا كاوندينيايانا

gurusbliss@gmail.com

تاريخ استلام البحث 2024/5/22 وتاريخ قبوله للنشر 2024/9/19.

A Review on Puncturing Potential: Microneedles' Present Landscape And Prospective Horizons

Boyeekati Mohammad Rizwan[1], Nawaz Mahammed[1*], Shaik Farheen Taj[1], V. Sivasai Bharath Kumar[1], B. Yamuna[1]

[1]Department of Pharmaceutics, Raghavendra Institute of Pharmaceutical Education and Research, K.R. Palli Cross, Anantapur, Chiyyedu, Andhra Pradesh-India

ABSTRACT

Microneedle technology has emerged as a promising approach for drug delivery, vaccination, diagnostics, and cosmetic treatments. This review provides an overview of microneedle technology, covering the various types of microneedles, fabrication techniques, applications, advantages, challenges, safety considerations, clinical translation, and future perspectives. Solid, hollow, dissolving, coated, and hydrogel-forming microneedles are discussed, along with their structures, materials, and fabrication methods. Applications in drug delivery, vaccination, diagnostics, and cosmetic treatments are explored, with an emphasis on emerging and novel uses. The review highlights the advantages of microneedle technology, including enhanced patient compliance, improved drug absorption, and reduced pain, as well as challenges such as manufacturing scalability and regulatory approval. Fabrication techniques, biocompatibility, safety issues, clinical translation, and commercialization aspects are examined, along with future directions and emerging trends such as multifunctional microneedles and personalized medicine. Overall, microneedle technology holds tremendous promise for revolutionizing healthcare and biomedical engineering, but further research and development are required to address current challenges and realize its full potential.

Keywords: Microneedles, drug delivery, vaccination, diagnostics, fabrication techniques, biocompatibility, clinical translation, future perspectives.

1. INTRODUCTION

1.1. Definition and Overview of Microneedle Technology:

Microneedle technology represents a breakthrough in drug delivery and biomedical engineering, offering a minimally invasive approach to administer therapeutics, vaccines, and diagnostics through the skin. These micron-scale structures, typically ranging from hundreds of micrometers to a few millimeters in length, puncture the outermost layer of the skin, known as the stratum corneum, to facilitate the delivery of bioactive compounds. Microneedles can be categorized into various types, including solid, hollow, dissolving, coated, and hydrogel-forming microneedles, each designed to address specific applications and requirements.

The development of microneedles has garnered significant interest due to their potential to overcome limitations associated with traditional drug delivery methods, such as oral administration and injections(1). They offer several advantages, including enhanced patient compliance, improved drug absorption, reduced pain and discomfort, and the ability to deliver a wide range of therapeutics, including small molecules, proteins, nucleic acids, and vaccines.

[*]***Corresponding author: Nawaz Mahammed***
mohammednawaz151@gmail.com
Received: 8/6/2024 Accepted: 21/9/2024.
DOI: https://doi.org/10.35516/jjps.v18i2.2763

Moreover, microneedles have shown promise in enabling targeted and controlled delivery of drugs, thereby minimizing systemic exposure and side effects(2).

1.2. Importance of Microneedles in Biomedical Engineering

Microneedles play a pivotal role in advancing biomedical engineering by offering innovative solutions to longstanding challenges in drug delivery and healthcare(3). Their importance stems from their ability to overcome the limitations of traditional delivery methods, such as oral administration and injections, by providing a minimally invasive and targeted approach for delivering therapeutics, vaccines, and diagnostics. This capability has significant implications for improving patient compliance, enhancing drug efficacy, and reducing side effects. In biomedical engineering, microneedles serve as versatile tools for delivering a wide range of substances, including small molecules, proteins, nucleic acids, and vaccines, across diverse patient populations and medical contexts. Their adaptability enables tailored approaches to address specific healthcare needs, such as personalized medicine, where precise dosing and targeted delivery are critical. Moreover, microneedles contribute to the development of wearable and implantable medical devices, enabling continuous monitoring and treatment of chronic conditions(4). Their integration with advanced materials, biosensors, and microelectronics opens new avenues for real-time diagnostics, therapy monitoring, and feedback-controlled drug delivery systems.

2. TYPES OF MICRONEEDLES

2.1. Solid Microneedles

Solid microneedles represent a significant advancement in drug delivery technology, offering a minimally invasive approach for transdermal delivery of therapeutics, vaccines, and diagnostics. These micron-scale structures, typically made of biocompatible materials such as silicon, polymers, or metals, feature sharp tips designed to penetrate the skin's outermost layer, the stratum corneum, without causing pain or tissue damage. Solid microneedles function by creating microchannels in the skin, allowing drugs to permeate through and reach the underlying tissue or systemic circulation. Unlike traditional hypodermic needles, solid microneedles do not require specialized handling or disposal procedures, making them safer and more convenient for both patients and healthcare providers. Furthermore, they offer precise control over drug dosage and release kinetics, enabling tailored treatment regimens and improved therapeutic outcomes. Solid microneedles have shown promise in a variety of applications, including insulin delivery for diabetes management, vaccination against infectious diseases, and transdermal administration of biologics and small molecules. Ongoing research aims to optimize microneedle design, fabrication techniques, and drug formulations to enhance their efficacy, stability, and patient acceptability(5).

2.2. Hollow Microneedles

Hollow microneedles are innovative devices designed to overcome the limitations of traditional injections by providing a minimally invasive and painless method for delivering drugs, vaccines, and other bioactive compounds. Unlike solid microneedles, hollow microneedles feature channels or lumens that allow fluids to be delivered directly into the skin or withdrawn from the body. These micron-scale needles, typically made of materials like silicon, polymers, or metals, offer several advantages, including precise control over drug dosage and delivery kinetics, reduced tissue damage, and improved patient comfort. Hollow microneedles can be used to administer a wide range of substances, including small molecules, biologics, and nanoparticles, with applications spanning from local anaesthesia and insulin delivery to vaccination and diagnostic sampling. The versatility of hollow microneedles makes them promising tools for various medical applications, including point-of-care diagnostics, continuous monitoring, and targeted drug delivery. Ongoing research focuses on optimizing

microneedle design, fabrication methods, and integration with advanced technologies such as microfluidics and biosensors to enhance their performance and functionality(6, 7).

2.3. Dissolving Microneedles

Dissolving microneedles are an innovative drug delivery technology that offers a painless and convenient approach for administering therapeutics, vaccines, and diagnostics. These micron-scale needles are typically composed of biocompatible polymers or sugar-based materials and are designed to dissolve or disintegrate upon insertion into the skin, releasing encapsulated drugs or payloads. Dissolving microneedles offer several advantages over traditional delivery methods, including improved patient compliance, reduced risk of needlestick injuries, and simplified disposal procedures. By bypassing the skin's stratum corneum and directly delivering drugs into the epidermis or dermis, they enable enhanced drug absorption and bioavailability, leading to improved therapeutic outcomes. These microneedles can be tailored to accommodate a wide range of drugs, including small molecules, biologics, and vaccines, with precise control over drug release kinetics and dosage. They have shown promise in various applications, such as pain management, vaccination campaigns, and point-of-care diagnostics, where their ease of use and rapid onset of action offer significant advantages(7).

2.4. Coated Microneedles

Coated microneedles are a cutting-edge drug delivery technology designed to enhance the efficiency and precision of transdermal drug delivery. These micron-scale needles are typically fabricated from biocompatible materials such as polymers or metals and are coated with drug-loaded or functionalized layers. The coating on these microneedles serves multiple purposes, including protecting the drug payload from degradation, controlling drug release kinetics, and targeting specific sites within the skin. Additionally, coatings can be engineered to enhance the mechanical properties of the microneedles, facilitating their insertion into the skin and ensuring optimal drug delivery(8). Coated microneedles offer several advantages over traditional delivery methods, including improved patient comfort, reduced risk of tissue damage, and enhanced bioavailability of drugs. By bypassing the skin's protective barrier and directly delivering drugs into the dermis or systemic circulation, they enable rapid onset of action and precise control over drug dosage. These microneedles have shown promise in a wide range of applications, including the delivery of small molecules, biologics, and vaccines, as well as in diagnostics and cosmetic treatments. Ongoing research in coated microneedles focuses on optimizing coating formulations, enhancing drug stability, and expanding their applicability to various therapeutic areas(8).

2.5. Hydrogel-forming Microneedles

Hydrogel-forming microneedles represent an innovative approach to transdermal drug delivery, combining the advantages of microneedle technology with the properties of hydrogels. These micron-scale needles are typically fabricated from biocompatible polymers that can absorb water and swell upon insertion into the skin, forming a hydrogel matrix that encapsulates and releases drugs. The unique properties of hydrogel-forming microneedles offer several advantages over conventional drug delivery methods. They provide a painless and minimally invasive approach for administering therapeutics, vaccines, and diagnostics, while also enabling controlled and sustained release of drugs over time. The hydrogel matrix formed within the skin enhances drug bioavailability and tissue penetration, leading to improved therapeutic efficacy. Hydrogel-forming microneedles are highly versatile and can be tailored to accommodate a wide range of drugs, including small molecules, biologics, and nanoparticles. They have shown promise in various applications, such as chronic disease management, vaccination campaigns, and cosmetic treatments, where their ease of use and precise drug delivery offer significant advantages(9).

2.6. Comparison of Different Microneedle Types

Table No:1 A Comprehensive Review of Microneedle Technologies for Transdermal Drug Delivery

Microneedle Type	Structure	Material	Drug Delivery Mechanism	Advantages	Disadvantages
Solid Microneedles	Micron-scale solid needles	Silicon, polymers, metals	Penetration of stratum corneum, drug diffusion	Simple fabrication, mechanical strength	Limited drug payload capacity, single-use only
Hollow Microneedles	Micron-scale needles with lumens	Silicon, polymers, metals	Fluid delivery or extraction	Precise dosing, versatile applications	Risk of clogging, complex fabrication
Dissolving Microneedles	Micron-scale needles with dissolvable matrix	Biocompatible polymers, sugars	Drug encapsulation and release upon dissolution	Pain-free application, enhanced bioavailability	Limited drug stability, formulation challenges
Coated Microneedles	Micron-scale needles with drug-loaded or functionalized coatings	Silicon, polymers, metals	Controlled drug release, protection from degradation	Enhanced drug stability, targeted delivery	Coating uniformity, potential delamination
Hydrogel-forming Microneedles	Micron-scale needles forming hydrogel matrix upon insertion	Biocompatible polymers	Drug encapsulation and sustained release	Enhanced tissue penetration, prolonged drug release	Hydrogel swelling, fabrication complexity

3. FABRICATION TECHNIQUES FOR MICRONEEDLES

3.1. Micromolding

Micromolding is a versatile and scalable fabrication technique used in the production of microneedles and other microscale structures(9). It involves the replication of micrometer-sized features from a master mold onto a substrate, typically using elastomeric materials such as polydimethylsiloxane (PDMS) or thermoplastics like polycarbonate or poly (methyl methacrylate) (PMMA). The process begins with the creation of a master mold, often fabricated using photolithography or other micromachining techniques. This master mold contains the desired microneedle geometry and is used as a template for replication. Liquid polymer precursor material is then poured or injected into the mold, where it undergoes curing or solidification to form the microneedle structures. After solidification, the molded substrate is demolded, resulting in an array of microneedles with precise dimensions and geometries(10). Micromolding offers several advantages, including high throughput, cost-effectiveness, and the ability to produce intricate microstructures with high fidelity(11). It is widely used in research and industry for the fabrication of microneedle arrays, microfluidic devices, lab-on-a-chip systems, and other microscale components for biomedical, pharmaceutical, and diagnostic applications(12).

3.2. Lithography

Lithography is a fundamental technique in microfabrication used to pattern and transfer geometric features onto substrates with high precision and resolution(13). It encompasses a variety of methods, including photolithography, electron beam lithography (EBL)(14), and nanoimprint lithography (NIL)(15), each with its own unique advantages and applications. In photolithography, a photosensitive resist is deposited onto

a substrate and exposed to ultraviolet (UV) light through a mask containing the desired pattern. The exposed regions of the resist undergo a chemical change, allowing selective removal of the unexposed regions through development, leaving behind the patterned features. Electron beam lithography (EBL) utilizes a focused beam of electrons to directly write patterns onto a substrate coated with a resist material. This technique offers unparalleled resolution and flexibility, making it ideal for prototyping and research applications requiring nanoscale features(14). Nanoimprint lithography (NIL) involves pressing a stamp or mold containing the desired pattern into a thermoplastic resist on a substrate, transferring the pattern through mechanical deformation. NIL is capable of producing high-resolution patterns over large areas and is used in the fabrication of microfluidic devices, optical components, and nanoelectronics(15).

3.3. Laser Ablation

Laser ablation is a versatile technique used in various fields, including materials science, microfabrication, and biomedical engineering, to precisely remove or modify material from a target surface using a laser beam(16). In laser ablation, a focused laser beam is directed onto the surface of the material, generating a high-intensity energy pulse that causes rapid heating and vaporization of the target material. The process of laser ablation can be used for various purposes, including cutting, drilling, patterning, and surface modification(17). It offers several advantages over traditional machining methods, including minimal heat-affected zones, high precision, and the ability to process a wide range of materials, including metals, ceramics, polymers, and biological tissues. Laser ablation is widely used in microfabrication processes such as micro structuring of semiconductor devices, fabrication of microfluidic channels, and patterning of biomaterials for tissue engineering applications(18). Additionally, it finds applications in biomedical research and clinical practice for procedures such as laser ablation therapy for cancer treatment, laser-assisted drug delivery, and laser-based diagnostics.

3.4. 3D Printing

3D printing, also known as additive manufacturing, is a transformative technology that enables the fabrication of three-dimensional objects layer by layer from digital design data(19). It offers unprecedented flexibility, speed, and customization compared to traditional manufacturing methods, making it increasingly popular across various industries, including aerospace, automotive, healthcare, and consumer goods(20). This digital model is then sliced into thin layers, and the 3D printer builds the object layer by layer, typically using materials such as plastics, metals, ceramics, or biomaterials. 3D printing offers several advantages, including rapid prototyping, cost-effectiveness for low-volume production, and design freedom to create complex geometries and customized parts. It also enables on-demand manufacturing, reducing lead times and waste compared to traditional manufacturing methods. In healthcare, 3D printing is revolutionizing medical device manufacturing, patient-specific implants, prosthetics, and anatomical models for surgical planning and education(21). In aerospace and automotive industries, it enables lightweight and complex components with improved performance and fuel efficiency.

3.5. Advantages and Limitations of Each Technique

Table No:2 Comparison of Microneedle Fabrication Techniques for Transdermal Drug Delivery Systems

Technique	Advantages	Limitations
Micromolding(22)	1. High throughput production	1. Limited to certain materials and geometries
	2. Cost-effective fabrication	2. Requires a master mold, which can be time-consuming and expensive
	3. Precise control over microneedle dimensions and geometries	3. Limited scalability for mass production
Lithography(23)	1. High resolution patterning	1. Expensive equipment and infrastructure
	2. Versatile applications in microfabrication	2. Complex process requiring expertise in photolithography or electron beam lithography
	3. Suitable for prototyping and large-scale production	3. Limited to planar substrates and small area patterning
Laser Ablation(24)	1. Minimal heat-affected zones	1. Limited to certain materials and thicknesses
	2. High precision and resolution	2. Limited scalability for large-area processing
	3. Versatile applications in materials processing and microfabrication	3. Potential for thermal damage to surrounding materials
3D Printing	1. Design freedom for complex geometries and customization	1. Limited resolution compared to lithography and laser ablation
	2. Rapid prototyping and on-demand manufacturing	2. Material limitations may affect mechanical properties and biocompatibility
	3. Reduced waste and lead times compared to traditional manufacturing methods	3. post-processing may be required for surface finishing and dimensional accuracy

4. APPLICATIONS OF MICRONEEDLES

4.1. Drug Delivery

Microneedles have emerged as a promising technology for drug delivery, offering several advantages over traditional methods such as oral administration and injections(25). By bypassing the skin's protective barrier, microneedles enable precise and targeted delivery of therapeutics, enhancing drug absorption and bioavailability while minimizing systemic side effects. This makes them particularly suitable for delivering drugs with poor oral bioavailability, large molecular size, or narrow therapeutic windows. Microneedles have shown promise in a wide range of drug delivery applications, including the delivery of small molecules, biologics, vaccines, and nucleic acids. They have been explored for the treatment of various medical conditions such as diabetes, cardiovascular diseases, cancer, and infectious diseases. Additionally, microneedles offer the potential for controlled and sustained release of drugs, enabling prolonged therapeutic effects and improved patient compliance. Furthermore, microneedle-based drug delivery systems can be tailored to specific patient needs, offering personalized treatment regimens and dosage adjustments. Ongoing research aims to optimize microneedle design, formulation strategies, and fabrication techniques to further enhance their efficacy, safety, and versatility for drug delivery applications. Overall, microneedles hold great promise for revolutionizing drug delivery and improving patient outcomes in diverse therapeutic areas(26).

4.2. Vaccination

Microneedles have emerged as a promising tool for vaccination, offering several advantages over traditional needle-based methods(27). By delivering vaccines directly into the skin's immune-rich layers, microneedles can enhance immune responses and improve vaccine efficacy. This is particularly advantageous for vaccines requiring enhanced immunogenicity or dose sparing. Microneedle-based vaccination offers several benefits, including improved patient compliance due to painless and minimally invasive administration, reduced risk of needlestick injuries for healthcare workers, and simplified vaccine administration in

resource-limited settings without the need for trained personnel or cold chain storage. Furthermore, microneedles enable precise control over vaccine delivery, allowing for dose optimization, antigen sparing, and the potential for combination vaccines. They have been explored for a wide range of vaccine targets, including infectious diseases such as influenza, measles, and COVID-19, as well as for emerging applications in cancer immunotherapy and personalized vaccines. Ongoing research aims to further optimize microneedle-based vaccination strategies, including vaccine stability, scalability, and integration with adjuvants or immune-modulating agents to enhance protective immune responses. Overall, microneedles hold great promise for revolutionizing vaccination efforts and improving global health outcomes(28).

4.3. Diagnostics

By penetrating the skin's outermost layer, microneedles can access interstitial fluid, blood, or other biological fluids containing biomarkers indicative of various health conditions(29). One of the key advantages of microneedle-based diagnostics is their ability to offer a less invasive alternative to traditional blood draws, reducing patient discomfort and anxiety associated with venipuncture. Microneedles also offer advantages in terms of sample volume requirements, allowing for smaller sample sizes compared to conventional blood collection methods. Microneedle-based diagnostic platforms have been developed for a wide range of applications, including monitoring glucose levels in diabetes management, detecting infectious diseases such as malaria and HIV, and assessing biomarkers for cancer diagnosis and monitoring. Additionally, microneedles have been explored for point-of-care testing in resource-limited settings, offering rapid and cost-effective diagnostic solutions outside of laboratory settings(30).

4.4. Cosmetic Treatments

Microneedles have emerged as a novel approach in the field of cosmetic treatments, offering minimally invasive and effective solutions for various skin conditions and aesthetic enhancements(31). By creating microchannels in the skin's surface, microneedles facilitate the delivery of cosmeceuticals, such as vitamins, peptides, growth factors, and hyaluronic acid, directly into the dermis or epidermis, where they can exert their beneficial effects. One of the key advantages of microneedle-based cosmetic treatments is their ability to enhance skin rejuvenation, improve texture, tone, and firmness, and address common concerns such as wrinkles, acne scars, hyperpigmentation, and stretch marks. Microneedling also promotes collagen production and enhances the absorption of topical formulations, leading to long-lasting improvements in skin health and appearance. Microneedle-based cosmetic procedures are versatile and customizable, allowing for tailored treatments based on individual skin types, concerns, and treatment goals. Additionally, microneedling is associated with minimal downtime and discomfort, making it a popular choice for patients seeking non-surgical and less invasive alternatives to traditional cosmetic procedures.

4.5. Emerging Applications

Microneedles have expanded beyond traditional applications, paving the way for innovative and emerging uses across various fields. One such application is in the field of biosensing, where microneedles are being explored as minimally invasive platforms for continuous monitoring of biomarkers in interstitial fluid or blood. These biosensing microneedles can detect analytes such as glucose, lactate, and ions, offering real-time monitoring for disease management, athletic performance optimization, and personalized healthcare. Another emerging application of microneedles is in the field of tissue engineering and regenerative medicine. Microneedles are being investigated as delivery vehicles for bioactive molecules, stem cells, and growth factors to promote tissue regeneration and wound healing(32). They offer precise control over the spatial distribution and release kinetics of therapeutic agents, enhancing tissue repair and regeneration in various clinical settings. Additionally, microneedles are being explored for drug

delivery to specialized tissues and organs, such as the eye, inner ear, and brain, where traditional delivery methods face challenges in accessing targeted sites. These targeted delivery approaches hold promise for treating ocular diseases, hearing disorders, and neurological conditions with improved efficacy and reduced side effects.

4.6. Case Studies Highlighting Successful Applications

Case studies showcasing successful applications of microneedles underscore their versatility and efficacy across various fields. In one notable example, microneedle-based influenza vaccination demonstrated improved immune responses compared to traditional intramuscular injection, highlighting the potential of microneedles for enhancing vaccine efficacy and compliance. In another case, microneedle patches loaded with lidocaine provided effective local anaesthesia for minor dermatological procedures, offering a painless and convenient alternative to needle-based anaesthesia. This demonstrates the utility of microneedles in pain management and procedural care. Furthermore, microneedle-based delivery of anti-inflammatory drugs has shown promising results in treating inflammatory skin conditions such as psoriasis and atopic dermatitis, offering targeted and localized therapy with reduced systemic side effects. In the field of biosensing, microneedle-based glucose monitoring systems have enabled continuous glucose monitoring for diabetes management, improving patient outcomes and quality of life(33).

5. ADVANTAGES AND CHALLENGES OF MICRONEEDLE TECHNOLOGY

5.1. Advantages:

5.1.1. Improved Patient Compliance

Microneedle technology offers several advantages that contribute to improved patient compliance in various healthcare applications. Firstly, microneedles provide a less invasive and painless alternative to traditional needle-based methods, reducing patient anxiety and fear associated with injections(34). This painless administration can alleviate needle phobia, particularly in pediatric and needle-sensitive populations, enhancing overall treatment adherence. Moreover, microneedles eliminate the need for healthcare professionals to administer injections, empowering patients to self-administer medications at home. This convenience promotes patient autonomy, reduces healthcare burdens, and increases treatment accessibility, especially for chronic conditions requiring frequent injections. Additionally, microneedles enable precise and controlled drug delivery, ensuring accurate dosing and minimizing medication errors. This reliability enhances treatment efficacy and reduces the risk of adverse reactions, fostering patient trust in the therapeutic regimen. Furthermore, the simplicity of microneedle-based delivery systems facilitates user-friendly interfaces, making them suitable for point-of-care applications and remote healthcare settings. This accessibility encourages patient engagement and facilitates continuous monitoring and management of health conditions.

5.1.2. Enhanced Drug Absorption

Microneedle technology offers significant advantages in enhancing drug absorption, revolutionizing drug delivery across various medical fields. By bypassing the skin's protective barrier, microneedles create microchannels that facilitate the direct delivery of therapeutics into the underlying dermis or systemic circulation, thereby improving drug absorption and bioavailability. One key advantage of microneedles is their ability to enhance the permeation of drugs, particularly macromolecules like proteins and peptides, which typically have poor transdermal absorption. The microneedle-mediated delivery enables these drugs to bypass enzymatic degradation in the gastrointestinal tract and first-pass metabolism in the liver, resulting in increased systemic exposure and therapeutic efficacy(35). Moreover, microneedles offer precise control over drug delivery kinetics, enabling tailored release profiles to

optimize drug absorption and maintain therapeutic concentrations over extended periods. This controlled release capability reduces the frequency of dosing and enhances patient compliance, particularly for medications requiring frequent administration. Furthermore, microneedles can improve drug absorption in patients with compromised skin barrier function, such as the elderly or those with dermatological conditions, offering new therapeutic options and improving treatment outcomes

5.1.3. Reduced Pain and Discomfort

Microneedle technology offers a significant advantage in reducing pain and discomfort associated with drug delivery and medical procedures, enhancing patient comfort and compliance. Traditional needle-based methods often cause pain, fear, and anxiety in patients, particularly in paediatric and needle-phobic populations. Microneedles provide a minimally invasive and virtually painless alternative, as their micrometer-scale dimensions enable gentle penetration of the skin without stimulating pain receptors or nerve endings. Furthermore, the design of microneedles, with their fine and tapered structures, minimizes tissue trauma and damage, further reducing discomfort during insertion. This gentle approach to drug delivery enhances patient acceptance and adherence to treatment regimens, particularly for individuals requiring frequent injections or long-term therapy. Moreover, microneedle-based delivery systems can be engineered to incorporate pain-reducing techniques, such as topical anaesthetics or vibration stimulation, further mitigating discomfort during administration. Additionally, the elimination of needle-related phobia and anxiety enhances patient satisfaction and trust in the healthcare provider, fostering positive therapeutic relationships and improving overall treatment outcomes(36).

5.2. Challenges

5.2.1. Manufacturing Scalability

Manufacturing scalability poses a significant challenge in the widespread adoption of microneedle technology for mass production and commercialization. While microneedles offer promising advantages in drug delivery, diagnostics, and other applications, their fabrication processes often require precise and intricate manufacturing techniques that may not be easily scalable to large volumes. Traditional micromolding and lithography methods used for microneedle fabrication are typically labor-intensive and time-consuming, making them unsuitable for high-throughput production(37). Additionally, these techniques may require expensive equipment and specialized expertise, further limiting scalability and increasing manufacturing costs. Furthermore, maintaining consistency and quality control in microneedle fabrication at scale presents additional challenges. Variations in material properties, microneedle geometries, and manufacturing processes can affect the performance and reliability of microneedle devices, posing challenges in achieving reproducibility and uniformity across large production batches. Addressing manufacturing scalability challenges requires the development of innovative fabrication techniques and scalable manufacturing processes tailored to microneedle production. Emerging approaches such as roll-to-roll manufacturing, additive manufacturing, and microfluidic-based fabrication offer promising solutions for high-throughput production of microneedle arrays while maintaining precision and quality control.

5.2.2. Skin Penetration Depth Control

Skin penetration depth control is a critical challenge in microneedle technology, as it directly impacts the efficacy, safety, and reproducibility of drug delivery and other applications. Achieving precise control over the penetration depth of microneedles is essential to ensure optimal delivery of therapeutics while minimizing tissue damage and discomfort. One of the main challenges lies in designing microneedles that can reliably penetrate the skin to the desired depth without causing pain or injury. Variations in skin thickness, elasticity, and composition among individuals present additional complexities in achieving consistent penetration depths across diverse

patient populations. Moreover, factors such as microneedle geometry, material properties, insertion speed, and application force influence the penetration depth and must be carefully optimized to ensure accurate and controlled delivery of drugs or sampling of biological fluids. Addressing the challenge of skin penetration depth control requires interdisciplinary approaches combining engineering, materials science, and dermatology(38). Advances in microneedle design, fabrication techniques, and insertion methods, along with computational modeling and in vivo testing, are essential for developing microneedle devices with improved penetration depth control and reproducibility.

5.2.3. Regulatory Approval and Safety Concerns

Regulatory approval and safety concerns represent significant challenges in the widespread adoption of microneedle technology for clinical and commercial applications. While microneedles offer promising advantages in drug delivery, diagnostics, and other biomedical fields, ensuring their safety, efficacy, and regulatory compliance is paramount for successful translation into clinical practice. One of the main challenges is establishing the safety profile of microneedle devices, particularly regarding their potential for skin irritation, allergic reactions, and infection risk. Microneedle materials and coatings must be thoroughly evaluated for biocompatibility, stability, and long-term safety to mitigate adverse effects on patients. Additionally, achieving regulatory approval for microneedle-based products requires adherence to stringent standards and guidelines set forth by regulatory agencies such as the FDA and EMA. Demonstrating the quality, safety, and performance of microneedle devices through preclinical studies, clinical trials, and comprehensive regulatory submissions is essential but often complex and time-consuming. Furthermore, the evolving nature of microneedle technology, with innovations in materials, designs, and applications, poses challenges in establishing standardized testing protocols and regulatory pathways for product approval. Addressing these challenges requires collaboration among researchers, clinicians, regulatory agencies, and industry stakeholders to develop robust safety assessment methodologies, streamline regulatory processes, and establish clear guidelines for microneedle-based products(39).

6. BIOCOMPATIBILITY AND SAFETY CONSIDERATIONS

6.1. Skin Irritation and Tissue Response

Biocompatibility and safety considerations are paramount in the development of microneedle technology, particularly regarding skin irritation and tissue response. While microneedles offer a minimally invasive approach to drug delivery and diagnostics, ensuring their compatibility with the skin and tissues is crucial for avoiding adverse reactions and promoting patient safety. Skin irritation and tissue response are primary concerns when assessing the biocompatibility of microneedle devices. The insertion of microneedles into the skin can elicit local tissue reactions, including erythema, edema, inflammation, and discomfort. These responses may vary depending on factors such as microneedle design, materials, insertion depth, and application duration. To mitigate skin irritation and tissue response, thorough preclinical evaluation of microneedle devices is essential. This involves conducting in vitro and in vivo studies to assess the biocompatibility, cytotoxicity, and immunogenicity of microneedle materials and formulations. Additionally, histological analysis of skin tissue following microneedle insertion provides valuable insights into the tissue response and inflammatory reactions. Furthermore, optimizing microneedle design and fabrication processes can help minimize tissue trauma and irritation during insertion. Strategies such as tapering microneedle tips, selecting biocompatible materials, and incorporating anti-inflammatory coatings can enhance the safety and tolerability of microneedle devices(40).

6.2. Infection Risk and Sterility

Biocompatibility and safety considerations extend beyond skin irritation to include infection risk and sterility in microneedle technology. Despite their minimally invasive nature, microneedle devices present a potential risk of infection due to their penetration of the skin barrier, making sterility a crucial aspect of their design and manufacturing process(41). To mitigate this risk, microneedle devices must undergo rigorous sterilization procedures to ensure the absence of pathogens and contaminants. Sterilization methods such as gamma irradiation, ethylene oxide gas, or autoclaving are commonly employed to achieve sterility while maintaining the integrity and functionality of microneedle materials. Additionally, the design of microneedle devices should incorporate features to minimize the risk of infection, such as smooth surfaces, aseptic handling procedures, and sterile packaging. Furthermore, maintaining strict quality control measures throughout the manufacturing process is essential to prevent microbial contamination and ensure product safety and efficacy. By addressing infection risk and maintaining sterility, microneedle technology can uphold patient safety and promote confidence in its use for drug delivery, diagnostics, and other biomedical applications(42). Ensuring compliance with regulatory standards and guidelines for sterilization and aseptic processing is essential for achieving regulatory approval and market acceptance of microneedle-based products.

6.3. Immune Responses and Allergic Reactions

Biocompatibility and safety considerations in microneedle technology extend to immune responses and allergic reactions, crucial factors that can impact the safety and efficacy of microneedle-based device(43). Immune responses to microneedles may manifest as local inflammation, immune cell infiltration, or systemic immune activation. Factors such as microneedle design, materials, and insertion depth can influence the magnitude and nature of immune responses. While mild inflammatory responses are common and typically resolve spontaneously, excessive or prolonged inflammation may compromise treatment outcomes and patient comfort. Allergic reactions to microneedle materials or components present another concern, particularly for individuals with known allergies or sensitivities. Certain materials used in microneedle fabrication, such as metals, polymers, or adhesives, may trigger allergic responses ranging from localized dermatitis to systemic hypersensitivity reactions. To mitigate immune responses and allergic reactions, thorough biocompatibility testing of microneedle materials and formulations is essential. Preclinical studies assessing immune compatibility, hypersensitivity reactions, and inflammatory markers can provide valuable insights into the safety profile of microneedle devices. Additionally, careful selection of biocompatible materials and coatings, along with adherence to regulatory guidelines for medical device safety, can help minimize the risk of adverse immune reactions and ensure the safe use of microneedle technology in clinical practice(44).

6.4. Strategies for Enhancing Biocompatibility and Safety

Table No:3 Advancements in Biocompatible Microneedle Technologies: Strategies for Enhanced Safety and Efficacy

Strategy	Description
Material Selection	Choose biocompatible materials for microneedle fabrication, such as medical-grade polymers (e.g., polylactic acid, polyethylene glycol), biodegradable materials (e.g., hyaluronic acid, gelatin), or metals (e.g., stainless steel, titanium) to minimize adverse tissue reactions and allergic responses.
Surface Modification	Apply coatings or surface treatments to microneedles to enhance biocompatibility and reduce tissue irritation. Examples include hydrophilic coatings to improve insertion and reduce friction, anti-inflammatory coatings to mitigate immune responses, or antimicrobial coatings to prevent infection risk.
Sterilization Techniques	Implement sterilization methods such as gamma irradiation, ethylene oxide gas, or autoclaving to achieve sterility and ensure the absence of pathogens and contaminants on microneedle devices. Maintain strict quality control measures throughout the sterilization process to preserve microneedle integrity and functionality.
Design Optimization	Optimize microneedle design parameters, including length, diameter, aspect ratio, and tip geometry, to minimize tissue trauma, enhance insertion efficiency, and improve patient comfort. Consider factors such as needle tapering, bevel angle, and spacing to optimize penetration depth and reduce pain during insertion.
Preclinical Testing	Conduct comprehensive biocompatibility testing using in vitro and in vivo models to evaluate the safety profile of microneedle materials and formulations. Assess parameters such as cytotoxicity, inflammation, immune compatibility, and tissue response to identify potential adverse effects and ensure regulatory compliance.
Regulatory Compliance	Adhere to regulatory standards and guidelines set forth by regulatory agencies (e.g., FDA, EMA) for medical device safety and biocompatibility. Ensure compliance with Good Manufacturing Practices (GMP) and ISO standards throughout the design, manufacturing, and testing of microneedle-based products.

7. CLINICAL TRANSLATION AND COMMERCIALIZATION

7.1. Current Status of Microneedle Technologies in Clinical Trials

Microneedle technologies have gained significant traction in clinical trials across various medical fields, reflecting their potential to revolutionize drug delivery, diagnostics, and therapeutic interventions. As of [current year], numerous clinical trials are underway to evaluate the safety, efficacy, and feasibility of microneedle-based devices in diverse patient populations and applications. In drug delivery, clinical trials are investigating microneedle patches for transdermal delivery of vaccines, insulin, contraceptives, and other medications, aiming to improve patient compliance, reduce pain, and enhance therapeutic outcomes. Additionally, microneedle-based systems are being evaluated for targeted delivery to specialized tissues and organs, such as the eye, inner ear, and mucosal surfaces, to address unmet clinical needs and overcome barriers to conventional drug administration routes. In offering potential advancements in disease management and personalized healthcare(45).

7.2. Commercial Products and Market Trends

Commercial products incorporating microneedle technology have witnessed significant growth and diversification in recent years, reflecting increasing demand for minimally invasive drug delivery, diagnostics, and cosmetic treatments. Microneedle-based patches, devices, and systems are now available across various market segments, with notable advancements in pharmaceuticals,

healthcare, and personal care industries. In the pharmaceutical sector, microneedle patches for transdermal drug delivery have garnered considerable attention for their potential to improve patient compliance and therapeutic outcomes(46). Commercial products include patches for insulin delivery, vaccination, pain management, and hormone therapy, catering to diverse patient needs and treatment regimens. In healthcare, microneedle-based biosensing platforms have emerged as valuable tools for continuous monitoring of biomarkers, offering real-time insights into health status and disease management. Commercial products encompass wearable sensors for glucose monitoring, lactate monitoring, and other diagnostic applications, enabling personalized healthcare solutions and remote patient monitoring. In the personal care industry, microneedle-based cosmetic treatments have gained popularity for their ability to rejuvenate skin, improve texture, and address various dermatological concerns. Commercial products include microneedle rollers, pens, and patches infused with skincare ingredients, offering consumers non-invasive alternatives to traditional cosmetic procedures. Market trends indicate continued growth and innovation in microneedle technology, driven by advancements in materials, fabrication techniques, and application domains. As microneedle products become increasingly accessible and diversified, they are poised to reshape healthcare delivery, diagnostics, and aesthetic treatments in the years to come(47).

7.3. Regulatory Pathways and Approval Processes

Regulatory pathways and approval processes for microneedle-based products are critical considerations in ensuring their safety, efficacy, and market accessibility. In the United States, the Food and Drug Administration (FDA) oversees the regulation of medical devices, including microneedle devices, through a rigorous premarket approval (PMA) or 510(k) clearance process. Classifying microneedle devices based on their intended use, risk profile, and technological characteristics is essential for determining the appropriate regulatory pathway(48). Microneedle devices intended for drug delivery or diagnostic purposes may require submission of a PMA application, which entails comprehensive preclinical and clinical data demonstrating safety, efficacy, and quality control. Alternatively, devices with substantially equivalent predicates may qualify for 510(k) clearance, expediting the approval process. Internationally, regulatory approval processes for microneedle devices vary by country, with regulatory agencies such as the European Medicines Agency (EMA) in the European Union and the Pharmaceuticals and Medical Devices Agency (PMDA) in Japan overseeing medical device approvals. Navigating regulatory pathways and approval processes for microneedle-based products necessitates close collaboration between manufacturers, regulatory consultants, and regulatory agencies(49).

7.4. Challenges in Scaling Up Production and Distribution

Scaling up production and distribution of microneedle-based products presents several challenges that must be addressed to meet growing demand and ensure widespread accessibility. One major challenge is optimizing manufacturing processes to achieve high throughput production while maintaining product quality and consistency. Traditional fabrication methods such as micromolding and lithography may be labor-intensive and time-consuming, requiring innovative approaches such as roll-to-roll manufacturing or automated assembly lines to increase efficiency. Additionally, sourcing raw materials and components for microneedle production at scale can be challenging, particularly for specialized materials or coatings. Ensuring a stable and reliable supply chain is crucial for uninterrupted manufacturing and timely delivery of products to market. Furthermore, establishing robust distribution networks and logistics infrastructure is essential for reaching diverse healthcare settings and consumer markets. Microneedle products may require specialized storage conditions or handling procedures, adding complexity to distribution channels and inventory management. Addressing these challenges requires

collaboration between manufacturers, suppliers, regulatory agencies, and distribution partners to develop scalable production processes, optimize supply chains, and implement effective quality control measures. By overcoming barriers to scaling up production and distribution, microneedle technology can realize its full potential in improving healthcare delivery and patient outcomes on a global scale(50).

8. FUTURE DIRECTIONS AND EMERGING TRENDS

8.1. Multifunctional Microneedles

Future directions in microneedle technology are increasingly focused on developing multifunctional microneedles capable of delivering multiple therapeutic agents or performing simultaneous diagnostic and therapeutic functions(51). This enables real-time monitoring of biomarkers or physiological parameters while delivering therapeutic agents, allowing for precise and personalized treatment adjustments based on individual patient responses. Additionally, multifunctional microneedles are being explored for targeted and combinatorial therapy approaches, where multiple drugs or therapeutic agents are co-delivered to specific tissue targets for synergistic effects or enhanced therapeutic outcomes. This strategy holds promise for treating complex diseases such as cancer, autoimmune disorders, and infectious diseases more effectively while minimizing side effects. Furthermore, advancements in materials science, microfabrication techniques, and biocompatible coatings are driving the development of multifunctional microneedles with enhanced capabilities and versatility. These innovations are poised to expand the scope of microneedle applications in healthcare and pave the way for personalized, patient-centric treatment approaches in the future(52).

8.2. Stimuli-Responsive Systems

Stimuli-responsive systems represent a promising future direction in microneedle technology, offering dynamic and adaptive capabilities for targeted drug delivery, diagnostics, and tissue engineering applications. These systems are designed to respond to specific environmental cues or external stimuli, triggering controlled release of therapeutic agents or modulation of biological processes in a precise and timely manner. One emerging trend is the development of stimuli-responsive microneedles that can actively respond to physiological changes within the body, such as variations in pH, temperature, glucose levels, or enzyme activity(53). By incorporating responsive materials or smart coatings into microneedle designs, researchers aim to create devices capable of on-demand drug release or sensing based on real-time physiological signals, enabling personalized and dynamic treatment regimens. Furthermore, stimuli-responsive microneedles are being explored for applications in tissue engineering and regenerative medicine, where they can deliver growth factors, cytokines, or cell therapies in response to specific cues within the local tissue microenvironment. This approach holds promise for enhancing tissue regeneration, wound healing, and functional tissue repair in various clinical settings.

8.3. Personalized Medicine Applications

Future directions in microneedle technology are increasingly oriented towards personalized medicine applications, leveraging the unique capabilities of microneedles to tailor treatments to individual patient needs and characteristics. Personalized medicine aims to optimize therapeutic outcomes by considering factors such as genetics, lifestyle, and disease state, and microneedle technology offers promising avenues for advancing this approach(54). One emerging trend is the development of personalized drug delivery systems using microneedles, where drug formulations and dosages are customized based on patient-specific factors. By integrating biosensing capabilities or utilizing patient-specific data, such as biomarker levels or genetic information, microneedle devices can deliver precise doses of therapeutics at optimal times, maximizing efficacy while minimizing side effects. Additionally, microneedles are being explored for point-of-care diagnostics and monitoring applications in personalized medicine,

enabling real-time assessment of biomarkers, disease progression, or treatment responses. These devices offer convenient and minimally invasive solutions for monitoring chronic conditions, managing medication regimens, and facilitating early disease detection. Furthermore, advances in materials science and microfabrication techniques are driving the development of customizable microneedle arrays tailored to individual patient needs, such as varying needle lengths, geometries, or drug release profiles. This customization enhances patient comfort, treatment adherence, and therapeutic outcomes, ultimately advancing the paradigm of personalized medicine with microneedle technology(55).

8.4. Integration with Wearable and Implantable Devices

The integration of microneedle technology with wearable and implantable devices represents a promising future direction in biomedical engineering, offering enhanced capabilities for drug delivery, diagnostics, and health monitoring. By combining microneedles with wearable or implantable platforms, researchers aim to create seamless and unobtrusive solutions for personalized healthcare management. One emerging trend is the integration of microneedle patches with wearable devices, such as smartwatches or adhesive sensors, for continuous monitoring of biomarkers or physiological parameters. Microneedles embedded within these wearable platforms can facilitate minimally invasive sampling of interstitial fluid or blood, enabling real-time monitoring of glucose levels, lactate levels, or other biomarkers relevant to health and disease. Additionally, microneedle-based implantable devices are being explored for sustained drug delivery or targeted therapy applications. These devices can be implanted beneath the skin or within specific tissue targets, providing controlled release of therapeutics over extended periods while minimizing systemic side effects. Integration with wireless communication technologies allows for remote programming and monitoring of implantable microneedle devices, enhancing patient convenience and treatment compliance.

8.5. Potential Impact on Healthcare and Biomedical Engineering

Table No:4 Transformative Potential of Microneedle Technologies: Advancing Healthcare Delivery and Therapeutic Outcomes

Potential Impact	Description
Enhanced Patient Compliance	Minimally invasive and painless microneedle-based drug delivery and diagnostics promote patient acceptance and adherence to treatment regimens, particularly for paediatric and needle-phobic populations, improving therapeutic outcomes and healthcare outcomes overall.
Personalized Medicine	Integration of biosensing capabilities and customizable drug delivery profiles enables tailored treatment regimens based on individual patient characteristics and disease states, advancing the paradigm of personalized medicine and optimizing therapeutic efficacy while minimizing adverse effects.
Remote Monitoring and Telemedicine	Wearable and implantable microneedle devices facilitate remote monitoring of biomarkers and physiological parameters, enabling real-time health assessment and disease management outside traditional healthcare settings. This promotes telemedicine and remote patient monitoring, improving access to healthcare and reducing healthcare disparities.
Targeted and Controlled Drug Delivery	Precise control over drug release kinetics and spatial distribution enables targeted delivery of therapeutics to specific tissues or organs, minimizing systemic side effects and maximizing therapeutic efficacy. Microneedle-based drug delivery systems offer potential advancements in treating localized diseases and overcoming biological barriers to drug delivery.
Point-of-Care Diagnostics	Microneedle-based biosensing platforms enable rapid and minimally invasive diagnostics at the point of care, facilitating early disease detection, monitoring of treatment responses, and management of chronic conditions. This enhances healthcare delivery by providing timely and actionable information for clinical decision-making and patient management.
Tissue Engineering and Regenerative Medicine	Microneedle-based delivery of bioactive molecules, stem cells, and growth factors promotes tissue regeneration and wound healing, offering potential applications in tissue engineering and regenerative medicine. Controlled release of therapeutic agents enhances tissue repair and regeneration, addressing unmet clinical needs in wound care and tissue reconstruction.

9. CONCLUSION

9.1. Summary of Key Findings and Insights

The review article provides a comprehensive overview of microneedle technology, exploring its evolution, current status, and future directions in healthcare and biomedical engineering. Key findings highlight the versatility and potential impact of microneedle-based devices across various applications, including drug delivery, diagnostics, tissue engineering, and personalized medicine. Microneedle technology offers several advantages, including minimally invasive administration, enhanced patient compliance, and targeted drug delivery, making it a promising tool for improving healthcare delivery and patient outcomes. Emerging trends such as multifunctional microneedles, stimuli-responsive systems, and integration with wearable devices underscore the innovation and potential for transformative advancements in personalized medicine and remote healthcare monitoring. Challenges such as manufacturing scalability, regulatory approval, and distribution logistics are also addressed, emphasizing the need for continued research and collaboration to overcome barriers to widespread adoption and commercialization.

9.2. Implications for Research, Industry, and Clinical

The implications of microneedle technology span across research, industry, and clinical practice, shaping the landscape of healthcare delivery and biomedical innovation. In research, continued exploration of microneedle technology holds promise for advancing our understanding of drug delivery mechanisms, biomarker detection, and tissue engineering. Future research efforts should focus on optimizing microneedle designs, materials, and fabrication techniques to enhance functionality, biocompatibility, and therapeutic efficacy. In industry, the commercialization of microneedle-based products presents opportunities for growth and innovation in pharmaceuticals, medical devices, and biotechnology sectors. Industry stakeholders should invest in scalable manufacturing processes, quality assurance systems, and regulatory compliance to bring microneedle products to market and meet growing demand for minimally invasive healthcare solutions. In clinical practice, the adoption of microneedle technology offers transformative benefits for patient care, enabling personalized medicine approaches, remote monitoring, and targeted therapy delivery. Healthcare providers should integrate microneedle-based devices into clinical workflows, leverage their capabilities for improved diagnostics and treatment outcomes, and educate patients on the benefits of these innovative technologies.

9.3. Future Directions and Recommendations for Further Study

Future directions in microneedle technology present exciting opportunities for further study and innovation, paving the way for advancements in healthcare delivery, biomedical engineering, and patient care. One key area for further study is the development of next-generation microneedle designs with enhanced functionality and versatility. Researchers should explore novel materials, fabrication techniques, and coating strategies to optimize microneedle performance for specific applications, such as targeted drug delivery, biosensing, and tissue engineering. Additionally, there is a need for comprehensive preclinical and clinical studies to evaluate the safety, efficacy, and long-term performance of microneedle-based devices in diverse patient populations. Future research efforts should focus on addressing challenges such as biocompatibility, scalability, and regulatory approval to facilitate translation of microneedle technologies from bench to bedside. Moreover, interdisciplinary collaborations between researchers, engineers, clinicians, and industry partners are essential for driving innovation and overcoming technical barriers in microneedle technology. Collaborative initiatives can accelerate the development of integrated microneedle platforms, personalized medicine approaches, and point-of-care solutions for improving healthcare delivery and patient outcomes.

REFERENCES

1. Vora LK, Moffatt K, Tekko IA, Paredes AJ, Volpe-Zanutto F, Mishra D, et al. Microneedle array systems for long-acting drug delivery. *European Journal of Pharmaceutics and Biopharmaceutics*. 2021;159:44-76.
2. Mdanda S, Ubanako P, Kondiah PP, Kumar P, Choonara YE. Recent advances in microneedle platforms for transdermal drug delivery technologies. *Polymers*. 2021;13(15):2405.
3. Kulkarni D, Gadade D, Chapaitkar N, Shelke S, Pekamwar S, Aher R, et al. Polymeric Microneedles: An Emerging Paradigm for Advanced Biomedical Applications. *Scientia Pharmaceutica*. 2023;91(2):27.
4. Erdem Ö, Eş I, Akceoglu GA, Saylan Y, Inci F. Recent advances in microneedle-based sensors for sampling, diagnosis and monitoring of chronic diseases. *Biosensors*. 2021;11(9):296.
5. Prausnitz MR. Microneedles for transdermal drug delivery. *Advanced drug delivery reviews*. 2004;56(5):581-7.
6. Cárcamo-Martínez Á, Mallon B, Domínguez-Robles J, Vora LK, Anjani QK, Donnelly RF. Hollow microneedles: A perspective in biomedical applications. *International journal of pharmaceutics*. 2021;599:120455.
7. Rajendhiran N, Bhattacharyya S. Preparation and Evaluation of Nanolipid Carriers of Bedaquiline-In vitro Evaluation and in silico Prediction. *Jordan Journal of Pharmaceutical Sciences*. 2024;17(3):450-67.
8. Dayyih WA, Hailat M, Albtoush S, Albtoush E, Dayah AA, Alabbadi I, et al. Nanomedicine Advancements in Cancer Therapy: A Scientific Review. *Jordan Journal of Pharmaceutical Sciences*. 2024;17(3):506-29.
9. Tucak A, Sirbubalo M, Hindija L, Rahić O, Hadžiabdić J, Muhamedagić K, et al. Microneedles: Characteristics, materials, production methods and commercial development. *Micromachines*. 2020;11(11):961.
10. Wang QL, Zhu DD, Chen Y, Guo XD. A fabrication method of microneedle molds with controlled microstructures. *Materials Science and Engineering: C*. 2016;65:135-42.
11. Yang C, Yin X-H, Cheng G-M. Microinjection molding of microsystem components: new aspects in improving performance. *Journal of Micromechanics and Microengineering*. 2013;23(9):093001.
12. Thanuja R, Kumar KV, Sree BD, Karthick S, Reshma T. A Comprehensive Review on Documentation Practices in the Pharmaceutical Manufacturing Industry. *Jordan Journal of Pharmaceutical Sciences*. 2024;17(4):829-47.
13. Mack C. Fundamental principles of optical lithography: the science of microfabrication. *John Wiley & Sons*. 2007.
14. Vieu C, Carcenac F, Pepin A, Chen Y, Mejias M, Lebib A, et al. Electron beam lithography: resolution limits and applications. *Applied surface science*. 2000;164(1-4):111-7.
15. Traub MC, Longsine W, Truskett VN. Advances in nanoimprint lithography. *Annual review of chemical and biomolecular engineering*. 2016;7:583-604.
16. Ahmed N, Darwish S, Alahmari AM. Laser ablation and laser-hybrid ablation processes: a review. *Materials and Manufacturing Processes*. 2016;31(9):1121-42.
17. Hazzan KE, Pacella M, See TL. Laser processing of hard and ultra-hard materials for micro-machining and surface engineering applications. *Micromachines*. 2021;12(8):895.
18. Limongi T, Tirinato L, Pagliari F, Giugni A, Allione M, Perozziello G, et al. Fabrication and applications of micro/nanostructured devices for tissue engineering. *Nano-micro letters*. 2017;9:1-13.
19. Praveena B, Lokesh N, Buradi A, Santhosh N, Praveena B, Vignesh R. A comprehensive review of emerging additive manufacturing (3D printing technology): Methods, materials, applications, challenges, trends and future potential. *Materials Today: Proceedings*. 2022;52:1309-13.

20. Nyirjesy SC, Heller M, von Windheim N, Gingras A, Kang SY, Ozer E, et al. The role of computer aided design/computer assisted manufacturing (CAD/CAM) and 3-dimensional printing in head and neck oncologic surgery: A review and future directions. *Oral Oncology*. 2022;132:105976.
21. Javaid M, Haleem A, Singh RP, Suman R. 3D printing applications for healthcare research and development. Global Health Journal. 2022;6(4):217-26.
22. Park J-H, Choi S-O, Kamath R, Yoon Y-K, Allen MG, Prausnitz MR. Polymer particle-based micromolding to fabricate novel microstructures. *Biomedical microdevices*. 2007;9:223-34.
23. Ozyilmaz ED, Turan A, Comoglu T. An overview on the advantages and limitations of 3D printing of microneedles. *Pharmaceutical Development and Technology*. 2021;26(9):923-33.
24. Nguyen HX, Banga AK. Delivery of methotrexate and characterization of skin treated by fabricated PLGA microneedles and fractional ablative laser. *Pharmaceutical research*. 2018;35:1-20.
25. Escobar-Chávez JJ, Bonilla-Martínez D, Angélica M, Molina-Trinidad E, Casas-Alancaster N, Revilla-Vázquez AL. Microneedles: a valuable physical enhancer to increase transdermal drug delivery. *The Journal of Clinical Pharmacology*. 2011;51(7):964-77.
26. Ganeson K, Alias AH, Murugaiyah V, Amirul A-AA, Ramakrishna S, Vigneswari S. Microneedles for efficient and precise drug delivery in cancer therapy. *Pharmaceutics*. 2023;15(3):744.
27. Gupta J, Gupta R, Vanshita. Microneedle technology: an insight into recent advancements and future trends in drug and vaccine delivery. *Assay and drug development technologies*. 2021;19(2):97-114.
28. Raikar AS, Kalaskar D, Bhilegaonkar S, Somnache SN, Bodaghi M. Revolutionizing drug delivery by bioinspired 4D transdermal microneedles: Advances and future horizons. *European Polymer Journal*. 2024:112952.
29. Rezania N. Design of minimally invasive diagnostic and dermal fluids sampling microneedle. 2024.
30. Saifullah KM, Faraji Rad Z. Sampling dermal interstitial fluid using microneedles: a review of recent developments in sampling methods and microneedle-based biosensors. *Advanced Materials Interfaces*. 2023;10(10):2201763.
31. Qu F, Geng R, Liu Y, Zhu J. Advanced nanocarrier-and microneedle-based transdermal drug delivery strategies for skin diseases treatment. *Theranostics*. 2022;12(7):3372.
32. Lyu S, Dong Z, Xu X, Bei H-P, Yuen H-Y, Cheung C-WJ, et al. Going below and beyond the surface: Microneedle structure, materials, drugs, fabrication, and applications for wound healing and tissue regeneration. *Bioactive Materials*. 2023;27:303-26.
33. Ribet F, Stemme G, Roxhed N. Real-time intradermal continuous glucose monitoring using a minimally invasive microneedle-based system. *Biomedical microdevices*. 2018;20:1-10.
34. Thakur Singh RR, Tekko I, McAvoy K, McMillan H, Jones D, Donnelly RF. Minimally invasive microneedles for ocular drug delivery. *Expert opinion on drug delivery*. 2017;14(4):525-37.
35. Paredes AJ, Volpe-Zanutto F, Vora LK, Tekko IA, Permana AD, Picco CJ, et al. Systemic delivery of tenofovir alafenamide using dissolving and implantable microneedle patches. *Materials Today Bio*. 2022;13:100217.
36. Romito B, Jewell J, Jackson M, Ernst K, Hill V, Hsu B, et al. Child life services. *Pediatrics*. 2021;147(1).
37. Rahbar M. Design, Fabrication and Testing of Magnetic Composite Polymer Actuators Integrated With Microfluidic Devices and Systems. 2016.
38. Korrapati PS, Karthikeyan K, Satish A, Krishnaswamy VR, Venugopal JR, Ramakrishna S. Recent advancements in nanotechnological strategies in selection, design and delivery of biomolecules for skin regeneration. *Materials Science and Engineering: C*. 2016;67:747-65.

39. Narayan SM, Wan EY, Andrade JG, Silva JNA, Bhatia NK, Deneke T, et al. Visions for digital integrated cardiovascular care: HRS Digital Health Committee perspectives. *Cardiovascular Digital Health Journal*. 2024;5(2):37-49.
40. Larrañeta E, Lutton RE, Woolfson AD, Donnelly RF. Microneedle arrays as transdermal and intradermal drug delivery systems: Materials science, manufacture and commercial development. *Materials Science and Engineering: R: Reports*. 2016;104:1-32.
41. Yang D, Chen M, Sun Y, Jin Y, Lu C, Pan X, et al. Microneedle-mediated transdermal drug delivery for treating diverse skin diseases. *Acta Biomaterialia*. 2021;121:119-33.
42. Pahal S, Badnikar K, Ghate V, Bhutani U, Nayak MM, Subramanyam DN, et al. Microneedles for extended transdermal therapeutics: a route to advanced healthcare. *European Journal of Pharmaceutics and Biopharmaceutics*. 2021;159:151-69.
43. Amarnani R, Shende P. Microneedles in diagnostic, treatment and theranostics: An advancement in minimally-invasive delivery system. *Biomedical Microdevices*. 2022;24(1):4.
44. Bullock CJ, Bussy C. Biocompatibility considerations in the design of graphene biomedical materials. *Advanced Materials Interfaces*. 2019;6(11):1900229.
45. Vranić E, Tucak A, Sirbubalo M, Rahić O, Elezović A, Hadžiabdić J, editors. Microneedle-based sensor systems for real-time continuous transdermal monitoring of analytes in body fluids. *CMBEBIH 2019: Proceedings of the International Conference on Medical and Biological Engineering, 16−18 May 2019, Banja Luka, Bosnia and Herzegovina*; 2020: Springer.
46. Wang R, Jiang G, Aharodnikau UE, Yunusov K, Sun Y, Liu T, et al. Recent advances in polymer microneedles for drug transdermal delivery: Design strategies and applications. *Macromolecular Rapid Communications*. 2022;43(8):2200037.
47. Aldawood FK, Andar A, Desai S. A comprehensive review of microneedles: Types, materials, processes, characterizations and applications. *Polymers*. 2021;13(16):2815.
48. Chen Y, Alba M, Tieu T, Tong Z, Minhas RS, Rudd D, et al. Engineering micro–nanomaterials for biomedical translation. *Advanced NanoBiomed Research*. 2021;1(9):2100002.
49. Arote KS, Salade DA, Patil NV. A Brief Review on Regulatory Affairs: Ensuring Compliance, Safety, and Market Access. *International Journal of Pharmaceutical Sciences*. 2023;1(09):1-.
50. Avcil M, Çelik A. Microneedles in drug delivery: progress and challenges. *Micromachines*. 2021;12(11):1321.
51. Ertas YN, Ertas D, Erdem A, Segujja F, Dulchavsky S, Ashammakhi N. Diagnostic, Therapeutic, and Theranostic Multifunctional Microneedles. *Small*. 2024:2308479.
52. Carou-Senra P, Rodríguez-Pombo L, Awad A, Basit AW, Alvarez-Lorenzo C, Goyanes A. Inkjet printing of pharmaceuticals. *Advanced Materials*. 2024;36(11):2309164.
53. Liu R, Li A, Lang Y, Cai H, Tang X, Li D, et al. Stimuli-responsive polymer microneedles: A rising transdermal drug delivery system and its applications in biomedical. *Journal of Drug Delivery Science and Technology*. 2023:104922.
54. Alzoubi L, Aljabali AA, Tambuwala MM. Empowering precision medicine: the impact of 3d printing on personalized therapeutic. *AAPS PharmSciTech*. 2023;24(8):228.
55. Awad A, Trenfield SJ, Pollard TD, Ong JJ, Elbadawi M, McCoubrey LE, et al. Connected healthcare: Improving patient care using digital health technologies. *Advanced Drug Delivery Reviews*. 2021;178:113958.

مراجعة حول القدرة على الاختراق: المشهد الحالي للميكرونيدلز وآفاقها المستقبلية

بوياكاتي محمد رضوان[1]، نواز محمد[1]، شيخ فرحين تاج [1]، ڤي .سيفاساي بهارات كومار[1]، بي .يامون[1]

[1]قسم الصيدلانيات، معهد راغافيندرا للتعليم والبحث الصيدلاني، تقاطع كيه. آر. بالي، أنانتابور، تشيبادو، أندرا براديش ، الهند

ملخص

تُعدّ تقنية الإبر الدقيقة نهجًا واعدًا لتوصيل الأدوية والتطعيم والتشخيص والعلاجات التجميلية. تقدم هذه المراجعة نظرة شاملة على تقنية الإبر الدقيقة، وتشمل الأنواع المختلفة من الإبر الدقيقة، وتقنيات التصنيع، والتطبيقات، والفوائد، والتحديات، واعتبارات السلامة، والترجمة السريرية، وآفاق المستقبل. يتم مناقشة الإبر الدقيقة الصلبة، والمجوفة، والقابلة للذوبان، والمطلية، وتلك المكونة من الهلام المائي، إلى جانب بنيتها، والمواد المستخدمة، وأساليب التصنيع. كما يتم استكشاف تطبيقات الإبر الدقيقة في توصيل الأدوية، والتطعيم، والتشخيص، والعلاجات التجميلية، مع التركيز على التطبيقات الناشئة والاستخدامات الجديدة. وتتناول المراجعة مزايا تقنية الإبر الدقيقة مثل زيادة التقبل من قبل المرضى، وتحسين امتصاص الدواء، وتقليل الألم، بالإضافة إلى التحديات مثل قابلية التصنيع على نطاق واسع والحصول على الموافقة التنظيمية. يتم مناقشة تقنيات التصنيع، والتوافق الحيوي، واعتبارات السلامة، والترجمة السريرية، وجوانب التسويق التجاري، إلى جانب الاتجاهات المستقبلية مثل الإبر الدقيقة متعددة الوظائف وتطبيقات الطب الشخصي. بشكل عام، تمتلك تقنية الإبر الدقيقة وعدًا كبيرًا لإحداث ثورة في الرعاية الصحية والهندسة الطبية الحيوية، لكن لا بد من إجراء المزيد من البحوث والتطوير لمعالجة التحديات وتحقيق كامل إمكاناتها.

الكلمات الدالة: الإبر الدقيقة، توصيل الأدوية، التطعيم، التشخيص، تقنيات التصنيع، التوافق الحيوي، الترجمة السريرية، آفاق المستقبل.

* ***المؤلف المراسل: نواز محمد***

mohammednawaz151@gmail.com

تاريخ استلام البحث 2024/6/8 وتاريخ قبوله للنشر 2024/9/21.

Jordan Journal of Pharmaceutical Sciences, Volume 18, No. 2, 2025

The Predictive Value of Neutrophil/Lymphocyte Ratio for CK-MB Elevation in Myocardial Infarction: A Study in Syrian ACS Patients

Issa Yusuf [1]*, ***Rama Ibrahim***[1]*

[1] Department of Biochemistry and Microbiology, Faculty of Pharmacy, Tishreen University, Latakia Syria

ABSTRACT

Acute coronary syndrome (ACS) is a serious cardiovascular condition associated with a high mortality rate. It typically arises from the rupture of an atherosclerotic plaque leading to thrombus formation and encompasses unstable angina (UA) and myocardial infarction (MI). The latter results in myocardial necrosis, which triggers an acute inflammatory response that contributes to disease progression. Few studies have explored the diagnostic utility of the neutrophil-to-lymphocyte ratio (NLR) as a complementary, inexpensive, and easily performed test for diagnosing MI, either alone or in conjunction with creatine kinase-MB (CK-MB). Therefore, this study aimed to evaluate the diagnostic accuracy of admission NLR as a biomarker for MI in ACS patients. This cross-sectional study included 89 patients with ACS who were admitted to the emergency department of Al-Basel Hospital between March 2023 and January 2024. The patients were categorized into two groups: MI (n = 41) and UA (n = 48). Baseline characteristics and specific inflammatory markers (WBC, neutrophils, lymphocytes, and NLR) were assessed and compared between the two groups. Our findings revealed that admission NLR values were significantly higher in the MI group compared to the UA group (4.62 vs. 2.56, $P < 0.01$). Moreover, NLR was significantly correlated with CK-MB activity in the MI group ($r = 0.45$, $P < 0.01$). A cutoff value of 2.78 for admission NLR yielded a sensitivity of 73% and a specificity of 62% for predicting MI in ACS patients. Notably, combining CK-MB and NLR measurements improved diagnostic performance, with a sensitivity of 88% and specificity of 93%. These findings suggest that a simple biomarker such as NLR could serve an adjunctive role in facilitating the diagnosis of MI in patients with ACS.

Keywords: neutrophil-to-lymphocyte ratio, CK-MB, acute coronary syndrome, myocardial infarction, inflammation.

1- INTRODUCTION

Cardiovascular diseases (CVDs) stand as a major global health concern, responsible for an estimated 17.9 million deaths worldwide [1, 2]. This high mortality rate is due to coronary artery disease (CAD), which is the first leading cause of global mortalities [3].

The main hallmark of CAD is atherosclerosis, a chronic inflammatory condition that affects the endothelial cells of arteries and causes a lipid-rich plaque that could enlarge over time, leading to the stenosis of the coronary arteries [4, 5]. Some plaques remain stable, others could rupture, leading to the formation of coronary thrombosis [6]. Thrombosis could cause partial or total occlusion of the lumen resulting in the development of acute coronary syndrome (ACS). it may present as unstable angina (UA), in semi-blockage of the coronary arteries, or myocardial infarction (MI), generally corresponding to complete occlusion of the coronary arteries and necrosis of myocardial cells [7].

*Corresponding author:
Issa Yusuf: issa.yusuf@tishreen.edu.sy
Rama Ibrahim: ramaibrahim@tishreen.edu.sy
Received: 13/6/2024 Accepted: 21/9/2024.
DOI: https://doi.org/10.35516/jjps.v18i2.2793

Plaque rupture leads to the activation of systemic inflammatory response, as evidenced by elevated levels of inflammatory biomarkers such as high-sensitive C-reactive protein (hs-CRP) and tumor necrosis factor α (TNF-α) in the peripheral blood of ACS patients [8, 9]. This inflammatory response is aggravated by the ischemic cellular injury following MI [10]. Studies have shown that inflammatory biomarkers, including CRP, IL-1β, ESR, and fibrinogen, are elevated in patients with MI compared to those in the healthy group [11, 12].

The neutrophil-to-lymphocyte ratio (NLR) is also used as an indicative biomarker of inflammatory status, it serves as an inexpensive, routinely available biomarker derived from the absolute neutrophil and lymphocyte counts [13, 14]. Various studies have emphasized the diagnostic and prognostic role of NLR in many diseases, including cancer, rheumatoid arthritis, Alzheimer's disease, and cardiovascular diseases [15-17]. However, there is a lack of research focusing on the utility of NLR as an adjunctive tool in the diagnosis of MI, particularly in combination with creatine kinase myocardial band isoform (CK-MB).

CK-MB is an enzyme that is expressed predominately in myocardial cells[18]. It persists as a biomarker for MI diagnosis especially when cardiac troponin assay is not available [19, 20]. This study aimed to investigate the individual or combined diagnostic accuracy of admission NLR as a biomarker of MI in patients presenting to the emergency department with anginal complaints consistent with MI. Those complaints are described as acute chest pain or discomfort, dyspnoea, or pain in the left or right arm or neck/jaw.

2- MATERIALS AND METHODS

2-1- Study population

We conducted a cross-sectional study involving a total of 89 patients diagnosed with ACS (48 with UA and 41 with MI) who were admitted to the emergency department of AL-Basel Hospital between March 2023 and January 2024.

The study was conducted according to the Declaration of Helsinki and all procedures undertaken in this study were approved by the Institutional Board of Tishreen University, confirmed by Ethical Approval No.123 dated 20/09/2022.

Patients presenting with ACS were initially diagnosed based on the presence of persistent and characteristic chest pain experienced at rest. Thereafter, the diagnosis was confirmed based on electrocardiography (ECG) and CK-MB measurements. Patients who presented with chest pain and subsequently showed no changes in either ECG or CK-MB were defined as having UA. Diagnosis of MI was established when an elevation of CK-MB was noted or when characteristic ECG changes, e.g. ST segment elevation or T wave inversion was recorded along with the presence of stenosis by cardiac coronary catheterization.

Patients diagnosed with ACS who had either acute or chronic infections, autoimmune diseases like rheumatoid arthritis or asthma, malignant tumors, or were undergoing steroid therapy were excluded from the study. Additionally, patients with hyperlipidemia who were receiving statin therapy were also excluded.

2-2- Demographic data

Demographic information was obtained using a standardized questionnaire. Information collected encompassed age, sex, current smoking and patient's medical history including diabetes and/or hypertension. Systolic blood pressure (SBP) and diastolic blood pressure (DBP) were also measured.

2-3- Laboratory analysis

Initial blood samples were drained from patients upon admission to the emergency unit, and a complete blood count (CBC) was performed using EDTA tubes on the QUINTUS 5-Part Hematology analyzer. We calculated NLR and platelet-to-lymphocyte (PLR) ratios by dividing the absolute neutrophil count and platelets count, respectively, by the absolute lymphocyte count. Biochemical tests for urea, creatinine, CK, and CK-MB were performed on BIOSYSTEMS BTS 350 Biochemistry analyzer using serum tubes.

2-4- Statistical analysis

The Shapiro-Wilk test was used to check the normality distribution of continuous variables. Categorical variables were presented as counts and percentages, while continuous variables were reported as mean ± standard deviation or median and interquartile range (25-75 percentile). The independent sample t-test and Mann-Whitney tests were conducted for continuous variables (according to their normal distribution), while chi-square test was used for categorical variables. Correlations were evaluated using Spearman's correlation test. Variables of interest were further analyzed by multivariate regression, and results were shown as odds ratio (OR) with 95% confidence intervals (CIs). Receiver Operating Characteristic (ROC) curve analysis was performed to determine the optimal NLR cut-off value with the best sensitivity and specificity for predicting MI. Results were considered statistically significant when P< 0.05. The statistical analysis was done using R statistical programming language.

3- RESULTS

The study included 89 patients with ACS, subdivided into 41 patients with MI (mean age: 55.9 ± 11.5 years; 73% male) and 48 patients with UA (mean age: 56.4 ± 11.2 years; 62.5% male). No significant differences were observed between the two groups in terms of gender distribution, smoking status, hypertension, or diabetes. Similarly, there were no statistically significant differences in mean age, diastolic blood pressure (DBP), systolic blood pressure (SBP), serum creatinine, urea, hemoglobin, absolute lymphocyte count, platelet count, or platelet-to-lymphocyte ratio. In contrast, the MI group exhibited significantly higher levels of WBC, absolute and relative neutrophil counts, relative lymphocyte count, NLR, CK, and CK-MB ($P < 0.05$), as presented in Table 1.

Table 1. Patients' baseline characteristics and laboratory findings of MI vs. UA groups.

	MI N=41	**UA N=48**	**P-value**
Males count	30 (73%)	30 (62.5%)	0.284
Smokers count	29 (70.7%)	28 (58.3%)	0.22
Hypertension	16 (39%)	23 (48%)	0.399
Diabetes	13 (31.7%)	15 (31.25%)	0.96
Hyperlipidemia	11 (26.83%)	17 (35.41%)	0.521
Age (years)	55.9±11.5	56.4±11.2	0.85
DBP (mmHg)	78.97±21.49	74.75±13.77	0.328
SBP (mmHg)	122.79±28.95	125.25±17.68	0.662
Urea (mg/dL)	37.01±13.61	36.73±12.11	0.92
Creatinine (mg/dL)	1.08±0.41	1.02±0.22	0.484
Hemoglobin (g/dL)	13.82±1.72	13.11±1.81	0.072
Platelets (*10^3/µL)	249.95±72.49	235.04±56.63	0.311
WBC (*10^9/L)$^+$	11.95(9.8-15.78)	7.7(7-9.8)	<0.001*
Neutrophils (*10^9/L)$^+$	9.02(6.3-12.5)	5.2(4.2-7.1)	<0.001*
Neutrophils %	74.87±10.96	66.96±6.91	<0.001*
Lymphocytes (*10^9/L)$^+$	2.05(1.4-2.8)	2.14(1.8-2.6)	0.91
Lymphocytes%	19.29±9.31	25.83±5.57	<0.001*
NLR$^+$	4.62(2.46-6.38)	2.56(1.9-3.4)	<0.001*
PLR$^+$	116(91.25-148.9)	110.36±(90.6-146.7)	0.546
CK (U/L)$^+$	315.5(130.75-520)	87.5(72-121.75)	<0.001*
CK-MB (U/L)$^+$	32.5(28-49.75)	11(8.8-16.3)	<0.001*

$^+$ Variable are not normally distributed, and expressed as median (interquartile range).
* The difference is considered statistically significant.

Admission NLR showed a significant positive correlation with serum CK-MB activity, whereas lymphocyte counts demonstrated a negative correlation with CK-MB in MI patients (Table 2).

Table 2. Spearman's correlation coefficients between CK-MB and inflammatory parameters in MI patients.

	CRP	WBC	Neutrophils	Lymphocytes*	NLR*
CK-MB					
rho	0.243	0.214	0.274	-0.412*	0.456*
P-value	0.302	0.204	0.101	<0.05*	<0.01*
* Variables are significantly correlated with CK-MB.					

Using multivariate logistic regression analysis, higher admission NLR values independently predicted MI among ACS patients (OR: 2.36, 95% CI: 14-4.5, P < .01; Table 3). In ROC analysis, a cut-off level of NLR > 2.78 had a sensitivity of 73% and a specificity of 62% for predicting MI [Area under the ROC curve (AUC) = 0.737, 95% CI: 0.620-0.852, P < .001; Figure 1]. The sensitivity and specificity of CK-MB were calculated to compare results with those of NLR, and the threshold value of 25 IU/L was selected based on the assay kit used for analysis (Biosystems immunoinhibition CK-MB kit "COD 11792"). As shown in Table 4, adding admission NLR measurement to CK-MB analysis demonstrated better sensitivity and specificity (0.88 and 0.93, respectively) for predicting MI than CK-MB alone (0.78 and 0.87, respectively).

Table 3. Multivariate logistic regression analysis for predictors of MI in ACS patients.

Predictors	Odds Ratio (95%CI)	P-value
NLR	2.35 (1.4-4.5)	<0.01*
CRP	0.95 (0.86-1.02)	0.21
Age	1 (0.9-1.08)	0.78
Male gender	2.68 (0.45-19.49)	0.29
Smoking	3.72 (0.58-36.76)	0.19
Hyperlipidemia	0.63(0.1-3.37)	0.59

Table 4. Sensitivity, specificity, Positive predictive value (PPV), negative predictive value (NPV) of CK-MB, NLR, and CK-MB+NLR for predicting MI in ACS patients.

	CK-MB	NLR	NLR+CK-MB
Sensitivity	0.78	0.73	0.88
Specificity	0.87	0.622	0.93
PPV	0.84	0.57	0.92
NPV	0.82	0.70	0.9

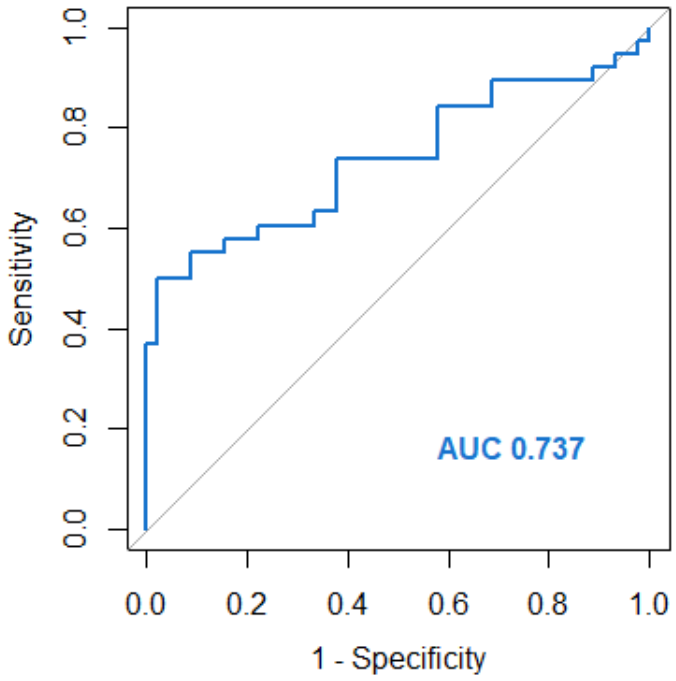

Figure1: The receiver–operating characteristic curve analysis of NLR for predicting MI.

4- DISCUSSION

Our study aimed to investigate the significance of NLR as an adjunctive biomarker in the diagnosis of MI in patients with ACS, in relation to the diagnostic performance of CK-MB within the first six hours of emergency admission.

This study showed that white blood cell and neutrophil counts were significantly higher in the MI group than in the UA group ($P < 0.01$). These results are consistent with the research of Marechal et al., who reported a significant difference in white blood cell count between patients with MI and those with stable and unstable angina. This difference was primarily attributed to variations in neutrophil count [21]. Likewise, Al-Fartosi et al., found that neutrophils were significantly higher in MI and UA groups compared to healthy controls, and also elevated in the MI group compared to the UA group [22]. Neutrophils are thought to participate in the pro-inflammatory response that follows the MI [23]. The cellular necrosis of cardiac muscle cells observed during MI results in the release of a variety of pro- and anti-inflammatory molecules. Of these, DAMPs (Damage-Associated Molecular Patterns) are nominated to play a crucial role in the inflammatory process. DAMPs bind to their receptors on the surface of innate immune cells, PRRs (Pattern Recognition Receptors), resulting in the induction of pro-inflammatory cytokines such as TNF-α and IL-1, which stimulate chemotaxis and recruitment of white blood cells to the site of necrosis, with neutrophils playing a primary role in the inflammatory response [24, 25]. Cellular necrosis is absent in UA, which explains the decreased neutrophil count compared to the MI. No significant difference was found in the number of lymphocytes between the MI and UA groups ($P > 0.05$), although the value was higher in the MI

group. This result was also reported by Tahto et al., and Marechal et al., who did not find any significant difference in absolute lymphocyte counts between the MI and UA groups [21, 26]. However, in our study, the difference in the relative lymphocyte count between the two groups was also investigated, because the higher count of WBC in the MI group could mislead the interpretation of the true difference in the lymphocyte count. Indeed, the mean relative lymphocyte count in the MI group was significantly lower than in the UA group ($P < 0.01$). Additionally, the relative lymphocyte count was below the reference limit in the MI group (19.3%) and within normal limits in the UA group (25.8%).

The role of lymphocytes in the pathogenesis of atherosclerosis remains ambiguous.

Mustafic et al., showed significantly lower relative lymphocyte values in patients with ACS compared to stable angina but without significant difference in absolute lymphocyte count [27]. Another study comparing absolute and relative lymphocyte counts between patients with stable and unstable angina showed no differences in either parameter [28]. These results together with ours imply that MI is the main contributor to the downregulation of lymphocytes in patients with ACS. To determine the mechanism underlying the reduction in lymphocyte count in MI patients, *in-vivo* experiments were conducted on MI-induced mice. The study found that MI mice exhibited glandular hypertrophy on the first day along with increased glucocorticoid production due to activation of the hypothalamic-pituitary-adrenal axis [29]. Plasma levels of glucocorticoids reduce lymphocyte count in peripheral blood by inducing reverse migration of lymphocytes to the bone marrow, promoting lymphocyte apoptosis and inhibiting their proliferation [29, 30]. We excluded patients undergoing steroid therapy because it affects lymphocyte counts. Admission NLR has been thoroughly studied as an inflammatory biomarker in a wide variety of medical conditions, including cardiovascular diseases [31], owing to its low cost, ease of measurement, and laboratory availability. Inflammation has a key role in ACS context, since atherosclerosis, which is the main cause of coronary heart disease, develops as a result of the chronic inflammatory process in damaged endothelial cells lining the arteries. Furthermore, plaque rupture and atherothrombosis trigger an acute local and systemic inflammation, that is exacerbated after myocardial cellular necrosis [32]. As atherothrombosis is an acute inflammatory response involving both innate and acquired immunity [33], a biomarker such as NLR which combines neutrophils and lymphocytes (representing the innate and acquired immunological response, respectively) could be considered as a biomarker with prognostic and diagnostic value in ACS and MI.

We found that NLR at admission was significantly increased in the MI group compared to the UA group ($P < 0.01$) and thus emerged as the biomarker with the strongest positive correlation with CK-MB values in patients with MI among other inflammatory indicators, i.e. WBC, lymphocytes, and neutrophils. In the study of Erturk et al., NLR was independently elevated in ACS patients compared to controls. Furthermore, the highest levels of NLR were observed in patients with STEMI followed by NSTEMI and UA. They also found that NLR was positively correlated with high-sensitivity troponin (hsTn) in ACS patients [34]. The results of our study support the above-mentioned conclusions and suggest that NLR could be used as an indicator to discriminate different types of ACS. Shumilah et al., investigated the diagnostic accuracy of NLR, mean platelet volume (MPV), PLR, and monocyte-to-lymphocyte ratio (MLR) for ACS, they found that NLR is the strongest predictive biomarker for ACS, while MLR was not significant [35]. This study highlights the diagnostic efficiency of NLR among other inflammatory biomarkers derived from complete blood count (CBC), thus supporting our choice of NLR as an inflammatory biomarker correlated with CK-MB during ACS. The mechanism that links MI to NLR involves the two phases of inflammation associated with MI: the inflammatory phase and the proliferative phase [36].

During the inflammatory phase, neutrophils play a crucial role by recruiting macrophages and removing cellular debris. Consequently, the neutrophil count in peripheral blood positively correlates with infarct size [37]. Lymphocytes are vital for myocardial remodeling after MI due to their anti-inflammatory properties. However, unlike neutrophils, lymphocyte levels decrease during the inflammatory phase, which contributes to the observed increase in NLR levels in the early stages of MI [38].

An NLR cutoff value of 2.78 showed a sensitivity of 0.73 and specificity of 0.62 for predicting ACS in patients with MI symptoms. Despite the low sensitivity and specificity of NLR compared to CK-MB, our study showed that integrating both biomarkers resulted in greater accuracy than using each biomarker individually. This suggests that NLR could help improve the accuracy of MI diagnosis when used in combination with CK-MB, a cardiac biomarker widely used in clinical practices. Similar conclusion was proposed by Korkmaz et al., who demonstrated that NLR was higher in the troponin-positive group and that a cut-off value of 2.80 had high sensitivity and specificity for predicting troponin elevation in ACS patients [39]. These findings indicate that NLR could serve as a useful biomarker in clinical practice. We recommend adding NLR to the routine hematorgram and considering it as an adjunctive diagnostic tool, as well as a biomarker for assessing the severity of inflammatory response.

5- CONCLUSION

Admission NLR is an adjunctive complementary tool in the diagnosis of MI in patients with ACS. It could also be a simple but potential biomarker of the inflammatory response that follows myocardial necrosis.

Admission NLR demonstrated a significant increase in MI compared to UA and a strong correlation with CK-MB levels, suggesting its relevance in discriminating ACS subtypes. While NLR alone has lower sensitivity and specificity than CK-MB, its use in combination with CK-MB could improve diagnostic accuracy in clinical practice. These findings highlight the need for further research into the role of inflammatory biomarkers in the diagnosis and management of ACS to optimize patient care.

6- LIMITATIONS

We were unable to study the prognostic value of NLR because there was a lack of long-term follow-up of patients. A cohort study design would be preferable for this purpose. The sample size is relatively small, which may have affected the significance of some results. Troponin was performed for MI screening initially but was later replaced by CK-MB due to its intermittent availability during the study period. The relationship between NLR and other inflammatory biomarkers, such as hs-CRP and TNF-α, could provide more details about the inflammatory response following MI.

7- DECLARATION

7-1- Competing interests

The author declares that there is no interest in the publication of the manuscript. In addition, the ethical issues, including plagiarism, informed consent, misconduct, data fabrication and/or falsification, double publication and/or submission, and redundancies have been completely observed by the author.

7-2- Author contributions

All work relevant to this study, from data collection, analysis, and writing of the article, was carried out by the authors I.Y and R.I.

7-3- Data sharing statement

The authors confirm that the data supporting the findings of this article are available within this article.

7-4- Acknowledgements

We deeply appreciate the commitment and efforts of the medical staff and healthcare professionals at "Al-Basel Hospital for Cardiology & Heart Surgery".

7-5- Funding

This work funded by Tishreen University in Syria.

7-6- Informed Consent Statement

Written consent was acquired from patients to ensure their informed participation.

REFERENCES

1. Alrob O.A. Cardiac energy metabolism: a potential novel therapeutic target in the treatment of ischemic heart diseases. *Jordan Journal of Pharmaceutical Sciences.* 2017; 10(3).
2. World Health Organization. Health topics: Cardiovascular diseases. Fact sheet. *Available online: http://www.who.int/cardiovascular_diseases/en/* (accessed on 11 December 2020). 2013.
3. Ralapanawa U., Sivakanesan R. Epidemiology and the magnitude of coronary artery disease and acute coronary syndrome: a narrative review. *Journal of Epidemiology and Global Health.* 2021; 11(2):169.
4. Al-Motassem Y., Bulatova N.L., AbuRuz S. Management of coronary artery disease in Jordan: cross-sectional comparative study. *Jordan Journal of Pharmaceutical Sciences.* 2008; 1(1).
5. Milutinović A., Šuput D., Zorc-Pleskovič R. Pathogenesis of atherosclerosis in the tunica intima, media, and adventitia of coronary arteries: an updated review. *Bosnian Journal of Basic Medical Sciences.* 2020; 20(1):21.
6. Bhatt D.L., Lopes R.D., Harrington R.A. Diagnosis and treatment of acute coronary syndromes: a review. *JAMA.* 2022; 327(7):662–675.
7. Komilovich E.B.Z. Coronary artery disease. *European Journal of Modern Medicine and Practice.* 2023; 3(12):81–87.
8. Sayfiddinovna S.A., et al. Comparative assessment of nonspecific inflammation markers and various key factors in patients with acute coronary syndrome. *European Science Review.* 2019; 2(1–2):210–213.
9. Tsioufis P., et al. The impact of cytokines in coronary atherosclerotic plaque: current therapeutic approaches. *International Journal of Molecular Sciences.* 2022; 23(24):15937.
10. Matter M.A., et al. Inflammation in acute myocardial infarction: the good, the bad and the ugly. *European Heart Journal.* 2024; 45(2):89–103.
11. Oprescu N., et al. Inflammatory markers in acute myocardial infarction and the correlation with the severity of coronary heart disease. *Annals of Medicine.* 2021; 53(1):1042–1048.
12. Wojtkowska A., et al. The inflammation link between periodontal disease and coronary atherosclerosis in patients with acute coronary syndromes: case–control study. *BMC Oral Health.* 2021; 21:1–17.
13. Guthrie G.J., et al. The systemic inflammation-based neutrophil–lymphocyte ratio: experience in patients with cancer. *Critical Reviews in Oncology/Hematology.* 2013; 88(1):218–230.
14. Han J.-B., et al. Predictive value of inflammation biomarkers in patients with portal vein thrombosis. *Journal of Clinical and Translational Hepatology.* 2021; 9(3):384.
15. Buonacera A., et al. Neutrophil to lymphocyte ratio: an emerging marker of the relationships between the immune system and diseases. *International Journal of Molecular Sciences.* 2022; 23(7):3636.
16. Li M., Xie L. Correlation between NLR, PLR, and LMR and disease activity, efficacy assessment in rheumatoid arthritis. *Evidence-Based Complementary and Alternative Medicine.* 2021; 2021:1–6.
17. Mosca M., et al. Neutrophil-to-lymphocyte ratio (NLR) in NSCLC, gastrointestinal, and other solid tumors: immunotherapy and beyond. *Biomolecules.* 2023; 13(12):1803.
18. Tilea I., Varga A., Serban R.C. Past, present, and future of blood biomarkers for the diagnosis of acute myocardial infarction—promises and challenges. *Diagnostics.* 2021; 11(5):881.
19. Byrne R.A., et al. 2023 ESC guidelines for the management of acute coronary syndromes: developed by the task force on the management of acute coronary syndromes of the European Society of Cardiology (ESC). *European Heart Journal: Acute Cardiovascular Care.* 2024; 13(1):55–161.

20. Al-Shatnawi S.F., Khasawneh R.A. Emergency research status in the Middle Eastern region. *Jordan Journal of Pharmaceutical Sciences.* 2022; 15(2):214–226.
21. Maréchal P., et al. Neutrophil phenotypes in coronary artery disease. *Journal of Clinical Medicine.* 2020; 9(5):1602.
22. Al-Fartosi K., Al-Salih R., Batah S.J. Study of relationship between blood parameters and oxidant-antioxidant status of patients with unstable angina pectoris and myocardial infractions. *Thi-Qar Medical Journal.* 2010; 4:47–64.
23. Puhl S.-L., Steffens S. Neutrophils in post-myocardial infarction inflammation: damage vs. resolution? *Frontiers in Cardiovascular Medicine.* 2019; 6:25.
24. Jiang K., Hwa J., Xiang Y. Novel strategies for targeting neutrophil against myocardial infarction. *Pharmacological Research.* 2024; 107256.
25. Ma Y., Yabluchanskiy A., Lindsey M.L. Neutrophil roles in left ventricular remodeling following myocardial infarction. *Fibrogenesis & Tissue Repair.* 2013; 6:1–10.
26. Tahto E., et al. Neutrophil-to-lymphocyte ratio and its relation with markers of inflammation and myocardial necrosis in patients with acute coronary syndrome. *Medical Archives.* 2017; 71(5):312.
27. Mustafic S., Ibralic A.M., Loncar D. Association of inflammatory and hemostatic parameters with values of high sensitive troponin in patients with acute coronary syndrome. *Medical Archives.* 2022; 76(2):84.
28. Zouridakis E.G., Garcia-Moll X., Kaski J.C. Usefulness of the blood lymphocyte count in predicting recurrent instability and death in patients with unstable angina pectoris. *American Journal of Cardiology.* 2000; 86(4):449–451.
29. Ma Y., et al. Circulating lymphocyte trafficking to the bone marrow contributes to lymphopenia in myocardial infarction. *American Journal of Physiology-Heart and Circulatory Physiology.* 2022; 322(4):H622–H635.
30. Jia W.-Y., Zhang J.-J. Effects of glucocorticoids on leukocytes: Genomic and non-genomic mechanisms. *World Journal of Clinical Cases.* 2022; 10(21):7187–7194.
31. Afari M.E., Bhat T. Neutrophil to lymphocyte ratio (NLR) and cardiovascular diseases: an update. *Expert Review of Cardiovascular Therapy.* 2016; 14(5):573–577.
32. Liuzzo G., et al. Inflammation and atherothrombosis. In: *Clinical Immunology.* Elsevier; 2019. p. 935–946.e1.
33. Cimmino G., et al. Evolving concepts in the pathophysiology of atherosclerosis: From endothelial dysfunction to thrombus formation through multiple shades of inflammation. *Journal of Cardiovascular Medicine.* 2023; 24(Suppl 2):e156–e167.
34. Özalp B., et al. Correlations between hematological indicators and other known markers in acute coronary syndromes. *EJCM.* 2017; 5(4):67–74.
35. Shumilah A.M., Othman A.M., Al-Madhagi A.K. Accuracy of neutrophil to lymphocyte and monocyte to lymphocyte ratios as new inflammatory markers in acute coronary syndrome. *BMC Cardiovascular Disorders.* 2021; 21:1–6.
36. Tudurachi B.-S., et al. Assessment of inflammatory hematological ratios (NLR, PLR, MLR, LMR and Monocyte/HDL–Cholesterol Ratio) in acute myocardial infarction and particularities in young patients. *International Journal of Molecular Sciences.* 2023; 24(18):14378.
37. Ma Y. Role of neutrophils in cardiac injury and repair following myocardial infarction. *Cells.* 2021; 10(7):1676.
38. Kologrivova I., et al. Cells of the immune system in cardiac remodeling: main players in resolution of inflammation and repair after myocardial infarction. *Frontiers in Immunology.* 2021; 12:664457.
39. Korkmaz A., et al. Utility of neutrophil–lymphocyte ratio in predicting troponin elevation in the emergency department setting. *Clinical and Applied Thrombosis/Hemostasis.* 2015; 21(7):667–671.

القيمة التنبؤيّة لنسبة العدلات إلى اللمفاويات في التنبؤ بارتفاع مستويات CK-MB في احتشاء العضلة القلبية: دراسة لدى مرضى ACS في سوريا

عيسى يوسف[1]، راما إبراهيم[1]

[1]قسم الكيمياء الحيوية والأحياء الدقيقة، كلية الصيدلة، جامعة تشرين، سوريا

ملخص

المتلازمة الإكليليّة الحادّة هي داء قلبي وعائي شديد مترافق مع معدل وفيات مرتفع. ينتج الداء عادةً من تمزّق لويحة التصلّب العصيدي ممّا يؤدي إلى تشكّل الخثرة العصيديّة. تتضمن المتلازمة الإكليليّة الحادّة كل من الخناق غير المستقر واحتشاء العضلة القلبيّة. يسبّب احتشاء العضلة القلبيّة تنخّراً للعضلة القلبيّة بالتالي تحريض استجابة التهابيّة حادّة تساهم في تقدّم المرض. قلّةٌ فقط من الدراسات قد تحرّت القدرة التشخيصيّة لنسبة العدلات إلى اللمفاويات باعتباره مشعر مساعد رخيص الثمن وسهل الإجراء لتشخيص احتشاء العضلة القلبيّة، وذلك لوحده أو بالمشاركة مع الكرياتين كيناز MB.بالتالي تهدف الدراسة إلى تحديد القدرة التشخيصية لنسبة العدلات إلى اللمفاويات عند القبول كمشعر لاحتشاء العضلة القلبية عند مرضى المتلازمة الإكليلية الحادّة. شارك 89 مريضاً بالمتلازمة الإكليلية الحادة في هذه الدراسة المقطعيّة والذين تم قبولهم في وحدة الإسعاف ضمن مشفى الباسل بين شهري آذار 2023 وكانون الثاني 2024. تم تقسيم المرضى إلى مجموعة احتشاء العضلة القلبية (عدد 41) ومجموعة الخناق غير المستقر (عدد 48). تم مقارنة وتقييم الخصائص الأساسية إضافةً لعدد من المشعرات الخلوية الالتهابية (تعداد الكريّات البيضاء والعدلات واللمفاويات ونسبة العدلات إلى اللمفاويات) بين مجموعتي الدراسة. أظهرت نتائجنا أن قيم نسبة العدلات إلى اللمفاويات عند القبول كانت أعلى عند مجموعة الاحتشاء منها عند مجموعة الخناق غير المستقر (4.62 مقابل 2.56، P <0.01)، كما كانت القيم مرتبطة مع فعالية الكرياتين كيناز في مجموعة الاحتشاء (معامل الارتباط=0.45، P <0.01). وجد أن القيمة الحديّة 2.78 لنسبة العدلات إلى اللمفاويات عند القبول كان لها حساسية73% ونوعية62% في التنبؤ باحتشاء العضلة القلبية عند مرضى المتلازمة الإكليلية الحادة. كما كان من المثير للاهتمام أن مشاركة نسبة العدلات إلى اللمفاويات مع الكرياتين كيناز MB أدّت إلى زيادة الحساسية والنوعية إلى (88% و93% على التوالي) أي أفضل من استخدام المشعرين بشكل منفصل. يدّل ذلك إلى أن مشعراً تشخيصيّاً بسيطاً كنسبة العدلات إلى اللمفاويات يمكن أن يكون له دور كعامل مساعد في تشخيص احتشاء العضلة القلبيّة عند المرضى المصابين بالمتلازمة الإكليليّة الحادّة.

الكلمات الدالة: نسبة العدلات إلى اللمفاويات، الكرياتين كيناز MB، المتلازمة الإكليلية الحادة، احتشاء العضلة القلبية، الالتهاب.

---

* ***المؤلف المراسل:***

عيسى يوسف: issa.yusuf@tishreen.edu.sy

راما إبراهيم: ramaibrahim@tishreen.edu.sy

تاريخ استلام البحث 2024/6/13 وتاريخ قبوله للنشر 2024/9/21.

Jordan Journal of Pharmaceutical Sciences, Volume 18, No. 2, 2025

Integrated Computational Exploring of Benzoyl Thienopyrimidine Derivatives as Potential ERα Regulators in Breast Cancer Treatment

Hassan Badaoui [1], Marwa Alaqarbeh[2*], Youness Moukhliss[1], Hanane Zaki[3], Moulay Ahfid El alaouy[1], M'barek Choukrad[1], Abdelouahid Sbai[1], Hamid Maghat[1], Tahar Lakhlifi[1], Mohammed Bouachrine[1]

[1]Molecular Chemistry and Natural Substances Laboratory, Faculty of Science, Moulay Ismail University of Meknes, Morocco.
[2] Basic Science Department, Prince Al Hussein bin Abdullah II Academy for Civil Protection, Al-Balqa Applied University, Al-Salt, Jordan.
[3] Biotechnology, Bioresources, and Bioinformatics Laboratory, Higher School of Technology, University of Sultan Moulay Sliman, Khenifra Morocco.

ABSTRACT

Estrogen receptor-positive (ER+) hormone-dependent breast cancer is the most common type in women, accounting for approximately 75% of all cases. This study aims to propose new potential therapeutic agents for breast cancer using computational methods. A 3D-QSAR study screened 22 compounds based on previous research, demonstrating strong predictive capabilities, as indicated by high Q^2 values of 0.516 and 0.787 for CoMFA and CoMSIA, respectively. Six new molecules (T1–T6) were proposed to enhance inhibitory activity, and the results of molecular docking analysis show that these drug candidates exhibit significant docking scores and form stable interactions within the receptor (PDB code: 1SJ0). The proposed compounds exhibited favorable pharmacokinetic and pharmacodynamic properties, except for T3, which showed mild toxicity. Molecular dynamics simulations also confirmed the stability of the T1–1SJ0 and 2D–1SJ0 complexes within the active site of ERα (estrogen receptor alpha). These findings highlight the potential of thienopyrimidine-based compounds as anti-breast cancer agents and open new avenues for experimental and clinical research.

Keywords: ADME/Tox, Breast cancer, Computational Modeling, 3D-QSAR, Thienopyrimidine.

1. INTRODUCTION

The broad family of nuclear receptors known as nuclear hormone receptors (NHR) functions as transcription factors. They are dispersed throughout the body and participate in cellular activities [1]. Estrone, estradiol (E2), and estriol are steroid hormones known as estrogens [2]. The most vital circulating estrogen is 17 β-estradiol, which plays a crucial role in maintaining and developing reproductive organs and controlling the activity of the immunological, circulatory, musculoskeletal, and central neurological systems. It also helps initiate and advance target tissue cancers and control energy homeostasis [3]. The estrogen receptor subtypes, ER-α and β, are crucial in mediating the physiological effects of estrogen. Estradiol binds to these receptors and activates multi-protein complexes that include coregulators. This process stimulates ER-mediated transcriptional activity through the involvement of ERα (Estrogen Receptor Alpha), AF1(Activation Function 1), and AF2 (Activation Function 2), leading to estrogenic effects [4]. The development of breast cancer occurs due to a disorder of coregulator activity, which may be

[*]***Corresponding author: Marwa Alaqarbeh***
marwaqabh@hotmail.com; marwa.aqarbeh@bau.edu.jo
Received: 17/6/2024 Accepted: 21/9/2024.
DOI: https://doi.org/10.35516/jjps.v18i2.2805

attributed to fluctuations in coregulator concentrations or genetic abnormalities [5]. AIB1 (Amplified in Breast Cancer 1) (ERα coregulator) increases, which induces PEA3 (Polyoma Enhancer Activator 3) mediated activation of MMP2 (matrix metalloproteinase 2) and MMP9 (Matrix Metalloproteinase 9) production, which promotes the spread of metastatic disease [6]. The process of breast cancer metastasis and invasion was facilitated by SRC-1 (Steroid Receptor Coactivator 1), an additional estrogen receptor (ER) coregulator, by its coactivation of PEA3 (Polyoma Enhancer Activator 3) mediated Twist expression. The study by Ali et al. showed that the coregulators of ERα had an impact on the modulation of gene expression in the context of metastasis [7]. Dydrogesterone is one of the essential non-acetylated pregnane derivatives and has many medical uses in treating and preventing miscarriage, supporting the luteal phase and part of menopausal treatment [8].

Heterocycle-based compounds are important in designing and developing potential drugs [9]. Pyrimidine [10], thiazole [11], quinoline [12], and imidazole [13] derivatives exhibit a variety of biological activities, among which pyrimidines are particularly important for the synthesize of antitumor drugs, including inhibitors of different cell lines [14]. Pregnanes containing imidazole rings, triazole rings, a glycoside moiety, and a piperazine ring have been demonstrated to possess anticancer and cytotoxic activity [15], antioxidant activity [16], and anti-leukemic properties [17], respectively. Recent studies have indicated that pyridines and pyrimidines are a category of heterocyclic nitrogen compounds with a wide range of applications in developing anticancer drugs [18]. These synthetic sources represent a potent class of compounds that can effectively treat breast cancer. Parveen et al. have developed a novel pyrimidine conjugate (Thienopyrimidine) that exhibits specific inhibitory effects in breast cancer [19]. The anti-proliferative efficacy of the synthesized conjugates was evaluated in the MCF-7 tumour cell line using the MTT assay [20].

The current study is divided into three sections. First, it uses the 3D-QSAR method to correlate the structure with the activity of a series of Benzoyl Thienopyrimidine molecules with anti-breast cancer activity. Second, it proposes new anti-breast cancer candidates with the best effect. Finally, an in-silico evaluation of the proposed molecule's ADME/Tox properties, molecular docking, and molecular dynamics predicted their stability in the target receptor. The ultimate objective is to forecast novel agents exhibiting activity surpassing that of the most potent compound within this series.

2. MATERIALS AND METHODS

2.1. Data sets

The dataset contains 22 anti-tubulin agent compounds synthesized by El-Sharkawy et al. [21]. Two arbitrary subsets were selected from this collection; one subset comprising 80% of the compounds was used for constructing the 3D QSAR model, while the other subset comprising 20% was used for model validation. The compounds' IC_{50} (μM) activity was expressed as $pIC_{50} = -\log IC_{50}$ (Table 1).

Table 1. Chemical structures and related activities of the compounds of the studied set.

N°	Molecules	X	R	Y
1a	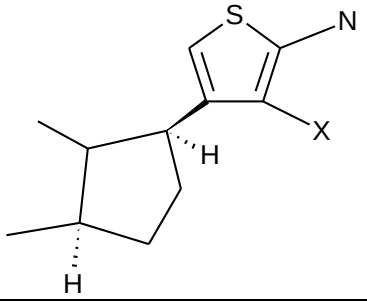	CN	-	-
1b		COOEt	-	-
2a	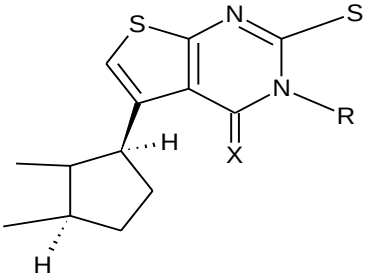	NH	Ph	-
2b		NH	COPh	-
2c		O	Ph	-
2d		O	COPh	-
6a	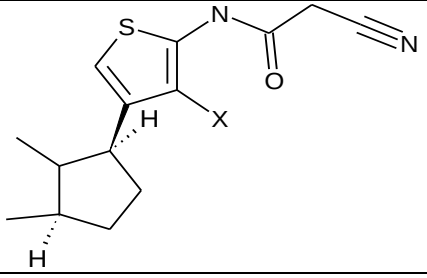	CN	-	-
6b		COOEt	-	-
8a	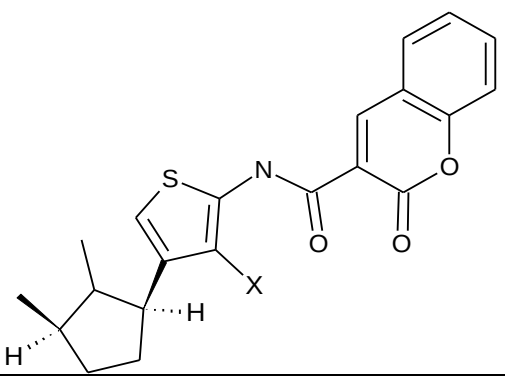	CN	-	-
8b		COOEt	-	-
7a	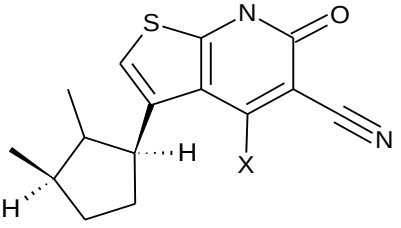	CN	-	-
7b		COOEt	-	-

N°	Molecules	X	R	Y
9a	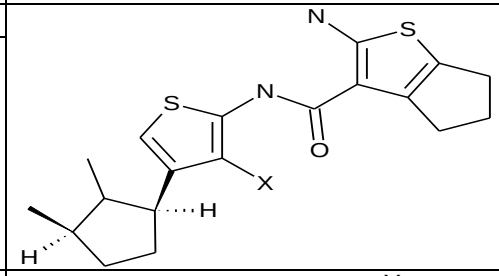	CN	-	-
9b		COOEt	-	-
10a	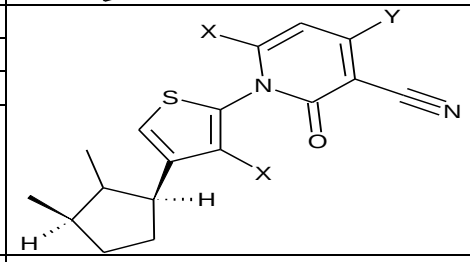	CN	-	H
10b		CN	-	CH_3
10c		COOEt	-	H
10d		COOEt	-	CH_3
12a	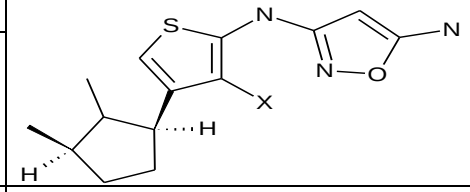	CN	-	-
12b		COOEt	-	-
14a	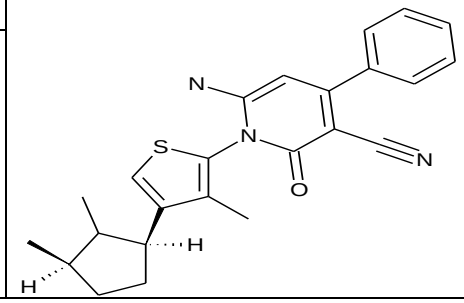	CN	-	-
14b		COOEt	-	

2.2. Minimization and molecular alignment

Molecular alignment is an essential stage in generating the best models of 3D-QSAR [22]. To model and optimize the chemical compounds in the studied set, a program Sybyl X-2.0 was utilized. The geometry of the compounds has been optimized using the field of Tripos forces in 1000 iterations[23]. Using the Gasteiger-Hückel concept, partial atomic loads have been computed with converge to 0.01 kcal/mol Å energy value [24]. As a result, the 2d compound, which is the most active in the compound set, is selected as a model. Other compounds have been aligned with their common maximal sub-structures (Figure 1).

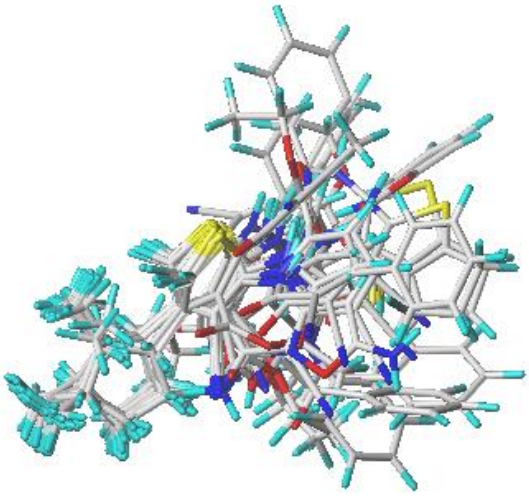

Fig. 1. Aligned compounds.

2.3. 3D QSAR studies

This study describes using the CoMFA and CoMSIA are abbreviations for Comparative Molecular Field Analysis and Comparative Molecular Similarity Indices Analysis, respectively techniques for 3D-QSAR modeling with the aid of the SYBYL-X 2.0 software[25]. Within the framework of the CoMFA modeling, a hybridized sp^3 carbon atoms with a 1.52 van der Waals radius was chosen to calculate the steric and electrostatic fields, with an energy coupling of 30 kcal/mol. The same grille was used by the CoMSIA model, allowing for the calculation of additional fields, including hydrophobicity, hydrogen bond donor and acceptor, and steric and electrostatic fields. These approaches provide an investigation of molecular properties, making them invaluable in developing and discovering pharmaceuticals.

2.4. Verification of the predictive capacity of the developed CoMFA and CoMSIA models

The model generated by the method of least squares partials (PLS) was internally validated using the coefficients of cross-validation square (Q^2), the number optimum de composants (ONC), the coefficient of cross-validation square (R^2), and the standard error estimation (SEE). These coefficients provide a gauge of the model's internal quality. The related expressions define Q^2 and R^2.

$$Q^2 = \frac{\sum (y_i - \hat{y}_i)^2}{\sum (y_i - \bar{y}_i)^2} > 0.5 \quad (1)$$

$$R^2 = \frac{\left[\sum (y_i - \bar{y}_i)(\hat{y}_i - \bar{\hat{y}}_i)\right]^2}{\sum (y_i - \bar{y}_i)^2 . \sum \hat{y}_i - \bar{\hat{y}}_i)^2} > 0.6 \quad (2)$$

y_i= experimental activity, $\hat{y}_i$ = calculated activity, $\bar{y}_i$= = average of experimental activity, and $\bar{\hat{y}}_i$ = average of calculated activity.

2.5. The prediction of ADME/Tox and bioavailability

2.5.1. Rules of Lipinski and Veber

SwissADME was used to calculate the similarity descriptors to the chosen medications using the Lipinski and Veber rules [26]. Lipinski's Rule of 5 guarantees a compound's applicability as an oral medication. A composition must meet at least two of the following requirements: molecules with PM < 500 Dalton, strong lipophilicity (LogP < 5), hydrogen bond donors (HBD < 5), and hydrogen bond acceptors (HBA < 10) [27]. Veber and colleagues have added two more relevant descriptors that are used to assess a compound's medicinal power: the number of rotative liaisons (NBR_{10}) and the surface polarity (PSA < 140 Å). The water solubility, lipophilicity,

and human intestinal absorption percentage (HIA) parameters have been used to predict absorption (LogS ≤ -10: insoluble; -10 < LogS ≤ –6). a little bit soluble; -6 < LogS ≤ -4: moderately soluble; -4 < LogS ≤ -2: soluble; -2 < LogS < 0: extremely soluble; 0 < LogS: highly soluble) [28].

2.5.2. Calculation of the ADME/Tox profile

The ADME/Tox (Absorption, Distribution, Metabolism, Elimination, and Toxicity) profile describes the chemical impact of drug candidates on health. It is a tool for predicting drug candidates' pharmacological and toxicological properties, avoiding costly late-stage preclinical and clinical failures in the preclinical phases [29].

2.6. Molecular docking

The expression of estrogen receptors characterizes MCF-7 cell lines targeted during the antiproliferative activity. The structure of the human estrogen receptor alpha domain (ERα) binding to the proposed selected 22 compounds is a target to be studied by molecular docking. Using the Auto Dock Vina program to predict the optimized binding conformation of the proposed selected 22 compounds (ligands) and understand receptor-ligand interactions [30]. After the compounds were drawn using SYBYL X2.0 software, molecular docking was carried out using Auto Dock Vina software[31].

2.6.1. Macromolecule Preparation

The RCSB database was used to retrieve the crystal structure of the human estrogen receptor alpha ligand-binding domain (ERα) in association with the antagonist (ligand 4-D) (PDB code: 1SJ0) [32]. The Discovery Studio 2016 program was used to remove the crystallized co-ligand, add polar hydrogens, and remove water molecules in the estrogen receptor (ERα).

2.6.2. Ligands Preparation

The most active compound in the database (2d) and the newly designed molecules (T1, T2, T3, T4, T5, and T6) were docked into the human estrogen receptor alpha (ER) [33]. The binding mode between the receptor and the docked molecules was studied, compared, and selected for further analysis.

2.7. Molecular dynamics simulations

Molecular dynamics (MD) computations were used to determine the ideal docking positions to comprehend the stability of the interaction between a (1SJ0) protein and (T1 and D2) ligands complexes [34]. The input files for the MD calculations were generated using the CHARMM force field parameters[35]. The CHARMM force field was utilized to build the ligand topology through the Param-Chem server. The five steps of the CHARMM GUI solution builder included solving the combination and reading the coordinates of the 1SJ0) protein and (T1 and D2) ligands complex.

The experiments took place within a triclinic container filled with TIP3P water models and balanced by the addition of Na^+ and Cl^- ions. Subsequently, the system underwent minimization utilizing the steepest descent technique. Following the energy minimization, the system was subjected to an NVT ensemble at 300 K for 100 ps, utilizing a v-rescale thermostat [36]. This was succeeded by an NPT ensemble at 300 K and 1 atm for 100 ps, employing a Parrinello-Rahman barostat [37] and a v-rescale thermostat [37]. Lastly, the production simulation was run at 300 K for 300 ns. The particle mesh Ewald algorithm [38] was used to figure out the electrostatic interactions, and the Linear Constraint Solver algorithm [36] was used to limit the covalent bonds.

2.7.1 Analysis of the Trajectory

Using GROMACS tools, the analysis of molecular dynamics simulations was carried out. The gmx_rms subroutine was used to calculate the ligand and the protein's root mean square deviations (RMSD) of the atom positions. Using gmx_rmsf, the quadrature-averaged fluctuations (RMSF) based on the protein's C-alpha atoms were calculated. Gmx_gyrate was used to calculate each protein's gyration radius, and Gmx_hbond was used to assess the number of hydrogen bonds at the protein-ligand interface. Also, the simulation has tracked the distance

between the protein's and the ligand's centers of mass thanks to the gmx_distance function. Finally, the trajectory visualization and frequency analysis of protein-ligand connections were conducted using the VMD 1.9.3 program [39].

2.7.2 MM/PBSA calculation of free energy of binding

A GROMACS tool called g_mmpbsa was used to perform MM/PBSA (Molecular Mechanics/Poisson-Boltzmann Surface Area) calculations for the systems chosen for additional research[40]. The free energy of binding between the (1SJ0) protein and (T1 and D2) ligands complexes in the solvent may be represented as follows:

$$\Delta G_{binding} = \Delta G_{complex} - (\Delta G_{protein} + \Delta G_{ligand})$$

To estimate the binding energy between a protein and ligand in a solvent, we use the isolated protein and ligand's total free energies and the protein-ligand complex's total free energies. An alternative method is to use g_mmpbsa to estimate the energy contribution of each residue to the binding energy. The binding energy can then be broken down by adding up the energy contribution of each residue. To compute g_mmpbsa's MM-PBSA, we need a binary run input file (.tpr) that reads files from specific versions of GROMACS. This file is created by GROMACS 5.1.4 [41].

3. RESULTS AND DISCUSSION

3.1. CoMFA and CoMSIA statistical findings

The real pIC_{50} about the calculated pIC_{50} for the CoMSIA and CoMFA models was illustrated in Fig. 2. The proximity of the red and blue dots creates a linear link between the observed and expected activity.

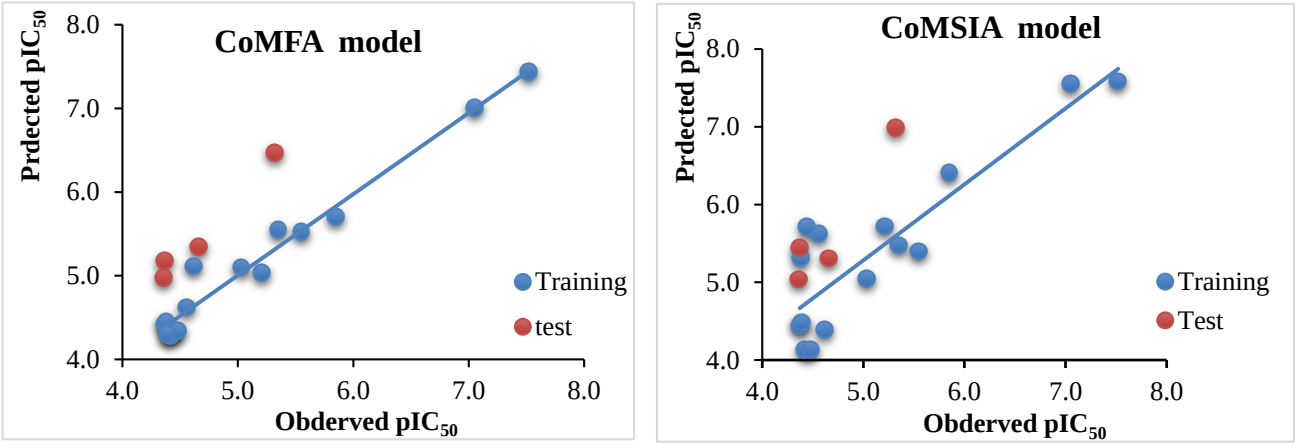

Fig. 2. Variation of the experimental activity versus the activity predicted by the CoMFA and CoMSIA models.

Tables 2 and 3 provide descriptions of the outcomes of the CoMFA and CoMSIA model validation. The outcomes satisfy all the criteria listed above.

Table 2. PLS statistical parameters.

							Fractions				
Model	**Q2**	**R2**	**SEE**	**F**	**N**	**R ext ^{2}**	**Ster**	**Elect**	**Acc**	**Don**	**Hyd**
CoMFA	0.516	0.970	0.194	118.276	3	0.972	0.480	0.520	-	-	-
CoMSIA	0.787	0.993	0.093	524.592	3	0.895	0.083	0.230	0.191	0.311	0.185

Table 3. Experimental and predicted pIC_{50} of 19 thiophene, pyrimidine, pyrazole, pyridine, coumarin and isoxazole derivatives

N°	**pIC_{50}**	**CoMFA**		**CoMSIA**	
		Predicted	**Residual**	**Predicted**	**Residual**
10a	5.85	5.703	0.147	6.407	-0.557
10c	5.55	5.522	0.028	5.398	0.152
10d	5.35	5.552	-0.202	5.477	-0.127
12a	4.62	5.111	-0.491	4.391	0.229
12b	4.37	4.419	-0.049	4.445	-0.075
2c	7.05	7.009	0.041	7.552	-0.502
2d	7.52	7.437	0.083	7.583	-0.063
6a	5.21	5.038	0.172	5.72	-0.51
6b	5.03	5.100	-0.07	5.046	-0.016
7a	4.42	4.28	0.14	4.130	0.29
7b	4.38	4.447	-0.067	5.320	-0.94
8a	4.56	4.624	-0.064	5.624	-1.064
8b	4.44	4.339	0.101	5.713	-1.273
9a	4.48	4.345	0.135	4.129	0.351
9b	4.39	4.293	0.097	4.486	-0.096
1a*	4.66	5.347	-0.687	5.309	-0.649
14a*	4.37	5.178	-0.808	5.444	-1.074
14b*	4.36	4.971	-0.611	5.037	-0.677
2b*	5.32	6.472	-1.152	6.983	-1.663

*** Molecule set test**

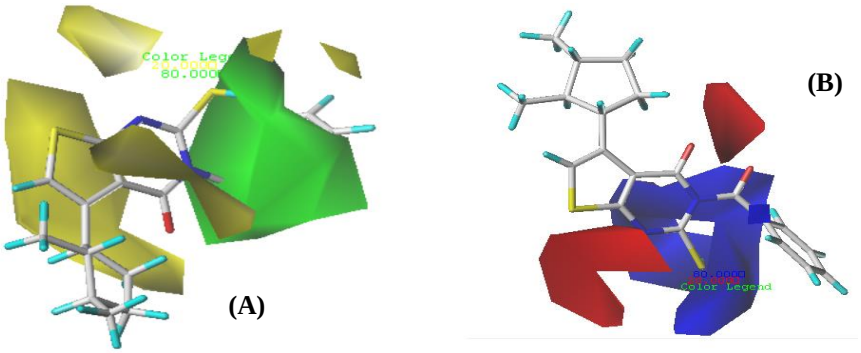

Fig. 3. (A) Steric field: yellow areas are sterically unfavorable, while green is sterically favorable. (B) Electrostatic field: blue indicates the zone where electropositive groups are favored, while red corresponds to the zone where negative groups are favored

3.2. Analysis of the results of the contour maps generated by the CoMFA model

Contextual data from contour maps is used to improve small molecule activity. On the contour maps, the most active chemical, 2d, was noted as a point of reference for interpretation.

Figure 3(A) illustrates electrostatic interactions using red and blue contours, whereas Figure 3(B) shows steric interactions of CoMFA using green and yellow contours. The green regions indicate a preference for bulky substituents, while the yellow regions indicate a preference against them. The blue sections show that nucleophilic groups are favored, while the red parts indicate that aromatization is not occurring. A) Steric specializations: the yellow outlines (20% contribution) indicate areas requiring large clusters to decrease activity, while the green contours (80% contribution) indicate regions requiring large clusters to boost activity. B) Regarding electrostatic fields, the blue contours (80% contribution) represent areas where positive charge clusters are more active. In comparison, the red contours (20% contribution) indicate areas where negative charge clusters are more active.

3.3. Analysis of the results of the contour maps generated by the CoMSIA model.

The CoMSIA analysis generated contour maps with a 2 Å grid spacing combined with compound 2D steric fields. The yellow contours (20% contribution) indicate areas where large groups are less active, while green contours (80% contribution) indicate areas of increased activity. Similarly, red contours (20% contribution) indicate areas in the electrostatic fields where electron-withdrawing groups are more active, and blue contours (80% contribution) indicate areas where they are less active. Fields with undesirable hydrophobic groups are characterized by white outlines that exhibit water-repelling properties (20% contribution), while hydrophobic groups are favored according to yellow contours (80% contribution). Magenta contours (80% contribution) indicate areas in H-bond acceptor fields where an H-bond acceptor substituent increases activity. On the other hand, red contours (20% contribution) indicate areas where an H-bond acceptor substituent decreases activity. Blue outlines (80% contribution) represent areas where the activities of the H-bond donor group increase, while purple outlines (20% contribution) indicate areas where H-bond

y [42].

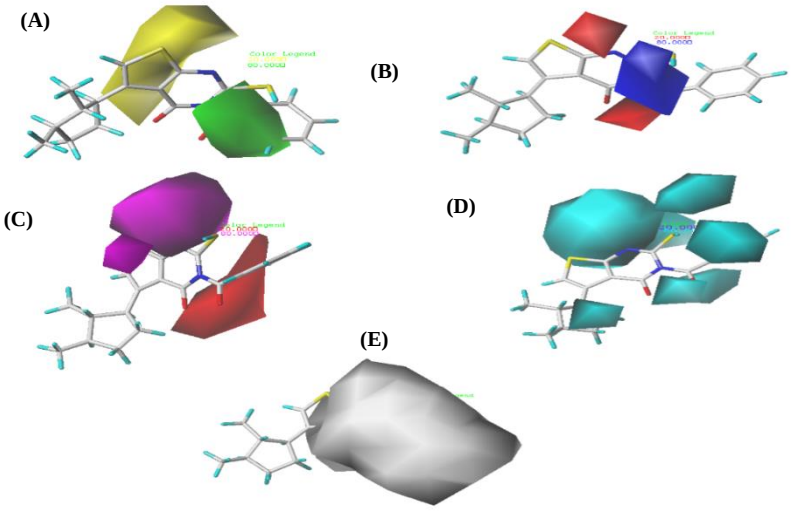

Fig. 4. 2d compound. A) Steric fields; B) Electrostatic fields.; C) H-bond acceptor fields; D) H-bond donor fields; E) Hydrophobic fields.

3.4. Drug Candidates and activity prediction

Finally, six medication candidates were recommended utilizing the field contour analysis results from the CoMFA and CoMSIA models. Table 3 illustrates the new candidates' organization and anticipated activities, and Table 4 illustrates the new candidates' structure and predicted activities.

Table 4. Newly designed drug candidates and their predicted activities.

Compound	pIC_{50}
T1 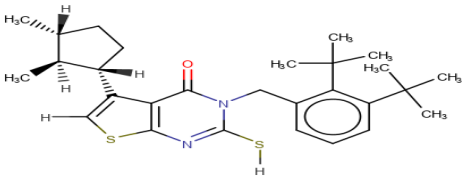	7.655
T2 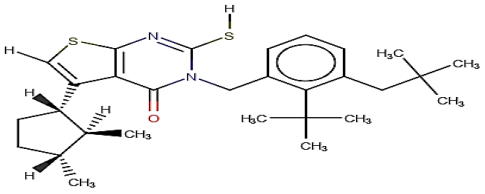	7.634
T3 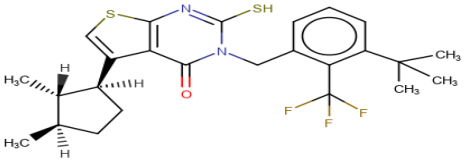	7.618
T4 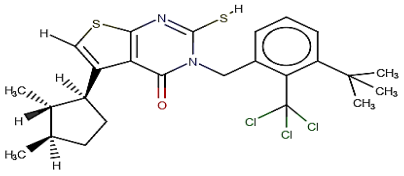	7.663
T5 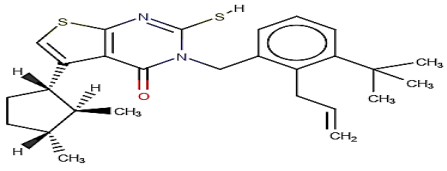	7.591
T6 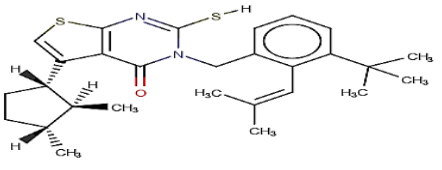	7.549

3.4.1. The prediction of ADME/Tox and bioavailability

3.4.1.1. Rules of Lipinski and Veber

Using Lipinski and Veber's rules, the similarity descriptors to the selected drugs were calculated with SwissADME (Table 5). Based on the results, the proposed drug candidates may be Lipinski drugs.

Table 5. ADME properties of newly designed compounds

	Property					
Rule	**LogP<5**	**HBD<5**	**HBA<10**	**TPSA**	**Nrotb<10**	**MW ≤500**
2d compound	4,58	1	6	119	2	384.526
T1	5.00	0	2	101.93	5	482.74
T2	4.64	0	2	101.93	6	496.77
T3	4.41	0	5	101.93	5	494.64
T4	4.47	0	2	101.93	5	544.00
T5	4.81	0	2	101.93	6	466.70
T6	5.14	1	5	101.93	4	480.73

3.4.1.2. Calculation of the ADME/Tox profile

The LogS values for our compounds ranged from -5.115 to -6.494, indicating that the compounds are highly soluble (Table 6).

The percentages of the proposed drug candidates absorbed from the human gut (% HIA) were predicted using pkCSM pharmacokinetics ranging from 86.129 to 91.511% (Table 6), indicating good absorption of the compounds studied.

Blood-brain barrier (BBB) permeability is a crucial factor in pharmacological control because it helps to limit molecular transport and diffusion via the BBB while still exerting therapeutic effects on the brain [43]. The validated blood-brain barrier (BBB) permeability value in the standard scale is higher than 0.3, while a number lower than -1 is unacceptable [44]. According to the BBB assessment, all chemicals proposed under study had average BBB permeability.

P-gp in various human tissues acts as an ATP-dependent drug extraction pump, as all the proposed drug candidates are not P-gp substrates.

CYP enzyme inhibition is an essential mechanism of drug interactions based on metabolism, which exerts another drug on the same enzymatic active site. Inhibiting CYP reduces toxicity or reduces medication effectiveness [45]. CYP2C9 is the main enzyme that metabolizes drugs [46]. It has a highly rearranged polymorphic structure, and how it is broken down differs for each person. Indeed, people with low CYP2D6 activity may not benefit as much from the drug or have harmful side effects. All proposed compounds, except T2, inhibit CYP2C9. As shown in Table 6, the compounds studied are not CYP2C19, CYP3A4, and CYP2D6 inhibitors, while they inhibit CYP1A2 [47].

Excretion is an effective method by which drugs are eliminated from the body. It is essential to determine dosing rates to achieve steady-state concentrations [48]. This descriptor's value varies between -0.361 and -0.158 ml/min/kg for the studied compounds.

AMES toxicity evaluates the potential carcinogenic effects of chemicals. When these mutant bacterial cells are exposed to mutagenic substances, the mutation in the bacterial cells is reversed, allowing the bacteria to thrive on a medium deficient in histidine [49]. T3 is the only compound that shows toxicity.

Table 6. Pharmacokinetic properties (ADMET) of new compounds.

Models	Compounds						
	T1	T2	T3	T4	T5	T6	2d
Absorption							
Water solubility	-5.228	-5.214	-6.494	-6.292	-6.077	-6.081	-5.115
Intestinal absorption (human) %	90.646	90.071	88.258	86.129	90.176	89.123	91.511
P-glycoprotein substrate	No	No	No	No	No	No	No
Distribution							
The blood-brain barrier (LogBB)	-0.065	-0.104	0.166	0.14	0.087	0.131	0.484
Metabolism							
CYP1A2	No	No	No	No	No	No	Yes
CYP2C9	**Yes**	**No**	**Yes**	**Yes**	**Yes**	**Yes**	**Yes**
CYP2D6	**Yes**	**Yes**	**Yes**	**Yes**	**Yes**	**Yes**	**Yes**
CYP2C19	**No**	**No**	**No**	**No**	**No**	**No**	**No**
CYP3A4	**No**	**No**	**No**	**No**	**No**	**No**	**Yes**
Excretion							
Total Clearance (ml/min/kg)	**-0.308**	**-0.361**	**-0.158**	**-0.320**	**-0.266**	**-0.336**	**-0.279**
Toxicity							
AMES toxicity	**No**	**No**	**Yes**	**No**	**No**	**No**	**No**

3.5. Docking results

Table 7 and Figure 5 show the interactions between the studied compounds and the target receptor and the corresponding free energy. According to the results, all the studied compounds interact with amino acids in the same pocket of the receptor's (PDB code 1SJ0) active site. Also, all the proposed compounds have a significant binding affinity.

Table 7. Different interactions between designed molecules and the receptor (ERα) (PDB code 1SJ0).

Designed molecules	Binding affinity [kcal/mol]	Conventional hydrogen bonding	Carbon Hydrogen	Charge attractive	Pi-Anion	Alkyl or Pi-alkyl	Pi-sigma	Pi-sulfur or Pi-stacked
T1	-6.6	Leu 536	None	None	None	Val A:533	Trp A:383	None
T2	-6.3	None	None	None	None	Val A:533 Ala A:350 Trp A:383 Leu A:354 Leu A:536	None	Tyr A:526
T4	-7.2	None	None	None	None	Leu A:354 Leu A:536	Trp A:383 Tyr A:526	Cys A:530
T5	-6.7	None	Cys 530	None	None	Leu A:354 Ala A:350 Trp A:383 Leu A:536	Tyr A:526	Tyr A:530
T6	-7.8	None	None	Asp 351	Asp 351	Leu A:354 Leu A:536 Leu A:525 Ala A:350	Trp A:383	None
2d	-7.4	None	None	None	None	Val A:533 Leu A:536	Trp A:383	Trp A:383

The affinity of the proposed compound and the active molecule of the (ERα) receptor ranged from -7.8 to -6.3 kcal/mol (Table 7). Compounds T1, T2, T4, T5, and T6 showed higher PIC50 activity than the active molecule 2d. Discovery Studio software elucidated the hydrogen and hydrophobic interactions between compounds T1, T2, T4, T5, and T6 and the more active molecule 2d. Compound 32 did not form any hydrogen bonds but demonstrated pi-sigma and pi-alkyl interactions with the (Me) groups and the residues Val (Valine, A533) and Leu (Leucine, A536). The limited number of bonds reduces the stability of this complex. In contrast, compound T1 established a hydrogen bond with the amine groups via the residues Leu (Leucine, A536), significantly enhancing the stability of the complex. Additionally, T1 formed two pi-sigma bonding interactions with the residues Trp (Tryptophan, A383) and Tyr (Tyrosine, A526). These important pi-sigma interactions contribute to a compact structure, with a lower binding affinity than the more active molecule. The proposed molecule T1 exhibits greater potency as an (ERα) receptor inhibitor than the 2d molecule due to its improved binding affinity and interaction stability. The other complexes (T2, T4, T5, and T6) show fewer hydrogen bonds and less effective interactions, making them less stable than T1. This demonstrates that T1 is the most stable complex among those analyzed.

Ligand	2D	3D
2d	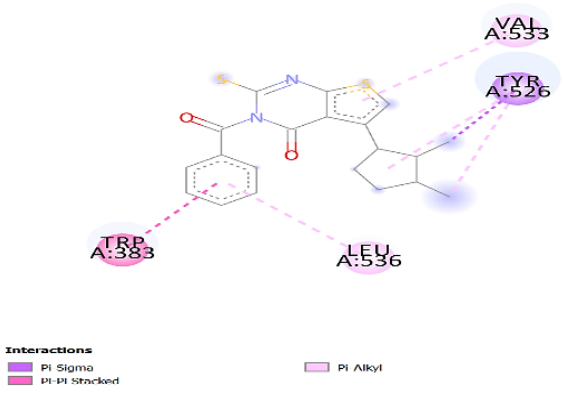	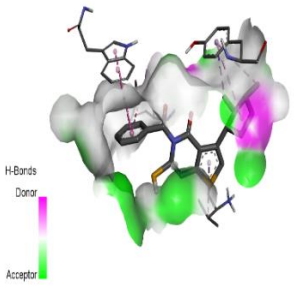
T1	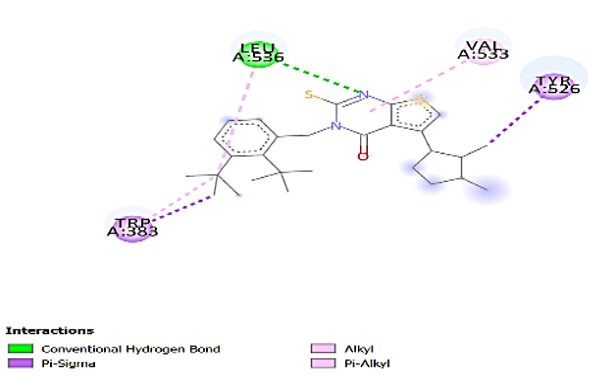	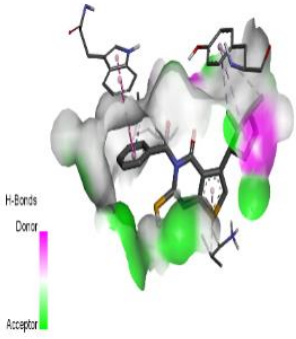

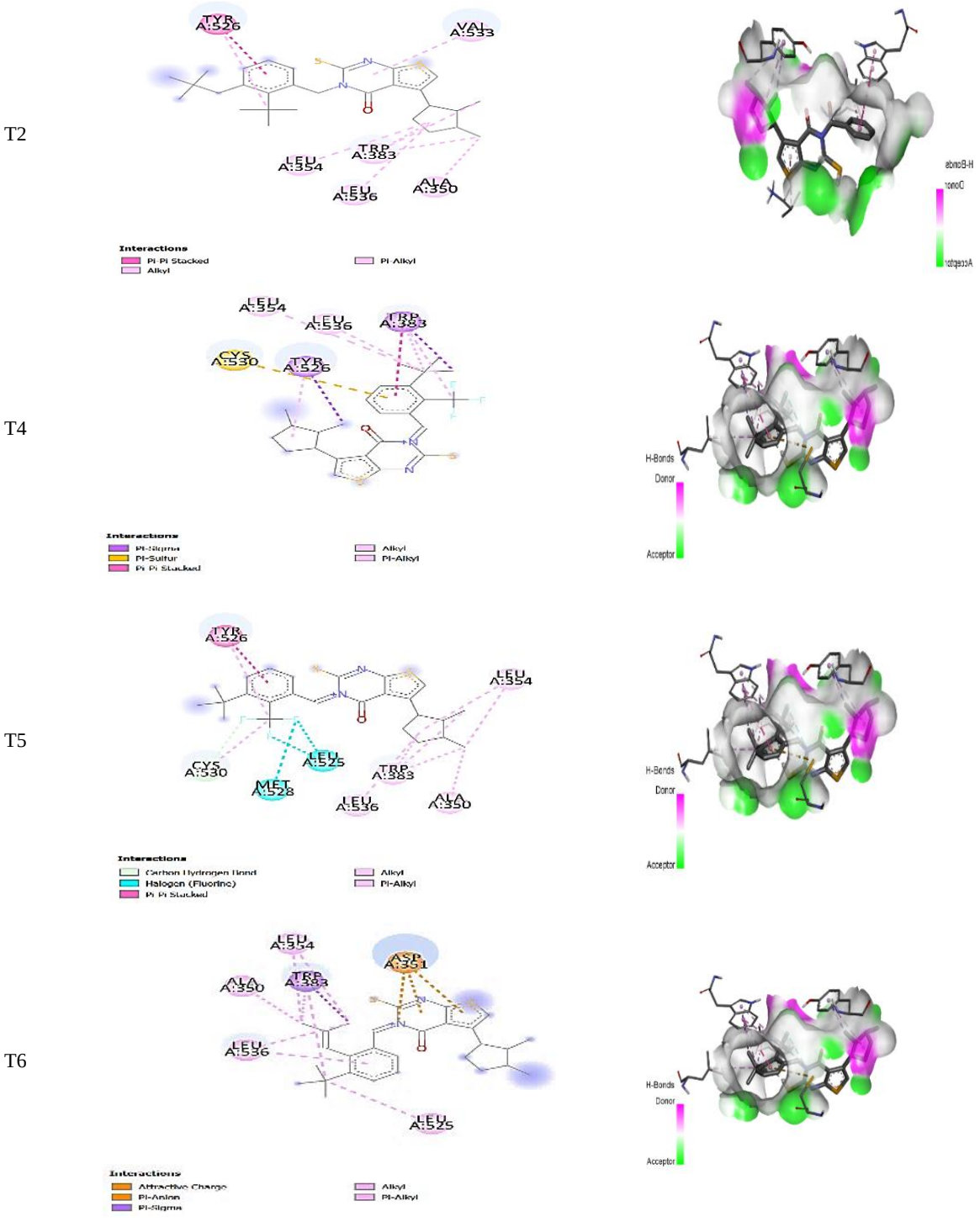

Fig. 5. Docking interaction of the representative compound in the estrogen receptor (ERα)

3.6. Molecular dynamics (MD) simulation of the stability of protein-ligand interactions

A one-hundred-nanosecond simulation using molecular dynamics (MD) was performed to assess the stability of the T1 and 2D complexes formed by the protein **1SJ0** and its associated ligands. Throughout the simulation, according to the trajectory analysis, every ligand maintained its link with the protein's gorge of liaison. Numerous parameters, including the RMSD, RMSF, gyration radius, hydrogen bonding, the average distance between the protein and ligand centers of mass (COM), and free energy of liaison (MMPBSA), have been computed to assess each structure's stability [50].

After the first ten simulation runs, the results showed very little variation, with the RMSD and RMSF values indicating the stability of the complexes [51]. The small variations observed in the radius of gyration suggest that the stability and compactness of the protein-ligand system are maintained. Throughout the simulation, the hydrogen bonds between the ligands and the protein persisted, and the COM's distance suggested strong stability, especially for ligand T1.

The free energy of binding (ΔG_{Bind}) obtained using the MM-PBSA method was -165.832 ± 20.069 kJ mol^{-1} for T1 and -135.295 ± 15.421 kJ mol^{-1} for 2D, confirming the strong affinity of the two ligands for the protein. The MM-PBSA calculations also provided the potential energy and the polar and non-polar energy of solvation, highlighting the stability of the interactions in the T1 and 2D complexes [52].

In summary, the simulations have shown the stability and robustness of protein-ligand complexes, offering vital information to comprehend their interaction and potential as therapeutic targets.

Table 8. Calculated binding free energies of the tested compounds [kJ/mol].

		ΔE_{MM} (kJ mol^{-1})		ΔG_{Sol} (kJ mol^{-1})	
Complex (Protein-ligand)	ΔG	**Van der Waal energy**	**Electrostatic energy**	**Polar solvation energy**	**SASA energy**
T1	-165.832+/-20.069	-194.756+/-16.084	-35.240+/-15.455	86.265+/- 5.823	-22.102+/-1.188
2D	-135.295+/-15.421	-147.225+/-10.945	-48.464+/-11.157	75.789+/- 9.759	-15.395+/- 1.469

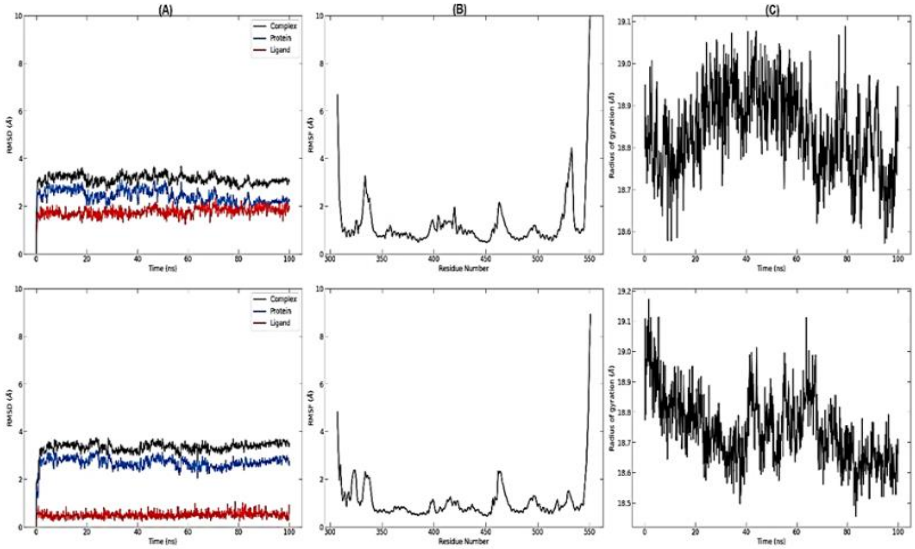

Fig. 6. (A) RMSD, (B) RMSF, and (C) gyratory radius, observed during 100ns MD simulation. T1 (top) and 2D (bottom) complexes.

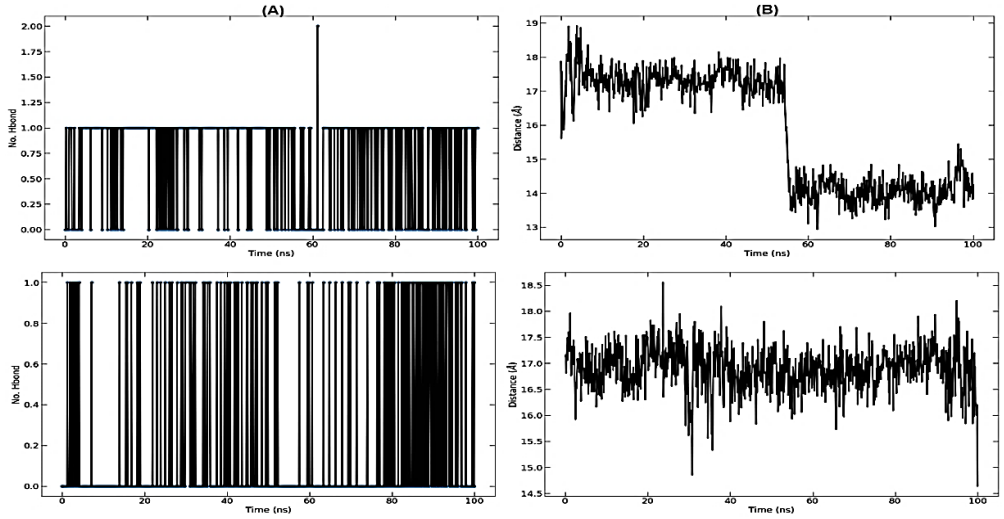

Fig. 7. From right to left: (A) Hydrogen bonds (protein (1SJ0)-ligand (T1 and 2D)) and (B) Average distance between ligand and protein for the complexes during the 100ns MD simulation. Compounds T1 (top) and 2D (bottom)

CONCLUSION

This study highlighted the potential of thienopyrimidine inhibitors for the treatment of ER+ breast cancer using advanced computational methods. Through robust 3D-QSAR analyses and molecular docking validation, six new molecules (T1-T6) were identified as promising candidates for estrogen receptor alpha inhibition. The results indicate that these compounds, except T3, which showed mild toxicity, have favorable pharmacokinetic and pharmacodynamic properties and maintain stability within the receptor's active site. Molecular dynamics simulations confirmed their stability, providing valuable insights into the development of new breast cancer drugs. These findings pave the way for future experimental and clinical research to improve therapeutic options for breast cancer patients.

Author Contributions

All participants contributed to the design and development of the study.

Hassan Badaoui, Youness Moukhliss, Moulay Ahfid Elalaouy, Hanane Zaki, and Marwa Alaqarbeh: creation and design of the research project, data collection, analysis, interpretation of the findings, and article writing; M'barek Choukrad, Hamid Maghat, Abdelouahid Sbai, Mohammed Bouachrine, and Tahar Lakhlifi: revising it critically for important intellectual content, and final approval of the version to be submitted.

Funding: The authors have no outside funding to declare.

Declarations

Conflict of interest: The authors declare no competing interests, as defined by Springer, or other interests that might be perceived to influence the results and/or discussion reported in this paper.

Ethical approval is Not applicable.

REFERENCES

1. Antebi A. Nuclear receptor signal transduction in *C. elegans*. In: *WormBook: The Online Review of C. elegans Biology*. WormBook. 2018.
2. Jeon S-Y., Hwang K-A., Choi K-C. Effect of steroid hormones, estrogen and progesterone, on epithelial mesenchymal transition in ovarian cancer development. *J Steroid Biochem Mol Biol.* 2016;158:1–8. https://doi.org/10.1016/j.jsbmb.2016.02.005
3. Merrheim J., Villegas J., Van Wassenhove J., Khansa R., Berrih-Aknin S., le Panse R., Dragin N. Estrogen, estrogen-like molecules and autoimmune diseases. *Autoimmun Rev.* 2020;19:102468. https://doi.org/10.1016/j.autrev.2020.102468
4. Speltz T.E., Mayne C.G., Fanning S.W., Siddiqui Z., Tajkhorshid E., Greene G.L., Moore T.W. A "Cross-Stitched" Peptide with Improved Helicity and Proteolytic Stability. *Org Biomol Chem.* 2018;16:3702–6. https://doi.org/10.1039/c8ob00790j
5. Hegde M., Girisa S., Naliyadhara N., Kumar A., Alqahtani M.S., Abbas M., Mohan C.D., Warrier S., Hui K.M., Rangappa K.S., Sethi G., Kunnumakkara A.B. Natural compounds targeting nuclear receptors for effective cancer therapy. *Cancer Metastasis Rev.* 2023;42:765–822. https://doi.org/10.1007/s10555-022-10068-w
6. Vishnoi K., Viswakarma N., Rana A., Rana B. Transcription Factors in Cancer Development and Therapy. *Cancers (Basel).* 2020;12:2296. https://doi.org/10.3390/cancers12082296
7. Taheri M., Shoorei H., Dinger M.E., Ghafouri-Fard S. Perspectives on the Role of Non-Coding RNAs in the Regulation of Expression and Function of the Estrogen Receptor. *Cancers (Basel).* 2020;12:2162. https://doi.org/10.3390/cancers12082162
8. Tetruashvili N., Domar A., Bashiri A. Prevention of Pregnancy Loss: Combining Progestogen Treatment and Psychological Support. *JCM.* 2023;12:1827. https://doi.org/10.3390/jcm12051827
9. Ali I., Lone M.N., Aboul-Enein H.Y. Imidazoles as potential anticancer agents †The authors declare no competing interests. *Medchemcomm.* 2017;8:1742–1773. https://doi.org/10.1039/c7md00067g
10. George S., Abrahamse H. Redox Potential of Antioxidants in Cancer Progression and Prevention. *Antioxidants (Basel).* 2020;9:1156. https://doi.org/10.3390/antiox9111156
11. Song S., Kim S., El-Sawy E.R., Cerella C., Orlikova-Boyer B., Kirsch G., Christov C., Dicato M., Diederich M. Anti-Leukemic Properties of Aplysinopsin Derivative EE-84 Alone and Combined to BH3 Mimetic A-1210477. *Mar Drugs.* 2021;19:285. https://doi.org/10.3390/md19060285
12. Ardevines S., Marqués-López E., Herrera R.P. Heterocycles in Breast Cancer Treatment: The Use of Pyrazole Derivatives. *Curr Med Chem.* 2023;30:1145–1174. https://doi.org/10.2174/0929867329666220829091830
13. Kolawole O.A., Banjo S. In Vitro Biological Estimation of 1,2,3-Triazolo[4,5-d]pyrimidine Derivatives as Anti-breast Cancer Agent: DFT, QSAR and Docking Studies. *Curr Pharm Biotechnol.* 2020;21:70–78. https://doi.org/10.2174/1389201020666190904163003
14. Thapa R., Flores R., Cheng K.H., Mochona B., Sikazwe D. Design and Synthesis of New Acyl Urea Analogs as Potential σ1R Ligands. *Molecules.* 2023;28:2319. https://doi.org/10.3390/molecules28052319

15. Aati H.Y., Attia H., Babtin R., Al-Qahtani N., Wanner J. Headspace solid phase micro-extraction of volatile constituents produced from Saudi *Ruta chalepensis* and molecular docking study of potential antioxidant activity. *Molecules.* 2023;28:1891. https://doi.org/10.3390/molecules28041891
16. Frant M.P., Trytek M., Deryło K., Kutyła M., Paduch R. Cellular localization of selected porphyrins and their effect on the in vitro motility of human colon tumors and normal cells. *Molecules.* 2023;28:2907. https://doi.org/10.3390/molecules28072907
17. [Author(s) missing] Antimicrobial, antibiofilm, and anticancer activities of *Syzygium aromaticum* essential oil nanoemulsion. *PMC.* [n.d.] https://www.ncbi.nlm.nih.gov/pmc/articles/PMC10421252/
18. Maimaitiming M., Lv L., Zhang X., Xia S., Li X., Wang P., Liu Z., Wang C.-Y. Semi-synthesis and biological evaluation of 25(R)-26-acetoxy-3β,5α-dihydroxycholest-6-one. *Mar Drugs.* 2023;21:191. https://doi.org/10.3390/md21030191
19. Thiriveedhi A., Nadh R.V., Srinivasu N., Bobde Y., Ghosh B., Sekhar K.V.G.C. Design, synthesis and anti-tumour activity of new pyrimidine-pyrrole appended triazoles. *Toxicol In Vitro.* 2019;60:87–96. https://doi.org/10.1016/j.tiv.2019.05.009
20. Kis B., Moacă E.-A., Tudoran L.B., Muntean D., Magyari-Pavel I.Z., Minda D.I., Lombrea A., Diaconeasa Z., Dehelean C.A., Dinu Ș., Danciu C. Green synthesis of silver nanoparticles using *Populi gemmae* extract: Preparation, physicochemical characterization, antimicrobial potential and in vitro antiproliferative assessment. *Materials (Basel).* 2022;15:5006. https://doi.org/10.3390/ma15145006
21. El-Sharkawy K.A., Bratty M.A., Alhazmi H.A., Najmi A. Design, synthesis, and biological activities of novel thiophene, pyrimidine, pyrazole, pyridine, coumarin and isoxazole: Dydrogesterone derivatives as antitumor agents. *Open Chemistry.* 2021;19:322–337. https://doi.org/10.1515/chem-2021-0028
22. Wilkes J.G., Stoyanova-Slavova I.B., Buzatu D.A. Alignment-independent technique for 3D QSAR analysis. *J Comput Aided Mol Des.* 2016;30:331–345. https://doi.org/10.1007/s10822-016-9909-0
23. Pan M., Cheng L., Wang Y., Lyu C., Hou C., Zhang Q. Exploration of 2D and 3D-QSAR analysis and docking studies for novel dihydropteridone derivatives as promising therapeutic agents targeting glioblastoma. *Front Pharmacol.* 2023;14:1249041. https://doi.org/10.3389/fphar.2023.1249041
24. Er-Rajy M., El Fadili M., Imtara H., Saeed A., Ur Rehman A., Zarougui S., Abdullah S.A., Alahdab A., Parvez M.K., Elhallaoui M. 3D-QSAR Studies, Molecular Docking, Molecular Dynamic Simulation, and ADMET Proprieties of Novel Pteridinone Derivatives as PLK1 Inhibitors for the Treatment of Prostate Cancer. *Life (Basel).* 2023;13:127. https://doi.org/10.3390/life13010127
25. Aouidate A., Ghaleb A., Ghamali M., Chtita S., Ousaa A., Choukrad M., Sbai A., Bouachrine M., Lakhlifi T. Computer aided drug design based on 3D-QSAR and molecular docking studies of 5-(1H-indol-5-yl)-1,3,4-thiadiazol-2-amine derivatives as PIM2 inhibitors: a proposal to chemists. *In Silico Pharmacol.* 2018;6:5. https://doi.org/10.1007/s40203-018-0043-7
26. Daina A., Michielin O., Zoete V. SwissADME: a free web tool to evaluate pharmacokinetics, drug-likeness and medicinal chemistry friendliness of small molecules. *Sci Rep.* 2017;7:42717. https://doi.org/10.1038/srep42717
27. Benet L.Z., Hosey C.M., Ursu O., Oprea T.I. BDDCS, the Rule of 5 and Drugability. *Adv Drug Deliv Rev.* 2016;101:89–98. https://doi.org/10.1016/j.addr.2016.05.007

28. O'Shea J.P., Augustijns P., Brandl M., Brayden D.J., Brouwers J., Griffin B.T., Holm R., Jacobsen A.-C., Lennernäs H., Vinarov Z., O'Driscoll C.M. Best practices in current models mimicking drug permeability in the gastrointestinal tract - An UNGAP review. *European Journal of Pharmaceutical Sciences.* 2022;170:106098. https://doi.org/10.1016/j.ejps.2021.106098
29. Durán-Iturbide N.A., Díaz-Eufracio B.I., Medina-Franco J.L. In Silico ADME/Tox Profiling of Natural Products: A Focus on BIOFACQUIM. *ACS Omega.* 2020;5:16076–16084. https://doi.org/10.1021/acsomega.0c01581
30. Sharma D., Kumar S., Narasimhan B. Estrogen alpha receptor antagonists for the treatment of breast cancer: a review. *Chem Cent J.* 2018;12:107. https://doi.org/10.1186/s13065-018-0472-8
31. Trott O., Olson A.J. AutoDock Vina: improving the speed and accuracy of docking with a new scoring function, efficient optimization, and multithreading. *J Comput Chem.* 2010;31:455–461. https://doi.org/10.1002/jcc.21334
32. Bank R.P.D. RCSB PDB - 1SJ0: Human Estrogen Receptor Alpha Ligand-binding Domain in Complex with the Antagonist Ligand 4-D. *RCSB Protein Data Bank.* [Online] Available from: https://www.rcsb.org/structure/1sj0
33. Kumar R., Zakharov M.N., Khan S.H., Miki R., Jang H., Toraldo G., Singh R., Bhasin S., Jasuja R. The Dynamic Structure of the Estrogen Receptor. *J Amino Acids.* 2011;2011:812540. https://doi.org/10.4061/2011/812540
34. Fu Y., Zhao J., Chen Z. Insights into the Molecular Mechanisms of Protein-Ligand Interactions by Molecular Docking and Molecular Dynamics Simulation: A Case of Oligopeptide Binding Protein. *Comput Math Methods Med.* 2018;2018:3502514. https://doi.org/10.1155/2018/3502514
35. Kognole A.A., Lee J., Park S.-J., Jo S., Chatterjee P., Lemkul J.A., Huang J., MacKerell A.D., Im W. CHARMM-GUI Drude prepper for molecular dynamics simulation using the classical Drude polarizable force field. *J Comput Chem.* 2022;43:359–375. https://doi.org/10.1002/jcc.26795
36. Kim S., Lee J., Jo S., Brooks C.L., Lee H.S., Im W. CHARMM-GUI Ligand Reader & Modeler for CHARMM Force Field Generation of Small Molecules. *J Comput Chem.* 2017;38:1879–1886. https://doi.org/10.1002/jcc.24829
37. Alencar W.L.M., da Silva Arouche T., Neto A.F.G., de Castro Ramalho T., de Carvalho Júnior R.N., de Jesus Chaves Neto A.M. Publisher Correction: Interactions of Co, Cu, and non-metal phthalocyanines with external structures of SARS-CoV-2 using docking and molecular dynamics. *Sci Rep.* 2022;12:4326. https://doi.org/10.1038/s41598-022-08312-y
38. Lee J., Cheng X., Swails J.M., Yeom M.S., Eastman P.K., Lemkul J.A., Wei S., Buckner J., Jeong J.C., Qi Y., Jo S., Pande V.S., Case D.A., Brooks C.L., MacKerell A.D., Klauda J.B., Im W. CHARMM-GUI Input Generator for NAMD, GROMACS, AMBER, OpenMM, and CHARMM/OpenMM Simulations Using the CHARMM36 Additive Force Field. *J Chem Theory Comput.* 2016;12:405–413. https://doi.org/10.1021/acs.jctc.5b00935
39. Pereira G.R.C., Abrahim-Vieira B. de A., de Mesquita J.F. In Silico Analyses of a Promising Drug Candidate for the Treatment of Amyotrophic Lateral Sclerosis Targeting Superoxide Dismutase I Protein. *Pharmaceutics.* 2023;15:1095. https://doi.org/10.3390/pharmaceutics15041095
40. Kumari R., Kumar R., Open Source Drug Discovery Consortium, Lynn A. g_mmpbsa--a GROMACS tool for high-throughput MM-PBSA calculations. *J Chem Inf Model.* 2014;54:1951–1962. https://doi.org/10.1021/ci500020m

41. Gundelach L., Fox T., Tautermann S.T., Skylaris C.-K. Protein–ligand free energies of binding from full-protein DFT calculations: convergence and choice of exchange–correlation functional. *Physical Chemistry Chemical Physics*. 2021; 23:9381–9393.
42. In silico studies of a novel scaffold of benzoxazole derivatives as anticancer agents by 3D-QSAR, molecular docking and molecular dynamics simulations. *RSC Advances*. 2023; DOI:10.1039/D3RA01316B.
43. Pandey P.K., Sharma A.K., Gupta U. Blood brain barrier: An overview on strategies in drug delivery, realistic in vitro modeling and in vivo live tracking. *Tissue Barriers*. 2016; 4:e1129476.
44. Wu Q., Yan R., Sun J. Probing the drug delivery strategies in ischemic stroke therapy. *Drug Delivery*. 2020; 27:1644–1655.
45. Iacopetta D., Ceramella J., Catalano A., Scali E., Scumaci D., Pellegrino M., Aquaro S., Saturnino C., Sinicropi M.S. Impact of Cytochrome P450 Enzymes on the Phase I Metabolism of Drugs. *Applied Sciences*. 2023; 13:6045.
46. Miners J.O., Birkett D.J. Cytochrome P4502C9: an enzyme of major importance in human drug metabolism. British Journal of Clinical Pharmacology. 1998; 45:525–538Jarvis, J.P., Peter, A.P., Shaman, J.A.: Consequences of CYP2D6 Copy-Number Variation for Pharmacogenomics in Psychiatry. *Frontiers in Psychiatry*. 10, (2019)
47. Sarkar P., Alheety M.A., Srivastava V. Molecular docking and ADMET study of spice-derived potential phytochemicals against human DNA topoisomerase III alpha. *Macromolecular Symposia.* 2023; 407:2200108.
48. Samiei M., Asgary S., Farajzadeh M., Bargahi N., Abdolrahimi M., Kananizadeh U., Dastmalchi S. Investigating the mutagenic effects of three commonly used pulpotomy agents using the Ames test. *Advanced Pharmaceutical Bulletin.* 2015; 5:121–125.
49. Al-Shaar M., Mando H., Alkhatib R. In silico antioxidant activity of six volatile constituents in *Capsella bursa-pastoris*. *Jordan Journal of Pharmaceutical Sciences.* 2025; 18(1):230–244.
50. Maslov O., Komisarenko M., Kolisnyk S., Derymedvid L. Evaluation of anti-inflammatory, antioxidant activities and molecular docking analysis of *Rubus idaeus* leaf extract. *Jordan Journal of Pharmaceutical Sciences.* 2024; 17(1):105–122.
51. Msafer B.A.A., Abbas M.A., Shaer W.A., Arafat S. Enhanced platelet activation induced by palbociclib treatment in MCF-7 breast cancer cells. *Jordan Journal of Pharmaceutical Sciences.* 2025; 18(1):10–20.

دراسة حوسبية متكاملة لمشتقات بنزويل ثينوبيريميدين كمنظمات محتملة لمستقبل الإستروجين Erα في علاج سرطان الثدي

حسن بداوي[1]، مروه العقاربه[*2]، يونس مخلص[1]، حنان زكي[3]، مولاي أحفيظ العلوي[1]، مبارك شوكراد[1]، عبد الواحد السباعي[1]، حميد مغات[1]، الطاهر الأخليفي[1]، محمد بوعشرين[1]

[1] مختبر الكيمياء الجزيئية والمواد الطبيعية، كلية العلوم، جامعة مولاي إسماعيل بمكناس، المغرب

[2] أكاديمية الأمير حسين بن عبدالله الثاني للحماية المدنية، جامعة البلقاء التطبيقية، السلط، الأردن

[3] مختبر التكنولوجيا الحيوية والموارد البيولوجية والمعلوماتية الحيوية، المدرسة العليا للتكنولوجيا، جامعة السلطان3 مولاي سليمان، خنيفرة، المغرب

ملخص

يُعدّ سرطان الثدي المعتمد على الهرمونات والموجب لمستقبلات الإستروجين (ER+) هو النوع الأكثر شيوعًا لدى النساء حيث يمثل حوالي 75٪ من جميع الحالات. تهدف هذه الدراسة إلى اقتراح عوامل علاجية جديدة محتملة لسرطان الثدي باستخدام الطرق الحوسبية تم إجراء دراسة ثلاثية الأبعاد للعلاقة الكمية بين البنية والنشاط (3 (D-QSARعلى 22) مركبًا مستندة إلى أبحاث سابقة، وقد أظهرت قدرة تنبؤية قوية كما يتضح من القيم العالية لـ Q^2، والتي بلغت 0.516 و0.787 لطريقتي CoMFA وCoMSIA على التوالي. تم اقتراح ست جزيئات جديدة (T1–T6) بهدف تعزيز النشاط المثبط، وقد أظهرت نتائج تحليل الارتباط الجزيئي أن الجزيئات المرشحة أحرزت نتائج مميزة واستقرت في موقع الارتباط داخل المستقبل رمز (PDB: 1SJ0) كما أظهرت المركبات المقترحة خصائص دوائية وحركية حيوية مناسبة، باستثناء T3 الذي أظهر سمية خفيفة. وأكدت محاكاة الديناميكيات الجزيئية أن المعقدين T1–1SJ0 وD–1SJ02 مستقران في الموقع الفعّال لمستقبل الإستروجين Erα تسلط هذه النتائج الضوء على إمكانيات المركبات المبنية على الثينوبيريميدين كمضادات محتملة لسرطان الثدي، مما يفتح آفاقًا جديدة للبحث التجريبي والسريري.

الكلمات الدالة: سرطان الثدي، النمذجة الحوسبية، الامتصاص والتوزيع والتمثيل والإخراج/السمّية،الثينوبيريميدين، العلاقة الكمية ثلاثية الأبعاد بين البنية والنشاط.

المؤلف المراسل: مروه العقاربه

marwaqabh@hotmail.com; marwa.aqarbeh@bau.edu.jo

تاريخ استلام البحث 2024/6/17 وتاريخ قبوله للنشر 2024/9/21.

الناشر

الجامعة الأردنية
عمادة البحث العلمي
عمان 11942 الأردن
فاكس: 00962 6 5300815

رقم الإيداع لدى دائرة المكتبة الوطنية
(2008/23.3/د)

عمادة البحث العلمي

المجلة الأردنية في العلوم الصيدلانية

تعريف بالمجلة الأردنية في العلوم الصيدلانية

تأسست المجلة الأردنية في العلوم الصيدلانية بقرار لجنة البحث العلمي/ وزارة التعليم العالي والبحث العلمي رقم 367/2/10 تاريخ 2007/1/11 بشأن إصدار "**المجلة الأردنية في العلوم الصيدلانية**" ضمن إصدارات المجلات الأردنية الوطنية، وهي مجلة علمية عالمية متخصصة ومحكمة، وتصدر بدعم من صندوق دعم البحث العلمي والجامعة الأردنية تعنى بنشر البحوث العلمية الأصيلة المقدمة إليها للنشر في كافة مجالات العلوم الصيدلانية والعلوم الأخرى المرتبطة بها. وتصدر عن عمادة البحث العلمي وضمان الجودة في الجامعة الأردنية باسم الجامعات الأردنية كافة، خدمة للمتخصصين والباحثين والمهتمين في هذه المجالات من داخل الأردن وخارجه. وهي مجلة تصدر أربع مرات في العام أعتبارا من 2021، ومواعيد صدورها (آذار وحزيران وأيلول وكانون أول) من كل عام.

وباسمي وباسم أعضاء هيئة التحرير نود أن نشكر الزملاء الذين أسهموا بإرسال أبحاثهم إلى مجلتنا وتمكنا من إخراج العدد الأول. ونأمل من جميع الزملاء بإرسال ملاحظاتهم الإيجابية إلينا لنتمكن من النهوض بمجلتكم بالشكل الذي يليق بها.

وهذه دعوة إلى كافة الزملاء لإرسال اسهاماتهم العلمية من الأبحاث الأصيلة إلى عنوان المجلة.

والله ولي التوفيق

رئيس هيئة التحرير
أ.د. إبراهيم العبادي
قسم الصيدلة الحيوية والسريرية
كلية الصيدلة– الجامعة الأردنية
عمان 11942–الأردن